Metallaelectro-Catalyzed C–H Activations by 3d Transition Metals

Dissertation

for the award of the degree

“Doctor rerum naturalium”

of the Georg-August-Universität Göttingen

within the doctoral program of chemistry

of the Georg-August-Universität School of Science (GAUSS)

Submitted by

Cong Tian

From Shijiazhuang (Hebei), China

Göttingen, 2020

Thesis Committee

Prof. Dr. Lutz Ackermann, Institute of Organic and Biomolecular Chemistry

Prof. Dr. Shoubhik Das, Universiteit Antwerpen

Members of the Examination Board

Reviewer: Prof. Dr. Lutz Ackermann, Institute of Organic and Biomolecular Chemistry

Second Reviewer: Prof. Dr. Shoubhik Das, Universiteit Antwerpen

Further members of the Examination Board

Prof. Dr. Sven Schneider, Institute of Inorganic Chemistry

Prof. Dr. Johannes Walker, Institute of Organic and Biomolecular Chemistry

Dr. Holm Frauendorf, Institute of Organic and Biomolecular Chemistry

Dr. Michael John, Institute of Organic and Biomolecular Chemistry

Date of the oral examination: 07.09.2020

Table of Contents

List of Abbreviations

Ac	acetyl
acac	acetyl acetonate
Alk	alkyl
AMLA	ambiphilic metal-ligand activation
aq.	aqueous
Ar	aryl
atm	atmospheric pressure
BHT	2,6-*di*-*tert*-butyl-4-methylphenol
BIES	base-assisted internal electrophilic substitution
Bn	benzyl
Boc	*tert*-butyloxycarbonyl
Bu	butyl
Bz	benzoyl
calc.	calculated
cat.	catalytic
CMD	concerted-metalation-deprotonation
conv.	conversion
Cp*	cyclopentadienyl
Cy	cyclohexyl
δ	chemical shift
d	doublet
DCE	1,2-dichloroethane
dd	doublet of doublet
DFT	density functional theory
DG	directing group
DME	dimethoxyethane
DMF	*N*,*N*-dimethylformamide

DMSO	dimethyl sulfoxide
DMPU	1,3-dimethyl-3,4,5,6-tetrahydro-2(1*H*)-pyrimidinone
dt	doublet of triplet
EI	electron ionization
equiv	equivalent
ES	electrophilic substitution
ESI	electronspray ionization
Et	ethyl
FG	functional group
g	gram
GC	gas chromatography
h	hour
Hal	halogen
Het	hetero atom
Hept	heptyl
Hex	hexyl
HPLC	high performance liquid chromatography
HR-MS	high resolution mass spectrometry
Hz	Hertz
i	*iso*
IR	infrared spectroscopy
IES	internal electrophilic substitution
J	coupling constant
KIE	kinetic isotope effect
L	ligand
m	*meta*
m	multiplet
M	molar
$[M]^+$	molecular ion peak

Me	methyl
Mes	mesityl
mg	milligram
MHz	megahertz
min	minute
mL	milliliter
mmol	millimol
M. p.	melting point
MS	mass spectrometry
m/z	mass-to-charge ratio
NCTS	*N*-cyano-4-methyl-*N*-phenyl benzenesulfonamide
NMTS	*N*-cyano-*N*-(4-methoxy)phenyl-*p*-toluenesulfonamide
NMP	*N-methylpyrrolidinone*
NMR	nuclear magnetic resonance
o	*ortho*
OA	oxidative addition
OPV	oil pump vacuum
p	*para*
Ph	phenyl
PMP	*para*-methoxyphenyl
Piv	pivaloyl
ppm	parts per million
Pr	propyl
PTSA	*p*-Toluenesulfonic acid
py	pyridyl
pym	pyrimidine
pyr	pyrazol
q	quartet
RT	room temperature

s	singlet
sat.	saturated
SPS	solvent purification system
t	*tert*
t	triplet
T	temperature
THF	tetrahydrofuran
TLC	thin layer chromatography
TM	transition metal
TMP	2,2,6,6-tetramethylpiperidine
TMS	trimethylsilyl
Ts	*para*-toluenesulfonyl
TS	transition state
wt%	weight by volume

1. Introduction

In the past century, along with further understanding of nature science, human civilization has undergone tremendous developments in industrial production, economy, cultural diversities and global population growth. Among other aspects of natural science research, organic synthesis has become one of the major driving forces to this progress.[1] Thus, organic synthesis enabled industrial scale product preparation, namely drugs, crop-protecting agents, nitrogen fertilizers, organic fuels and polymer materials. Despite diverse applications provided by organic chemistry in life-saving pharmaceuticals, agrochemicals and material science, chemical industry was considered as one of the most polluting industries, due to the chemical wastes generation, toxic reagents usage during the process and greenhouse gases emission.[2] With our increasing acknowledgement towards the ecological impact of chemical production processes, new concept and sustainable approaches were required in designing novel synthetic routes.[3]

In order to overcome the environmental drawbacks of chemical processes, environmentally friendly synthetic methods development has become one of the major goals for chemists nowadays. In this context, new concepts of sustainable chemistry have been introduced in the last few decades. In 1991, *Trost* proposed the concept of atom economy,[4] which has been considered as a guideline for developing sustainable synthetic methodologies. In 1998, *Anastas* and *Warner* published the “12 Principles of Green Chemistry”,[5] which refined how chemists design their synthetic approaches by detailed guidance towards environmental-benign chemical processes. Among other principles of green chemistry, catalysis, by using catalytic quantities of a reagent instead of stoichiometric amounts, stands out as a fundamental tool to achieve sustainable chemistry, especially in industry-scale reactions. Catalysis does not only minimize the environmental footprint of chemical processes by reducing the waste generation, but also holds potential towards a resource economy[6] for organic

chemistry.

1.1 Transition Metal-Catalyzed C–H Activation

Enabled by organic synthesis methodologies, strategies for molecular construction and engineering with applications towards bioactive reagents, material science as well as pharmaceutical and agrochemical industries, have been developed over the last century. Thus far, due to a high demand for efficient formation of C–C/C–Het bonds in molecular synthesis, strategies for selective C–C/C–Het bonds architecture have been well-established, especially in transition metal-catalyzed cross-coupling reactions.[7] Major achievements in the field of C–C construction using diverse coupling partners have been realized by pioneering researchers, giving numerous name reactions, for instance *Suzuki–Miyaura*,[8] *Mizoroki-Heck*,[9] *Tsuji-Trost*,[10] *Buchwald–Hartwig*[11] and *Sonogashira–Hagihara*[12] cross-coupling reactions. Palladium-catalyzed cross-couplings are nowadays a readily available tool for organic synthesis with wide applications in molecular design, late-stage diversification and drug development within academia as well as industry.[13] Due to these contributions, the Nobel Prize in Chemistry 2010 was awarded jointly to *R. F. Heck*, *E. Negishi* and *A. Suzuki* “for palladium-catalyzed cross couplings in organic synthesis”.[14]

However, despite indisputable progress, the cross-coupling reactions possess inherent drawbacks that cannot be ignored when ecological impacts are taken into consideration. Indeed, traditional cross-coupling transformations largely rely not only on prefunctionalized substrates and sensitive, hard-to-handle organometallic reagents, but also noble, rare and often toxic transition metal catalysts. These major drawbacks lead to multi-step procedures to synthesize the starting materials, stochiometric amounts of by-product generation and hazardous, environmentally harmful waste. To address these limitations, different strategies have been developed, namely the use of low-toxic base metal catalysts,[15] the application of biomass-derived solvents[16] and

development of renewable noble catalysts.[17] These approaches exploited and advanced the sustainability of cross-coupling chemistry, however, the major issues concerning low level of step-economy and atom-economy of cross-coupling reactions stay unfortunately unsolved.

With continuing growth of ecological awareness in novel synthetic strategies design, the direct functionalization of otherwise inert C–H bonds appears to be a highly attractive alternative to conventional cross-coupling approaches (Scheme 1.1). In contrast to cross-couplings, the direct site-selective C–H functionalization replaces the organometallic reagents by simple C–H bonds, thus improving the step-economy as well as the atom-economy of the overall process. In this context, the past decade has witnessed significant development of C–H functionalizations as an efficient and sustainable tool for organic synthesis, with notable applications to natural products synthesis,[18] material sciences[19] and pharmaceutical development,[20] among others. However, the functionalization of C–H bonds largely relies on organic (pseudo-)halide electrophiles as coupling partners, which results in stoichiometric quantities of undesired by-products. Therefore, to achieve better resource economy, the formation of C–C bonds can be realized by activation of two C–H bonds in a dehydrogenative fashion. Nearly full atom-economy can be achieved by oxidative C–H activations with molecular hydrogen as the only by-product, while the step-economy is improved by avoiding the use of prefunctionalized substrates. Recently, merged with electrochemistry, the often toxic, sacrificial chemical oxidants for oxidative C–H activations can be replaced by sustainable electricity as redox reagents, which further developed oxidative metallaelectro-catalyzed C–H activations[21] with oxidant-economy nature.

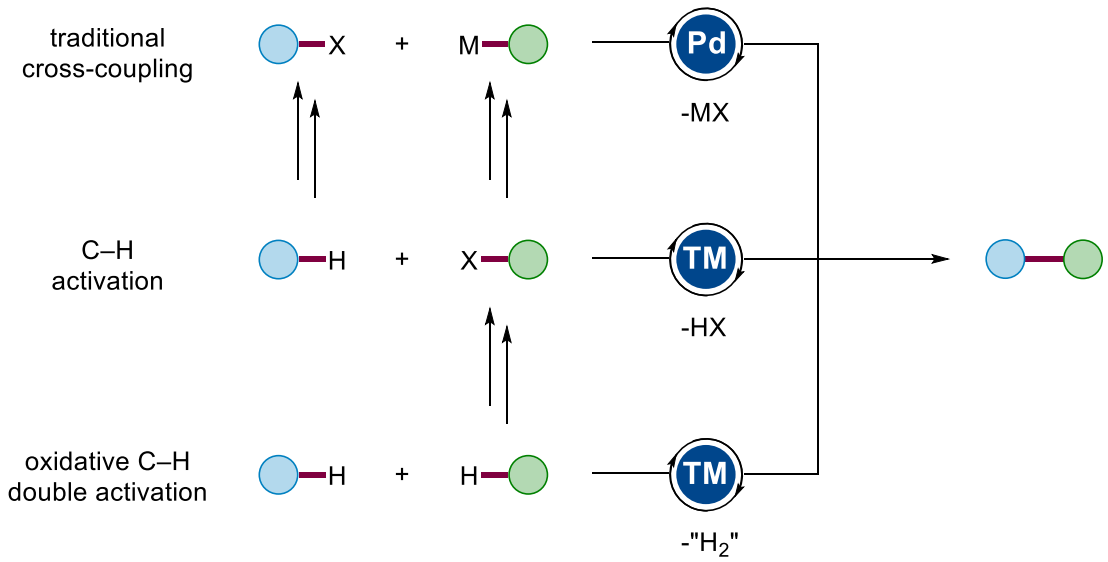

Scheme 1.1. Comparison of traditional cross-coupling with C–H activation strategies.

Along with the increasing advance in transition metal catalyzed C–H functionalizations, detail mechanistic insights[22] gained from experimental and computational studies provided an improved understanding of the reaction mechanism. Herein, a general catalytic cycle containing three main steps for C–H functionalization can be summarized (Scheme 1.2): (i) C–H activation, (ii) organometallic intermediate functionalization, and (iii) regeneration of the active catalyst species as well as release of the desired product.

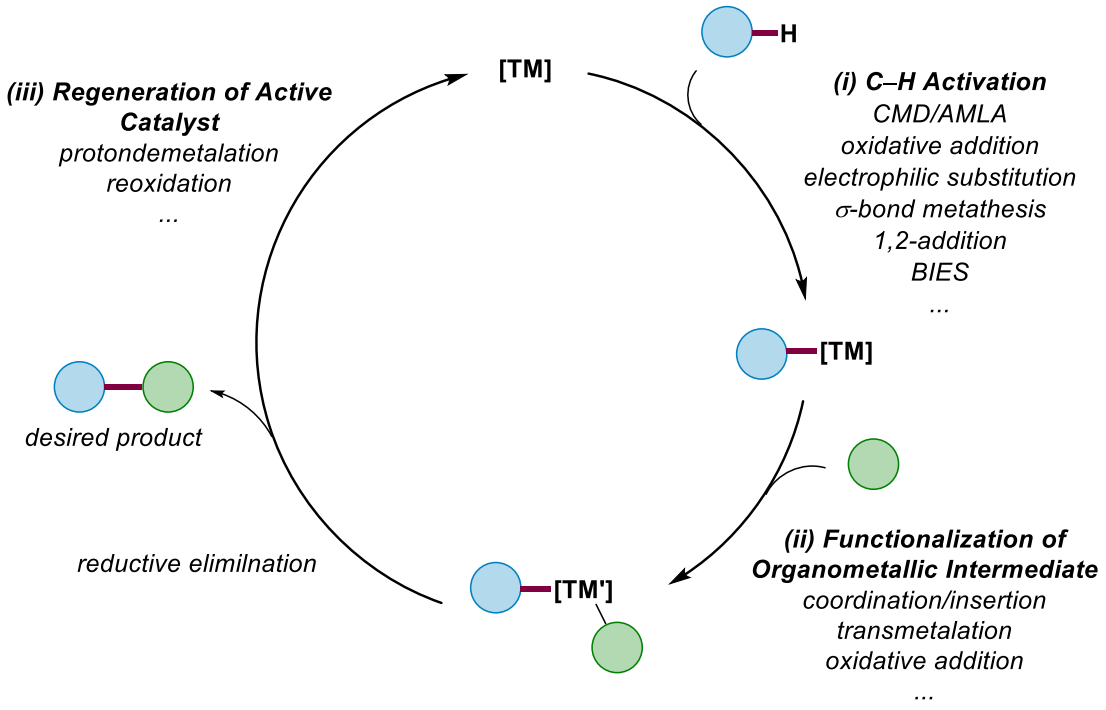

Scheme 1.2. General catalytic cycle for transition metal-catalyzed C–H activation.

To understand C–H functionalization process, the C–H cleavage, as the key step of the general mechanism proposed above, has been extensively studied. These mechanistic findings result in a profound understanding of modes of action for the C–H metalation procedure, which are governed by the nature of the substrate, the catalyst, the ligand and the oxidation state of catalyst.[23] Within this regime, five pathways have been proposed, including oxidative addition, σ-bond metathesis, electrophilic substitution, 1,2-additon and base-assisted metalation (Scheme 1.3). The oxidative addition of C–H bonds is often observed with electron-rich, low-valent complexes of late transition metals, which have readily accessible oxidation state. For early transition metals with a d^0 electron configuration, as well as lanthanides and actinides, σ-bond metathesis is the prevalent pathway through the concerted formation and breaking of the C–M and C–H bonds without any changes in oxidation state. In contrast to early transition metals, late transition metals in higher transition states typically undergo an electrophilic substitution pathway. Within this regime, electrophilic attack of the metal takes place, forming the putative intermediate. Transformations occurred via 1,2-

additon pathway are usually observed for early transition metals complexes bearing a metal-ligand unsaturated M=R bond. The base-assisted metalation C–H activation is featured by the simultaneous formation of a new C–M bond and transformation of the proton to the coordinated carboxylate.

(a) oxidative addition

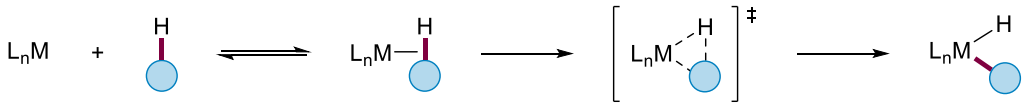

(b) σ-bond metathesis

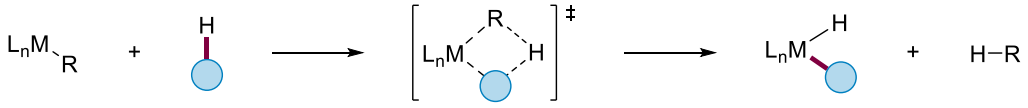

(c) electrophilic substitiution

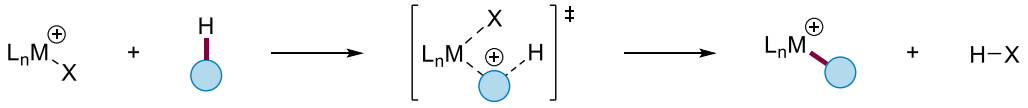

(d) 1,2-addition

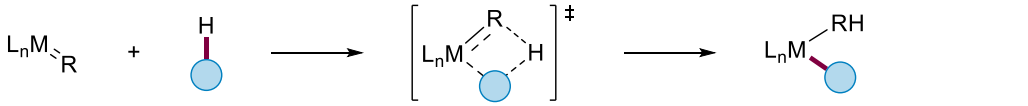

(e) base-assisted metalation

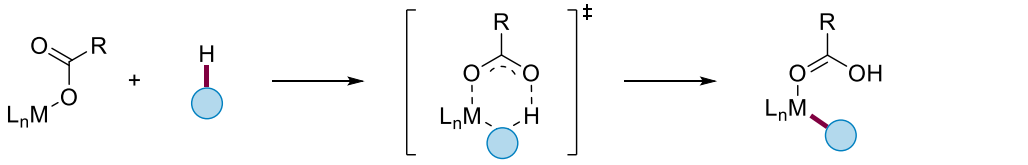

Scheme 1.3. Mechanistic pathways for organometallic C–H activation.

Detailed mechanistic studies on base-assisted metalation C–H activation manifolds have unraveled several possible scenarios for the key C–H bond cleavage process (Scheme 1.4). By proposing a six-membered deprotonative transition state, the concept of concerted metalation-deprotonation (CMD) was developed by *Gorelsky* and *Fagnou*.[24] A similar mechanism with an agostic interaction between the metal and the

C–H bond was suggested by *Davies* and *Macgregor*, which was named ambiphilic metal ligand activation (AMLA).[23d, 25] For the reactions with alkoxide bases involved, a four-membered ring transition state pathway was proposed as an internal electrophilic substitution (IES).[26] Recently, base-assisted internal electrophilic substitution (BIES) was introduced by *Ackermann*, explaining the preference for electron-rich substrates in most catalytic processes by undergoing an electrophilic substitution-type pathway.[23a, 27]

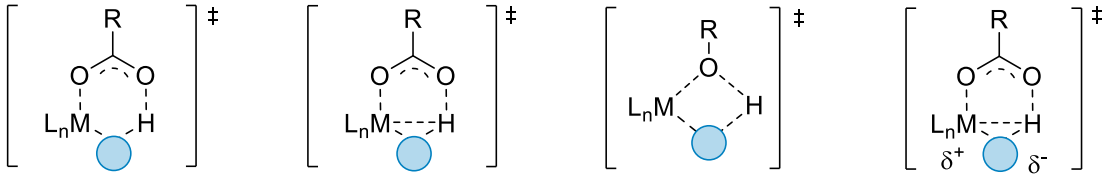

CMD *AMLA* *IES* *BIES*

Scheme 1.4. Transition states of C–H cleavage through base-assisted C–H metalation.

One of the major challenges of C–H activation chemistry is the selectivity control of omnipresent C–H bonds, which have almost identical bond dissociation energies in organic molecules. Various strategies have been developed to face this challenge (Scheme 1.5). Among these approaches, electronic bias and steric bias require heterocycle and/or particular substituents in the substrates, which limit the viable scope to a narrowed number of viable manifolds. In stark contrast, the introduction of directing groups (DG) expands the selectivity-control of C–H activations.[28] Over the years, a variety of directing groups have been applied, for instance amides and N-heterocyclic bidentate directing groups, to achieve *ortho*-selective activations of arenes.[29] However, the incorporation of the directing group remains a limitation for selective C–H activations. Therefore, recently, the strategies of applying weakly-coordinating,[30] removable[31] and transient[32] directing groups in C–H activation attracted considerable attention.

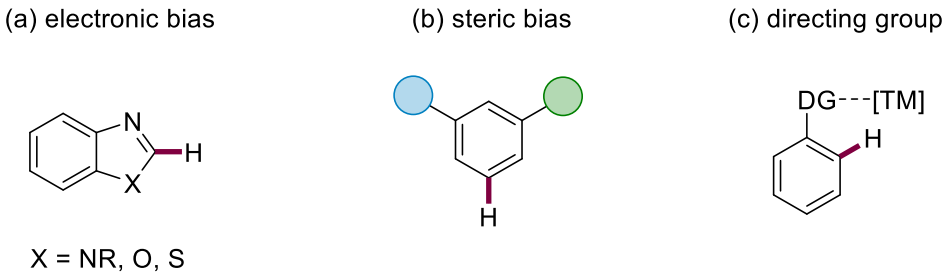

Scheme 1.5. Selectivity control of C–H activation.

Major progress in transition metal catalyzed C–H activations have been accomplished by the development of precious 4d and 5d transition metals catalysis, such as palladium,[33] iridium,[34] rhodium[22b, 35] and ruthenium.[36] However, these noble metal catalysts suffer not only their high costs, but also generally high toxicity. In contrast, applying less-toxic, earth-abundant 3d transition metals as catalysts for functionalization of C–H bonds has emerged as a more sustainable alternative in the last decade.[37]

Recent years have witnessed a remarkable renaissance of organic electrosynthesis,[38] especially with significant advances in electrocatalysis. Merged with oxidative C–H transformations, metallaelectro-catalysis has become an important platform for molecular syntheses.[21, 39] By replacing stoichiometric amounts of often toxic redox reagents with renewable electricity, the sustainable nature of C–H activation has been significantly improved through metallaelectro-catalysis. Early examples of electrochemical C–H activations developed by *Jutand*[40] and *Kakiuchi*[41] for noble palladium catalysis used indirect electrolysis with redox mediators. These approaches were restricted to the combination of precious palladium catalysts and redox mediators, which lowered the resource-economy of the electrochemical processes. Consequently, earth-abundant 3d metals catalyzed electrochemical C–H activation was in high demand as a cost-efficient, low-toxic alternative strategy. To this end, *Ackermann*[21, 42] and later *Mei*,[39a] among others, have disclosed various methodologies in cobaltaelectro-catalysis, nickelaelectro-cataysis as well as cupraelectro-catalysis. Based on these pioneering works, further developments in the field of 3d metals

catalyzed electrochemical C–H activation are foreseeable in the near future.

1.2 Cobalt-Catalyzed C–H Activation

Over the last century, cobalt, as an earth-abundant 3d base metal, has been widely studied in the field of catalysis due to the cost-efficient nature and identified as versatile catalysts for organic transformations. In 1938, while studying the *Fischer-Tropsch* process, *Roelen* disclosed the promoting effect of cobalt, and further developed hydrocarbonylation of ethylene using cobalt catalyst.[43] Thereafter, notable achievements have been made in organic chemistry using cobalt catalysts, namely, the coupling of Grignard reagents in the *Kharasch*-coupling,[44] the *Pauson-Khand* reaction,[45] the *Nicholas* reaction,[46] cross-coupling reactions[47] and C–H activations.[48]

1.2.1. Early Contributions

Indeed, cobalt-catalyzed C–H functionalization is not without precedence.[48] In 1955, the first chelation-assisted C–H functionalization by cobalt-catalysis has been reported by *S. Murahashi*.[49] By applying high pressure carbon monoxide to benzaldimine **1**, the synthesis of 2-phenylphthalimidine **2** was achieved with catalytic amounts of a cobalt catalyst (Scheme 1.6). The scope of this protocol was later expanded to include azobenzene substrates.[50]

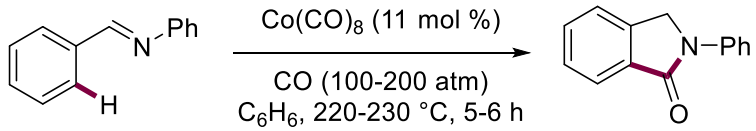

1 **2**

Scheme 1.6. Cobalt-catalyzed carbonalytion of benzaldimine **1**.

The development of cobalt-catalyzed C–H activation remained scarce until 1990s. An

example of cyclometalation reaction with azobenzene **3** was disclosed by *Klein* using a well-defined cobalt complex $[Co(CH_3)(PMe_3)_4]$ **4** (Scheme 1.7).[51] Due to the high reactivity of the cobalt complex, further exploration revealed challenging four-membered ring metallacycles[52] were also obtainable by this cobalt complex.

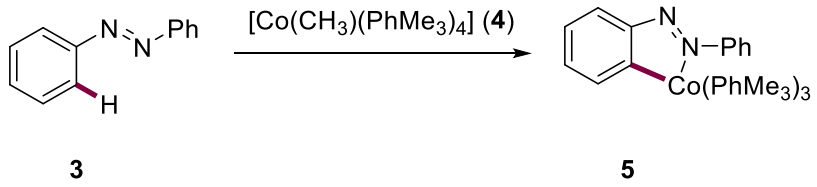

3 **5**

Scheme 1.7. Cyclometalation reaction with well-defined cobalt complex.

Another major contribution in cobalt-catalyzed C–H activation was disclosed in 1994 by *Kisch*, who reported the hydroarylation of azobenzene **3** with diphenylacetylene **6a** using a well-defined cobalt-hydride complex $[Co(H)(N_2)(PPh_3)_3]$ **7** as catalyst (scheme 1.8).[53] This work was considered as the first C–H hydroarylation of alkynes enabled by cobalt complex.

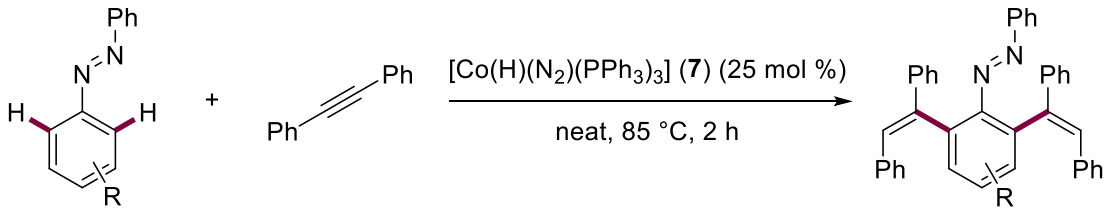

3 **6a** **8**

Scheme 1.8. Hydroarylation of azobenzene **3** by cobalt complex.

1.2.2. Low-Valent Cobalt-Catalyzed C–H Activation

Ever since the pioneering early research of the first cobalt-catalyzed hydroarylation reaction developed by *Kisch* using cobalt(I) complex,[53] the potential of the so-called low-valent cobalt catalysis has been further explored with various approaches. Due to the instability of the catalytic active species towards moisture and air, these

approaches are typically achieved with well-defined cobalt complexes or *in situ* generated cobalt complexes, which are formed by the action between cobalt(II) salts and Grignard reagents.[37] The combination of a cobalt-NHC catalyst and a Grignard reagent enables selectively aromatic C–H functionalizations with electrophiles.

In 2010, *Yoshikai* and co-workers reported cobalt-catalyzed C–H hydroarylations of internal alkyne **6** with phenylpyridine **9** using $PMePh_2$ as the ligand and the stoichiometric reductant MeMgCl (Scheme 1.9a).[54] In contrast to a well-defined cobalt complex, a simple $CoBr_2$ was introduced as catalyst. Thereafter, the same group expanded this approach to aryl imines **11**.[55] Hydroarylated products were successfully converted at room temperature (Scheme 1.9b).

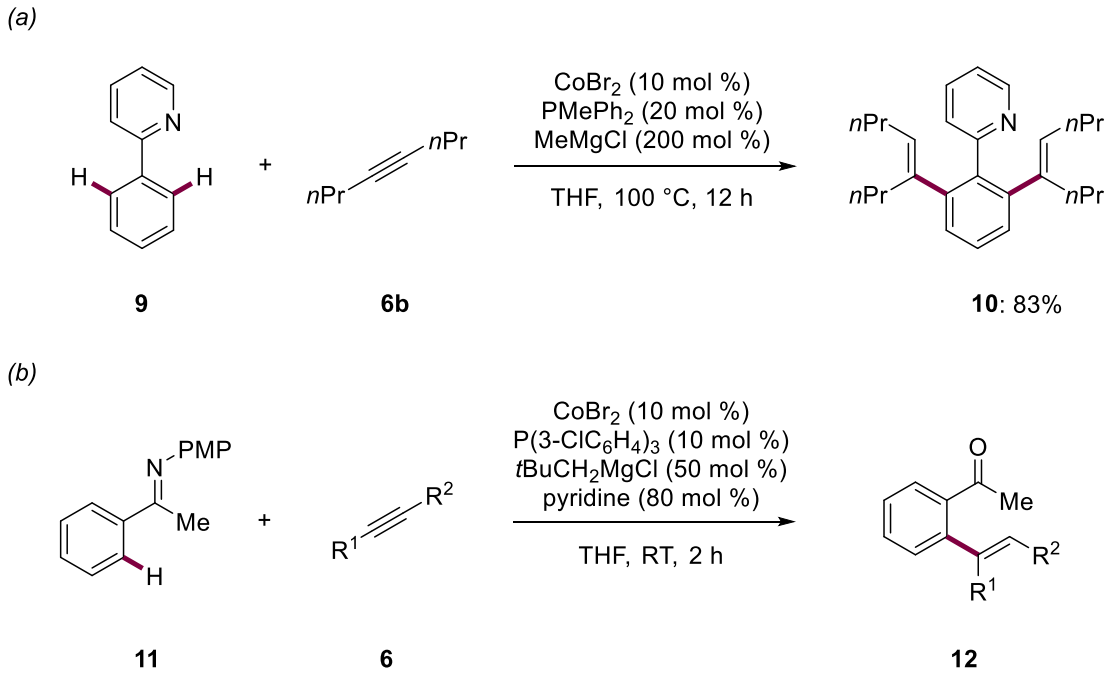

Scheme 1.9. Cobalt-catalyzed hydroarylation of alkynes **6**.

Based on the well-established cobalt-catalyzed C–H hydroarylation reactions with alkynes **6**, the hydroarylation of alkenes **13** proved to be viable by cobalt catalysis as well. *Yoshikai* developed the hydroarylation of phenylpyridine **9** with alkenes **13** under similar reaction conditions.[56] By applying different combinations of ligand and

Grignard reagent, regioselective formation of linear product **14a** and branched product **14b** can be achieved (Scheme 1.10).

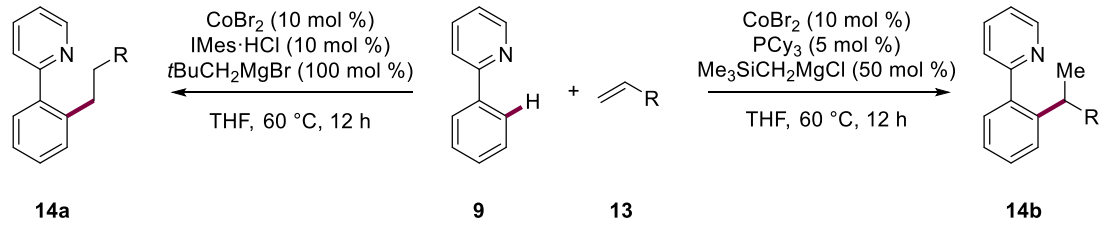

Scheme 1.10. Regioselectivity-controlled cobalt-catalyzed hydroarylation.

Based on the early example of *Kharasch* coupling reactions,[44] *Nakamura* explored cobalt-catalyzed C–H alkylation of amides (Scheme 1.11).[57] By applying $Co(acac)_3$ as the catalyst with Grignard reagents, an *in situ* generated low-valent cobalt catalytic species was proposed and successfully delivering the *ortho*-alkylated product **17**. Direct alkylation reactions were accomplished without phosphine ligand at room temperature.

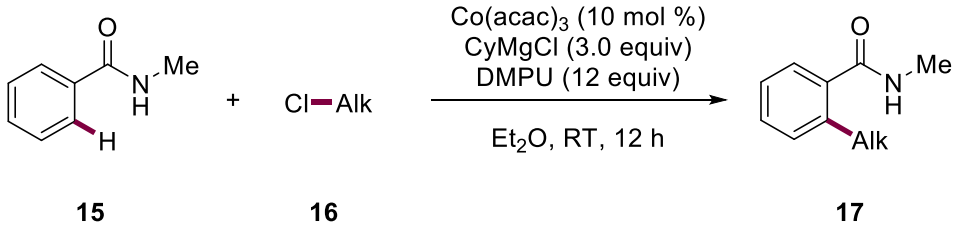

Scheme 1.11. Cobalt-catalyzed direct alkylation of amide **15**.

Apart from direct alkylations, C–H arylation reactions were also achieved by low-valent cobalt catalysis. *Ackermann* reported the cobalt-catalyzed C–H arylations with electrophiles (Scheme 1.12).[58] Arylations of phenylpyridine **9** with various organic electrophiles, including aryl carbamates **18a**, sulfamates **18b** and aryl chloride **18c**, have been developed using $Co(acac)_2$ as the catalyst with cyclohexylmagnesium chloride to generate the corresponding cobalt complex *in situ*.

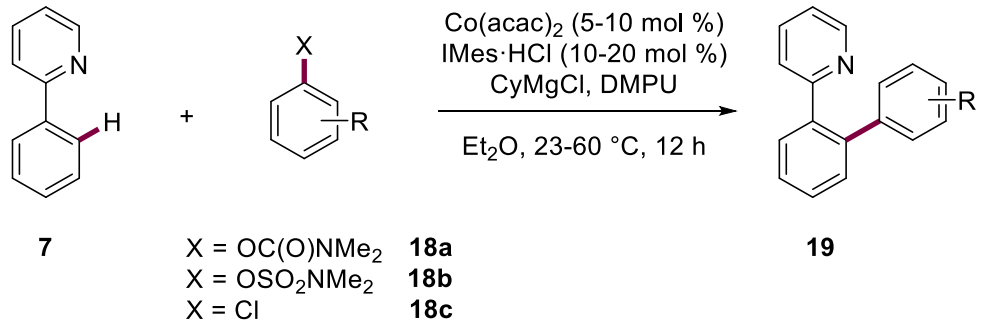

7 X = $OC(O)NMe_2$ **18a**; X = OSO_2NMe_2 **18b**; X = Cl **18c** **19**

Scheme 1.12. Cobalt-catalyzed C–H arylation with electrophiles **18**.

In 2012, *Yoshikai* developed a similar cobalt-catalyzed C–H arylation with aryl chloride **18c** (Scheme 1.13).[59] This approach expanded the substrate scope of arylation reactions to aryl imines **11**.

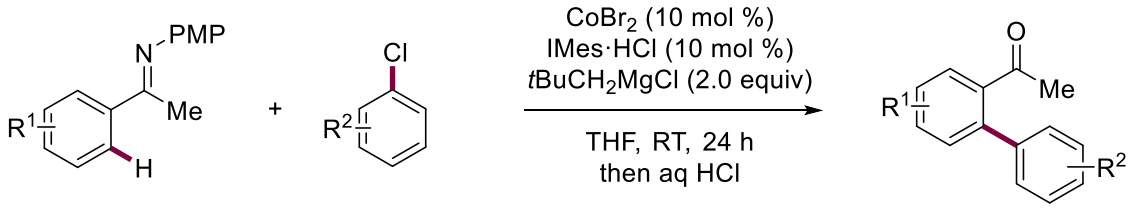

11 **18c** **20**

Scheme 1.13. Cobalt-catalyzed C–H arylation of aryl imines **9**.

Furthermore, Ackermann and co-workers disclosed the application of low-valent cobalt catalysis to C–H alkenylation reactions. The first direct alkenylation of (hetero)arenes **21** with readily accessible enol esters **22** has thus been developed using a combination of a cobalt(II) catalyst and a Grignard reagent in the presence of DMPU (Scheme 1.14).[60]

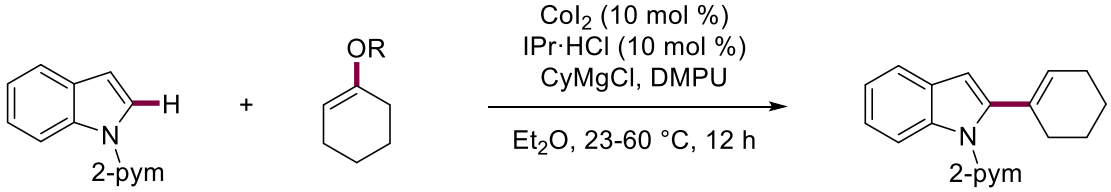

21 R = $CONMe_2$ **22a**; R = $P(O)(OEt)_2$ **22b**; R = C(O)OEt **22c**; R = Ac **22d**; **23**

Scheme 1.14. Cobalt-catalyzed C–H alkenylations.

1.2.3. High-Valent Cobalt-Catalyzed C–H Activation

The introduction of cyclopentadienyl-rhodium(III) catalysts enabled notable developments in transition metal catalyzed C–H activation.[35b, 61] However, the less-abundant and cost-inefficient nature of rhodium catalysts largely limit the wide applicability of these approaches. Therefore, the development of alternative earth-abundant 3d metal catalysts is of high demand. In this context, high-valent cobalt-catalyzed C–H activations were developed using well-defined Cp*Co(III) complexes as catalysts, which represent bench-stable compounds and easy-to-handle reaction protocols.

In 2013, *Matsunaga*, *Kanai* and coworkers identified the cationic $[Cp^*Co(C_6H_6)](PF_6)_2]$ (**24**) can be a high active catalyst for C–H activation.[62] It is notable to mention that even though the Cp*Co(III) complex **24** have been reported previously,[63] but the use of it in C–H activation remained without precedence. This Cp*Co(III) complex **24** showed high reactivity in addition reactions of phenylpyridine **9** onto *α*,*β*-unsaturated ketones **25** or *N*-sulfonyl imines **26** (Scheme 1.15).

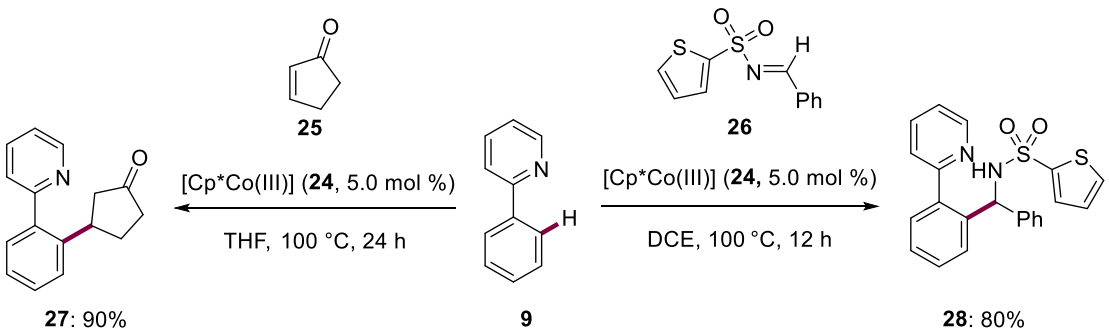

Scheme 1.15. Cobalt(III)-catalyzed hydroarylation of *α*,*β*-unsaturated ketones **25** and *N*-sulfonyl imines **26**.

Inspired by the elegant work of *Matsunaga* and *Kanai*, various C–H activation reactions using Cp*Co(III) complexes as catalysts have been developed. Typical examples of the high-valent Cp*Co(III)-catalyzed C–H activation reactions are discussed in this thesis. In 2015, *Ackermann* and coworkers reported the first cyanation of (hetero)arenes by Cp*Co(III)-catalyzed C–H activation (Scheme 1.16).[64] Different types of heteroarenes, including phenylpyridine **7** and *N*-pyrimidylindoles **19**, were selectively cyanated with *N*-cyano-*N*-phenyl-*p*-toluenesulfonamide **27** reagent. High functional group tolerance and ample substrate scope have been achieved within this regime, as well as the traceless removal of the pyrimidyl group.

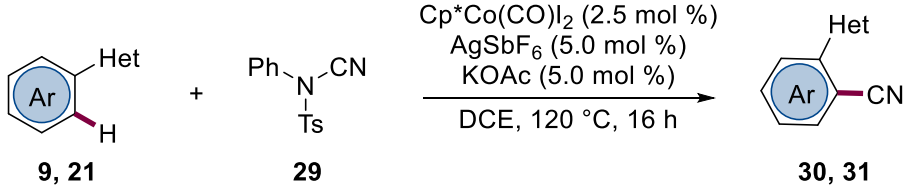

Scheme 1.16. Cp*Co(III)-catalyzed C–H cyanation.

A plausible catalytic cycle was proposed for Cp*Co(III)-catalyzed C–H cyanation reactions to have an insight of the catalyst's mode of action. Reversible C–H bond cobaltation of substrate **9** with active cationic cobalt species **32,** gives raise to cobalt intermediate **33**, which undergoes coordination with cyanating reagent **29** and insertion, affording complex **35**. The desired product **30** is obtained by *β*-elimination and the

cobalt(III) species **32** is regenerated by proto-demetalation (Scheme 1.17).

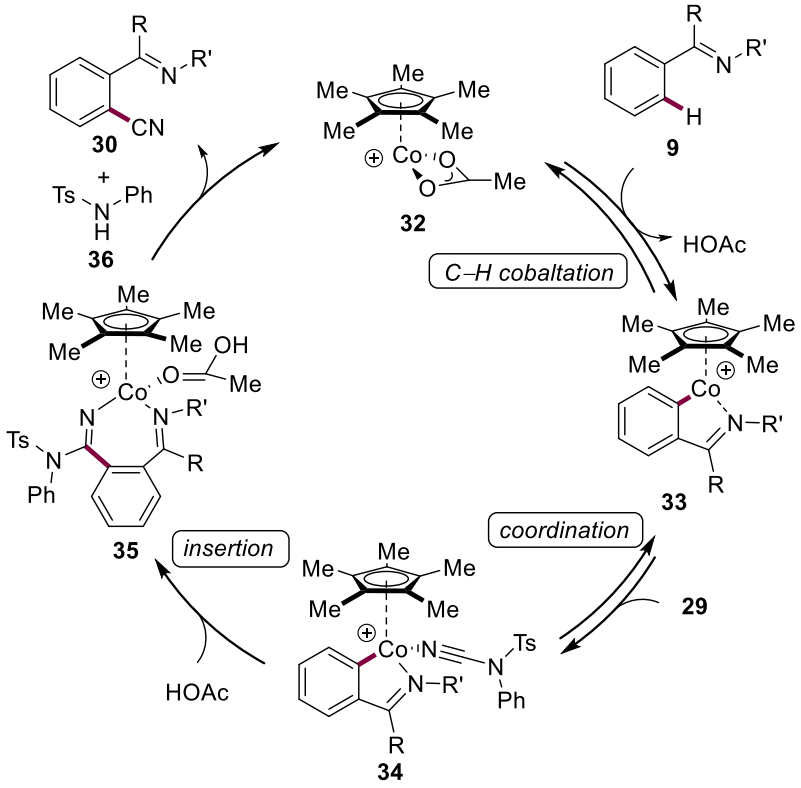

Scheme 1.17. Plausible catalytic cycle for Cp*Co(III)-catalyzed C–H cyanation.

High-valent cobalt-catalyzed C–H allylations of *N*-pyrimidylindoles **21** were developed by *Glorius* and coworkers with allyl carbonates **13b** using Cp*Co(CO)I_2 catalyst (scheme 1.18).[65] Notably, 0.5 mol % of the cobalt catalyst proved to be necessary in this manifold, giving the desired allylation products in excellent yield.

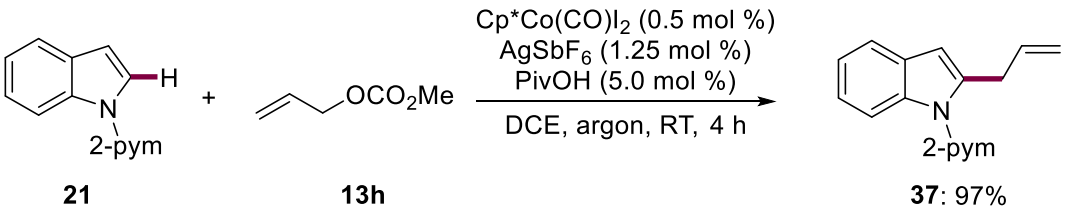

21 **13h** **37**: 97%

Scheme 1.18. Cp*Co(III)-catalyzed C–H allylation with allyl methyl carbonate **13b**.

Concurrently, *Ackermann* and coworkers disclosed versatile cobalt-catalyzed C–H

allylations using well-defined Cp* cobalt complex as catalyst. Highly selective *N*-pyrimidylindoles **21** allylations were achieved with allyl acetate **13c** (Scheme 1.19a)[66] and later *Z*-selective allylations *via* C–H/C–O activation (Scheme 1.19b).[67] The allylation approaches were not limited to indole substrates, various (hetero)arenes proved to be applicable.[66-67]

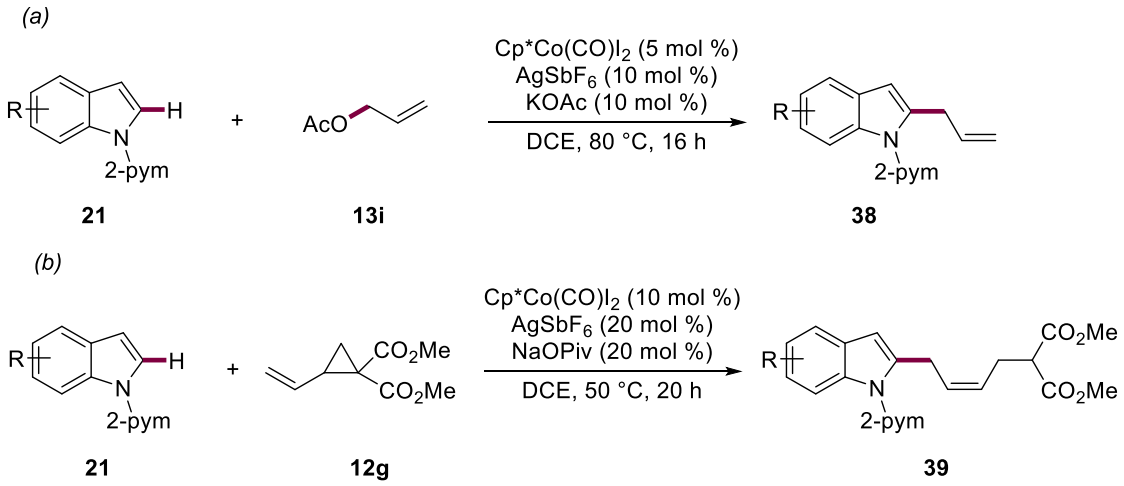

Scheme 1.19. Cp*Co(III)-catalyzed C–H allylation *via* C–H/C–C activation.

Matsunaga, *Kanai* and coworkers further developed Co(III) catalysis for C–H cascade annulations by alkenylation, using the cationic $[Cp^*Co(C_6H_6)](PF_6)_2]$ (**24**) catalyst (Scheme 1.20).[68] The annulations of *N*-carbamoyl indoles **40** with internal alkynes **6** were enabled by alkenylation addition of Cp* cobalt complex, and cascade annulation to deliver the desired products **41**.

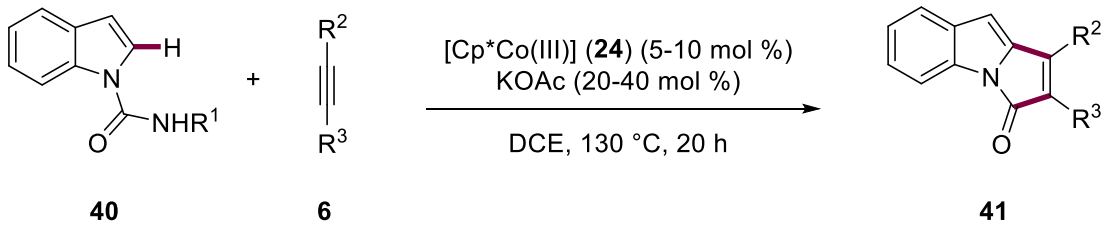

Scheme 1.20. Cp*Co(III)-catalyzed C–H cascade annulation.

Major contributions in Co(III) catalyzed C–H annulation were reported by *Ackermann*

and coworkers for the synthesis of indoles **43** and isoquinolines **45** (Scheme 1.21).[69] Employing various internal alkynes **6**, broad scope and good functional group tolerance were achieved.

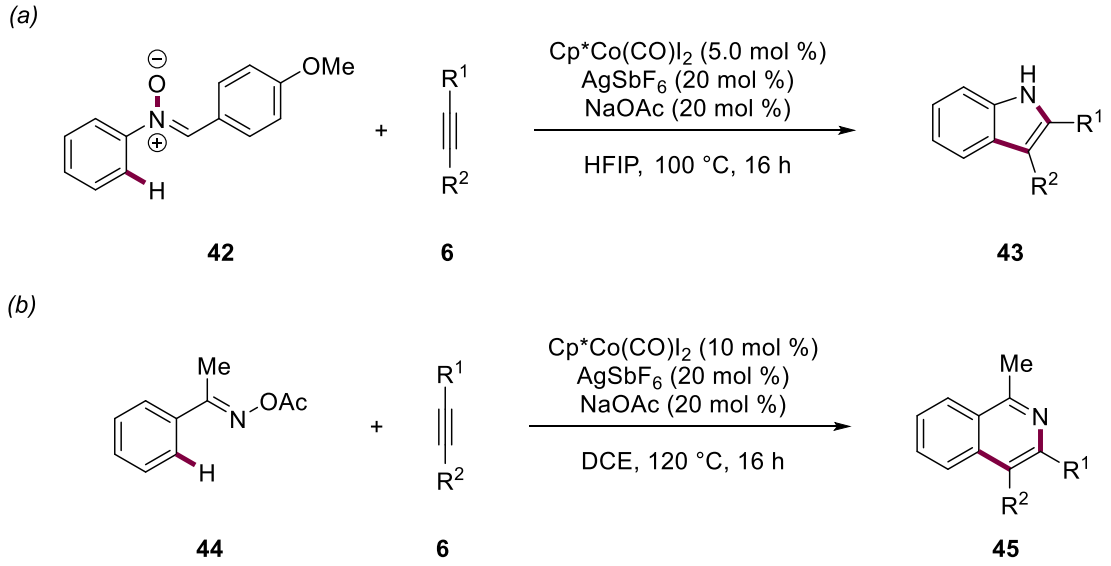

Scheme 1.21. Cp*Co(III)-catalyzed C–H annulation for synthesis of indoles **43** and isoquinolines **45**.

Cobalt(III)-catalyzed C–H activation reactions are not limited to cyanation, allylation or annulation, but cobalt(III)-catalyzed C–H hydroarylation with unactivated alkenes **13** was realized by *Ackermann* and coworkers as well (Scheme 1.22).[27b] By tuning the reaction conditions, the *anti-Markovnikov* isomer **47** was obtained in the absence of carboxylic acid additive, while the branched product **48** was selectively obtained in the presence of 1-AdCO_2H. Notably, this manifold also provided support as a proof-of-concept pathway to develop an asymmetric approach when chiral carboxylic acids were applied.

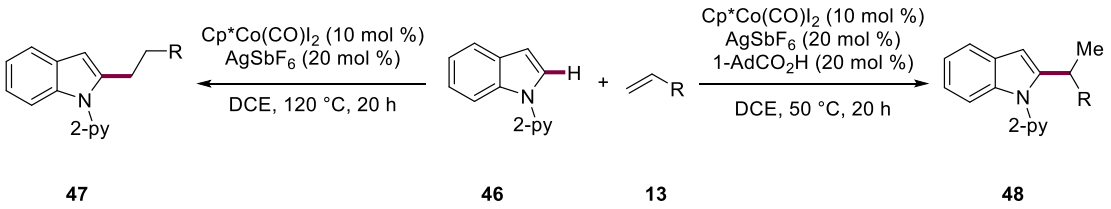

Scheme 1.22. Full selectivity control in Co(III)-catalyzed C–H alkylation.

Based on previous hydroarylation results,[27b] *Ackermann* and coworkers explored the possibility of asymmetric alkylation by cobalt catalysis. Indeed, the first enantioselective cyclopentadienyl-cobalt(III)-catalyzed C–H activation was developed and promoted by a novel chiral carboxylic acid **50** (Scheme 1.23).[70] High regio- and enantio-selective alkylations of indoles **49** with alkenes **13** were thus achieved. Furthermore, the 5-methylpyridine group proved to be easily removeable, yielding a free indole final product.

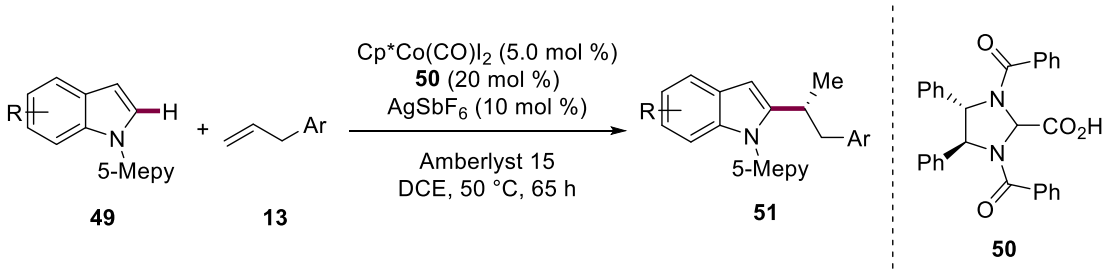

Scheme 1.23. Enantioselective Co(III)-catalyzed C–H alkylation of indole **49**.

Indeed, major achievements have been made in Cp*Co(III)-catalyzed C(sp^2)–H bond functionalizations over the last decade. Unfortunately, only a few reports have been devoted to C(sp^3)–H bond activation in the field of cobalt(III) catalysis. In this context, *Sundararaju* and coworkers disclosed the C(sp^3)–H alkenylation of 8-methylquinolines **52** (Scheme 1.24).[71] Applying catalytic amounts of Cp*Co(CO)I_2, alkenylated products were obtained with internal alkynes **6**. However, major drawbacks, such as low yields of desired products and a narrow scope of alkynes, limited further applications of this manifold thus far.

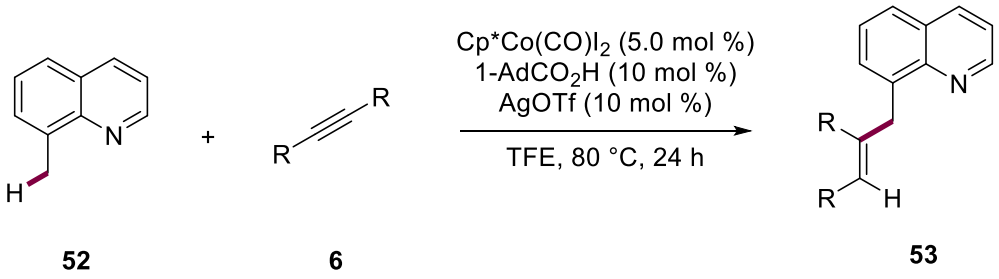

52 **6** **53**

Scheme 1.24. Cp*Co(III)-catalyzed C(sp^3)–H alkenylation.

1.2.4. Cobalt-Catalyzed Oxidative C–H Activation

Despite indisputable developments in low-valent cobalt-catalysis with Grignard reagents and high-valent cobalt-catalysis with well-defined cobalt(III) complexes, major drawbacks in cobalt-catalyzed C–H activations remain unsolved. As discussed above, the low-valent cobalt-catalysis largely depends on a combination of a cobalt-NHC pre-catalysts with sensitive and highly reactive Grignard reagents, which enables aromatic C–H functionalizations with electrophiles. In this context, Grignard reagents are not only highly reactive, but also bear the drawbacks of air- and moisture-sensitivity. Therefore, bench-stable and easy-to-handle high-valent cobalt-catalysis with well-defined cyclopentadienyl-cobalt(III) catalysts were widely studied. However, multi-step syntheses of Cp*Co(III) complexes are inevitable for these approaches. Thus, another major class of cobalt-catalyzed C–H functionalization known as oxidative cobalt-catalyzed C–H activation was introduced. With the assistance of external or internal oxidants, the direct utilization of cost-efficient, air-stable cobalt(II) salts as pre-catalysts has been realized.

Based on the early work within palladium-catalyzed C–H activation by *Daugulis* in 2005,[72] the use of 8-aminoquinoline (Q) auxiliary and other directing groups was further developed into the concept of bidentate directing groups and have been explored with various transition metals.[29b, 73] However, not until 2014, the first application of 8-aminoquinoline directing group in cobalt-catalyzed oxidative alkyne **6** annulation reactions has been introduced by *Daugulis* and co-workers (Scheme

1.25).[74] Employing stoichiometric amounts of $Mn(OAc)_2$ oxidant, oxidative C–H/N–H annulation reactions with broad scope and excellent functional group tolerance have been achieved. The same group later expanded the scope of this approach to alkenes **13**.[75]

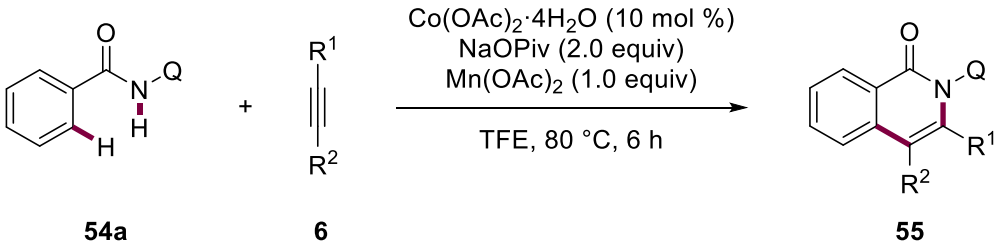

54a **6** **55**

Scheme 1.25. Cobalt-catalyzed C–H/N–H oxidative annulation with benzamide **54a**.

Thereafter, cobalt-catalyzed C–H/Het–H annulation reactions have been widely explored for the synthesis of cyclic phosphoramides,[76] sultamamides[77] and isocoumarines.[78] Notably, *Ackermann* and co-workers reported the first cobalt-catalyzed oxidative C–H/N–H annulation using molecular oxygen as the terminal oxidant (Scheme 1.26).[79] Applying the bidentate 2-pyridyl-*N*-oxide (PyO) directing group, a site- and rigo-selective C–H activation of amides **56** was achieved with both terminal and internal alkynes **6**.

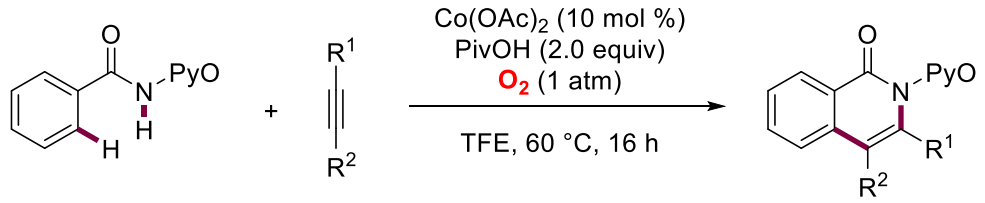

56a **6** **57**

Scheme 1.26. Cobalt-catalyzed C–H/N–H oxidative annulation by molecular oxygen oxidant.

Further studies conducted by *Ackermann* and co-workers revealed electron-deficient alkenes **11** are also well suited within the regime of cobalt-catalyzed C–H annulation

reactions (Scheme 1.27).[80] Access to synthetically-useful isoindolones **58** were realized by cobalt-catalysis with a wide range of substituted benzamides **54**.

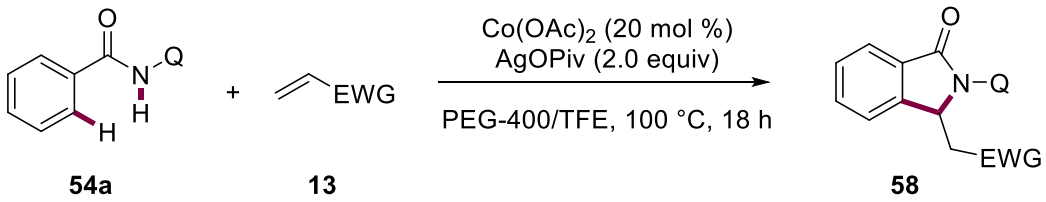

Scheme 1.26. Cobalt-catalyzed isoindolones **58** synthesis.

A plausible mechanism was proposed to explain the oxidative annulation process (Scheme 1.27). The catalytic cycle is initiated by base-assisted C–H activation forming the cobalt intermediate **59**. Subsequent alkene **13** insertion and *β*-hydride elimination yield the desired product **58**. Oxidation of the cobalt species **62** regenerates the active catalyst **63**.

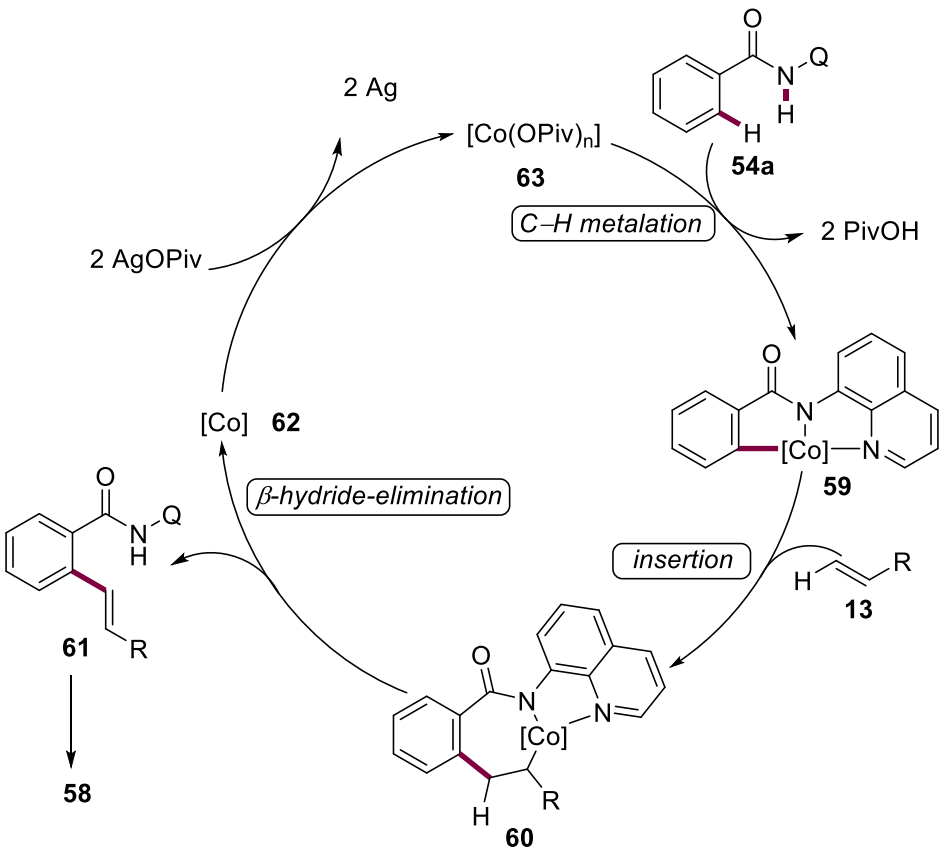

Scheme 1.27. Proposed catalytic cycle for cobalt-catalyzed oxidative C–H annulation.

The selective construction of C–O bonds by C–H oxygenation using cobalt-catalyzed oxidative C–H activation was realized by *Song* and *Chatani*. *Song* reported cobalt-catalyzed alkoxylation reactions of 2-pyridyl-*N*-oxide (PyO) benzamides **56** using the corresponding alcohols **64** as the solvent (Scheme 1.28a).[81] *Chatani* disclosed the acyloxylation of quinolinamides **54** with carboxylic acids **66** (Scheme 1.28b).[82] Good functional group tolerance and product yields have been achieved in both cases.

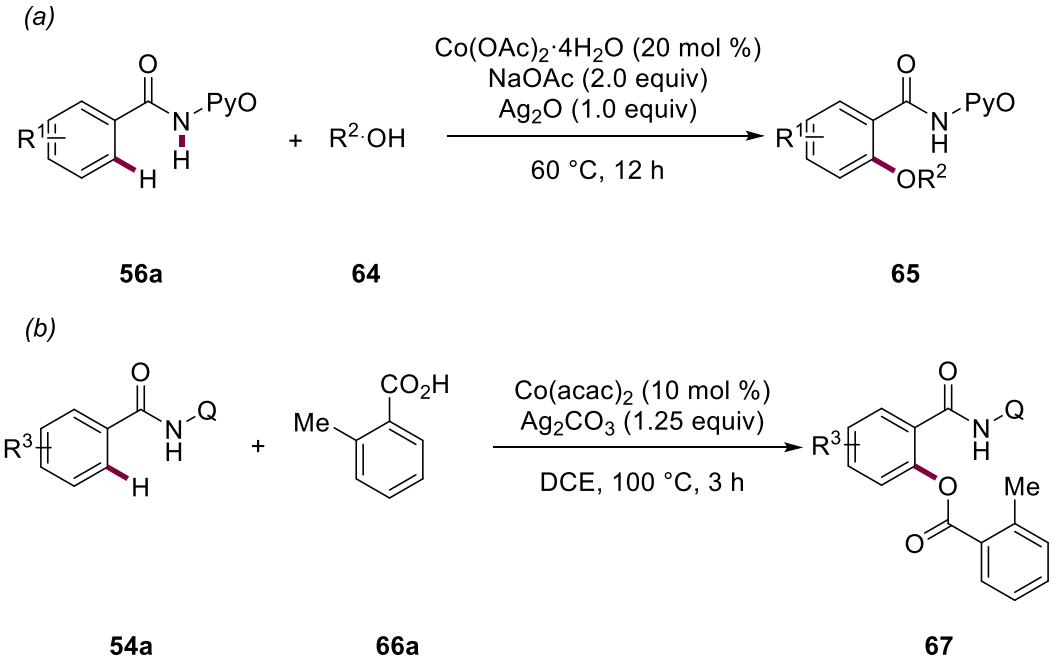

Scheme 1.28. Cobalt-catalyzed oxidative C–H oxygenation.

In 2016, *Balaraman* reported the cobalt-catalyzed oxidative C–H alkynylation reactions of benzamides **54** (Scheme 1.29).[83] Applying bromoalkynes **70**, dialkynylated products **69** were formed under oxidative conditions. The functional group tolerance of amides is in general good, but the narrow scope of alkynes **70** is one of the major drawbacks in this manifold.

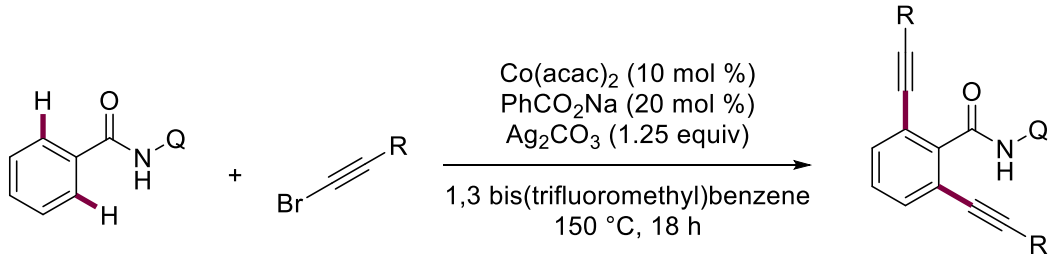

54a **68** **69**

Scheme 1.29. Cobalt-catalyzed oxidative C–H alkynylation.

The formation of C–C bonds by using cobalt-catalysis is not limited to alkynylations, additionally oxidative allylations by cobalt-catalyzed C–H activation were reported by *Maiti*.[84] Applying Ag_2SO_4 as the external oxidant, C–H allylations were achieved using preferentially *ortho*-substituted benzamides **54** with non-activated alkenes **13** (Scheme 1.30). Almost at the same time, *Chatani* developed a similar cobalt-catalyzed allylation process independently.[85]

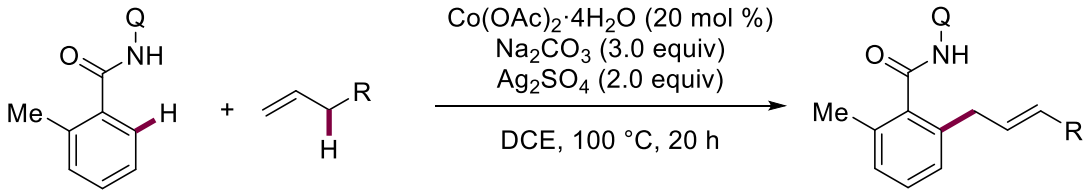

54b **13** **70**

Scheme 1.30. Cobalt-catalyzed oxidative C–H allylation.

Moreover, the oxidative cobalt-catalyzed C–H halogenation was developed by *Chatani* and co-workers using molecular iodine **72** as the iodination reagent (Scheme 1.31).[86] Diverse benzamides **71** with various functional groups were found applicable. It is noteworthy that the commonly applied quinoline directing group needed to be modified by this manifold to prevent undesired side reactions.

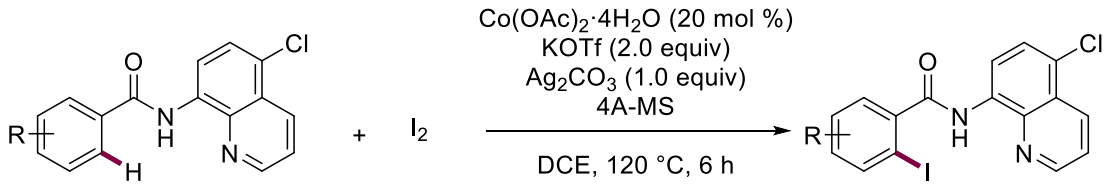

Scheme 1.31. Cobalt-catalyzed oxidative C–H iodination.

The oxidative cobalt-catalyzed C–H activation manifolds were further expanded to challenging C(sp^3)–H bonds by versatile cobalt-catalysis. Several cyclization strategies have thus been developed. In 2015, an intramolecular C(*sp*^{3})–H amination was reported by *Ge* and co-workers (Scheme 1.32).[87] The use of the quinoline directing group provided an access to the four-membered cyclization product **75**.

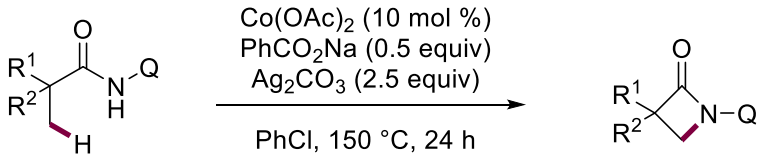

Scheme 1.32. Intramolecular cobalt-catalyzed oxidative C(sp^3)–H amination.

Oxidative cobalt-catalyzed cyclization reactions of C(sp^3)–H bonds are not limited to intramolecular reactions. Indeed, an elegant example of aliphatic amides **74** cyclization with terminal alkynes **76** was developed by *Zhang* and co-workers using oxidative cobalt-catalysis (scheme 1.33a).[88] In the presence of $Co(OAc)_2 \cdot 4H_2O$ as the catalyst and Ag_2CO_3 as the oxidant, the desired pyrrolidones **77** were formed. Another approach of C(sp^3)–H cyclization using bidentate chelating group were found with carbonylation reactions with carbon monoxide.[89] In this context, intramolecular oxidative C–H/N–H activation of aliphatic amides **74** was achieved, delivering the carbonylated product in good yield (Scheme 1.33b).

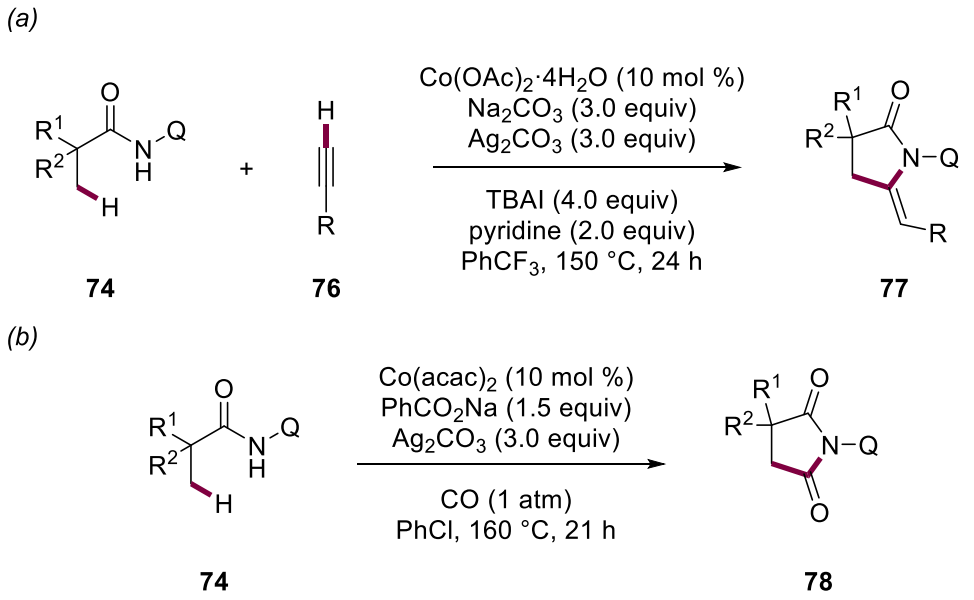

Scheme 1.33. Cobalt-catalyzed oxidative C(*sp*^{3})–H cyclization of aliphatic amides **74**.

1.2.5. Cobaltaelectro-Catalyzed C–H Activation

Oxidative cobalt-catalyzed C–H activations enabled the direct use of cost-efficient and bench-stable cobalt(II) salts as pre-catalysts, which have significantly broadened the toolbox of cobalt-catalysis. However, the success of these strategies greatly depends on the external chemical oxidants. The oxidants give rise to a higher oxidation state of the cobalt(II) pre-catalysts, which are generated *in situ* during the reactions and serve as the active catalyst species in the catalytic cycle. However, traditional chemical oxidants, namely silver(I) and copper(II) salts are rather expensive and toxic, which stoichiometric amounts are needed usually. The application of oxidants compromises the overall sustainable nature of C–H activations. In recent years, merging with electrochemistry, transition metal catalyzed oxidative C–H transformations have been largely advanced by replacing the traditional chemical redox reagents with renewable, environmental-friendly electricity, which largely improved the environmentally friendly nature of C–H activation. In this context, cobaltaelectro-catalyzed C–H activations, as the pioneering works in the field of 3d earth-abundant metal catalyzed electrochemical C–H activation, were established by *Ackermann* and later *Lei*.[21, 38c, 42a]

In 2017, *Ackermann* and co-workers reported the first cobaltaelectro-catalyzed C–H oxygenation reactions with alcohols **64** (Scheme 1.34).[90] By applying electricity as external oxidant, the silver oxidant used in previous example[81] was avoided and a milder condition of room temperature was realized by the electrochemical approach as well. Detail mechanistic studies using cyclic voltammograms revealed the oxidation process of the cobalt(II) catalyst enabled by the electricity.

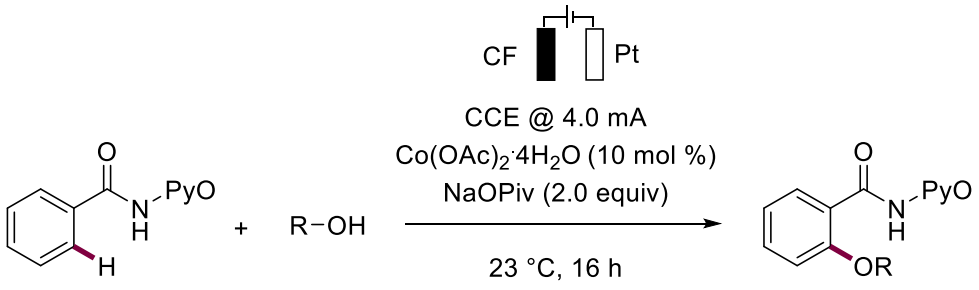

56a **64** **65**

Scheme 1.34. Cobaltaelectro-catalyzed C–H oxygenation.

Later, *Ackermann* and co-workers expanded the cobaltaelectro-catalysis to C–H amination reactions with amines **79** using biomass-derived, renewable *γ*-valerolactone (GVL) (Scheme 1.34).[91] A broad substrate scope with excellent functional group tolerance has thereby been achieved. Notably, the use of React-IR analysis in the process showed the reaction profile and kinetic studies in great detail. Almost at the same time, *Lei* published a similar cobalt-catalyzed electrochemical amination reaction with a *N*,*N*-bidentate directing group.[92]

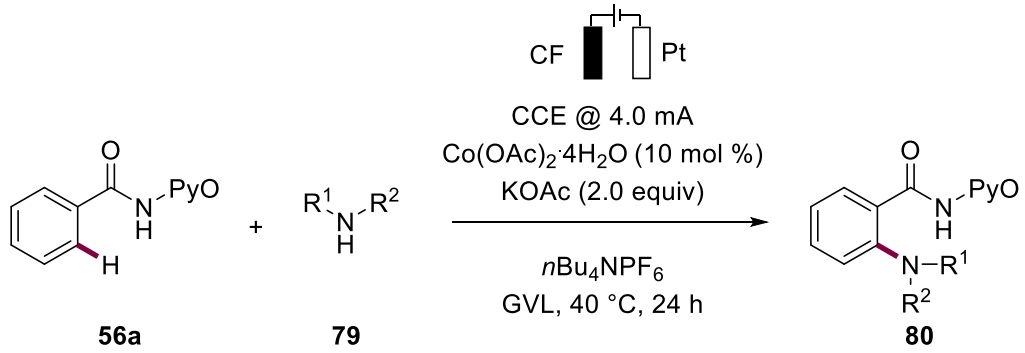

Scheme 1.35. Cobaltaelectro-catalyzed C–H amination.

Based on previous reports,[93] *Ackermann* and co-workers disclosed the cobaltaelectro-catalyzed C–H/N–H annulation reactions using a bidentate directing group strategy (Scheme 1.36).[94] Cobalt-catalyzed oxidative C−H/N−H activations with internal alkynes **5** were achieved using a traceless removable hydrazide directing group. Thereafter, several other manifolds of cobalt-catalyzed electrochemical C−H/N−H annulations have been developed, including annulations with olefins,[95] allenes,[96] diynes[97] and with renewable forms of solar and wind energy.[98]

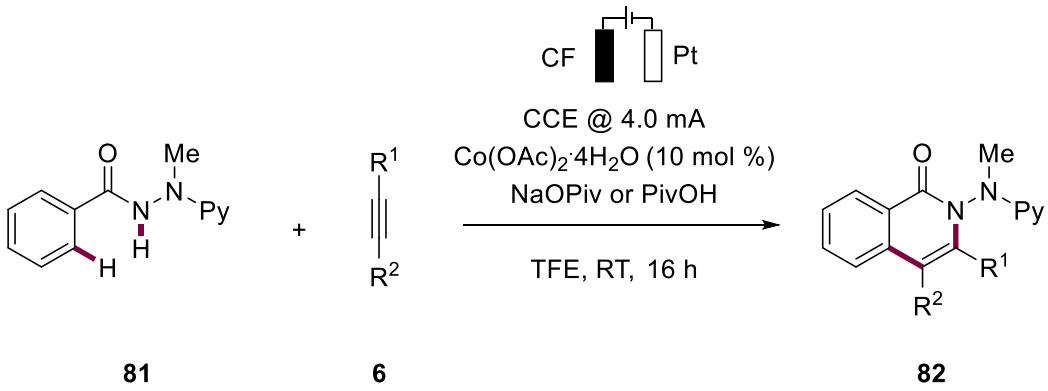

Scheme 1.36. Cobaltaelectro-catalyzed C–H annulation.

The cobaltaelectro-catalyzed C–H activation reactions were not limited to oxygenations, aminations and annulations. Indeed, cobalt-catalyzed oxidative electrochemical carbonylations[99] with CO gas were reported recently. Cobalt catalysis was identified as a versatile tool for the carbon monoxide insertion of benzamides **81** under electrochemical conditions (Scheme 1.37).

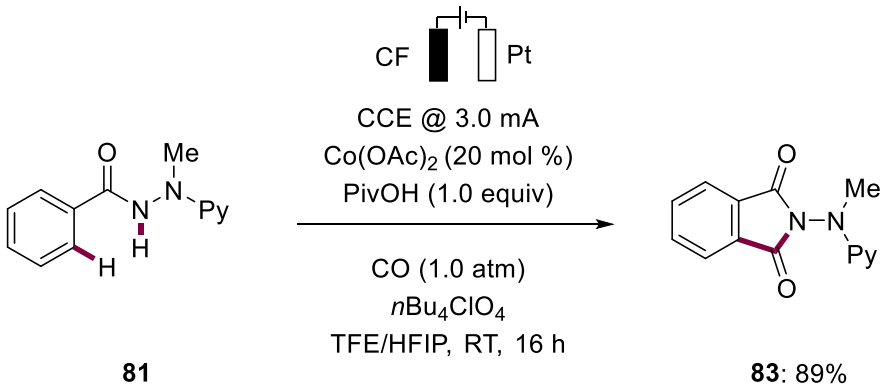

81 **83**: 89%

Scheme 1.37. Cobaltaelectro-catalyzed C–H carbonylation of CO gas.

1.3 Copper-Catalyzed C–H Activation

Compared to other transition metals, especially noble 4d transition metals, copper possesses indisputable advantages in natural abundance and low toxicity.[37] Apart from these advantages, copper complexes, as important catalysts in 3d transition metal-catalyzed C–H functionalizations, have readily accessible oxidation states, which enabled both radical pathway and one- or two-electron transfer manifolds. Due to these innate properties of copper-catalysis, numerous attentions have been attracted to develop various C–H activation reactions using copper catalysts. Therefore, copper-catalyzed C–H activation witnessed considerable development in the past few decades.

1.3.1. Copper-Catalyzed Oxidative C–H Activation

Early studies of copper-catalysis can be traced back to the beginning of 20th century. In 1905, *Ullmann* disclosed the first example for catalytical utilization of copper as a catalyst in C–O bond formations (Scheme 1.38a).[100] One year later, *Goldberg* reported the arylation of aniline derivative **85** with a broad scope using copper catalysis (Scheme 1.38b).[101]

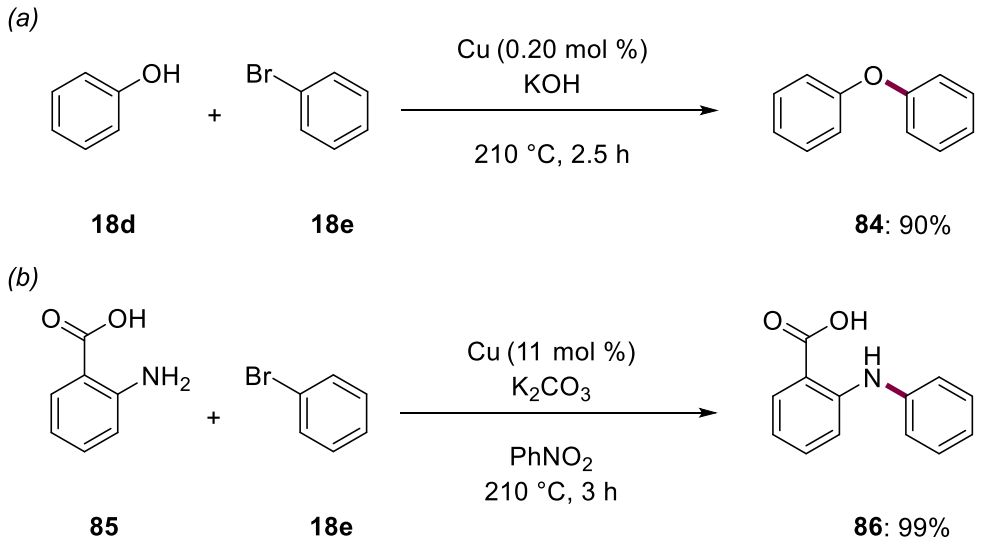

Scheme 1.38. Early examples of copper-catalyzed arylation.

Inspired by these pioneering works, tremendous attention has been attracted by the field of copper-catalysis. However, recently significant momentum has been gained by copper-catalyzed activation of inert C–H bonds. In 2007, *Daugulis* and co-workers explored the copper-catalyzed C–H arylation of benzoxazole **87** (Scheme 1.39a).[102] The addition of alkoxide base allows a facile generation of the organo-copper intermediate in the catalytic cycle. Later, the same group expanded the scope of this manifold into different types of heterocycle substrates (scheme 1.39b).[103]

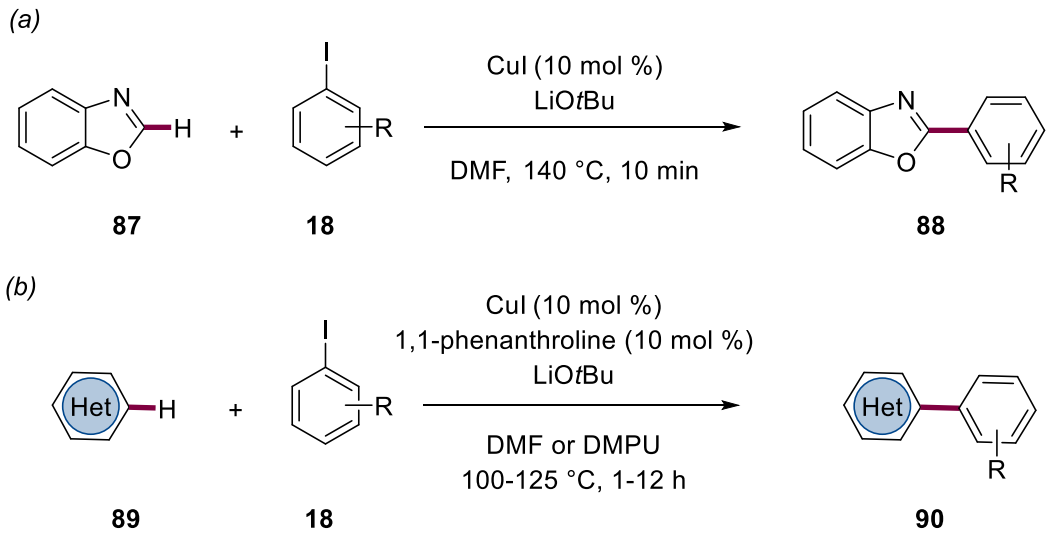

Scheme 1.39. Copper-catalyzed arylation of benzoxazole **87** and heterocycles **89**.

Independently, *Ackermann* and co-workers developed the copper-catalyzed arylation on 1,2,3-triazoles **91** (scheme 1.40).[104] Diversely substituted triazoles **92** syntheses have been enabled with high level of regioselectivity for the formation of decorated 1,2,3-triazoles **91**.

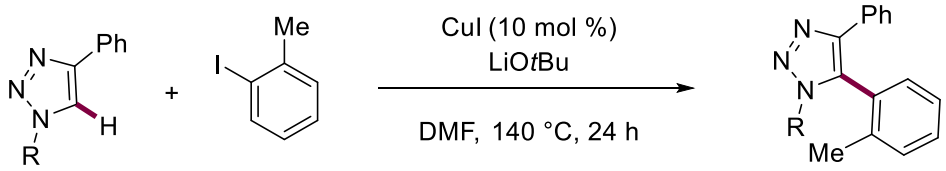

91 **18g** **92**

Scheme 1.40. Copper-catalyzed arylation of 1,2,3-triazoles **91**.

After these primary developments of copper-catalyzed C–H activations, oxidative copper-catalyzed arylations with organoboron reagents **94** have recently been achieved by *Dai* and *Yu* (Scheme 1.41).[105] By introducing an oxazoline-based bidentate directing group strategy, *ortho*-arylated benzamides **95** products were formed using stoichiometric amount of Ag_2O as oxidant.

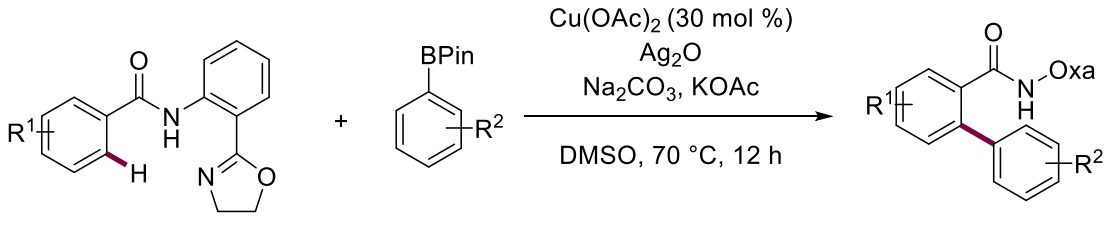

93 **94** **95**

Scheme 1.41. Oxidative copper-catalyzed C–H arylation.

The oxidative copper-catalysis was not limited to arylation reactions. Indeed, *Yu* and co-workers developed the copper-mediated selective oxidative C–H alkynylation with terminal alkynes **76** (Scheme 1.42).[106] Broad substrate scope of functionalized

benzamides **93** and alkynes **76** has been noted. Later, *Zhang* and co-workers further developed this manifold and applied catalytic amounts of copper acetate as the catalyst and stoichiometric amounts of silver carbonate as oxidant, resulting in the alkynylation and cascade annulation with C(sp^3)–H and C(sp^2)–H bonds activations in a decarboxylative fashion.[107]

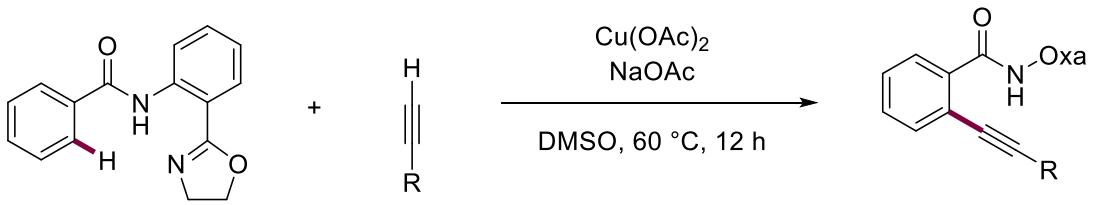

93 **76** **96**

Scheme 1.42. Oxidative copper-catalyzed C–H arylation.

As copper-catalyzed C–H activations are well-developed for the C–C bond construction, copper-catalyzed C–Het bond formations gained much attention. Indeed, *Yu* reported in one of his early works on the C–H acyloxylation reactions (Scheme 1.43).[108] Using O_2 as external oxidant, copper-catalyzed C–H acyloxylation reactions were achieved, converting diverse decorated 2-arylpyridines **9** into the corresponding acyloxylated product **97**.

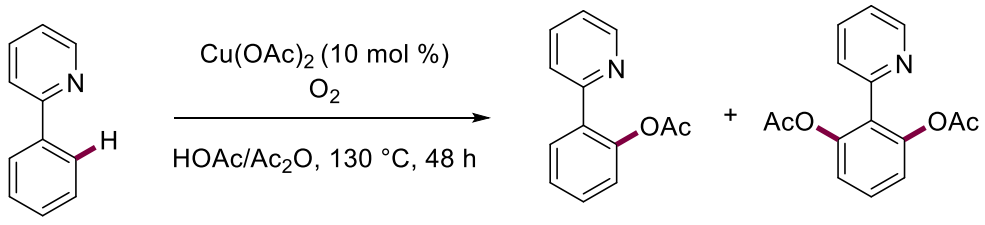

9 **97**: 37% **97'**: 56%

Scheme 1.43. Copper-catalyzed C–H acyloxylation.

Additionally, selective copper-catalyzed C–H amination reactions were reported by the group of *Daugulis* with the assistance of a bidentate quinoline directing group (Scheme

1.44).[109] Applying morpholine **79a**, the *ortho*-aminated benzamides **98** were formed in good yield.

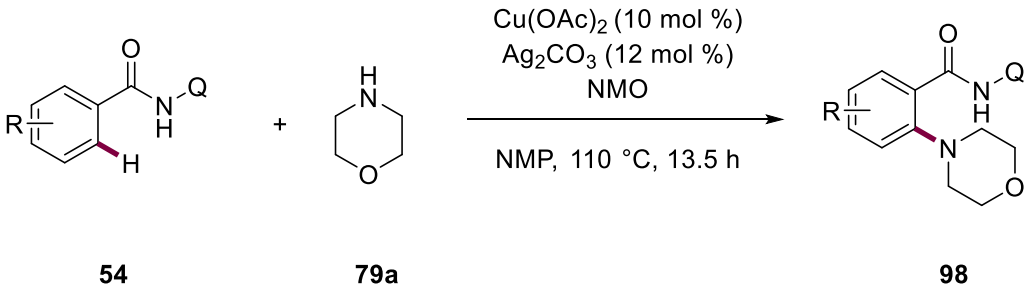

54 **79a** **98**

Scheme 1.44. Copper-catalyzed C–H amination.

In 2009, *Fukuzawa* and co-workers disclosed the copper-catalyzed C–H sulfenylation of benzoxazoles **87** in an oxidative fashion (Scheme 1.45).[110] By applying catalytic amount of copper(I) iodide in the presence of O_2 as the terminal oxidant, sulfenylated products **100** were generated in excellent yields.

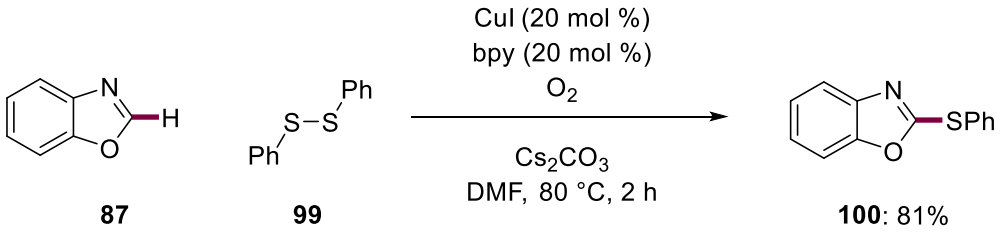

87 **99** **100**: 81%

Scheme 1.45. Copper-catalyzed C–H sulfenylation.

1.3.2. Cupraelectro-Catalyzed C–H Activation

The last decade has witnessed a renaissance on electrochemistry.[21, 38a, 38e] Merged with transition metal catalyzed C–H activation, new strategies for electrosynthesis have been developed and applied to exploit the innate reactivity of otherwise inert C–H bonds. Among other manifolds, 3d transition metal catalyzed electrochemical C–H activations attracted much attention due to the cost-efficient and low-toxic nature of the catalysis. As discussed previously, cobaltaelectro-catalysis has undergone

tremendous development with various oxidative C–H activation reactions, including annulation, oxygenation, amination, carbonylation and allylation. These achievements largely inspired the exploration of other 3d earth-abundant metal catalyzed electrochemical C–H activations. In this context, nickel, iron, manganese and very recently copper have been devised for metallaelectro-catalyzed C−H activations.[21] Among others, cupraeletro-catalyzed C–H activation will be discussed in detail in this thesis.

In 2018, *Mei* developed the cupraelectro-catalyzed C–H amination reactions of arenes **101** with secondary amines **79** (scheme 1.46).[111] Using a redox mediator, the copper-catalysis can be carried out in an undivided cell, without copper disposition on the cathode. Detailed mechanistic studies revealed two single electron transfer (SET) processes in the oxidation of copper pre-catalyst.

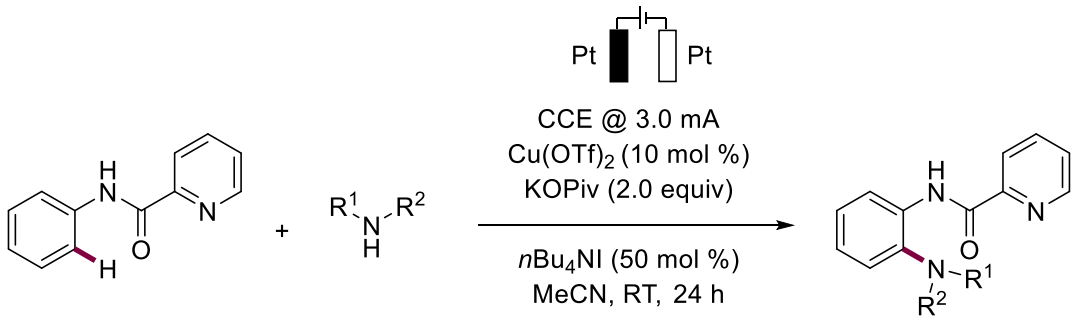

Scheme 1.46. Cupraelectro-catalyzed C–H amination using secondary amines **79**.

Later on, a similar amination reaction was reported by *Nicholls* and co-workers.[112] Using a commonly applied quinoline directing group, aminations of benzamides **54** have been achieved in good yields with further applications using pharmaceutical compounds as the amination source (Scheme 1.47).

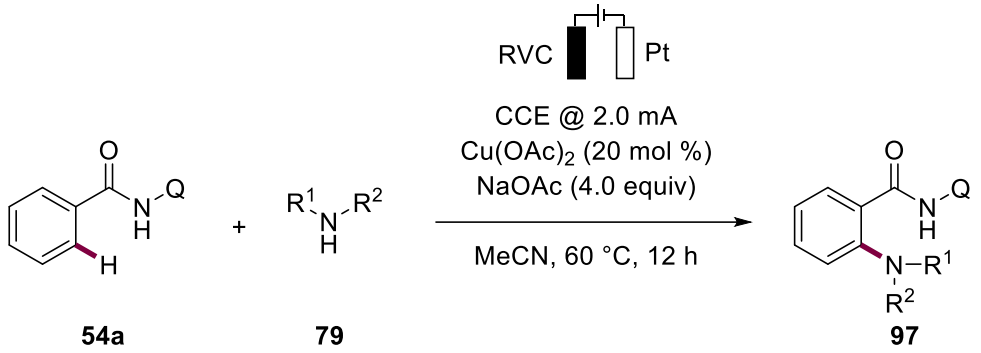

Scheme 1.47. Cupraelectro-catalyzed C–H amination with benzamides **54**.

Very recently, *Fang* and *Mei* disclosed a cupraelectro-catalyzed C–H bromination with quinoline benzamides **54** (Scheme 1.48).[113] Site-selective brominated quinoline products **103** were formed using electricity as the external oxidant under rather mild conditions.

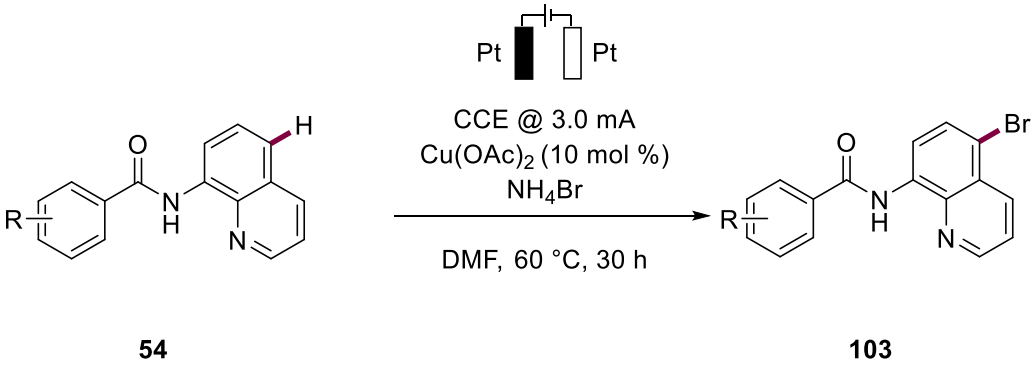

Scheme 1.48. Cupraelectro-catalyzed C–H bromination with benzamides **54**.

2. Objectives

In recent years, transition metal-catalyzed C–H transformation has emerged as an increasingly powerful tool for molecular syntheses. Merged with electrocatalysis, the sustainable nature of oxidative C–H transformations has been significantly improved. The effective utilization of renewable electricity bears considerable potential towards an environmentally friendly resource economy.[39b] Thereby, stoichiometric amounts of often toxic traditional chemical oxidants can be replaced by green, renewable electricity. Despite indisputable progress in metallaelectro-catalyzed C–H activation using noble transition metals,[21, 39a, 39b] 3d base metal-catalyzed electrochemical C–H activation continuous to be underdeveloped. Hence, we became attracted to inexpensive, earth-abundant 3d base metal-catalyzed electrochemical C–H activations.

Recently, earth-abundant, cost-efficient 3d base metal cobalt has been identified as a versatile catalyst for C–H transformations.[48] In this context, C–H/N–H activation with terminal alkyne has been accomplished by cobalt-catalysis with traditional chemical oxidants,[74, 79] which led to undesired by-products and/or generated stoichiometric amount of metal waste. To this end, electrochemistry holds great potential for more sustainable oxidative C–H transformation by minimizing the waste generation, with H_2 as the only by-product. Therefore, we tested cobaltaelectro-catalyzed C–H/N–H annulation with terminal alkyne (Scheme 2.1).

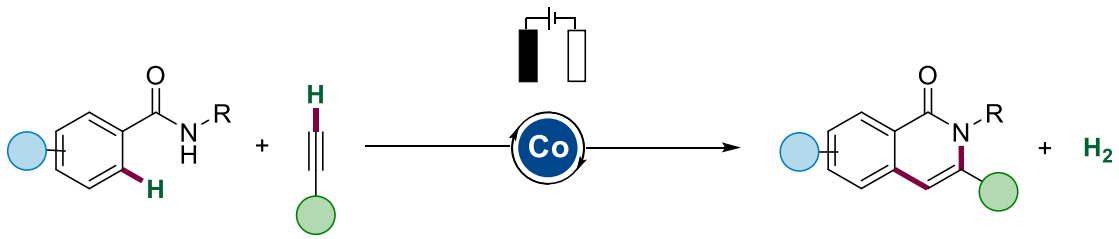

Scheme 2.1. Cobaltaelectro-catalyzed C–H/N–H annulation with terminal alkyne.

Based on our pervious report on cobaltaelectro-catalyzed C–H/N–H annulation of terminal alkyne, we became intrigued by the possibility of electrochemical alkynylation

by terminal alkyne and decarboxylative alkynylations by alkynyl carboxylic acids. Oxidative alkynylation using copper catalysts have been well-developed in the last few years,[106] while the cupraelectro-catalyzed C–H transformations remain scarce.[111-112] In this context, we developed the cupraelectro-catalyzed cascade annulation by C–H alkynylation and decarboxylative C–H/C–C manifolds with alkynyl carboxylic acids (Scheme 2.2).

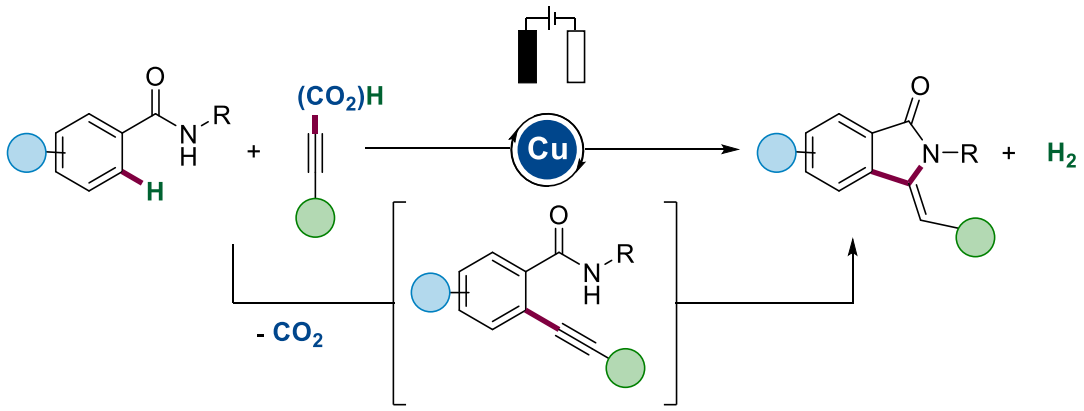

Scheme 2.2. Cupraelectro-catalyzed cascade annulation by C–H alkynylation.

Cobalt catalyzed electrochemical C–H activations have been widely applied in the formation of C–N,[91-92] C–C[93-96, 98] and C–O[90] bonds. Inspired by our previous work on cobaltaelectro-catalyzed C–H alkoxylation with alcohols,[90] we further expanded this regime of electrochemical construction of C–O band to C–H acyloxylation reactions with carboxylic acids (scheme 2.3).

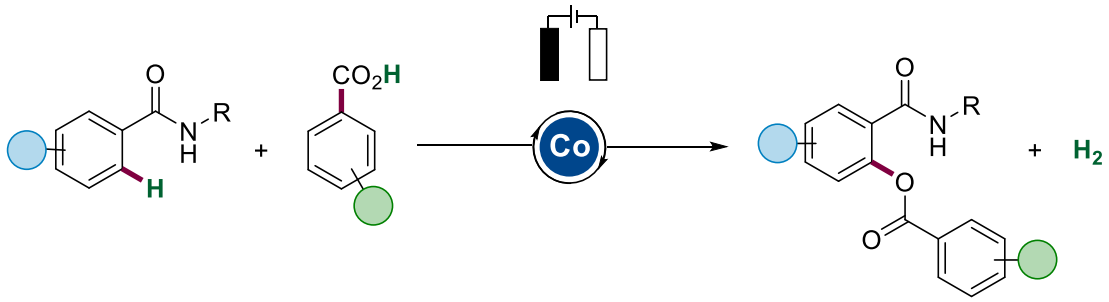

Scheme 2.3. Cobaltaelectro-catalyzed C–H acyloxylation.

Electrochemical C–H activations with alkenes have been reported using precious transition metals such as palladium,[114] rhodium[115] and iridium[116] but were largely limited to electronically activated styrenes and acrylates. The utilization of non-activated alkenes by metallaelectro-catalyzed C−H activation is unknown. Herein, we disclose the first cobaltaelectro-catalyzed chemo-selective C−H allylation with non-activated alkenes (scheme 2.4).

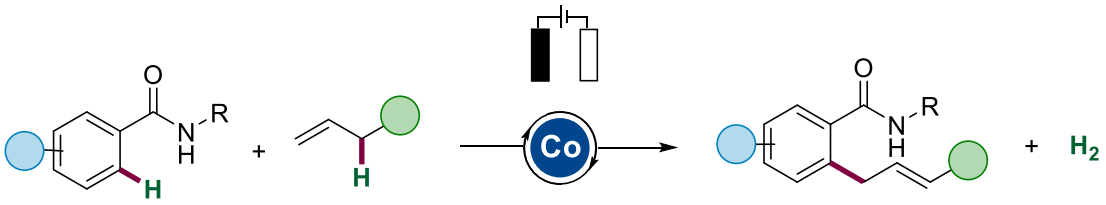

Scheme 2.4. Cobaltaelectro-catalyzed oxidative C−H allylation with non-activated alkenes.

3. Result and Discussion

3.1 Water-Tolerant Cobaltaelectro-Catalyzed C–H/N–H Activation at Room Temperature

Heterocycle syntheses enabled by C–H/N–H activations have been achieved with various transition metal catalysts over the last decade.[37, 117] Among these, the versatile cobalt catalysis proved to be a powerful tool in C–H/N–H alkyne annulations, enabling step-economical isoquinolone synthesis.[74, 79] Despite indisputable advances, these approaches normally required high reaction temperature and stoichiometric amounts of toxic metal salts as the sacrificial oxidants. In sharp contrast, merging the metallaelectro-catalysis with oxidative C–H activations, the use of expensive and toxic oxidants has been avoided by anodic oxidation, enhancing the inherent sustainable nature of C–H activation. In this context, we disclosed the first unprecedented cobaltaelectro-catalyzed C–H/N–H activation for an isoquinolone synthesis at ambient temperature with full water-tolerant. The novel electrochemical C–H/N–H functionalization is operative in a considerably resource-economical fashion as compared to the traditional approaches.

3.1.1. Optimization Studies

To initiate our studies on cobaltaelectro-catalyzed annulation reactions, we probed different reaction conditions for the C–H/N–H activation using terminal alkyne **76a** (Table 3.1). The desired product **104aa** was formed within the cobaltaelectro-catalysis manifold, using NaOPiv as the optimal additive (entries 1-3). The robust cobalt complex was fully tolerant of H_2O (entries 5-6). The highest catalyst performance was obtained in a mixture of MeOH and H_2O 1:1 with 10 mol % of the cobalt catalyst (entries 3-9). It should be noted that unlike the previous reported cobaltaelectro-catalyzed oxygenation reactions with alcohols,[90] the addition of large access of free alcohols as cosolvent did not lead to the oxygenation of benzamide **56a**, but selectively delivered

the annulated product **104aa**. Furthermore, control experiments illuminated the essential roles of the additive, the cobalt catalyst and the electricity (entries 10-12). Nevertheless, several typical 3d or 4d transition metal catalysts were tested. All proved to be ineffective (entries 13-17).

Table 3.1. Optimization of the cobaltaelectro-catalyzed C–H/N–H alkyne annulation.[a]

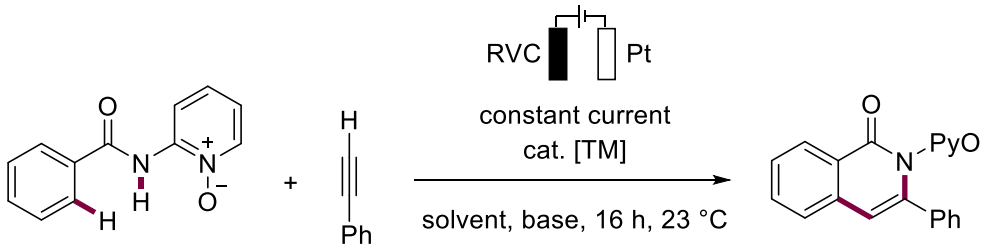

56a **76a** **104aa**

Entry	[Co]	Solvent	Base	Yield [%]
1	$Co(OAc)_2{\cdot}4H_2O$	DMSO	NaOAc	28
2	$Co(OAc)_2{\cdot}4H_2O$	DMSO	Na_2CO_3	-
3	$Co(OAc)_2{\cdot}4H_2O$	DMSO	NaOPiv	31
4	$Co(OAc)_2{\cdot}4H_2O$	TFE	NaOPiv	50
5	$Co(OAc)_2{\cdot}4H_2O$	H_2O	NaOPiv	62
6	$CoCl_2{\cdot}6H_2O$	H_2O	NaOPiv	56
7	$Co(OAc)_2{\cdot}4H_2O$	MeOH	NaOPiv	64[b]
8	$Co(OAc)_2{\cdot}4H_2O$	H_2O/MeOH (1:1)	NaOPiv	76
9	**$Co(OAc)_2{\cdot}4H_2O$**	**H_2O/MeOH (1:1)**	**NaOPiv**	**76**[c]
10	$Co(OAc)_2{\cdot}4H_2O$	H_2O/MeOH (1:1)	NaOPiv	-[d]
11	-	H_2O/MeOH (1:1)	NaOPiv	-
12	$Co(OAc)_2{\cdot}4H_2O$	H_2O/MeOH (1:1)	-	-
13	$MnBr(CO)_5$	H_2O/MeOH (1:1)	NaOPiv	-[c]
14	$Ni(OAc)_2$	H_2O/MeOH (1:1)	NaOPiv	-[c]
15	$[RuCl_2(p\text{-cymene})]_2$	H_2O/MeOH (1:1)	NaOPiv	-[c]
16	$AuMePPh_3$	H_2O/MeOH (1:1)	NaOPiv	-[c]
17	$PtCl_2$	H_2O/MeOH (1:1)	NaOPiv	-[c]

[a] Reaction conditions: Undivided cell, **56** (0.5 mmol), **76** (1.0 mmol), [Co] (20 mol %), base (2.0 equiv), solvent (10 mL), 23 ºC, 4.0 mA, 16 h, CF anode, Pt-plate cathode. [b] Oxygenation product also formed (17%). [c] [TM] (10 mol %). [d] No electricity.

3.1.2. Scope of Cobaltaelectro-Catalyzed C–H/N–H Annulation

With the optimized reaction conditions in hand, we became interested in the key factor of *N*,*O*-bidentate coordination pattern of cobaltaelectro-catalysis. Hence, we performed a set of electrochemical annulation experiments using different directing groups (Scheme 3.1). Quinoline bidentate motif **54** proved to be able to provide the corresponding annulated product, albeit with reduced product yield. While, simple pyridine group **56b** or *N*-methylbenzamide **15** failed to deliver any product under the electrochemical conditions.

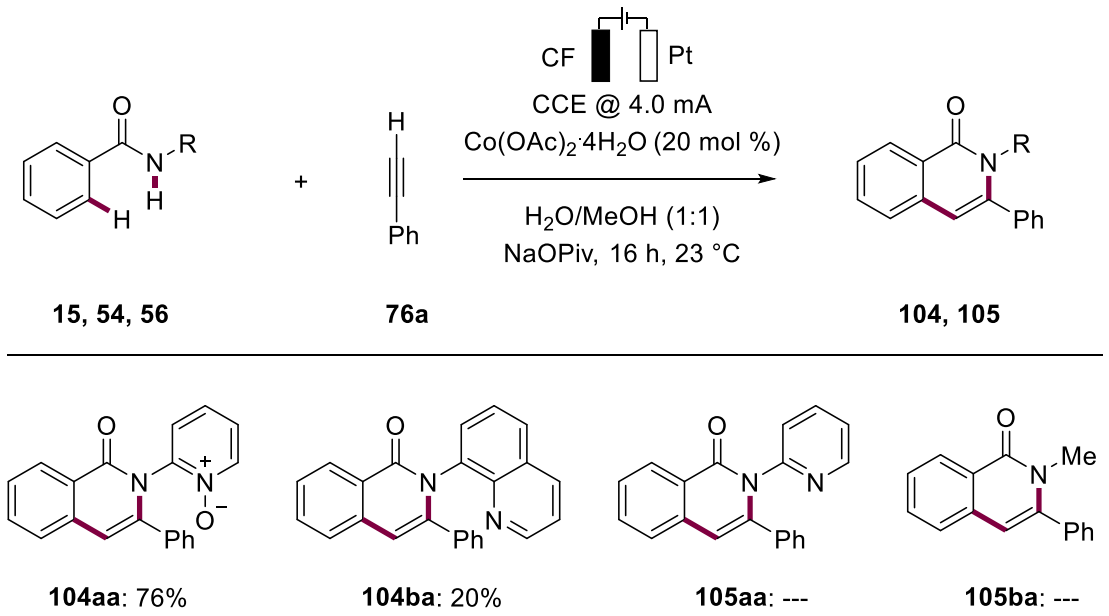

Scheme 3.1. Effect of *N*-substitution on cobaltaelectro-catalyzed C–H/N–H activation.

Thereafter, we explored the versatility of the cobaltaelectro-catalyzed C–H/N–H annulation regime with various decorated benzamides **56** under the optimized reaction condition (Scheme 3.2). Electron-rich as well as electron-poor arenes **56c-56e** were amenable to yield the corresponding isoquinolones **104** with excellent chemo- and positional-selectivity. Notably, synthetically-useful halides such as fluorides, bromides and iodides, were well tolerated under the electrochemical conditions with H_2O as cosolvent, while reductive couplings[118] were not detected. The robust cobaltaelectro-

catalysis enabled highly efficient C–H/N–H activation on amides **56c-56j** with *para*-, *meta*- or *ortho*-substitution pattern, as well as di-substituted and tri-substituted amides **56k-56m**. The cobalt catalysis was not limited to arene annulation, but C–H/N–H activations of alkenes were also effective delivering the corresponding pyridines **104na-104oa** under the electrochemical reaction conditions.

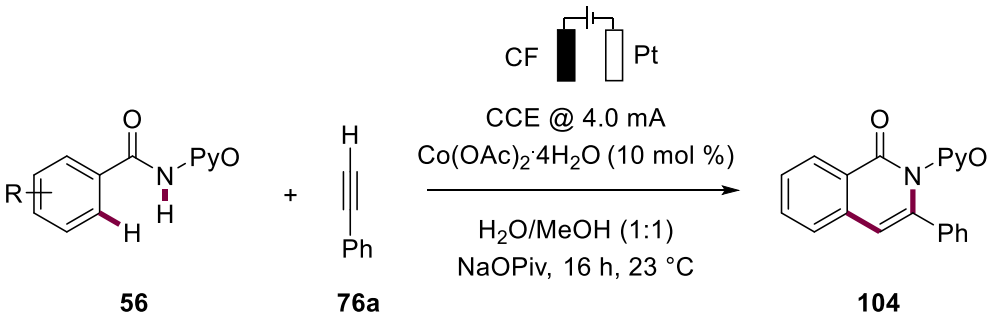

56 **76a** **104**

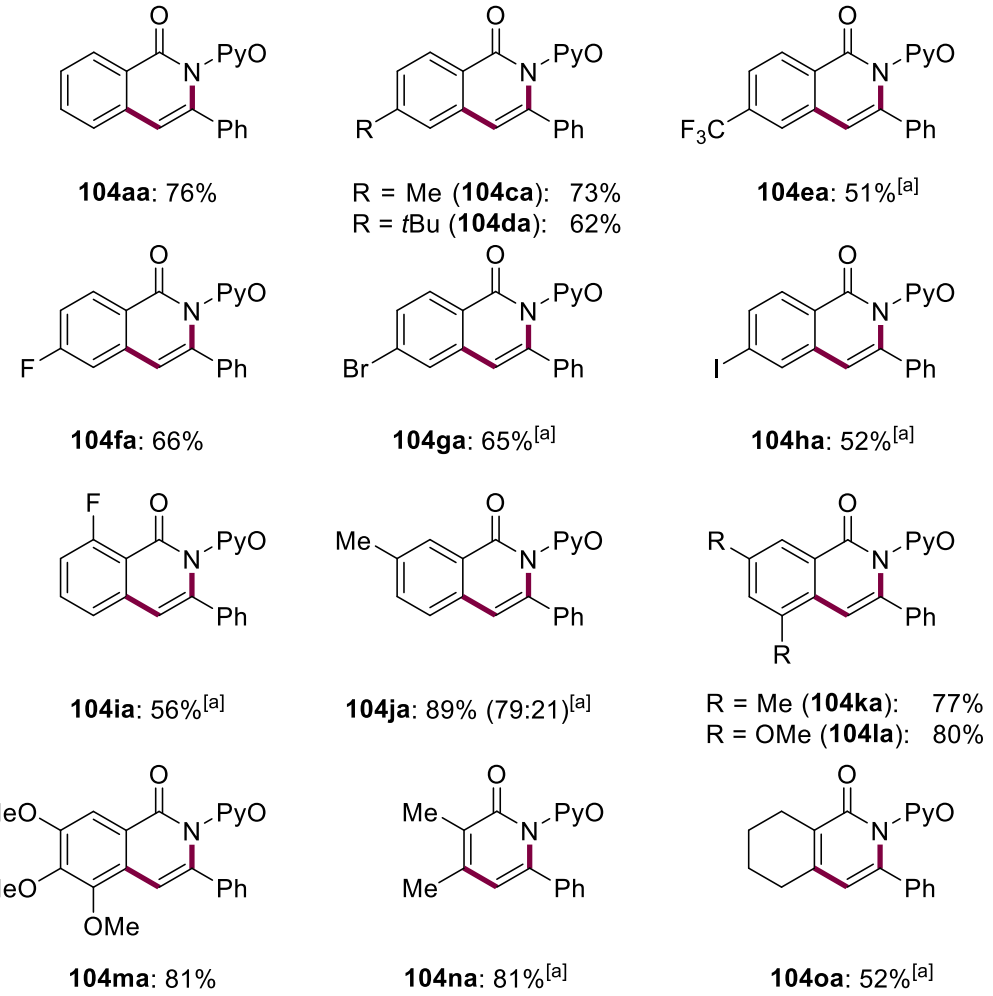

104aa: 76%

R = Me (**104ca**): 73%
R = *t*Bu (**104da**): 62%

104ea: 51%[a]

104fa: 66%

104ga: 65%[a]

104ha: 52%[a]

104ia: 56%[a]

104ja: 89% (79:21)[a]

R = Me (**104ka**): 77%
R = OMe (**104la**): 80%

104ma: 81%

104na: 81%[a]

104oa: 52%[a]

Scheme 3.2. Cobaltaelectro-catalyzed C–H/N–H activation of benzamides **56**. [a] $Co(OAc)_2{\cdot}4H_2O$ (20 mol %).

Likewise, we tested the versatility of representative alkynes **76** (Scheme 3.3). The versatile cobaltaelectro-catalysis proved effective with electron-rich and electron-deficient acetylenes **76b-76d**. Alkyl alkynes **76e-76g**, as well as functional cyclopropyl alkyne **76h**, afforded the desired annulated products in good to excellent yield. Valuable alkynes with ester **76i-76j** and alkyl chloride **76k** functional groups were fully tolerated by the cobaltaelectro-catalysis manifold.

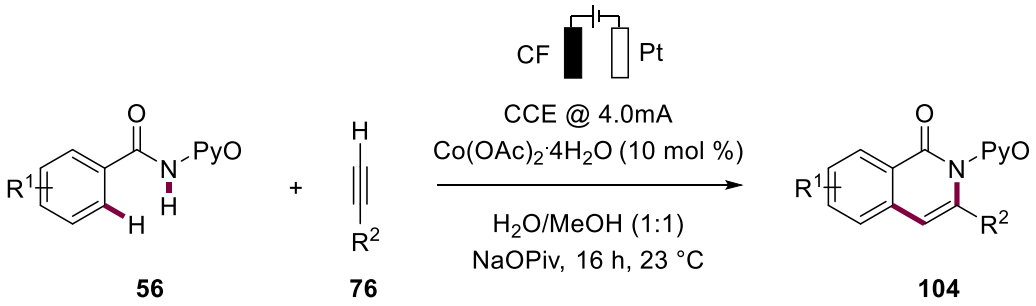

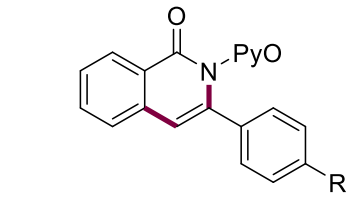

R= Me (**104ab**): 82%[a]
R= OMe (**104ac**): 82%[a]

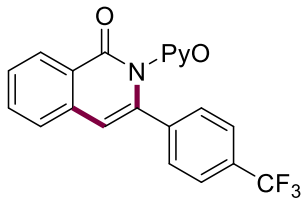

104ad: 53%[a]

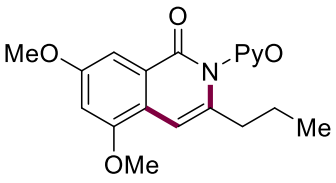

104le: 85%[a]

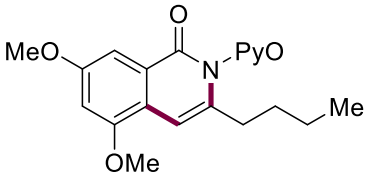

104lf: 74%[a]

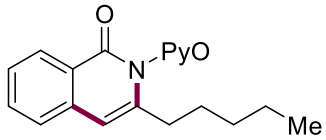

104ag: 55%[a]

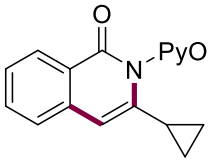

104ah: 64%[a]

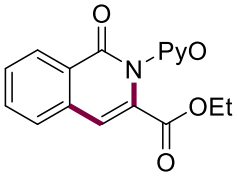

104ai: 65%

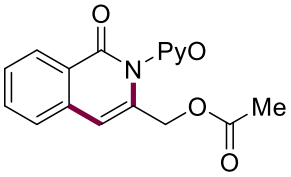

104aj: 55%[a]

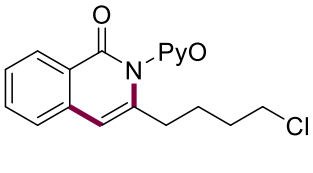

104ak: 60%[a]

Scheme 3.3. Cobaltaelectro-catalyzed C–H/N–H activation of alkynes **76**. [a] $Co(OAc)_2{\cdot}4H_2O$ (20 mol %).

Furthermore, the robustness of the cobaltaelectro-catalyzed C–H/N–H annulation was reflected by applying H_2O as the sole reaction medium. Substituted benzamide, alkene and functional ester group-containing alkyne were chemo-selectively transformed into the corresponding isoquinolones and pyridines **104** in moderate yields (Scheme 3.4).

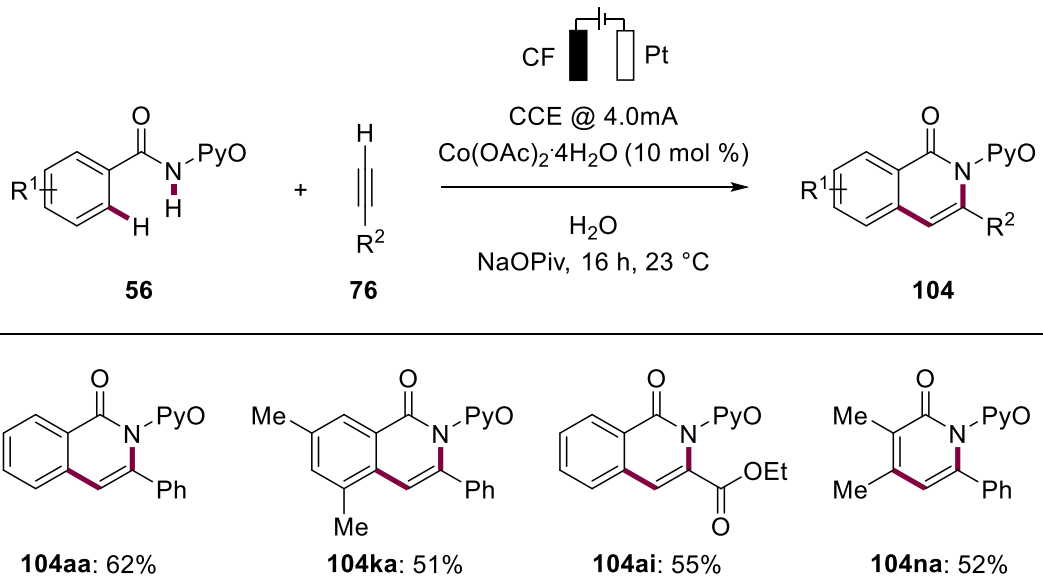

Scheme 3.4. Cobaltaelectro-catalyzed C–H/N–H annulation in H_2O.

3.1.3. Mechanistic Studies

3.1.3.1. Competition Experiments

Intrigued by the unique cobaltaelectro-catalyzed C–H/N–H annulation manifold, we further explored the catalyst's mode of action. To this end, we started the mechanistic studies with intermolecular competition experiments (Scheme 3.5). Different *para*-substituted benzamides **56** and acetylenes **76** were submitted under the optimized reaction conditions with 20 mol % of the cobalt catalyst to conduct competition experiments between electron-donating and electron-withdrawing substrates. In both cases, electron-donating substrates proved to feature superior reactivities. The ratio of electron-rich benzamide **56c** to electron-deficient benzamide **56e** is 1.4:1, while a ratio of 1.3:1 for electron-rich isoquinolones **104ab** to electron-deficient isoquinolones

104ad were obtained in the intermolecular competition experiment with substituted acetylenes **76**. The finding of the competition between benzamides highlighted the inherent nature of a base-assisted internal electrophilic substitution (BIES)[27] pattern.

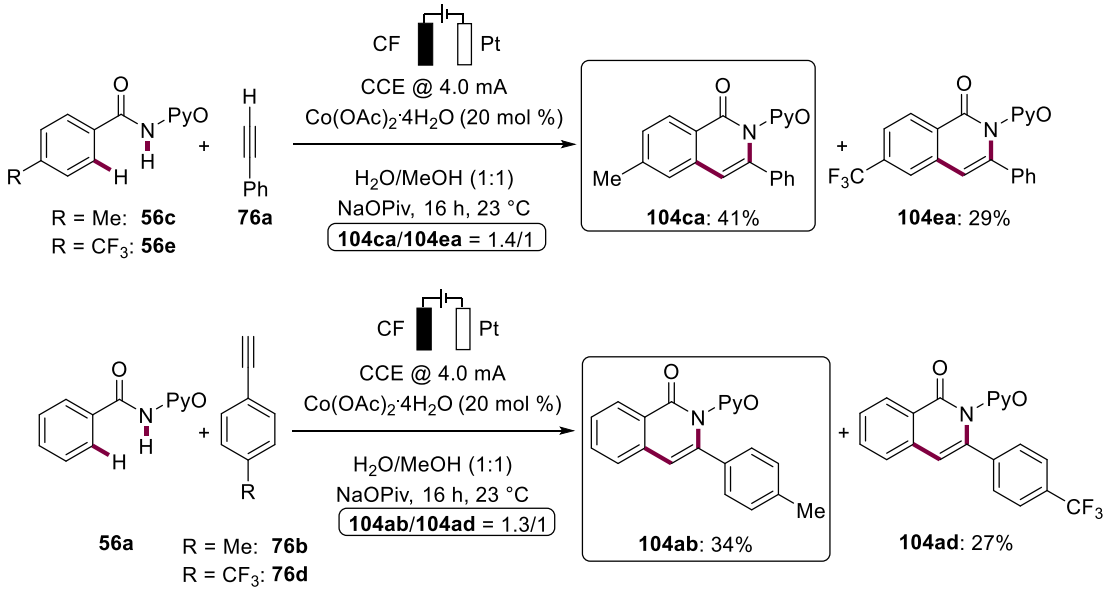

Scheme 3.5. Intermolecular competition experiments.

3.1.3.2. H/D Exchange Experiment

Thereafter, a reaction with isotopically labelled solvent was conducted under the electrochemical conditions (Scheme 3.6). Since H_2O as the sole reaction medium was able to deliver the desired product, isotopically labelled D_2O was introduced to perform the H/D exchange experiment. No H/D exchange can be found at the *ortho*-position of ether recovered benzamide **56a** or isoquinolone product **104aa**, which revealed the C–H cleavage was irreversible.

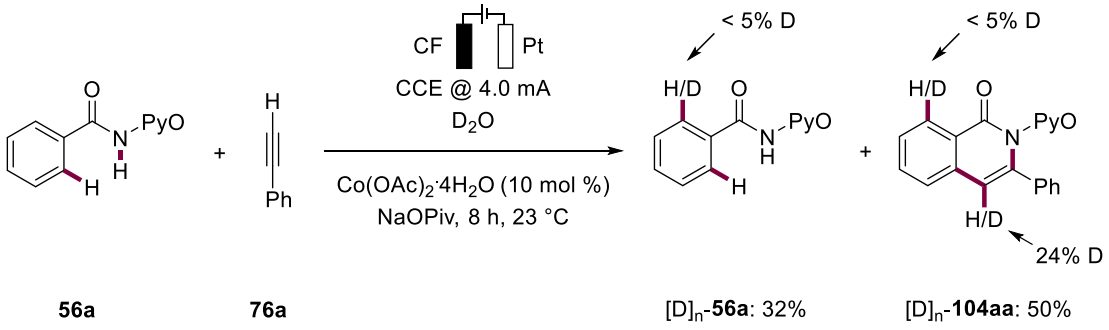

Scheme 3.6. Cobaltaelectro-catalyzed C–H/N–H annulation in D_2O.

3.1.3.3. Kinetic Isotope Effect Studies

Subsequently, kinetic isotope effect (KIE) studies were performed with two parallel reactions using D_5-benzamide [D_5]-**56a** and the standard substrate **56a**. Initial rates of both experiments were recorded within 20% of product yield (Scheme 3.7). A KIE value of k_H/k_D = 1.1 was obtained, suggesting a facile C–H scission.

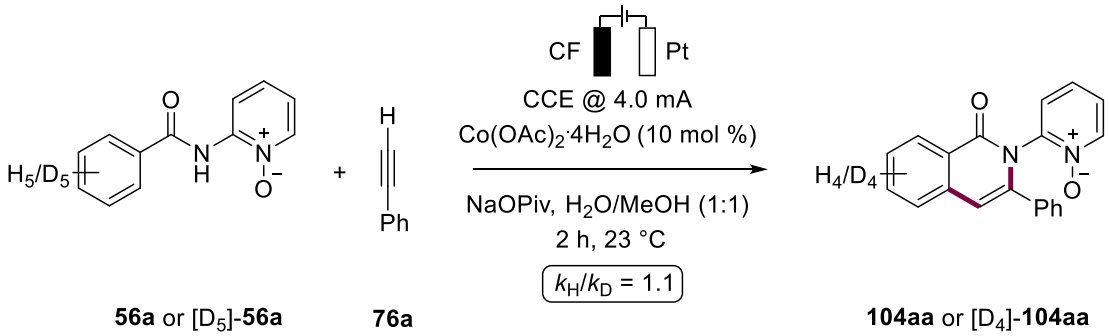

56a or [D_5]-**56a** **76a** **104aa** or [D_4]-**104aa**

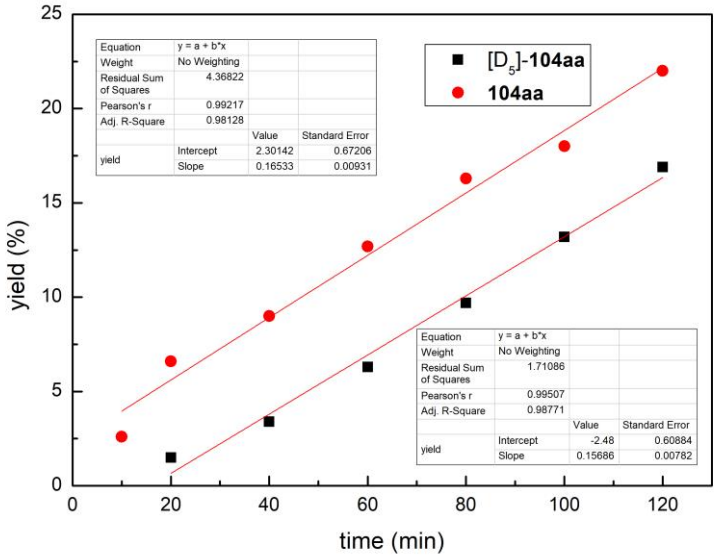

Scheme 3.7. Kinetic isotope effect experiments.

3.1.3.4. Attempted Cyclization

Moreover, the independently prepared *ortho*-alkynylated substrate **105** was tested under the optimized electrochemical condition, which failed to form the desired annulated product **104aa** (Scheme 3.8). Thus, an organometallic alkyne annulation process was suggestive in the catalytic cycle.

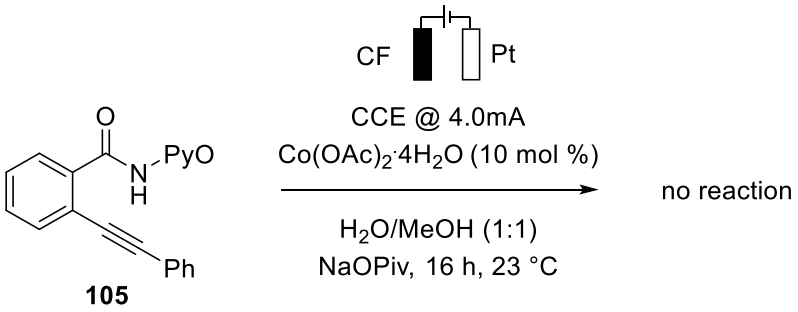

Scheme 3.8. Attempted cyclization experiment.

3.1.3.5. Cyclic Voltammetry Studies

Detailed cyclic voltammetry studies were conducted by *T. H. Meyer* to gain mechanistic insights into the cobaltaelectro-catalyzed C–H/N–H annulation (Figure 3.1). In the absence of the cobalt catalyst, benzamide **56a** exhibited an oxidation potential of 1.51 V versus SCE, while the oxidation potential of cobalt catalyst was found to be 1.19 V versus SCE. The oxidation potential of the catalyst was 320 mV lower than substrate **56a**, which provides support for a single-electron oxidation process happening between the cobalt catalyst species and the benzamide. No distinguishable redox activity was observed on the case of phenylacetylene **76a** alone, suggesting an organometallic alkyne annulation manifold, which coincides with the attempted cyclization reaction result.

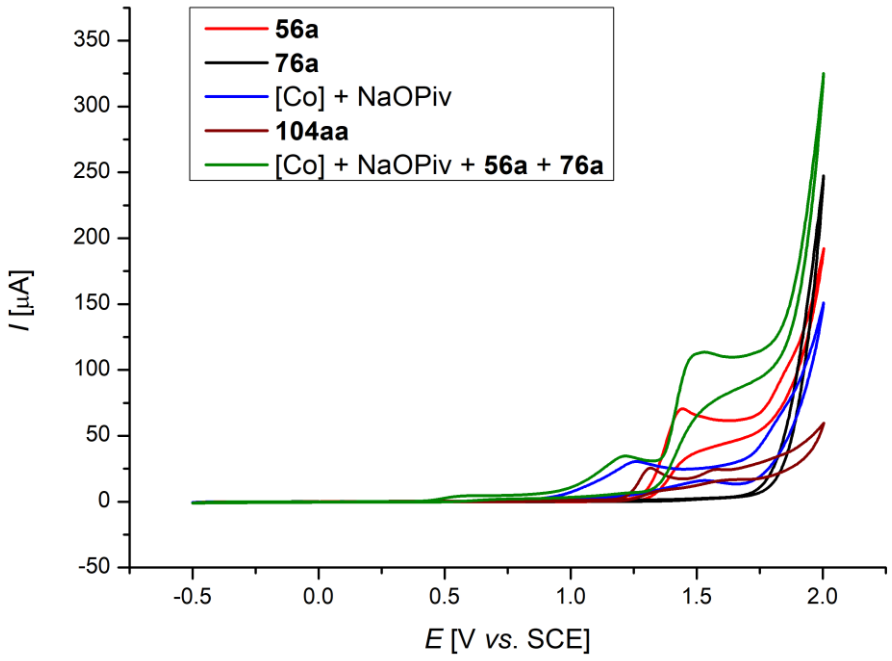

Figure 3.1. Cyclic voltammograms at 100 mVs^{-1}: *n*-Bu_4NPF_6 (0.1 M in MeOH), concentration of substrates 1 mM (NaOPiv 4 mM).

3.1.4. Proposed Mechanism

Based on these mechanistic studies, a plausible catalytic cycle can be proposed to illuminate the cobaltaelectro-catalyzed C–H/N–H annulation manifold (Scheme 3.9). Initiated by the anodic oxidation of Co(II) into Co(III) catalytically active carboxylate species **106**, benzamide substrate undergoes a BIES C–H cleavage[27] to deliver intermediate **107**. Thereafter, insertion of alkyne give rise to cobalt complex **108** and reductive elimination gives desired product **104** while releasing a putative cobalt(I) species **109**. Finally, the catalytically active cobalt(III) species **106** is regenerated by anodic oxidation and cathodic reduction gives the only byproduct H_2 at the cathode surface.

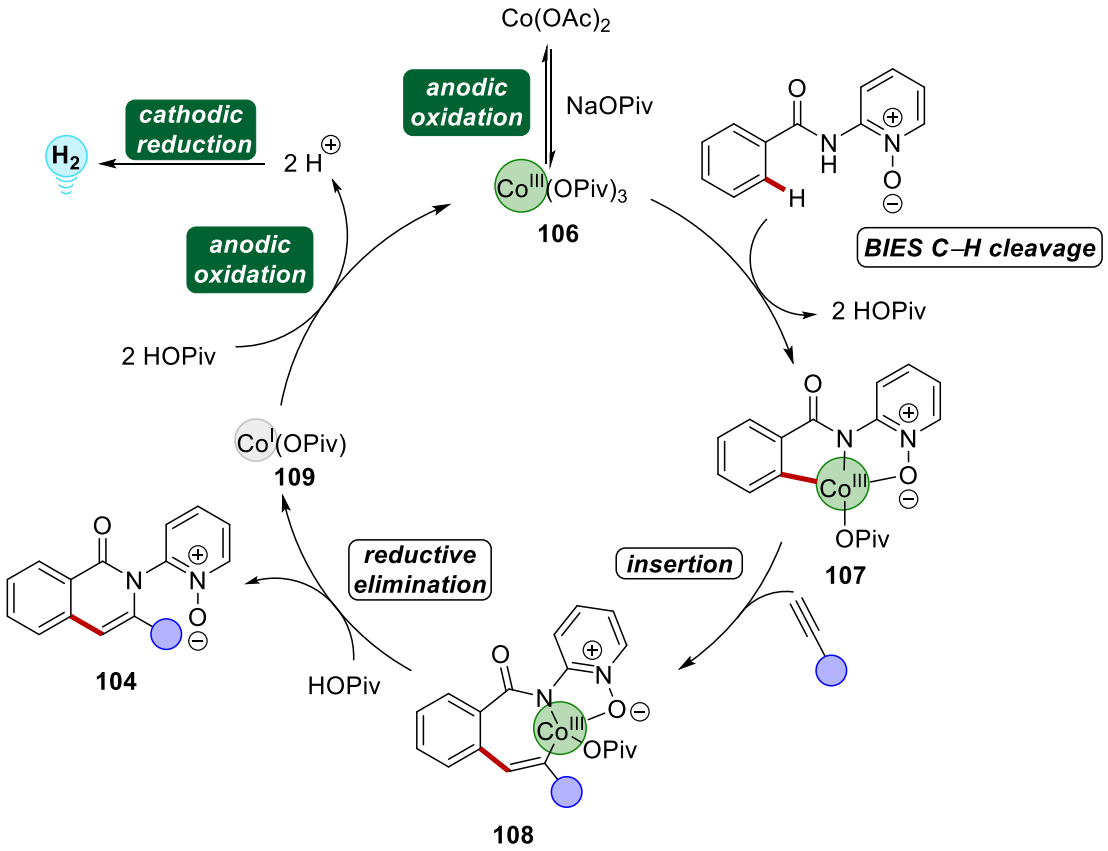

Scheme 3.9. Pausible catalytic cycle.

3.2 Cupraelectro-Catalyzed Cascade Annulation by C–H Alkynylation and Decarboxylative C–H/C–C Manifolds

The merger of oxidative C–H transformation with electrocatalysis has substantially improved the sustainability of earth-abundant 3d transition metal catalyzed oxidative C–H activation.[21, 39b] In this context, stoichiometric amounts of sacrificial chemical oxidants are replaced by environmentally-friendly electricity. Thereby, the environmental impacts have been minimized and no chemical wastes have been generated during the electrochemical process, with H_2 as the sole by-product from cathodic reduction. Thus, recent momentum was gained by 3d transition metal catalyzed electrochemical C–H transformations using cobalt,[90-97, 99, 119] nickel,[120] copper,[111-113, 121] manganese[122] and iron[122] catalysts. Despite these inspiring achievements, cupraelectro-catalyzed C–H activations remain rare. In this context,

only one example of copper-catalyzed electrochemical C–H aminations with electron-rich anilides has been reported by Mei[111] in 2018. However, electrocatalyzed C–H alkynylations have thus far proven elusive. Herein, we disclosed the first cupraelectro-catalyzed oxidative alkyne cascade annulation enabled by a C–H alkynylation manifold, which also set the stage for cupraelectro-catalyzed C–H/C–C decarboxylative annulations. Unlike the cobaltaelectro-catalyzed C–H/N–H annulations for isoquinolone synthesis,[93] cupraelectro-catalyzed C–H alkynylations selectively delivered five-membered bioactive isoindolones.[123]

3.2.1. Optimization Studies

We initiated our studies by probing different reaction conditions for the envisioned cupraelectro-catalyzed oxidative alkyne C–H annulation using constant current electrolysis (CCE) in an operationally-friendly undivided cell setup (Table 3.2). First, a set of commonly used organic solvents were tested under electrochemical condition, and we found DMA to be the optimal solvent for cupraelectro-catalyzed isoindolone synthesis, while *t*AmOH, MeCN, MeOH, DMF and NMP proved to be inefficient (entries 1-6). Second, the test of additives and copper catalysts revealed a combination of NaOPiv with $Cu(OAc)_2 \cdot H_2O$ giving the best catalytic performance for the electrolysis (entries 6-10). Higher or lower reaction temperatures did not give rise to higher yields (entries 11-12). Unlike the copper-catalyzed electrochemical C–H aminations,[111] the addition of redox mediators such as TBAI or TEMPO reduced the isoindolone yield, BQ even prevented the product formation completely (entries 13-15). The cupraelectro-catalyzed C–H alkynylation was also conducted in a potentiostatic manifold at 2.0 V, giving a similar result as was obtained in the galvanostatic regime (entry 16). Control experiments verified the essential roles of the electricity, the additive and the copper catalyst, with a minor influence of oxygen in the reaction atmosphere (entries 17-21). Other representative transition metal catalysts were further tested under otherwise identical conditions (entries 22-28). Manganese, cobalt, nickel,

ruthenium, rhodium, iridium, and palladium failed to deliver the desired products. Notably, when using cobalt(II) acetate tetrahydrate as catalysts, the corresponding isoquinolone product was obtained instead of the five-membered isoindolone.

Table 3.2. Optimization of the cupraelectro-catalyzed isoindolones synthesis.[a]

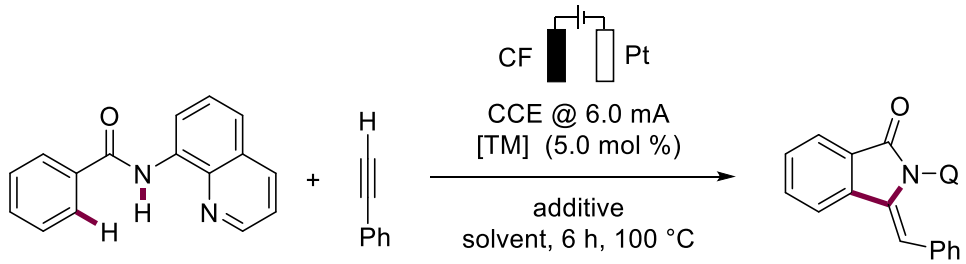

54a **76a** **110aa**

Entry	Solvent	Additive	[TM]	*E*/*Z*	Yield [%]
1	*t*AmOH	NaOPiv	$Cu(OAc)_2·H_2O$	–	–
2	DMF	NaOPiv	$Cu(OAc)_2·H_2O$	1:3	56
3	MeCN	NaOPiv	$Cu(OAc)_2·H_2O$	–	–
4	MeOH	NaOPiv	$Cu(OAc)_2·H_2O$	–	–
5	NMP	NaOPiv	$Cu(OAc)_2·H_2O$	1:8	80
6	**DMA**	**NaOPiv**	**$Cu(OAc)_2·H_2O$**	**1:13**	**90**
7	DMA	NaOAc	$Cu(OAc)_2·H_2O$	1:6	58
8	DMA	Na_2CO_3	$Cu(OAc)_2·H_2O$	1:4	44
9	DMA	KOPiv	$Cu(OAc)_2·H_2O$	1:1	51
10	DMA	NaOPiv	$Cu(OPiv)_2$	1:12	74
11	DMA	NaOPiv	$Cu(OAc)_2·H_2O$	1:6	84[b]
12	DMA	NaOPiv	$Cu(OAc)_2·H_2O$	1:8	73[c]
13	DMA	NaOPiv	$Cu(OAc)_2·H_2O$	1:10	76[d]
14	DMA	NaOPiv	$Cu(OAc)_2·H_2O$	1:8	81[e]
15	DMA	NaOPiv	$Cu(OAc)_2·H_2O$	–	–[f]
16	DMA	NaOPiv	$Cu(OAc)_2·H_2O$	1:12	86[g]
17	DMA	NaOPiv	$Cu(OAc)_2·H_2O$	1:8	18[h]
18	DMA	NaOPiv	$Cu(OAc)_2·H_2O$	1:11	90[i]
19	DMA	NaOPiv	$Cu(OAc)_2·H_2O$	1:9	5[j]
20	DMA	NaOPiv	–	–	–
21	DMA	–	$Cu(OAc)_2·H_2O$	–	–
22	DMA	NaOPiv	$Co(OAc)_2·4H_2O$	–	–[k]
23	DMA	NaOPiv	$Mn(OAc)_2$	–	–
24	DMA	NaOPiv	$[RuCl_2(p\text{-cymene})]_2$	–	–
25	DMA	NaOPiv	$Ni(OAc)_2·4H_2O$	–	–
26	DMA	NaOPiv	$[Cp^*RhCl_2]_2$	–	–
27	DMA	NaOPiv	$[Cp^*IrCl_2]_2$	–	–
28	DMA	NaOPiv	$Pd(OAc)_2$	–	–

[a] Reaction conditions: Undivided cell, **54a** (0.25 mmol), **76a** (0.50 mmol) [TM] (5.0 mol %), additive (1.0 equiv), solvent (4.0 mL), 100 °C, constant current at 6.0 mA, 6 h, CF anode, Pt-plate cathode. All yields are reported as isolated yield. [b] 80 °C. [c] 120 °C. [d] TBAI (50 mol %) as redox mediator. [e] TEMPO (20 mol %) as redox mediator. [f] BQ (50 mol %) as redox mediator. [g] Constant potential at 2.0 V (silver wire as reference electrode). [h] No electricity. [i] Under N_2. [j] Without electricity, under N_2. [k] Isoquinolone product formed in 65% yield.

3.2.2. Scope of Cupraelectro-Catalyzed Cascade Annulation

With the optimized conditions in hand, we evaluated the coordination mode of *N*-substitution pattern for the cupraelectro-catalyzed cascade annulation by C–H alkynylation (Scheme 3.10). Therefore, a set of cupraelectro-catalysis experiments using different *N*-substitutions was carried out. Benzamide with the phenyl oxazoline **93** directing group was able to give the corresponding isoindolinones **111aa** product but resulted in reduced yield. *N*,*O*-bidentate type pyridine-*N*-oxide **56a** proved to be ineffective, as was the same result when simple *N*-phenylbenzamide **15b** was applied.

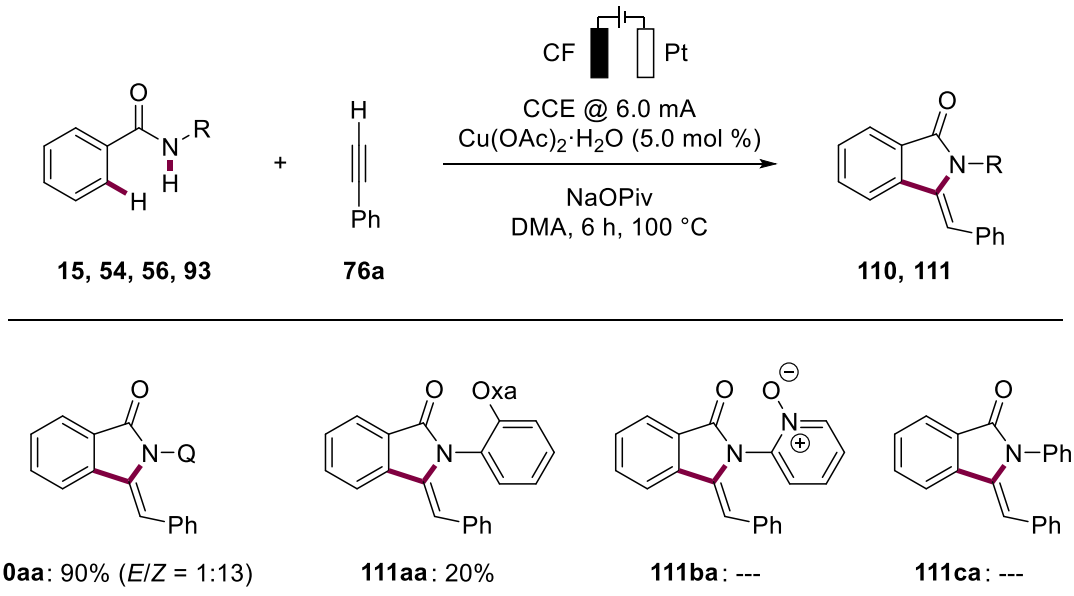

Scheme 3.10. Effect of the *N*-substitution on the cupraelectro-catalysis.

Furthermore, we probed the versatility of cupraelectro-catalyzed cascade annulation by C–H alkynylation with various substituted benzamides **54** and terminal alkynes **76** (Scheme 3.11). The experiment for the product **110al** synthesis was performed by *U. Dhawa*. A wide variety of benzamides **54** with electron-rich and electron-deficient substituted arenes **54b**-**54g** were amenable to cupraelectro-catalyzed cascade annulation regime, affording the desired isoindolinones in good to excellent yields. *ortho*-, *meta*- and *para*-substituted benzamides **54b**-**54d** successfully delivered the corresponding products under the electrochemical reaction conditions. Notably, the positional selectivity for *meta*-substituted arenes **54c** and **54k** was dominated by steric interactions. The robust cupraelectro-catalysis tolerated a wide array of halide functionalized benzamides **54h**-**54g**, which provided access to further late-stage diversifications. Synthetically-useful electrophilic functional groups, including thioether (**54m**) and cyano (**54n**), were introduced in cupraelectro-catalyzed cascade annulation by C–H alkynylation, selectively providing corresponding decorated isoindolinones. The copper-catalysis was not limited to benzamides, differently substituted alkynes **76b** and **76d** were efficiently transformed into desired product. To be noted, terminal alkyne bearing an amino acid functional group **76l** was efficiently converted by the cupraelectro-catalysis.

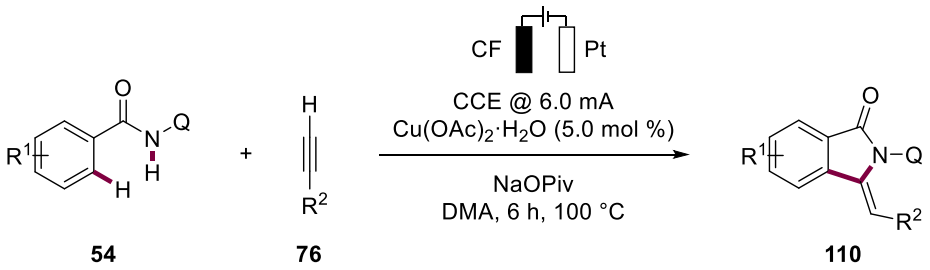

54 **76** **110**

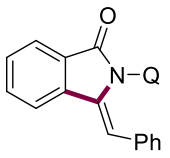

110aa: 90% (*E*/*Z* = 1:13)

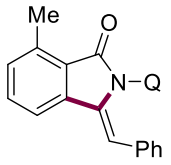

110ba: 83% (*E*/*Z* = 1:10)

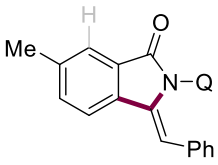

110ca: 87% (*E*/*Z* = 1:13)

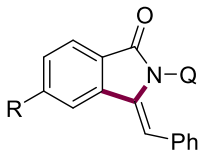

R = Me (**110da**): 72% (*E*/*Z* = 1:12)
R = Ph (**110ea**): 72% (*E*/*Z* = 1:8)

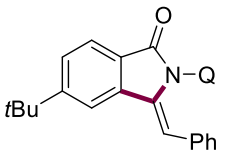

110fa: 56%

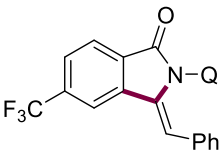

110ga: 77% (*E*/*Z* = 1:12)

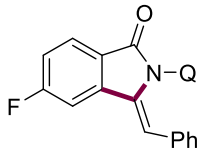

110ha: 77%

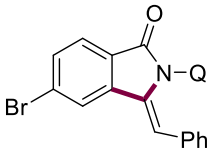

110ia: 76%

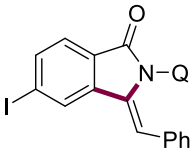

110ja: 59%

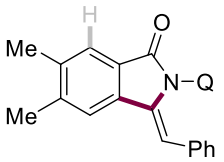

110ka: 52% (*E*/*Z* = 1:10)

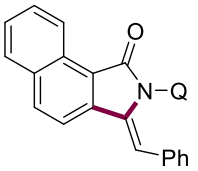

110la: 54% (*E*/*Z* = 1:5)

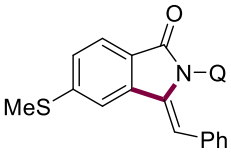

110ma: 82% (*E*/*Z* = 1:2)

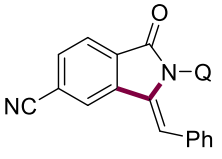

110na: 55%

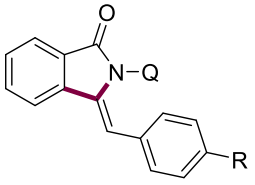

R = Me (**110ab**): 77% (*E*/*Z* = 1:6)
R = CF_3 (**110ad**): 60% (*E*/*Z* = 1:20)

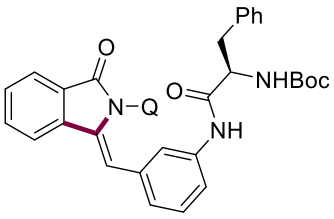

110al: 70% (*E*/*Z* = 1:6)[a]

Scheme 3.11. Cupraelectro-catalyzed C–H alkynylation for isoindolones **110**. [a] $Cu(OAc)_2·H_2O$ (10 mol %).

The green and user-friendly nature of the cupraelectro-catalysis for C–H activations was further illustrated by the gram-scale synthesis of isoindolone **110aa** (Scheme 3.12). Slight modifications of the electrochemical setup were necessary for the gram-scale synthesis. With appropriate scale-up on electrochemical cell volume for proper substrate concentration, stirring device for sufficient mass transfer and electrode size for larger current density, the copper-catalyzed electrochemical isoindolones synthesis was efficiently proceeded with high catalytic performance on a scale-up experiment using 50 mA within 11.5 h, yielding 1.14 g of the desired product **110aa**.

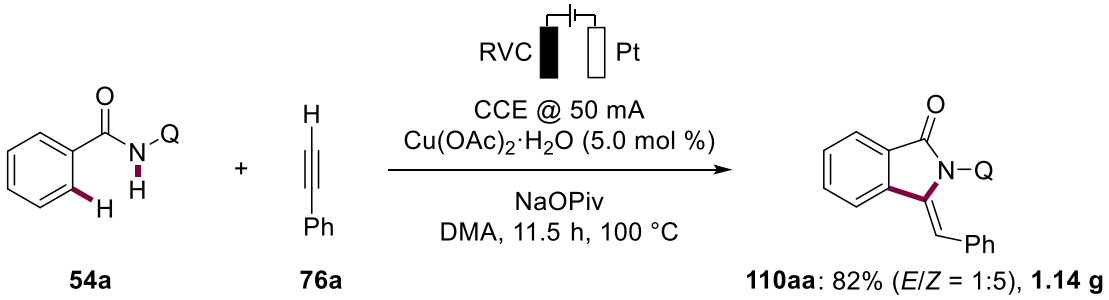

54a **76a** **110aa**: 82% (*E*/*Z* = 1:5), **1.14 g**

Scheme 3.12. Gram-scale cupraelectro-catalyzed isoindolone synthesis.

The robustness of cupraelectro-catalyzed C–H alkynylation regime was not limited to terminal alkynes **76**. Indeed, by applying easily accessible carboxylic acids **112**, an alternative approach to isoindolones synthesis was realized under otherwise identical electrochemical conditions (Scheme 3.13). Substituted alkynyl carboxylic acids **112b**-**112d** with electron-donating groups as well as electron-withdrawing groups were effectively converted to the desired five-membered isoindolones by decarboxylative C–H/C–C scission.

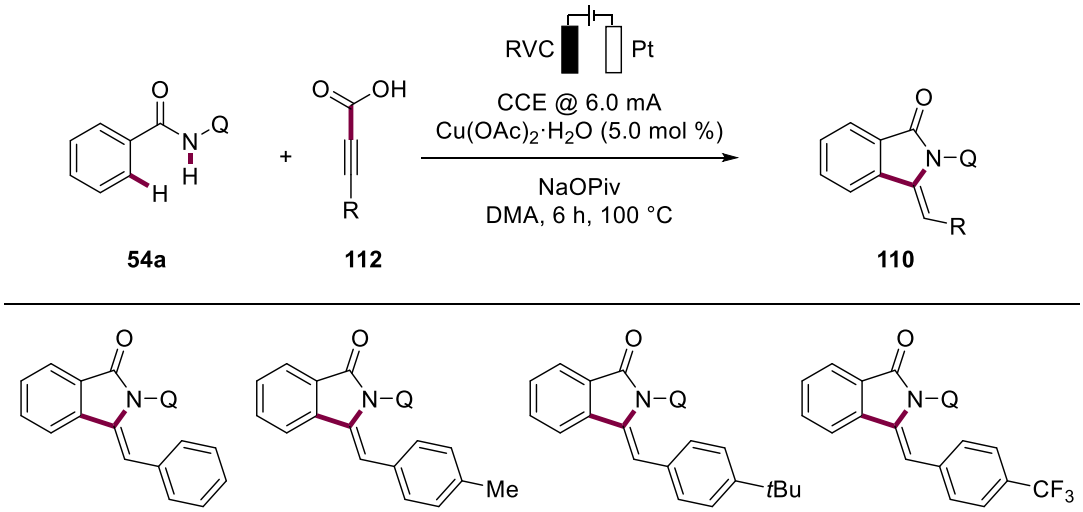

110aa: 61% (*E*/*Z* = 1:10) **110ab**: 51% (*E*/*Z* = 1:7) **110ac**: 52% (*E*/*Z* = 1:20) **110ad**: 56% (*E*/*Z* = 1:2)

Scheme 3.13. Decarboxylative cupraelectro-catalyzed C–H/C–C scission.

3.2.3. Mechanistic Studies

3.2.3.1. Competition Experiments

Intrigued by the unique catalytic performance of the electrochemical copper-catalyzed cascade annulation by C–H alkynylation, we became interested in understanding the catalyst's mode of action. To this end, a set of mechanistic studies was initiated with intermolecular competition experiments (Scheme 3.14). Benzamides with electron-rich and electron-deficient para-substitution were conducted under the optimized electrochemical reaction conditions. As a result, electron-deficient substrate **54g** revealed to be inherently superior. Likewise, competition experiment between electron-donating and electron-withdrawing terminal alkynes was converted under the same condition. A similar result of electron-withdrawing alkyne **76d** provided better reactivity. In both cases, substrates with electron-deficient groups proved to be inherently favorable, which clearly highlights the complementary nature of our approach comparing to the former copper-catalyzed electrochemical C–H amination[111-112] with electron-rich anilides by a single electron transform (SET) pathway.

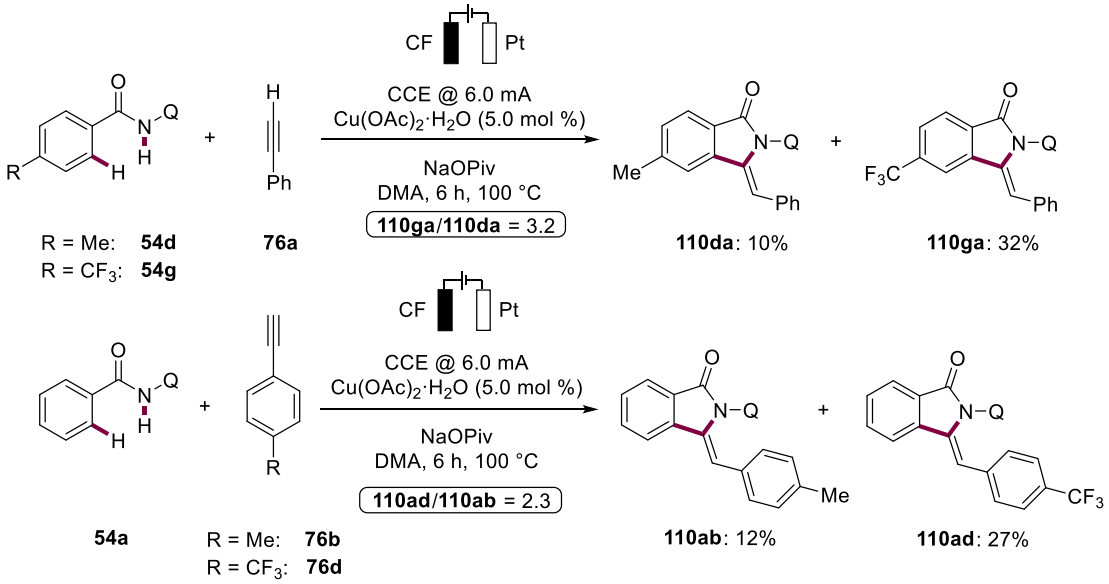

Scheme 3.14. Intermolecular competition experiments.

3.2.3.2. H/D Exchange Experiments

Thereafter, H/D exchange reactions in the presence of isotopically labelled compounds were further tested (Scheme 3.15). By applying isotopically labelled CD_3OD as co-solvent under otherwise identical optimized electrochemical condition, the cupraelectro-catalysis delivered the corresponding isotopically labelled annulated isoindolone product. No H/D exchange was found in either the reisolated benzamide **54a** or product **110aa**, which suggested the C–H cleavage step is irreversible.

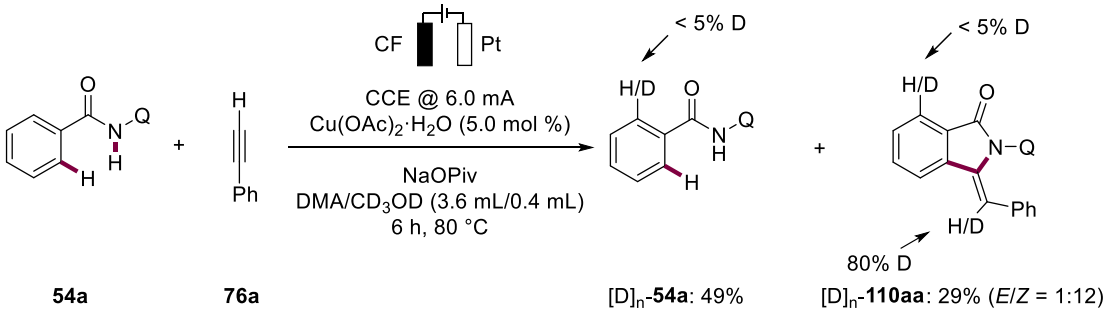

Scheme 3.15. H/D exchange experiment.

3.2.3.3. Kinetic Isotope Effect Studies

Furthermore, KIE studies were conducted with two parallel experiments using *in-operando* React-IR (Scheme 3.16). Initial rates of both [D_5]-**54a** and **54a** substrates were analyzed using the data obtained within 2 h of reactions. A KIE value of k_H/k_D = 1.2 was obtained, providing support for a facile C–H scission.

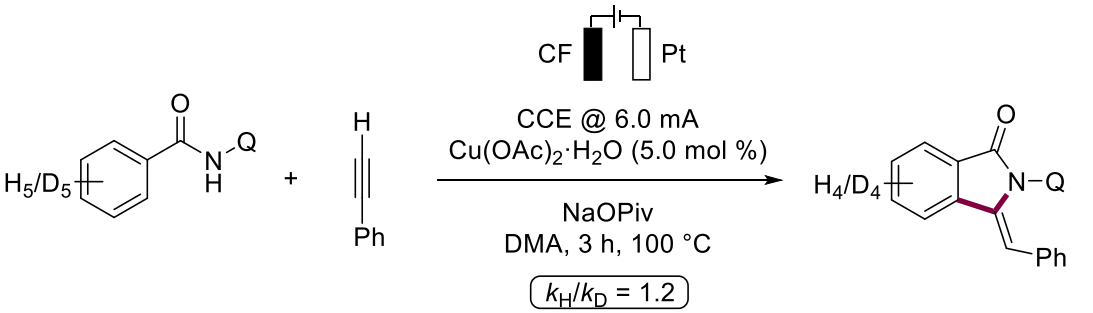

54a or $[D]_5$-**54a** **76a** **110aa** or $[D]_4$-**110aa**

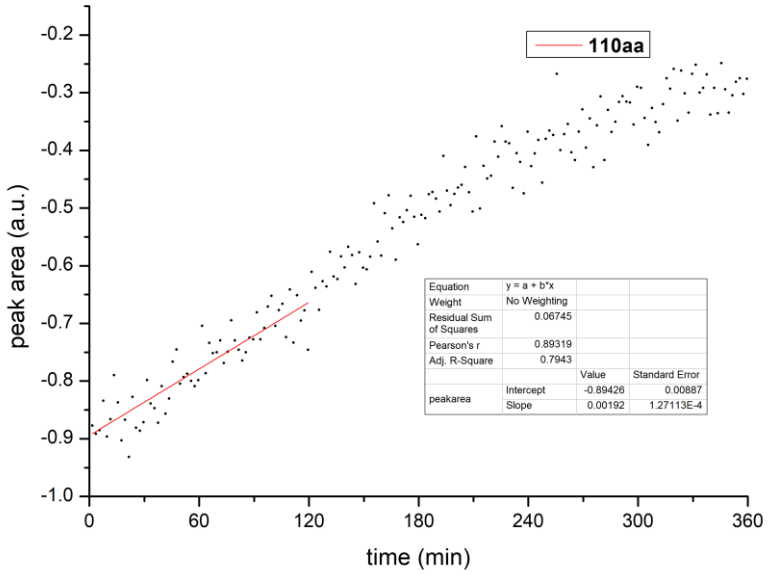

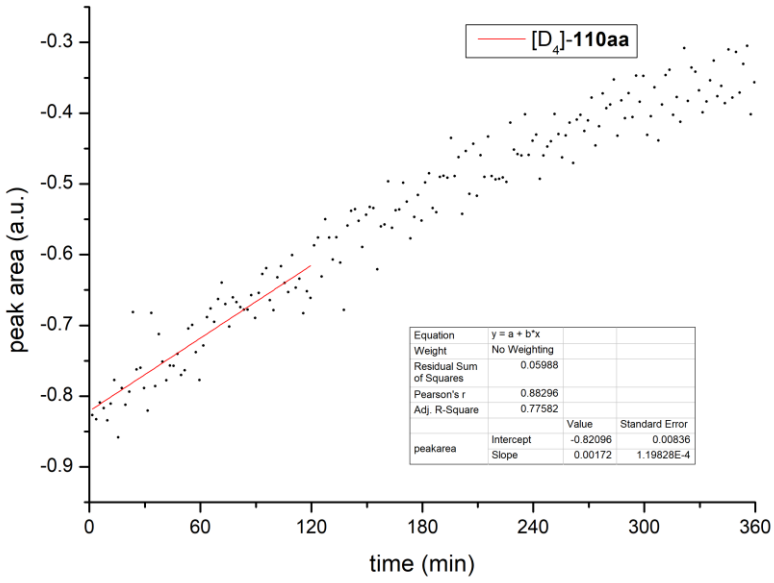

Scheme 3.16. Kinetic isotope effect experiments by *in-operando* React-IR.

3.2.3.4. Kinetic Profile

With the assistance of *in-operando* React-IR analysis, we were able to track the electrochemical copper C–H alkynylation reaction profiles by *in situ* IR study (Figure 3.2). A kinetic profile over the entire reaction time can be plotted with the IR data generated by React-IR, using surface plot at 1109 cm^{-1} and 1327 cm^{-1} as product **110aa** generation and benzamide **54a** consumption respectively.

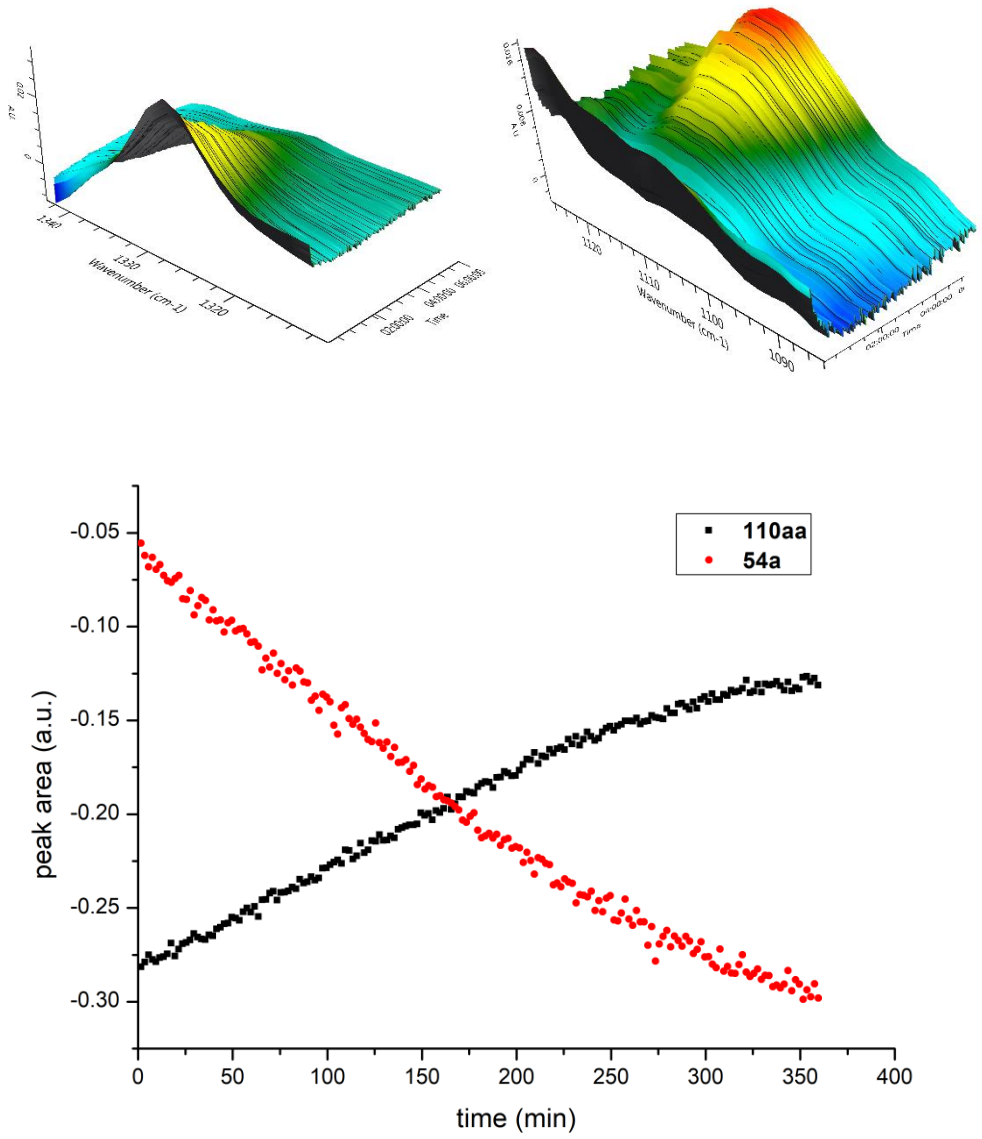

Figure 3.2. Kinetic profile by in-operando React-IR at 1109 cm^{-1} and 1327 cm^{-1}.

3.2.3.5. Attempted Cyclization

To gain further mechanistic insights in the alkynylation manifold of the cupraelectro-catalyzed cascade C–H annulation, we conducted cyclization reactions with an independently prepared *ortho*-alkynylated substrate **54o** (Scheme 3.17). Unlike the cobaltaelectro-catalyzed C–H/N–H annulation presented above, which formed no product with similar studies, *ortho*-alkynylated substrate **54o** successfully delivered the desired isoindolone product with or without electricity. Therefore, a cascade annulation manifold initiated by C–H alkynylation is suggested instead of the organometallic alkyne annulation process in the cobalt catalyzed base-mediated cascade electrochemical C–H annulation.[93]

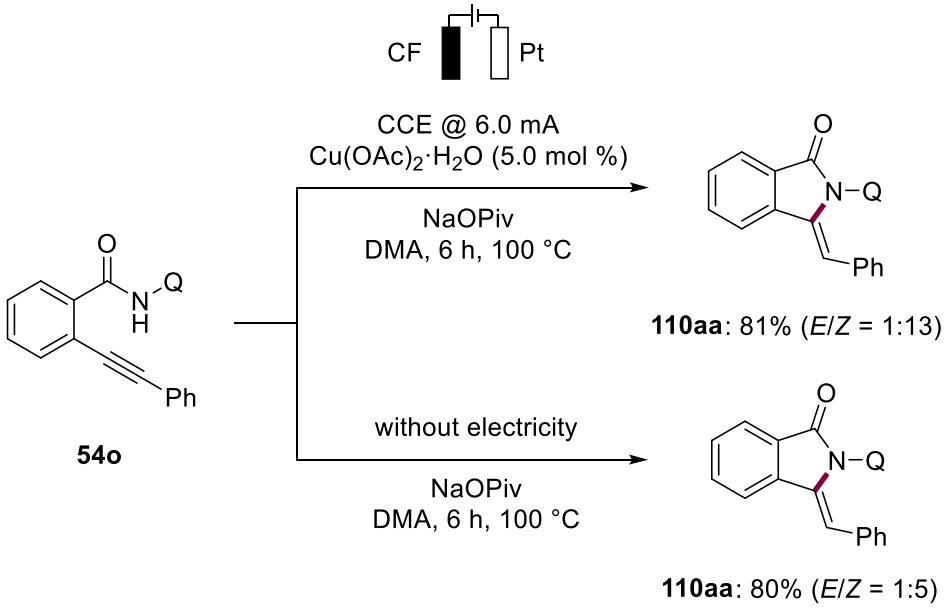

Scheme 3.17. Cyclization experiments.

3.2.3.6. Headspace GC Analysis

Moreover, headspace GC analysis was applied to detect the byproduct generation of molecular hydrogen by cathodic proton reduction (Scheme 3.18). The reaction vapor

phase was collected and submitted to headspace GC, H_2 production was hence confirmed at 1.59 min in the chromatogram.

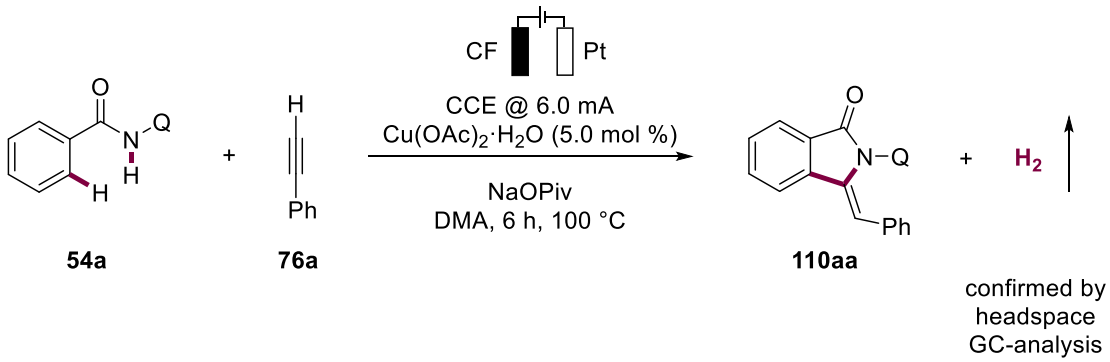

Scheme 3.18. Headspace GC analysis for cupraelectro-catalysis.

3.2.3.7. Cyclic Voltammetry Studies

Finally, we probed the cupraelectro-catalyzed C–H alkynylation with detailed cyclic voltammetry studies by *A. Scheremetjew*. With the addition of benzamide **54a**, the copper(II) catalyst exhibited a clear oxidative potential at 0.95 V *versus* SCE, while the copper(II) catalyst alone revealed no significant oxidation potential. These findings give support to the formation of a copper(II) complex **113** in the catalytic cycle, which further undergoes anodic oxidation to the copper(III) intermediate **114**. For the reoxidation process of copper catalyst species, the cyclic voltammetry study of copper(I) acetate provided support for a facile generation of the initial copper(II) catalyst **118** with a low oxidation potential of 0.05 V *versus* SCE.

3.2.4. Proposed Mechanism

Based on these mechanistic studies, a plausible catalytic cycle is proposed to commence with the formation of copper(II) complex **113** by substrate coordination of benzamide **52** (scheme 3.19). Thus, under electrochemical conditions, subsequent anodic oxidation gives raise to copper(III) species **114**. Thereafter, facile carboxylate

assisted C–H activation provides the intermediate **115**, which undergoes the ligand exchange with terminal alkyne to generate the copper(III) intermediate **116**. Then, reductive elimination delivers the alkynylated product **54o**, and forms the copper(I) species **117**. The alkynylated product **54o** further cyclizes the desired isoindolone **108** with the presence of NaOPiv. The putative copper(I) species **117** is oxidized at the anode and regenerates the initial copper(II) catalyst **118**.

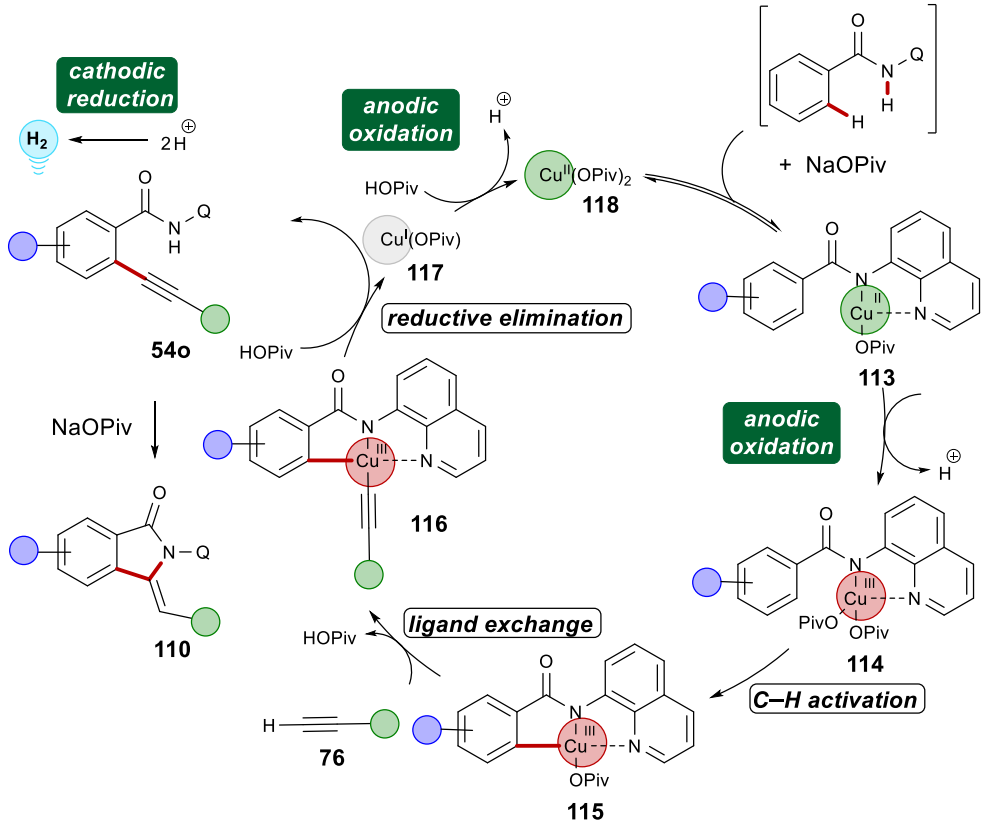

Scheme 3.19. Pausible catalytic cycle.

3.3 Cobaltaelectro-Catalyzed C–H Acyloxylation with Carboxylic Acids

The sustainability of oxidative C–H activation approach has been largely advanced by metallaelectro-catalyzed C–H activation, which replaced chemical oxidants by renewable green electricity. In this context, merging bio-mass derived solvents[124] with

electrochemical C–H transformations[91, 98] brings the environmentally friendly nature of C–H activation to the next level. Despite significant progress discussed above on 3d transition metallaelectro-catalysis, electrochemical formation of C–O bond by 3d transition metal catalyzed C–H activations remains scarce. Except one report of cobaltaelectro-catalyzed oxygenation developed by *Ackermann*[90] and palladium-catalyzed electrochemical acyloxylation reported by *Mei*.[125] Herein, we explored the cobaltaelectro-catalyzed C–H acyloxylation with free carboxylic acids using biomass derived renewable *γ*-valerolactone (GVL)[124, 126] as green solvent.

3.3.1. Optimization Studies

The exploration of cobaltaelectro-catalyzed C–H acyloxylation were initiated by probing various reaction conditions, using user-friendly undivided cell setup with a galvanostatic regime at 5.0 mA (Table 3.3). Our preliminary result of acyloxylated product formation was achieved with DCE as the solvent at 60 °C under electrochemical conditions (entry 1). Thus, we tested a set of commonly used additives for cobalt catalysis. Among others, Na_2CO_3 proved to be the optimal additive for electrochemical C–H acyloxylation (entries 2-4). Reducing the loading of the cobalt catalyst from 20 mol % to 10 mol % led to lower desired product yield (entry 5). Different representative organic solvents were probed in cobaltaelectro-catalysis (entries 8-16). To our delight, in the presence of biomass derived GVL, the cobalt catalyst provided the best catalytic performance in electrochemical oxidative C–H acyloxylation. Solvent mixtures with GVL as the co-solvent were further probed in cobaltaelectro-catalysis but failed to produce higher yields (entries 17-19). Higher or lower reaction temperatures did not improve the catalyst performance (entries 20-22). Other cobalt sources were tested under electrochemical conditions, but $CoCl_2$, $CoSO_4{\cdot}7H_2O$, $Co(acac)_2$ and $Co(acac)_3$ were found to be inefficient (entries 6-7 and entries 23-24). Control experiments provided strong support for the essential roles of electricity and cobalt catalyst (entries 25-26).

Table 3.3. Optimization of cobaltaelectro-catalyzed C–H acyloxylation.[a]

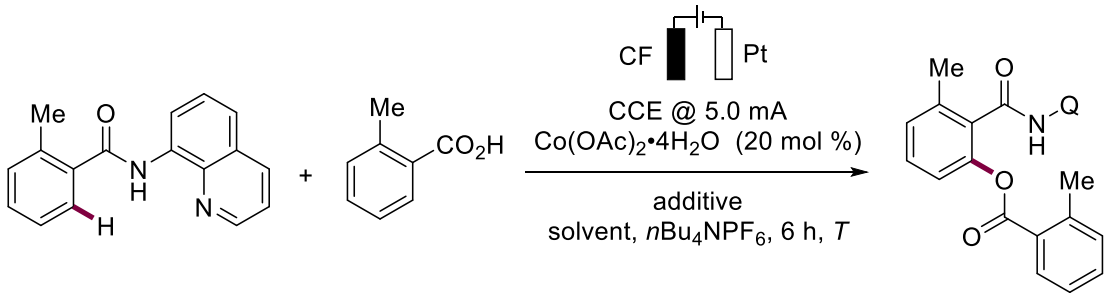

54b **66a** **67ba**

Entry	Solvent	Additive	T [ºC]	Yield [%]
1	DCE	Na_2CO_3	60	25
2	DCE	$NaHCO_3$	80	27
3	DCE	NaOAc	80	22
4	DCE	Na_2CO_3	80	51
5	DCE	Na_2CO_3	80	37[b]
6	DCE	Na_2CO_3	80	29[c]
7	DCE	Na_2CO_3	80	45[d]
8	DMF	Na_2CO_3	80	13
9	*t*AmOH	Na_2CO_3	80	-
10	1,4-dioxane	Na_2CO_3	80	38
11	*i*PrOH	Na_2CO_3	80	-
12	NMP	Na_2CO_3	80	40
13	MeCN	Na_2CO_3	80	29
14	H_2O	Na_2CO_3	80	-
15	DCE/MeCN (1:1)	Na_2CO_3	80	22
16	**GVL**	**Na_2CO_3**	**80**	**66 (22)**
17	GVL/H_2O (1:1)	Na_2CO_3	80	-
18	GVL/DCE (1:1)	Na_2CO_3	80	55
19	GVL/MeCN (1:1)	Na_2CO_3	80	31
20	GVL	Na_2CO_3	40	20
21	GVL	Na_2CO_3	60	55
22	GVL	Na_2CO_3	100	50
23	GVL	Na_2CO_3	80	41[e]
24	GVL	Na_2CO_3	80	44[f]
25	GVL	Na_2CO_3	80	-[g]
26	GVL	Na_2CO_3	80	-[h]

[a] Reaction conditions: Undivided cell, **54b** (0.25 mmol), **66a** (0.50 mmol), [Co] (20 mol %),

additive (2.0 equiv), nBu$_4$NPF$_6$ (0.25 mmol), solvent (3.0 mL), constant current at 5.0 mA, 6 h, CF anode, Pt-plate cathode, under air, in parenthesis reisolated **54b**. [b] [Co] 10 mol %. [c] Co(acac)$_2$ as catalyst. [d] $CoCl_2$ as catalyst. [e] Co(acac)$_3$ as catalyst. [f] $CoSO_4 \cdot 7H_2O$ as catalyst. [g] In the absence of a cobalt source. [h] No electricity.

3.3.2. Scope of Cobaltaelectro-Catalyzed C–H Acyloxylation

With the optimized conditions in hand, we tested the versatility of cobaltaelectro-catalyzed C–H acyloxylation with a set of substituted benzamides **54** (Scheme 3.20), experiments of substrate **54p** and **54s** were conducted by *U. Dhawa*. Various *ortho*-, *meta*- and *para*-substituted benzamides **54p**-**54s** were probed and selectively delivered the corresponding ester products **67** under electrochemical oxidative conditions. The sterically congestion on arene, such as in substrates **54p** and **54l**, did not affect the catalytic performance of cobalt. These benzamides **54** converted the desired products in moderate to good yields.

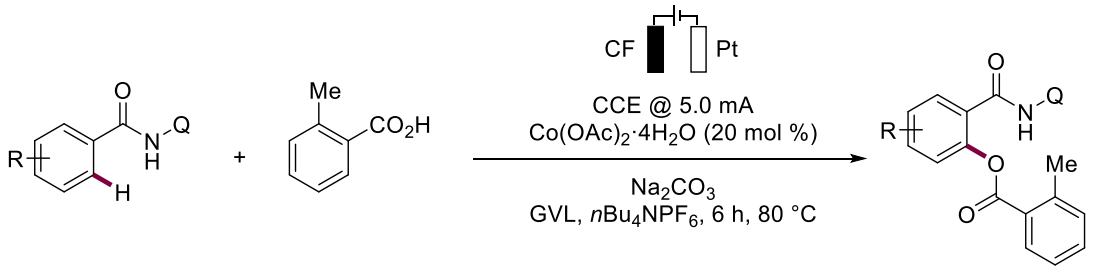

54 **66a** **67**

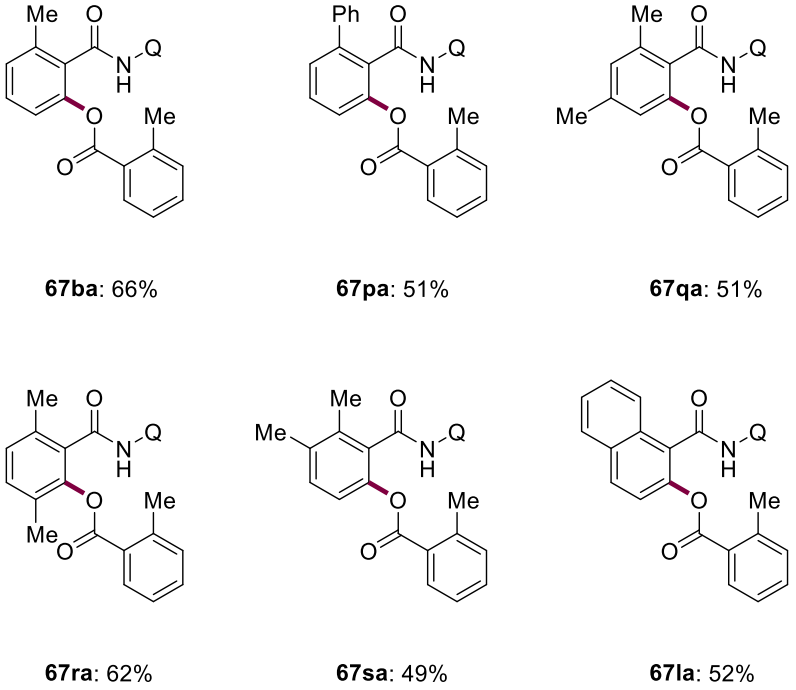

67ba: 66% **67pa**: 51% **67qa**: 51%

67ra: 62% **67sa**: 49% **67la**: 52%

Scheme 3.20. Cobaltaelectro-catalyzed C–H acyloxylation of benzamides **54**.

The robustness of the cobaltaelectro-catalyzed C–H acyloxylation was not limited to benzamides **54**, different decorated carboxylic acids **66** were appliable in this manifold (Scheme 3.21). Substituted carboxylic acids **66b**-**66e** bearing *para*-, *meta*- and *ortho*-substitution were well-tolerated in cobaltaelectro-catalysis with high level of chemo-selectivity. Benzoic acids **66g** bearing halide functional group was able to convert into the desired aromatic ester. Disubstituted benzyl acids **66g**-**66i** proved amenable to cobaltaelectro-catalyzed acyloxylation regime, affording the corresponding ester in modest yield. To be noted, aliphatic carboxylic acid **66j** successfully delivered the desired product, albeit in a slightly reduced fashion.

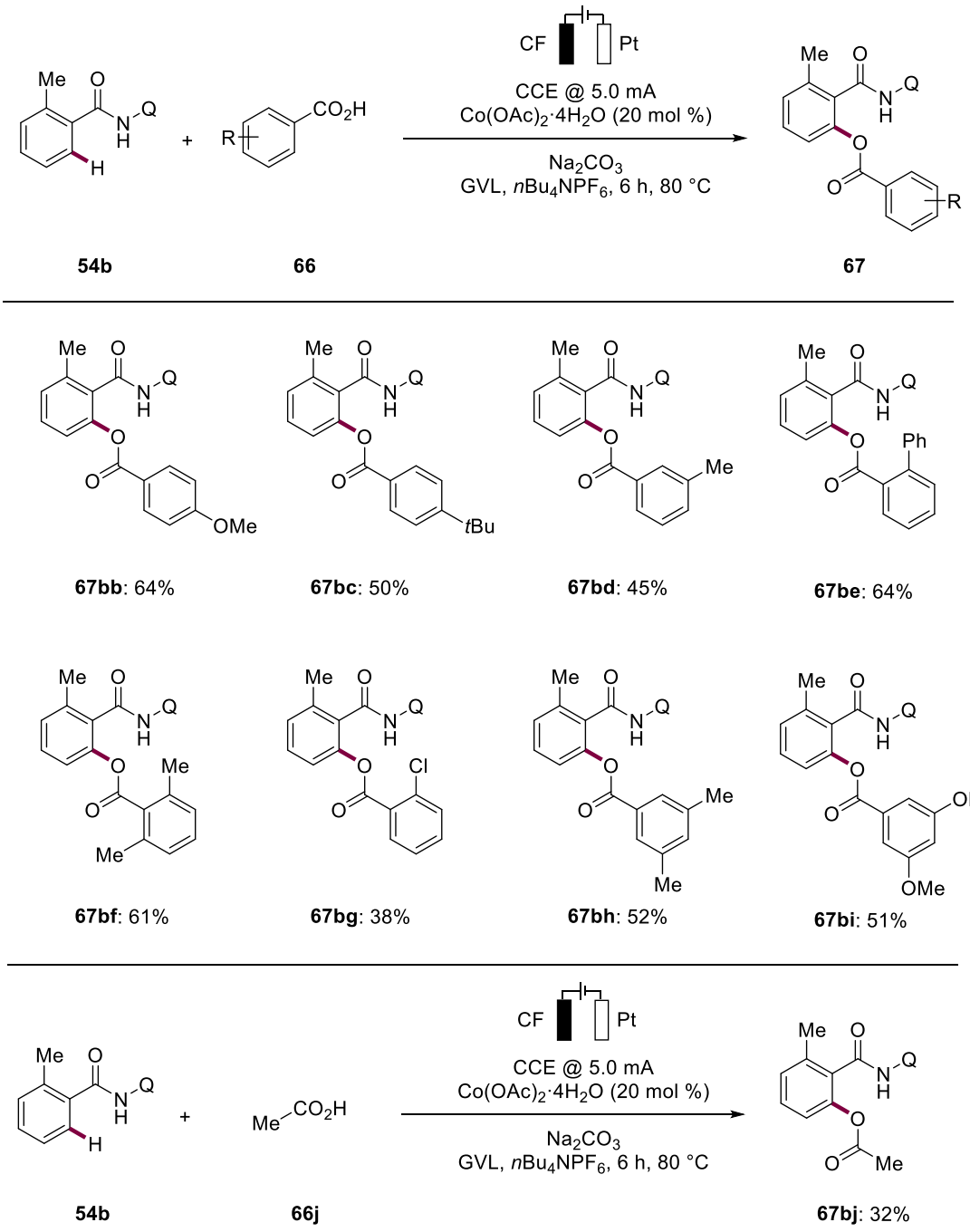

Scheme 3.21. Cobaltaelectro-catalyzed C–H acyloxylation of carboxylic acids **66**.

3.3.3. Mechanistic Studies

3.3.3.1. Competition Experiment

Intrigued by the unique catalytic performance of electrochemical cobalt acyloxylation, we became interested in exploring the catalyst's mode of action. To this end, we started

the mechanistic studies with intermolecular competition experiment (Scheme 3.22). Competition reaction between electron-rich and electron-deficient carboxylic acids **66d** and **66k** under optimal electrochemical conditions was conducted with benzamide **54b**. Both acyloxylated products were obtained, while electron-donating ester **67bd** proved to be inherently more reactive. This result supported a BIES mechanism for the key C–H scission, which is in good agreement with our previous results on cobaltaelectrocatalysis.[93]

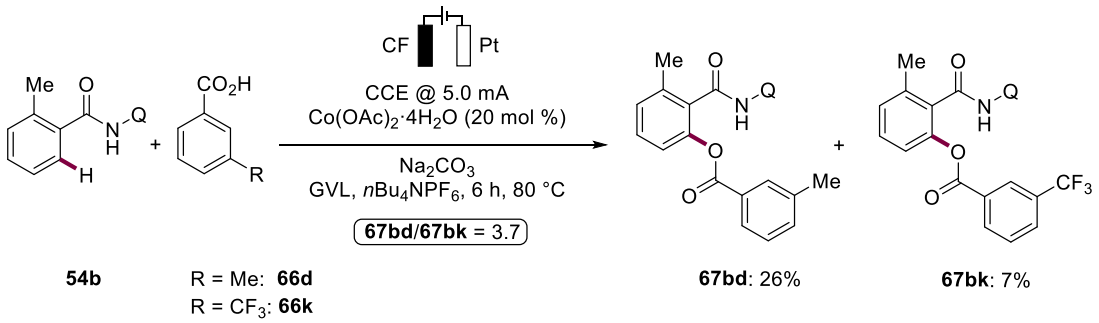

Scheme 3.22. Intermolecular competition experiment.

3.3.3.2. H/D Exchange Experiment

Moreover, H/D exchange reaction using isotopically labelled compound in electrochemical condition was further tested (Scheme 3.23). In the presence of isotopically labelled CD_3OD as the co-solvent, benzamide **54b** can be successfully converted to corresponding ester. However, we were unable to observe any significant H/D exchange in both the reisolated benzamide substrate and the desired aromatic ester product. This observation suggests that the C–H cleavage is not reversible.

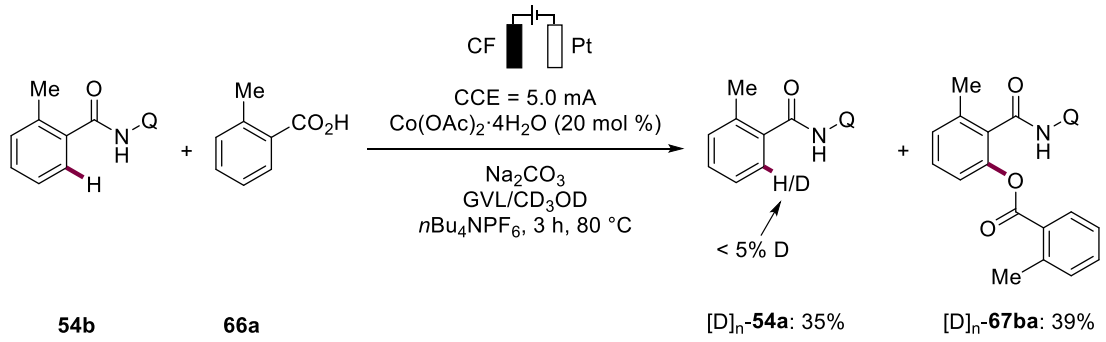

Scheme 3.23. H/D exchange experiment.

3.3.3.3. Headspace GC Analysis

Thereafter, to confirm the H_2 byproduct formation during the cathodic reduction process, we applied headspace GC analysis in cobaltaelectro-catalyzed C–H acyloxylation (Scheme 3.24). The gas phase was collected and submitted to headspace GC analysis. Thus, H_2 formation can be detected at 1.59 min in GC-chromatogram.[91, 121]

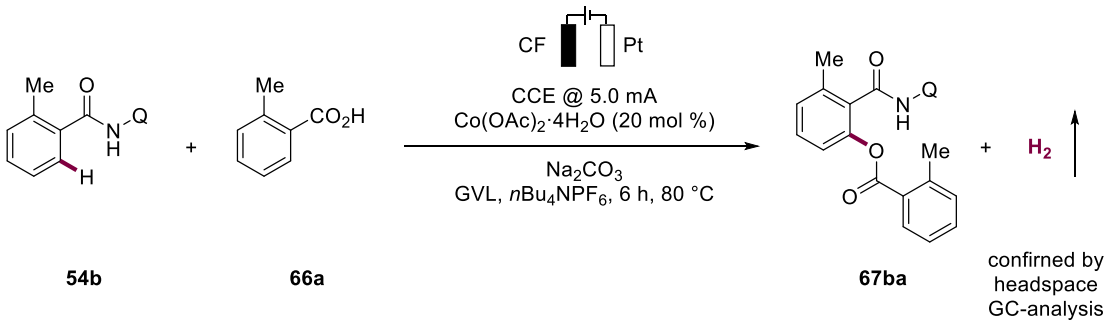

Scheme 3.24. Headspace GC analysis for cobaltaelectro-catalyzed acyloxylation.

3.3.3.4. Cyclic Voltammetry Studies

To illustrate the key oxidation and reduction events of cobaltaelectro-catalyzed C–H acyloxylation, *J. Struwe* preformed detailed cyclic voltammetry studies (Figure 3.4). An irreversible oxidation of benzamide **54b** was revealed at 1.46 V versus $Fc^{+/0}$, while carboxylic acid **66a** showed no relevant oxidation in MeOH. Meanwhile, cobalt(II)

catalyst featured a lower oxidative potential at 1.13 V versus $Fc^{+/0}$ without addition of any other substrates, which is in good agreement with our pervious findings on cobaltaelectro-catalysis.[93] The mixture of substrate **54b** and cobalt(II) acetate catalyst did not give rise to any significant oxidation potential, which indicates the formation of cobalt(III) intermediate **119** by anodic oxidation.

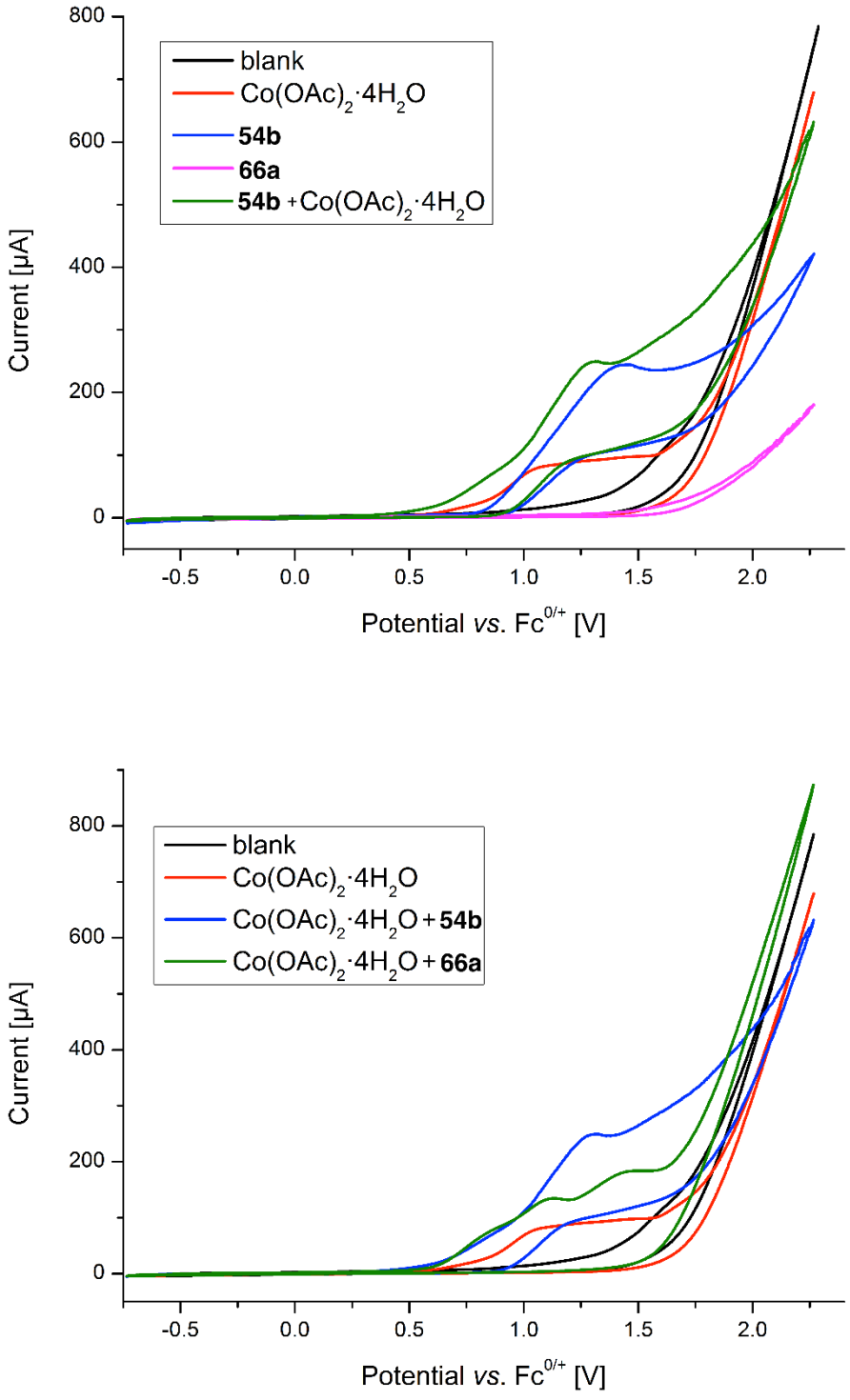

Figure 3.4. Cyclic voltammograms at 100 mV/s preformed by *J. Struwe*: General condition: MeOH, 0.1 M nBu$_4$NPF$_6$, 5 mM substrates.

3.3.4. Proposed Mechanism

Based on our mechanistic findings, a plausible catalytic cycle for electrochemical cobalt catalyzed C–H acyloxylation is proposed (scheme 3.25). To initiate the cycle, an anodic oxidation of cobalt(II) acetate is suggested, forming the catalytically active cobalt(III) species **119**. Thus, carboxylate-assisted C–H activation provides the cyclometalated intermediate **120**, further salt metathesis with carboxylic acid **66** delivers cobalt(III) complex **121**. Thereafter, reductive elimination provides ester product **67** and cobalt(I) complex **122**. Finally, the catalytically active cobalt(III) species **119** is regenerated at anode.

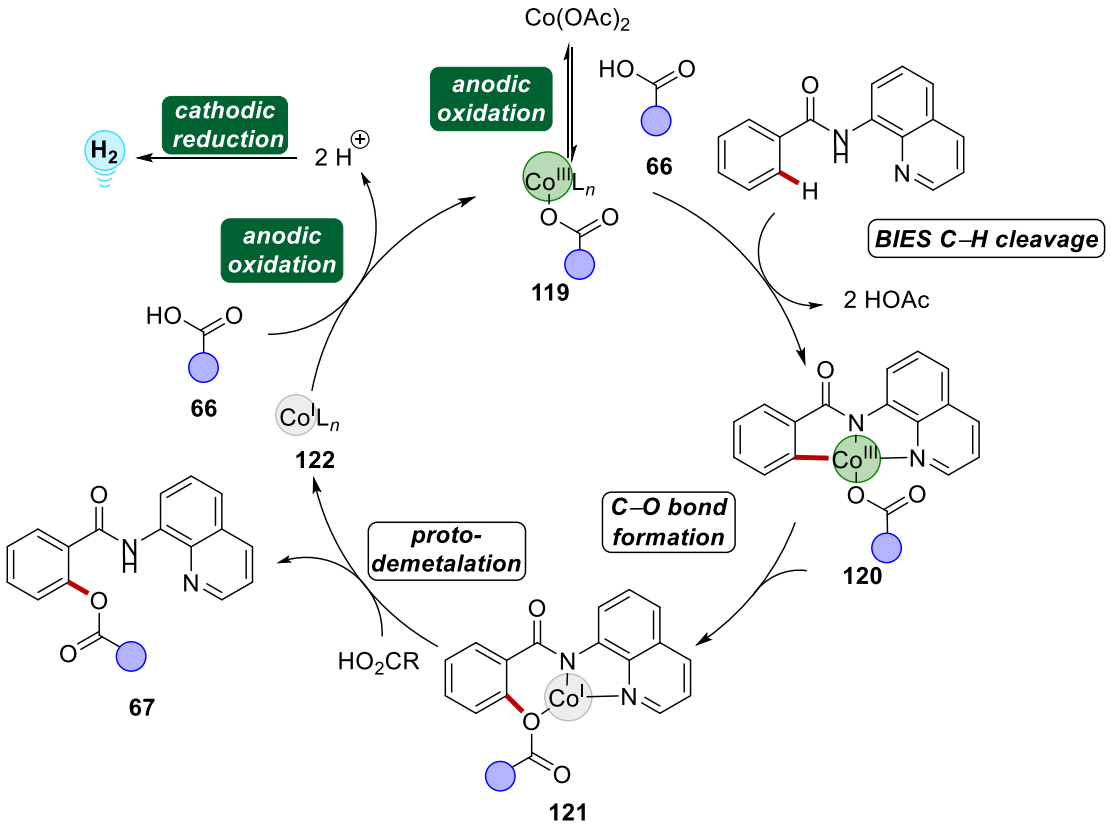

Scheme 3.25. Pausible catalytic cycle.

3.4 Cobaltaelectro-Catalyzed C–H Allylation with Non-activated Alkene

The merger of electrochemistry with oxidative C–H activation has become an increasingly powerful platform for molecular syntheses, with transformative potential applications towards late-stage diversification,[127] material sciences[19] and pharmaceutical industries.[20] One of the appealing advantages of C–H activation is the ability to attain full positional- and chemo-selectivity control. Despite the indisputable progress on electrochemical C–H transformations in recent years,[21, 38c, 39a] chemo-selective alkene allylation via metallaelectro-catalysis was as of yet unprecedented. Herein, we disclosed the first cobaltaelectro-catayzed C–H allylation with non-activated alkenes using biomass derived GVL as solvent.

3.4.1. Optimization Studies

Our studies were initiated by probing different conditions for the envisioned cobaltaelectro-catalyzed C–H allylation with inactivated alkene **54b** (Table 3.4). After considerable preliminary experimentations, we were delighted to observe that the allylated product **70ba** was formed by cobaltaelectro-cataylsis at 4.0 mA in GVL, with NaOPiv as the additive at 100 °C (entry 1). A larger access of nBu$_4$NPF$_6$ electrolyte did not affect the electrolysis process (entries 2-3). Lowering the additive amount from 2 equivalent to 1 equivalent decreased the yield of desired product (entry 4). While applying higher current in cobaltaelectro-catalyzed allylation failed to achieve a higher yield (entries 5-6).

Table 3.4. Optimization of cobaltaelectro-catalyzed C–H allylation.[a]

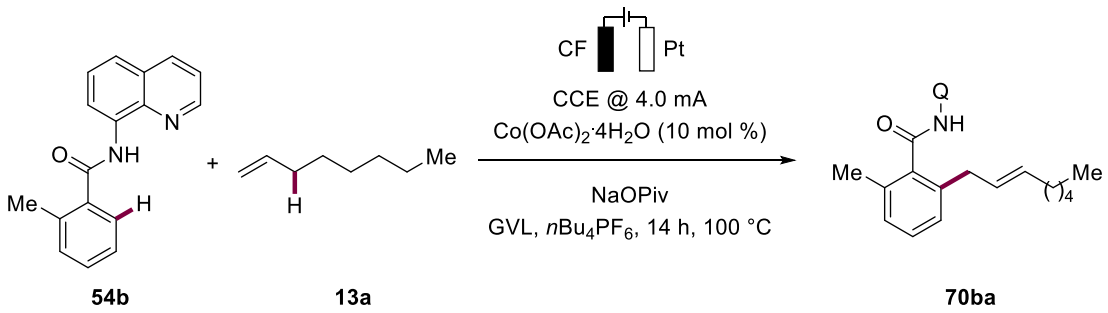

54b **13a** **70ba**

Entry	Deviation from standard condition	Yield [%]
1	**none**	**58**
2	0.50 mmol of nBu$_4$NPF$_6$	55
3	1.0 mmol of nBu$_4$NPF$_6$	56
4	1.0 equiv of NaOPiv	32
5	8.0 mA, 7 h	42
6	6.0 mA, 9 h	48

[a] Reaction conditions: Undivided cell, **54b** (0.50 mmol), **13a** (1.5 mmol), Co(OAc)$_2$·4H$_2$O (10 mol %), NaOPiv (2.0 equiv), nBu$_4$NPF$_6$ (0.25 mmol), GVL (4.0 mL), constant current at 4.0 mA, 14 h, CF anode, Pt-plate cathode, under ambient air.

3.4.2. Scope of Cobaltaelectro-Catalyzed C–H Allylation

With the optimized reaction conditions in hand, we explored the versatility of cobaltaelectro-catalyzed C–H allylation using non-activated *n*-octene **13a** with different substituted benzamides **54** (Scheme 3.20). Diverse *ortho*-substituted benzamides **54q**-**54v** were evaluated and chemo-selectively delivered the corresponding allylated product **70** under electrochemical reaction conditions. Notably, synthetically-useful halide groups in benzamides **54t**-**54v** were well tolerated by the cobaltaelectro-catalyzed C–H allylation, which provided valuable application for further late-stage diversification. Quinoline amide **54w** proved to be unsuitable in electrochemical cobalt allylation.

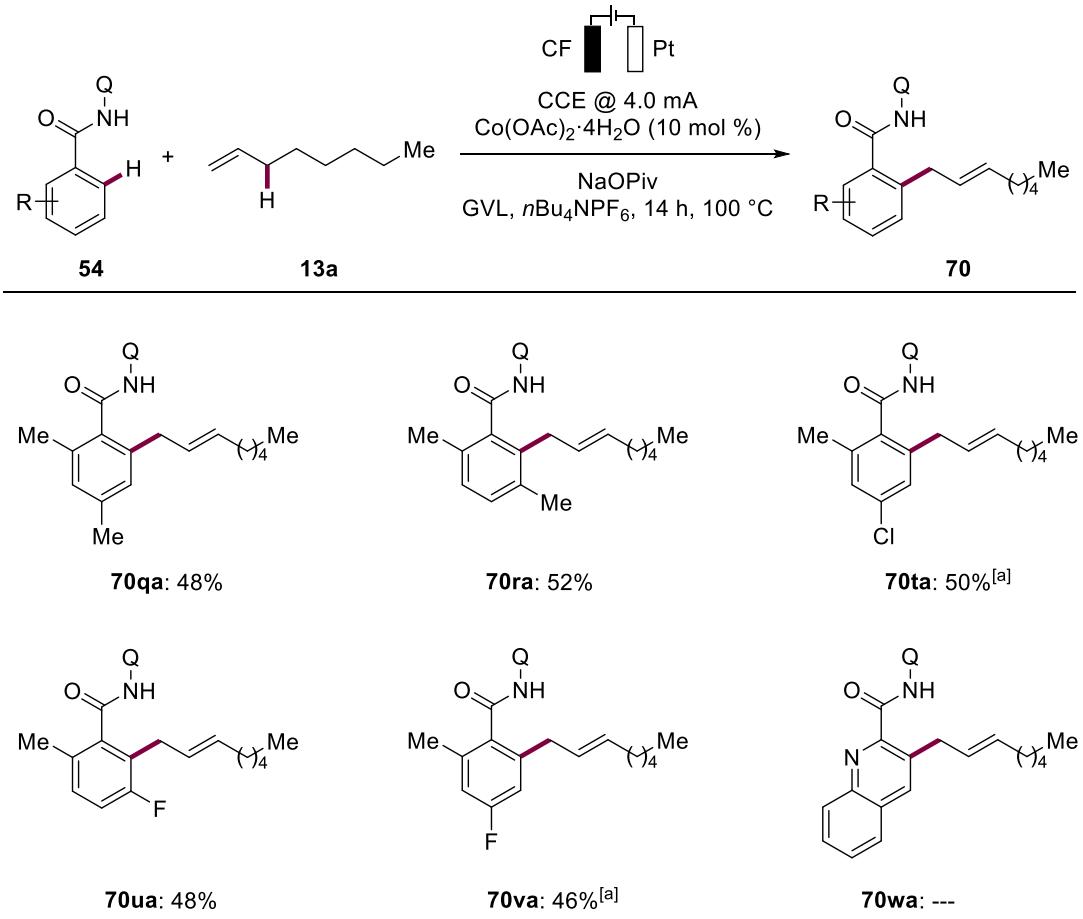

Scheme 3.26. Cobaltaelectro-catalyzed C–H allylation of benzamides **54**. [a] $Co(OAc)_2{\cdot}4H_2O$ (20 mol %).

Likewise, various non-activated alkenes **13** were tested in cobaltaelectro-catalyzed C–H allylation (Scheme 3.27). Aliphatic alkenes **13b**-**13c** proved to be applicable under electrochemical conditions, providing the allylated product with modest yield. Allylbiphenyl **13e** and homoallylbenzene **13d** olefins were well tolerated, chemo-selectively transformed towards desired product. Unfortunately, *para*-functionalized allylbenzene **13f-13g** failed to deliver the corresponding allylated benzamide product **70**.

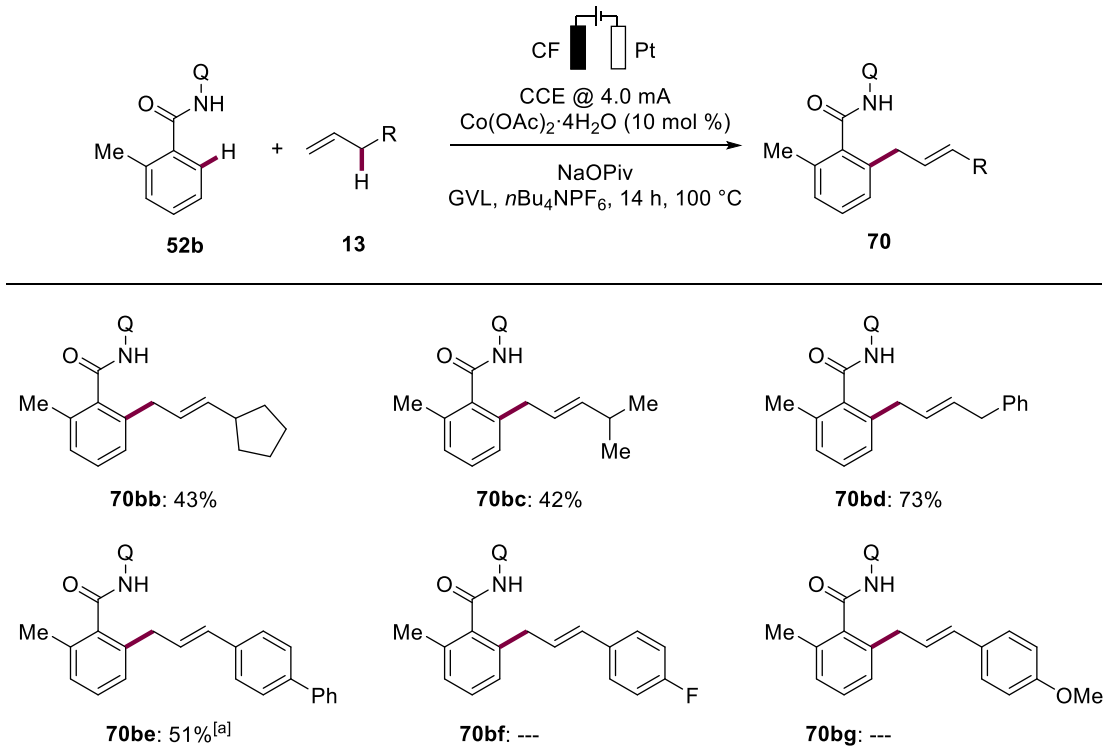

Scheme 3.27. Cobaltaelectro-catalyzed C–H allylation of alkene **13**. [a] $Co(OAc)_2{\cdot}4H_2O$ (20 mol %).

3.4.3. Mechanistic Studies

3.4.3.1. Headspace GC Analysis

Intrigued by the unique catalytic performance of electrochemical cobalt allylation, we became attracted to illuminate the catalyst's mode of action. The mechanistic studies were initiated with headspace GC analysis to confirm the byproduct H_2 formation during the reduction process at the cathode (Scheme 3.28).[119, 121]

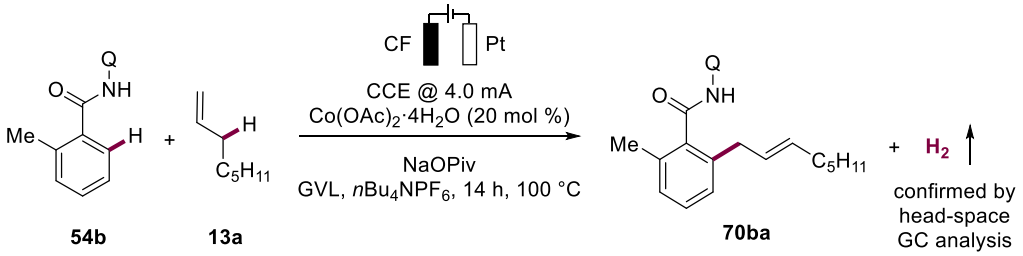

Scheme 3.28. Headspace GC analysis for cobaltaelectro-catalyzed allylation.

3.4.3.2. Cyclic Voltammetry Studies

Thereafter, cyclic voltammetry studies were preformed to gain mechanistic insights of oxidation and reduction events during cobaltaelectro-catalyzed C–H allylation (figure 3.5). The oxidation potential of benzamide **54b** was found at 1.46 V *versus* SCE, while the olefin **13a** revealed no relevant oxidation. After addition of substrate **54b** to the cobalt(II) catalyst, a significant oxidation potential was showed at 1.13 V *versus* SCE, which is lower than the oxidation potential of the benzamide **54b** itself. These findings support an anodic single-electron oxidation happening to the cobalt(II) complex **123**, and forming catalytic active cobalt(III) species **124**, which is in good agreement with our previous reports on CV studies on cobaltaelectro-cataylsis.[93, 119]

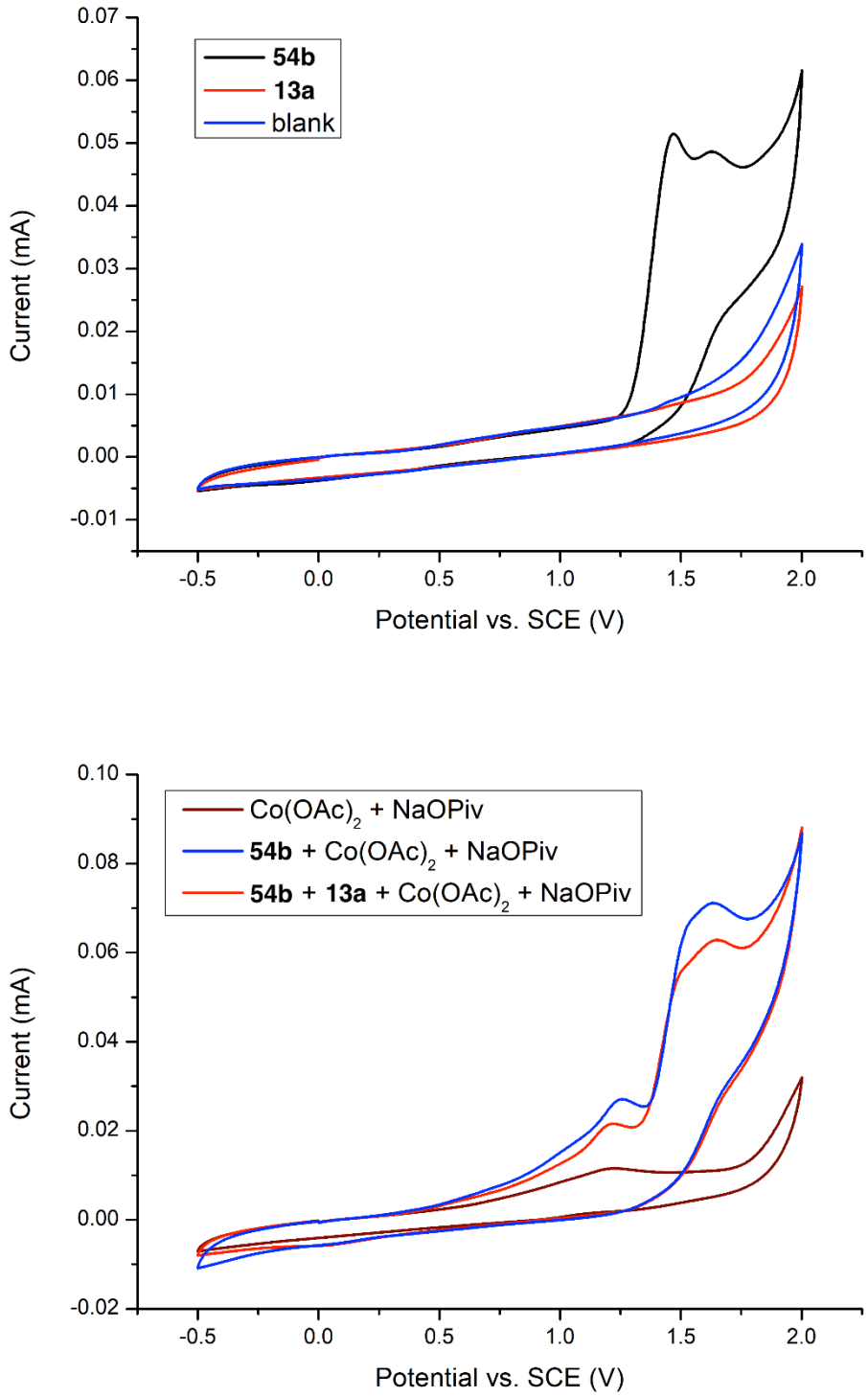

Figure 3.5. Cyclic voltammograms at 100 mV/s: General condition: MeCN, 0.1 M nBu$_4$NPF$_6$, 5 mM substrates.

3.4.4. Proposed Mechanism

Based on our mechanistic findings, a plausible catalytic cycle for cobaltaelectro-catalyzed C–H allylation is proposed herein (sheme 3.26). After adding the benzamide substrate **54**, a cobalt(II) intermediate **123** is formed, which undergoes the single-electron oxidation to generate the cobalt(III) complex **124**. Further carboxylate-assisted C–H cleavage and insertion of olefin **13** provide cobalt(III) species **127**. Reductive elimination releases desired allylated product **70** and cobalt(I) complex **128**. Finally, the catalytically active cobalt(III) species **124** is regenerated by anodic oxidation.

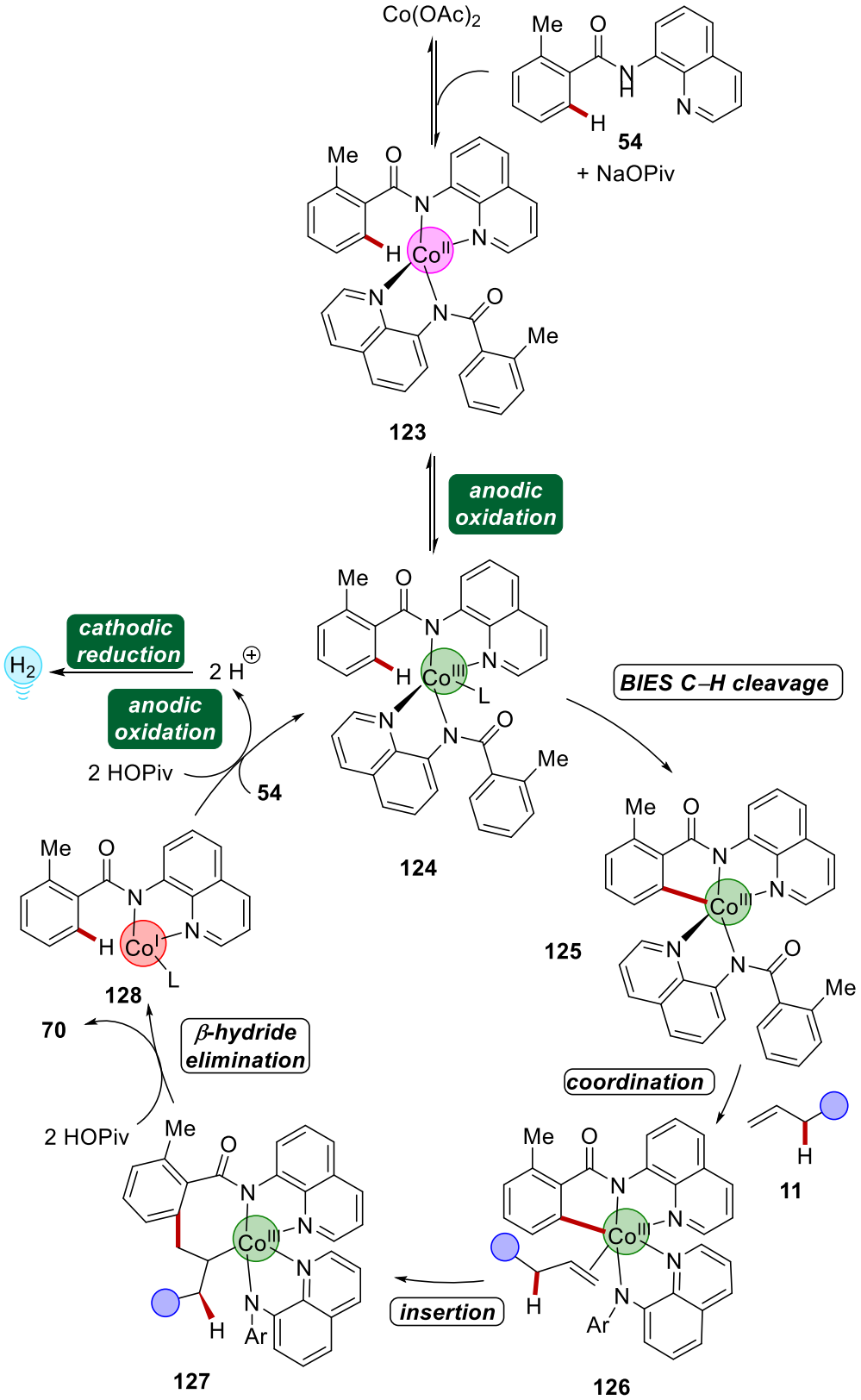

Scheme 3.26. Pausible catalytic cycle.

4. Summary and Outlook

Oxidative C–H activation has been considered as an increasingly powerful platform for organic synthesis, with applications to material sciences, late-stage diversifications and pharmaceutical industries. Merging with metallaelectro-catalysis, the sustainability of oxidative C–H activation has been significantly advanced by replacing the often toxic, stoichiometric amount of traditional chemical oxidant with green, sustainable electricity. In this context, electrochemical C–H activation approaches fulfill the inherent nature of resource economy. Despite major progress on noble transition metals, namely, palladium, iridium, ruthenium, and rhodium in electrochemical C–H activation, our focus has shifted to inexpensive, earth-abundant 3d base metals catalyzed electrochemical oxidative C–H activation. Especially less expensive and less toxic cobalt and copper catalysts further develop the environmentally friendly nature of oxidative electrochemical C–H activation.

In the first project, we disclosed the first electrochemical alkyne annulation by 3d transition-metal-catalyzed C–H/N–H activation under ambient reaction conditions. The mild C–H/N–H functionalization occurred efficiently with full tolerance of H_2O at room temperature for arenes and alkenes alike (scheme 4.1). Utilizing a versatile cobalt-catalysis regime, a sustainable isoquinolone synthesis was achieved with resource-economical electricity as external oxidant. Ample substrate scope with respect to functionalized benzamides, alkenes and alkynes were proved to be applicable in cobaltaelectro-catalysis. Detailed mechanistic studies illuminated a base-assisted internal electrophilic substitution (BIES) pathway, a facile C–H cleavage and an organometallic alkyne annulation process were involved in the catalytic cycle.

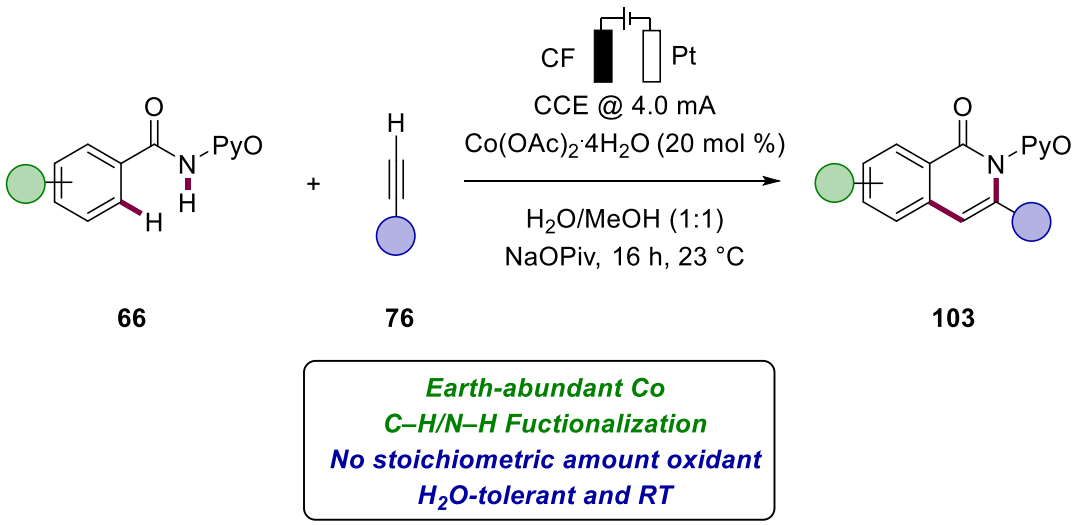

Scheme 4.1. Water-tolerant cobaltaelectro-catalyzed C–H/N–H activation at room temperature.

In the second project, the first electrochemical oxidative cascade annulation was achieved by copper-catalyzed C–H alkynylation (scheme 4.2). The cupraelectro-catalysis enabled the bioactive isoindolone synthesis in the absence of sacrificial oxidants and generated molecular hydrogen as sole by-product. Thus, the versatile cupraelectro-catalyzed domino regime enabled excellent access to synthetically useful functional groups and broad substrate scope, including electron-deficient benzamides. Applying the earth-abundant and non-toxic copper-catalysis manifold, decarboxylative metallaelectro-catalysis for C–H/C–C functionalization has been realized in a similar fashion. Further mechanistic studies revealed the key C–H alkynylation step in cupraelectro-catalysis manifold.

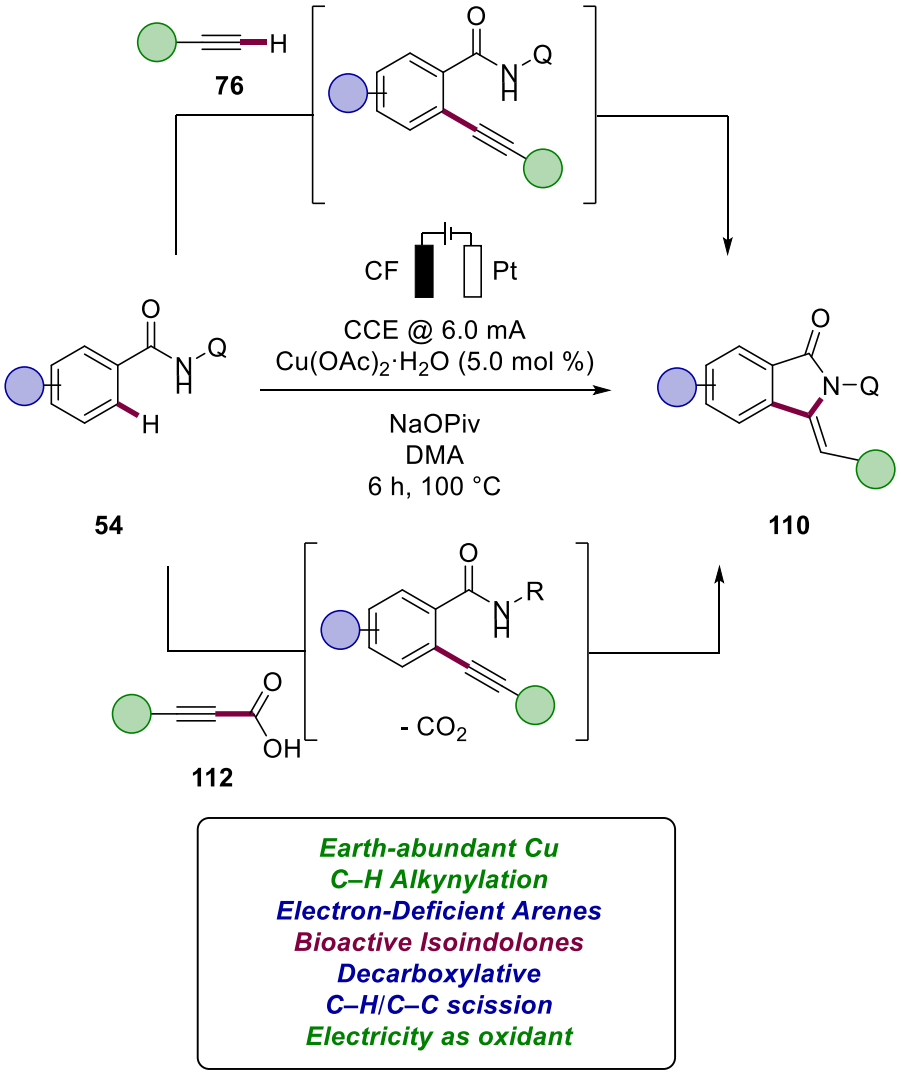

Scheme 4.2. Cupraelectro-catalyzed cascade annulation by C–H alkynylation and decarboxylative C–H/C–C manifolds.

In the third project, we reported the first electrochemical cobalt-catalyzed C–H acyloxylation (scheme 4.3). Enabled by versatile cobaltaelectro-catalysis, oxygenations of functionalized benzamides were accomplished in the absence of toxic and expensive silver(I) oxidants, generating H_2 as the sole by-product. A broad scope of substituted benzamides and carboxylic acids proved applicable in the cobaltaelectro-catalyzed C–H acyloxylation regime. Using the biomass-derived γ-valerolactone as a renewable solvent, the sustainable nature of metallaelectro-catalysis has been further advanced.

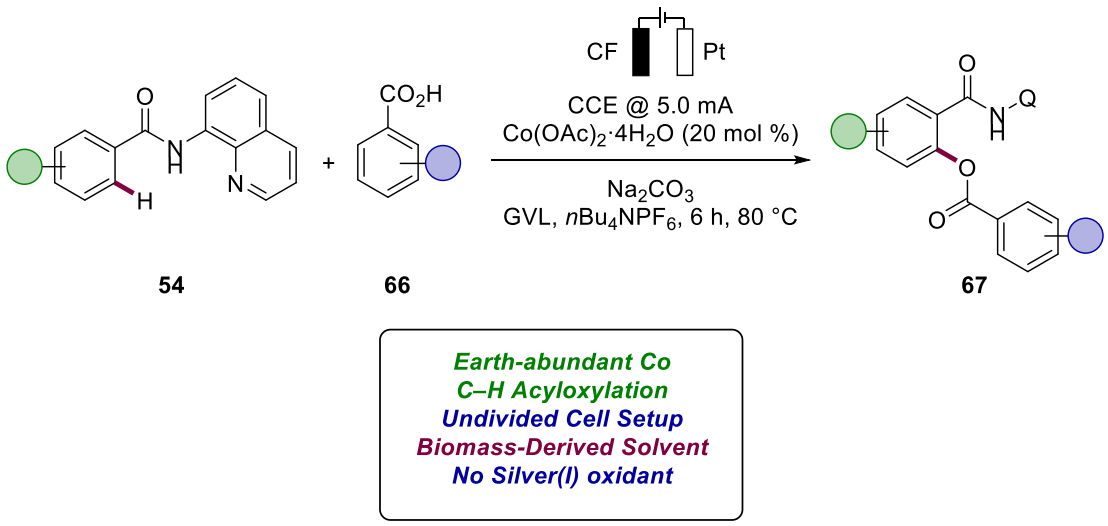

Scheme 4.3. Cobaltaelectro-catalyzed C–H acyloxylation with carboxylic acids.

In the fourth project, we disclosed the first cobaltaelectro-catalyzed C–H allylation with electronically non-activated alkenes (scheme 4.4). High levels of chemo-, position- and regio-selectivity have been achieved by the versatile cobaltaelectro-catalysis. Instead of stoichiometric amount of sacrificial chemical oxidants, sustainable electricity has been applied in C–H allylation. The cobaltaelectro-catalysis was characterized by a broad substrate scope and excellent functional group tolerance, and proceeded efficiently in biomass-derived green γ-valerolactone (GVL) as the reaction media.

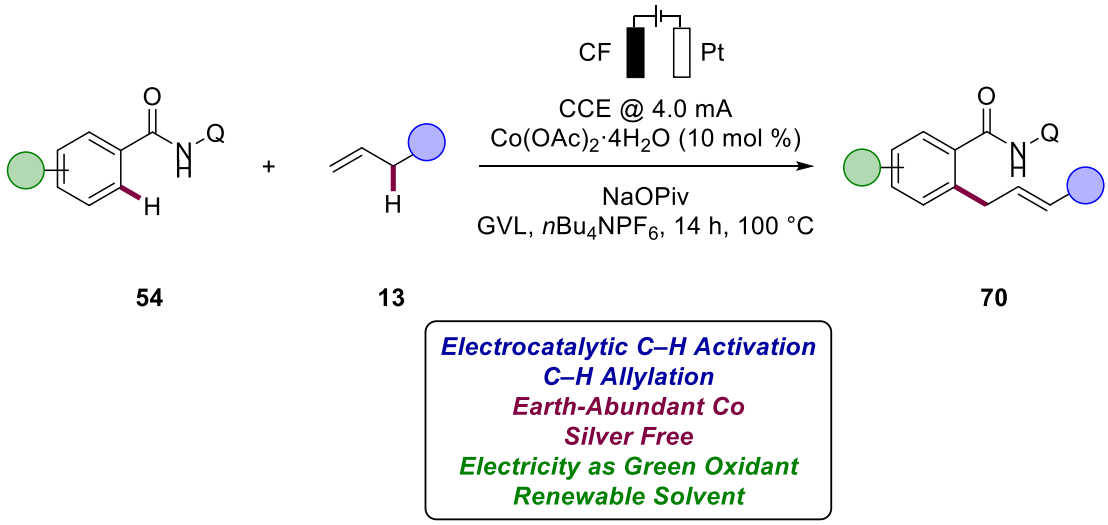

Scheme 4.4. Cobaltaelectro-catalyzed C–H allylation with nonactivated alkene.

With the successful applications of 3d transition metal catalyzed electrochemical C–H activations displayed herein, great potential of merging C–H activation with metallaelectro-catalysis has been highlighted. Further developments of sustainable approaches for oxidative C–H transformations with environmentally-benign electricity can be expected in the near future. New strategies to develop novel electrochemical C–H activation can be applied to achieve full energy and atom economy, such as paired electrolysis[128] and photoelectrocatalysis.[129] Other approaches applied in electrolysis, for example electrode materials design[130] and artificial intelligence[131] assisted reaction development, also provided unique synthetic possibilities to achieve electrochemical C–H activation in a resource-economic[39b] fashion.

5. Experiment Section

5.1 General Remarks

The catalysis in water or under an atmosphere of air was conducted in sealed tubes or Schlenk tubes. Unless otherwise noted, other reactions were performed under N_2 atmosphere using pre-dried glassware and standard Schlenk techniques. If not otherwise noted, yields refer to isolated compounds, estimated to be >95% pure as determined by ^{1}H-NMR.

Vacuum

The following pressures were measured on the used vacuum pump and were not corrected: membrane pump vacuum (MPV): 0.5 mbar, oil pump vacuum (OPV): 0.1 mbar.

Melting Points (M.p.)

Melting points were measured using a Stuart® Melting Point Apparatus *SMP3* from BARLOWORLD SCIENTIFIC. The reported values are uncorrected.

Chromatography

Analytical thin layer chromatography (TLC) was performed on 0.25 mm silica gel 60F-plates (MACHEREY-NAGEL) with 254 nm fluorescent indicator from MERCK. Plates were visualized under UV-light or developed by treatment with a $KMnO_4$ solution followed by careful applying a heat gun. Chromatographic purification of products was accomplished by flash column chromatography on MERCK silica gel, grade 60 (0.040-0.063 mm and 0.063-0.200 mm).

Gas Chromatograpgy (GC)

The conversions of the reactions were monitored applying coupled gas chromatography/mass spectrometry using G1760C GCDplus with mass detector *HP*

5971, 5890 Series II with mass detector *HP 5972* from HEWLETT-PACKARD and *7890A GC-System* with mass detector *5975C (Triplex-Axis-Detector)* from AGILENT TECHNOLOGIES equipped with *HP-5MS* columns (30 m × 0.25 mm × 0.25 m) were used.

Gel permeation chromatography (GPC)

GPC purifications were performed on a JAI system (*JAI-LC-9260 II NEXT*) equipped with two sequential columns (*JAIGEL-2HR*, gradient rate: 5.000; *JAIGEL-2.5HR*, gradient rate: 20.000; internal diameter = 20 mm; length = 600 mm; Flush rate = 10.0 mL/min and chloroform (HPLC-quality with 0.6% ethanol as stabilizer) was used as the eluent.

Infrared Spectroscopy

Infrared spectra was recorded at a BRUKER *Alpha-P ATR FT-IR* spectrometer. Liquid samples were measured as a film and solid samples were measured neat. The analysis of the spectra was carried out using the software from BRUKER *OPUS 6*. The absorption is given in wave numbers (cm^{-1}) and the spectra were recorded in the range of 4000-400 cm^{-1}. *In situ*-IR studies were performed on METTLER TOLEDO *ReactIR*^{TM} 15 with an *iC IR 4.3* software.

Mass Spectrometry

Electrospray Ionization high resolution mass spectra were recorded on a quadrupole - time-of-flight instrument *maXis* and a time-of-flight mass spectrometer *micrOTOF* both from BRUKER DALTONIK.

Nuclear Magnetic Resonance Spectroscopy (NMR)

Nuclear magnetic resonance (NMR) spectra were recorded on VARIAN *Inova 500, 600*, VARIAN *Mercury 300, VX 300*, VARIAN *Avance 300*, VARIAN *VNMRS 300* and BRUKER *Avance III 300, 400* and *HD 500* spectrometers. All chemical shifts are given

as *δ*-values in ppm relative to the residual proton peak of the deuterated solvent or its carbon atom, respectively. ^{1}H and ^{13}C NMR spectra were referenced using the residual proton or solvent carbon peak (see table), respectively. ^{13}C and ^{19}F NMR were measured as proton-decoupled spectra.

	^{1}H-NMR	^{13}C-NMR
$CDCl_3$	7.26	77.16
$[D]_6$-DMSO	2.50	39.52

The observed resonance-multiplicities were described by the following abbreviations: s (singlet), d (doublet), t (triplet), q (quartet), hept (heptet), m (multiplet) or analogous representations. The coupling constants *J* are reported in Hertz (Hz). Analysis of the recorded spectra was carried out with *MestReNova 10* software.

Electrochemistry

Platinum electrodes (10 mm × 25 mm × 0.125 mm, 99.9%; obtained from ChemPur® Karlsruhe, Germany) and CF electrodes (10 mm × 25 mm × 6 mm, SIGRACELL®GFA 6 EA, obtained from SGL Carbon, Wiesbaden, Germany) were connected using stainless steel adapters. Electrolysis was conducted using an AXIOMET *AX-3003P* potentiostat in constant current mode, CV studies were performed using a Metrohm Autolab *PGSTAT204* workstation and *Nova 2.0* software. Divided cells separated by a P4-glassfrit were obtained from Glasgerätebau Ochs Laborfachhandel e. K. (Bovenden, Germany).

Solvents

Solvents for column chromatography or reactions not sensitive to air and moisture were distilled under reduced pressure prior to use. All solvents for reactions involving air- or moisture-sensitive compounds were dried, distilled and stored under inert atmosphere according to the following procedures:

Toluene (PhMe), Tetrahydrofuran (THF), Dichloromethane (DCM), *N,N*-

dimethylformamide (DMF) and **ethyl ether (Et_2O)** were purified using a solvent purification system (*SPS-800*) from M. BRAUN.

1,2-Dichloroethane (DCE), ***N*-methyl-2-pyrrolidone (NMP)**, ***N*,*N*-dimethylacetamide (DMA), dimethylsulfoxide (DMSO)** and ***γ*-Valerolactone (GVL)** were dried over CaH_2 for 8 h, degassed and distilled under reduced pressure under N_2.

Methanol (MeOH), *t*-amylalcohol (*t*-AmOH) and **1,4-dioxane** were dried over Na for 8 h, degassed and distilled under reduced pressure under N_2.

2,2,2-Trifluoroethanol (TFE) was stirred over $CaSO_4$ and distilled under reduced pressure.

Acetonitrile (MeCN) was dried over 3 Å molecular sieves and degassed using multiple cycles of *Freeze-Pump-Thaw* degassing procedure.

Water (H_2O) was degassed by repeated *Freeze-Pump-Thaw* degassing procedure.

Isopropyl alcohol (*i*-PrOH) was used as received from Merck.

Chemicals

Chemicals obtained from commercial sources with purity above 95% were used without further purification. The following compounds are known and were synthesized according to previously described methods:

The following compounds were kindly synthesized and provided by the persons listed below:

Reagents

Chemicals obtained from commercial sources with purity above 95% were used without further purification. The following compounds are known and were synthesized according to previously described methods:

2-pyridyl-*N*-oxide benzamides **56**,[79] quinoline benzamides **54**,[132] oxazoline benzamide **93**,[106] alkynyl carboxylic acids **112**.[107]

The following compounds were obtained by the generous courtesy of the following persons:

Karsten Rauch: $[RuCl_2(p\text{-cymene})]_2$, $[Cp^*RhCl_2]_2$, dry and/or degassed DCE, NMP, H_2O, DMA solvents.

Shou-Kun Zhang: Benzamides **54f**-**54j**, **54n**, **54p**, deuterated compound $[D_5]$-**54a**.
Dr. Ruhuai Mei: Benzamides **56a**., deuterated compound $[D_5]$-**56a**.
Dr. Ramesh Chandra Samanta: Benzamide **54w**.

5.2 General Procedures

General Procedure A: Water-Tolerant Cobaltaelectro-Catalyzed C–H/N–H Activation at Room Temperature

The electrocatalysis was carried out in an undivided cell, with a CF anode (10 mm × 25 mm × 6 mm) and a platinum cathode (10 mm × 25 mm × 0.125 mm). Benzamide **56** (0.50 mmol, 1.0 equiv), alkyne **76** (1.00 mmol, 2.0 equiv), NaOPiv (124 mg, 1.0 mmol, 2.0 equiv) and $Co(OAc)_2 \cdot 4H_2O$ (12.7 mg, 10 mol %) were placed in a 20 mL cell and dissolved in 10 mL of H_2O/MeOH (1:1). Electrocatalysis was performed at ambient temperature of 23 °C with a constant current of 4.0 mA maintained for 16 h. The reaction was stopped by adding saturated aqueous $NaHCO_3$ (10 mL). The CF anode was washed with CH_2Cl_2 (3 × 10 mL) in an ultrasonic bath. The washings were added to the reaction mixture and the combined phases were extracted with CH_2Cl_2 (4 × 10 mL), then dried over Na_2SO_4. Evaporation of the solvent and subsequent column chromatography on silica gel afforded the corresponding products **104**.

General Procedure B: Cupraelectro-Catalyzed Cascade Annulation by C–H Alkynylation and Decarboxylative C–H/C–C Manifolds

The electrocatalysis was carried out in an undivided cell, with a CF anode (10 mm × 25 mm × 6 mm) and a platinum cathode (10 mm × 25 mm × 0.125 mm). Benzamide **54** (0.25 mmol, 1.0 equiv), alkyne **76** or alkynyl carboxylic acids **112** (0.50 mmol, 2.0 equiv), NaOPiv (31 mg, 0.25 mmol, 1.0 equiv) and $Cu(OAc)_2 \cdot H_2O$ (2.5 mg, 5.0 mol %) were placed in a 10 mL cell and dissolved in DMA (4.0 mL). Electrocatalysis was performed at 100 °C with a constant current of 6.0 mA maintained for 6 h. At ambient temperature, saturated aqueous $NaHCO_3$ (4.0 mL) was added. The CF anode was washed with EtOAc (3 × 10 mL) in an ultrasonic bath. The washings were added to the reaction mixture and the combined phases were extracted with EtOAc (4 × 10 mL),

then dried over Na_2SO_4. Evaporation of the solvent and subsequent column chromatography on silica gel afforded the corresponding products **110**.

General Procedure C: Cobaltaelectro-Catalyzed C–H Acyloxylation with Carboxylic Acids

The electrocatalysis was carried out in an undivided cell, with a CF anode (10 mm × 25 mm × 6 mm) and a platinum cathode (10 mm × 25 mm × 0.125 mm). Benzamide **54** (0.25 mmol, 1.0 equiv), carboxylic acid **66** (0.50 mmol, 2.0 equiv), Na_2CO_3 (53 mg, 0.5 mmol, 2.0 equiv) and $Co(OAc)_2{\cdot}4H_2O$ (12.7 mg, 20 mol %) were placed in a 10 mL cell and dissolved in GVL (3.0 mL). Electrocatalysis was performed at 80 °C with a constant current of 5.0 mA maintained for 6 h. At ambient temperature, the reaction was stopped by adding saturated aqueous $NaHCO_3$ (4.0 mL). The CF anode was washed with acetone (3 × 10 mL) in an ultrasonic cleaner. The washings were added to the reaction mixture and the combined organic phases were evaporated. After evaporation of solvents, the mixture was extracted with pentane (4 × 10 mL) and successively with EtOAc (3 × 10 mL) then dried over Na_2SO_4. Evaporation of the solvent and subsequent column chromatography on silica gel afforded the products **67**.

General Procedure D: Cobaltaelectro-Catalyzed C–H Allylation with Nonactivated Alkene

The electrocatalysis was carried out in an undivided cell, with a CF anode (10 mm × 25 mm × 6 mm) and a platinum cathode (10 mm × 25 mm × 0.125 mm). Benzamide **54** (0.50 mmol, 1.0 equiv), alkene **13** (1.5 mmol, 3.0 equiv), NaOPiv (124 mg, 1.0 mmol, 1.0 equiv) , nBu$_4$NPF$_6$ (97.0 mg, 0.25 mmol, 0.50 equiv) and $Co(OAc)_2{\cdot}4H_2O$ (12.7 mg, 10 mol %) were placed in a 10 mL cell and dissolved in GVL (4.0 mL). Electrocatalysis was performed at 100 °C with a constant current of 4.0 mA maintained for 14 h. At ambient temperature, the reaction was stopped by adding saturated aqueous $NaHCO_3$

(4 mL). The CF anode was washed with acetone (3 × 10 mL) in an ultrasonic cleaner. The washings were added to the reaction mixture and evaporated. The mixture was extracted with pentane (4 × 10 mL) and successively with EtOAc (3 × 10 mL) then dried over Na_2SO_4. Evaporation of the solvent and subsequent column chromatography on silica gel afforded the products **70**.

5.3 Experimental Procedures and Analytical Data

5.3.1. Water-Tolerant Cobaltaelectro-Catalyzed C–H/N–H Activation at Room Temperature

5.3.1.1. Characterization Data

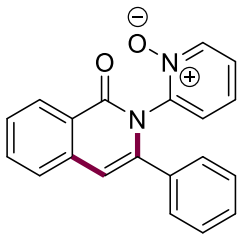

2-[1-Oxo-3-phenylisoquinolin-2(1*H*)-yl]-pyridine-2-oxide (104aa)

The general procedure **A** was followed using benzamide **56a** (107 mg, 0.50 mmol) and alkyne **76a** (102 mg, 1.00 mmol). Purification by column chromatography on silica gel (CH_2Cl_2/acetone 3:1) yielded **104aa** (119 mg, 76%) as a white solid. M. p.: 225–226 °C. ^{1}H-NMR (300 MHz, $CDCl_3$): δ = 8.46–8.37 (m, 1H), 8.23–8.14 (m, 1H), 7.73–7.63 (m, 1H), 7.53 (dt, J = 7.2, 0.7 Hz, 1H), 7.51–7.44 (m, 1H), 7.44–7.35 (m, 2H), 7.28–7.16 (m, 3H), 7.16–7.08 (m, 2H), 7.08–7.00 (m, 1H), 6.59 (s, 1H). ^{13}C-NMR (125 MHz, $CDCl_3$): δ = 161.7 (C_q), 145.3 (C_q), 142.4 (C_q), 139.8 (CH), 136.9 (C_q), 134.7 (C_q), 133.2 (CH), 128.9 (CH), 128.2 (CH), 128.0 (CH), 127.8 (CH), 127.5 (CH), 126.9 (CH), 126.2 (CH), 125.3 (CH), 124.9 (CH), 124.8 (C_q), 107.9 (CH). IR (ATR): 1664, 1624, 1490, 1261, 889, 843, 764, 526 cm^{-1}. MS (ESI) *m/z* (relative intensity): 353 (5), 337 (30) $[M+Na]^+$, 315 (60) $[M+H]^+$, 221 (20). HR-MS (ESI) *m/z* calcd for $C_{20}H_{15}N_2O_2$ $[M+H]^+$: 315.1128, found: 315.1128.

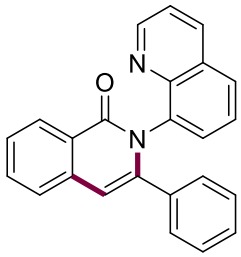

3-Phenyl-2-(quinolin-8-yl)-isoquinolin-1(*2H*)-one (104ba)

The slightly changed general procedure **A** was followed using benzamide **54a** (124 mg, 0.50 mmol) and alkyne **76a** (102 mg, 1.00 mmol) with $Co(OAc)_2{\cdot}4H_2O$ (25.7 mg, 20

mmol %). Purification by column chromatography on silica gel (CH_2Cl_2/acetone 3:1) yielded **104ba** (34 mg, 20%) as a white solid. M. p.: 210–211 °C. ^{1}H-NMR (400 MHz, $CDCl_3$): δ = 8.90 (dd, J = 4.2, 1.7 Hz, 1H), 8.51–8.45 (m, 1H), 8.08 (dd, J = 8.3, 1.7 Hz, 1H), 7.75–7.67 (m, 2H), 7.63–7.59 (m, 1H), 7.54–7.48 (m, 2H), 7.44–7.39 (m, 1H), 7.36 (dd, J = 8.3, 4.2 Hz, 1H), 7.15–7.09 (m, 2H), 7.06–6.99 (m, 1H), 6.98–6.92 (m, 2H), 6.65 (s, 1H). ^{13}C-NMR (100 MHz, $CDCl_3$): δ = 163.2 (C_q), 150.9 (CH), 144.8 (C_q), 144.5 (C_q), 137.3 (C_q), 137.2 (C_q), 136.3 (C_q), 136.0 (CH), 132.6 (CH), 130.7 (CH), 128.7 (CH), 128.6 (CH), 128.4 (CH), 127.9 (CH), 127.2 (CH), 126.6 (CH), 126.1 (CH), 125.7 (CH), 125.5 (C_q), 121.5 (CH), 107.3 (CH). IR (ATR): 3058, 1656, 1624, 1594, 1382, 1156, 829, 760 cm^{-1}. MS (EI) *m/z* (relative intensity): 348 (100) $[M]^+$, 347 (30), 319 (20), 271 (95), 242 (10), 217 (15). HR-MS (EI) *m/z* calcd for $C_{24}H_{16}N_2O$ $[M]^+$: 348.1263, found: 348.1268.

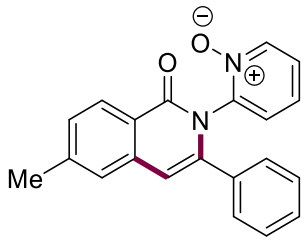

2-[6-Methyl-1-oxo-3-phenylisoquinolin-2(1*H*)-yl]-pyridine-2-oxide (104ca)

The general procedure **A** was followed using benzamide **56c** (114 mg, 0.50 mmol) and alkyne **76a** (102 mg, 1.00 mmol). Purification by column chromatography on silica gel (CH_2Cl_2/acetone 3:1) yielded **104ca** (121 mg, 73%) as a white solid. M. p. = 220–221 °C. ^{1}H-NMR (300 MHz, $CDCl_3$): δ = 8.29 (d, J = 8.0 Hz, 1H), 8.21-8.10 (m, 1H), 7.43–7.36 (m, 2H), 7.34–7.27 (m, 2H), 7.25–7.17 (m, 3H), 7.17–7.10 (m, 2H), 7.06–6.97 (m, 1H), 6.52 (s, 1H), 2.48 (s, 3H). ^{13}C-NMR (125 MHz, $CDCl_3$): δ = 161.8 (C_q), 145.7 (C_q), 143.9 (C_q), 142.5 (C_q), 140.0 (CH), 137.0 (C_q), 134.8 (C_q), 128.8 (CH), 128.5 (CH), 128.2 (CH), 128.0 (CH), 127.8 (CH), 127.6 (CH), 126.0 (CH), 125.1 (CH), 125.0 (CH), 122.6 (C_q), 107.8 (CH), 21.9 (CH_3). IR (ATR): 3059, 1664, 1626, 1486, 1260, 909, 769, 727 cm^{-1}. MS (EI) *m/z* (relative intensity): 328 (25) $[M]^+$, 283 (15), 208 (25), 181 (100), 165 (15), 78 (65). HR-MS (EI) *m/z* calcd for $C_{21}H_{16}N_2O_2$ $[M]^+$: 328.1212, found: 328.1213.

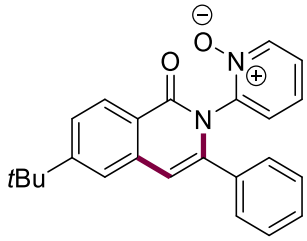

2-[6-(*tert*-Butyl)-1-oxo-3-phenylisoquinolin-2(1*H*)-yl]-pyridine-2-oxide (104da)

The general procedure **A** was followed using benzamide **56d** (135 mg, 0.50 mmol) and alkyne **76a** (102 mg, 1.00 mmol). Purification by column chromatography on silica gel (CH_2Cl_2/acetone 3:1) yielded **104da** (115 mg, 62%) as a white solid. M. p.: 243–244 °C. ^{1}H-NMR (300 MHz, $CDCl_3$): δ = 8.35 (d, J = 8.5 Hz, 1H), 8.20 (d, J = 6.3 Hz, 1H), 7.56 (dd, J = 8.5, 1.9 Hz, 1H), 7.52 (d, J = 1.8 Hz, 1H), 7.45–7.34 (m, 2H), 7.29–7.17 (m, 3H), 7.17–7.09 (m, 2H), 7.08–6.99 (m, 1H), 6.60 (s, 1H), 1.40 (s, 9H). ^{13}C-NMR (125 MHz, $CDCl_3$): δ = 161.7 (C_q), 156.9 (C_q), 145.5 (C_q), 142.4 (C_q), 139.9 (CH), 136.9 (C_q), 134.9 (C_q), 128.8 (CH), 128.1 (CH), 128.0 (CH), 127.8 (CH), 127.6 (CH), 125.2 (CH), 125.1 (CH), 124.8 (CH), 122.5 (C_q), 122.3 (CH), 108.4 (CH), 35.2 (C_q), 31.1 (CH_3). IR (ATR): 1673, 1627, 1608, 1490, 1272, 932, 766, 701 cm^{-1}. MS (EI) *m/z* (relative intensity): 370 (15) $[M]^+$, 354 (12), 250 (15), 235 (20), 181 (100), 78 (35). HR-MS (EI) *m/z* calcd for $C_{24}H_{22}N_2O_2$ $[M]^+$: 370.1681, found: 370.1672.

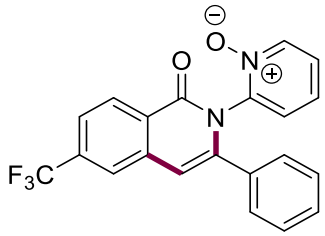

2-[6-Trifluoromethyl-1-oxo-3-phenylisoquinolin-2(1*H*)-yl]-pyridine-2-oxide (104ea)

The slightly modified general procedure **A** was followed using benzamide **56e** (141 mg, 0.50 mmol) and alkyne **76a** (102 mg, 1.00 mmol) with $Co(OAc)_2{\cdot}4H_2O$ (25.7 mg, 20 mmol %). Purification by column chromatography on silica gel (CH_2Cl_2/acetone 3:1) yielded **104ea** (97.2 mg, 51%) as a white solid. M. p.: 190–191 °C. ^{1}H-NMR (400 MHz, $CDCl_3$): δ = 8.57–8.52 (m, 1H), 8.24 (d, J = 6.4 Hz, 1H), 7.87–7.82 (m, 1H), 7.74–7.66 (m, 1H), 7.44–7.37 (m, 2H), 7.32–7.22 (m, 3H), 7.21–7.14 (m, 2H), 7.13–7.07 (m, 1H),

6.66 (s, 1H). ^{13}C-NMR (100 MHz, $CDCl_3$): δ = 161.1 (C_q), 145.1 (C_q), 144.3 (C_q), 140.1 (CH), 137.1 (C_q), 134.9 (q, $^2J_{C-F}$ = 32.6 Hz, C_q), 134.3 (C_q), 129.5 (CH), 129.5 (CH), 128.4 (CH), 127.9 (CH), 127.6 (CH), 127.1 (C_q), 125.7 (CH), 125.3 (CH), 125.0 (q, $^1J_{C-F}$ = 273.4 Hz, C_q), 123.6 (q, $^3J_{C-F}$ = 3.9 Hz, CH), 123.1 (q, $^3J_{C-F}$ = 3.2 Hz, CH), 107.5 (CH). ^{19}F-NMR (376 MHz, $CDCl_3$) δ = –63.13 (s). IR (ATR): 1672, 1490, 1431, 1319, 1126, 920, 729, 698 cm^{-1}. MS (EI) *m/z* (relative intensity): 382 (30) $[M]^+$, 365 (20), 337 (20), 262 (30), 181 (100), 78 (85). HR-MS (EI) *m/z* calcd for $C_{21}H_{13}F_3N_2O_2$ $[M]^+$: 382.0929, found: 382.0928.

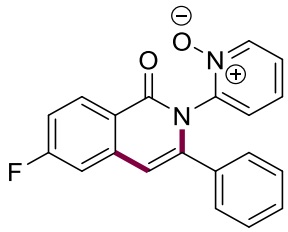

2-[6-Fluoro-1-oxo-3-phenylisoquinolin-2(1*H*)-yl]-pyridine-2-oxide (104fa)

The general procedure **A** was followed using benzamide **56f** (116 mg, 0.50 mmol) and alkyne **76a** (102 mg, 1.00 mmol). Purification by column chromatography on silica gel (CH_2Cl_2/acetone 6:1) yielded **104fa** (110 mg, 66%) as a white solid. M. p.: 190–191 °C. ^{1}H-NMR (300 MHz, $CDCl_3$): δ = 8.46–8.37 (m, 1H), 8.18 (d, *J* = 5.8 Hz, 1H), 7.42–7.34 (m, 2H), 7.29–7.19 (m, 3H), 7.19–7.12 (m, 3H), 7.12–7.10 (m, 1H), 7.09–7.01 (m, 1H), 6.53 (s, 1H). ^{13}C-NMR (125 MHz, $CDCl_3$): δ = 165.9 (d, $^1J_{C-F}$ = 254.2 Hz, C_q), 161.2 (C_q), 145.3 (C_q), 144.1 (C_q), 140.1 (CH), 139.4 (d, $^3J_{C-F}$ = 10.6 Hz, C_q), 134.5 (C_q), 131.8 (d, $^3J_{C-F}$ = 10.0 Hz, CH), 129.3 (CH), 128.3 (CH), 127.9 (CH), 127.6 (CH), 125.6 (CH), 125.1 (CH), 121.5 (d, $^4J_{C-F}$ = 1.9 Hz, C_q), 115.7 (d, $^2J_{C-F}$ = 23.4 Hz, CH), 111.3 (d, $^2J_{C-F}$ = 22.2 Hz, CH), 107.4 (d, $^4J_{C-F}$ = 3.1 Hz, CH). ^{19}F-NMR (471 MHz, $CDCl_3$): δ = –104.73 (td, *J* = 8.9, 5.8 Hz). IR (ATR): 1671, 1617, 1504, 1482, 1431, 1272, 868, 758 cm^{-1}. MS (ESI) *m/z* (relative intensity): 417 (5), 371 (5), 359 (4), 355 (100) $[M+Na]^+$, 333 (30) $[M+H]^+$. HR-MS (ESI) *m/z* calcd for $C_{20}H_{14}FN_2O_2$ $[M+H]^+$: 333.1034, found: 333.1034.

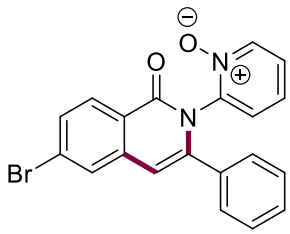

2-[6-Bromo-1-oxo-3-phenylisoquinolin-2(1*H*)-yl]-pyridine-2-oxide (104ga)

The slightly modified general procedure **A** was followed using benzamide **56g** (146 mg, 0.50 mmol) and alkyne **76a** (102 mg, 1.00 mmol) with $Co(OAc)_2 \cdot 4H_2O$ (25.7 mg, 20 mmol %). Purification by column chromatography on silica gel (CH_2Cl_2/acetone 3:1) yielded **104ga** (127 mg, 65%) as a white solid. M. p.: 212–215 °C. ^{1}H-NMR (300 MHz, $CDCl_3$): δ = 8.24 (d, J = 8.6 Hz, 1H), 8.19 (d, J = 6.2 Hz, 1H), 7.69 (d, J = 1.9 Hz, 1H), 7.56 (dd, J = 8.6, 1.9 Hz, 1H), 7.41–7.34 (m, 2H), 7.30–7.17 (m, 3H), 7.17–7.09 (m, 2H), 7.09–7.00 (m, 1H), 6.49 (s, 1H). ^{13}C-NMR (125 MHz, $CDCl_3$): δ = 161.2 (C_q), 145.1 (C_q), 144.0 (C_q), 139.9 (CH), 138.3 (C_q), 134.3 (C_q), 130.2 (CH), 130.0 (CH), 129.2 (CH), 128.6 (CH), 128.4 (C_q), 128.1 (CH), 127.7 (CH), 127.5 (CH), 125.4 (CH), 124.9 (CH), 123.5 (C_q), 106.7 (CH). IR (ATR): 1666, 1627, 1491, 1428, 1368, 1255, 900, 727 cm^{-1}. MS (EI) *m/z* (relative intensity): 394 (10) [M$^+$] (^{81}Br), 392 (10) [M$^+$] (^{79}Br), 377 (15), 349 (15), 274 (10), 268 (15), 181 (100), 165 (10), 78 (55). HR-MS (EI) *m/z* calcd for $C_{20}H_{13}{}^{79}BrN_2O_2$ [M$^+$] 392.0160, found 392.0160.

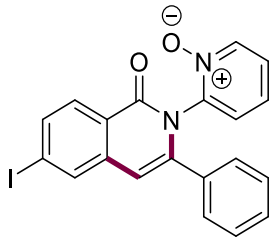

2-[6-Iodo-1-oxo-3-phenylisoquinolin-2(1*H*)-yl]-pyridine-2-oxide (104ha)

The slightly modified general procedure **A** was followed using benzamide **56h** (170 mg, 0.50 mmol) and alkyne **76a** (102 mg, 1.00 mmol) with $Co(OAc)_2 \cdot 4H_2O$ (25.7 mg, 20 mmol %). Purification by column chromatography on silica gel (CH_2Cl_2/acetone 6:1) yielded **104ha** (114 mg, 52%) as a white solid. M. p.: 246–248 °C. ^{1}H-NMR (300 MHz, $CDCl_3$): δ = 8.19 (d, J = 6.3 Hz, 1H), 8.09 (d, J = 8.5 Hz, 1H), 7.94 (d, J = 1.6 Hz, 1H), 7.78 (dd, J = 8.5, 1.7 Hz, 1H), 7.41–7.34 (m, 2H), 7.28–7.18 (m, 3H), 7.18–7.10 (m,

2H), 7.10–7.01 (m, 1H), 6.47 (s, 1H). ^{13}C-NMR (100 MHz, $CDCl_3$): δ = 161.7 (C_q), 145.3 (C_q), 144.0 (C_q), 140.1 (CH), 138.4 (C_q), 136.0 (CH), 135.1 (CH), 134.5 (C_q), 129.8 (CH), 129.3 (CH), 128.3 (CH), 127.8 (CH), 127.6 (CH), 125.5 (CH), 125.0 (CH), 124.1 (C_q), 106.6 (CH), 101.4 (C_q). IR (ATR): 1667, 1625, 1598, 1584, 1269, 895, 764, 728 cm^{-1}. MS (EI) *m/z* (relative intensity): 440 (25) $[M]^+$, 423 (10), 395 (15), 320 (20), 181 (100), 78 (55). HR-MS (EI) *m/z* calcd for $C_{20}H_{13}IN_2O_2$ $[M]^+$: 440.0022, found: 440.0022.

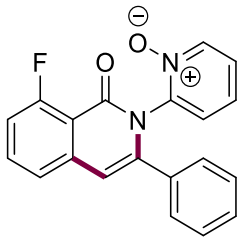

2-[8-Fluoro-1-oxo-3-phenylisoquinolin-2(1*H*)-yl]-pyridine-2-oxide (104ia)

The slightly modified general procedure **A** was followed using benzamide **56i** (116 mg, 0.50 mmol) and alkyne **76a** (102 mg, 1.00 mmol) with $Co(OAc)_2{\cdot}4H_2O$ (25.7 mg, 20 mmol %). Purification by column chromatography on silica gel (CH_2Cl_2/acetone 3:1) yielded **104ia** (92.8 mg, 56%) as a colorless oil. ^{1}H-NMR (500 MHz, $CDCl_3$): δ = 8.27–7.97 (m, 1H), 7.62 (td, *J* = 8.0, 4.8 Hz, 1H), 7.45–7.36 (m, 2H), 7.34–7.29 (m, 1H), 7.29–7.20 (m, 4H), 7.20–7.15 (m, 1H), 7.12 (ddd, *J* = 11.2, 8.1, 1.1 Hz, 1H), 7.07–6.88 (m, 1H), 6.56 (d, *J* = 2.0 Hz, 1H). ^{13}C-NMR (125 MHz, $CDCl_3$): δ = 162.9 (d, $^1J_{C–F}$ = 266.2 Hz, C_q), 159.1 (d, $^3J_{C–F}$ = 4.7 Hz, C_q), 143.9 (C_q), 140.4 (CH), 139.7 (C_q), 134.4 (C_q), 134.4 (d, $^3J_{C–F}$ = 9.8 Hz, CH), 132.0 (CH), 129.3 (CH), 129.1 (CH), 128.3 (CH), 127.9 (C_q), 127.8 (CH), 125.2 (CH), 122.1 (d, $^4J_{C–F}$ = 4.5 Hz, CH), 114.0 (d, $^2J_{C–F}$ = 5.8 Hz, CH), 114.0 (d, $^2J_{C–F}$ = 21.3 Hz, C_q), 107.3 (d, $^4J_{C–F}$ = 2.6 Hz, CH). ^{19}F-NMR (471 MHz, $CDCl_3$) δ = –109.10 (dd, *J* = 11.8, 4.8 Hz). IR (ATR): 1675, 1630, 1612, 1492, 1432, 1034, 838, 763 cm^{-1}. MS (EI) *m/z* (relative intensity): 332 (25) $[M]^+$, 316 (30), 287 (40), 212 (20), 181 (100), 78 (80). HR-MS (EI) *m/z* calcd for $C_{20}H_{13}FN_2O_2$ $[M]^+$: 332.0961, found: 332.0971.

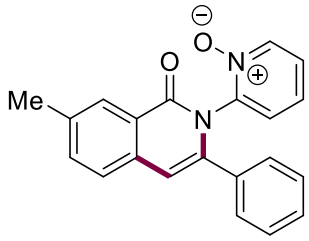
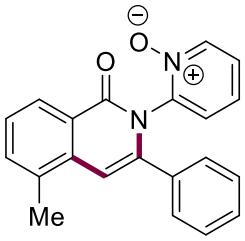

2-[7-Methyl-1-oxo-3-phenylisoquinolin-2(1*H*)-yl]-pyridine-2-oxide (104ja)

The slightly modified general procedure **A** was followed using benzamide **56j** (114 mg, 0.50 mmol) and alkyne **76a** (102 mg, 1.00 mmol) with $Co(OAc)_2{\cdot}4H_2O$ (25.7 mg, 20 mmol %). Purification by column chromatography on silica gel (CH_2Cl_2/acetone 3:1) yielded **104ja**/**104ja'** (146 mg, 89%) as a white solid. M. p.: 230–232 °C. The ratio of **104ja**/**104ja'** (79:21) was determined by ^{1}H-NMR spectroscopy. Resonances are reported for **104ja**. ^{1}H-NMR (500 MHz, $CDCl_3$): δ = 8.24–8.20 (m, 2H), 7.53 (dd, J = 8.0, 1.8 Hz, 1H), 7.46 (d, J = 8.1 Hz, 1H), 7.41–7.38 (m, 2H), 7.25–7.19 (m, 3H), 7.15–7.11 (m, 2H), 7.08–7.06 (m, 1H), 6.58 (s, 1H), 2.50 (s, 3H). ^{13}C-NMR (125 MHz, $CDCl_3$): δ = 161.9 (C_q), 145.6 (C_q), 141.6 (C_q), 140.0 (CH), 137.3 (C_q), 135.0 (C_q), 134.8 (CH), 134.7 (C_q), 128.9 (CH), 128.2 (CH), 128.0 (CH), 127.9 (CH), 127.7 (CH), 126.2 (CH), 125.3 (CH), 125.0 (CH), 124.8 (C_q), 108.0 (CH), 21.5 (CH_3). IR (ATR): 1669, 1491, 1433, 1376, 1271, 848, 760, 706 cm^{-1}. MS (ESI) *m/z* (relative intensity): 353 (24), 351 (100) $[M+Na]^+$, 340 (5), 329 (18) $[M+H]^+$. HR-MS (ESI) *m/z* calcd for $C_{21}H_{17}N_2O_2$ $[M+H]^+$: 329.1285, found: 329.1285.

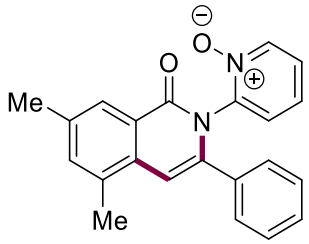

2-[5,7-Dimethyl-1-oxo-3-phenylisoquinolin-2(1*H*)-yl]-pyridine-2-oxide (104ka)

The general procedure **A** was followed using benzamide **104k** (121 mg, 0.50 mmol) and alkyne **76a** (102 mg, 1.00 mmol). Purification by column chromatography on silica gel (CH_2Cl_2/acetone 3:1) yielded **104ka** (132 mg, 77%) as a white solid. M. p.: 238–239 °C. ^{1}H-NMR (300 MHz, $CDCl_3$): δ = 8.24–8.17 (m, 1H), 8.15–8.07 (m, 1H), 7.47–7.39 (m, 2H), 7.39–7.34 (m, 1H), 7.29–7.18 (m, 3H), 7.17–7.10 (m, 2H), 7.10–7.02 (m,

1H), 6.68 (d, *J* = 0.8 Hz, 1H), 2.51 (s, 3H), 2.45 (s, 3H). ^{13}C-NMR (125 MHz, $CDCl_3$): *δ* = 162.0 (C_q), 145.6 (C_q), 141.1 (C_q), 139.9 (CH), 136.7 (C_q), 135.6 (CH), 135.2 (C_q), 133.4 (C_q), 133.4 (C_q), 128.8 (CH), 128.1 (CH), 128.0 (CH), 127.6 (CH), 125.9 (CH), 125.2 (CH), 125.0 (C_q), 124.8 (CH), 104.8 (CH), 21.4 (CH_3), 18.9 (CH_3). IR (ATR): 1711, 1668, 1491, 1268, 843, 755, 703, 577 cm^{-1}. MS (EI) *m/z* (relative intensity): 342 (10) $[M]^+$, 326 (30), 297 (20), 222 (28), 181 (100), 78 (70). HR-MS (EI) *m/z* calcd for $C_{22}H_{18}N_2O_2$ $[M]^+$: 342.1368, found: 342.1363.

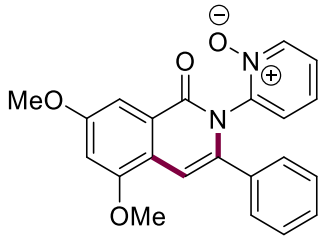

2-[5,7-Dimethoxy-1-oxo-3-phenylisoquinolin-2(1*H*)-yl]-pyridine-2-oxide (104la)

The general procedure **A** was followed using benzamide **56l** (137 mg, 0.50 mmol) and alkyne **76a** (102 mg, 1.00 mmol). Purification by column chromatography on silica gel (CH_2Cl_2/acetone 3:1) yielded **104la** (150 mg, 80%) as a white solid. M. p.: 246–247 °C. ^{1}H-NMR (300 MHz, $CDCl_3$): *δ* = 8.25–8.18 (m, 1H), 7.42 (d, *J* = 2.4 Hz, 1H), 7.40–7.34 (m, 2H), 7.23–7.15 (m, 3H), 7.15–7.06 (m, 2H), 7.06–6.99 (m, 1H), 6.92 (d, *J* = 0.6 Hz, 1H), 6.73 (d, *J* = 2.3 Hz, 1H), 3.89 (s, 3H), 3.88 (s, 3H). ^{13}C-NMR (125 MHz, $CDCl_3$): *δ* = 161.2 (C_q), 159.4 (C_q), 155.9 (C_q), 145.7 (C_q), 139.8 (CH), 139.4 (C_q), 135.2 (C_q), 128.6 (CH), 128.0 (CH), 127.9 (CH), 127.4 (CH), 126.4 (C_q), 125.2 (CH), 124.7 (CH), 122.6 (C_q), 103.8 (CH), 102.4 (CH), 99.6 (CH), 55.9 (CH_3), 55.6 (CH_3). IR (ATR): 1664, 1606, 1488, 1433, 1366, 1046, 784, 753 cm^{-1}. MS (EI) *m/z* (relative intensity): 374 (15) $[M]^+$, 330 (10), 269 (10), 254 (15), 181 (100), 78 (60). HR-MS (EI) *m/z* calcd for $C_{22}H_{18}N_2O_4$ $[M]^+$: 374.1267, found: 374.1264.

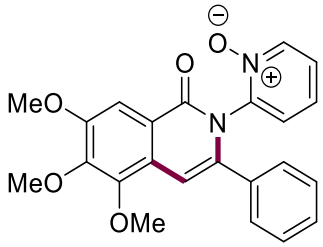

2-[5,6,7-Trimethoxy-1-oxo-3-phenylisoquinolin-2(1*H*)-yl]-pyridine-2-oxide

(104ma)

The general procedure **A** was followed using benzamide **56m** (137 mg, 0.50 mmol) and alkyne **76a** (102 mg, 1.00 mmol). Purification by column chromatography on silica gel (CH_2Cl_2/acetone 3:1) yielded **104ma** (163 mg, 81%) as a white solid. M. p.: 219–221 °C. ^{1}H-NMR (300 MHz, $CDCl_3$): δ = 8.27–8.18 (m, 1H), 7.67 (s, 1H), 7.43–7.34 (m, 2H), 7.25–7.17 (m, 3H), 7.17–7.11 (m, 1H), 7.11–7.00 (m, 2H), 6.84 (s, 1H), 4.00 (s, 3H), 3.97 (s, 3H), 3.95 (s, 3H). ^{13}C-NMR (125 MHz, $CDCl_3$): δ = 161.0 (C_q), 153.2 (C_q), 147.8 (C_q), 146.6 (C_q), 145.6 (C_q), 140.6 (C_q), 139.9 (CH), 135.1 (C_q), 128.8 (CH), 128.1 (CH), 127.9 (CH), 127.5 (CH), 126.7 (C_q), 125.2 (CH), 124.8 (CH), 120.8 (C_q), 104.8 (CH), 102.3 (CH), 61.5 (CH_3), 61.1 (CH_3), 56.2 (CH_3). IR (ATR): 1665, 1593, 1483, 1430, 1377, 1129, 843, 758 cm^{-1}. MS (EI) *m/z* (relative intensity): 404 (10) $[M]^+$, 388 (50), 373 (15), 195 (25), 181 (100), 78 (50). HR-MS (EI) *m/z* calcd for $C_{23}H_{20}N_2O_5$ $[M]^+$: 404.1372, found: 404.1384.

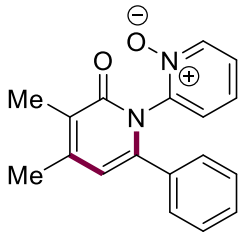

3,4-Dimethyl-2-oxo-6-phenyl-2*H*-[1,2'-bipyridine]-2'-oxide (104na)

The slightly modified general procedure **A** was followed using alkene **56n** (96 mg, 0.50 mmol) and alkyne **76a** (102 mg, 1.00 mmol) with $Co(OAc)_2{\cdot}4H_2O$ (25.7 mg, 20 mmol %). Purification by column chromatography on silica gel (CH_2Cl_2/acetone 1:1) yielded **104na** (118 mg, 81%) as a white solid. M. p.: 202–204 °C. ^{1}H-NMR (400 MHz, $CDCl_3$): δ = 8.20 (d, J = 6.5 Hz, 1H), 7.41–7.29 (m, 2H), 7.26–7.16 (m, 3H), 7.16–7.09 (m, 1H), 7.09–7.00 (m, 2H), 6.14 (s, 1H), 2.24 (s, 3H), 2.15 (s, 3H). ^{13}C-NMR (100 MHz, $CDCl_3$): δ = 162.1 (C_q), 147.2 (C_q), 145.7 (C_q), 144.3 (C_q), 140.0 (CH), 134.4 (C_q), 129.1 (CH), 128.2 (CH), 127.7 (CH), 127.3 (CH), 125.4 (C_q), 125.3 (CH), 125.0 (CH), 111.2 (CH), 20.0 (CH_3), 12.4 (CH_3). IR (ATR): 1654, 1551, 1490, 1430, 1267, 846, 767, 702 cm^{-1}. MS (EI) *m/z* (relative intensity): 292 (30) $[M]^+$, 276 (15), 198 (100), 181 (45), 169 (25), 78 (65). HR-MS (EI) *m/z* calcd for $C_{18}H_{16}N_2O_2$ $[M]^+$: 292.1212,

found: 292.1205.

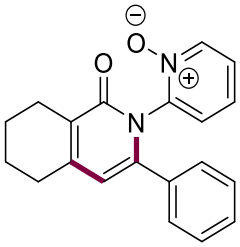

2-[1-Oxo-3-phenyl-5,6,7,8-tetrahydroisoquinolin-2(1*H*)-yl]-pyridine-2-oxide (104oa)

The slightly modified general procedure **A** was followed using alkene **56o** (109 mg, 0.50 mmol) and alkyne **76a** (102 mg, 1.00 mmol) with $Co(OAc)_2 \cdot 4H_2O$ (25 mg, 20 mmol %). Purification by column chromatography on silica gel (CH_2Cl_2/acetone 1:1) yielded **104oa** (82.4 mg, 52%) as a colorless oil. ^{1}H-NMR (400 MHz, $CDCl_3$): δ = 8.18 (d, J = 6.4 Hz, 1H), 7.36–7.29 (m, 2H), 7.25–7.15 (m, 3H), 7.12 (td, J = 6.6, 3.0 Hz, 1H), 7.09–7.00 (m, 2H), 6.05 (s, 1H), 2.74–2.43 (m, 4H), 1.87–1.69 (m, 4H). ^{13}C-NMR (100 MHz, $CDCl_3$): δ = 161.8 (C_q), 148.4 (C_q), 145.5 (C_q), 144.1 (C_q), 140.0 (CH), 134.5 (C_q), 129.0 (CH), 128.2 (CH), 127.7 (CH), 127.4 (CH), 126.5 (C_q), 125.3 (CH), 125.0 (CH), 110.0 (CH), 29.5 (CH_2), 23.3 (CH_2), 21.9 (CH_2), 21.8 (CH_2). IR (ATR): 2931, 1653, 1490, 1432, 1264, 908, 842, 728 cm^{-1}. MS (EI) *m/z* (relative intensity): 318 (25) $[M]^+$, 302 (15), 224 (100), 195 (20), 181 (65), 78 (60). HR-MS (EI) *m/z* calcd for $C_{20}H_{18}N_2O_2$ $[M]^+$: 318.1368, found: 318.1367.

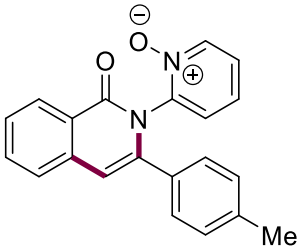

2-[1-Oxo-3-(*p*-tolyl)isoquinolin-2(1*H*)-yl]-pyridine-2-oxide (104ab)

The slightly modified general procedure **A** was followed using benzamide **56a** (107 mg, 0.50 mmol) and alkyne **76b** (116 mg, 1.00 mmol) with $Co(OAc)_2 \cdot 4H_2O$ (25.7 mg, 20 mmol %). Purification by column chromatography on silica gel (CH_2Cl_2/acetone 2:1) yielded **104ab** (135 mg, 82%) as a white solid. M. p.: 242–243 °C. ^{1}H-NMR (300 MHz, $CDCl_3$): δ = 8.46–8.39 (m, 1H), 8.26–8.20 (m, 1H), 7.73–7.64 (m, 1H), 7.58–7.52 (m,

1H), 7.52–7.45 (m, 1H), 7.32–7.25 (m, 2H), 7.19–7.06 (m, 3H), 7.04–6.98 (m, 2H), 6.58 (s, 1H), 2.27 (s, 3H). ^{13}C-NMR (125 MHz, $CDCl_3$): δ = 161.9 (C_q), 145.5 (C_q), 142.6 (C_q), 139.9 (CH), 139.0 (C_q), 137.1 (C_q), 133.2 (CH), 131.9 (C_q), 128.8 (CH), 128.3 (CH), 127.7 (CH), 127.6 (CH), 126.9 (CH), 126.1 (CH), 125.3 (CH), 124.9 (CH), 124.8 (C_q), 107.8 (CH), 21.3 (CH_3). IR (ATR): 1670, 1626, 1482, 1433, 1272, 1024, 817, 760 cm^{-1}. MS (EI) *m/z* (relative intensity): 328 (25) $[M]^+$, 283 (15), 208 (30), 195 (100), 165 (15), 78 (65). HR-MS (EI) *m/z* calcd for $C_{21}H_{16}N_2O_2$ $[M]^+$: 328.1212, found: 328.1210.

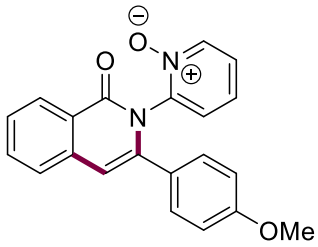

2-[1-Oxo-3-(4-methoxy)-isoquinolin-2(1*H*)-yl]-pyridine-2-oxide (104ac)

The slightly modified general procedure **A** was followed using benzamide **56a** (107 mg, 0.50 mmol) and alkyne **76c** (132 mg, 1.00 mmol) with $Co(OAc)_2{\cdot}4H_2O$ (25.7 mg, 20 mmol %). Purification by column chromatography on silica gel (CH_2Cl_2/acetone 3:1) yielded **104ac** (141 mg, 82%) as a white solid. M. p.: 228–230 °C. ^{1}H-NMR (300 MHz, $CDCl_3$): δ = 8.44–8.38 (m, 1H), 8.25–8.19 (m, 1H), 7.72–7.64 (m, 1H), 7.56–7.51 (m, 1H), 7.50–7.45 (m, 1H), 7.35–7.30 (m, 2H), 7.18–7.11 (m, 2H), 7.11–7.05 (m, 1H), 6.76–6.70 (m, 2H), 6.57 (s, 1H), 3.74 (s, 3H). ^{13}C-NMR (125 MHz, $CDCl_3$): δ = 162.0 (C_q), 160.0 (C_q), 145.6 (C_q), 142.4 (C_q), 140.0 (CH), 137.2 (C_q), 133.3 (CH), 129.3 (CH), 128.3 (CH), 127.7 (CH), 127.3 (C_q), 126.9 (CH), 126.2 (CH), 125.4 (CH), 125.1 (CH), 124.8 (C_q), 113.6 (CH), 107.8 (CH), 55.1 (CH_3). IR (ATR): 2359, 2010, 1670, 1511, 1251, 1028, 762, 561 cm^{-1}. MS (ESI) *m/z* (relative intensity): 368 (23), 367 (100) $[M+Na]^+$, 345 (30) $[M+H]^+$, 337 (5). HR-MS (ESI) *m/z* calcd for $C_{21}H_{17}N_2O_3$ $[M+H]^+$: 345.1234, found: 345.1232.

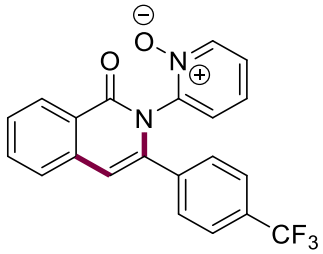

2-[1-Oxo-3-(4-trifluoro)-isoquinolin-2(1*H*)-yl]-pyridine-2-oxide (104ad)

The slightly modified general procedure **A** was followed using benzamide **56a** (107 mg, 0.50 mmol) and alkyne **76d** (170 mg, 1.00 mmol) with $Co(OAc)_2 \cdot 4H_2O$ (25.7 mg, 20 mmol %). Purification by column chromatography on silica gel (CH_2Cl_2/acetone 3:1) yielded **104ad** (110 mg, 58%) as colorless oil. ^{1}H-NMR (300 MHz, $CDCl_3$): δ = 8.45–8.39 (m, 1H), 8.24–8.15 (m, 1H), 7.76–7.68 (m, 1H), 7.60–7.51 (m, 4H), 7.51–7.46 (m, 2H), 7.23–7.16 (m, 2H), 7.16–7.09 (m, 1H), 6.61 (s, 1H). ^{13}C-NMR (125 MHz, $CDCl_3$): δ = 161.6 (C_q), 144.9 (C_q), 141.0 (C_q), 140.0 (CH), 138.2 (C_q), 136.6 (C_q), 133.4 (CH), 131.0 (q, $^2J_{C-F}$ = 32.7 Hz, C_q), 128.4 (CH), 127.6 (CH), 127.5 (CH), 126.4 (CH), 125.7 (CH), 125.5 (q, $^1J_{C-F}$ = 273.0 Hz, C_q), 125.2 (CH), 125.1 (C_q), 125.1 (q, $^3J_{C-F}$ = 4.0 Hz, CH), 124.9 (CH), 108.6 (CH). ^{19}F-NMR (283 MHz, $CDCl_3$) δ = –62.85 (S). IR (ATR): 1669, 1491, 1321, 1262, 1123, 1020, 760, 730 cm^{-1}. MS (EI) *m/z* (relative intensity): 382 (20) $[M]^+$, 337 (15), 262 (25), 249 (90), 193 (15), 78 (100). HR-MS (EI) *m/z* calcd for $C_{21}H_{13}F_3N_2O_2$ $[M]^+$: 382.0929, found: 382.0930.

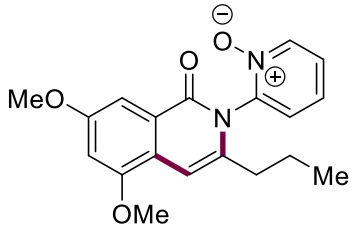

2-[5,7-Methoxy-1-oxo-3-*n*-propylisoquinolin-2(1*H*)-yl]-pyridine-2-oxide (104le)

The slightly modified general procedure **A** was followed using benzamide **56l** (137 mg, 0.50 mmol) and alkyne **76e** (68.1 mg, 1.00 mmol) with $Co(OAc)_2 \cdot 4H_2O$ (25.7 mg, 20 mmol %). Purification by column chromatography on silica gel (CH_2Cl_2/acetone 1:1) yielded **104le** (144 mg, 85%) as a yellow oil. ^{1}H-NMR (300 MHz, $CDCl_3$): δ = 8.44–8.36 (m, 1H), 7.48–7.42 (m, 1H), 7.42–7.35 (m, 2H), 7.34 (d, *J* = 2.4 Hz, 1H), 6.76 (s, 1H), 6.70 (d, *J* = 2.4 Hz, 1H), 3.92 (s, 3H), 3.87 (s, 3H), 2.40–2.05 (m, 2H), 1.65–1.50

(m, 2H), 0.87 (t, *J* = 7.3 Hz, 3H). ^{13}C-NMR (125 MHz, $CDCl_3$): *δ* = 162.1 (C_q), 158.8 (C_q), 155.4 (C_q), 144.7 (C_q), 140.5 (CH), 139.0 (C_q), 127.7 (CH), 125.9 (C_q), 125.8 (CH), 125.1 (CH), 123.2 (C_q), 103.8 (CH), 99.4 (CH), 99.2 (CH), 55.9 (CH_3), 55.7 (CH_3), 34.1 (CH_2), 21.0 (CH_2), 13.8 (CH_3). IR (ATR): 2340, 2167, 1666, 1604, 1379, 1204, 1045, 840 cm^{-1}. MS (EI) *m/z* (relative intensity): 340 (15) $[M]^+$, 323 (30), 294 (40), 279 (50), 147 (100), 78 (40). HR-MS (EI) *m/z* calcd for $C_{19}H_{20}N_2O_4$ $[M]^+$: 340.1423, found: 340.1414.

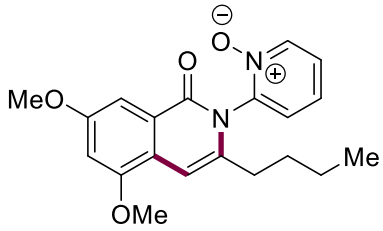

2-[5,7-Methoxy-1-oxo-3-*n*-butylisoquinolin-2(1*H*)-yl]-pyridine-2-oxide (104lf)

The slightly modified general procedure **A** was followed using benzamide **56l** (137 mg, 0.50 mmol) and alkyne **76f** (82.2 mg, 1.00 mmol) with $Co(OAc)_2{\cdot}4H_2O$ (25.7 mg, 20 mmol %). Purification by column chromatography on silica gel (CH_2Cl_2/acetone 1:1) yielded **104lf** (131 mg, 74%) as a yellow oil. ^{1}H-NMR (300 MHz, $CDCl_3$): *δ* = 8.44–8.36 (m, 1H), 7.48–7.41 (m, 1H), 7.41–7.35 (m, 2H), 7.34 (dd, *J* = 2.4, 0.6 Hz, 1H), 6.78–6.74 (m, 1H), 6.70 (d, *J* = 2.4 Hz, 1H), 3.92 (s, 3H), 3.87 (s, 3H), 2.36–2.14 (m, 2H), 1.58–1.46 (m, 2H), 1.31–1.21 (m, 2H), 0.82 (t, *J* = 7.3 Hz, 3H). ^{13}C-NMR (125 MHz, $CDCl_3$): *δ* = 162.1 (C_q), 158.8 (C_q), 155.4 (C_q), 144.7 (C_q), 140.5 (CH), 139.3 (C_q), 127.8 (CH), 125.9 (C_q), 125.8 (CH), 125.1 (CH), 123.2 (C_q), 103.8 (CH), 99.4 (CH), 99.2 (CH), 55.9 (CH_3), 55.7 (CH_3), 31.8 (CH_2), 29.9 (CH_2), 22.3 (CH_2), 13.8 (CH_3). IR (ATR): 2358, 1668, 1509, 1431, 1379, 1048, 842, 765 cm^{-1}. MS (EI) *m/z* (relative intensity): 354 (10) $[M]^+$, 337 (40), 294 (45), 279 (50), 161 (100), 78 (40). HR-MS (EI) *m/z* calcd for $C_{20}H_{22}N_2O_4$ $[M]^+$: 354.1580, found: 354.1571.

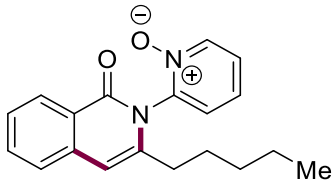

2-[3-*n*-Pentyl-1-oxoisoquinolin-2(1*H*)-yl]-pyridine-2-oxide (104ag)

The slightly modified general procedure **A** was followed using benzamide **56a** (107 mg, 0.50 mmol) and alkyne **76g** (96.2 mg, 1.00 mmol) with $Co(OAc)_2 \cdot 4H_2O$ (25.7 mg, 20 mmol %). Purification by column chromatography on silica gel (CH_2Cl_2/acetone 3:1) yielded **104ag** (85.2 mg, 55%) as a yellow oil. ^{1}H-NMR (400 MHz, $CDCl_3$): δ = 8.43–8.37 (m, 1H), 8.36–8.29 (m, 1H), 7.69–7.60 (m, 1H), 7.50–7.44 (m, 2H), 7.44–7.40 (m, 1H), 7.40–7.36 (m, 2H), 6.44 (s, 1H), 2.41–2.09 (m, 2H), 1.62–1.47 (m, 2H), 1.28–1.18 (m, 4H), 0.84 (t, J = 6.9 Hz, 3H). ^{13}C-NMR (100 MHz, $CDCl_3$): δ = 162.6 (C_q), 144.5 (C_q), 142.5 (C_q), 140.6 (CH), 137.5 (C_q), 133.2 (CH), 128.2 (CH), 128.0 (CH), 126.3 (CH), 126.0 (CH), 125.7 (CH), 125.3 (CH), 124.4 (C_q), 104.9 (CH), 31.9 (CH_2), 31.2 (CH_2), 27.2 (CH_2), 22.2 (CH_2), 13.8 (CH_3). IR (ATR): 2358, 2001, 1667, 1634, 1258, 824, 773, 749 cm^{-1}. MS (EI) *m/z* (relative intensity): 308 (45) $[M]^+$, 291 (80), 251 (60), 234 (100), 171 (35), 78 (60). HR-MS (EI) *m/z* calcd for $C_{19}H_{20}N_2O_2$ $[M]^+$: 308.1525, found: 308.1529.

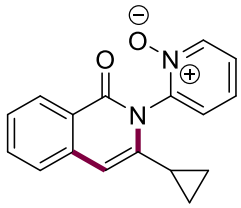

2-[3-Cyclopropyl-1-oxoisoquinolin-2(1*H*)-yl]-pyridine-2-oxide (104ah)

The slightly modified general procedure **A** was followed using benzamide **56a** (107 mg, 0.50 mmol) and alkyne **76h** (66.1 mg, 1.00 mmol) with $Co(OAc)_2 \cdot 4H_2O$ (25.7 mg, 20 mmol %). Purification by column chromatography on silica gel (CH_2Cl_2/acetone 3:1) yielded **104ah** (89.6 mg, 64%) as a white solid. M. p.: 216–218 °C. ^{1}H-NMR (300 MHz, $CDCl_3$): δ = 8.43–8.38 (m, 1H), 8.38–8.31 (m, 1H), 7.67–7.60 (m, 1H), 7.51–7.40 (m, 3H), 7.40–7.38 (m, 1H), 7.38–7.36 (m, 1H), 6.39 (s, 1H), 1.59–1.47 (m, 1H), 0.98–0.90 (m, 1H), 0.68–0.49 (m, 3H). ^{13}C-NMR (125 MHz, $CDCl_3$): δ = 162.4 (C_q), 145.0 (C_q), 143.2 (C_q), 140.4 (CH), 137.3 (C_q), 133.0 (CH), 128.1 (CH), 127.8 (CH), 126.4 (CH), 125.8 (CH), 125.7 (CH), 125.3 (CH), 124.7 (C_q), 104.7 (CH), 13.1 (CH), 7.3 (CH_2), 5.2 (CH_2). IR (ATR): 1667, 1631, 1602, 1431, 1390, 1264, 761, 728 cm^{-1}. MS (EI) *m/z* (relative intensity): 278 (40) $[M]^+$, 261 (85), 234 (80), 193 (50), 145 (55), 78 (100). HR-

MS (EI) *m/z* calcd for $C_{17}H_{14}N_2O_2$ $[M]^+$: 278.1055, found: 278.1057.

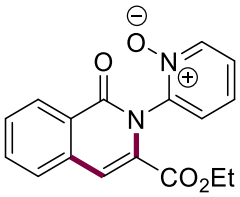

2-[3-(Ethoxycarbonyl)-1-oxoisoquinolin-2(1*H*)-yl]-pyridine-2-oxide (104ai)

The general procedure **A** was followed using benzamide **56a** (107 mg, 0.50 mmol) and alkyne **76i** (100 mg, 1.00 mmol). Purification by column chromatography on silica gel (CH_2Cl_2/acetone 3:1) yielded **104ai** (101 mg, 65%) as a white solid. M. p.: 173–175 °C. ^{1}H-NMR (300 MHz, $CDCl_3$): δ = 8.44–8.37 (m, 1H), 8.26 (dd, *J* = 7.6, 5.3 Hz, 1H), 7.78–7.70 (m, 1H), 7.68–7.64 (m, 1H), 7.63–7.55 (m, 2H), 7.48 (s, 1H), 7.40 (td, *J* = 7.8, 1.5 Hz, 1H), 7.34–7.27 (m, 1H), 4.22 (q, *J* = 7.1 Hz, 2H), 1.28 (t, *J* = 7.1 Hz, 3H). ^{13}C-NMR (125 MHz, $CDCl_3$): δ = 161.4 (C_q), 161.2 (C_q), 144.2 (C_q), 139.6 (CH), 134.8 (C_q), 133.5 (CH), 131.3 (C_q), 129.2 (CH), 128.6 (CH), 127.8 (CH), 127.4 (C_q), 127.0 (CH), 125.4 (CH), 124.7 (CH), 112.7 (CH), 62.0 (CH_2), 14.0 (CH_3). IR (ATR): 1720, 1673, 1491, 1433, 1402, 1255, 1215, 766 cm^{-1}. MS (EI) *m/z* (relative intensity): 310 (30) $[M]^+$, 237 (100), 109 (95), 181 (20), 89 (40), 78 (90). HR-MS (ESI) *m/z* calcd for $C_{17}H_{15}N_2O_4$ $[M+H^+]$: 311.1026, found: 311.1021.

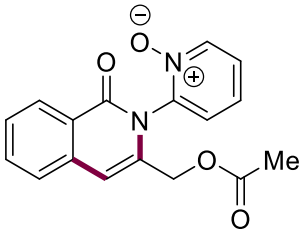

2-[3-(Acetyloxy)ethyl-1-oxoisoquinolin-2(1*H*)-yl]-pyridine-2-oxide (104aj)

The slightly modified general procedure **A** was followed using benzamide **56a** (107 mg, 0.50 mmol) and alkyne **76j** (98.1 mg, 1.00 mmol) with $Co(OAc)_2{\cdot}4H_2O$ (25.7 mg, 20 mmol %). Purification by column chromatography on silica gel (CH_2Cl_2/acetone 3:1) yielded **104aj** (85.5 mg, 55%) as a white solid. M. p.: 198–200 °C. ^{1}H-NMR (300 MHz, $CDCl_3$): δ = 8.40–8.27 (m, 2H), 7.73–7.64 (m, 1H), 7.59–7.46 (m, 3H), 7.44–7.28 (m, 2H), 6.73 (s, 1H), 4.92–4.57 (m, 2H), 1.96 (s, 3H). ^{13}C-NMR (125 MHz, $CDCl_3$): δ =

169.5 (C_q), 162.1 (C_q), 140.7 (CH), 136.3 (C_q), 135.9 (C_q), 133.3 (CH), 128.2 (CH), 128.1 (CH), 127.6 (CH), 126.4 (CH), 126.0 (CH), 125.5 (C_q), 125.3 (C_q), 125.3 (CH), 109.1 (CH), 62.4 (CH_2), 20.6 (CH_3). IR (ATR): 1731, 1670, 1636, 1603, 1484, 1398, 1030, 762 cm^{-1}. MS (EI) *m/z* (relative intensity): 310 (30) $[M]^+$, 267 (90), 251 (100), 234 (70), 173 (40), 78 (65). HR-MS (EI) *m/z* calcd for $C_{17}H_{14}N_2O_4$ $[M]^+$: 310.0954, found: 310.0944.

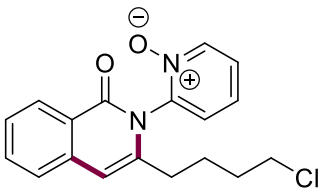

2-[3-(4-Chloro)-1-oxoisoquinolin-2(1*H*)-yl]-pyridine-2-oxide (104ak)

The slightly modified general procedure **A** was followed using benzamide **56a** (107 mg, 0.50 mmol) and alkyne **76k** (117 mg, 1.00 mmol) with $Co(OAc)_2{\cdot}4H_2O$ (25.7 mg, 20 mmol %). Purification by column chromatography on silica gel (CH_2Cl_2/acetone 3:1) yielded **104ak** (98.6 mg, 60%) as a white solid. M. p.: 176–177 °C. ^{1}H-NMR (300 MHz, $CDCl_3$): δ = 8.43–8.33 (m, 1H), 8.30 (dt, J = 7.4, 0.6 Hz, 1H), 7.68–7.58 (m, 1H), 7.49–7.43 (m, 2H), 7.43–7.38 (m, 1H), 7.38–7.32 (m, 2H), 6.43 (s, 1H), 3.54–3.36 (m, 2H), 2.42–2.14 (m, 2H), 1.78–1.62 (m, 4H). ^{13}C-NMR (125 MHz, $CDCl_3$): δ = 162.6 (C_q), 144.2 (C_q), 141.6 (C_q), 140.6 (CH), 137.2 (C_q), 133.2 (CH), 128.1 (CH), 128.0 (CH), 126.5 (CH), 126.1 (CH), 125.7 (CH), 125.5 (CH), 124.5 (C_q), 105.1 (CH), 44.4 (CH_2), 31.6 (CH_2), 31.1 (CH_2), 24.7 (CH_2). IR (ATR): 2342, 2003, 1669, 1631, 1484, 1431, 1266, 761 cm^{-1}. MS (EI) *m/z* (relative intensity): 328 (40) $[M]^+$, 311 (45), 265 (20), 251 (60), 234 (100), 195 (35). HR-MS (EI) *m/z* calcd for $C_{18}H_{17}ClN_2O_2$ $[M]^+$: 328.0979, found: 328.0976.

5.3.1.2. Competition Experiments

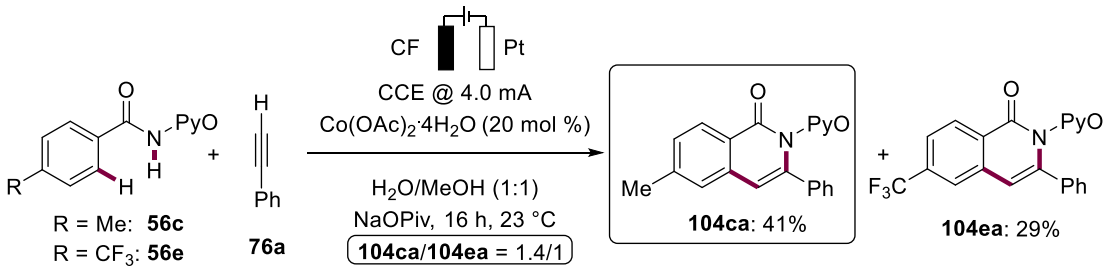

The electrocatalysis was carried out in an undivided cell, with a CF anode (10 mm × 25 mm × 6 mm) and a platinum cathode (10 mm × 25 mm × 0.125 mm). Benzamide **56c** (114 mg, 0.50 mmol), benzamide **56e** (141 mg, 0.50 mmol), alkyne **76a** (0.50 mmol, 1.0 equiv), NaOPiv (124 mg, 1.0 mmol, 2.0 equiv) and $Co(OAc)_2{\cdot}4H_2O$ (25.7 mg, 20 mol %) were dissolved in H_2O/MeOH (1:1, 10 mL). Electrocatalysis was performed at ambient temperature with a constant current of 4.0 mA maintained for 16 h. The reaction was stopped by adding saturated aqueous $NaHCO_3$ solution (10 mL). The CF anode was washed with CH_2Cl_2 (3 × 10 mL) in an ultrasonic bath. The washings were added to the reaction mixture and the combined phases were extracted with CH_2Cl_2 (4 × 10 mL), then dried over Na_2SO_4. Evaporation of the solvent and subsequent column chromatography using CH_2Cl_2/acetone 6:1 yielded **104ca** (68 mg, 41%) and **104ea** (55 mg, 29%).

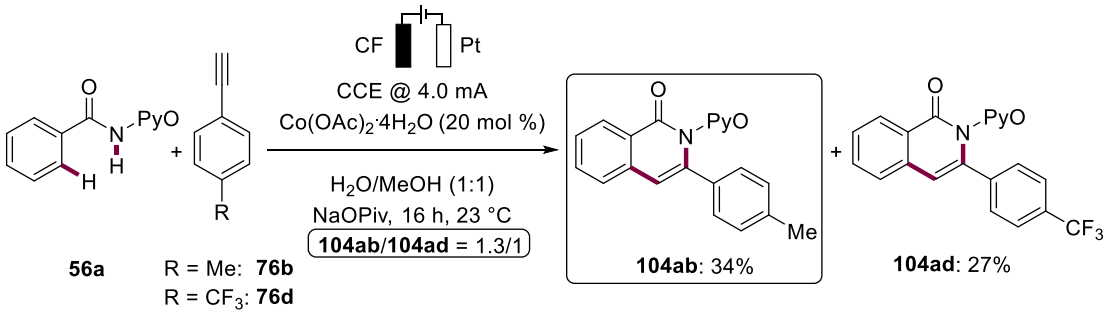

The electrocatalysis was carried out in an undivided cell, with a CF anode (10 mm × 25 mm × 6 mm) and a platinum cathode (10 mm × 25 mm × 0.125 mm). Benzamide **56a** (107 mg, 0.50 mmol), alkyne **76b** (0.50 mmol, 1.0 equiv), alkyne **76d** (0.50 mmol, 1.0 equiv), NaOPiv (124 mg, 1.0 mmol, 2.0 equiv) and $Co(OAc)_2{\cdot}4H_2O$ (25.7 mg, 20 mol %) were dissolved in H_2O/MeOH (1:1, 10 mL). Electrocatalysis was performed at

ambient temperature with a constant current of 4.0 mA maintained for 16 h. The reaction was stopped by adding saturated aqueous $NaHCO_3$ solution (10 mL). The CF anode was washed with CH_2Cl_2 (3 × 10 mL) in an ultrasonic bath. The washings were added to the reaction mixture and the combined phases were extracted with CH_2Cl_2 (4 × 10 mL), then dried over Na_2SO_4. Evaporation of the solvent and subsequent column chromatography using CH_2Cl_2/acetone 6:1 yielded **104ab** (55.5 mg, 34%) and **104ad** (51.5 mg, 27%).

5.3.1.3. H/D Exchange Experiments

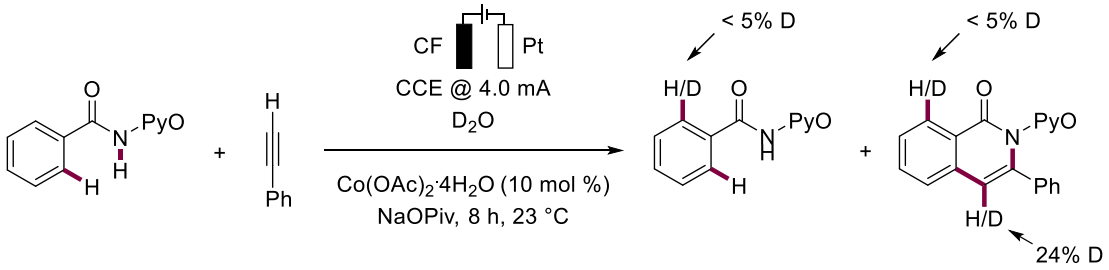

56a **76a** [D]$_n$-**56a**: 32% [D]$_n$-**104aa**: 50%

The electrocatalysis was carried out in an undivided cell, with a CF anode (10 mm × 25 mm × 6 mm) and a platinum cathode (10 mm × 25 mm × 0.125 mm). Benzamide **56a** (107 mg, 0.50 mmol, 1.0 equiv), alkyne **76a** (102 mg, 2.0 equiv), NaOPiv (124 mg, 1.0 mmol, 2.0 equiv) and $Co(OAc)_2{\cdot}4H_2O$ (25.7 mg, 20 mol %) were placed in a 20 mL cell and dissolved in D_2O (10 mL). Electrocatalysis was performed at ambient temperature with a constant current of 4.0 mA maintained for 8 h. The reaction was stopped by adding saturated aqueous $NaHCO_3$ solution (10 mL). The CF anode was washed with CH_2Cl_2 (3 × 10 mL) in an ultrasonic bath. The washings were added to the reaction mixture and the combined phases were extracted with CH_2Cl_2 (4 × 10 mL), then dried over Na_2SO_4. Evaporation of the solvent and subsequent column chromatography (CH_2Cl_2/acetone 3:1) yielded [D]$_n$-**104aa** (78.9 mg, 50%) as a white solid (figure 5.1) and [D]$_n$-**56a** (30 mg, 28%) as a white solid (figure 5.2). The D-incorporation was estimated by ^{1}H-NMR spectroscopy.

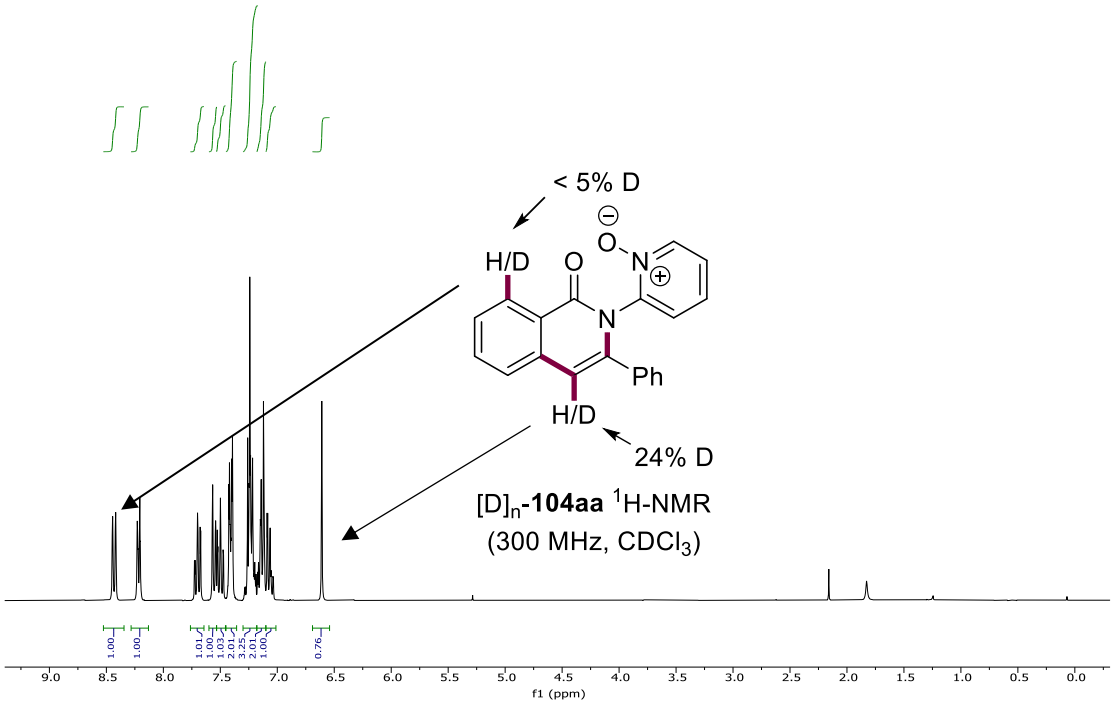

Figure 5.1. ^{1}H-NMR of **104aa** from the deuteration study.

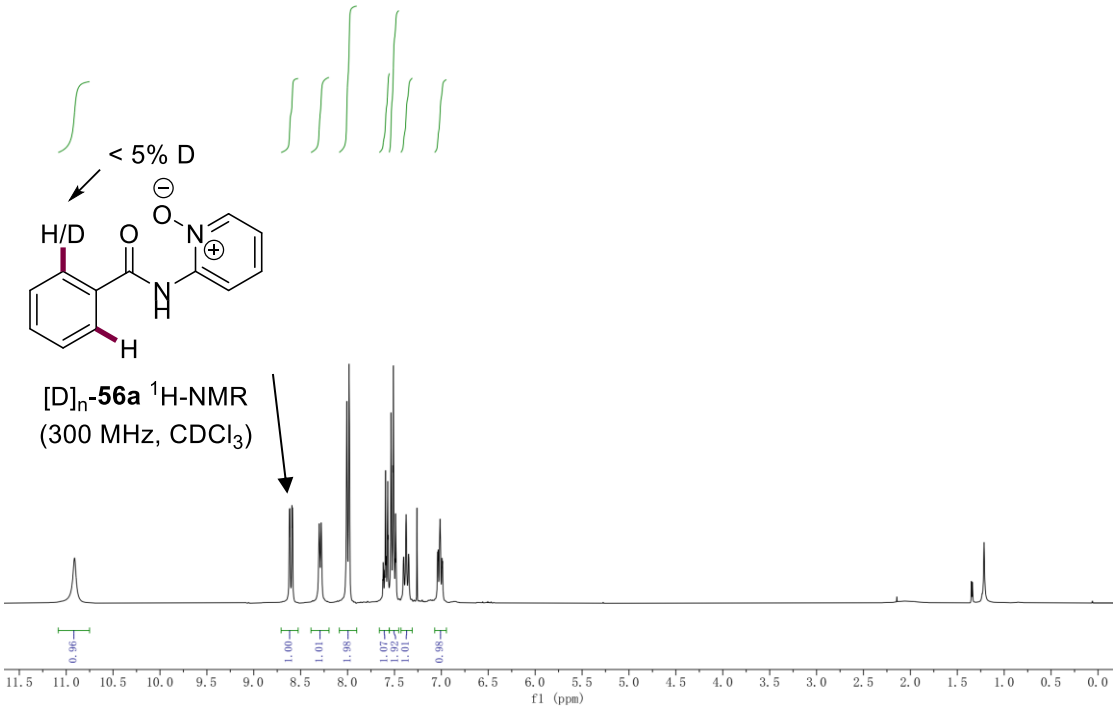

Figure 5.2. ^{1}H-NMR of reisolated **56a** from the deuteration study.

5.3.1.4. Kinetic Isotope Effect Studies

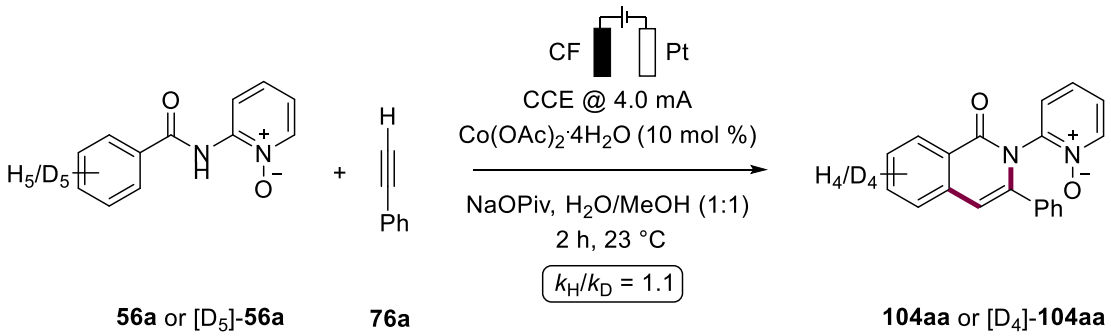

56a or [D_5]-**56a** **76a** **104aa** or [D_4]-**104aa**

Two parallel reactions using substrates **56a** and [D_5]-**56a** (0.50 mmol each) were carried out to determine the KIE by comparison of the initial rates (figure 5.3). After 10 minutes to reach a stable constant current of 4.0 mA, aliquots of 0.40 mL were removed from the cell every twenty minutes. The reaction mixture was extracted with CH_2Cl_2 (3 × 2.0 mL). After evaporation of solvent, the crude mixture was analyzed by ^{1}H-NMR spectroscopy using 1,3,5-trimethoxybenzene as an internal standard.

Time [min]	10	20	40	60	80	100	120
104aa [%]	2.6	4.8	9.0	12.7	16.3	18.0	22.0
[D_4]-**104aa** [%]	-	1.5	3.4	6.3	9.7	13.2	16.9

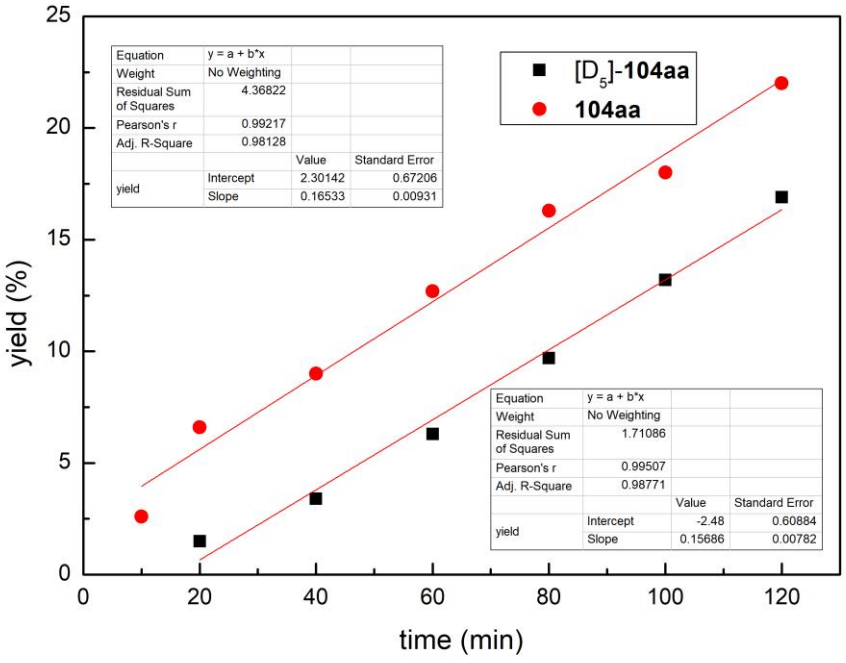

Figure 5.3. Initial rates analysis of **104aa** and [D_4]-**104aa**.

5.3.1.5. Cyclization Reactions

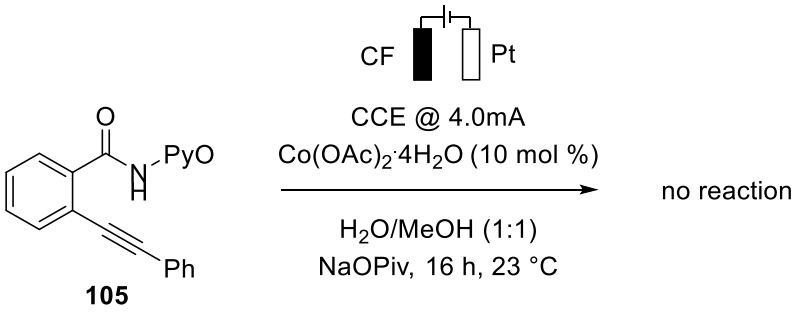

The electrocatalysis was carried out in an undivided cell, with a CF anode (10 mm × 25 mm × 6 mm) and a platinum cathode (10 mm × 25 mm × 0.125 mm). **105** (157 mg, 0.50 mmol), NaOPiv (124 mg, 1.0 mmol, 2.0 equiv) and $Co(OAc)_2 \cdot 4H_2O$ (25.7 mg, 20 mol %) were placed in a 20 mL cell and dissolved in 10 mL of H_2O/MeOH (1:1). Electrocatalysis was performed at ambient temperature with a constant current of 4.0 mA maintained for 16 h. The reaction was stopped by adding saturated aqueous $NaHCO_3$ (10 mL). The CF anode was washed with CH_2Cl_2 (3 × 10 mL) in an ultrasonic bath. The washings were added to the reaction mixture and the combined phases were extracted with CH_2Cl_2 (4 × 10 mL), then dried over Na_2SO_4. No product formation was detected by GC-MS analysis.

5.3.2. Cupraelectro-Catalyzed Cascade Annulation by C–H Alkynylation and Decarboxylative C–H/C–C Manifolds

5.3.2.1. Characterization Data

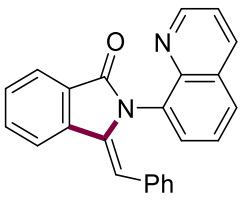

(*Z*)-3-Benzylidene-2-(quinolin-8-yl) isoindolin-1-one (110aa)

The general procedure **B** was followed using benzamide **54a** (62 mg, 0.25 mmol) and alkyne **76a** (51 mg, 0.50 mmol). Purification by column chromatography on silica gel (*n*-hexane/EtOAc: 5/1) yielded **110aa** (78.7 mg, 90%, *E*/*Z* = 1:13) as a white solid.

Mixture with M. p.: 210–215 °C. Resonances are reported for (*Z*)-**110aa**. ^{1}H-NMR (300 MHz, $CDCl_3$): δ = 8.85 (dd, *J* = 4.2, 1.7 Hz, 1H), 8.02–7.94 (m, 2H), 7.88 (d, *J* = 7.7 Hz, 1H), 7.68 (td, *J* = 7.5, 1.2 Hz, 1H), 7.61–7.53 (m, 2H), 7.48 (dd, *J* = 7.4, 1.5 Hz, 1H), 7.34–7.27 (m, 2H), 6.81 (s, 0.93H, *Z*), 6.71–6.64 (m, 1H), 6.60–6.48 (m, 4H), 6.02 (s, 0.07H, *E*). ^{13}C-NMR (125 MHz, $CDCl_3$): δ = 167.9 (C_q), 150.2 (CH), 144.3 (C_q), 138.6 (C_q), 136.0 (C_q), 135.6 (CH), 134.1 (C_q), 133.4 (C_q), 132.1 (CH), 129.9 (CH), 128.9 (CH), 128.7 (C_q), 128.2 (C_q), 128.2 (CH), 128.0 (CH), 126.2 (CH), 125.9 (CH), 125.5 (CH), 123.8 (CH), 121.1 (CH), 119.5 (CH), 107.2 (CH). IR (ATR): 3061, 1704, 1596, 1472, 1377, 1221, 1024, 716 cm^{-1}. MS (ESI) *m/z* (relative intensity): 371 (10) $[M+Na]^+$, 349 (60) $[M+H]^+$. HR-MS (ESI) *m/z* calcd for $C_{24}H_{17}N_2O$ $[M+H]^+$: 349.1335, found: 349.1324.

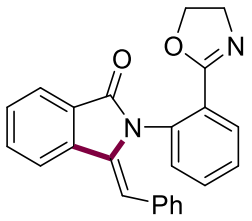

(*Z*)-3-Benzylidene-2-(2-(4,5-dihydrooxazol-2-yl) phenyl) isoindolin-1-one (109aa)

The general procedure **B** was followed using benzamide **91a** (67 mg, 0.25 mmol) and alkyne **76a** (51 mg, 0.50 mmol). Purification by column chromatography on silica gel (*n*-hexane/EtOAc: 5/1) yielded **109aa** (18 mg, 20%) as colorless oil. ^{1}H-NMR (400 MHz, $CDCl_3$): δ = 7.92 (d, *J* = 7.6 Hz, 1H), 7.86–7.83 (m, 1H), 7.73 (dd, *J* = 7.7, 1.7 Hz, 1H), 7.66 (dd, *J* = 7.6, 1.2 Hz, 1H), 7.54 (dd, *J* = 7.5, 0.9 Hz, 1H), 7.13 (dd, *J* = 7.6, 1.4 Hz, 1H), 7.06 (dd, *J* = 7.6, 1.5 Hz, 1H), 6.97–6.87 (m, 6H), 6.81 (s, 1H), 4.21 (t, *J* = 9.2 Hz, 2H), 3.98–3.85 (m, 2H). ^{13}C-NMR (100 MHz, $CDCl_3$): δ = 167.8 (C_q), 163.1 (C_q), 138.8 (C_q), 135.1 (C_q), 134.9 (C_q), 133.5 (C_q), 132.2 (CH), 130.5 (CH), 130.0 (CH), 129.4 (CH), 129.0 (CH), 128.8 (CH), 128.1 (C_q), 127.4 (CH), 127.2 (CH), 126.5 (CH), 126.3 (C_q), 123.8 (CH), 119.4 (CH), 107.0 (CH), 67.4 (CH_2), 55.1 (CH_2). IR (ATR): 2928, 1712, 1650, 1493, 1396, 1188, 1051, 944 cm^{-1}. MS (ESI) *m/z* (relative intensity): 389 (10) $[M+Na]^+$, 367 (100) $[M+H]^+$. HR-MS (ESI) *m/z* calcd for $C_{24}H_{19}N_2O_2$ $[M+H]^+$: 367.1441, found: 367.1444.

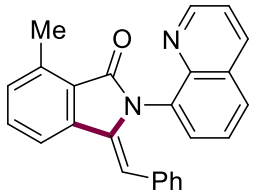

(*Z*)-3-Benzylidene-7-methyl-2-(quinolin-8-yl) isoindolin-1-one (110ba)

The general procedure **B** was followed using benzamide **54b** (66 mg, 0.25 mmol) and alkyne **76a** (51 mg, 0.50 mmol). Purification by column chromatography on silica gel (*n*-hexane/EtOAc: 5/1) yielded **110ba** (75.4 mg, 83%, *E*/*Z* = 1:10) as a white solid. M. p.: 215–220 °C. Resonances are reported for (*Z*)-**110ba**. ^{1}H-NMR (300 MHz, $CDCl_3$): δ = 8.88 (dd, *J* = 4.2, 1.7 Hz, 1H), 7.97 (dd, *J* = 8.3, 1.7 Hz, 1H), 7.71 (d, *J* = 7.9 Hz, 1H), 7.60–7.50 (m, 2H), 7.45 (dd, *J* = 7.4, 1.4 Hz, 1H), 7.33–7.31 (m, 1H), 7.31–7.24 (m, 2H), 6.77 (s, 0.91H, *Z*), 6.71–6.63 (m, 1H), 6.61–6.48 (m, 4H), 5.96 (s, 0.09H, *E*), 2.78 (s, 3H). ^{13}C-NMR (125 MHz, $CDCl_3$): δ = 168.7 (C_q), 150.2 (CH), 144.4 (C_q), 139.1 (C_q), 137.9 (C_q), 135.9 (C_q), 135.6 (CH), 134.3 (C_q), 133.7 (C_q), 131.6 (CH), 130.9 (CH), 129.9 (CH), 128.7 (C_q), 128.3 (CH), 128.1 (CH), 126.1 (CH), 125.8 (CH), 125.5 (CH), 125.4 (C_q), 121.0 (CH), 117.0 (CH), 106.3 (CH), 17.6 (CH_3). IR (ATR): 3059, 2925, 1708, 1597, 1474, 1397, 1110, 888 cm^{-1}. MS (EI) *m/z* (relative intensity): 362 (90) $[M]^+$, 333 (10), 318 (10), 285 (100), 242 (10), 189 (10). HR-MS (EI) *m/z* calcd for $C_{25}H_{18}N_2O$ $[M]^+$: 362.1419, found: 362.1413.

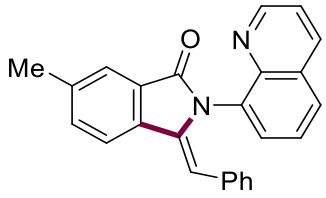

(*Z*)-3-Benzylidene-6-methyl-2-(quinolin-8-yl) isoindolin-1-one (110ca)

The general procedure **B** was followed using benzamide **54c** (66 mg, 0.25 mmol) and alkyne **76a** (51 mg, 0.50 mmol). Purification by column chromatography on silica gel (*n*-hexane/EtOAc: 5/1) yielded **110ca** (78.8 mg, 87%, *E*/*Z* = 1:13) as yellow oil. Resonances are reported for (*Z*)-**110ca**. ^{1}H-NMR (400 MHz, $CDCl_3$): δ = 8.84 (dd, *J* = 4.2, 1.7 Hz, 1H), 7.96 (dd, *J* = 8.3, 1.8 Hz, 1H), 7.81–7.78 (m, 1H), 7.76 (d, *J* = 7.9 Hz, 1H), 7.57 (dd, *J* = 8.2, 1.4 Hz, 1H), 7.51–7.45 (m, 2H), 7.31–7.25 (m, 2H), 6.74 (s, 0.93H, *Z*), 6.69–6.62 (m, 1H), 6.57–6.49 (m, 4H), 5.96 (s, 0.07H, *E*), 2.52 (s, 3H). ^{13}C-

NMR (100 MHz, $CDCl_3$): δ = 168.2 (C_q), 150.2 (CH), 144.4 (C_q), 139.3 (C_q), 136.2 (C_q), 136.1 (C_q), 135.7 (CH), 134.3 (C_q), 133.6 (C_q), 133.2 (CH), 129.9 (CH), 128.8 (C_q), 128.4 (C_q), 128.2 (CH), 128.1 (CH), 126.2 (CH), 125.8 (CH), 125.5 (CH), 123.9 (CH), 121.1 (CH), 119.4 (CH), 106.5 (CH), 21.5 (CH_3). IR (ATR): 3051, 2157, 1713, 1596, 1474, 1399, 1188, 803 cm^{-1}. MS (EI) *m/z* (relative intensity): 362 (80) $[M]^+$, 333 (15), 318 (15), 285 (100), 273 (10), 165 (10). HR-MS (ESI) *m/z* calcd for $C_{25}H_{19}N_2O$ $[M+H]^+$: 363.1492, found: 363.1494.

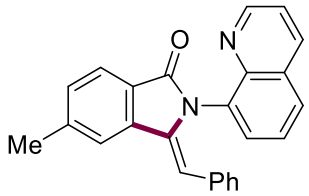

(*Z*)-4-Benzylidene-6-methyl-2-(quinolin-8-yl) isoindolin-1-one (110da)

The general procedure **B** was followed using benzamide **54d** (66 mg, 0.25 mmol) and alkyne **76a** (51 mg, 0.50 mmol). Purification by column chromatography on silica gel (*n*-hexane/EtOAc: 2/1) yielded **110da** (65.2 mg, 72%, *E/Z* = 1:12) as white solid. M. p.: 170–176 °C. Resonances are reported for (*Z*)-**110da**. ^{1}H-NMR (400 MHz, $CDCl_3$): δ = 8.82 (dd, *J* = 4.2, 1.7 Hz, 1H), 7.94 (dd, *J* = 8.3, 1.8 Hz, 1H), 7.85 (d, *J* = 7.8 Hz, 1H), 7.66 (s, 1H), 7.55 (d, *J* = 8.2 Hz, 1H), 7.45 (dd, *J* = 7.4, 1.4 Hz, 1H), 7.35 (d, *J* = 7.8 Hz, 1H), 7.31–7.24 (m, 2H), 6.75 (s, 0.92H, *Z*), 6.69–6.60 (m, 1H), 6.57–6.45 (m, 4H), 5.96 (s, 0.08H, *E*), 2.54 (s, 3H). ^{13}C-NMR (100 MHz, $CDCl_3$): δ = 168.2 (C_q), 150.3 (CH), 144.5 (C_q), 142.9 (CH), 139.1 (C_q), 136.2 (C_q), 135.7 (CH), 134.4 (C_q), 133.7 (C_q), 130.2 (CH), 130.0 (CH), 128.9 (C_q), 128.3 (C_q), 128.2 (CH), 126.3 (CH), 126.0 (C_q), 125.9 (CH), 125.6 (CH), 123.8 (CH), 121.2 (CH), 120.0 (CH), 106.9 (CH), 22.2 (CH_3). IR (ATR): 3020, 1755, 1620, 1464, 1232, 745 cm^{-1}. MS (ESI) *m/z* (relative intensity): 385 (30) $[M+Na]^+$, 363 (100) $[M+H]^+$. HR-MS (ESI) *m/z* calcd for $C_{25}H_{19}N_2O$ $[M+H]^+$: 363.1492, found: 363.1495.

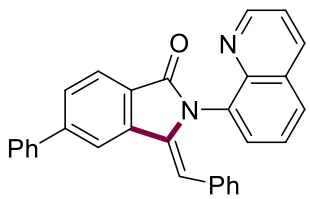

(*Z*)-3-Benzylidene-5-phenyl-2-(quinolin-8-yl) isoindolin-1-one (110ea)

The general procedure **B** was followed using benzamide **54e** (81 mg, 0.25 mmol) and alkyne **76a** (51 mg, 0.50 mmol). Purification by column chromatography on silica gel (*n*-hexane/EtOAc: 5/1) yielded **110ea** (76.5 mg, 72%, *E*/*Z* = 1:8) as yellow oil. Resonances reported for (*Z*)-**110ea**: ^{1}H-NMR (400 MHz, $CDCl_3$): δ = 8.86 (dd, *J* = 4.2, 1.7 Hz, 1H), 8.09–8.03 (m, 2H), 7.97 (dd, *J* = 8.3, 1.7 Hz, 1H), 7.79 (dd, *J* = 7.9, 1.5 Hz, 1H), 7.74–7.71 (m, 2H), 7.59 (dd, *J* = 8.2, 1.4 Hz, 1H), 7.53–7.50 (m, 2H), 7.47–7.39 (m, 2H), 7.34–7.28 (m, 2H), 6.89 (s, 1H), 6.72–6.66 (m, 1H), 6.60–6.53 (m, 4H). ^{13}C-NMR (100 MHz, $CDCl_3$): δ = 167.9 (C_q), 150.3 (CH), 145.6 (C_q), 144.3 (C_q), 140.6 (C_q), 139.2 (C_q), 136.1 (C_q), 135.7 (CH), 134.2 (C_q), 133.5 (C_q), 130.0 (CH), 128.9 (CH), 128.8 (CH), 128.8 (C_q), 128.4 (CH), 128.3 (CH), 128.1 (CH), 127.5 (CH), 127.1 (C_q), 126.2 (CH), 126.0 (CH), 125.6 (CH), 124.3 (CH), 121.1 (CH), 118.3 (CH), 107.4 (CH). Resonances reported for (*E*)-**110ea**: ^{1}H-NMR (400 MHz, $CDCl_3$): δ = 8.93 (dd, *J* = 4.2, 1.7 Hz, 1H), 8.23 (dd, *J* = 8.3, 1.7 Hz, 1H), 8.03 (dd, *J* = 7.4, 1.3 Hz, 1H), 7.98–7.95 (m, 1H), 7.86 (dd, *J* = 7.3, 1.4 Hz, 1H), 7.74–7.72 (m, 1H), 7.71–7.68 (m, 2H), 7.53–7.53 (m, 1H), 7.53–7.52 (m, 2H), 7.40–7.37 (m, 2H), 7.36–7.35 (m, 1H), 7.34–7.33 (m, 1H), 6.60–6.53 (m, 4H), 6.07 (s, 1H). ^{13}C-NMR (100 MHz, $CDCl_3$): δ = 166.8 (C_q), 151.2 (CH), 144.9 (C_q), 144.7 (C_q), 140.3 (C_q), 138.9 (C_q), 136.2 (CH), 135.3 (C_q), 132.9 (C_q), 131.3 (CH), 129.6 (C_q), 129.5 (CH), 129.4 (CH), 129.2 (C_q), 128.8 (CH), 128.4 (CH), 127.9 (CH), 127.5 (CH), 127.1 (C_q), 127.1 (CH), 126.3 (CH), 126.2 (CH), 124.1 (CH), 121.9 (CH), 121.8 (CH), 112.1 (CH). IR (ATR): 3060, 1777, 1709, 1597, 1474, 1376, 1179, 886 cm^{-1}. MS (EI) *m/z* (relative intensity): 424 (90) $[M]^+$, 347 (100), 318 (10), 252 (15), 212 (10), 77 (5). HR-MS (EI) *m/z* calcd for $C_{30}H_{20}N_2O$ $[M]^+$: 424.1576, found: 424.1569.

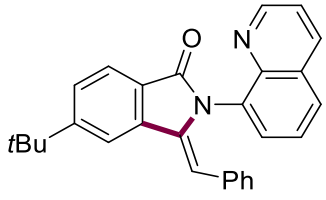

(*Z*)-3-Benzylidene-5-(*tert*-butyl)-2-(quinolin-8-yl) isoindolin-1-one (110fa)

The general procedure **B** was followed using benzamide **54f** (76 mg, 0.25 mmol) and alkyne **76a** (51 mg, 0.50 mmol). Purification by column chromatography on silica gel

(*n*-hexane/EtOAc: 5/1) yielded **110fa** (56.2 mg, 56%) as a yellow solid. M. p.: 213–219 °C. ^{1}H-NMR (300 MHz, $CDCl_3$): δ = 8.84 (dd, *J* = 4.2, 1.7 Hz, 1H), 7.97–7.89 (m, 3H), 7.63 (dd, *J* = 8.0, 1.6 Hz, 1H), 7.57 (dd, *J* = 8.2, 1.5 Hz, 1H), 7.49 (dd, *J* = 7.4, 1.4 Hz, 1H), 7.33–7.29 (m, 1H), 7.29–7.26 (m, 1H), 6.83 (s, 1H), 6.70–6.63 (m, 1H), 6.58–6.49 (m, 4H), 1.46 (s, 9H). ^{13}C-NMR (125 MHz, $CDCl_3$): δ = 167.9 (C_q), 156.0 (C_q), 150.1 (CH), 144.3 (C_q), 138.5 (C_q), 136.3 (C_q), 135.6 (CH), 134.2 (C_q), 133.6 (C_q), 130.0 (CH), 128.7 (C_q), 128.1 (CH), 128.0 (CH), 126.7 (CH), 126.1 (CH), 125.8 (C_q), 125.8 (CH), 125.5 (CH), 123.5 (CH), 121.0 (CH), 116.1 (CH), 106.6 (CH), 35.6 (C_q), 31.4 (CH_3). IR (ATR): 2963, 1712, 1597, 1475, 1396, 1221, 1101, 791 cm^{-1}. MS (EI) *m/z* (relative intensity): 404 (85) $[M]^+$, 387 (20), 327 (100), 311 (20), 202 (10), 165 (10). HR-MS (EI) *m/z* calcd for $C_{28}H_{24}N_2O$ $[M]^+$: 404.1889, found: 404.1892.

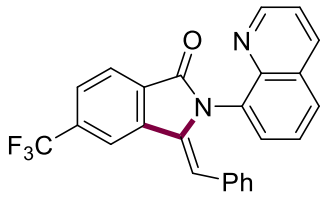

(*Z*)-3-Benzylidene-2-(quinolin-8-yl)-5-(trifluoromethyl) isoindolin-1-one (110ga)

The general procedure **B** was followed using benzamide **54g** (79 mg, 0.25 mmol) and alkyne **76a** (51 mg, 0.50 mmol). Purification by column chromatography on silica gel (*n*-hexane/EtOAc: 5/1) yielded **110ga** (80 mg, 77%, *E*/*Z* = 1:12) as a yellow solid. M. p.: 215–220 °C. Resonances are reported for (*Z*)-**110ga**. ^{1}H-NMR (400 MHz, $CDCl_3$): δ = 8.83 (dd, *J* = 4.2, 1.7 Hz, 1H), 8.17–8.14 (m, 1H), 8.11 (dd, *J* = 8.0, 0.7 Hz, 1H), 7.97 (dd, *J* = 8.3, 1.7 Hz, 1H), 7.85–7.81 (m, 1H), 7.61 (dd, *J* = 8.2, 1.4 Hz, 1H), 7.50 (dd, *J* = 7.3, 1.4 Hz, 1H), 7.37–7.29 (m, 2H), 6.90 (s, 0.92H, *Z*), 6.73–6.67 (m, 1H), 6.55 (d, *J* = 4.5 Hz, 4H), 6.14 (s, 0.08H, *E*). ^{13}C-NMR (100 MHz, $CDCl_3$): δ = 166.7 (C_q), 150.4 (CH), 144.1 (C_q), 138.8 (C_q), 135.8 (CH), 135.1 (C_q), 134.1 (q, $^{2}J_{C–F}$ = 32.5 Hz, C_q), 133.7 (C_q), 132.8 (C_q), 131.0 (C_q), 129.9 (CH), 128.8 (C_q), 128.6 (CH), 128.0 (CH), 126.4 (CH), 126.3 (CH), 125.8 (q, $^{3}J_{C–F}$ = 3.6 Hz, CH), 125.6 (CH), 124.6 (CH), 123.8 (q, $^{1}J_{C–F}$ = 273.4 Hz, C_q), 121.3 (CH), 117.1 (q, $^{3}J_{C–F}$ = 4.1 Hz, CH), 109.2 (CH). ^{19}F-NMR (375 MHz, $CDCl_3$): δ = –62.43 (s, *Z*), –62.77 (s, *E*). IR (ATR): 3060, 1715, 1596, 1501, 1398, 1322, 1127, 694 cm^{-1}. MS (EI) *m/z* (relative intensity): 416 (95) $[M]^+$, 387

(25), 347 (10), 339 (100), 242 (10), 159 (5). HR-MS (EI) *m/z* calcd for $C_{25}H_{15}F_3N_2O$ $[M]^+$: 416.1136, found: 416.1116.

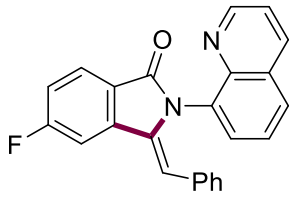

(*Z*)-3-Benzylidene-5-fluoro-2-(quinolin-8-yl) isoindolin-1-one (110ha)

The general procedure **B** was followed using benzamide **1o** (67 mg, 0.25 mmol) and alkyne **76a** (51 mg, 0.50 mmol). Purification by column chromatography on silica gel (*n*-hexane/EtOAc: 5/1) yielded **110ha** (70.2 mg, 77%) as yellow oil. ^{1}H-NMR (400 MHz, $CDCl_3$): δ = 8.84 (dd, J = 4.2, 1.7 Hz, 1H), 7.99–7.95 (m, 2H), 7.58 (dd, J = 8.2, 1.4 Hz, 1H), 7.53 (dd, J = 8.3, 2.3 Hz, 1H), 7.48 (dd, J = 7.4, 1.4 Hz, 1H), 7.32–7.27 (m, 2H), 7.26–7.23 (m, 1H), 6.75 (s, 1H), 6.71–6.66 (m, 1H), 6.56–6.52 (m, 4H). ^{13}C-NMR (100 MHz, $CDCl_3$): δ = 167.0 (C_q), 165.8 (d, $^1J_{C–F}$ = 251.3 Hz, C_q), 150.3 (CH), 144.2 (C_q), 141.1 (d, $^3J_{C–F}$ = 10.4 Hz, C_q), 135.7 (CH), 135.3 (d, $^4J_{C–F}$ = 3.6 Hz, C_q), 133.9 (C_q), 133.0 (C_q), 129.9 (CH), 128.8 (C_q), 128.4 (CH), 128.0 (CH), 126.3 (CH), 126.2 (CH), 126.1 (d, $^3J_{C–F}$ = 10.0 Hz, CH), 125.6 (CH), 124.4 (d, $^4J_{C–F}$ = 1.9 Hz, C_q), 121.2 (CH), 116.9 (d, $^2J_{C–F}$ = 24.0 Hz, CH), 108.3 (CH), 106.7 (d, $^2J_{C–F}$ = 24.8 Hz, CH). ^{19}F-NMR (376 MHz, $CDCl_3$): δ = –106.42 (m). IR (ATR): 3060, 1711, 1618, 1475, 1398, 1243, 776, 699 cm^{-1}. MS (EI) *m/z* (relative intensity): 366 (65) $[M]^+$, 337 (15), 289 (100), 277 (60), 183 (15), 128 (10). HR-MS (ESI) *m/z* calcd for $C_{24}H_{16}FN_2O$ $[M+H]^+$: 367.1241, found: 367.1241.

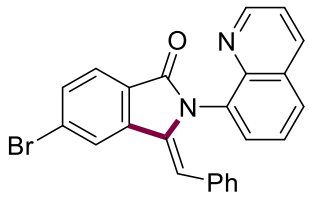

(*Z*)-3-Benzylidene-5-bromo-2-(quinolin-8-yl) isoindolin-1-one (110ia)

The general procedure **B** was followed using benzamide **54i** (82 mg, 0.25 mmol) and alkyne **76a** (51 mg, 0.50 mmol). Purification by column chromatography on silica gel (*n*-hexane/EtOAc: 5/1) yielded **110ia** (81.3 mg, 76%) as a white solid. M. p.: 217–224 °C. ^{1}H-NMR (300 MHz, $CDCl_3$): δ = 8.82 (d, J = 3.7 Hz, 1H), 8.05–8.01 (m, 1H),

7.95 (d, *J* = 8.1 Hz, 1H), 7.85 (d, *J* = 8.0 Hz, 1H), 7.71–7.66 (m, 1H), 7.58 (d, *J* = 8.3 Hz, 1H), 7.47 (d, *J* = 7.4 Hz, 1H), 7.33–7.24 (m, 2H), 6.76 (s, 1H), 6.72–6.64 (m, 1H), 6.55–6.50 (m, 4H). ^{13}C-NMR (125 MHz, $CDCl_3$): *δ* = 167.0 (C_q), 150.2 (CH), 144.1 (C_q), 140.2 (C_q), 135.6 (CH), 134.8 (C_q), 133.7 (C_q), 132.9 (C_q), 132.1 (CH), 129.8 (CH), 128.7 (C_q), 128.4 (CH), 127.9 (CH), 126.9 (C_q), 126.9 (C_q), 126.2 (CH), 126.1 (CH), 125.5 (CH), 125.2 (CH), 122.9 (CH), 121.1 (CH), 108.5 (CH). IR (ATR): 2992, 2206, 1720, 1498, 1398, 1045, 791, 395 cm^{-1}. MS (EI) *m/z* (relative intensity): 428 (65) $[M]^+$ (^{81}Br), 426 (60) $[M]^+$ (^{79}Br), 397 (10), 351 (100), 318 (30), 242 (15), 176 (20). HR-MS (ESI) *m/z* calcd for $C_{24}H_{16}{}^{79}BrN_2O$ $[M+H]^+$: 427.0441, found: 427.0443.

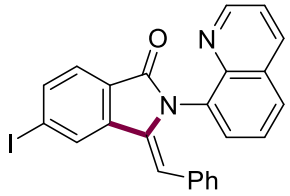

(*Z*)-3-Benzylidene-5-iodo-2-(quinolin-8-yl) isoindolin-1-one (110ja)

The general procedure **B** was followed using benzamide **54j** (93 mg, 0.25 mmol) and alkyne **76a** (51 mg, 0.50 mmol). Purification by column chromatography on silica gel (*n*-hexane/EtOAc: 5/1) yielded **110ja** (70.2 mg, 59%) as a white solid. M. p.: 243–247 °C. ^{1}H-NMR (300 MHz, $CDCl_3$): *δ* = 8.83 (dd, *J* = 4.2, 1.7 Hz, 1H), 8.26 (d, *J* = 1.3 Hz, 1H), 7.96 (dd, *J* = 8.3, 1.7 Hz, 1H), 7.90 (dd, *J* = 8.0, 1.3 Hz, 1H), 7.72 (d, *J* = 8.0 Hz, 1H), 7.58 (dd, *J* = 8.2, 1.5 Hz, 1H), 7.47 (dd, *J* = 7.4, 1.5 Hz, 1H), 7.34–7.24 (m, 2H), 6.76 (s, 1H), 6.72–6.63 (m, 1H), 6.58–6.47 (m, 4H). ^{13}C-NMR (125 MHz, $CDCl_3$): *δ* = 167.2 (C_q), 150.2 (CH), 144.0 (C_q), 140.1 (C_q), 137.9 (CH), 135.7 (CH), 134.7 (C_q), 133.7 (C_q), 133.0 (C_q), 129.9 (CH), 128.9 (CH), 128.7 (C_q), 128.4 (CH), 127.9 (CH), 127.5 (C_q), 126.2 (CH), 126.1 (CH), 125.5 (CH), 125.2 (CH), 121.2 (CH), 108.5 (CH), 99.1 (C_q). IR (ATR): 3057, 2890, 2029, 1716, 1599, 1396, 788, 695 cm^{-1}. MS (EI) *m/z* (relative intensity): 474 (100) $[M]^+$, 445 (10), 397 (90), 346 (20), 270 (25), 242 (10), 176 (10). HR-MS (EI) *m/z* calcd for $C_{24}H_{15}IN_2O$ $[M]^+$: 474.0229, found: 474.0228.

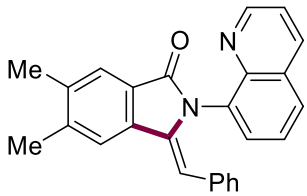

(*Z*)-3-Benzylidene-5,6-dimethyl-2-(quinolin-8-yl) isoindolin-1-one (110ka)

The general procedure **B** was followed using benzamide **54k** (69 mg, 0.25 mmol) and alkyne **76a** (51 mg, 0.50 mmol). Purification by column chromatography on silica gel (*n*-hexane/EtOAc: 5/1) yielded **110ka** (48.6 mg, 52%, *E*/*Z* = 1:10) as colorless oil. Resonances are reported for (*Z*)-**110ka**. ^{1}H-NMR (400 MHz, $CDCl_3$): δ = 8.84 (dd, *J* = 4.2, 1.7 Hz, 1H), 7.95 (dd, *J* = 8.3, 1.7 Hz, 1H), 7.76–7.73 (m, 1H), 7.64 (s, 1H), 7.56 (dd, *J* = 8.2, 1.4 Hz, 1H), 7.46 (dd, *J* = 7.4, 1.4 Hz, 1H), 7.31–7.25 (m, 2H), 6.72 (s, 0.91H, *Z*), 6.69–6.63 (m, 1H), 6.59–6.46 (m, 4H), 5.93 (s, 0.09H, *E*), 2.45 (s, 3H), 2.42 (s, 3H). ^{13}C-NMR (100 MHz, $CDCl_3$): δ = 168.4 (C_q), 150.2 (CH), 144.4 (C_q), 141.7 (C_q), 138.2 (C_q), 136.9 (C_q), 136.3 (C_q), 135.7 (CH), 134.4 (C_q), 133.8 (C_q), 130.0 (CH), 128.8 (C_q), 128.1 (CH), 128.1 (CH), 126.3 (C_q), 126.2 (CH), 125.7 (CH), 125.6 (CH), 124.3 (CH), 121.1 (CH), 120.4 (CH), 106.2 (CH), 20.7 (CH_3), 20.1 (CH_3). IR (ATR): 3059, 1714, 1596, 1474, 1395, 1221, 1108, 806 cm^{-1}. MS (EI) *m/z* (relative intensity): 376 (75) $[M]^+$, 347 (10), 332 (10), 299 (100), 243 (10), 91 (20). HR-MS (ESI) *m/z* calcd for $C_{26}H_{21}N_2O$ $[M+H]^+$: 377.1648, found: 377.1633.

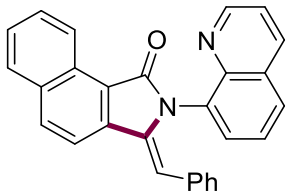

(*Z*)-3-Benzylidene-2-(quinolin-8-yl)-2,3-dihydro-1H-benzo[*e*]isoindol-1-one (110la)

The general procedure **B** was followed using benzamide **110l** (74 mg, 0.25 mmol) and alkyne **76a** (51 mg, 0.50 mmol). Purification by column chromatography on silica gel (*n*-hexane/EtOAc: 5/1) yielded **110la** (53.5 mg, 54%, *E*/*Z* = 1:5) as a brown solid. M. p.: 219–226 °C. Resonances are reported for (*Z*)-**110la**: ^{1}H-NMR (400 MHz, $CDCl_3$): δ = 9.16 (d, *J* = 8.4 Hz, 1H), 8.87 (dd, *J* = 4.1, 1.7 Hz, 1H), 8.12 (d, *J* = 8.5 Hz, 1H), 8.00 (dd, *J* = 8.3, 1.7 Hz, 1H), 7.98–7.85 (m, 2H), 7.71–7.65 (m, 1H), 7.64–7.56 (m, 2H), 7.53 (dd, *J* = 7.3, 1.4 Hz, 1H), 7.37–7.28 (m, 2H), 6.94 (s, 1H), 6.73–6.68 (m, 1H), 6.67–6.52 (m, 4H). ^{13}C-NMR (100 MHz, $CDCl_3$): δ = 169.0 (C_q), 150.4 (CH), 144.7 (C_q), 138.5 (C_q), 136.5 (C_q), 135.8 (CH), 134.4 (C_q), 133.9 (C_q), 133.7 (C_q), 133.0 (CH),

130.2 (CH), 129.3 (C_q), 128.9 (C_q), 128.4 (CH), 128.3 (CH), 128.2 (CH), 128.2 (CH), 126.7 (CH), 126.4 (CH), 126.2 (CH), 125.7 (CH), 124.6 (CH), 122.1 (C_q), 121.2 (CH), 117.0 (CH), 109.1 (CH). Resonances are reported for (*E*)-**110la**: ^{1}H-NMR (400 MHz, $CDCl_3$): δ = 9.25 (dd, *J* = 8.3, 1.1 Hz, 1H), 8.94 (dd, *J* = 4.2, 1.7 Hz, 1H), 8.27 (dd, *J* = 8.3, 1.8 Hz, 1H), 7.98–7.85 (m, 2H), 7.82 (d, *J* = 8.7 Hz, 1H), 7.74 (dd, *J* = 8.3, 7.3 Hz, 1H), 7.47–7.42 (m, 3H), 7.41–7.35 (m, 2H), 6.73–6.68 (m, 1H), 6.67–6.52 (m, 4H), 6.17 (s, 1H). ^{13}C-NMR (100 MHz, $CDCl_3$): δ = 168.0 (C_q), 151.3 (CH), 145.3 (C_q), 138.9 (C_q), 136.3 (CH), 135.4 (C_q), 135.3 (C_q), 133.9 (C_q), 132.2 (CH), 133.0 (C_q), 131.7 (CH), 129.7 (CH), 129.6 (C_q), 129.4 (CH), 129.3 (C_q), 128.5 (CH), 128.2 (CH), 127.9 (CH), 127.8 (CH), 127.0 (CH), 124.9 (CH), 122.1 (C_q), 121.8 (CH), 120.4 (CH), 113.5 (CH), 110.0 (CH). IR (ATR): 3060, 2057, 1693, 1499, 1398, 1146, 828, 697 cm^{-1}. MS (EI) *m/z* (relative intensity): 398 (80) $[M]^+$, 369 (15), 321 (100), 309 (55), 279 (15), 226 (10). HR-MS (EI) *m/z* calcd for $C_{28}H_{18}N_2O$ $[M]^+$: 398.1419, found: 398.1417.

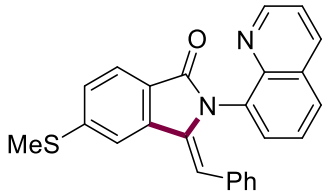

(*Z*)-3-Benzylidene-5-(methylthio)-2-(quinolin-8-yl) isoindolin-1-one (110ma)

The general procedure **B** was followed using benzamide **54m** (74 mg, 0.25 mmol) and alkyne **76a** (51 mg, 0.50 mmol). Purification by column chromatography on silica gel (*n*-hexane/EtOAc: 5/1) yielded **110ma** (80.8 mg, 82%, *E*/*Z* = 1:2) as yellow oil. Resonances reported for (*Z*)-**110ma**: ^{1}H-NMR (300 MHz, $CDCl_3$): δ = 8.83 (dd, *J* = 4.1, 1.5 Hz, 1H), 7.99–7.92 (m, 1H), 7.87 (d, *J* = 8.3 Hz, 1H), 7.73–7.65 (m, 1H), 7.57 (dd, *J* = 8.2, 1.4 Hz, 1H), 7.48 (dd, *J* = 7.4, 1.2 Hz, 1H), 7.40–7.38 (m, 1H), 7.37–7.34 (m, 1H), 7.32–7.28 (m, 1H), 6.78 (s, 1H), 6.72–6.62 (m, 1H), 6.57–6.48 (m, 4H), 2.61 (s, 3H). ^{13}C-NMR (125 MHz, $CDCl_3$): δ = 167.5 (C_q), 150.1 (CH), 144.6 (C_q), 144.2 (C_q), 139.2 (C_q), 135.6 (C_q), 135.6 (CH), 134.0 (C_q), 133.3 (C_q), 129.9 (CH), 129.3 (CH), 128.7 (C_q), 128.3 (CH), 127.9 (CH), 125.0 (C_q), 126.5 (CH), 126.1 (CH), 125.9 (CH), 123.9 (CH), 121.0 (CH), 116.2 (CH), 107.3 (CH), 15.6 (CH_3). Resonances reported for (*E*)-**110ma**: ^{1}H-NMR (300 MHz, $CDCl_3$): δ = 8.92 (dd, *J* = 4.2, 1.5 Hz, 1H), 8.23 (dd, *J*

= 8.3, 1.7 Hz, 1H), 7.99–7.92 (m, 1H), 7.87 (d, *J* = 8.3 Hz, 1H), 7.85–7.82 (m, 1H), 7.73–7.65 (m, 1H), 7.46–7.42 (m, 1H), 7.42–7.40 (m, 1H), 7.40–7.38 (m, 1H), 7.37–7.34 (m, 1H), 7.34–7.32 (m, 1H), 7.32–7.28 (m, 1H), 7.28–7.25 (m, 1H), 7.22 (d, *J* = 1.5 Hz, 1H), 6.03 (s, 1H), 2.24 (s, 3H). ^{13}C-NMR (125 MHz, $CDCl_3$): *δ* = 166.5 (C_q), 151.0 (CH), 144.8 (C_q), 143.9 (C_q), 138.5 (C_q), 136.3 (C_q), 136.1 (CH), 135.2 (C_q), 132.7 (C_q), 131.2 (CH), 129.4 (C_q), 129.3 (CH), 128.1 (CH), 127.6 (CH), 126.9 (C_q), 126.9 (CH), 126.2 (CH), 125.5 (CH), 123.5 (CH), 121.7 (CH), 119.1 (CH), 111.9 (CH), 15.0 (CH_3). IR (ATR): 3059, 1775, 1706, 1601, 1474, 1396, 1222, 764 cm^{-1}. MS (EI) *m/z* (relative intensity): 394 (80) $[M]^+$, 378 (15), 317 (100), 302 (30), 229 (10), 159 (10). HR-MS (EI) *m/z* calcd for $C_{25}H_{18}N_2OS$ $[M]^+$: 394.1140, found: 394.1136.

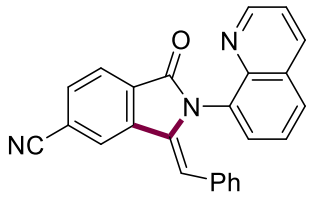

(*Z*)-3-Benzylidene-1-oxo-2-(quinolin-8-yl) isoindoline-5-carbonitrile (110na)

The general procedure **B** was followed using benzamide **54n** (68 mg, 0.25 mmol) and alkyne **76a** (51 mg, 0.50 mmol). Purification by column chromatography on silica gel (*n*-hexane/EtOAc: 5/1) yielded **110na** (51.7 mg, 55%) as a white solid. M. p.: 235–238 °C. ^{1}H-NMR (400 MHz, $CDCl_3$): *δ* = 8.82 (d, *J* = 4.1 Hz, 1H), 8.22–8.16 (m, 1H), 8.09 (d, *J* = 7.8 Hz, 1H), 7.98 (d, *J* = 8.3 Hz, 1H), 7.83 (d, *J* = 7.9 Hz, 1H), 7.61 (d, *J* = 8.2 Hz, 1H), 7.49 (d, *J* = 7.3 Hz, 1H), 7.36–7.28 (m, 2H), 6.87 (s, 1H), 6.76–6.65 (m, 1H), 6.60–6.48 (m, 4H). ^{13}C-NMR (100 MHz, $CDCl_3$): *δ* = 166.3 (C_q), 150.5 (CH), 144.0 (C_q), 138.9 (C_q), 135.9 (CH), 134.4 (C_q), 133.4 (C_q), 132.6 (C_q), 132.2 (CH), 131.4 (C_q), 129.9 (CH), 128.9 (C_q), 128.8 (CH), 128.0 (CH), 126.6 (CH), 126.4 (CH), 125.7 (CH), 124.9 (CH), 124.0 (CH), 121.4 (CH), 118.3 (C_q), 115.7 (C_q), 110.0 (CH). IR (ATR): 3048, 2231, 1715, 1501, 1474, 1399, 797, 690 cm^{-1}. MS (EI) *m/z* (relative intensity): 373 (70) $[M]^+$, 344 (25), 296 (100), 267 (10), 270 (25), 190 (10), 101 (5). HR-MS (EI) *m/z* calcd for $C_{25}H_{15}N_3O$ $[M]^+$: 373.1215, found: 373.1210.

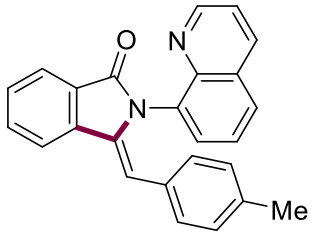

(*Z*)-3-(4-Methybenzylidene)-2-(quinolin-8-yl) isoindolin-1-one (110ab)

The general procedure **B** was followed using benzamide **54a** (62 mg, 0.25 mmol) and alkyne **76b** (58 mg, 0.50 mmol). Purification by column chromatography on silica gel (*n*-hexane/EtOAc: 2/1) yielded **110ab** (69.7 mg, 77%, *E*/*Z* = 1:6) as a yellow oil. Resonances reported for (*Z*)-**110ab**: ^{1}H-NMR (400 MHz, $CDCl_3$): δ = 8.82 (d, *J* = 3.2 Hz, 1H), 7.97 (d, *J* = 7.2 Hz, 2H), 7.86 (d, *J* = 7.8 Hz, 1H), 7.66 (t, *J* = 7.6 Hz, 1H), 7.61–7.55 (m, 1H), 7.52 (dd, *J* = 7.5, 0.8 Hz, 1H), 7.45 (dd, *J* = 7.4, 1.2 Hz, 1H), 7.33–7.24 (m, 2H), 6.77 (s, 1H), 6.41 (d, *J* = 7.8 Hz, 2H), 6.30 (d, *J* = 7.8 Hz, 2H), 2.00 (s, 3H). ^{13}C-NMR (100 MHz, $CDCl_3$): δ = 168.1 (C_q), 150.3 (CH), 144.4 (C_q), 138.7 (C_q), 135.8 (C_q), 135.8 (CH), 135.6 (C_q), 134.3 (C_q), 132.1 (CH), 130.5 (C_q), 130.0 (CH), 129.1 (CH), 128.9 (CH), 128.8 (C_q), 128.2 (C_q), 128.0 (CH), 126.9 (CH), 125.6 (CH), 123.9 (CH), 121.2 (CH), 119.6 (CH), 107.5 (CH), 20.8 (CH_3). Resonances reported for (*E*)-**3ab**: ^{1}H-NMR (400 MHz, $CDCl_3$): δ = 8.91 (dd, *J* = 4.2, 1.5 Hz, 1H), 8.22 (dd, *J* = 8.1, 1.3 Hz, 1H), 7.99–7.93 (m, 2H), 7.82 (dd, *J* = 7.3, 1.2 Hz, 1H), 7.71–7.68 (m, 1H), 7.52–7.51 (m, 1H), 7.50–7.47 (m, 1H), 7.43–7.36 (m, 2H), 7.25 (d, *J* = 3.7 Hz, 2H), 7.14 (d, *J* = 7.9 Hz, 2H), 5.98 (s, 1H), 2.35 (s, 3H). ^{13}C-NMR (100 MHz, $CDCl_3$): δ = 167.0 (C_q), 151.2 (CH), 145.0 (C_q), 138.5 (C_q), 137.4 (C_q), 136.2 (CH), 135.6 (C_q), 132.9 (C_q), 132.2 (C_q), 131.6 (CH), 131.4 (CH), 130.4 (C_q), 129.6 (C_q), 129.4 (CH), 129.2 (CH), 128.0 (CH), 126.9 (CH), 126.3 (CH), 123.7 (CH), 123.3 (CH), 121.8 (CH), 112.3 (CH), 21.3 (CH_3). IR (ATR): 2922, 1718, 1630, 1565, 1255, 1203, 891, 724 cm^{-1}. MS (ESI) *m/z* (relative intensity): 385 (10) $[M+Na]^+$, 363 (100) $[M+H]^+$. HR-MS (ESI): *m/z* calcd for $C_{25}H_{19}N_2O$ $[M+H]^+$: 363.1495, found: 363.1492.

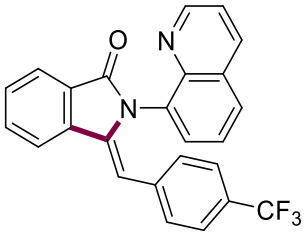

(*Z*)-2-(Quinolin-8-yl)-3-(4-(trifluoromethyl) benzylidene) isoindolin-1-one (110ad)

The general procedure **B** was followed using benzamide **54a** (73 mg, 0.25 mmol) and alkyne **76d** (85 mg, 0.50 mmol). Purification by column chromatography on silica gel (*n*-hexane/EtOAc: 2/1) yielded **110ad** (62.6 mg, 60%, *E*/*Z* = 1:20) as a yellow oil. Resonances are reported for (*Z*)-**110ad**: ^{1}H-NMR (400 MHz, $CDCl_3$): δ = 8.82 (dd, *J* = 4.2, 1.7 Hz, 1H), 8.03 (dd, *J* = 7.6, 1.0 Hz, 1H), 7.95 (dd, *J* = 8.3, 1.7 Hz, 1H), 7.91 (dd, *J* = 7.8, 1.0 Hz, 1H), 7.73 (dd, *J* = 7.6, 1.2 Hz, 1H), 7.62 (dd, *J* = 7.8, 1.2 Hz, 2H), 7.56 (dd, *J* = 7.6, 1.4 Hz, 1H), 7.37 (dd, *J* = 8.3, 7.6 Hz, 1H), 7.31 (dd, *J* = 8.3, 4.2 Hz, 1H), 6.80–6.72 (m, 3H), 6.68–6.61 (m, 2H). ^{13}C-NMR (100 MHz, $CDCl_3$): δ = 167.9 (C_q), 150.4 (CH), 144.1 (C_q), 138.3 (C_q), 137.5 (C_q), 137.4 (C_q), 135.9 (CH), 133.9 (C_q), 132.5 (CH), 130.2 (CH), 129.5 (CH), 128.9 (C_q), 128.7 (CH), 128.4 (C_q), 128.2 (CH), 127.7 (q, $^{2}J_{C–F}$ = 34.2 Hz, C_q), 125.8 (CH), 124.1 (CH), 123.4 (q, $^{1}J_{C–F}$ = 270 Hz, C_q), 122.8 (q, $^{3}J_{C–F}$ = 3.4 Hz, CH), 121.4 (CH), 119.8 (CH), 105.2 (CH). ^{19}F-NMR (375 MHz, $CDCl_3$): δ = –63.1 (m). IR (ATR): 3022, 1711, 1609, 1511, 1221, 827, 798, 728 cm^{-1}. MS (ESI) *m/z* (relative intensity): 417 (100) $[M+H]^+$. HR-MS (ESI): *m/z* calcd for $C_{25}H_{16}F_3N_2O$ $[M+H]^+$: 417.1209, found: 417.1218.

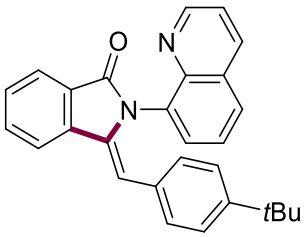

(*Z*)-3-(4-(tert-butyl)benzylidene)-2-(quinolin-8-yl)isoindolin-1-one (110ac)

The general procedure **B** was followed using benzamide **54a** (62 mg, 0.25 mmol) and alkyne **76c** (79 mg, 0.50 mmol). Purification by column chromatography on silica gel (*n*-hexane/EtOAc: 2/1) yielded **110ac** (81.8 mg, 81%, *E*/*Z* = 1:20) as yellow oil. Resonances are reported for (*Z*)-**110ac**. ^{1}H-NMR (300 MHz, $CDCl_3$): δ = 8.86 (dd, *J* =

4.2, 1.6 Hz, 1H), 8.02 (d, *J* = 7.6 Hz, 1H), 7.98–7.88 (m, 2H), 7.70 (dd, *J* = 7.6, 1.2 Hz, 1H), 7.63–7.48 (m, 3H), 7.36–7.27 (m, 2H), 6.83 (s, 0.94H, *Z*), 6.54 (d, *J* = 8.2 Hz, 2H), 6.48 (d, *J* = 8.2 Hz, 2H), 6.01 (s, 0.06H, *E*), 1.11 (s, 9H). ^{13}C-NMR (100 MHz, $CDCl_3$): δ = 168.0 (C_q), 150.2 (CH), 148.7 (C_q), 144.4 (C_q), 138.6 (C_q), 136.1 (C_q), 135.6 (CH), 134.3 (C_q), 132.1 (CH), 130.5 (C_q), 130.1 (CH), 128.9 (CH), 128.8 (C_q), 128.3 (C_q), 128.2 (CH), 127.7 (CH), 125.6 (CH), 123.9 (CH), 123.0 (CH), 121.1 (CH), 119.6 (CH), 107.5 (CH), 34.1 (C_q), 30.9 (CH_3). IR (ATR): 2962, 1721, 1607, 1501, 1268, 828, 790, 718 cm^{-1}. MS (ESI) *m/z* (relative intensity): 427 (20) $[M+Na]^+$, 405 (100) $[M+H]^+$. HR-MS (ESI): *m/z* calcd for $C_{28}H_{24}N_2ONa$ $[M+Na]^+$: 427.1781, found: 427.1791.

5.3.2.2. Gram-Scale Reaction

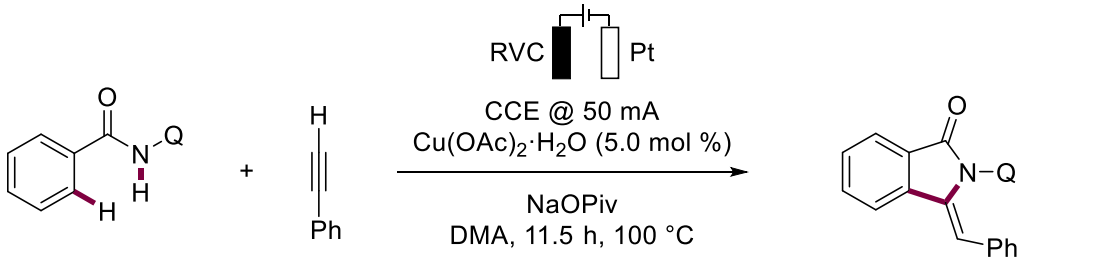

54a **76a** **54aa**: 82% (*E*/*Z* = 1:5), **1.14 g**

The electrocatalysis was carried out in an undivided cell, with a CF anode (50 mm × 50 mm × 6 mm) and a platinum cathode (50 mm × 50 mm × 0.125 mm). Benzamide **54a** (0.99 g, 4.0 mmol, 1.0 equiv), alkyne **76a** (0.61 g, 6.0 mmol, 2.0 equiv), NaOPiv (0.50 g, 4.0 mmol, 1.0 equiv) and $Cu(OAc)_2{\cdot}H_2O$ (40 mg, 5.0 mol %) were placed in a 50 mL cell and dissolved in DMA (20 mL). Electrocatalysis was proformed at 100 °C with a constant current of 50 mA maintained for 11.5 h. At ambient temperature, saturated aqueous $NaHCO_3$ (20 mL) was added. The CF anode was washed with EtOAc (3 × 20 mL) in an ultrasonic bath. The washings were added to the reaction mixture and the combined phases were extracted with EtOAc (4 × 20 mL), then dried over Na_2SO_4. Evaporation of the solvent and subsequent column chromatography on silica gel (*n*-hexane/EtOAc: 3/1) yielded **110aa** (1.14 g, 82%, *E*/*Z* = 1:4) as a white solid.

5.3.2.3. Competition Experiments

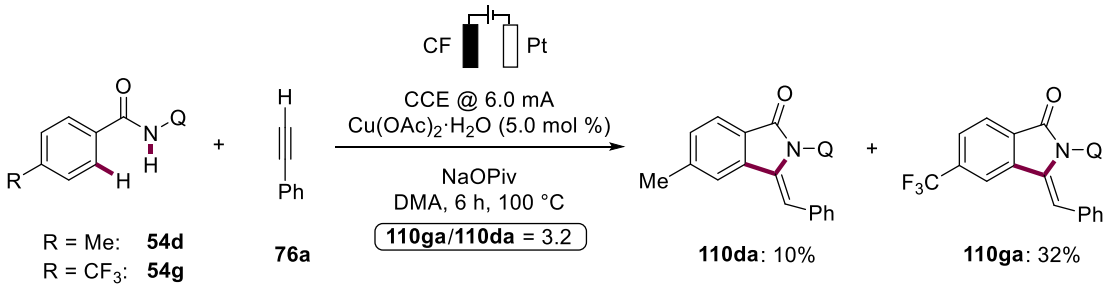

The electrocatalysis was carried out in an undivided cell, with a CF anode (10 mm × 25 mm × 6 mm) and a platinum cathode (10 mm × 25 mm × 0.125 mm). Benzamide **54d** (66 mg, 0.25 mmol), benzamide **54g** (79 mg, 0.25 mmol), alkyne **76a** (26 mg, 0.50 mmol), NaOPiv (31 mg, 0.25 mmol) and $Cu(OAc)_2 \cdot H_2O$ (2.5 mg, 5.0 mol %) were placed in a 10 mL cell and dissolved in DMA (4.0 mL). Electrocatalysis was proformed at 100 °C with a constant current of 6.0 mA maintained for 6 h. At ambient temperature, saturated aqueous $NaHCO_3$ (4.0 mL) was added. The CF anode was washed with EtOAc (3 × 10 mL) in an ultrasonic bath. The combined phases were extracted with EtOAc (4 × 10 mL), then dried over Na_2SO_4. After removal of the solvents *in vacuo*, **110da** and **110ga** were isolated together by column chromatography on silica gel using *n*-hexane/EtOAc 5:1 as eluent. The ratio of **110da** and **110ga** was determined by means of GC which corresponds to **110da** (10%) and **110ga** (32%).

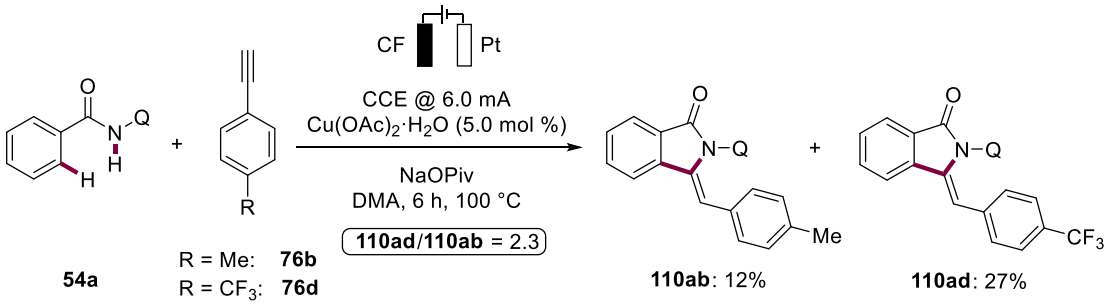

The electrocatalysis was carried out in an undivided cell, with a CF anode (10 mm × 25 mm × 6 mm) and a platinum cathode (10 mm × 25 mm × 0.125 mm). Benzamide **54a** (62 mg, 0.25 mmol), alkyne **76b** (29 mg, 0.25 mmol), alkyne **76d** (43 mg, 0.25 mmol), NaOPiv (31 mg, 0.25 mmol) and $Cu(OAc)_2 \cdot H_2O$ (2.5 mg, 5.0 mol %) were

placed in a 10 mL cell and dissolved in DMA (4.0 mL). Electrocatalysis was proformed at 100 °C with a constant current of 6.0 mA maintained for 6 h. At ambient temperature, saturated aqueous $NaHCO_3$ (4.0 mL) was added. The CF anode was washed with EtOAc (3 × 10 mL) in an ultrasonic bath. The combined phases were extracted with EtOAc (4 × 10 mL), then dried over Na_2SO_4. After removal of the solvents *in vacuo*, **110ab** and **110ad** were isolated together by column chromatography on silica gel using *n*-hexane/EtOAc 5:1. The ratio of **110ab** and **110ad** was determined by means of ^{1}H-NMR spectroscopy which corresponds to **110ab** (12%) and **110ad** (27%).

5.3.2.4. H/D Exchange Experiments

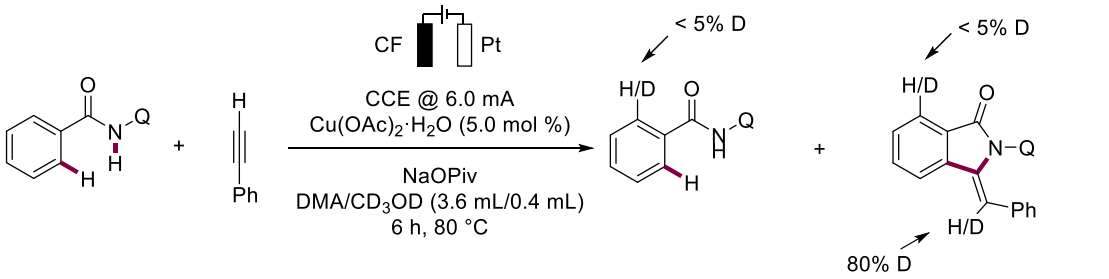

The electrocatalysis was carried out in an undivided cell, with a RVC anode (10 mm × 25 mm × 6 mm) and a platinum cathode (10 mm × 25 mm × 0.125 mm). Benzamide **54a** (62 mg, 0.25 mmol), alkyne **76a** (51 mg, 0.50 mmol), NaOPiv (31 mg, 0.25 mmol) and $Cu(OAc)_2 \cdot H_2O$ (2.5 mg, 5.0 mol %) were placed in a 10 mL cell and dissolved in DMA (3.6 mL) and CD_3OD (0.40 mL). Electrocatalysis was preformed at 80 °C with a constant current of 6.0 mA maintained for 6 h. At ambient temperature, saturated aqueous $NaHCO_3$ (4.0 mL) was added. The RVC anode was washed with EtOAc (3 × 10 mL) in an ultrasonic bath. The combined phases were extracted with EtOAc (4 × 10 mL), then dried over Na_2SO_4. Evaporation of the solvent and subsequent column chromatography (*n*-hexane/EtOAc: 10/1) yielded $[D]_n$-**54a** (30.5 mg, 49%) (figure 5.4) as a white solid and $[D]_n$-**110aa** (25.3 mg, 29%, *E*/*Z* = 1:12) (figure 5.5) as a white solid. The D-incorporation was estimated by ^{1}H-NMR spectroscopy.

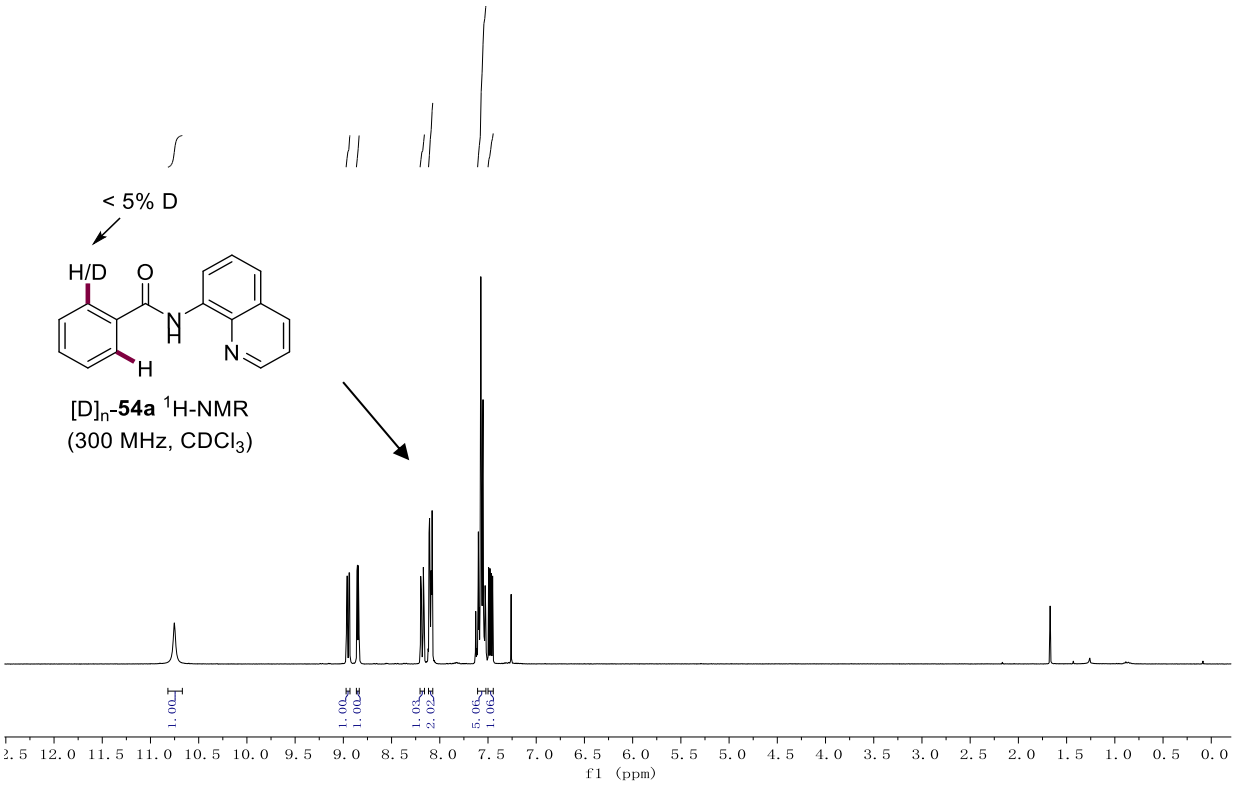

Figure 5.4. ^{1}H-NMR of reisolated [D]$_n$-**54a** from the deuteration study.

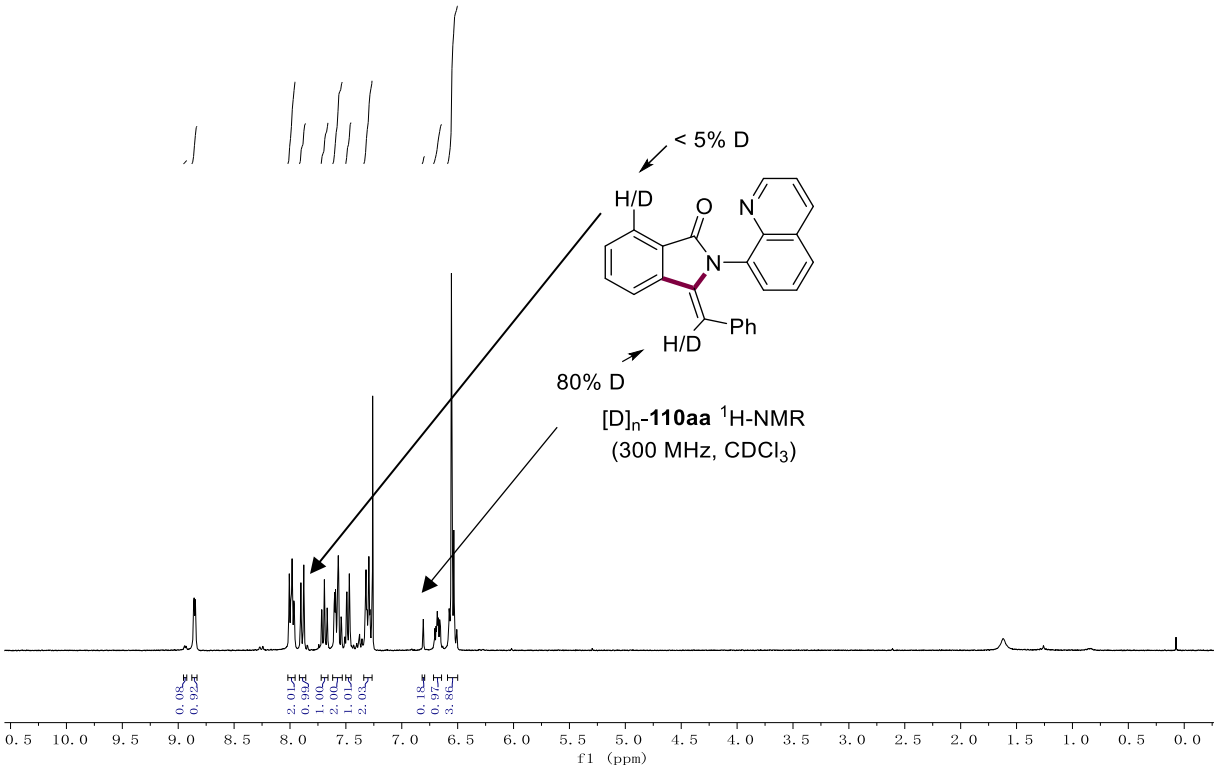

Figure 5.5. ^{1}H-NMR of [D]$_n$-**110aa** from the deuteration study.

5.3.2.5. Kinetic Isotope Effect Studies

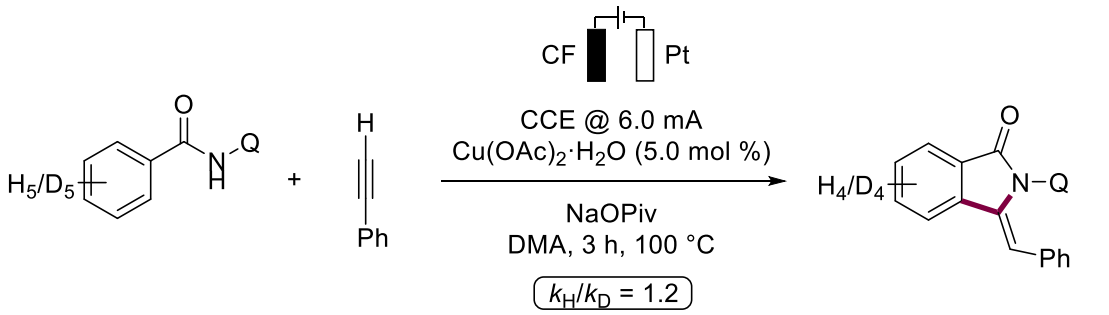

54a or $[D]_5$-**54a** **76a** **110aa** or $[D]_4$-**110aa**

Two parallel reactions were carried out following the general procedure **B** by React-IR studies using substrates **54a** (0.50 mmol) and $[D_5]$-**54a** (0.50 mmol). An IR spectrum was recorded every two minutes, and the KIE was determined by the analysis of the initial rates of the increase of the peak at 1721 cm^{-1} (figure 5.6 and 5.7). The peakarea of first 2 h was plotted to analyze the initial rates of the reaction and a linear fit revealed a KIE of $k_H/k_D \approx 1.2$.

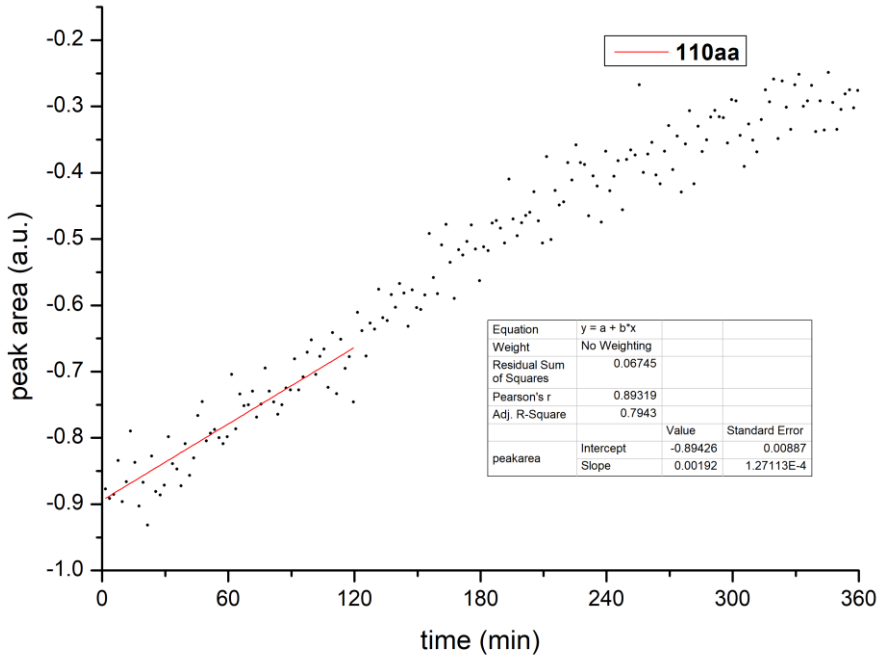

Figure 5.6. Initial rates analysis of **110aa**.

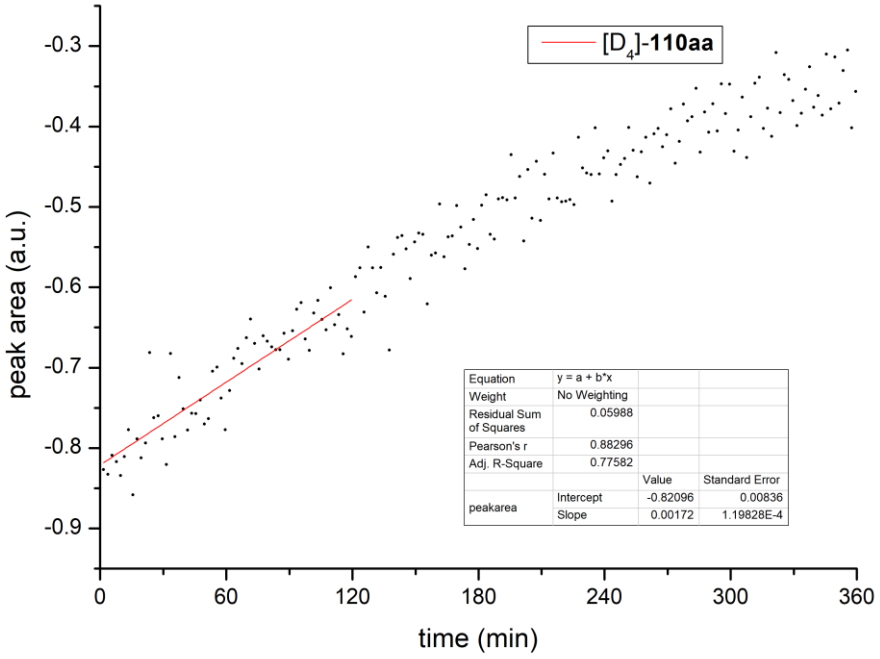

Figure 5.7. Initial rates analysis of [D_4]-**110aa**.

5.3.2.6. Kinetic Profile

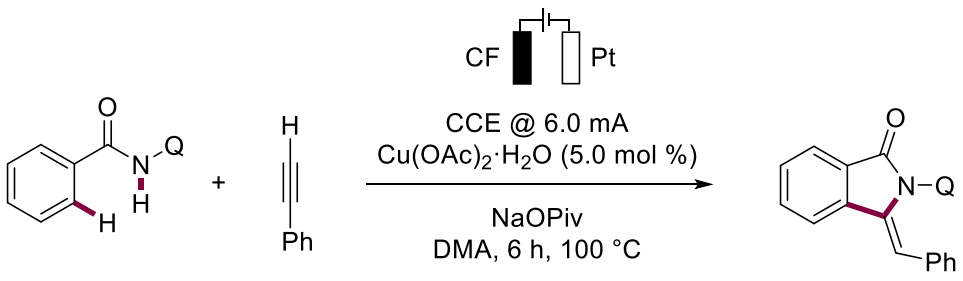

54a **76a** **110aa**

The reaction was carried out following the general procedure **B** by React-IR studies using substrates **54a** (0.50 mmol). IR spectrum was recorded every two minutes. Peaks at 1327 cm^{-1} and 1109 cm^{-1} were identified to belong to the starting material **54a** and the product **110aa**, respectively (figure 5.8 and 5.9).

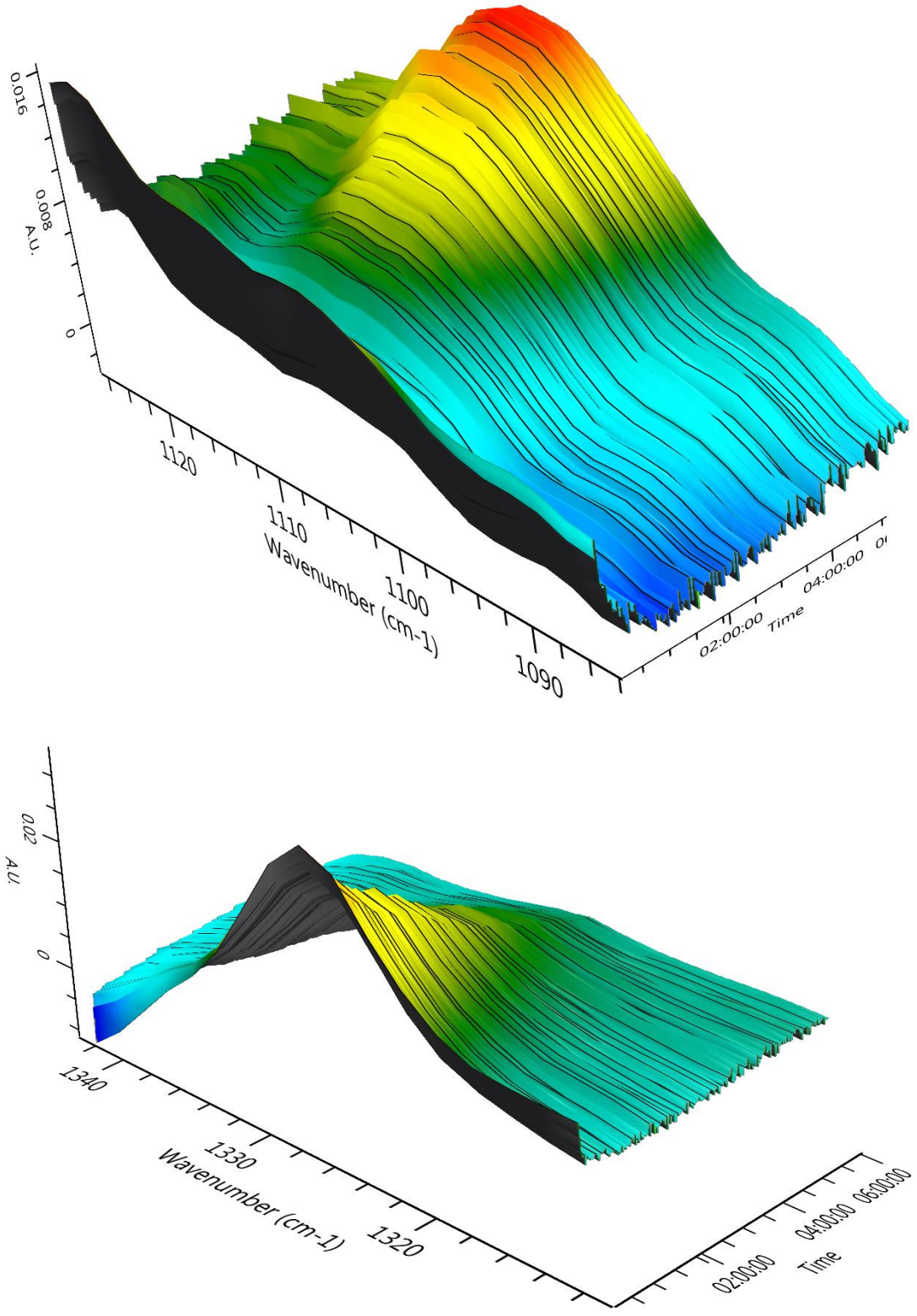

Figure 5.8. 3D-Surface plot of the observed vibrations at 1109 cm^{-1} and 1327 cm^{-1}.

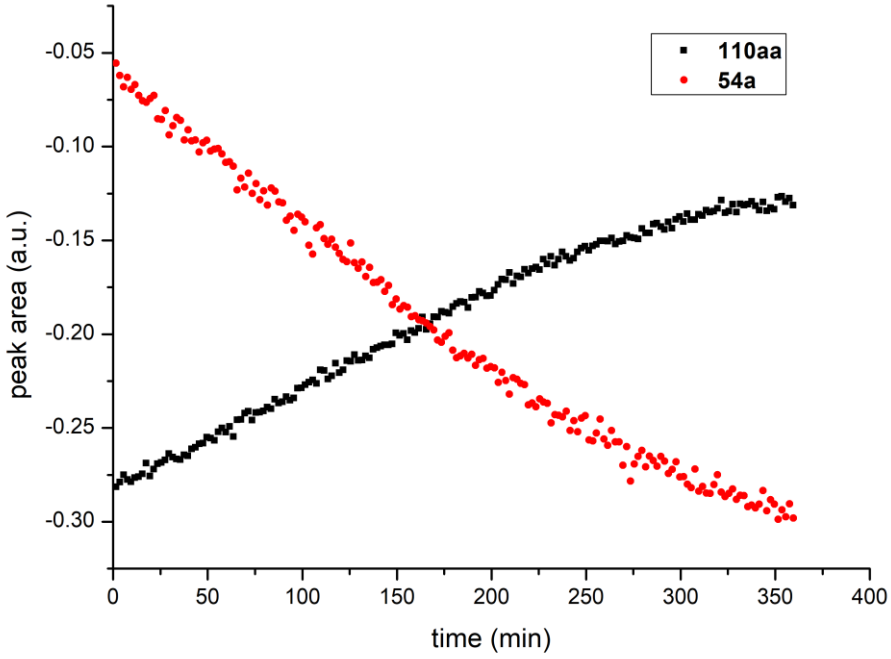

Figure 5.9. Plot of the observed vibrations over time.

5.3.2.7. Cyclization Reactions

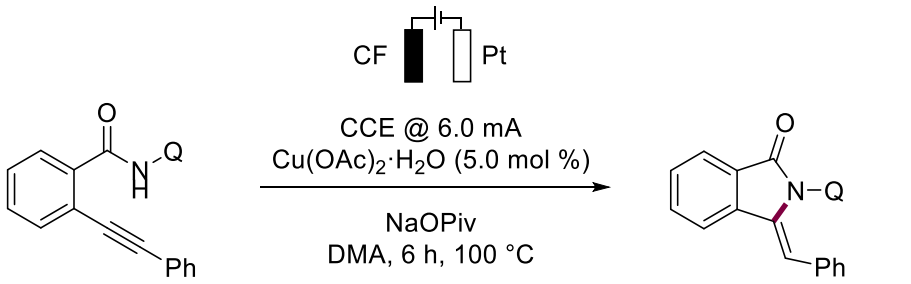

54o **110aa**: 81% (*E*/*Z* = 1:13)

The electrocatalysis was carried out in an undivided cell, with a CF anode (10 mm × 25 mm × 6 mm) and a platinum cathode (10 mm × 25 mm × 0.125 mm). **54o** (87 mg, 0.25 mmol), NaOPiv (31 mg, 0.25 mmol) and $Cu(OAc)_2 \cdot H_2O$ (2.5 mg, 5.0 mol %) were placed in a 10 mL cell and dissolved in DMA (4.0 mL). Electrocatalysis was performed at 100 °C with a constant current of 6.0 mA maintained for 6 h. At ambient temperature, saturated aqueous $NaHCO_3$ (4.0 mL) was added. The CF anode was washed with EtOAc (3 × 10 mL) in an ultrasonic bath. The washings were added to the reaction

mixture and the combined phases were extracted with EtOAc (4 × 10 mL), then dried over Na_2SO_4. After removal of the solvents *in vacuo*, **110aa** was isolated by column chromatography on silica gel using *n*-hexane/EtOAc 5:1 yield **110aa** (70.5 mg, 81%, *E*/*Z* = 1:13).

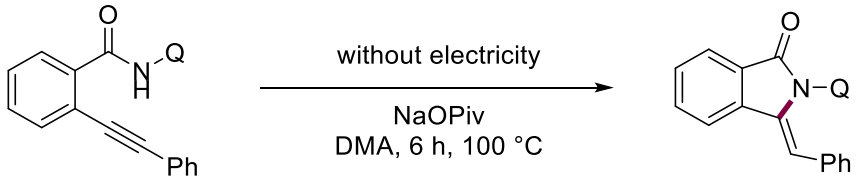

54o **110aa**: 80% (*E*/*Z* = 1:5)

The reaction was carried out in an undivided cell, with a CF anode (10 mm × 25 mm × 6 mm) and a platinum cathode (10 mm × 25 mm × 0.125 mm). **54o** (87 mg, 0.25 mmol), NaOPiv (31 mg, 0.25 mmol) were placed in a 10 mL cell and dissolved in DMA (4.0 mL) at 100 °C for 6 h. At ambient temperature, saturated aqueous $NaHCO_3$ (4.0 mL) was added. The RVC anode was washed with EtOAc (3 × 10 mL) in an ultrasonic bath. The washings were added to the reaction mixture and the combined phases were extracted with EtOAc (4 × 10 mL), then dried over Na_2SO_4. After removal of the solvents *in vacuo*, **110aa** was isolated by column chromatography on silica gel using *n*-hexane/EtOAc 5:1 yield **110aa** (69.3 mg, 80%, *E*/*Z* = 1:5).

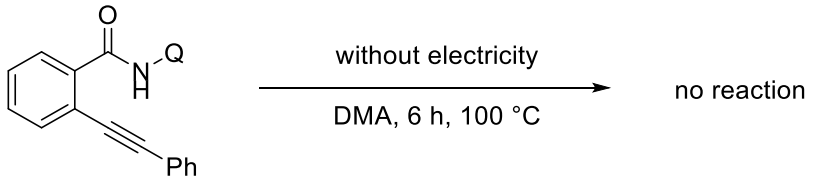

54o

The reaction was carried out in an undivided cell, with a CF anode (10 mm × 25 mm × 6 mm) and a platinum cathode (10 mm × 25 mm × 0.25 mm). **54o** (87 mg, 0.25 mmol) was placed in a 10 mL cell and dissolved in DMA (4.0 mL) at 100 °C for 6 h. At ambient temperature, saturated aqueous $NaHCO_3$ (4.0 mL) was added. No product formation was detected by GC-MS analysis.

5.3.2.8. Headspace GC analysis

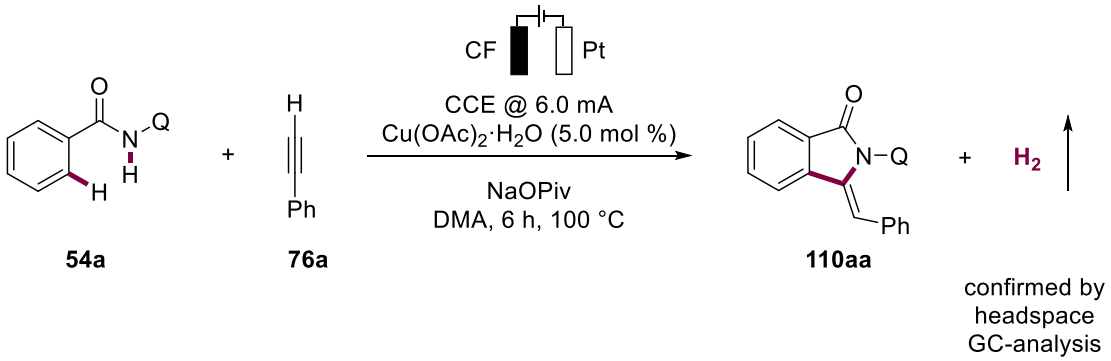

The electrocatalysis was carried out in an undivided cell, with a CF anode (10 mm × 25 mm × 6 mm) and a platinum cathode (10 mm × 25 mm × 0.125 mm). Benzamide **54a** (62 mg, 0.25 mmol), alkyne **76a** (51 mg, 0.50 mmol), NaOPiv (31 mg, 0.25 mmol) and $Cu(OAc)_2 \cdot H_2O$ (2.5 mg, 5.0 mol %) were placed in a 10 mL cell and dissolved in DMA (4.0 mL) under N_2. Electrocatalysis was proformed at 100 °C with a constant current of 6.0 mA for 6 h. After cooling to ambient temperature, 1.0 mL of the headspace volume was removed for GC analysis (figure 5.10). At ambient temperature, saturated aqueous $NaHCO_3$ (4.0 mL) was added. The CF anode was washed with EtOAc (3 × 10 mL) in an ultrasonic bath. The combined phases were extracted with EtOAc (4 × 10 mL), then dried over Na_2SO_4. Evaporation of the solvent and subsequent column chromatography on silica gel (*n*-hexane/EtOAc: 5/1) yielded **110aa** (85%).

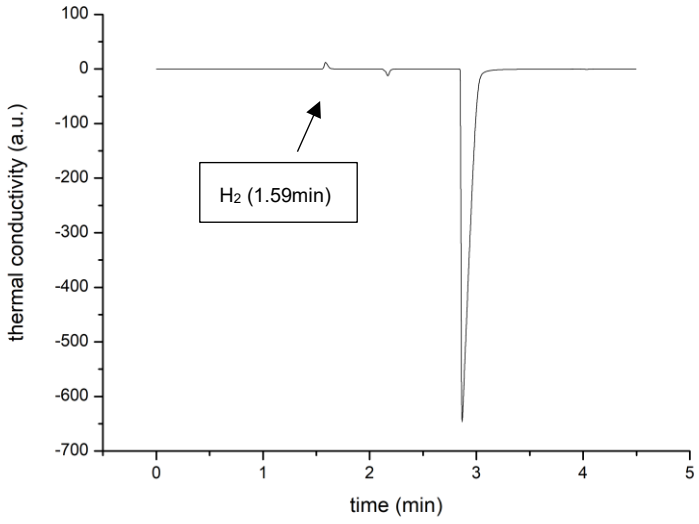

Figure 5.10. Headspace-GC analysis **110aa**.

5.3.2.9. Cyclic voltammograms studies

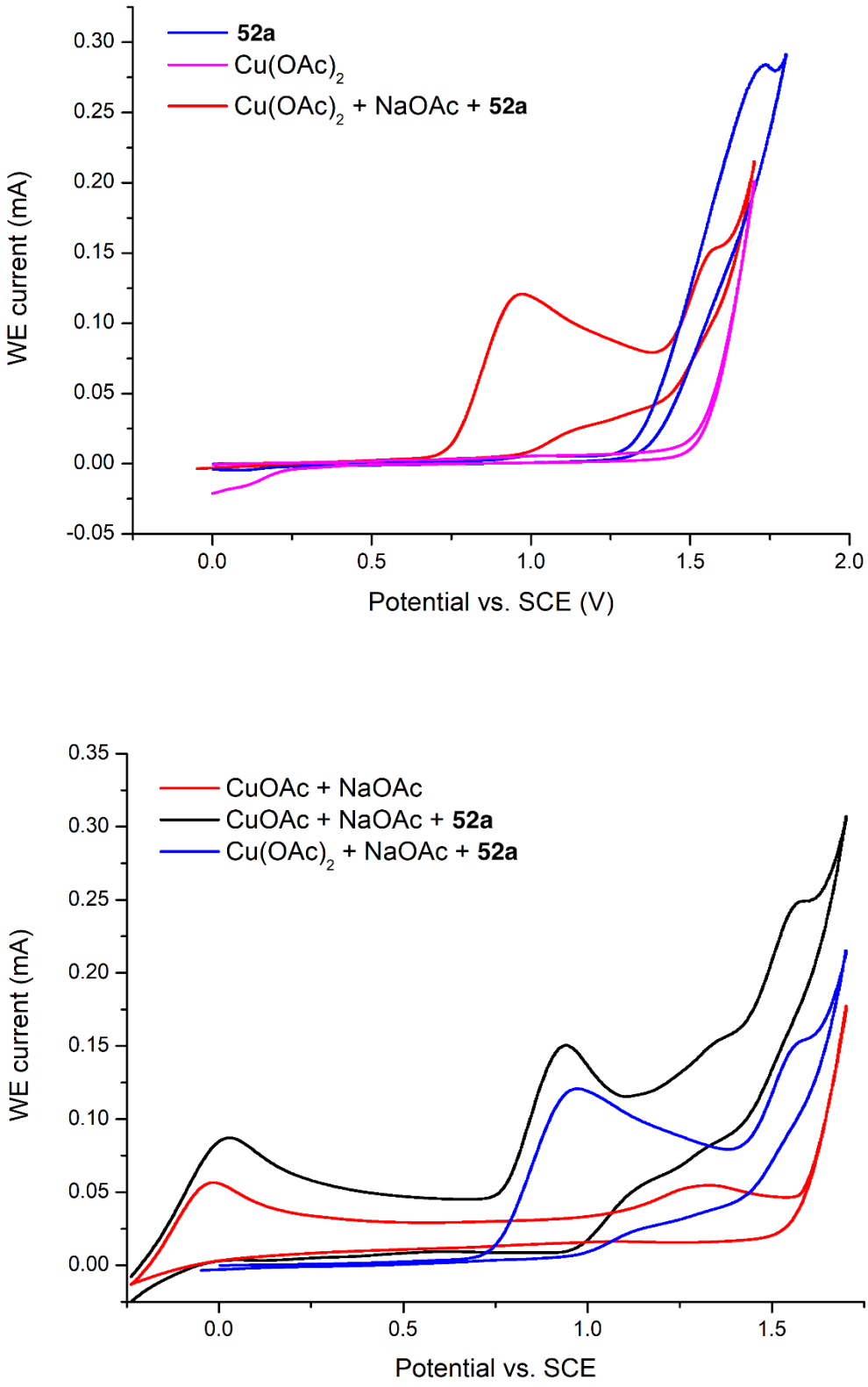

Figure 5.11. Cyclic voltammograms at 100 mVs^{-1}: General condition: DMA, 0.1 M

nBu_4NPF_6, 5 mM HOAc, 5 mM substrates, 100 mV/s.

5.3.3. Cobaltaelectro-Catalyzed C–H Acyloxylation with Carboxylic Acids

5.3.3.1. Characterization Data

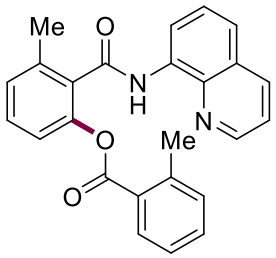

3-Methyl-2-(quinolin-8-ylcarbamoyl) phenyl 2-methylbenzoate (67ba)

The general procedure **C** was followed using benzamide **54b** (66 mg, 0.25 mmol) and caboxylic acid **66a** (68 mg, 0.5 mmol). Purification by column chromatography on silica gel (*n*-hexane/EtOAc: 10/1) yielded **67ba** (65.5 mg, 66%) as colorless oil. ^{1}H-NMR (300 MHz, $CDCl_3$): δ = 10.13 (s, 1H), 8.89 (dd, *J* = 6.7, 2.3 Hz, 1H), 8.73 (dd, *J* = 4.2, 1.7 Hz, 1H), 8.10 (dd, *J* = 8.3, 1.7 Hz, 1H), 7.98 (dd, *J* = 7.9, 1.5 Hz, 1H), 7.55–7.48 (m, 2H), 7.43–7.36 (m, 2H), 7.28–7.18 (m, 3H), 7.08 (d, *J* = 7.7 Hz, 1H), 6.96–6.90 (m, 1H), 2.54 (s, 3H), 2.49 (s, 3H). ^{13}C-NMR (125 MHz, $CDCl_3$): δ = 165.5 (C_q), 164.8 (C_q), 148.0 (CH), 147.6 (C_q), 141.1 (C_q), 138.2 (C_q), 137.4 (C_q), 136.0 (CH), 134.1 (C_q), 132.4 (CH), 131.4 (CH), 131.1 (CH), 130.9 (C_q), 129.9 (CH), 128.0 (CH), 127.8 (C_q), 127.7 (C_q), 127.1 (CH), 125.4 (CH), 121.8 (CH), 121.4 (CH), 120.3 (CH), 116.6 (CH), 21.6 (CH_3), 19.5 (CH_3). IR (ATR): 2130, 1524, 1219, 1038, 840, 818, 734, 495 cm^{-1}. MS (ESI) *m/z* (relative intensity): 419 (30) $[M+Na]^+$, 397 (100) $[M+H]^+$, 253 (20). HR-MS (ESI) *m/z* calcd for $C_{25}H_{21}N_2O_3$ $[M+H]^+$: 397.1547, found: 397.1544.

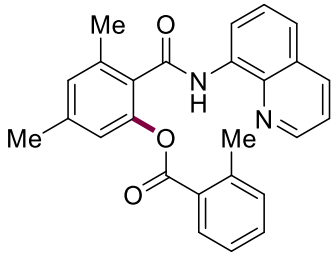

3,5-Dimethyl-2-(quinolin-8-ylcarbamoyl) phenyl 2-methylbenzoate (67qa)

The general procedure **C** was followed using benzamide **54q** (69 mg, 0.25 mmol) and caboxylic acid **66a** (68 mg, 0.5 mmol). Purification by column chromatography on silica gel (*n*-hexane/EtOAc: 10/1) yielded **67qa** (52.7 mg, 51%) as colorless oil. ^{1}H-NMR (400 MHz, $CDCl_3$): δ = 10.10 (s, 1H), 8.87 (dd, *J* = 7.0, 2.0 Hz, 1H), 8.72 (dd, *J* = 4.2, 1.7 Hz, 1H), 8.11 (dd, *J* = 8.3, 1.7 Hz, 1H), 7.97 (dd, *J* = 7.9, 1.4 Hz, 1H), 7.54–7.45 (m, 2H), 7.39 (dd, *J* = 8.3, 4.2 Hz, 1H), 7.27–7.21 (m, 1H), 7.08 (d, *J* = 7.7 Hz, 1H), 7.05–6.98 (m, 2H), 6.97–6.89 (m, 1H), 2.49 (s, 3H), 2.48 (s, 3H), 2.41 (s, 3H). ^{13}C-NMR (100 MHz, $CDCl_3$): δ = 165.8 (C_q), 165.1 (C_q), 148.1 (CH), 147.7 (C_q), 141.2 (C_q), 140.5 (C_q), 138.4 (C_q), 137.3 (C_q), 136.1 (CH), 134.4 (C_q), 132.4 (CH), 131.5 (CH), 131.3 (CH), 129.0 (CH), 128.2 (C_q), 128.0 (C_q), 127.8 (C_q), 127.3 (CH), 125.5 (CH), 121.8 (CH), 121.5 (CH), 120.9 (CH), 116.6 (CH), 21.6 (CH_3), 21.3 (CH_3), 19.5 (CH_3). IR (ATR): 2253, 1735, 1672, 1523, 907, 731, 650, 420 cm^{-1}. MS (EI) *m/z* (relative intensity): 410 (10) $[M]^+$, 291 (5), 267 (35), 218 (5), 119 (100), 91 (50). HR-MS (EI) *m/z* calcd for $C_{26}H_{22}N_2O_3$ $[M]^+$: 410.1630, found: 410.1647.

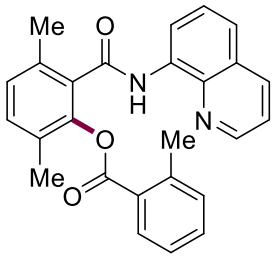

3,6-Dimethyl-2-(quinolin-8-ylcarbamoyl)phenyl 2-methylbenzoate (67ra)

The general procedure **C** was followed using benzamide **54r** (69 mg, 0.25 mmol) and caboxylic acid **66a** (68 mg, 0.5 mmol). Purification by column chromatography on silica gel (*n*-hexane/EtOAc: 10/1) yielded **67ra** (64 mg, 62%) as colorless oil. ^{1}H-NMR (300 MHz, $CDCl_3$): δ = 10.11 (s, 1H), 8.87 (dd, *J* = 6.4, 2.6 Hz, 1H), 8.75 (dd, *J* = 4.2, 1.7 Hz, 1H), 8.09 (dd, *J* = 8.3, 1.7 Hz, 1H), 8.02 (dd, *J* = 7.8, 1.5 Hz, 1H), 7.50–7.45 (m, 2H), 7.39 (dd, *J* = 8.3, 4.2 Hz, 1H), 7.30–7.22 (m, 2H), 7.15–7.05 (m, 2H), 7.02 (dd, *J* = 7.6, 1.2 Hz, 1H), 2.48 (s, 3H), 2.43 (s, 3H), 2.26 (s, 3H). ^{13}C-NMR (75 MHz, $CDCl_3$): δ = 165.5 (C_q), 165.5 (C_q), 148.2 (CH), 146.3 (C_q), 141.1 (C_q), 138.4 (C_q), 136.1 (CH), 134.6 (C_q), 134.3 (C_q), 132.5 (CH), 131.7 (CH), 131.5 (CH), 131.5 (C_q), 131.2 (CH),

128.7 (C_q), 128.2 (CH), 128.0 (C_q), 127.8 (C_q), 127.2 (CH), 125.6 (CH), 122.0 (CH), 121.6 (CH), 116.7 (CH), 21.4 (CH_3), 19.1 (CH_3), 16.3 (CH_3). IR (ATR): 2253, 1734, 1524, 1385, 1052, 907, 730, 650 cm^{-1}. MS (ESI) *m/z* (relative intensity): 433 (40) $[M+Na]^+$, 411 (80) $[M+H]^+$, 357 (5), 335 (5). HR-MS (ESI): *m/z* calcd for $[C_{26}H_{22}N_2O_3+H]^+$: 411.1703, found: 411.1708.

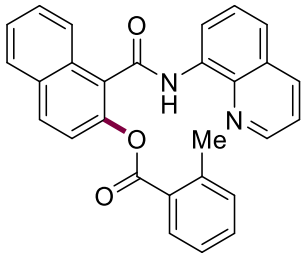

1-(Quinolin-8-ylcarbamoyl) naphthalen-2-yl 2-methylbenzoate (67la)

The general procedure **C** was followed using benzamide **54l** (75 mg, 0.25 mmol) and caboxylic acid **66a** (68 mg, 0.5 mmol). Purification by column chromatography on silica gel (*n*-hexane/EtOAc: 10/1) yielded **67la** (56.4 mg, 52%) as colorless oil. ^{1}H-NMR (400 MHz, $CDCl_3$): δ = 10.37 (s, 1H), 9.04 (dd, *J* = 7.5, 1.5 Hz, 1H), 8.68 (dd, *J* = 4.2, 1.7 Hz, 1H), 8.23–8.18 (m, 1H), 8.10 (td, *J* = 7.9, 1.6 Hz, 2H), 8.03 (d, *J* = 8.7 Hz, 1H), 7.95–7.92 (m, 1H), 7.61–7.50 (m, 4H), 7.48 (d, *J* = 8.9 Hz, 1H), 7.37 (dd, *J* = 8.3, 4.2 Hz, 1H), 7.28 (td, *J* = 7.7, 1.4 Hz, 1H), 7.12 (d, *J* = 7.7 Hz, 1H), 7.01–6.95 (m, 1H), 2.54 (s, 3H). ^{13}C-NMR (100 MHz, $CDCl_3$): δ = 165.7 (C_q), 164.4 (C_q), 148.1 (CH), 145.4 (C_q), 141.4 (C_q), 138.3 (C_q), 136.1 (CH), 134.3 (C_q), 132.6 (CH), 131.6 (CH), 131.6 (C_q), 131.4 (CH), 131.0 (CH), 131.0 (C_q), 128.2 (CH), 127.8 (C_q), 127.7 (C_q), 127.6 (CH), 127.2 (CH), 126.7 (C_q), 126.2 (CH), 125.5 (CH), 125.2 (CH), 122.1 (CH), 121.7 (CH), 121.5 (CH), 116.8 (CH), 21.6 (CH_3). IR (ATR): 1737, 1673, 1521, 1484, 1207, 1044, 827, 735 cm^{-1}. MS (EI) *m/z* (relative intensity): 432 (15) $[M]^+$, 313 (5), 289 (20), 262 (20), 119 (100), 91 (45). HR-MS (EI) *m/z* calcd for $C_{28}H_{20}N_2O_3$ $[M]^+$: 432.1474, found: 432.1460.

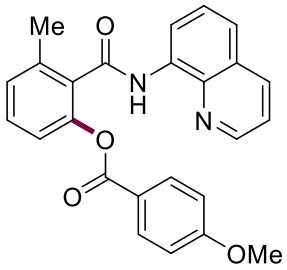

3-Methyl-2-(quinolin-8-ylcarbamoyl) phenyl 4-methoxybenzoate (67bb)

The general procedure **C** was followed using benzamide **54b** (66 mg, 0.25 mmol) and caboxylic acid **66b** (76 mg, 0.5 mmol). Purification by column chromatography on silica gel (*n*-hexane/EtOAc: 10/1) yielded **67bb** (66.4 mg, 64%) as colorless oil. ^{1}H-NMR (400 MHz, $CDCl_3$): δ = 10.09 (s, 1H), 8.86 (dd, *J* = 7.0, 2.0 Hz, 1H), 8.74 (dd, *J* = 4.2, 1.7 Hz, 1H), 8.11 (dd, *J* = 8.3, 1.7 Hz, 1H), 7.96 (dd, *J* = 9.0, 2.8 Hz, 2H), 7.54–7.46 (m, 2H), 7.44–7.38 (m, 2H), 7.24–7.19 (m, 2H), 6.65 (dd, *J* = 9.0, 2.8 Hz, 2H), 3.74 (s, 3H), 2.52 (s, 3H). ^{13}C-NMR (100 MHz, $CDCl_3$): δ = 164.9 (C_q), 164.6 (C_q), 163.6 (C_q), 148.2 (CH), 147.8 (C_q), 138.4 (C_q), 137.6 (C_q), 136.1 (CH), 134.3 (C_q), 132.3 (CH), 130.8 (C_q), 130.0 (CH), 127.9 (CH), 127.8 (C_q), 127.3 (CH), 121.9 (CH), 121.5 (CH), 121.3 (C_q), 120.4 (CH), 116.7 (CH), 113.4 (CH), 55.3 (CH_3), 19.5 (CH_3). IR (ATR): 2140, 1957, 1732, 1604, 1523, 1224, 1166, 1067 cm^{-1}. MS (EI) *m/z* (relative intensity): 412 (15) $[M]^+$, 278 (5), 269 (50), 218 (5), 135 (100), 77 (20). HR-MS (EI) *m/z* calcd for $C_{25}H_{20}N_2O_4$ $[M]^+$: 412.1423, found: 412.1436. The analytical data correspond with those reported in the literature.[2]

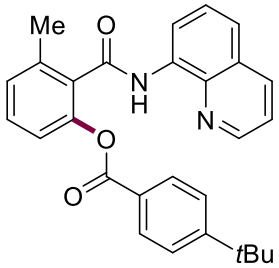

3-Methyl-2-(quinolin-8-ylcarbamoyl) phenyl 4-(*tert*-butyl)benzoate (67bc)

The general procedure **C** was followed using benzamide **54b** (66 mg, 0.25 mmol) and caboxylic acid **66c** (89 mg, 0.5 mmol). Purification by column chromatography on silica gel (*n*-hexane/EtOAc: 10/1) yielded **67bc** (55.2 mg, 50%) as colorless oil. ^{1}H-NMR (400 MHz, $CDCl_3$): δ = 10.09 (s, 1H), 8.86 (dd, *J* = 7.3, 1.7 Hz, 1H), 8.72 (dd, *J* = 4.2,

1.7 Hz, 1H), 8.09 (dd, *J* = 8.3, 1.7 Hz, 1H), 7.92 (dt, *J* = 8.8, 2.2 Hz, 2H), 7.54–7.45 (m, 2H), 7.45–7.37 (m, 2H), 7.25–7.15 (m, 4H), 2.53 (s, 3H), 1.22 (s, 9H). ^{13}C-NMR (100 MHz, $CDCl_3$): δ = 164.9 (C_q), 164.8 (C_q), 157.0 (C_q), 148.1 (CH), 147.7 (C_q), 138.3 (C_q), 137.5 (C_q), 136.0 (CH), 134.3 (C_q), 130.7 (C_q), 130.0 (CH), 129.9 (CH), 127.9 (CH), 127.7 (C_q), 127.2 (CH), 126.1 (C_q), 125.0 (CH), 121.8 (CH), 121.4 (CH), 120.3 (CH), 116.6 (CH), 34.9 (C_q), 30.9 (CH_3), 19.5 (CH_3). IR (ATR): 2252, 1735, 1524, 1385, 1224, 905, 729, 650 cm^{-1}. MS (EI) *m/z* (relative intensity): 438 (20) $[M]^+$, 295 (60), 260 (10), 161 (100), 146 (15), 118 (15). HR-MS (EI) *m/z* calcd for $C_{28}H_{26}N_2O_3$ $[M]^+$: 438.1943, found: 438.1961.

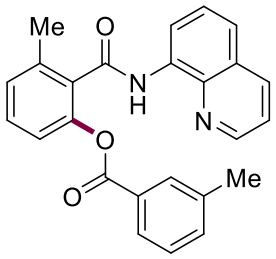

3-Methyl-2-(quinolin-8-ylcarbamoyl) phenyl 3-methylbenzoate (67bd)

The general procedure **C** was followed using benzamide **54b** (66 mg, 0.25 mmol) and caboxylic acid **66d** (68 mg, 0.5 mmol). Purification by column chromatography on silica gel (*n*-hexane/EtOAc: 10/1) yielded **67bd** (44.5 mg, 45%) as colorless oil. ^{1}H-NMR (400 MHz, $CDCl_3$): δ = 10.13 (s, 1H), 8.88 (dd, *J* = 6.9, 2.1 Hz, 1H), 8.75 (dd, *J* = 4.2, 1.7 Hz, 1H), 8.11 (dd, *J* = 8.3, 1.7 Hz, 1H), 7.83–7.75 (m, 2H), 7.54–7.47 (m, 2H), 7.45–7.38 (m, 2H), 7.28–7.24 (m, 1H), 7.22 (dt, *J* = 7.6, 0.9 Hz, 1H), 7.20–7.16 (m, 1H), 7.08 (t, *J* = 7.6 Hz, 1H), 2.54 (s, 3H), 2.06 (s, 3H). ^{13}C-NMR (100 MHz, $CDCl_3$): δ = 165.0 (C_q), 164.8 (C_q), 148.2 (CH), 147.7 (C_q), 138.3 (C_q), 137.9 (C_q), 137.6 (C_q), 136.1 (CH), 134.3 (C_q), 134.1 (CH), 130.7 (C_q), 130.5 (CH), 130.0 (CH), 128.9 (C_q), 128.0 (CH), 127.8 (C_q), 127.3 (CH), 127.2 (CH), 121.9 (CH), 121.5 (CH), 120.2 (CH), 116.7 (CH), 20.8 (CH_3), 19.5 (CH_3). IR (ATR): 2253, 1736, 1525, 1485, 1227, 907, 731, 650 cm^{-1}. MS (EI) *m/z* (relative intensity): 396 (15) $[M]^+$, 379 (5), 253 (40), 119 (100), 91 (40), 65 (15). HR-MS (EI) *m/z* calcd for $C_{25}H_{20}N_2O_3$ $[M]^+$: 396.1474, found: 396.1479.

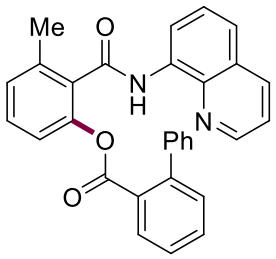

3-Methyl-2-(quinolin-8-ylcarbamoyl) phenyl [1,1'-biphenyl]-2-carboxylate (67be)

The general procedure **C** was followed using benzamide **54b** (66 mg, 0.25 mmol) and caboxylic acid **66e** (99 mg, 0.5 mmol). Purification by column chromatography on silica gel (*n*-hexane/EtOAc: 10/1) yielded **67be** (73.3 mg, 64%) as colorless oil. ^{1}H-NMR (400 MHz, $CDCl_3$): δ = 10.05 (s, 1H), 8.93 (dd, *J* = 7.1, 1.9 Hz, 1H), 8.73 (dd, *J* = 4.2, 1.7 Hz, 1H), 8.15 (dd, *J* = 8.3, 1.7 Hz, 1H), 7.70 (dd, *J* = 7.8, 1.2 Hz, 1H), 7.60–7.52 (m, 2H), 7.42 (dd, *J* = 8.3, 4.2 Hz, 1H), 7.38 (td, *J* = 7.6, 1.4 Hz, 1H), 7.34–7.24 (m, 7H), 7.15 (d, *J* = 7.7 Hz, 1H), 7.06 (td, *J* = 7.6, 1.3 Hz, 1H), 6.84 (d, *J* = 8.2 Hz, 1H), 2.48 (s, 3H). ^{13}C-NMR (100 MHz, $CDCl_3$): δ = 166.6 (C_q), 164.7 (C_q), 148.2 (CH), 147.5 (C_q), 143.0 (C_q), 140.8 (C_q), 138.4 (C_q), 137.3 (C_q), 136.1 (CH), 134.3 (C_q), 131.5 (CH), 130.8 (C_q), 130.6 (CH), 130.1 (CH), 130.0 (CH), 129.4 (C_q), 128.5 (CH), 128.0 (CH), 127.9 (CH), 127.8 (C_q), 127.2 (CH), 126.8 (CH), 121.9 (CH), 121.6 (CH), 119.8 (CH), 116.7 (CH), 19.4 (CH_3). IR (ATR): 2253, 1746, 1524, 1220, 1040, 907, 730 cm^{-1}. MS (EI) *m/z* (relative intensity): 458 (20) $[M]^+$, 315 (30), 278 (5), 181 (100), 152 (40), 144 (15). HR-MS (EI) *m/z* calcd for $C_{30}H_{22}N_2O_3$ $[M]^+$: 458.1630, found: 458.1643.

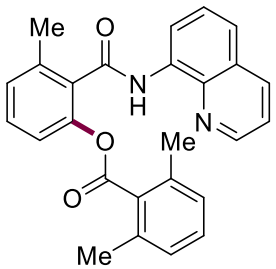

3-Methyl-2-(quinolin-8-ylcarbamoyl) phenyl 2,6-dimethylbenzoate (67bf)

The general procedure **C** was followed using benzamide **54b** (66 mg, 0.25 mmol) and caboxylic acid **66f** (75 mg, 0.5 mmol). Purification by column chromatography on silica gel (*n*-hexane/EtOAc: 10/1) yielded **67bf** (62.4 mg, 61%) as colorless oil. ^{1}H-NMR (400 MHz, $CDCl_3$): δ = 10.15 (s, 1H), 8.92 (dd, *J* = 6.9, 2.1 Hz, 1H), 8.71 (dd, *J* = 4.2, 1.7

Hz, 1H), 8.15 (dd, *J* = 8.3, 1.7 Hz, 1H), 7.60–7.53 (m, 2H), 7.46–7.39 (m, 2H), 7.24 (dt, *J* = 7.7, 0.9 Hz, 1H), 7.19 (dt, *J* = 8.1, 0.9 Hz, 1H), 7.10 (t, *J* = 7.6 Hz, 1H), 6.90 (d, *J* = 7.8 Hz, 2H), 2.51 (s, 3H), 2.25 (s, 6H). ^{13}C-NMR (100 MHz, $CDCl_3$): *δ* = 168.4 (C_q), 164.9 (C_q), 148.3 (CH), 147.3 (C_q), 138.4 (C_q), 137.3 (C_q), 136.1 (CH), 135.5 (C_q), 134.3 (C_q), 132.5 (C_q), 131.5 (C_q), 130.1 (CH), 129.7 (CH), 128.2 (CH), 127.8 (C_q), 127.5 (CH), 127.2 (CH), 122.1 (CH), 121.6 (CH), 120.1 (CH), 116.8 (CH), 19.7 (CH_3), 19.4 (CH_3). IR (ATR): 2253, 1675, 1486, 1219, 906, 729, 650, 419 cm^{-1}. MS (EI) *m/z* (relative intensity): 410 (10) $[M]^+$, 267 (10), 218 (5), 133 (100), 105 (35), 79 (15). HR-MS (EI) *m/z* calcd for $C_{26}H_{22}N_2O_3$ $[M]^+$: 410.1630, found: 410.1636.

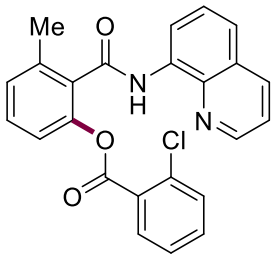

3-methyl-2-(quinolin-8-ylcarbamoyl) phenyl 2-chlorobenzoate (67bg)

The general procedure **C** was followed using benzamide **54b** (66 mg, 0.25 mmol) and caboxylic acid **66g** (78 mg, 0.5 mmol). Purification by column chromatography on silica gel (*n*-hexane/EtOAc: 10/1) yielded **67bg** (39.5 mg, 38%) as colorless oil. ^{1}H-NMR (400 MHz, $CDCl_3$): *δ* = 10.10 (s, 1H), 8.90 (dd, *J* = 7.0, 2.0 Hz, 1H), 8.73 (dd, *J* = 4.2, 1.7 Hz, 1H), 8.13 (dd, *J* = 8.3, 1.7 Hz, 1H), 7.81 (dd, *J* = 7.8, 1.7 Hz, 1H), 7.58–7.51 (m, 2H), 7.44–7.39 (m, 2H), 7.32–7.22 (m, 4H), 7.01–6.96 (m, 1H), 2.53 (s, 3H). ^{13}C-NMR (100 MHz, $CDCl_3$): *δ* = 164.8 (C_q), 163.7 (C_q), 148.3 (CH), 147.4 (C_q), 138.4 (C_q), 137.5 (C_q), 136.1 (CH), 134.4 (C_q), 134.2 (C_q), 132.9 (CH), 131.9 (CH), 130.9 (CH), 130.8 (C_q), 130.1 (CH), 128.6 (C_q), 128.4 (CH), 127.8 (C_q), 127.2 (CH), 126.3 (CH), 122.0 (CH), 121.6 (CH), 120.3 (CH), 116.8 (CH), 19.5 (CH_3). IR (ATR): 3017, 1737, 1674, 1524, 1215, 826, 766, 669 cm^{-1}. MS (EI) *m/z* (relative intensity): 418 (10) [^{37}Cl-M]$^+$, 416 (25) [^{35}Cl-M]$^+$, 399 (5), 273 (40), 139 (100), 111 (25), 77 (10). HR-MS (ESI) *m/z* calcd for $C_{24}H_{17}{}^{35}ClN_2O_3$ $[M+H]^+$: 417.1000, found: 417.1001.

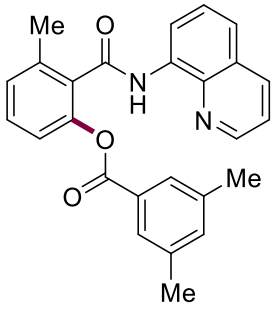

3-Methyl-2-(quinolin-8-ylcarbamoyl) phenyl 3,5-dimethylbenzoate (67bh)

The general procedure **C** was followed using benzamide **54b** (66 mg, 0.25 mmol) and caboxylic acid **66h** (75 mg, 0.5 mmol). Purification by column chromatography on silica gel (*n*-hexane/EtOAc: 10/1) yielded **67bh** (53.2 mg, 52%) as colorless oil. ^{1}H-NMR (400 MHz, $CDCl_3$): δ = 10.14 (s, 1H), 8.90 (dd, *J* = 7.0, 2.0 Hz, 1H), 8.75 (dd, *J* = 4.2, 1.7 Hz, 1H), 8.12 (dd, *J* = 8.3, 1.7 Hz, 1H), 7.61–7.55 (m, 2H), 7.55–7.46 (m, 2H), 7.44–7.42 (m, 1H), 7.42–7.39 (m, 1H), 7.29–7.25 (m, 1H), 7.21 (dt, *J* = 7.6, 0.9 Hz, 1H), 7.02–6.96 (m, 1H), 2.54 (s, 3H), 2.04 (s, 6H). ^{13}C-NMR (100 MHz, $CDCl_3$): δ = 165.1 (C_q), 164.8 (C_q), 148.2 (CH), 147.8 (C_q), 138.3 (C_q), 137.8 (C_q), 137.7 (C_q), 136.1 (CH), 135.0 (CH), 134.3 (C_q), 130.6 (C_q), 130.0 (CH), 128.8 (C_q), 128.0 (CH), 127.8 (CH), 127.8 (C_q), 127.3 (CH), 121.8 (CH), 121.5 (CH), 120.2 (CH), 116.7 (CH), 20.7 (CH_3), 19.5 (CH_3). IR (ATR): 1736, 1675, 1525, 1486, 1309, 907, 730, 650 cm^{-1}. MS (EI) *m/z* (relative intensity): 410 (15) $[M]^+$, 267 (50), 171 (5), 133 (100), 105 (35), 79 (15). HR-MS (EI) *m/z* calcd for $C_{26}H_{22}N_2O_3$ $[M]^+$: 410.1630, found: 410.1616.

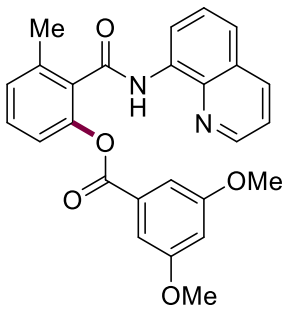

3-Methyl-2-(quinolin-8-ylcarbamoyl) phenyl 3,5-dimethoxybenzoate (67bi)

The general procedure **C** was followed using benzamide **54b** (66 mg, 0.25 mmol) and caboxylic acid **66i** (91 mg, 0.5 mmol). Purification by column chromatography on silica gel (*n*-hexane/EtOAc: 10/1) yielded **67bi** (56.2 mg, 51%) as colorless oil. ^{1}H-NMR (400 MHz, $CDCl_3$): δ = 10.10 (s, 1H), 8.89 (dd, *J* = 6.7, 2.3 Hz, 1H), 8.73 (dd, *J* = 4.3, 1.7

Hz, 1H), 8.12 (dd, *J* = 8.2, 1.7 Hz, 1H), 7.53–7.49 (m, 2H), 7.43–7.38 (m, 2H), 7.28–7.21 (m, 2H), 7.13 (d, *J* = 2.3 Hz, 2H), 6.48 (t, *J* = 2.4 Hz, 1H), 3.53 (s, 6H), 2.53 (s, 3H). ^{13}C-NMR (100 MHz, $CDCl_3$): *δ* = 164.8 (C_q), 164.7 (C_q), 160.4 (C_q), 148.3 (CH), 147.7 (C_q), 138.4 (C_q), 137.6 (C_q), 136.1 (CH), 134.3 (C_q), 130.9 (C_q), 130.7 (C_q), 130.1 (CH), 128.1 (CH), 127.9 (C_q), 127.3 (CH), 122.0 (CH), 121.6 (CH), 120.2 (CH), 116.7 (CH), 107.5 (CH), 106.6 (CH), 55.3 (CH_3), 19.5 (CH_3). IR (ATR): 2166, 1738, 1676, 1524, 1304, 1047, 908 cm^{-1}. MS (EI) *m/z* (relative intensity): 442 (20) $[M]^+$, 299 (55), 264 (5), 165 (100), 137 (25), 122 (20). HR-MS (EI) *m/z* calcd for $C_{26}H_{22}N_2O_5$ $[M]^+$: 442.1529, found: 442.1516.

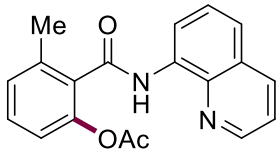

3-Methyl-2-(quinolin-8-ylcarbamoyl) phenyl acetate (67bj)

The general procedure **C** was followed using benzamide **54b** (66 mg, 0.25 mmol) and caboxylic acid **66j** (60 mg, 1.0 mmol). Purification by column chromatography on silica gel (*n*-hexane/EtOAc: 10/1) yielded **67bj** (25.8 mg, 32%) as colorless oil. ^{1}H-NMR (400 MHz, $CDCl_3$): *δ* = 10.02 (s, 1H), 8.94 (dd, *J* = 7.0, 2.0 Hz, 1H), 8.78 (dd, *J* = 4.2, 1.7 Hz, 1H), 8.18 (dd, *J* = 8.3, 1.7 Hz, 1H), 7.63–7.55 (m, 2H), 7.45 (q, *J* = 4.1 Hz, 1H), 7.37 (t, *J* = 7.9 Hz, 1H), 7.18 (d, *J* = 7.5 Hz, 1H), 7.07–7.04 (m, 1H), 2.50 (s, 3H), 2.10 (s, 3H). ^{13}C-NMR (100 MHz, $CDCl_3$): *δ* = 169.5 (C_q), 164.8 (C_q), 148.4 (CH), 147.4 (C_q), 138.5 (C_q), 137.5 (C_q), 136.3 (CH), 134.3 (C_q), 130.7 (C_q), 130.0 (CH), 128.2 (CH), 128.0 (C_q), 127.3 (CH), 122.1 (CH), 121.7 (CH), 120.3 (CH), 116.8 (CH), 20.8 (CH_3), 19.5 (CH_3). IR (ATR): 1769, 1679, 1524, 1484, 1326, 1195, 828, 793 cm^{-1}. MS (EI) *m/z* (relative intensity): 320 (20) $[M]^+$, 259 (30), 186 (10), 144 (100), 135 (75), 43 (40). HR-MS (EI) *m/z* calcd for $C_{19}H_{16}N_2O_3$ $[M]^+$: 320.1161, found: 320.1160.

5.3.3.2. Competition Experiment

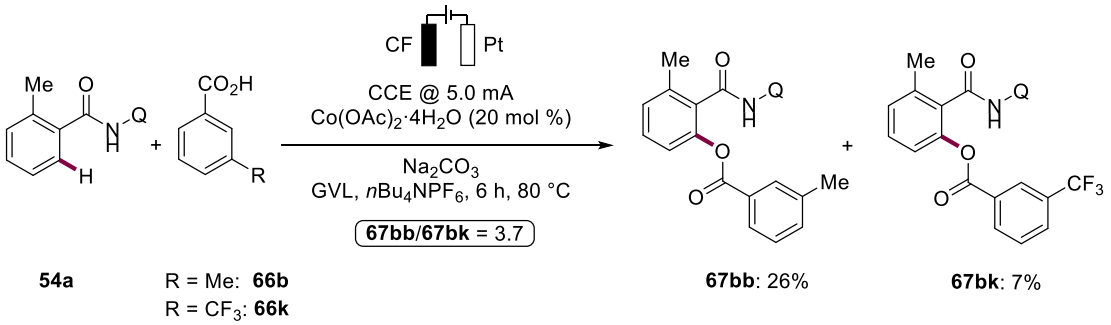

The electrocatalysis was carried out in an undivided cell, with a CF anode (10 mm × 25 mm × 6 mm) and a platinum cathode (10 mm × 25 mm × 0.125 mm). Benzamide **54a** (66 mg, 0.25 mmol), carboxylic acid **66b** (34 mg, 0.25 mmol), carboxylic acid **66k** (48 mg, 0.25 mmol), Na_2CO_3 (53 mg, 0.50 mmol, 2.0 equiv) and $Co(OAc)_2{\cdot}4H_2O$ (12.7 mg, 20 mol %) were dissolved in GVL (3.0 mL). Electrocatalysis was performed at 80 °C with a constant current of 5.0 mA maintained for 6 h. At ambient temperature, the reaction was stopped by adding saturated aqueous $NaHCO_3$ (10 mL). The CF anode was washed with acetone (3 × 10 mL) in an ultrasonic bath. The CF anode was washed with acetone (3 × 10 mL) in an ultrasonic cleaner. The washings were added to the reaction mixture and the combined organic phases were evaporated. After evaporation of acetone the mixture was extracted with pentane (4 × 10 mL), and successively with EtOAc (3 × 10 mL) then dried over Na_2SO_4. After removal of the solvents *under vacuo*, **67bb** and **67bk** were isolated together by column chromatography on silica gel using *n*-hexane/EtOAc 20:1. The ratio of **67bb** and **67bk** was determined by means of GC which corresponds to **67bb** (26%) and **67bk** (7%).

5.3.3.3. H/D Exchange Experiment

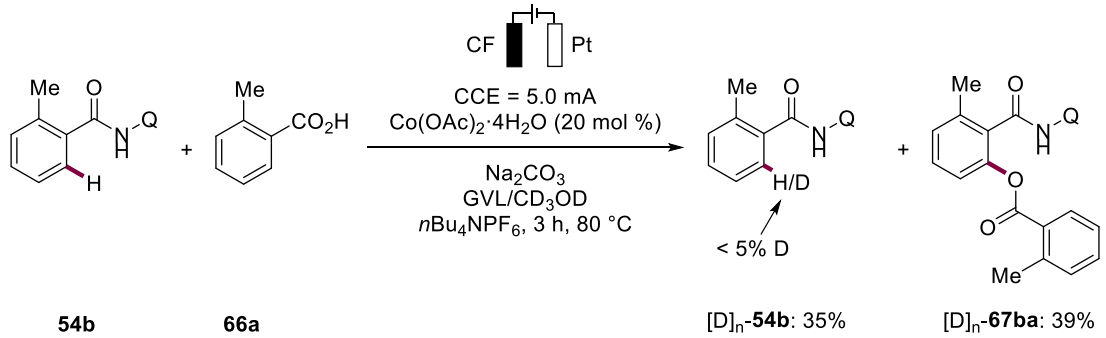

In an undivided cell with a CF anode (10 mm × 25 mm × 6 mm) and a platinum cathode (10 mm × 25 mm × 0.125 mm), benzamide **54b** (66 mg, 0.25 mmol), carboxylic acid **66a** (68 mg, 0.50 mmol, 2.0 equiv), Na_2CO_3 (53 mg, 0.50 mmol, 2.0 equiv) and $Co(OAc)_2{\cdot}4H_2O$ (12.5 mg, 20 mol %) were placed in a 10 mL cell and dissolved in GVL/CD_3OD (5:1, 3.0 mL). Electrocatalysis was performed at 80 °C with a constant current of 5.0 mA maintained for 3 h. The reaction was stopped by adding saturated aqueous $NaHCO_3$ (10 mL). The CF anode was washed with acetone (3 × 10 mL) in an ultrasonic bath. The washings were added to the reaction mixture and the combined organic phases were evaporated. After evaporation of acetone the mixture was extracted with pentane (4 × 10 mL), and successively with EtOAc (3 × 10 mL) then dried over Na_2SO_4. Evaporation of the solvent and subsequent column chromatography on silica gel using *n*-hexane/EtOAc 15:1 yielded **54b** (23.1 mg, 35%) (figure 5.12) as a white solid and **67ba** (38.9 mg, 39%) (figure 5.13) as colorless oil. The D-incorporation was estimated by ^{1}H-NMR spectroscopy.

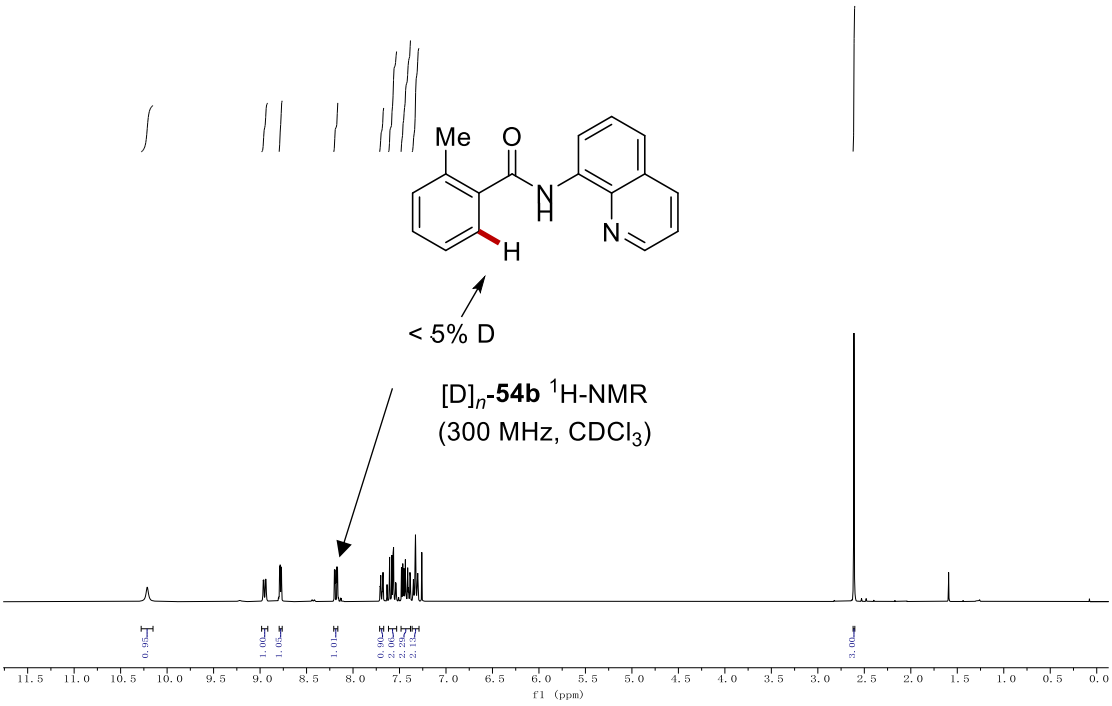

Figure 5.12. ^{1}H-NMR of **54b** from the deuteration study.

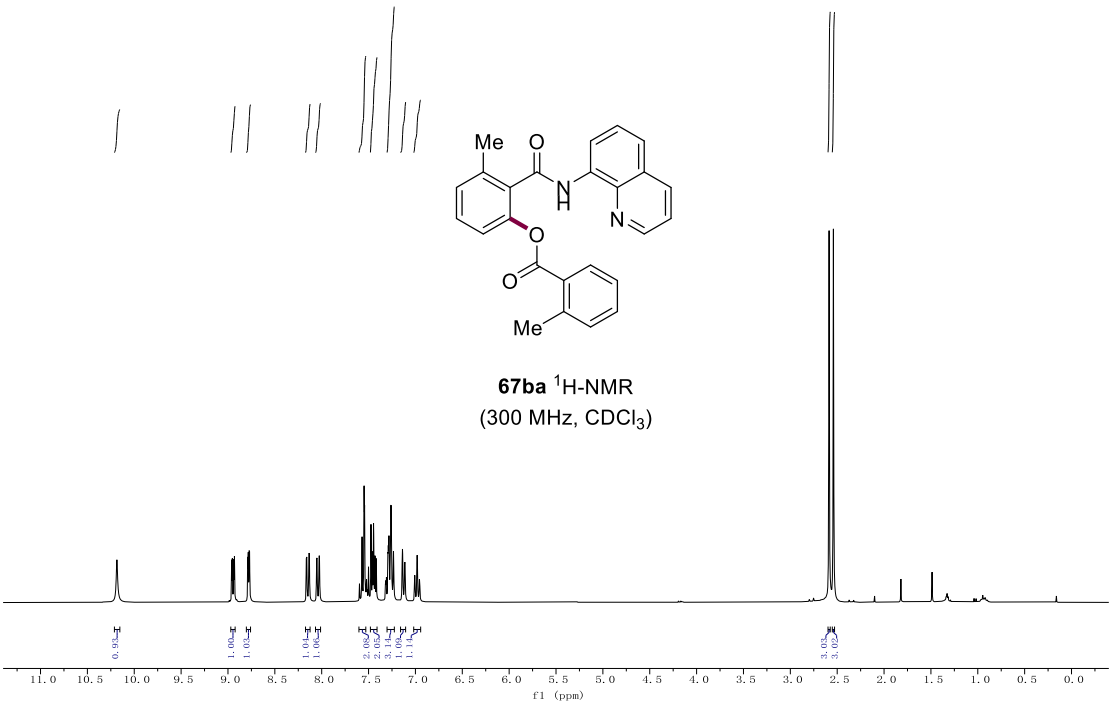

Figure 5.13. ^{1}H-NMR of product **67ba**.

5.3.3.4. Headspace GC analysis

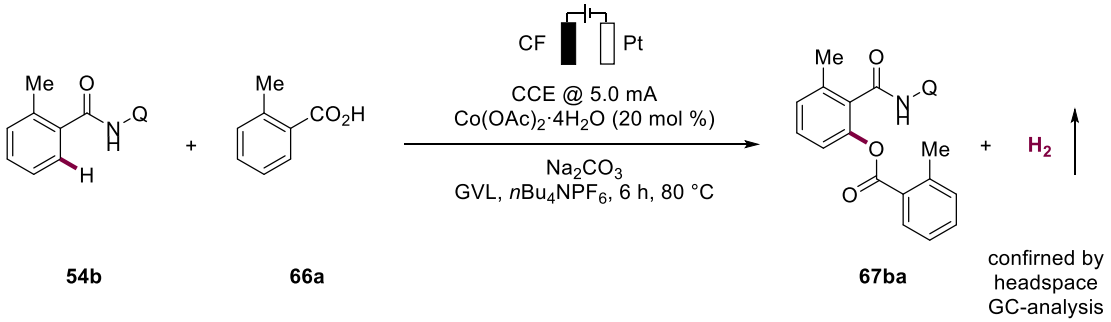

54b **66a** **67ba**

The electrocatalysis was carried out in an undivided cell, with a CF anode (10 mm × 25 mm × 6 mm) and a platinum cathode (10 mm × 25 mm × 0.125 mm). Benzamide **54b** (66 mg, 0.25 mmol), carboxylic acid **66a** (68 mg, 0.50 mmol), Na_2CO_3 (53 mg, 0.50 mmol, 2.0 equiv) and $Co(OAc)_2{\cdot}4H_2O$ (12.7 mg, 20 mol %) were placed in a 10 mL cell and dissolved in GVL (3.0 mL) under N_2. Electrocatalysis was performed at 80 °C with a constant current of 5.0 mA maintained for 6 h. After cooling to ambient temperature, 1.0 mL of the headspace volume was taken for GC analysis (figure 5.14). The CF anode was washed with acetone (3 × 10 mL) in an ultrasonic bath. The washings were added to the reaction mixture and the combined organic phases were evaporated. The mixture was extracted with pentane (4 × 10 mL) and successively with EtOAc (3 × 10 mL) then dried over Na_2SO_4. Evaporation of the solvent and subsequent column chromatography on silica gel (*n*-hexane/EtOAc: 10/1) yielded **67ba** (62%).

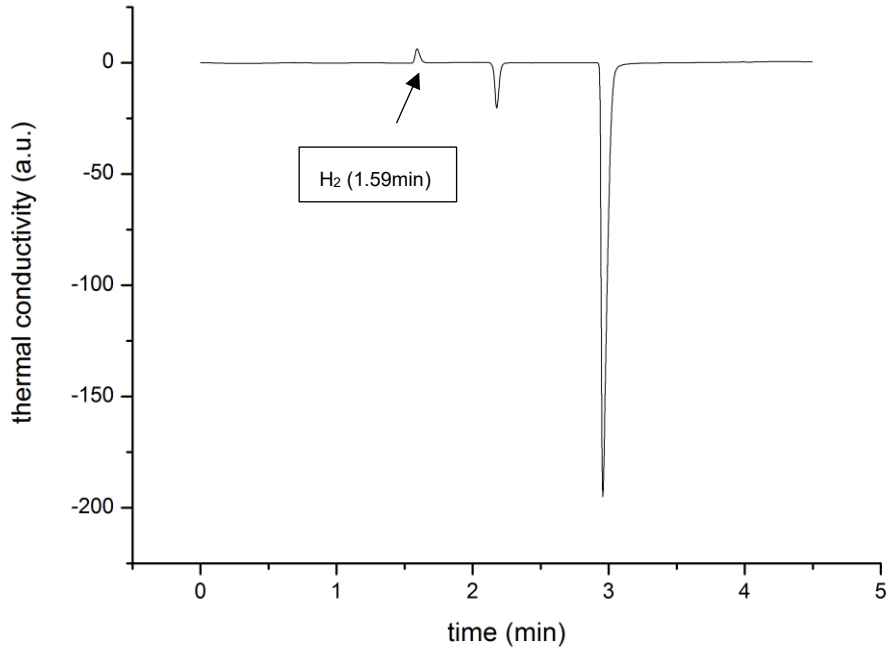

Figure 5.14. Headspace-GC analysis **67ba**.

5.3.4. Cobaltaelectro-Catalyzed C–H Acyloxylation with Carboxylic Acids

5.3.4.1. Characterization Data

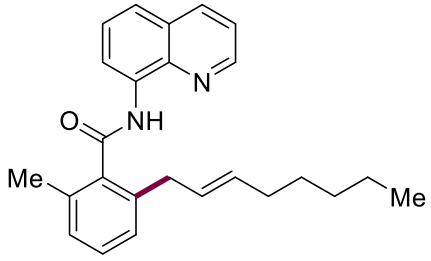

(*E*)-2-Methyl-6-(oct-2-en-1-yl)-*N*-(quinolin-8-yl)benzamide (70ba)

The general procedure **D** was followed using benzamide **54b** (131.1 mg, 0.50 mmol) and alkene **13a** (168.0 mg, 1.5 mmol). Isolation by column chromatography (*n*-hexane/EtOAc = 10:1) yielded **70ba** (112.0 mg, 60%) as a colourless oil. ^{1}H-NMR (400 MHz, $CDCl_3$): δ = 9.95 (s, 1H), 9.03 (dd, *J* = 7.4, 1.7 Hz, 1H), 8.75 (dd, *J* = 4.2, 1.7 Hz, 1H), 8.20 (dd, *J* = 8.3, 1.7 Hz, 1H), 7.66–7.61 (m, 1H), 7.59 (dd, *J* = 8.3, 1.7 Hz, 1H),

7.46 (dd, *J* = 8.3, 4.2 Hz, 1H), 7.31 (dd, *J* = 7.4, 1.7 Hz, 1H), 7.21–7.12 (m, 2H), 5.59 (dtt, *J* = 14.7, 6.6, 1.4 Hz, 1H), 5.44 (dtt, *J* = 14.7, 6.6, 1.4 Hz, 1H), 3.48 (d, *J* = 6.6 Hz, 2H), 2.47 (s, 3H), 1.93–1.79 (m, 2H), 1.22–1.11 (m, 6H), 0.82 (t, *J* = 6.2 Hz, 3H). ^{13}C-NMR (100 MHz, $CDCl_3$): δ = 168.7 (C_q), 148.2 (CH), 138.5 (C_q), 137.8 (C_q), 137.7 (C_q), 136.3 (CH), 134.7 (C_q), 134.4 (C_q), 132.5 (CH), 129.1 (CH), 128.1 (CH), 128.1 (CH), 128.0 (C_q), 127.4 (CH), 127.0 (CH), 121.9 (CH), 121.6 (CH), 116.8 (CH), 36.7 (CH_2), 32.4 (CH_2), 31.4 (CH_2), 28.9 (CH_2), 22.4 (CH_2), 19.5 (CH_3), 14.0 (CH_3). IR (ATR): 2947, 1675, 1582, 1429, 1296, 970, 800, 710 cm^{-1}. MS (ESI) *m*/*z* (relative intensity): 395 (20) $[M+Na]^+$, 373 (100) $[M+H]^+$. HR-MS (ESI): *m*/*z* calcd. for $[C_{25}H_{28}N_2O+Na]^+$ 395.2094 found 395.2087.

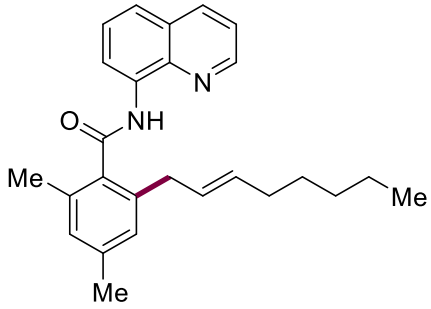

(*E*)-2,4-Dimethyl-6-(oct-2-en-1-yl)-*N*-(quinolin-8-yl)benzamide (70qa)

The general procedure **D** was followed using benzamide **54q** (138.0 mg, 0.50 mmol) and alkene **13a** (168.0 mg, 1.5 mmol). Purification by column chromatography on silica gel (*n*-hexane/EtOAc = 40:1) yielded **70qa** (93.5 mg, 48%) as a colorless oil. ^{1}H-NMR (400 MHz, $CDCl_3$): δ = 9.92 (s, 1H), 9.00 (dd, *J* = 7.5, 1.5 Hz, 1H), 8.72 (dd, *J* = 4.2, 1.7 Hz, 1H), 8.17 (dd, *J* = 8.3, 1.7 Hz, 1H), 7.64–7.58 (m, 1H), 7.55 (dd, *J* = 8.3, 1.5 Hz, 1H), 7.43 (dd, *J* = 8.3, 4.2 Hz, 1H), 7.00–6.93 (m, 2H), 5.57 (dtt, *J* = 14.8, 6.7, 1.3 Hz, 1H), 5.41 (dtt, *J* = 14.8, 6.7, 1.3 Hz, 1H), 3.43 (d, *J* = 6.7 Hz, 2H), 2.41 (s, 3H), 2.36 (s, 3H), 1.84 (dd, *J* = 6.7, 1.2 Hz, 2H), 1.22–1.10 (m, 6H), 0.80 (t, *J* = 6.8 Hz, 3H). ^{13}C-NMR (100 MHz, $CDCl_3$): δ = 168.9 (C_q), 148.1 (CH), 138.8 (C_q), 138.5 (C_q), 137.7 (C_q), 136.2 (CH), 135.0 (C_q), 134.6 (C_q), 134.5 (C_q), 132.3 (CH), 128.8 (CH), 128.2 (CH), 128.0 (C_q), 127.6 (CH), 127.4 (CH), 121.7 (CH), 121.6 (CH), 116.7 (CH), 36.6 (CH_2), 32.3 (CH_2), 31.4 (CH_2), 28.8 (CH_2), 22.4 (CH_2), 21.2 (CH_3), 19.4 (CH_3), 14.0 (CH_3). IR (ATR): 2923, 2854, 1737, 1675, 1519, 1240, 1045, 792 cm^{-1}. MS (ESI) *m/z* (relative

intensity): 409 (100) $[M+Na]^+$, 387 (15) $[M+H]^+$. HR-MS (ESI) *m/z* calcd for $C_{26}H_{31}N_2O$ $[M+H]^+$: 387.2431, found: 387.2429.

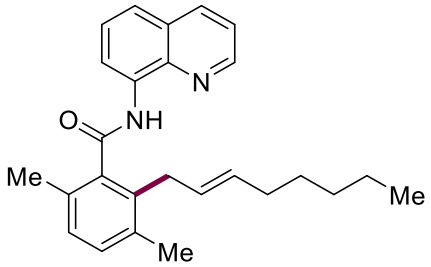

(*E*)-3,6-Dimethyl-2-(oct-2-en-1-yl)-*N*-(quinolin-8-yl)benzamide (70ra)

The general procedure **D** was followed using benzamide **54r** (138.0 mg, 0.50 mmol) and alkene **13a** (168.0 mg, 1.5 mmol). Purification by column chromatography on silica gel (*n*-hexane/EtOAc = 50:1) yielded **70ra** (101.2 mg, 52%) as a colorless oil. ^{1}H-NMR (400 MHz, $CDCl_3$): δ = 9.93 (s, 1H), 9.04 (dd, *J* = 7.5, 1.5 Hz, 1H), 8.72 (dd, *J* = 4.2, 1.7 Hz, 1H), 8.16 (dd, *J* = 8.3, 1.7 Hz, 1H), 7.61 (t, *J* = 7.5 Hz, 1H), 7.56 (dd, *J* = 8.3, 1.5 Hz, 1H), 7.43 (dd, *J* = 8.3, 4.2 Hz, 1H), 7.15 (d, *J* = 7.8 Hz, 1H), 7.06 (d, *J* = 7.7 Hz, 1H), 5.58–5.48 (m, 1H), 5.37–5.27 (m, 1H), 3.45 (dd, *J* = 6.1, 1.2 Hz, 2H), 2.41 (s, 3H), 2.34 (s, 3H), 1.86–1.78 (m, 2H), 1.18–1.09 (m, 6H), 0.79 (t, *J* = 7.0 Hz, 3H). ^{13}C-NMR (100 MHz, $CDCl_3$): δ = 169.2 (C_q), 148.1 (CH), 138.5 (C_q), 138.4 (C_q), 136.2 (CH), 135.0 (C_q), 134.7 (C_q), 134.4 (C_q), 132.0 (C_q), 131.7 (CH), 130.9 (CH), 128.0 (CH), 128.0 (C_q), 127.3 (CH), 127.1 (CH), 121.8 (CH), 121.5 (CH), 116.7 (CH), 34.0 (CH_2), 32.3 (CH_2), 31.3 (CH_2), 28.8 (CH_2), 22.3 (CH_2), 19.2 (CH_3), 19.2 (CH_3), 13.9 (CH_3). IR (ATR): 2983, 1737, 1680, 1521, 1234, 1044, 793, 607 cm^{-1}. MS (ESI) *m/z* (relative intensity): 409 (100) $[M+Na]^+$, 387 (20) $[M+H]^+$. HR-MS (ESI) *m/z* calcd for $C_{26}H_{31}N_2O$ $[M+H]^+$: 387.2431, found: 387.2432.

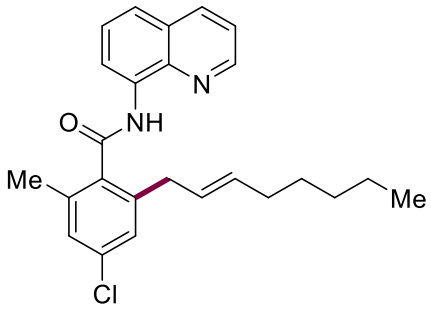

(*E*)-4-Chloro-2-methyl-6-(oct-2-en-1-yl)-*N*-(quinolin-8-yl)benzamide (70ta)

The slightly modified procedure **D** was followed using benzamide **54t** (148.0 mg, 0.50 mmol) and alkene **13a** (168.0 mg, 1.5 mmol) with $Co(OAc)_2 \cdot 4H_2O$ (25.7 mg, 20 mol %) . Purification by column chromatography on silica gel (*n*-hexane/EtOAc = 30:1) yielded **70ta** (100.0 mg, 50%) as a colorless oil. ^{1}H-NMR (400 MHz, $CDCl_3$): δ = 9.90 (s, 1H), 8.96 (dd, *J* = 7.2, 1.8 Hz, 1H), 8.74 (dd, *J* = 4.2, 1.7 Hz, 1H), 8.18 (dd, *J* = 8.3, 1.7 Hz, 1H), 7.64–7.55 (m, 2H), 7.45 (dd, *J* = 8.3, 4.2 Hz, 1H), 7.13 (s, 2H), 5.57–5.49 (m, 1H), 5.43 (dtt, *J* = 15.1, 6.5, 1.0 Hz, 1H), 3.42 (d, *J* = 6.5 Hz, 2H), 2.41 (s, 3H), 1.90–1.81 (m, 2H), 1.22–1.10 (m, 6H), 0.81 (t, *J* = 6.8 Hz, 3H). ^{13}C-NMR (100 MHz, $CDCl_3$): δ = 167.7 (C_q), 148.3 (CH), 139.9 (C_q), 138.5 (C_q), 136.7 (C_q), 136.3 (CH), 136.1 (C_q), 134.7 (C_q), 134.2 (C_q), 133.3 (CH), 128.0 (C_q), 128.0 (CH), 127.4 (CH), 127.2 (CH), 127.0 (CH), 122.1 (CH), 121.7 (CH), 116.8 (CH), 36.4 (CH_2), 32.3 (CH_2), 31.4 (CH_2), 28.8 (CH_2), 22.4 (CH_2), 19.4 (CH_3), 14.0 (CH_3). IR (ATR): 2984, 1736, 1372, 1233, 1043, 847, 608, 463 cm^{-1}. MS (ESI) *m/z* (relative intensity): 429 (100) $[M+Na]^+$, 407 (10) $[M+H]^+$. HR-MS (ESI) *m/z* calcd for $C_{25}H_{28}{}^{35}ClN_2O$ $[M+H]^+$: 407.1885, found: 407.1884.

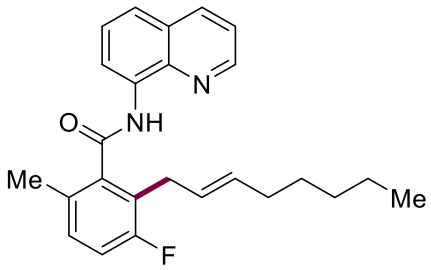

(*E*)-3-Fluoro-6-methyl-2-(oct-2-en-1-yl)-*N*-(quinolin-8-yl)benzamide (70ua)

The general procedure **D** was followed using benzamide **54u** (140.0 mg, 0.50 mmol) and alkene **13a** (168.0 mg, 1.5 mmol). Purification by column chromatography on silica

gel (*n*-hexane/EtOAc = 50:1) yielded **70ua** (93.1 mg, 48%) as a colorless oil. ^{1}H-NMR (400 MHz, $CDCl_3$): δ = 9.91 (s, 1H), 8.97 (d, J = 7.2 Hz, 1H), 8.78–8.69 (m, 1H), 8.18 (d, J = 8.2 Hz, 1H), 7.67–7.55 (m, 2H), 7.45 (dd, J = 8.4, 4.2 Hz, 1H), 7.15–6.98 (m, 2H), 5.54 (dt, J = 14.6, 6.6 Hz, 1H), 5.36 (dt, J = 14.6, 6.6 Hz, 1H), 3.44 (d, J = 6.6 Hz, 2H), 2.39 (s, 3H), 1.81–1.72 (m, 2H), 1.15–1.00 (m, 6H), 0.76 (t, J = 6.7 Hz, 3H). ^{13}C-NMR (100 MHz, $CDCl_3$): δ = 167.3 (d, $^{4}J_{C–F}$ = 3.1 Hz, C_q), 159.4 (d, $^{1}J_{C–F}$ = 244.7 Hz, C_q), 148.3 (CH), 139.2 (d, $^{4}J_{C–F}$ = 3.7 Hz, C_q), 138.5 (C_q), 136.3 (CH), 134.2 (C_q), 132.3 (CH), 130.3 (d, $^{4}J_{C–F}$ = 3.7 Hz, C_q), 129.4 (d, $^{2}J_{C–F}$ = 8.1 Hz, C_q), 128.0 (C_q), 127.4 (CH), 126.6 (CH), 124.9 (d, $^{3}J_{C–F}$ = 17.4 Hz, CH), 122.1 (CH), 121.7 (CH), 116.9 (CH), 115.9 (d, $^{2}J_{C–F}$ = 22.4 Hz, CH), 32.3 (CH_2), 31.4 (CH_2), 30.1 (d, $^{3}J_{C–F}$ = 2.8 Hz, CH_2), 28.7 (CH_2), 22.4 (CH_2), 18.9 (CH_3), 14.0 (CH_3). ^{19}F-NMR (282 MHz, $CDCl_3$): δ = –120.8. IR (ATR): 2984, 1737, 1372, 1233, 1043, 938, 847, 608 cm^{-1}. MS (ESI) *m/z* (relative intensity): 413 (100) $[M+Na]^+$, 391 (20) $[M+H]^+$. HR-MS (ESI) *m/z* calcd for $C_{25}H_{28}FN_2O$ $[M+H]^+$: 391.2180, found: 391.2180.

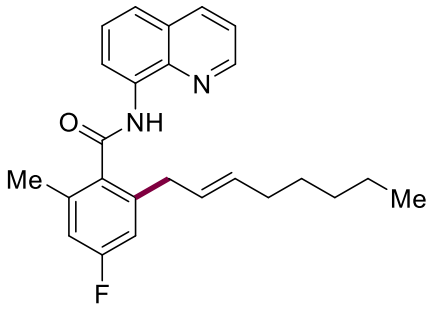

(*E*)-4-Fluoro-6-methyl-2-(oct-2-en-1-yl)-*N*-(quinolin-8-yl)benzamide (70va)

The slightly modified general procedure **D** was followed using benzamide **54v** (140.0 mg, 0.50 mmol) and alkene **13a** (168.0 mg, 1.5 mmol) with $Co(OAc)_2{\cdot}4H_2O$ (25.7 mg, 20 mol %). Purification by column chromatography on silica gel (*n*-hexane/EtOAc = 50:1) yielded **70va** (90.1 mg, 46%) as a colorless oil. ^{1}H-NMR (400 MHz, $CDCl_3$): δ = 9.92 (s, 1H), 8.99 (dd, J = 7.3, 1.7 Hz, 1H), 8.75 (dd, J = 4.2, 1.7 Hz, 1H), 8.17 (dd, J = 8.3, 1.7 Hz, 1H), 7.63–7.55 (m, 2H), 7.44 (dd, J = 8.3, 4.2 Hz, 1H), 6.91–6.79 (m, 2H), 5.62–5.50 (m, 1H), 5.49–5.39 (m, 1H), 3.45 (dd, J = 6.5, 1.3 Hz, 2H), 2.44 (s, 3H), 1.91–1.83 (m, 2H), 1.24–1.12 (m, 6H), 0.81 (t, J = 6.9 Hz, 3H). ^{13}C-NMR (100 MHz, $CDCl_3$): δ = 167.9 (C_q), 162.7 (d, $^{1}J_{C–F}$ = 247.6 Hz, C_q), 148.2 (CH),

140.7 (d, $^{3}J_{C–F}$ = 7.8 Hz, C_q), 138.4 (C_q), 137.5 (d, $^{3}J_{C–F}$ = 8.5 Hz, C_q), 136.3 (CH), 134.2 (C_q), 133.8 (d, $^{4}J_{C–F}$ = 3.1 Hz, C_q), 133.2 (CH), 128.0 (C_q), 127.3 (CH), 127.2 (CH), 122.0 (CH), 121.6 (CH), 116.7 (CH), 114.7 (d, $^{2}J_{C–F}$ = 21.5 Hz, CH), 113.6 (d, $^{2}J_{C–F}$ = 21.4 Hz, CH), 36.5 (d, $^{4}J_{C–F}$ = 1.7 Hz, CH_2), 32.3 (CH_2), 31.3 (CH_2), 28.7 (CH_2), 22.4 (CH_2), 19.6 (d, $^{4}J_{C–F}$ = 1.8 Hz, CH_3) 13.9 (CH_3). ^{19}F-NMR (377 MHz, $CDCl_3$): δ = –112.6. IR (ATR): 2927, 1737, 1519, 1237, 1138, 1045, 791, 607 cm^{-1}. MS (ESI) *m/z* (relative intensity): 413 (100) $[M+Na]^+$, 391 (20) $[M+H]^+$. HR-MS (ESI) *m/z* calcd for $C_{25}H_{28}FN_2O$ $[M+H]^+$: 391.2180, found: 391.2179.

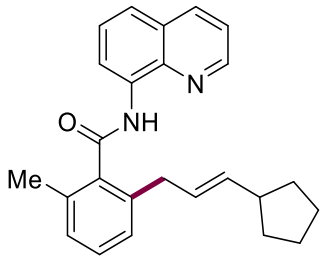

(*E*)-2-(3-Cyclopentylallyl)-6-methyl-*N*-(quinolin-8-yl)benzamide (70bb)

The general procedure **D** was followed using benzamide **54b** (131.1 mg, 0.50 mmol) and alkene **13b** (165.0 mg, 1.5 mmol). Purification by column chromatography on silica gel (*n*-hexane/EtOAc = 40:1) yielded **70bb** (78.8 mg, 43%) as a colorless oil. ^{1}H-NMR (400 MHz, $CDCl_3$): δ = 9.93 (s, 1H), 9.00 (dd, *J* = 7.4, 1.6 Hz, 1H), 8.73 (dd, *J* = 4.2, 1.7 Hz, 1H), 8.18 (dd, *J* = 8.3, 1.7 Hz, 1H), 7.64–7.58 (m, 1H), 7.56 (dd, *J* = 8.3, 1.6 Hz, 1H), 7.44 (dd, *J* = 8.3, 4.2 Hz, 1H), 7.29 (t, *J* = 7.6 Hz, 1H), 7.18–7.10 (m, 2H), 5.61–5.48 (m, 1H), 5.48–5.36 (m, 1H), 3.46 (d, *J* = 6.7 Hz, 2H), 2.44 (s, 3H), 2.27 (q, *J* = 8.0 Hz, 1H), 1.63–1.54 (m, 2H), 1.52–1.38 (m, 4H), 1.15–1.04 (m, 2H). ^{13}C-NMR (100 MHz, $CDCl_3$): δ = 168.6 (C_q), 148.2 (CH), 138.5 (C_q), 137.8 (C_q), 137.7 (C_q), 136.9 (CH), 136.3 (CH), 134.6 (C_q), 134.4 (C_q), 129.0 (CH), 128.0 (CH), 128.0 (C_q), 127.4 (CH), 127.0 (CH), 126.2 (CH), 121.9 (CH), 121.6 (CH), 116.7 (CH), 42.9 (CH), 36.6 (CH_2), 32.8 (CH_2), 25.0 (CH_2), 19.5 (CH_3). IR (ATR): 2984, 1737, 1447, 1372, 1235, 1045, 847, 608 cm^{-1}. MS (ESI) *m/z* (relative intensity): 393 (80) $[M+Na]^+$, 371 (90) $[M+H]^+$. HR-MS (ESI) *m/z* calcd for $C_{25}H_{27}N_2O$ $[M+H]^+$: 371.2118, found: 371.2118.

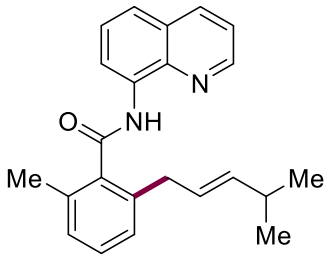

(*E*)-2-Methyl-6-(4-methylpent-2-en-1-yl)-*N*-(quinolin-8-yl)benzamide (70bc)

The general procedure **D** was followed using benzamide **54b** (131.1 mg, 0.50 mmol) and alkene **13c** (126 mg, 1.5 mmol). Purification by column chromatography on silica gel (*n*-hexane/EtOAc = 40:1) yielded **70bc** (72.0 mg, 42%) as a colorless oil. ^{1}H-NMR (400 MHz, $CDCl_3$): δ = 9.95 (s, 1H), 9.02 (dd, *J* = 7.4, 1.5 Hz, 1H), 8.73 (dd, *J* = 4.2, 1.7 Hz, 1H), 8.17 (dd, *J* = 8.3, 1.7 Hz, 1H), 7.65–7.59 (m, 1H), 7.56 (dd, *J* = 8.3, 1.5 Hz, 1H), 7.44 (dd, *J* = 8.3, 4.2 Hz, 1H), 7.30 (d, *J* = 7.6 Hz, 1H), 7.18–7.13 (m, 2H), 5.60–5.50 (m, 1H), 5.42 (ddt, *J* = 15.3, 6.5, 1.3 Hz, 1H), 3.47 (d, *J* = 6.5 Hz, 2H), 2.46 (s, 3H), 2.13 (q, *J* = 6.8 Hz, 1H), 0.83 (d, *J* = 6.8 Hz, 6H). ^{13}C-NMR (100 MHz, $CDCl_3$): δ = 168.6 (C_q), 148.2 (CH), 139.3 (CH), 138.4 (C_q), 137.8 (C_q), 137.6 (C_q), 136.2 (CH), 134.6 (C_q), 134.3 (C_q), 129.0 (CH), 128.0 (CH), 127.9 (C_q), 127.3 (CH), 126.9 (CH), 125.2 (CH), 121.9 (CH), 121.6 (CH), 116.7 (CH), 36.5 (CH_2), 30.7 (CH), 22.2 (CH_3), 19.4 (CH_3). IR (ATR): 2924, 1676, 1522, 1483, 1326, 826, 637, 575 cm^{-1}. MS (ESI) *m/z* (relative intensity): 367 (80) $[M+Na]^+$, 345 (100) $[M+H]^+$. HR-MS (ESI) *m/z* calcd for $C_{23}H_{25}N_2O$ $[M+H]^+$: 345.1961, found: 345.1963.

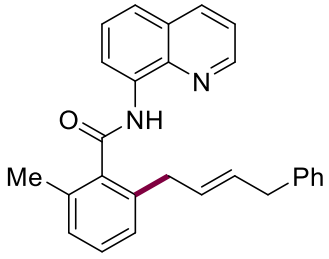

(*E*)-2-Methyl-6-(4-phenylbut-2-en-1-yl)-*N*-(quinolin-8-yl)benzamide (70bd)

The general procedure **D** was followed using benzamide **54b** (131.1 mg, 0.50 mmol) and alkene **13d** (198.0 mg, 1.5 mmol). Purification by column chromatography on silica gel (*n*-hexane/EtOAc: 35/1) yielded **70bd** (143.0 mg, 73%) as a colorless oil. ^{1}H-NMR (400 MHz, $CDCl_3$): δ = 10.01 (s, 1H), 9.07 (d, *J* = 7.4 Hz, 1H), 8.76 (d, *J* = 4.0 Hz, 1H),

8.19 (dd, *J* = 8.2, 2.1 Hz, 1H), 7.69–7.57 (m, 2H), 7.46 (dd, *J* = 8.4, 4.1 Hz, 1H), 7.34 (t, *J* = 7.6 Hz, 1H), 7.25–7.12 (m, 5H), 7.08 (d, *J* = 7.5 Hz, 2H), 5.75 (dtt, *J* = 14.8, 6.4, 1.2 Hz, 1H), 5.65 (dtt, *J* = 14.8, 6.4, 1.2 Hz, 1H), 3.57 (d, *J* = 6.4 Hz, 2H), 3.25 (d, *J* = 6.4 Hz, 2H), 2.51 (s, 3H). ^{13}C-NMR (100 MHz, $CDCl_3$): *δ* = 168.7 (C_q), 148.3 (CH), 140.5 (C_q), 138.6 (C_q), 137.8 (C_q), 137.4 (C_q), 136.4 (CH), 134.8 (C_q), 134.4 (C_q), 130.9 (CH), 130.0 (CH), 129.3 (CH), 128.5 (CH), 128.3 (CH), 128.3 (CH), 128.1 (C_q), 127.5 (CH), 127.2 (CH), 125.9 (CH), 122.1 (CH), 121.8 (CH), 116.9 (CH), 38.9 (CH_2), 36.7 (CH_2), 19.6 (CH_3). IR (ATR): 2924, 1676, 1522, 1483, 1326, 826, 637, 575 cm^{-1}. MS (ESI) *m/z* (relative intensity): 415 (90) $[M+Na]^+$, 393 (80) $[M+H]^+$. HR-MS (ESI) *m/z* calcd for $C_{27}H_{25}N_2O$ $[M+H]^+$: 393.1961, found: 393.1963.

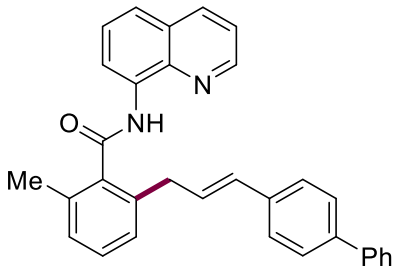

(*E*)-2-(3-([1,1'-biphenyl]-4-yl)allyl)-6-methyl-N-(quinolin-8-yl)benzamide (70be)

The slightly modified general procedure **D** was followed using benzamide **54b** (131.1 mg, 0.50 mmol) and alkene **13e** (198.0 mg, 1.5 mmol) with $Co(OAc)_2{\cdot}4H_2O$ (25.7 mg, 20 mol %). Purification by column chromatography on silica gel (*n*-hexane/EtOAc = 40:1) yielded **70be** (115.1 mg, 51%) as a colorless oil. ^{1}H-NMR (400 MHz, $CDCl_3$): *δ* = 9.95 (s, 1H), 9.00 (dd, *J* = 7.6, 1.4 Hz, 1H), 8.47 (dd, *J* = 4.2, 1.7 Hz, 1H), 8.07 (dd, *J* = 8.3, 1.7 Hz, 1H), 7.59 (dd, *J* = 7.9, 1.7 Hz, 1H), 7.54–7.50 (m, 3H), 7.44–7.39 (m, 2H), 7.34–7.28 (m, 5H), 7.21 (d, *J* = 7.5 Hz, 1H), 7.17 (d, *J* = 7.5 Hz, 1H), 7.13–7.08 (m, 2H), 6.45–6.26 (m, 2H), 3.66 (d, *J* = 6.2 Hz, 2H), 2.46 (s, 3H). ^{13}C-NMR (100 MHz, $CDCl_3$): *δ* = 168.6 (C_q), 148.1 (CH), 140.8 (C_q), 139.4 (C_q), 138.4 (C_q), 138.0 (C_q), 136.7 (C_q), 136.2 (C_q), 136.1 (CH), 134.9 (C_q), 134.3 (C_q), 130.8 (CH), 129.2 (CH), 128.7 (CH), 128.7 (CH), 128.4 (CH), 127.9 (C_q), 127.3 (CH), 127.3 (CH), 127.1 (CH), 126.8 (CH), 126.8 (CH), 126.3 (CH), 121.9 (CH), 121.5 (CH), 116.7 (CH), 37.3 (CH_2), 19.5 (CH_3). IR (ATR): 2984, 1737, 1372, 1233, 1043, 938, 847, 607 cm^{-1}. MS (ESI) *m/z* (relative intensity): 477 (90) $[M+Na]^+$, 455 (100) $[M+H]^+$. HR-MS (ESI)

m/z calcd for $C_{32}H_{27}N_2O$ $[M+H]^+$: 455.2118, found: 455.2121.

5.3.4.2. Headspace GC analysis

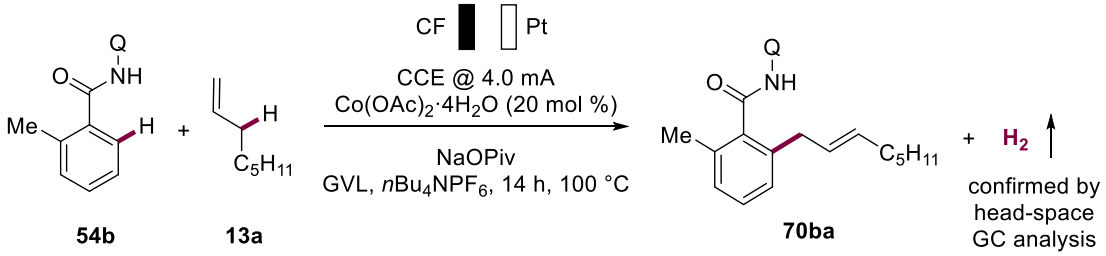

The electrocatalysis was carried out in an undivided cell, with a CF anode (10 mm × 25 mm × 6 mm) and a platinum cathode (10 mm × 25 mm × 0.125 mm). Benzamide **54b** (131.1 mg, 0.50 mmol), *n*-octene **13a** (168.4 mg, 1.50 mmol), NaOPiv (124.0 mg, 1.0 mmol), *n*-Bu_4NPF_6 (97.0 mg, 0.25 mmol) and $Co(OAc)_2·4H_2O$ (12.7 mg, 10 mol %) were placed in a 10 mL cell and dissolved in GVL (4.0 mL). Electrocatalysis was performed at 100 °C with a constant current of 4.0 mA maintained for 14 h under N_2. After cooling to ambient temperature, 1.0 mL of the headspace volume was removed for GC analysis (figure 5.15).

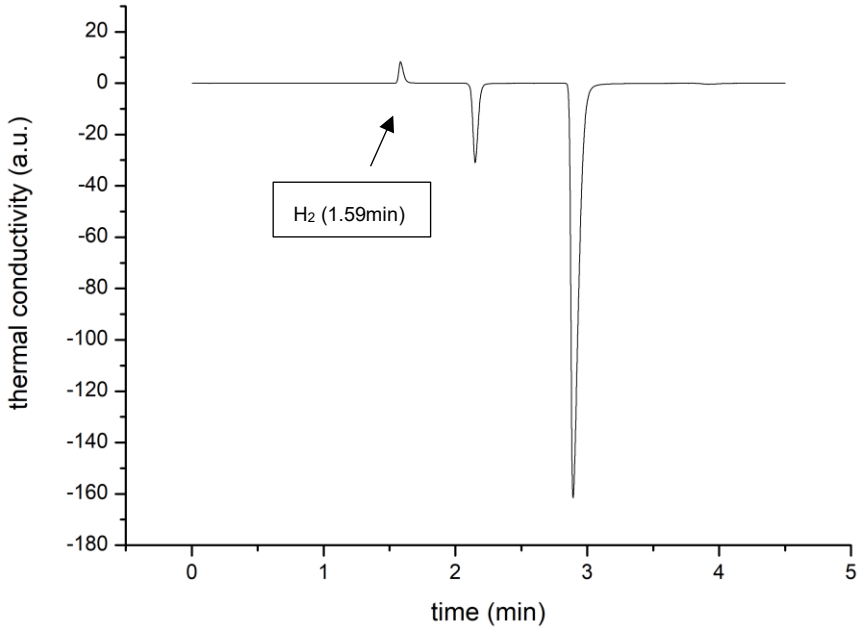

Figure 5.15. Headspace-GC analysis for **70ba**.

5.3.4.3. Cyclic Voltammetry

The cyclic voltammetry was carried out with a Metrohm Autolab PGSTAT204 workstation and the analysis was performed with the Nova 2.0 software (figure 5.16). A glassy-carbon electrode (3 mm-diameter, disc-electrode) was used as the working electrode, a Pt wire as the auxiliary electrode and a saturated calomel electrode (SCE) was employed as the reference. The measurements were carried out at a scan rate of 100 mVs^{-1}.

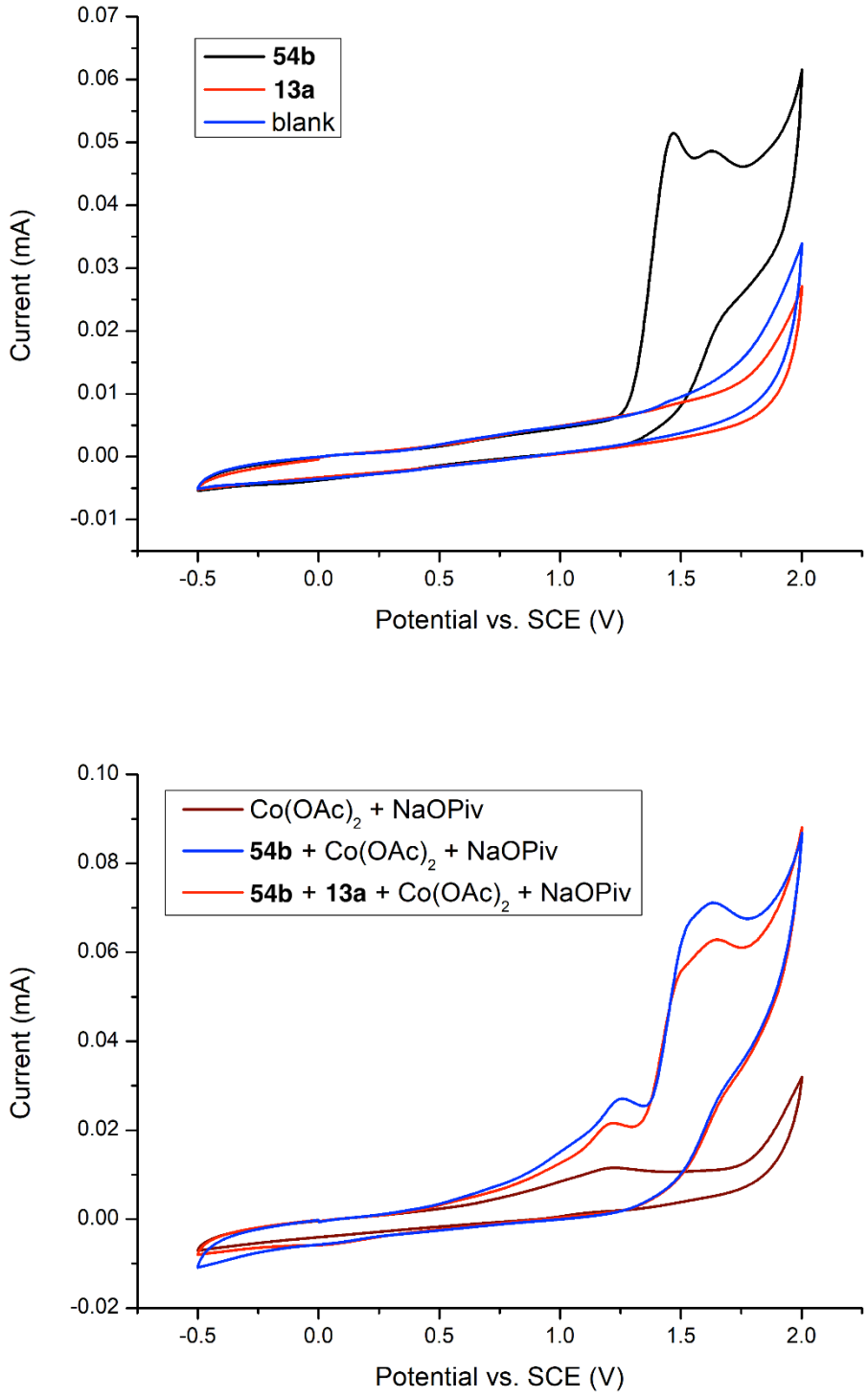

Figure 5.16. Cyclic voltammograms at 100 mVs^{-1}: *n*-Bu_4NPF_6 (0.1 M) in MeCN, concentrations of **54a**, **13a**, $Co(OAc)_2$ and NaOPiv 5 mM.

6. References

[1] a) B. R. Stockwell, *Nature* **2004**, *432*, 846-854; b) J. W. Szostak, D. P. Bartel, P. L. Luisi, *Nature* **2001**, *409*, 387-390.

[2] a) B. H. Lipshutz, N. A. Isley, J. C. Fennewald, E. D. Slack, *Angew. Chem. Int. Ed.* **2013**, *52*, 10952-10958; b) E. B. Pinxterhuis, M. Giannerini, V. Hornillos, B. L. Feringa, *Nat. Commun.* **2016**, *7*, 11698; c) S. Chu, Y. Cui, N. Liu, *Nat. Mater.* **2017**, *16*, 16-22.

[3] R. G. Bergman, *Nature* **2007**, *446*, 391-393.

[4] B. M. Trost, *Science* **1991**, *254*, 1471-1477.

[5] P. T. Anastas, J. C. Warner, *Green Chemistry: Theory and Practice*, Oxford University Press, Oxford, UK, **1998**.

[6] T. H. Meyer, L. H. Finger, P. Gandeepan, L. Ackermann, *Trends Chem.* **2019**, *1*, 63-76.

[7] C. C. C. Johansson Seechurn, M. O. Kitching, T. J. Colacot, V. Snieckus, *Angew. Chem. Int. Ed.* **2012**, *51*, 5062-5085.

[8] a) N. Miyaura, A. Suzuki, *Chem. Rev.* **1995**, *95*, 2457-2483; b) N. Miyaura, K. Yamada, A. Suzuki, *Tetrahedron Lett.* **1979**, *20*, 3437-3440; c) N. Miyaura, A. Suzuki, *J. Chem. Soc., Chem. Commun.* **1979**, 866-867.

[9] a) R. F. Heck, J. P. Nolley, *J. Org. Chem.* **1972**, *37*, 2320-2322; b) M. Tsutomu, M. Kunio, O. Atsumu, *Bull. Chem. Soc. Jpn.* **1971**, *44*, 581-581.

[10] a) B. M. Trost, D. L. Van Vranken, *Chem. Rev.* **1996**, *96*, 395-422; b) B. M. Trost, P. E. Strege, *J. Am. Chem. Soc.* **1977**, *99*, 1649-1651; c) B. M. Trost, T. J. Fullerton, *J. Am. Chem. Soc.* **1973**, *95*, 292-294; d) J. Tsuji, H. Takahashi, M. Morikawa, *Tetrahedron Lett.* **1965**, *6*, 4387-4388.

[11] a) A. S. Guram, S. L. Buchwald, *J. Am. Chem. Soc.* **1994**, *116*, 7901-7902; b) F. Paul, J. Patt, J. F. Hartwig, *J. Am. Chem. Soc.* **1994**, *116*, 5969-5970.

[12] a) R. Chinchilla, C. Nájera, *Chem. Soc. Rev.* **2011**, *40*, 5084-5121; b) R. Chinchilla, C. Nájera, *Chem. Rev.* **2007**, *107*, 874-922; c) K. Sonogashira, *J.*

Organomet. Chem. **2002**, *653*, 46-49; d) K. Sonogashira, Y. Tohda, N. Hagihara, *Tetrahedron Lett.* **1975**, *16*, 4467-4470.

[13] J.-P. Corbet, G. Mignani, *Chem. Rev.* **2006**, *106*, 2651-2710.

[14] The Nobel Prize in Chemistry 2010, https://www.nobelprize.org/prizes/chemistry/2010/summary/, accessed on 2020.04.06

[15] A. Piontek, E. Bisz, M. Szostak, *Angew. Chem. Int. Ed.* **2018**, *57*, 11116-11128.

[16] S. Santoro, F. Ferlin, L. Luciani, L. Ackermann, L. Vaccaro, *Green Chem.* **2017**, *19*, 1601-1612.

[17] Á. Molnár, *Chem. Rev.* **2011**, *111*, 2251-2320.

[18] a) R. R. Karimov, J. F. Hartwig, *Angew. Chem. Int. Ed.* **2018**, *57*, 4234-4241; b) S. K. Sinha, G. Zanoni, D. Maiti, *Asian J. Org. Chem.* **2018**, *7*, 1178-1192; c) Y. Qiu, S. Gao, *Nat. Prod. Rep.* **2016**, *33*, 562-581; d) J. Yamaguchi, A. D. Yamaguchi, K. Itami, *Angew. Chem. Int. Ed.* **2012**, *51*, 8960-9009.

[19] a) J. Zhang, L. J. Kang, T. C. Parker, S. B. Blakey, C. K. Luscombe, S. R. Marder, *Molecules* **2018**, *23*, 922; b) J.-R. Pouliot, F. Grenier, J. T. Blaskovits, S. Beaupré, M. Leclerc, *Chem. Rev.* **2016**, *116*, 14225-14274.

[20] a) M. Seki, *Org. Process Res. Dev.* **2016**, *20*, 867-877; b) L. Ackermann, *Org. Process Res. Dev.* **2015**, *19*, 260-269.

[21] L. Ackermann, *Acc. Chem. Res.* **2020**, *53*, 84-104.

[22] a) D. L. Davies, S. A. Macgregor, C. L. McMullin, *Chem. Rev.* **2017**, *117*, 8649-8709; b) D. A. Colby, R. G. Bergman, J. A. Ellman, *Chem. Rev.* **2010**, *110*, 624-655.

[23] a) C. Shan, L. Zhu, L.-B. Qu, R. Bai, Y. Lan, *Chem. Soc. Rev.* **2018**, *47*, 7552-7576; b) L. Ackermann, *Chem. Rev.* **2011**, *111*, 1315-1345; c) D. Balcells, E. Clot, O. Eisenstein, *Chem. Rev.* **2010**, *110*, 749-823; d) Y. Boutadla, D. L. Davies, S. A. Macgregor, A. I. Poblador-Bahamonde, *Dalton Trans.* **2009**, 5820-5831.

[24] a) D. Lapointe, K. Fagnou, *Chem. Lett.* **2010**, *39*, 1118-1126; b) S. I. Gorelsky, D. Lapointe, K. Fagnou, *J. Am. Chem. Soc.* **2008**, *130*, 10848-10849.

[25] a) R. A. Alharis, C. L. McMullin, D. L. Davies, K. Singh, S. A. Macgregor, *J. Am. Chem. Soc.* **2019**, *141*, 8896-8906; b) Y. Boutadla, D. L. Davies, S. A. Macgregor, A. I. Poblador-Bahamonde, *Dalton Trans.* **2009**, 5887-5893.

[26] J. Oxgaard, W. J. Tenn, R. J. Nielsen, R. A. Periana, W. A. Goddard, *Organometallics* **2007**, *26*, 1565-1567.

[27] a) E. Tan, O. Quinonero, M. Elena de Orbe, A. M. Echavarren, *ACS Catal.* **2018**, *8*, 2166-2172; b) D. Zell, M. Bursch, V. Müller, S. Grimme, L. Ackermann, *Angew. Chem. Int. Ed.* **2017**, *56*, 10378-10382; c) W. Ma, R. Mei, G. Tenti, L. Ackermann, *Chem. Eur. J.* **2014**, *20*, 15248-15251.

[28] a) C. Sambiagio, D. Schönbauer, R. Blieck, T. Dao-Huy, G. Pototschnig, P. Schaaf, T. Wiesinger, M. F. Zia, J. Wencel-Delord, T. Besset, B. U. W. Maes, M. Schnürch, *Chem. Soc. Rev.* **2018**, *47*, 6603-6743; b) Z. Chen, B. Wang, J. Zhang, W. Yu, Z. Liu, Y. Zhang, *Org. Chem. Front.* **2015**, *2*, 1107-1295; c) M. Zhang, Y. Zhang, X. Jie, H. Zhao, G. Li, W. Su, *Org. Chem. Front.* **2014**, *1*, 843-895; d) L. Ackermann, *Top. Organomet. Chem.* **2007**, *24*, 35-60.

[29] a) G. Rouquet, N. Chatani, *Angew. Chem. Int. Ed.* **2013**, *52*, 11726-11743; b) O. Daugulis, J. Roane, L. D. Tran, *Acc. Chem. Res.* **2015**, *48*, 1053-1064.

[30] S. De Sarkar, W. Liu, S. I. Kozhushkov, L. Ackermann, *Adv. Synth. Catal.* **2014**, *356*, 1461-1479.

[31] a) W. Ma, P. Gandeepan, J. Li, L. Ackermann, *Org. Chem. Front.* **2017**, *4*, 1435-1467; b) F. Zhang, D. R. Spring, *Chem. Soc. Rev.* **2014**, *43*, 6906-6919.

[32] P. Gandeepan, L. Ackermann, *Chem* **2018**, *4*, 199-222.

[33] a) O. Baudoin, *Acc. Chem. Res.* **2017**, *50*, 1114-1123; b) S. R. Neufeldt, M. S. Sanford, *Acc. Chem. Res.* **2012**, *45*, 936-946; c) C.-L. Sun, B.-J. Li, Z.-J. Shi, *Chem. Commun.* **2010**, *46*, 677-685; d) X. Chen, K. M. Engle, D.-H. Wang, J.-Q. Yu, *Angew. Chem. Int. Ed.* **2009**, *48*, 5094-5115.

[34] a) M. Nagamoto, T. Nishimura, *ACS Catal.* **2017**, *7*, 833-847; b) J. Kim, S. Chang, *Angew. Chem. Int. Ed.* **2014**, *53*, 2203-2207; c) S. Pan, T. Shibata, *ACS Catal.* **2013**, *3*, 704-712; d) T. Suzuki, *Chem. Rev.* **2011**, *111*, 1825-1845.

[35] a) T. Piou, T. Rovis, *Acc. Chem. Res.* **2018**, *51*, 170-180; b) G. Song, F. Wang, X. Li, *Chem. Soc. Rev.* **2012**, *41*, 3651-3678; c) D. A. Colby, A. S. Tsai, R. G. Bergman, J. A. Ellman, *Acc. Chem. Res.* **2012**, *45*, 814-825.

[36] a) P. Nareddy, F. Jordan, M. Szostak, *ACS Catal.* **2017**, *7*, 5721-5745; b) J. A. Leitch, C. G. Frost, *Chem. Soc. Rev.* **2017**, *46*, 7145-7153; c) V. S. Thirunavukkarasu, S. I. Kozhushkov, L. Ackermann, *Chem. Commun.* **2014**, *50*, 29-39; d) L. Ackermann, *Acc. Chem. Res.* **2014**, *47*, 281-295; e) S. I. Kozhushkov, L. Ackermann, *Chem. Sci.* **2013**, *4*, 886-896; f) P. B. Arockiam, C. Bruneau, P. H. Dixneuf, *Chem. Rev.* **2012**, *112*, 5879-5918; g) L. Ackermann, R. Vicente, *Top. Curr. Chem.* **2010**, *292*, 211-229.

[37] P. Gandeepan, T. Müller, D. Zell, G. Cera, S. Warratz, L. Ackermann, *Chem. Rev.* **2019**, *119*, 2192-2452.

[38] a) A. Wiebe, T. Gieshoff, S. Mohle, E. Rodrigo, M. Zirbes, S. R. Waldvogel, *Angew. Chem. Int. Ed.* **2018**, *57*, 5594-5619; b) M. Yan, Y. Kawamata, P. S. Baran, *Angew. Chem. Int. Ed.* **2018**, *57*, 4149-4155; c) S. Tang, Y. Liu, A. Lei, *Chem* **2018**, *4*, 27-45; d) K. D. Moeller, *Chem. Rev.* **2018**, *118*, 4817-4833; e) M. Yan, Y. Kawamata, P. S. Baran, *Chem. Rev.* **2017**, *117*, 13230-13319; f) J. Yoshida, K. Kataoka, R. Horcajada, A. Nagaki, *Chem. Rev.* **2008**, *108*, 2265-2299; g) A. Jutand, *Chem. Rev.* **2008**, *108*, 2300-2347.

[39] a) K.-J. Jiao, Y.-K. Xing, Q.-L. Yang, H. Qiu, T.-S. Mei, *Acc. Chem. Res.* **2020**, *53*, 300-310; b) T. H. Meyer, L. H. Finger, P. Gandeepan, L. Ackermann, *Trends Chem.* **2019**, *1*, 63-76; c) N. Sauermann, T. H. Meyer, Y. Qiu, L. Ackermann, *ACS Catal.* **2018**, *8*, 7086-7103.

[40] C. Amatore, C. Cammoun, A. Jutand, *Adv. Synth. Catal.* **2007**, *349*, 292-296.

[41] a) H. Aiso, T. Kochi, H. Mutsutani, T. Tanabe, S. Nishiyama, F. Kakiuchi, *J. Org. Chem.* **2012**, *77*, 7718-7724; b) F. Kakiuchi, T. Kochi, H. Mutsutani, N.

Kobayashi, S. Urano, M. Sato, S. Nishiyama, T. Tanabe, *J. Am. Chem. Soc.* **2009**, *131*, 11310-11311.

[42] a) N. Sauermann, T. H. Meyer, L. Ackermann, *Chem. Eur. J.* **2018**, *24*, 16209-16217; b) S.-K. Zhang, R. C. Samanta, A. Del Vecchio, L. Ackermann, *Chem. Eur. J.* **2020**, 10.1002/chem.202001318.

[43] F. Hebrard, P. Kalck, *Chem. Rev.* **2009**, *109*, 4272-4282.

[44] M. S. Kharasch, E. K. Fields, *J. Am. Chem. Soc.* **1941**, *63*, 2316-2320.

[45] a) I. U. Khand, G. R. Knox, P. L. Pauson, W. E. Watts, *J. Chem. Soc., Perkin Trans. 1* **1973**, 975-977; b) I. U. Khand, G. R. Knox, P. L. Pauson, W. E. Watts, *J. Chem. Soc. D* **1971**, 36a-36a.

[46] K. M. Nicholas, R. Pettit, *J. Organomet. Chem.* **1972**, *44*, C21-C24.

[47] G. Cahiez, A. Moyeux, *Chem. Rev.* **2010**, *110*, 1435-1462.

[48] a) M. Moselage, J. Li, L. Ackermann, *ACS Catal.* **2016**, *6*, 498-525; b) L. Ackermann, *J. Org. Chem.* **2014**, *79*, 8948-8954.

[49] S. Murahashi, *J. Am. Chem. Soc.* **1955**, *77*, 6403-6404.

[50] S. Murahashi, S. Horiie, *J. Am. Chem. Soc.* **1956**, *78*, 4816-4817.

[51] H.-F. Klein, M. Helwig, U. Koch, U. Flörke, H.-J. Haupt, *Z. Naturforsch. B* **1993**, *48*, 778-784.

[52] H.-F. Klein, S. Schneider, M. He, U. Floerke, H.-J. Haupt, *Eur. J. Inorg. Chem.* **2000**, 2295-2301.

[53] G. Halbritter, F. Knoch, A. Wolski, H. Kisch, *Angew. Chem. Int. Ed.* **1994**, *33*, 1603-1605.

[54] K. Gao, P.-S. Lee, T. Fujita, N. Yoshikai, *J. Am. Chem. Soc.* **2010**, *132*, 12249-12251.

[55] P.-S. Lee, T. Fujita, N. Yoshikai, *J. Am. Chem. Soc.* **2011**, *133*, 17283-17295.

[56] K. Gao, N. Yoshikai, *J. Am. Chem. Soc.* **2011**, *133*, 400-402.

[57] L. Ilies, Q. Chen, X. Zeng, E. Nakamura, *J. Am. Chem. Soc.* **2011**, *133*, 5221-5223.

[58] a) J. Li, L. Ackermann, *Chem. Eur. J.* **2015**, *21*, 5718-5722; b) R. Mei, L. Ackermann, *Adv. Synth. Catal.* **2016**, *358*, 2443-2448; c) B. Punji, W. Song, G. A. Shevchenko, L. Ackermann, *Chem. Eur. J.* **2013**, *19*, 10605-10610; d) W. Song, L. Ackermann, *Angew. Chem. Int. Ed.* **2012**, *51*, 8251-8254.

[59] K. Gao, P.-S. Lee, C. Long, N. Yoshikai, *Org. Lett.* **2012**, *14*, 4234-4237.

[60] M. Moselage, N. Sauermann, S. C. Richter, L. Ackermann, *Angew. Chem. Int. Ed.* **2015**, *54*, 6352-6355.

[61] T. Yoshino, S. Matsunaga, *Adv. Synth. Catal.* **2017**, *359*, 1245-1262.

[62] T. Yoshino, H. Ikemoto, S. Matsunaga, M. Kanai, *Angew. Chem. Int. Ed.* **2013**, *52*, 2207-2211.

[63] U. Koelle, B. Fuss, M. V. Rajasekharan, B. L. Ramakrishna, J. H. Ammeter, M. C. Boehm, *J. Am. Chem. Soc.* **1984**, *106*, 4152-4160.

[64] J. Li, L. Ackermann, *Angew. Chem. Int. Ed.* **2015**, *54*, 3635-3638.

[65] D.-G. Yu, T. Gensch, F. de Azambuja, S. Vásquez-Céspedes, F. Glorius, *J. Am. Chem. Soc.* **2014**, *136*, 17722-17725.

[66] M. Moselage, N. Sauermann, J. Koeller, W. Liu, D. Gelman, L. Ackermann, *Synlett* **2015**, *26*, 1596-1600.

[67] D. Zell, Q. Bu, M. Feldt, L. Ackermann, *Angew. Chem. Int. Ed.* **2016**, *55*, 7408-7412.

[68] H. Ikemoto, T. Yoshino, K. Sakata, S. Matsunaga, M. Kanai, *J. Am. Chem. Soc.* **2014**, *136*, 5424-5431.

[69] a) H. Wang, M. Moselage, M. J. González, L. Ackermann, *ACS Catal.* **2016**, *6*, 2705-2709; b) H. Wang, J. Koeller, W. Liu, L. Ackermann, *Chem. Eur. J.* **2015**, *21*, 15525-15528.

[70] F. Pesciaioli, U. Dhawa, J. C. A. Oliveira, R. Yin, M. John, L. Ackermann, *Angew. Chem. Int. Ed.* **2018**, *57*, 15425-15429.

[71] M. Sen, B. Emayavaramban, N. Barsu, J. R. Premkumar, B. Sundararaju, *ACS Catal.* **2016**, *6*, 2792-2796.

[72] V. G. Zaitsev, D. Shabashov, O. Daugulis, *J. Am. Chem. Soc.* **2005**, *127*, 13154-13155.

[73] a) S. Rej, Y. Ano, N. Chatani, *Chem. Rev.* **2020**, *120*, 1788-1887; b) Y. Kommagalla, N. Chatani, *Coord. Chem. Rev.* **2017**, *350*, 117-135.

[74] L. Grigorjeva, O. Daugulis, *Angew. Chem. Int. Ed.* **2014**, *53*, 10209-10212.

[75] L. Grigorjeva, O. Daugulis, *Org. Lett.* **2014**, *16*, 4684-4687.

[76] T. T. Nguyen, L. Grigorjeva, O. Daugulis, *ACS Catal.* **2016**, *6*, 551-554.

[77] a) O. Planas, C. J. Whiteoak, A. Company, X. Ribas, *Adv. Synth. Catal.* **2015**, *357*, 4003-4012; b) D. Kalsi, B. Sundararaju, *Org. Lett.* **2015**, *17*, 6118-6121.

[78] N. T. Thanh, G. Liene, D. Olafs, *Angew. Chem. Int. Ed.* **2018**, *57*, 1688-1691.

[79] R. Mei, H. Wang, S. Warratz, S. A. Macgregor, L. Ackermann, *Chem. Eur. J.* **2016**, *22*, 6759-6763.

[80] W. Ma, L. Ackermann, *ACS Catal.* **2015**, *5*, 2822-2825.

[81] L.-B. Zhang, X.-Q. Hao, S.-K. Zhang, Z.-J. Liu, X.-X. Zheng, J.-F. Gong, J.-L. Niu, M.-P. Song, *Angew. Chem. Int. Ed.* **2015**, *54*, 272-275.

[82] R. Ueno, S. Natsui, N. Chatani, *Org. Lett.* **2018**, *20*, 1062-1065.

[83] V. G. Landge, G. Jaiswal, E. Balaraman, *Org. Lett.* **2016**, *18*, 812-815.

[84] S. Maity, R. Kancherla, U. Dhawa, E. Hoque, S. Pimparkar, D. Maiti, *ACS Catal.* **2016**, *6*, 5493-5499.

[85] T. Yamaguchi, Y. Kommagalla, Y. Aihara, N. Chatani, *Chem. Commun.* **2016**, *52*, 10129-10132.

[86] Y. Kommagalla, K. Yamazaki, T. Yamaguchi, N. Chatani, *Chem. Commun.* **2018**, *54*, 1359-1362.

[87] X. Wu, K. Yang, Y. Zhao, H. Sun, G. Li, H. Ge, *Nat. Commun.* **2015**, *6*, 6462.

[88] J. Zhang, H. Chen, C. Lin, Z. Liu, C. Wang, Y. Zhang, *J. Am. Chem. Soc.* **2015**, *137*, 12990-12996.

[89] a) L. Zeng, S. Tang, D. Wang, Y. Deng, J.-L. Chen, J.-F. Lee, A. Lei, *Org. Lett.* **2017**, *19*, 2170-2173; b) P. Williamson, A. Galvan, M. J. Gaunt, *Chem. Sci.*

2017, *8*, 2588-2591; c) N. Barsu, S. K. Bolli, B. Sundararaju, *Chem. Sci.* **2017**, *8*, 2431-2435.

[90] N. Sauermann, T. H. Meyer, C. Tian, L. Ackermann, *J. Am. Chem. Soc.* **2017**, *139*, 18452-18455.

[91] N. Sauermann, R. Mei, L. Ackermann, *Angew. Chem. Int. Ed.* **2018**, *57*, 5090-5094.

[92] X. Gao, P. Wang, L. Zeng, S. Tang, A. Lei, *J. Am. Chem. Soc.* **2018**, *140*, 4195-4199.

[93] C. Tian, L. Massignan, T. H. Meyer, L. Ackermann, *Angew. Chem. Int. Ed.* **2018**, *57*, 2383-2387.

[94] R. Mei, N. Sauermann, J. C. A. Oliveira, L. Ackermann, *J. Am. Chem. Soc.* **2018**, *140*, 7913-7921.

[95] S. Tang, D. Wang, Y. Liu, L. Zeng, A. Lei, *Nat. Commun.* **2018**, *9*, 798.

[96] T. H. Meyer, J. C. A. Oliveira, S. C. Sau, N. W. J. Ang, L. Ackermann, *ACS Catal.* **2018**, *8*, 9140-9147.

[97] R. Mei, W. Ma, Y. Zhang, X. Guo, L. Ackermann, *Org. Lett.* **2019**, *21*, 6534-6538.

[98] T. H. Meyer, G. A. Chesnokov, L. Ackermann, *ChemSusChem* **2020**, *13*, 668-671.

[99] a) S. C. Sau, R. Mei, J. Struwe, L. Ackermann, *ChemSusChem* **2019**, *12*, 3023-3027; b) L. Zeng, H. Li, S. Tang, X. Gao, Y. Deng, G. Zhang, C.-W. Pao, J.-L. Chen, J.-F. Lee, A. Lei, *ACS Catal.* **2018**, *8*, 5448-5453.

[100] F. Ullmann, P. Sponagel, *Ber. Dtsch. Chem. Ges.* **1905**, *38*, 2211-2212.

[101] I. Goldberg, *Ber. Dtsch. Chem. Ges.* **1906**, *39*, 1691-1692.

[102] H.-Q. Do, O. Daugulis, *J. Am. Chem. Soc.* **2007**, *129*, 12404-12405.

[103] H.-Q. Do, R. M. K. Khan, O. Daugulis, *J. Am. Chem. Soc.* **2008**, *130*, 15185-15192.

[104] L. Ackermann, H. K. Potukuchi, D. Landsberg, R. Vicente, *Org. Lett.* **2008**, *10*, 3081-3084.

[105] M. Shang, S.-Z. Sun, H.-X. Dai, J.-Q. Yu, *Org. Lett.* **2014**, *16*, 5666-5669.

[106] M. Shang, H.-L. Wang, S.-Z. Sun, H.-X. Dai, J.-Q. Yu, *J. Am. Chem. Soc.* **2014**, *136*, 11590-11593.

[107] J. Zhang, D. Li, H. Chen, B. Wang, Z. Liu, Y. Zhang, *Adv. Synth. Catal.* **2016**, *358*, 792-807.

[108] X. Chen, X.-S. Hao, C. E. Goodhue, J.-Q. Yu, *J. Am. Chem. Soc.* **2006**, *128*, 6790-6791.

[109] L. D. Tran, J. Roane, O. Daugulis, *Angew. Chem. Int. Ed.* **2013**, *52*, 6043-6046.

[110] S.-i. Fukuzawa, E. Shimizu, Y. Atsuumi, M. Haga, K. Ogata, *Tetrahedron Lett.* **2009**, *50*, 2374-2376.

[111] Q.-L. Yang, X.-Y. Wang, J.-Y. Lu, L.-P. Zhang, P. Fang, T.-S. Mei, *J. Am. Chem. Soc.* **2018**, *140*, 11487-11494.

[112] S. Kathiravan, S. Suriyanarayanan, I. A. Nicholls, *Org. Lett.* **2019**, *21*, 1968-1972.

[113] X. Yang, Q.-L. Yang, X.-Y. Wang, H.-H. Xu, T.-S. Mei, Y. Huang, P. Fang, *J. Org. Chem.* **2020**, *85*, 3497-3507.

[114] C. Amatore, C. Cammoun, A. Jutand, *Adv. Synth. Catal.* **2007**, *349*, 292-296.

[115] a) Y. Qiu, A. Scheremetjew, L. Ackermann, *J. Am. Chem. Soc.* **2019**, *141*, 2731-2738; b) Y. Qiu, W.-J. Kong, J. Struwe, N. Sauermann, T. Rogge, A. Scheremetjew, L. Ackermann, *Angew. Chem. Int. Ed.* **2018**, *57*, 5828-5832.

[116] a) Y. Qiu, M. Stangier, T. H. Meyer, J. C. A. Oliveira, L. Ackermann, *Angew. Chem. Int. Ed.* **2018**, *57*, 14179-14183; b) Q.-L. Yang, Y.-K. Xing, X.-Y. Wang, H.-X. Ma, X.-J. Weng, X. Yang, H.-M. Guo, T.-S. Mei, *J. Am. Chem. Soc.* **2019**, *141*, 18970-18976.

[117] a) C. Borie, L. Ackermann, M. Nechab, *Chem. Soc. Rev.* **2016**, *45*, 1368-1386; b) B. Ye, N. Cramer, *Acc. Chem. Res.* **2015**, *48*, 1308-1318.

[118] a) P. Gomes, C. Gosmini, J. Périchon, *Tetrahedron* **2003**, *59*, 2999-3002; b) P. Gomes, C. Gosmini, J. Périchon, *J. Org. Chem.* **2003**, *68*, 1142-1145; c) P.

Gomes, H. Fillon, C. Gosmini, E. Labbé, J. Périchon, *Tetrahedron* **2002**, *58*, 8417-8424.

[119] C. Tian, U. Dhawa, J. Struwe, L. Ackermann, *Chin. J. Chem.* **2019**, *37*, 552-556.

[120] a) S.-K. Zhang, J. Struwe, L. Hu, L. Ackermann, *Angew. Chem. Int. Ed.* **2020**, *59*, 3178-3183; b) Y. Kawamata, J. C. Vantourout, D. P. Hickey, P. Bai, L. Chen, Q. Hou, W. Qiao, K. Barman, M. A. Edwards, A. F. Garrido-Castro, J. N. deGruyter, H. Nakamura, K. Knouse, C. Qin, K. J. Clay, D. Bao, C. Li, J. T. Starr, C. Garcia-Irizarry, N. Sach, H. S. White, M. Neurock, S. D. Minteer, P. S. Baran, *J. Am. Chem. Soc.* **2019**, *141*, 6392-6402; c) S. K. Zhang, R. C. Samanta, N. Sauermann, L. Ackermann, *Chem. Eur. J.* **2018**, *24*, 19166-19170.

[121] C. Tian, U. Dhawa, A. Scheremetjew, L. Ackermann, *ACS Catal.* **2019**, *9*, 7690-7696.

[122] C. Zhu, M. Stangier, J. C. A. Oliveira, L. Massignan, L. Ackermann, *Chem. Eur. J.* **2019**, *25*, 16382-16389.

[123] a) M. Lamblin, A. Couture, E. Deniau, P. Grandclaudon, *Org. Biomol. Chem.* **2007**, *5*, 1466-1471; b) Y. Kato, H. Ebiike, K. Achiwa, N. Ashizawa, T. Kurihara, F. Kobayashi, *Chem. Pharm. Bull.* **1990**, *38*, 2060-2062.

[124] a) P. Gandeepan, N. Kaplaneris, S. Santoro, L. Vaccaro, L. Ackermann, *ACS Sustain. Chem. Eng.* **2019**, *7*, 8023-8040; b) S. Santoro, F. Ferlin, L. Luciani, L. Ackermann, L. Vaccaro, *Green Chem.* **2017**, *19*, 1601-1612; c) F. Ferlin, S. Santoro, L. Ackermann, L. Vaccaro, *Green Chem.* **2017**, *19*, 2510-2514.

[125] a) A. Shrestha, M. Lee, A. L. Dunn, M. S. Sanford, *Org. Lett.* **2018**, *20*, 204-207; b) Q.-L. Yang, Y.-Q. Li, C. Ma, P. Fang, X.-J. Zhang, T.-S. Mei, *J. Am. Chem. Soc.* **2017**, *139*, 3293-3298; c) Y.-Q. Li, Q.-L. Yang, P. Fang, T.-S. Mei, D. Zhang, *Org. Lett.* **2017**, *19*, 2905-2908; d) Y. B. Dudkina, D. Y. Mikhaylov, T. V. Gryaznova, A. I. Tufatullin, O. N. Kataeva, D. A. Vicic, Y. H. Budnikova, *Organometallics* **2013**, *32*, 4785-4792.

[126] S. Santoro, A. Marrocchi, D. Lanari, L. Ackermann, L. Vaccaro, *Chem. Eur. J.* **2018**, *24*, 13383-13390.

[127] W. Wang, M. M. Lorion, J. Shah, A. R. Kapdi, L. Ackermann, *Angew. Chem. Int. Ed.* **2018**, *57*, 14700-14717.

[128] R. S. Sherbo, R. S. Delima, V. A. Chiykowski, B. P. MacLeod, C. P. Berlinguette, *Nat. Catal.* **2018**, *1*, 501-507.

[129] a) Y. Qiu, A. Scheremetjew, L. H. Finger, L. Ackermann, *Chem. Eur. J.* **2020**, *26*, 3241-3246; b) H. Yan, Z.-W. Hou, H.-C. Xu, *Angew. Chem. Int. Ed.* **2019**, *58*, 4592-4595.

[130] Y. Imada, Y. Okada, K. Noguchi, K. Chiba, *Angew. Chem. Int. Ed.* **2019**, *58*, 125-129.

[131] M. Zhong, K. Tran, Y. Min, C. Wang, Z. Wang, C.-T. Dinh, P. De Luna, Z. Yu, A. S. Rasouli, P. Brodersen, S. Sun, O. Voznyy, C.-S. Tan, M. Askerka, F. Che, M. Liu, A. Seifitokaldani, Y. Pang, S.-C. Lo, A. Ip, Z. Ulissi, E. H. Sargent, *Nature* **2020**, *581*, 178-183.

[132] R. Ueno, S. Natsui, N. Chatani, *Org. Lett.* **2018**, *20*, 1062-1065.

7. NMR Spectra

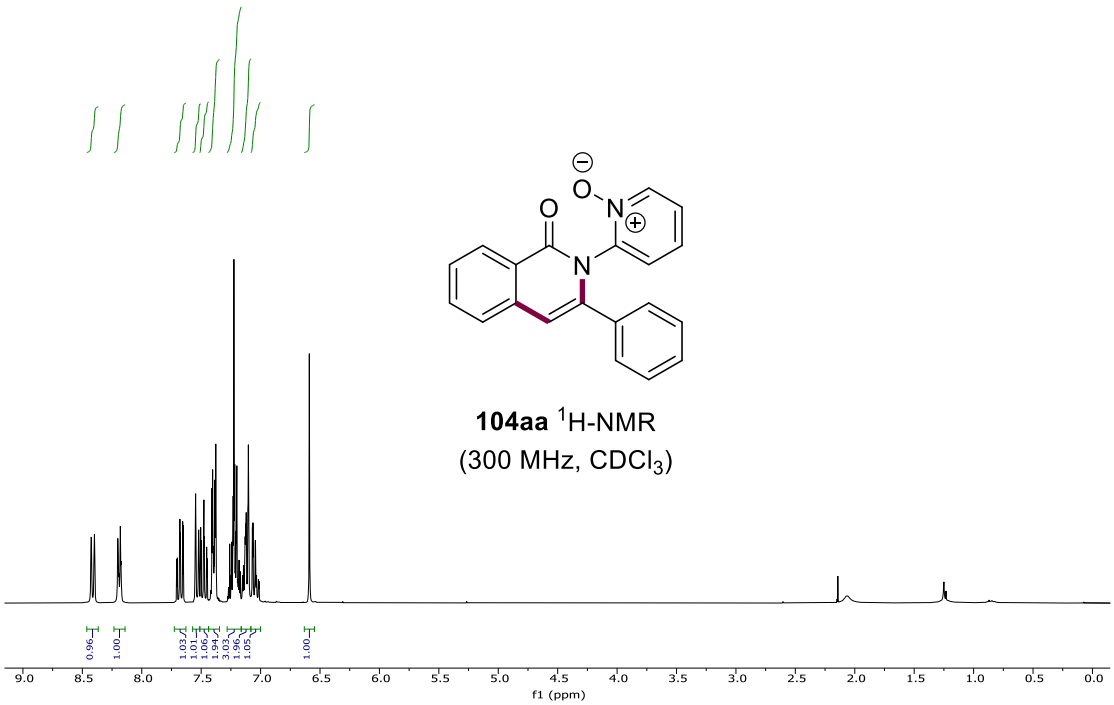

104aa ^{1}H-NMR
(300 MHz, $CDCl_3$)

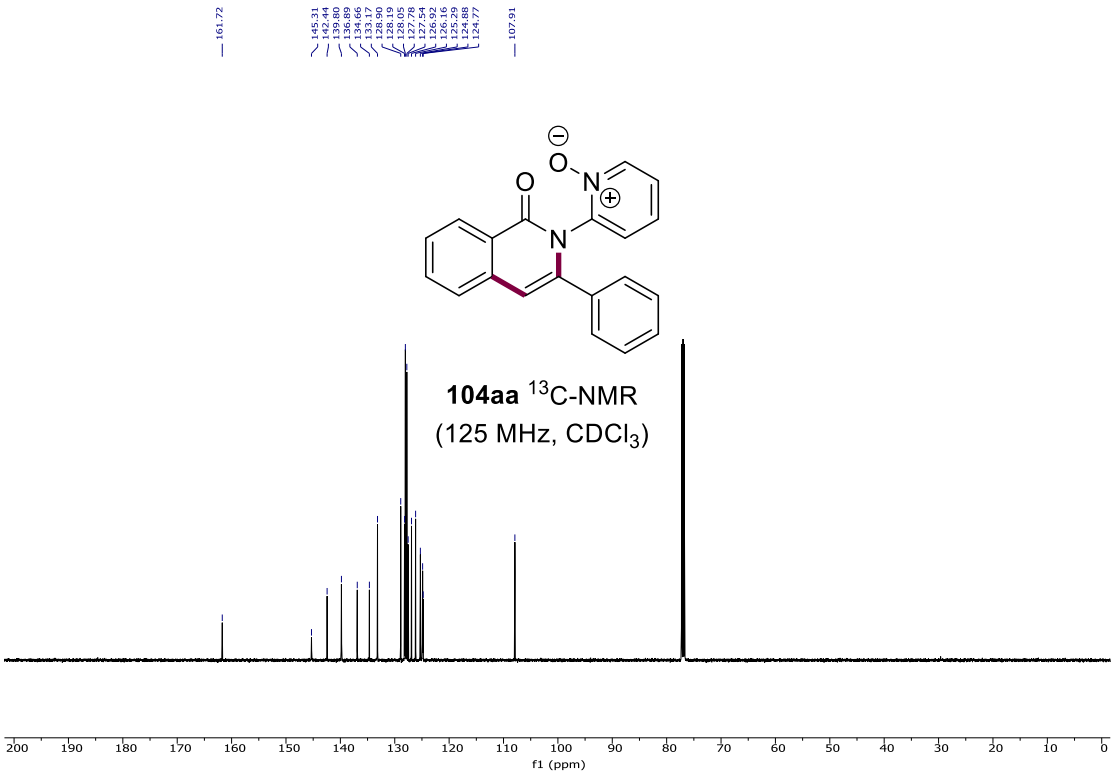

104aa ^{13}C-NMR
(125 MHz, $CDCl_3$)

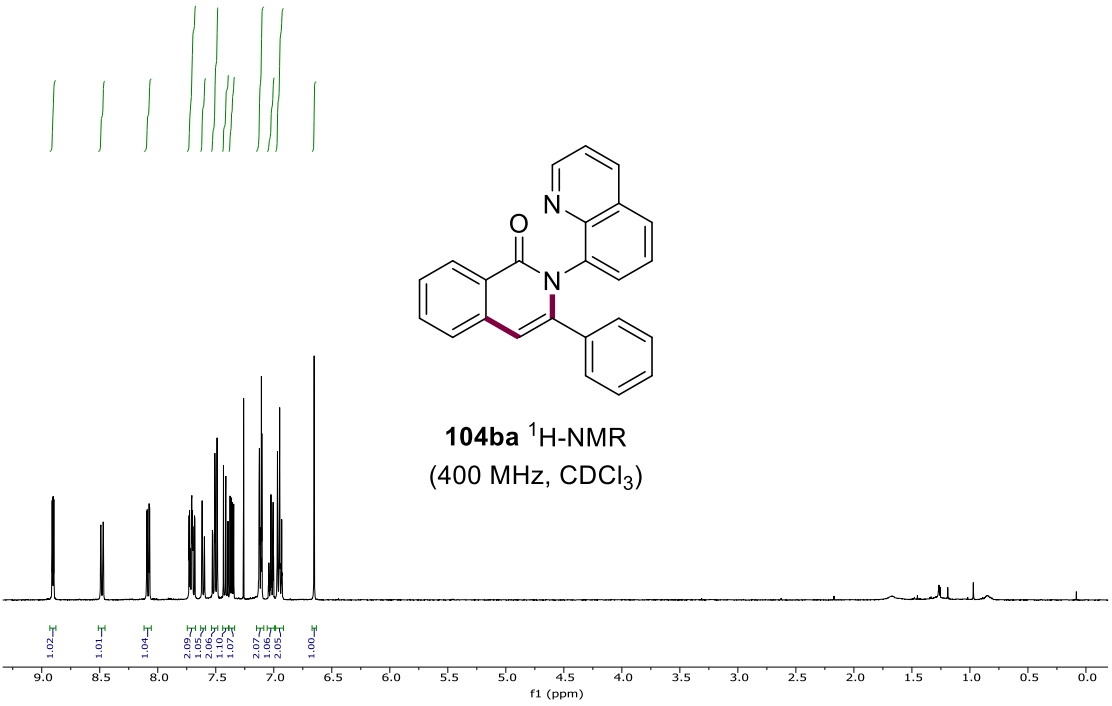

104ba ^{1}H-NMR
(400 MHz, $CDCl_3$)

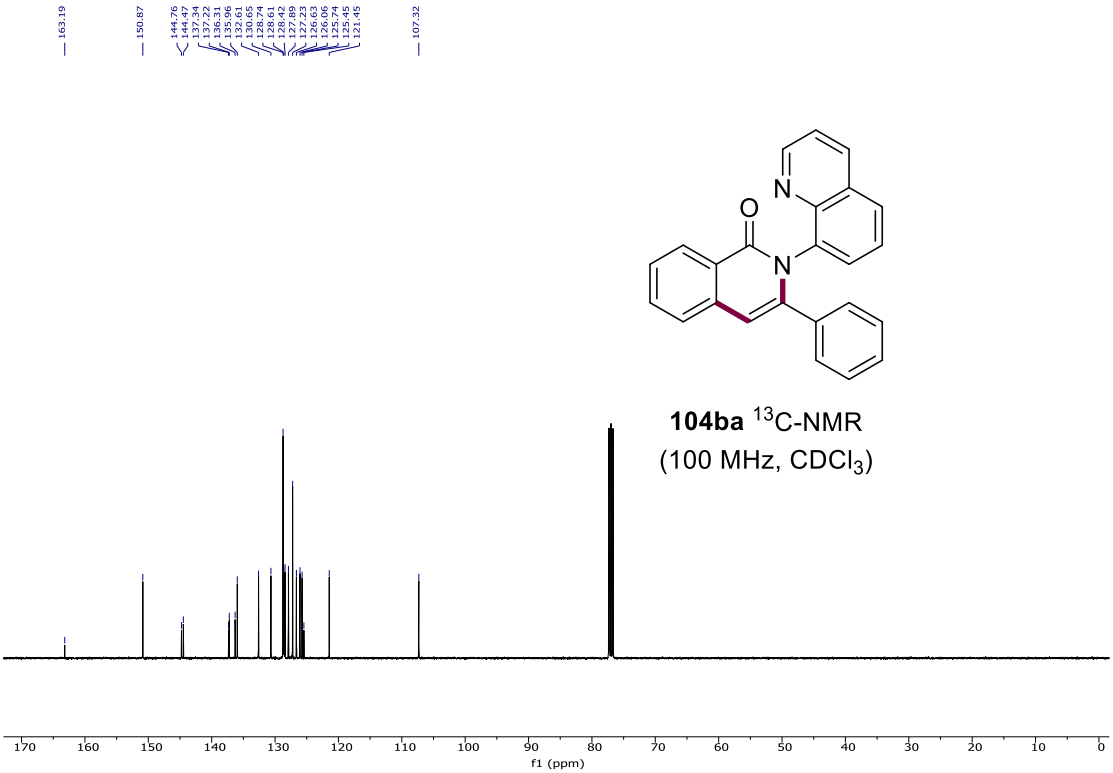

104ba ^{13}C-NMR
(100 MHz, $CDCl_3$)

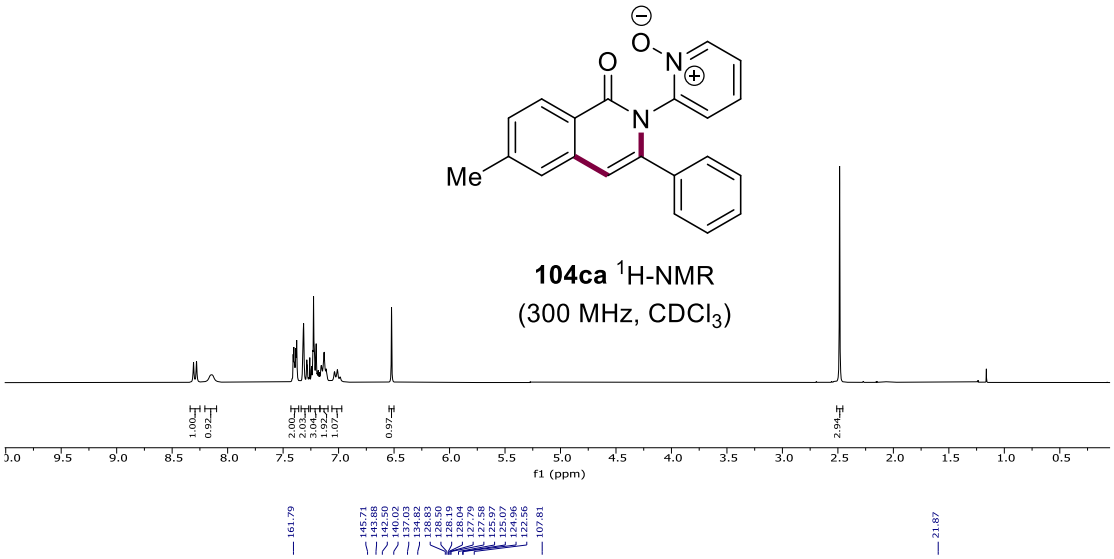
Me
104ca 1H-NMR
(300 MHz, CDCl3)
f1 (ppm)

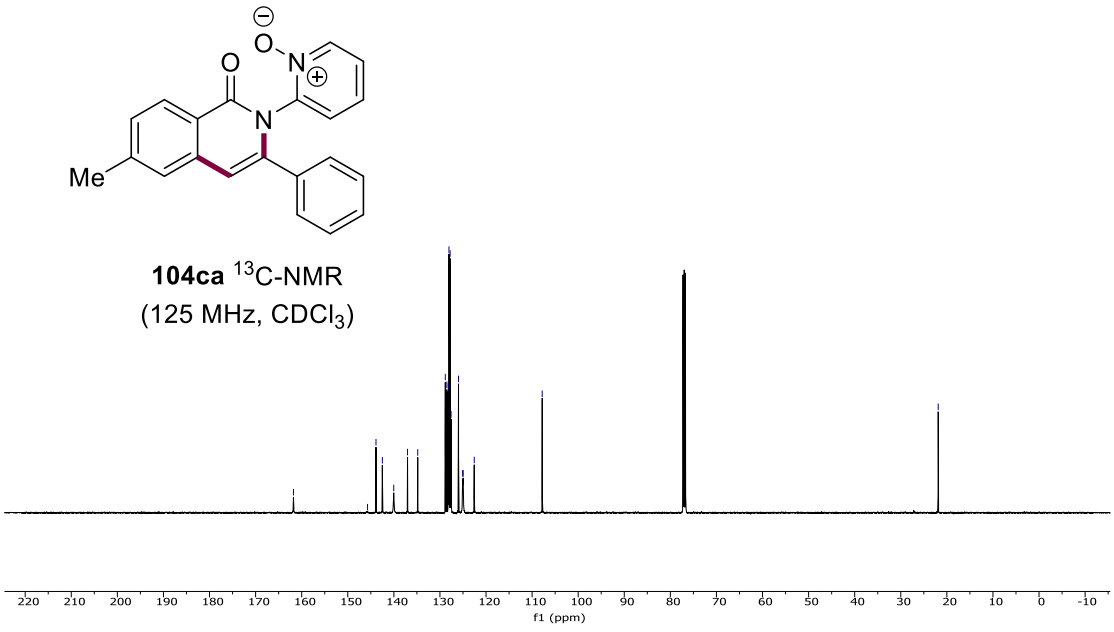
Me
104ca 13C-NMR
(125 MHz, CDCl3)
f1 (ppm)

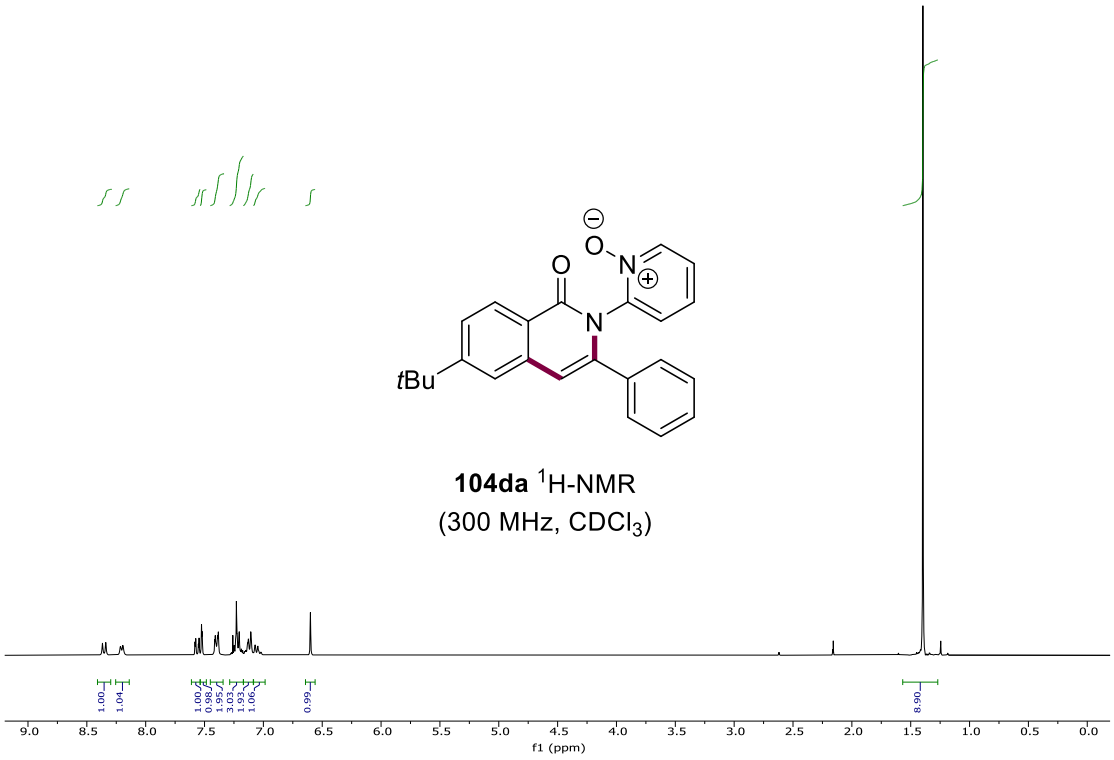

104da ^{1}H-NMR
(300 MHz, $CDCl_3$)

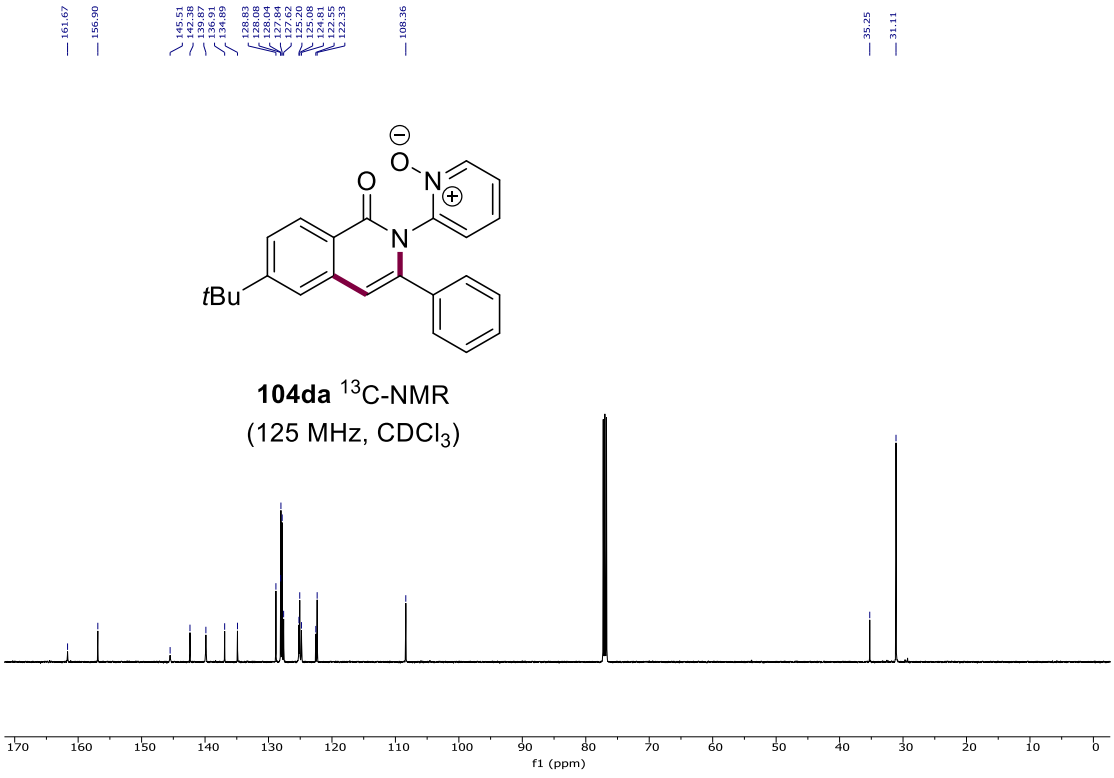

104da ^{13}C-NMR
(125 MHz, $CDCl_3$)

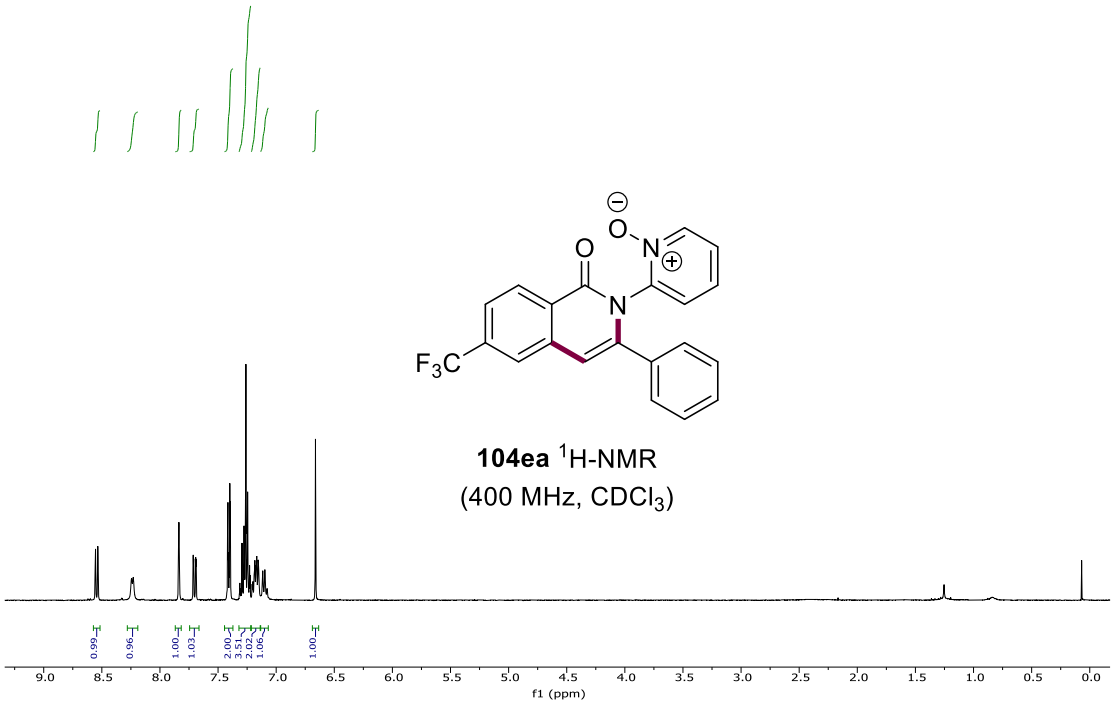

104ea ^{1}H-NMR
(400 MHz, $CDCl_3$)

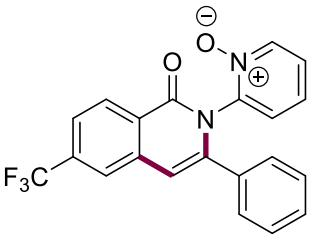

104ea ^{13}C-NMR
(100 MHz, $CDCl_3$)

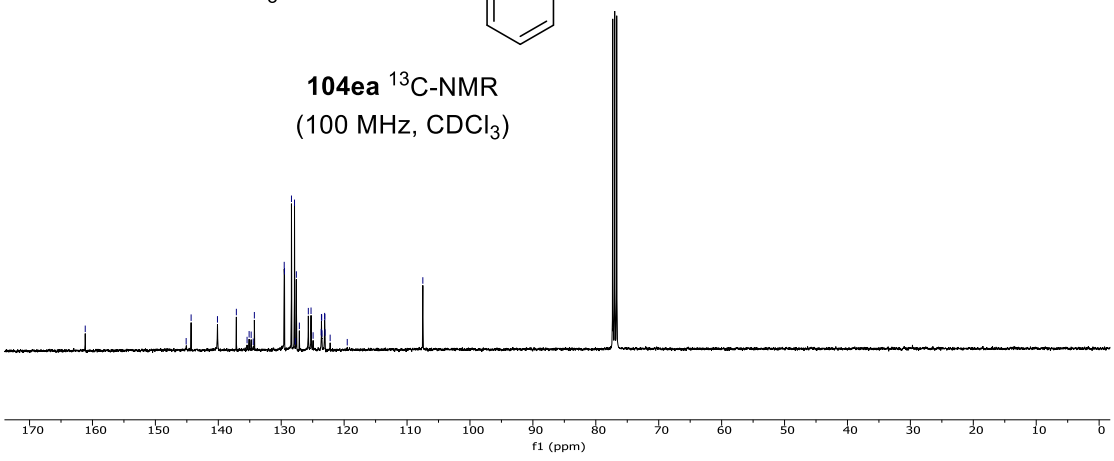

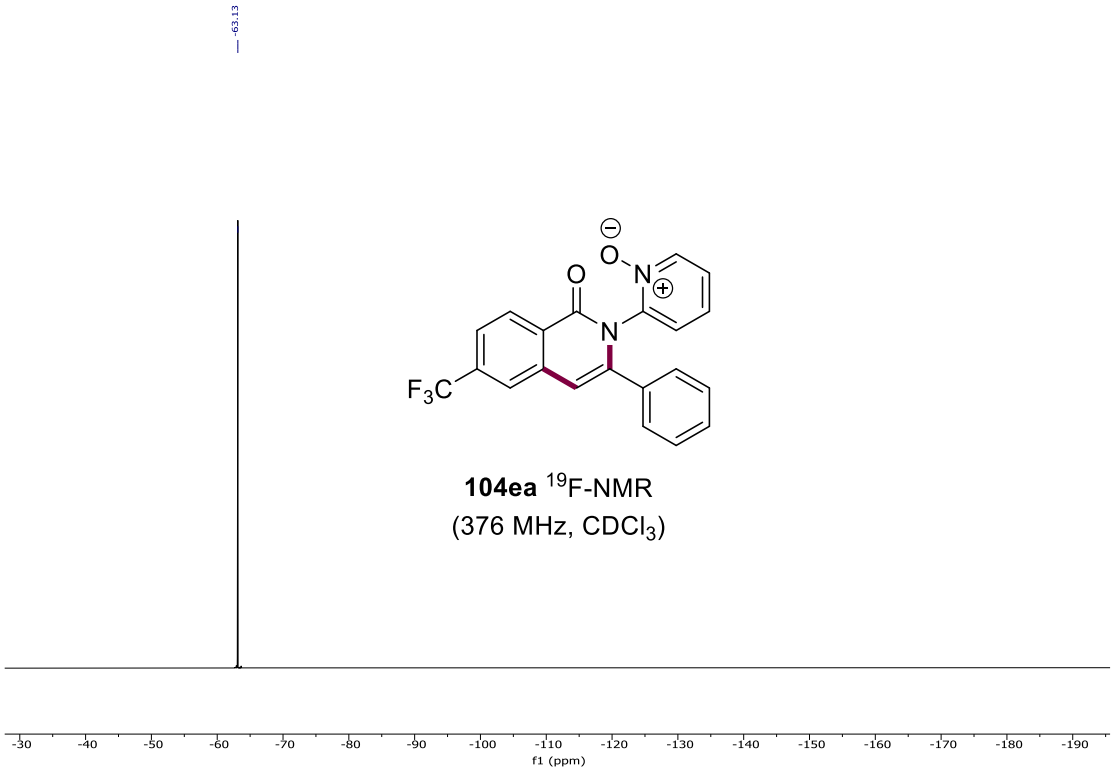

104ea ^{19}F-NMR
(376 MHz, $CDCl_3$)

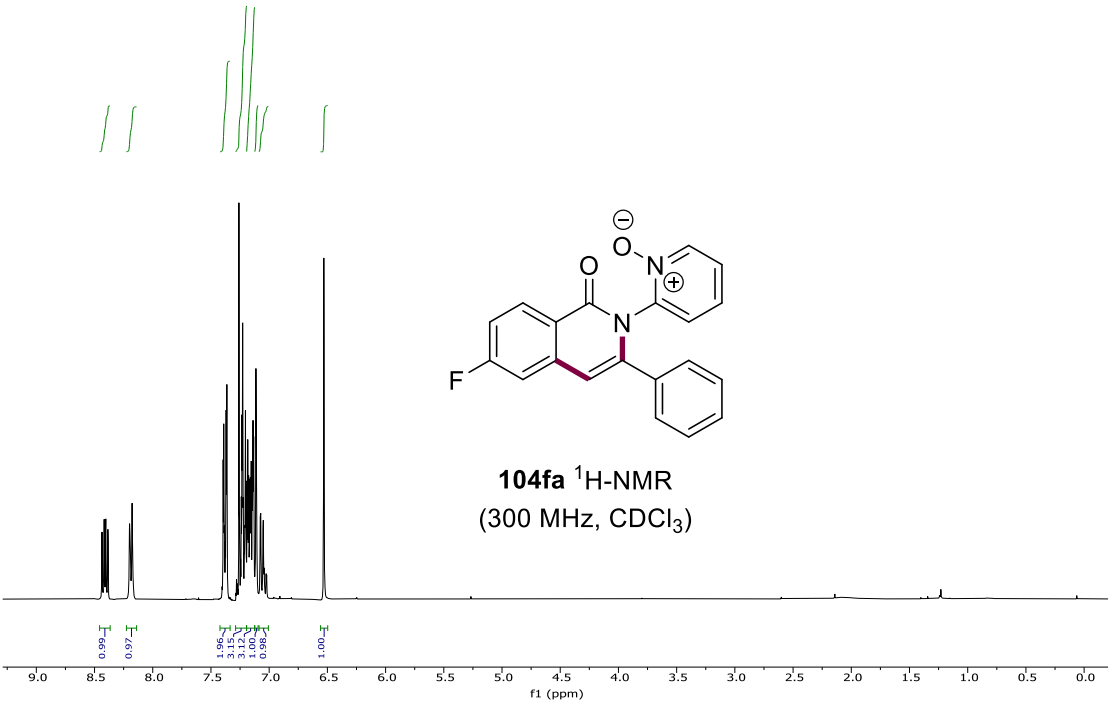

104fa ^{1}H-NMR
(300 MHz, $CDCl_3$)

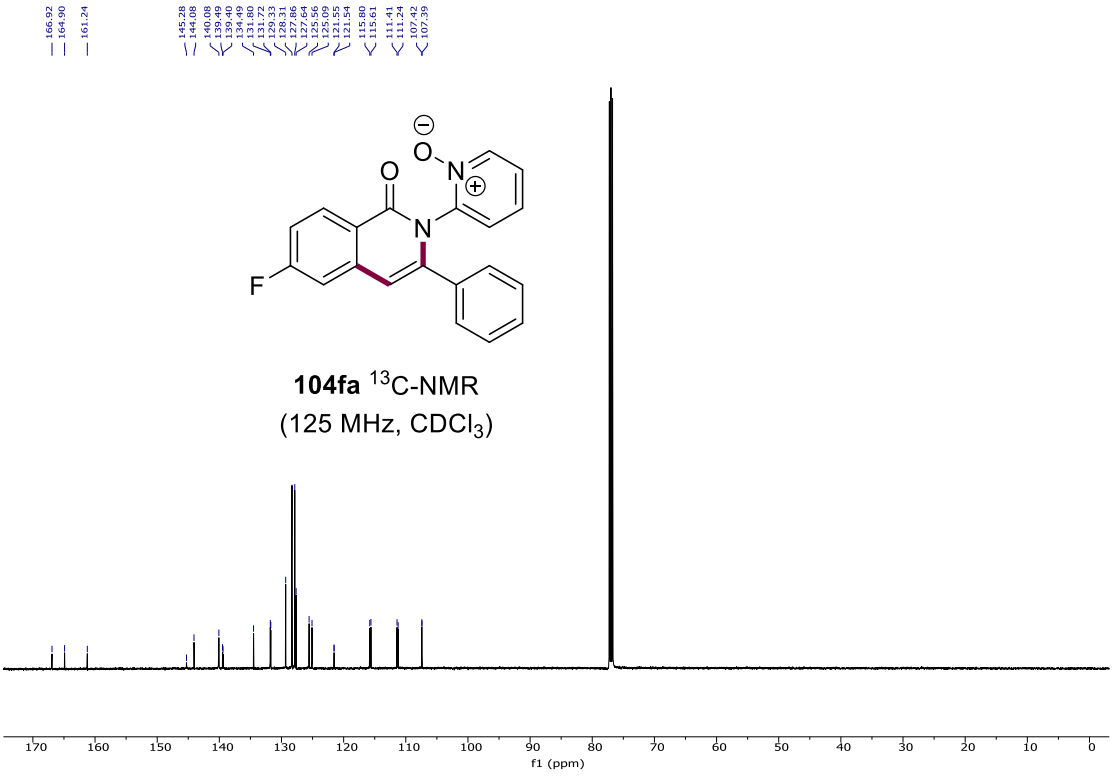

104fa ^{13}C-NMR
(125 MHz, $CDCl_3$)

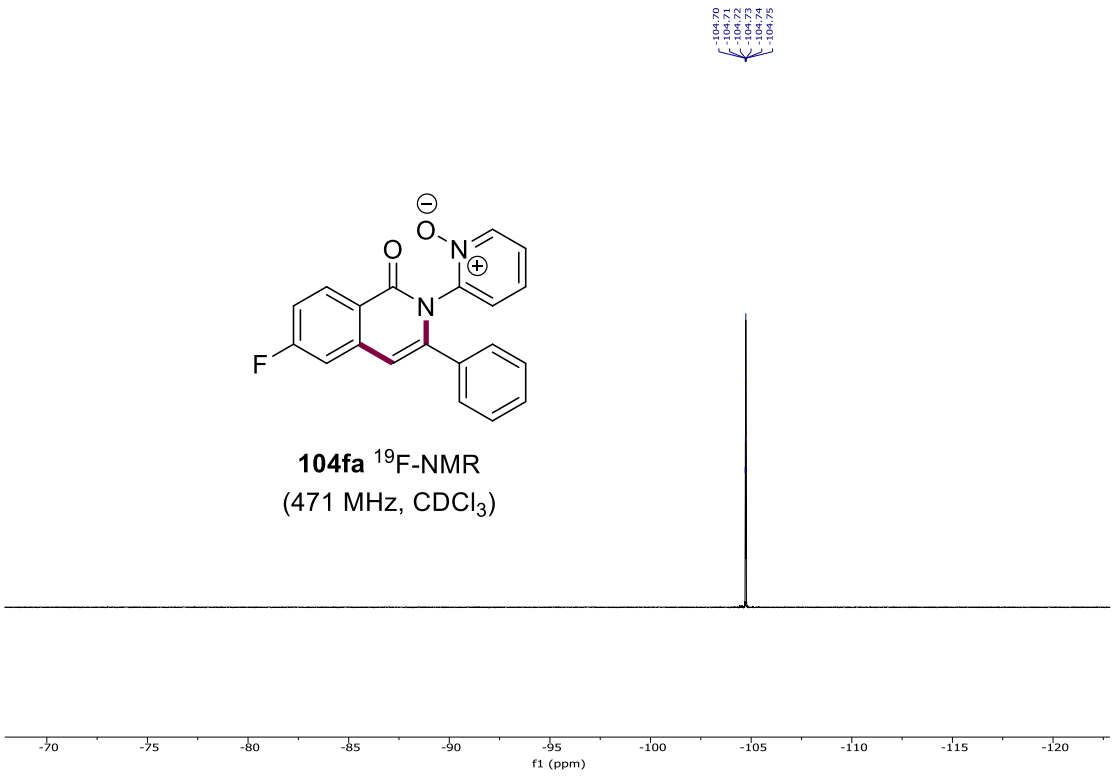

104fa ^{19}F-NMR
(471 MHz, $CDCl_3$)

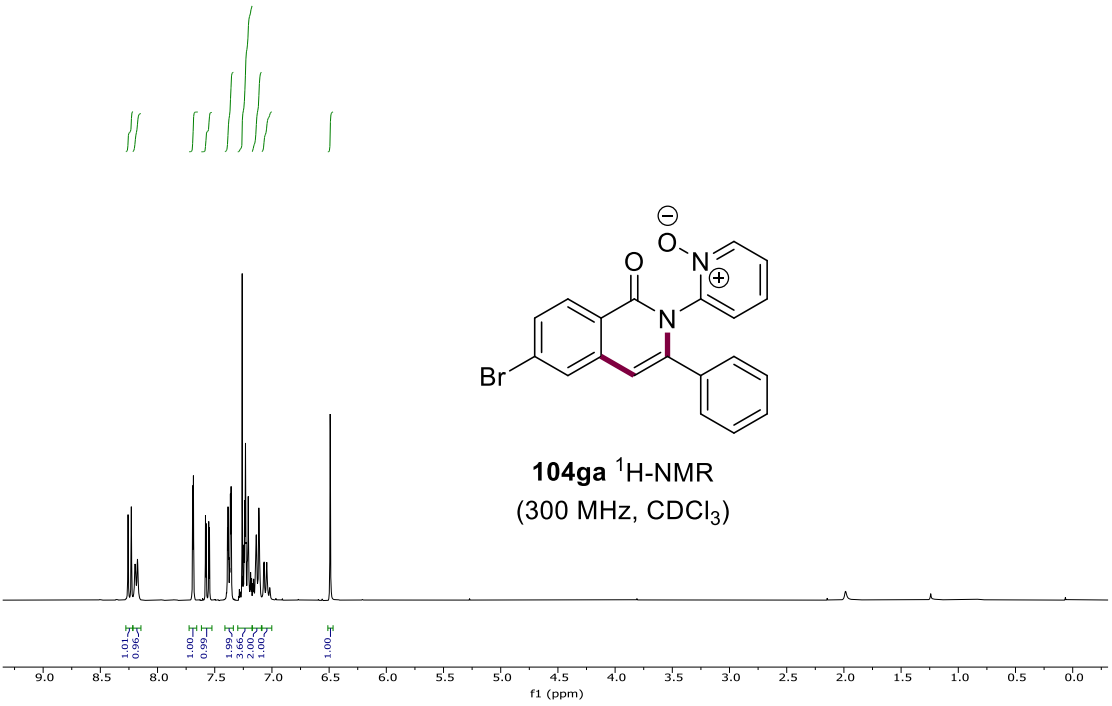

104ga ^{1}H-NMR
(300 MHz, $CDCl_3$)

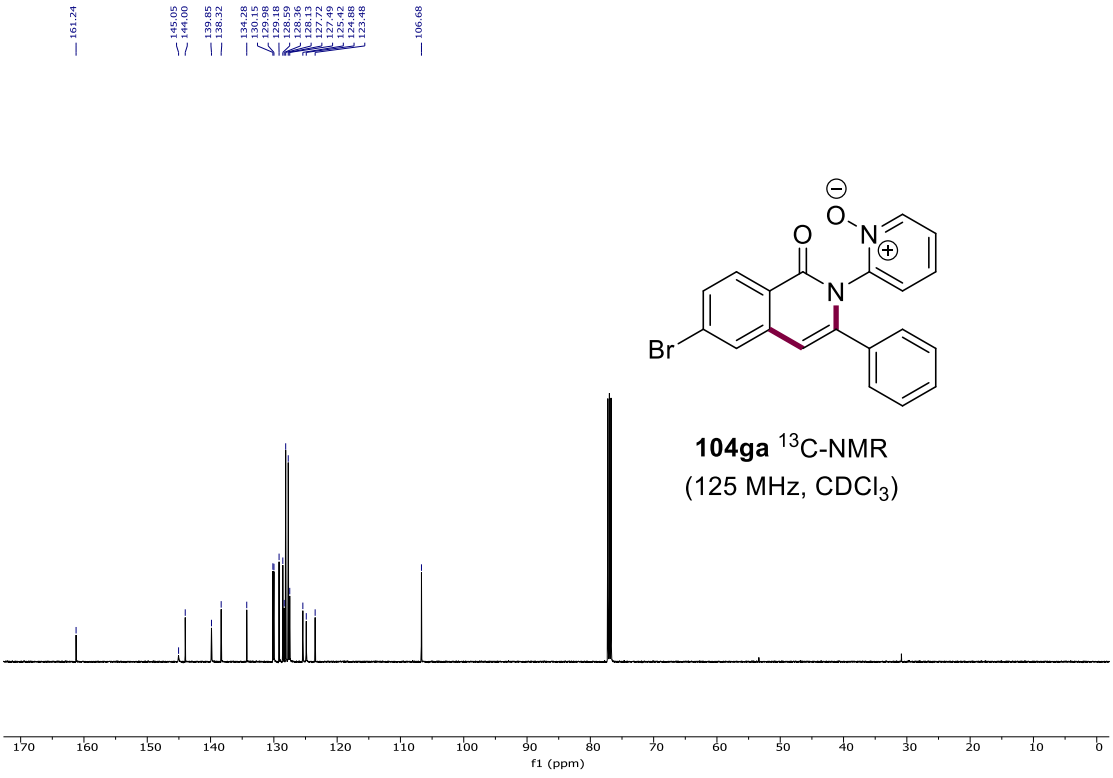

104ga ^{13}C-NMR
(125 MHz, $CDCl_3$)

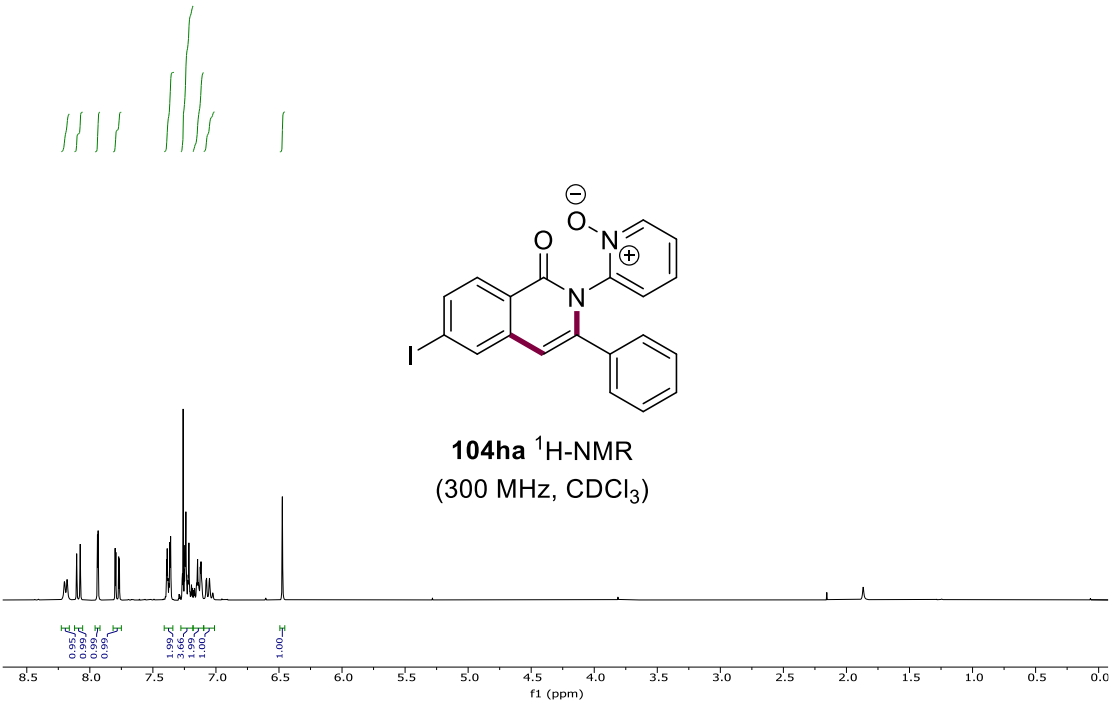

104ha ^{1}H-NMR
(300 MHz, $CDCl_3$)

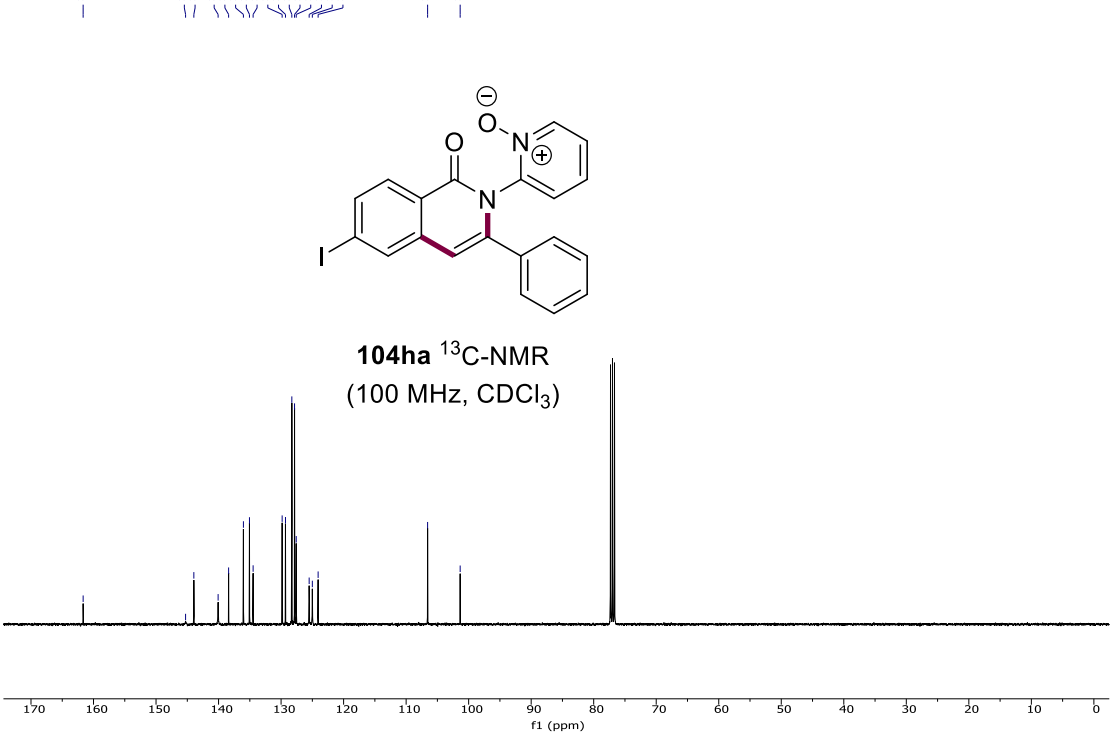

104ha ^{13}C-NMR
(100 MHz, $CDCl_3$)

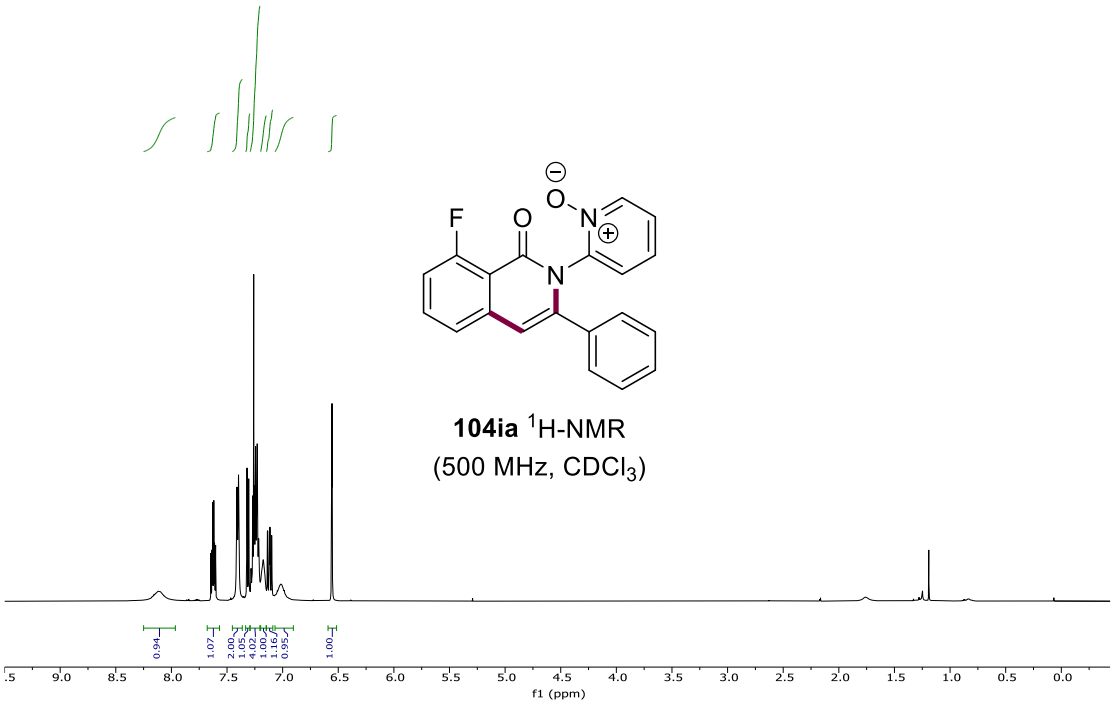

104ia ^{1}H-NMR
(500 MHz, $CDCl_3$)

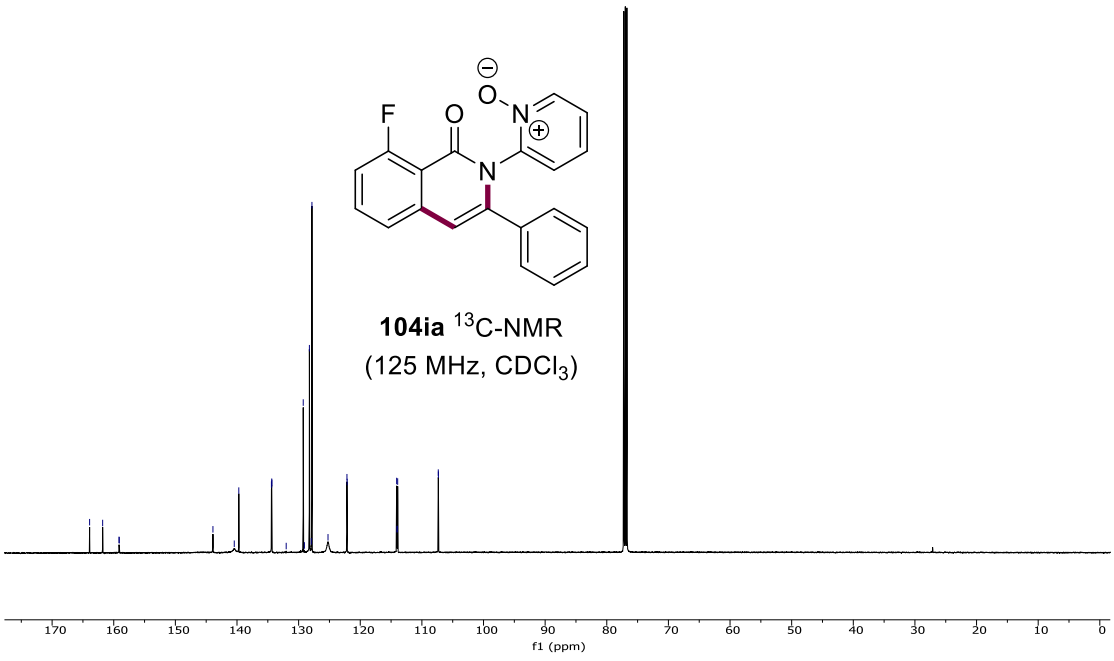

104ia ^{13}C-NMR
(125 MHz, $CDCl_3$)

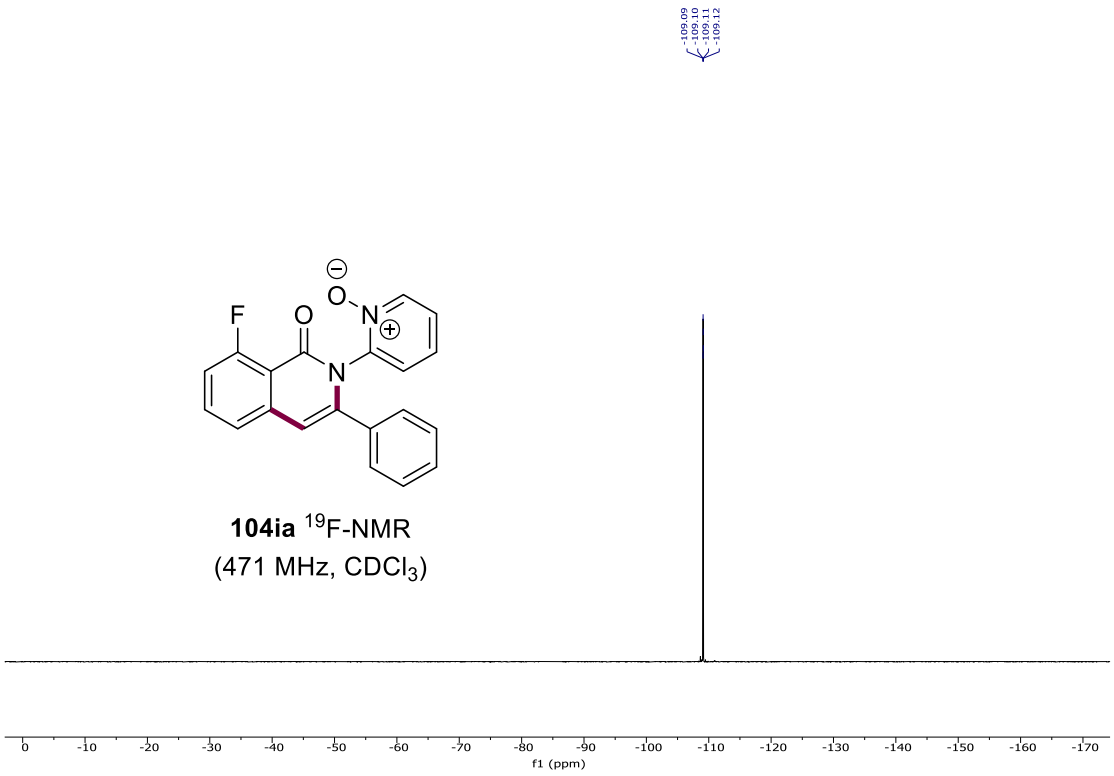

104ia ^{19}F-NMR
(471 MHz, $CDCl_3$)

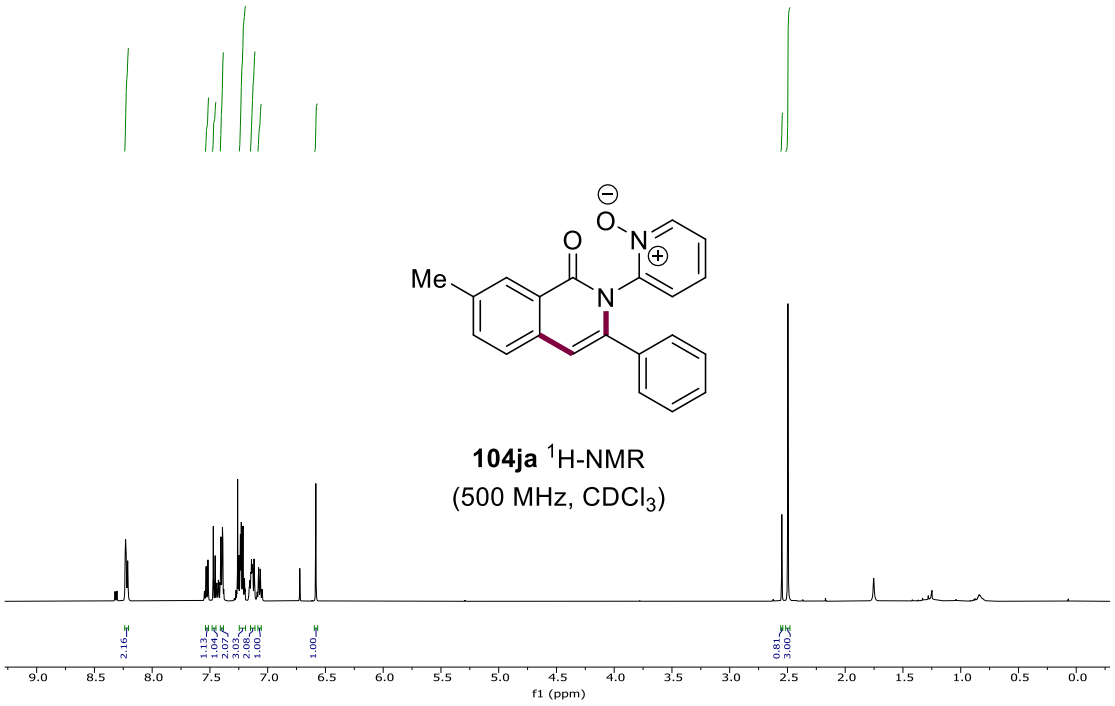
Me
O
N
O
N
104ja 1H-NMR
(500 MHz, CDCl3)
f1 (ppm)

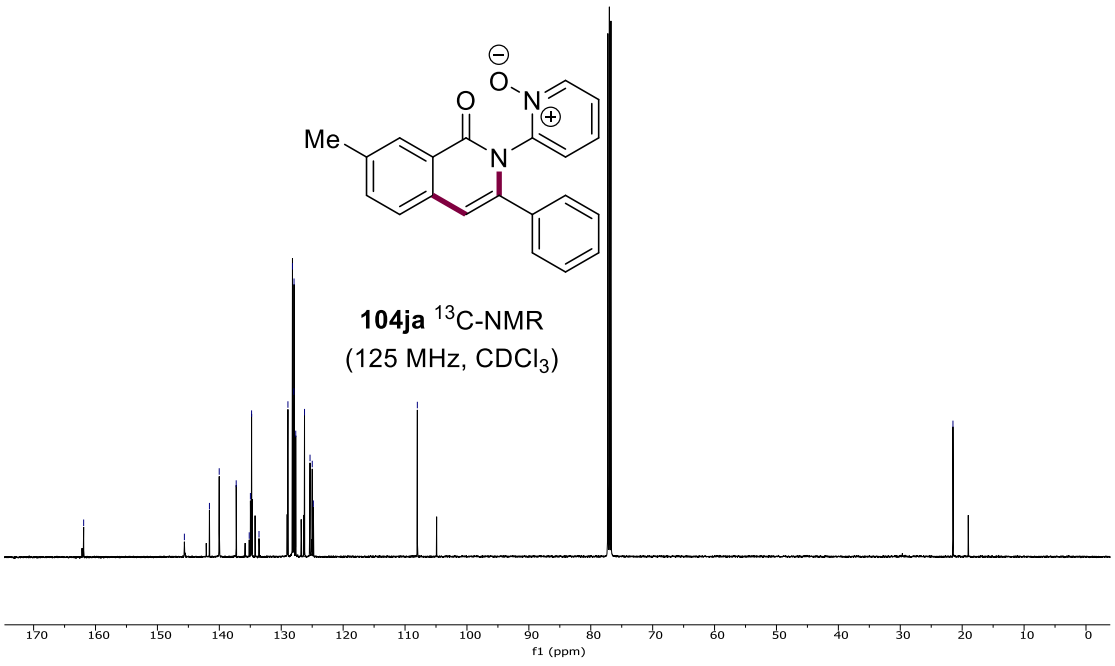
Me
O
N
O
N
104ja 13C-NMR
(125 MHz, CDCl3)
f1 (ppm)

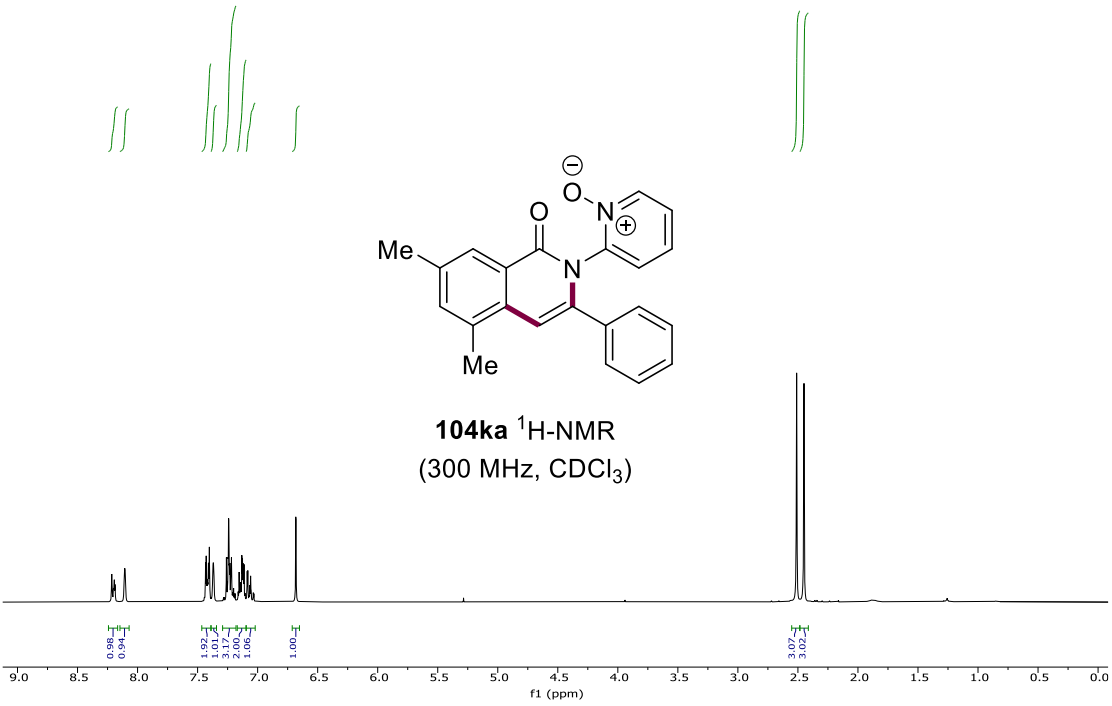

104ka ^{1}H-NMR
(300 MHz, $CDCl_3$)

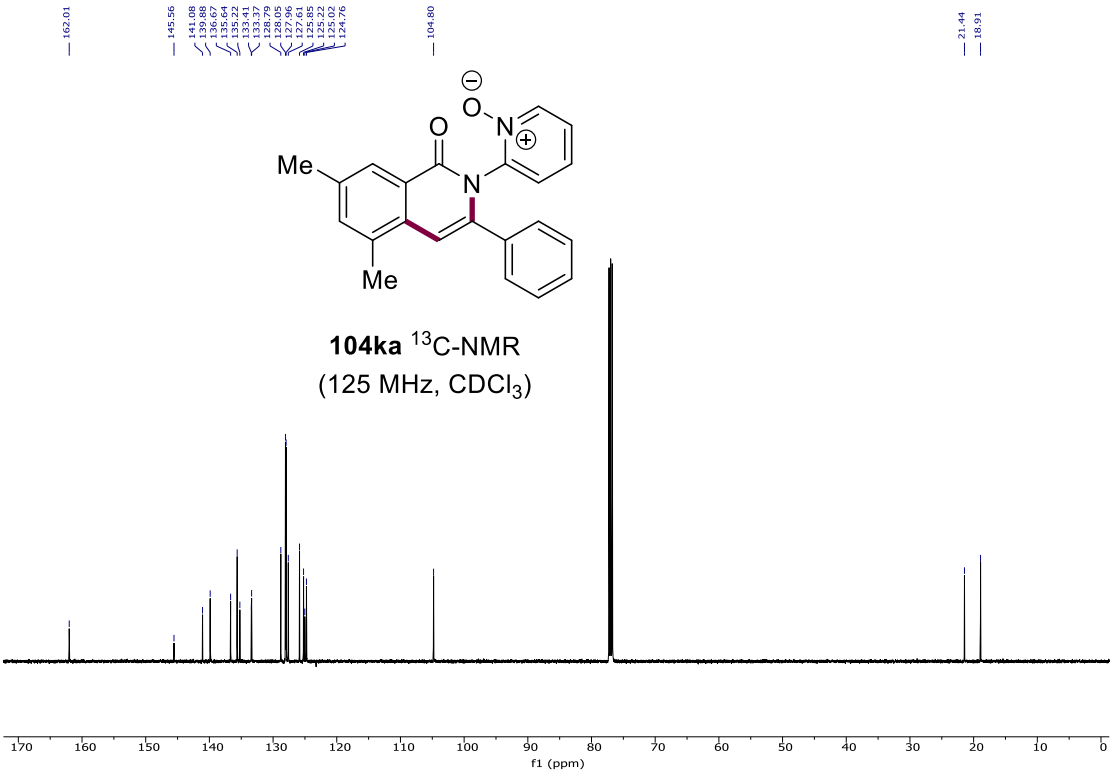

104ka ^{13}C-NMR
(125 MHz, $CDCl_3$)

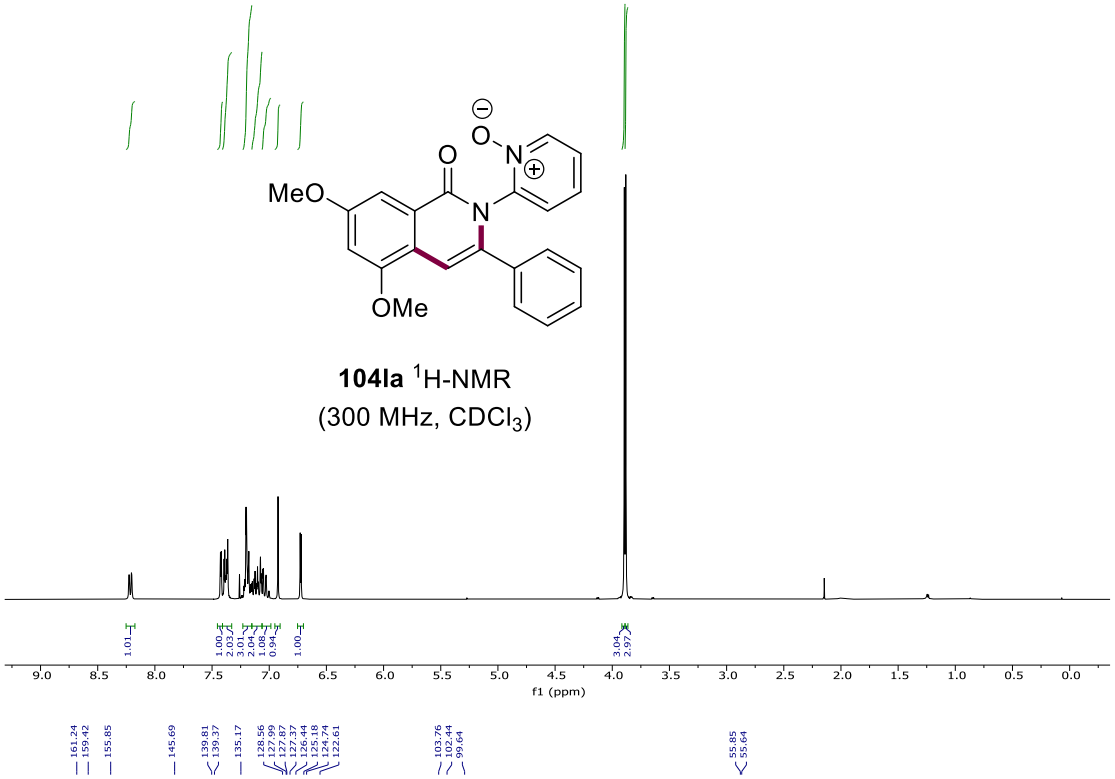
MeO
OMe
O
N
O
N
104la 1H-NMR
(300 MHz, CDCl3)
f1 (ppm)

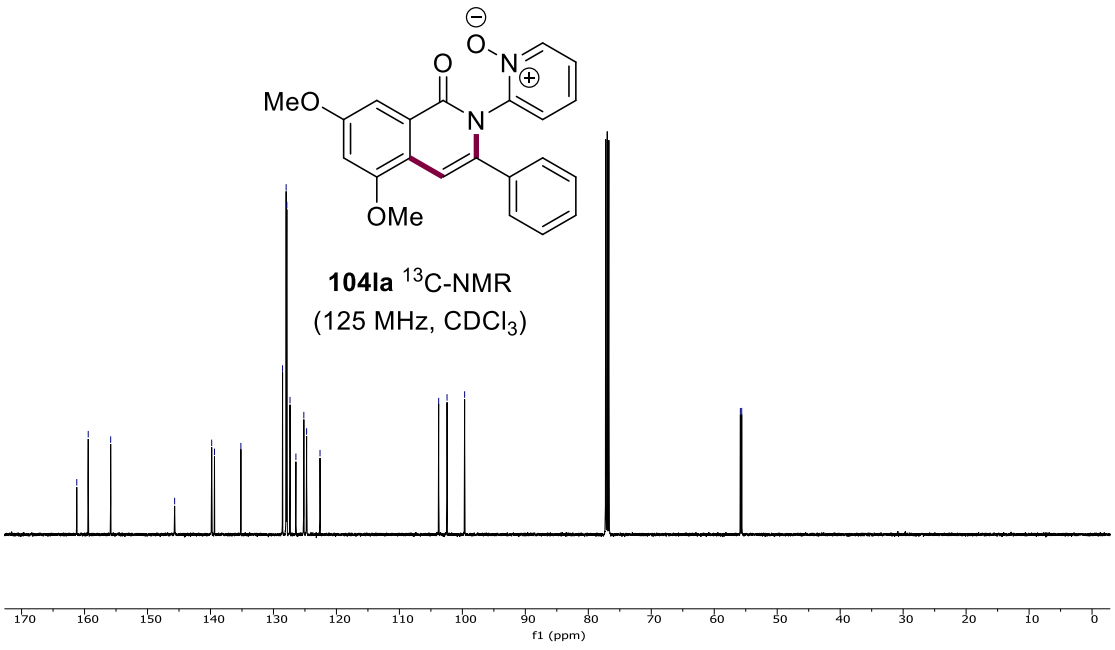
MeO
OMe
O
N
O
N
104la 13C-NMR
(125 MHz, CDCl3)
f1 (ppm)

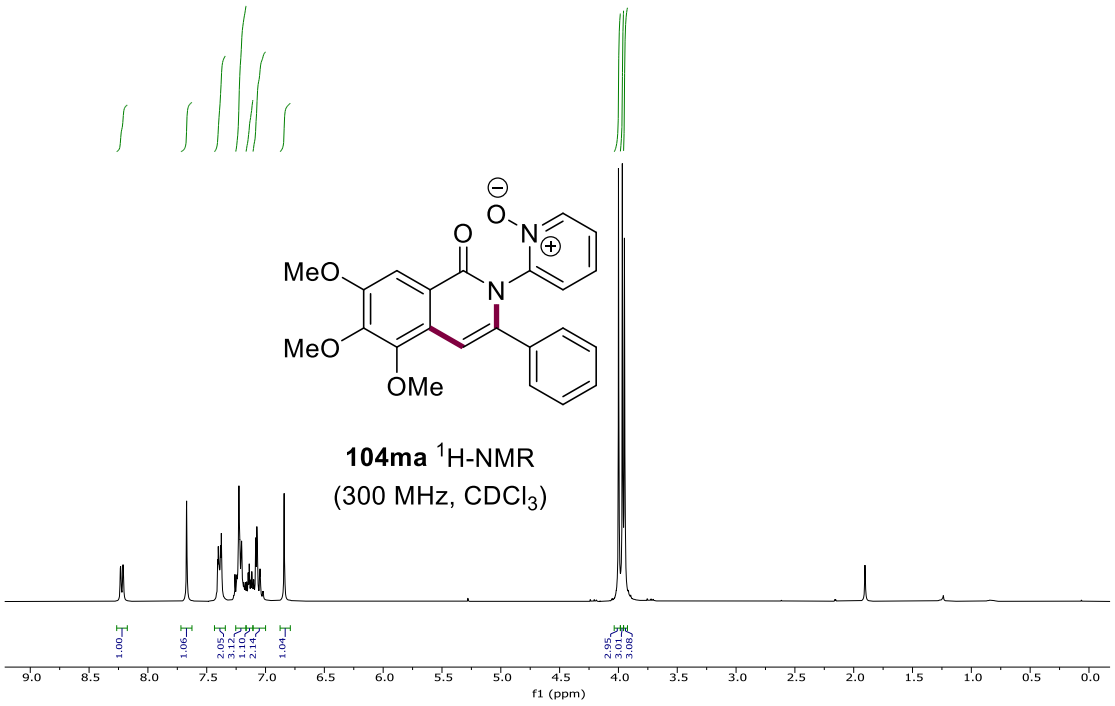
MeO
MeO
OMe
O
N
O
N
104ma 1H-NMR
(300 MHz, CDCl3)
f1 (ppm)

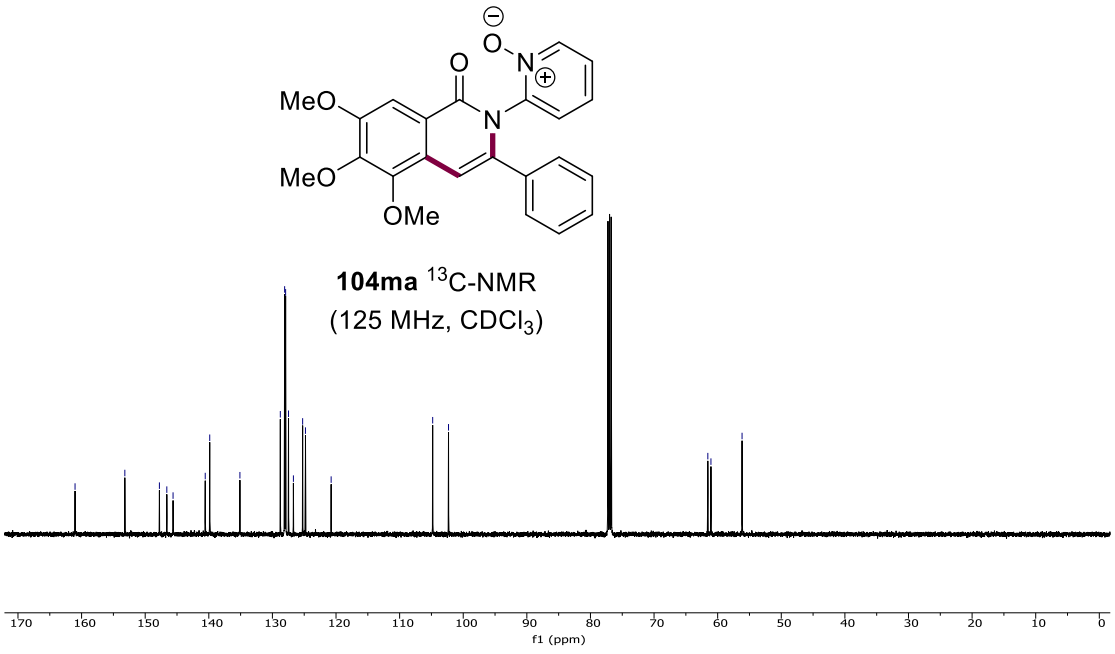
MeO
MeO
OMe
O
N
O
N
104ma 13C-NMR
(125 MHz, CDCl3)
f1 (ppm)

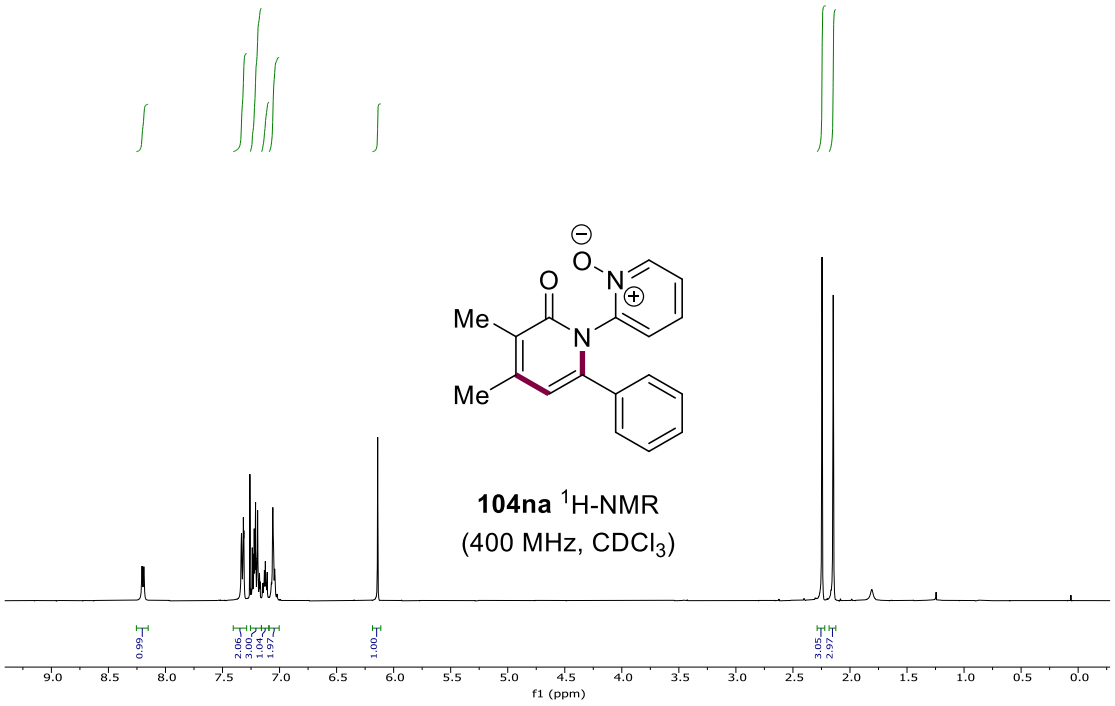

104na ^{1}H-NMR
(400 MHz, $CDCl_3$)

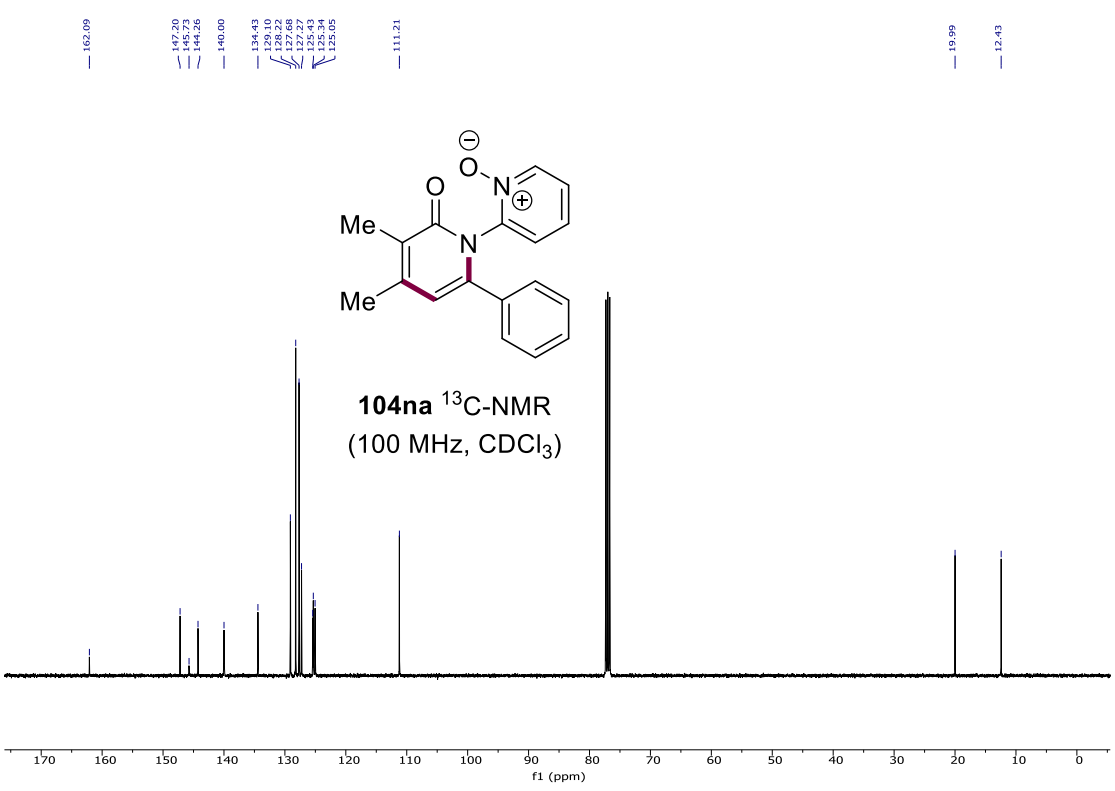

104na ^{13}C-NMR
(100 MHz, $CDCl_3$)

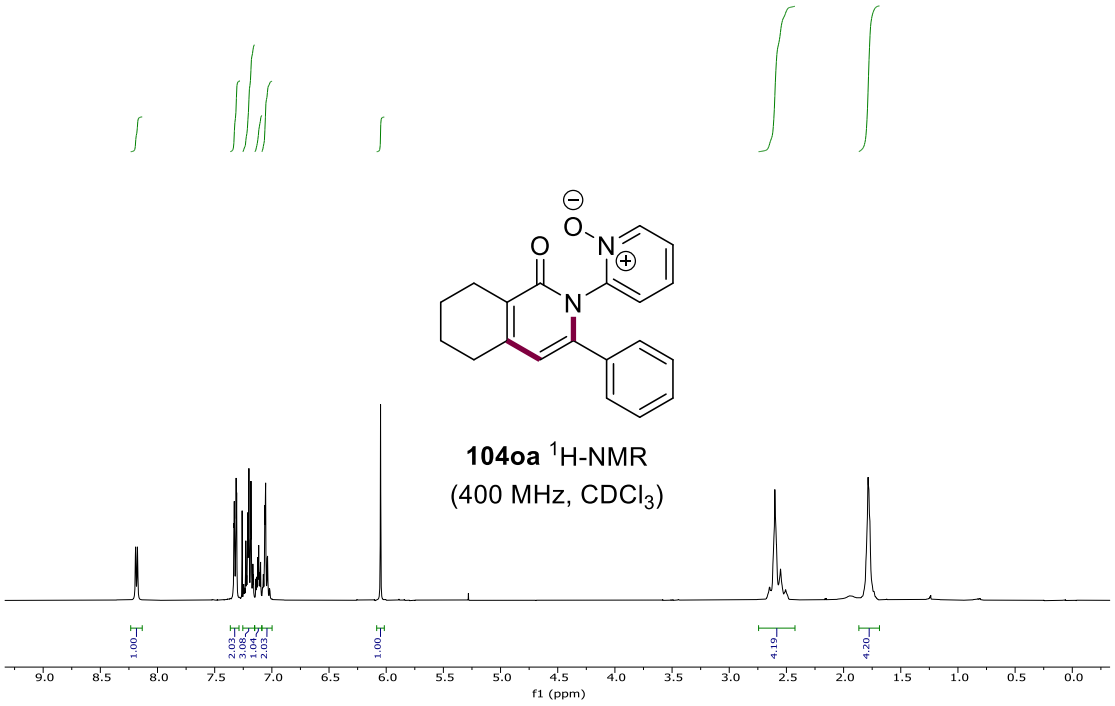
104oa 1H-NMR
(400 MHz, CDCl3)
f1 (ppm)

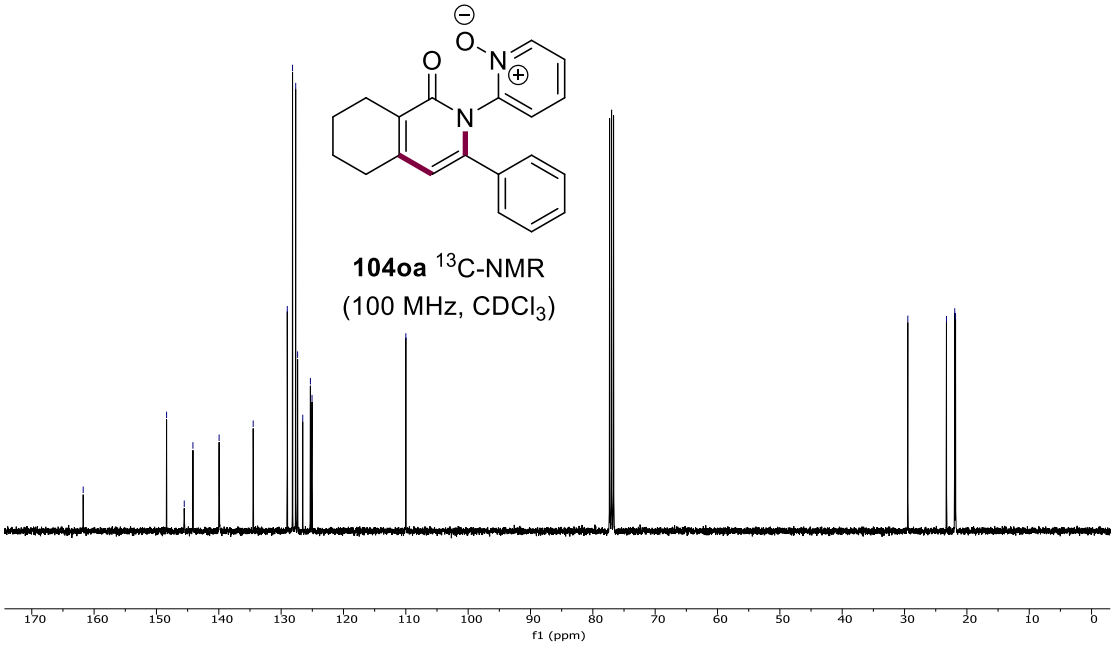
104oa 13C-NMR
(100 MHz, CDCl3)
f1 (ppm)

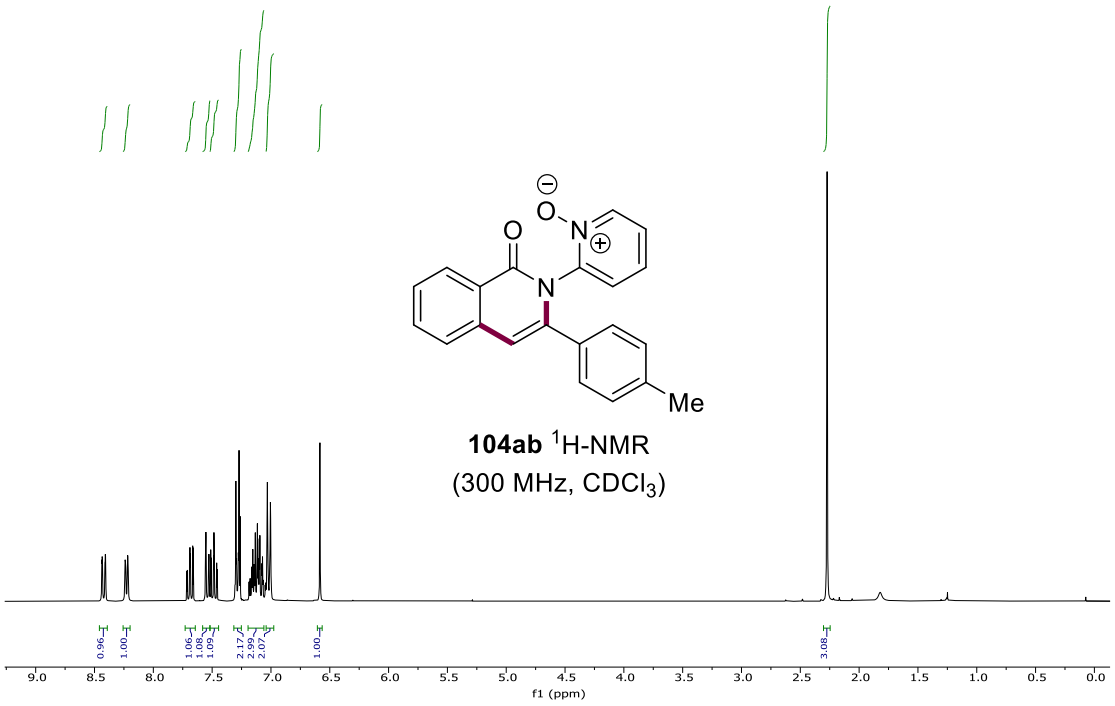

104ab ^{1}H-NMR
(300 MHz, $CDCl_3$)

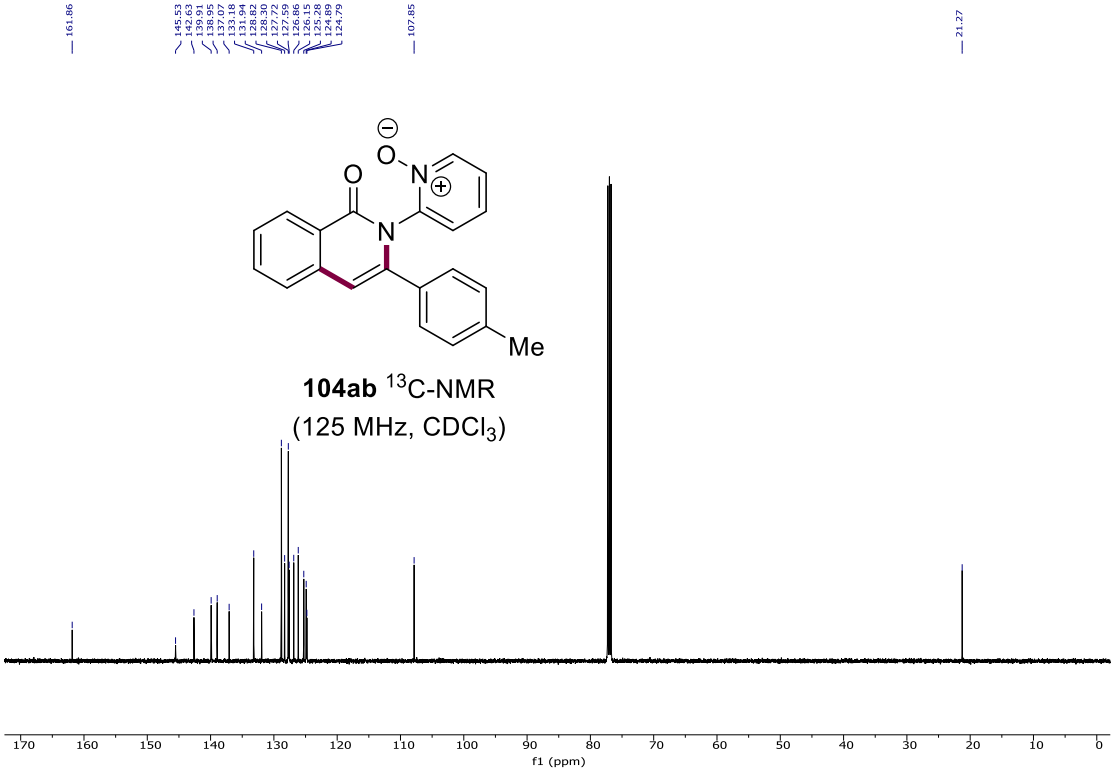

104ab ^{13}C-NMR
(125 MHz, $CDCl_3$)

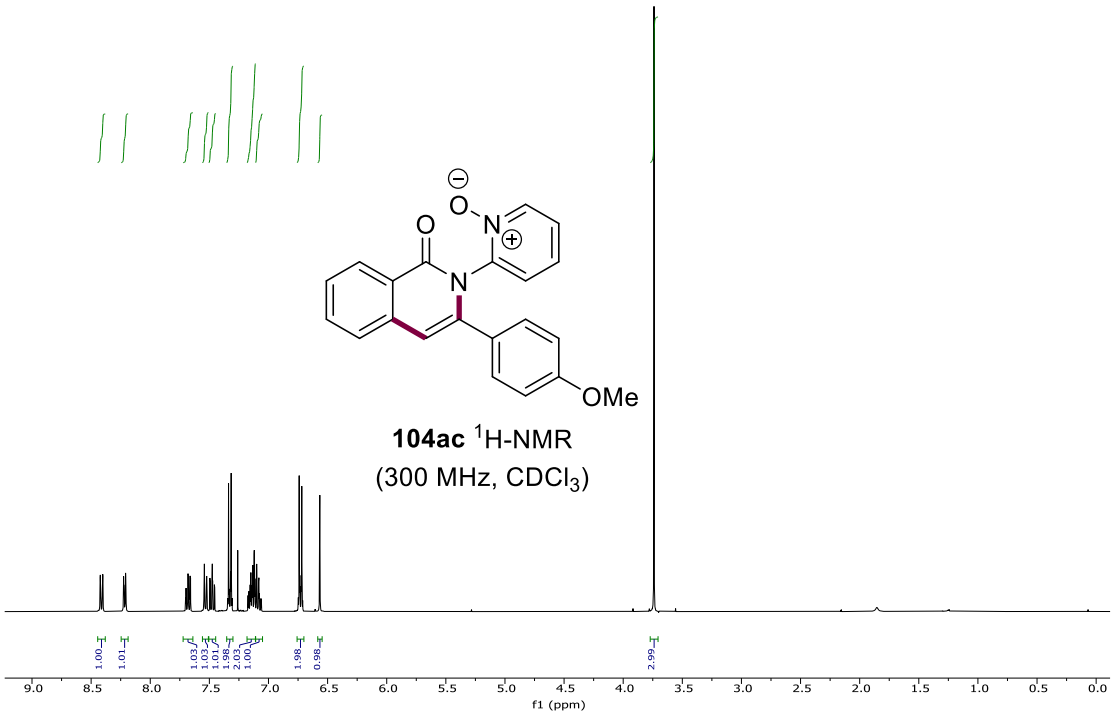
OMe
104ac 1H-NMR
(300 MHz, CDCl3)
f1 (ppm)

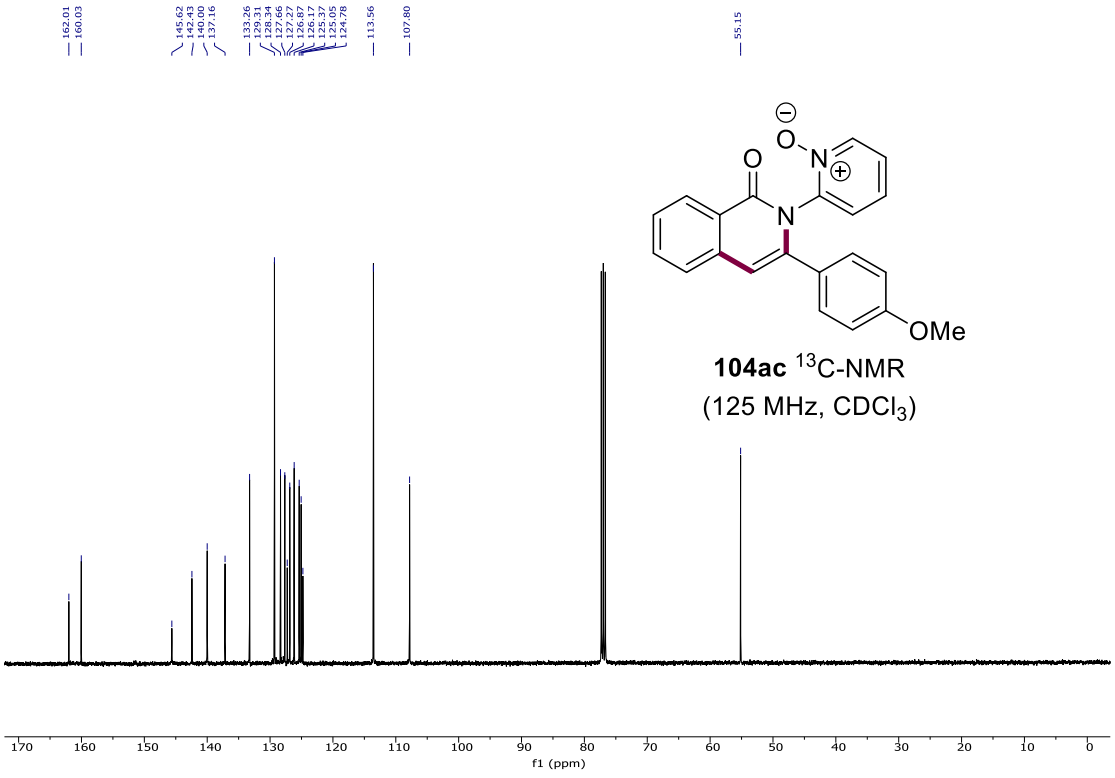
OMe
104ac 13C-NMR
(125 MHz, CDCl3)
f1 (ppm)

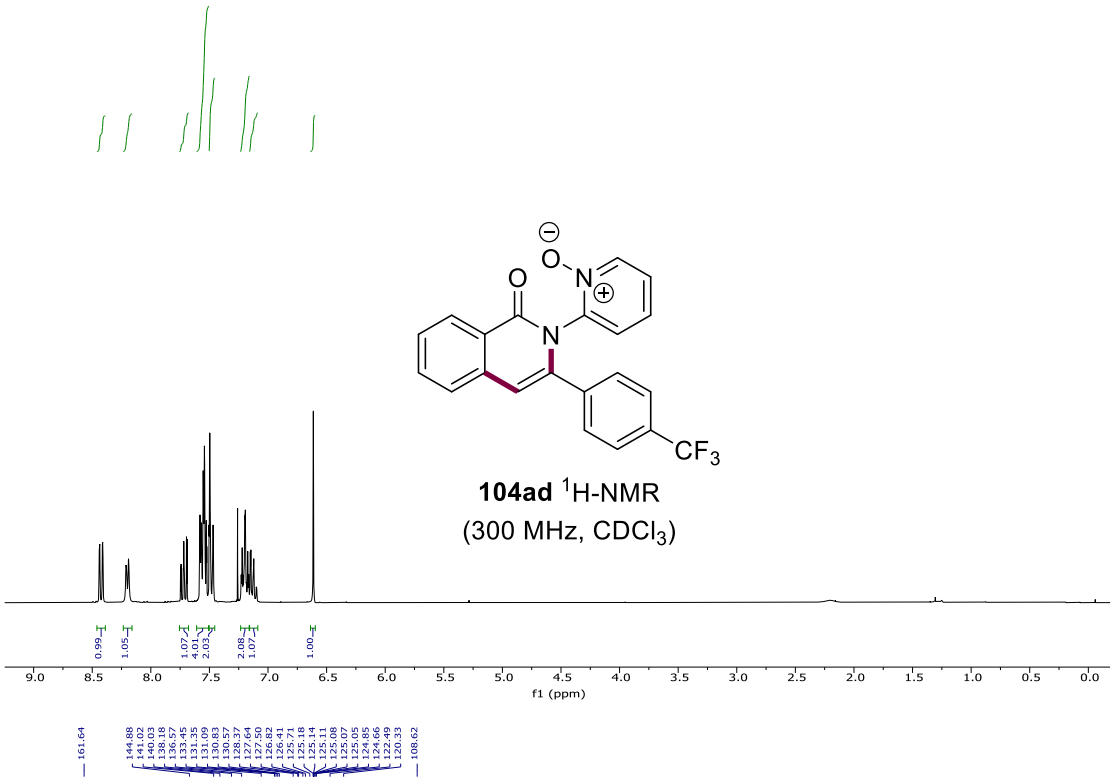
O
N
N
CF3
104ad 1H-NMR
(300 MHz, CDCl3)
f1 (ppm)

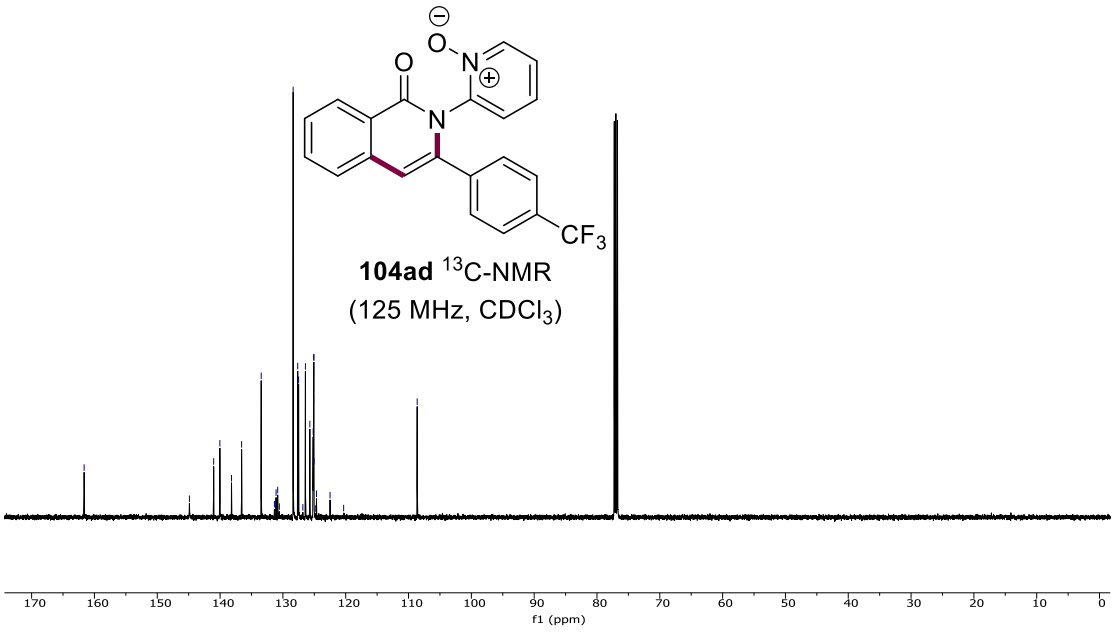
O
N
N
CF3
104ad 13C-NMR
(125 MHz, CDCl3)
f1 (ppm)

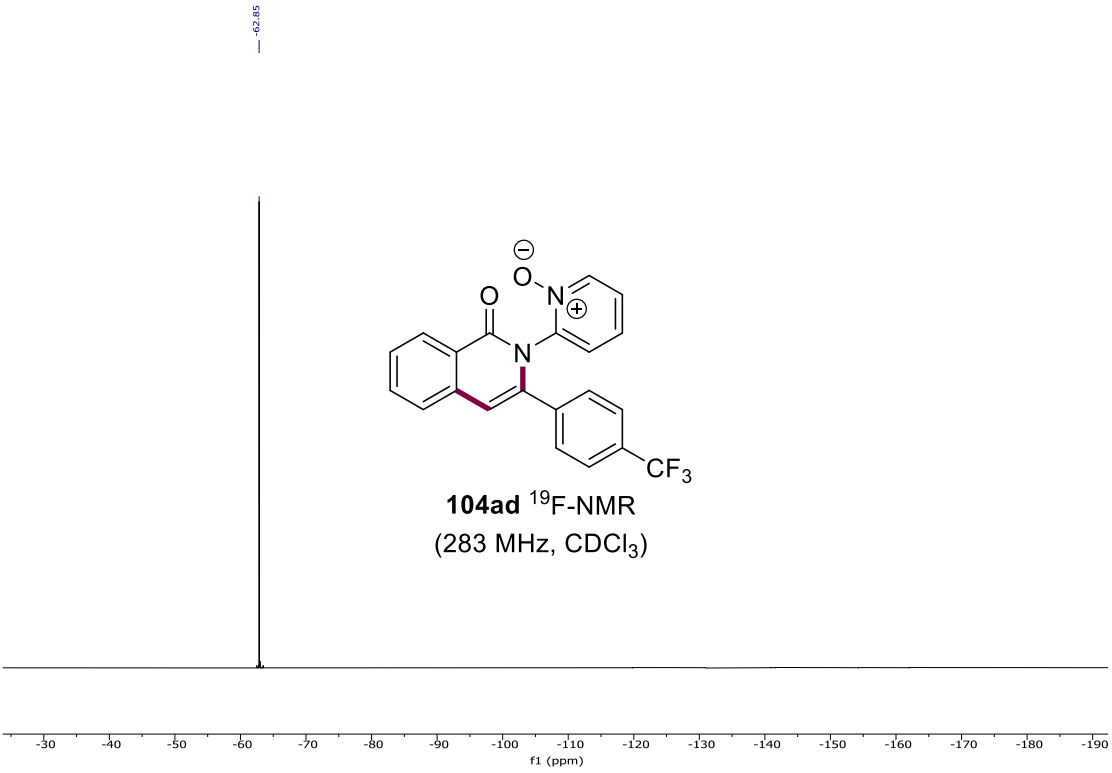

104ad ^{19}F-NMR
(283 MHz, $CDCl_3$)

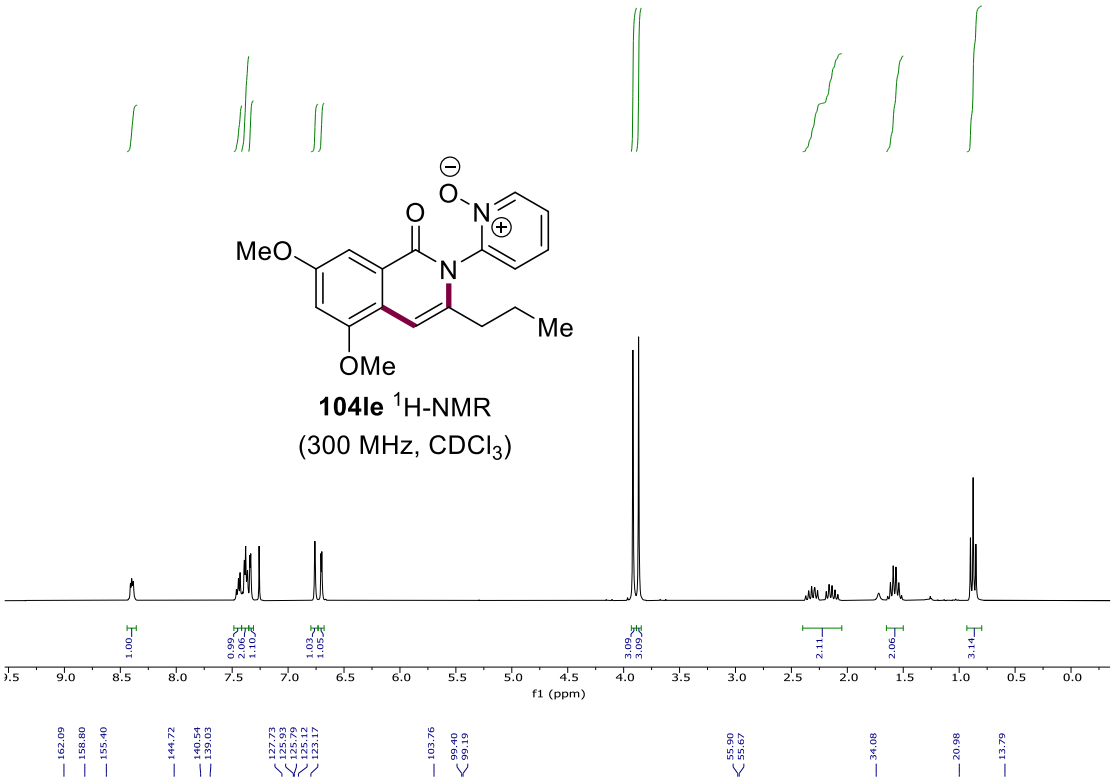

104le ^{1}H-NMR
(300 MHz, $CDCl_3$)

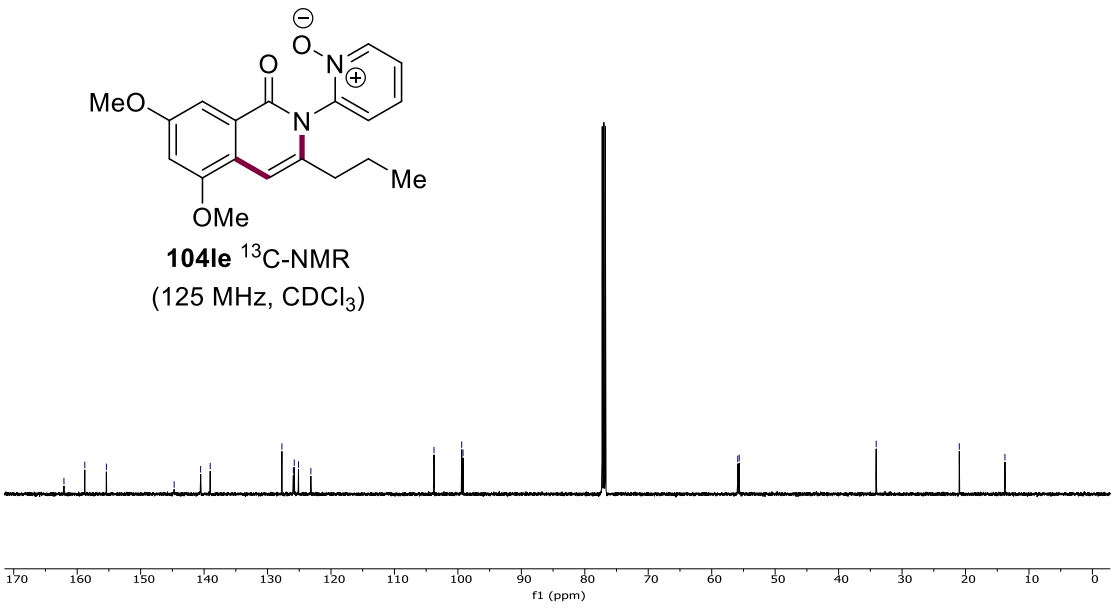

104le ^{13}C-NMR
(125 MHz, $CDCl_3$)

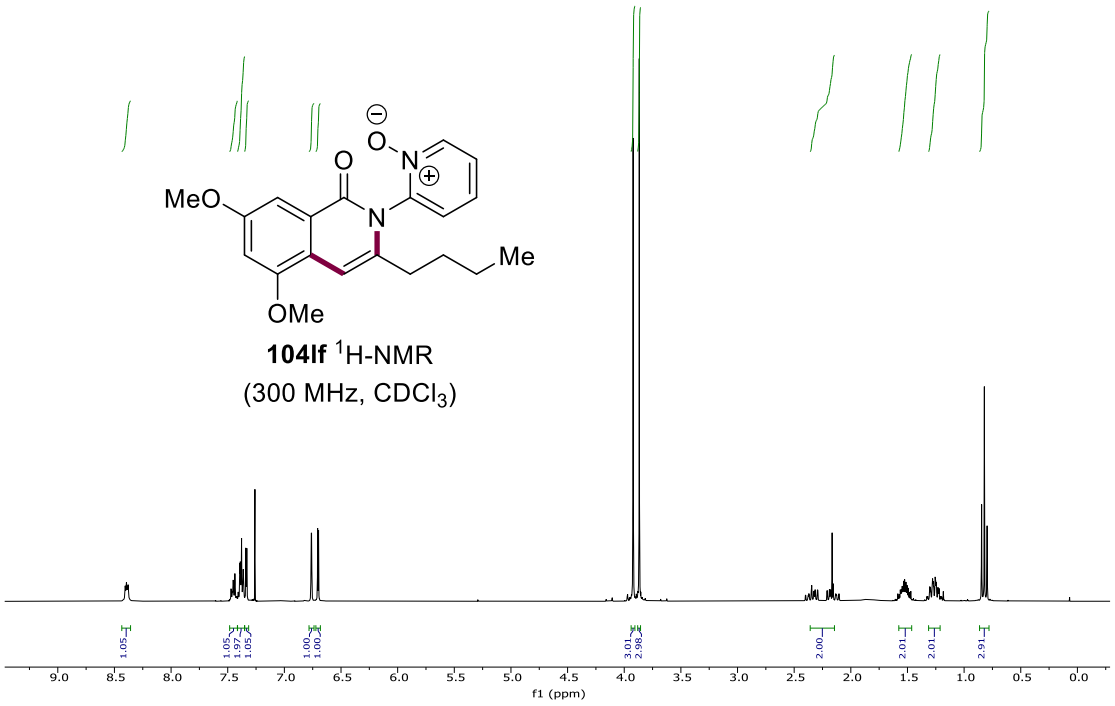

104lf ^{1}H-NMR
(300 MHz, $CDCl_3$)

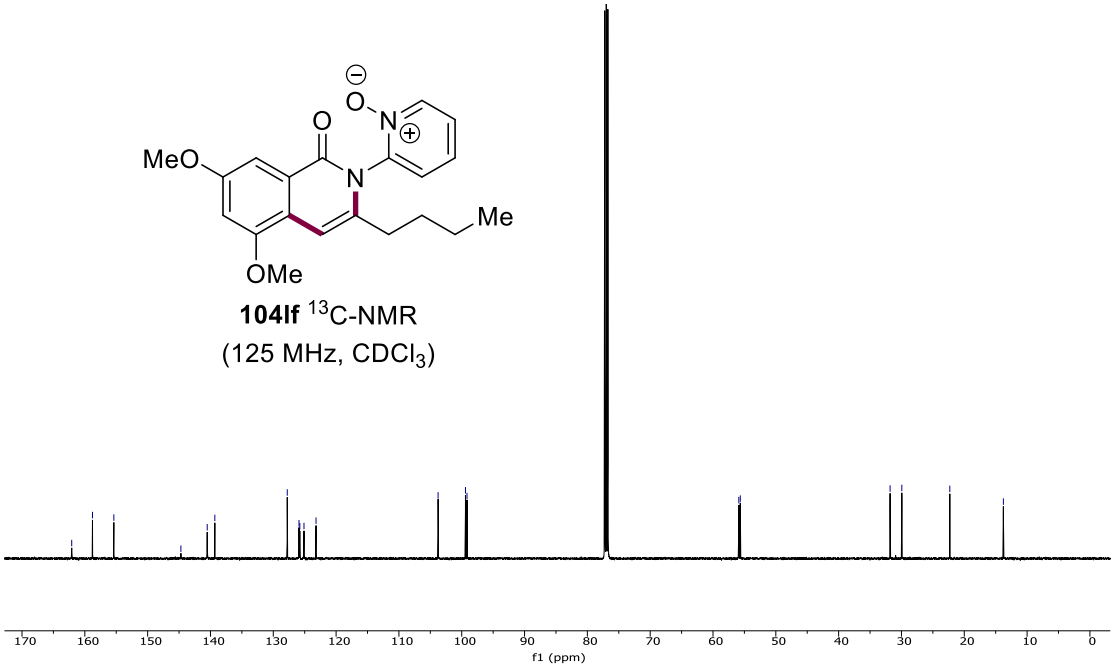

104lf ^{13}C-NMR
(125 MHz, $CDCl_3$)

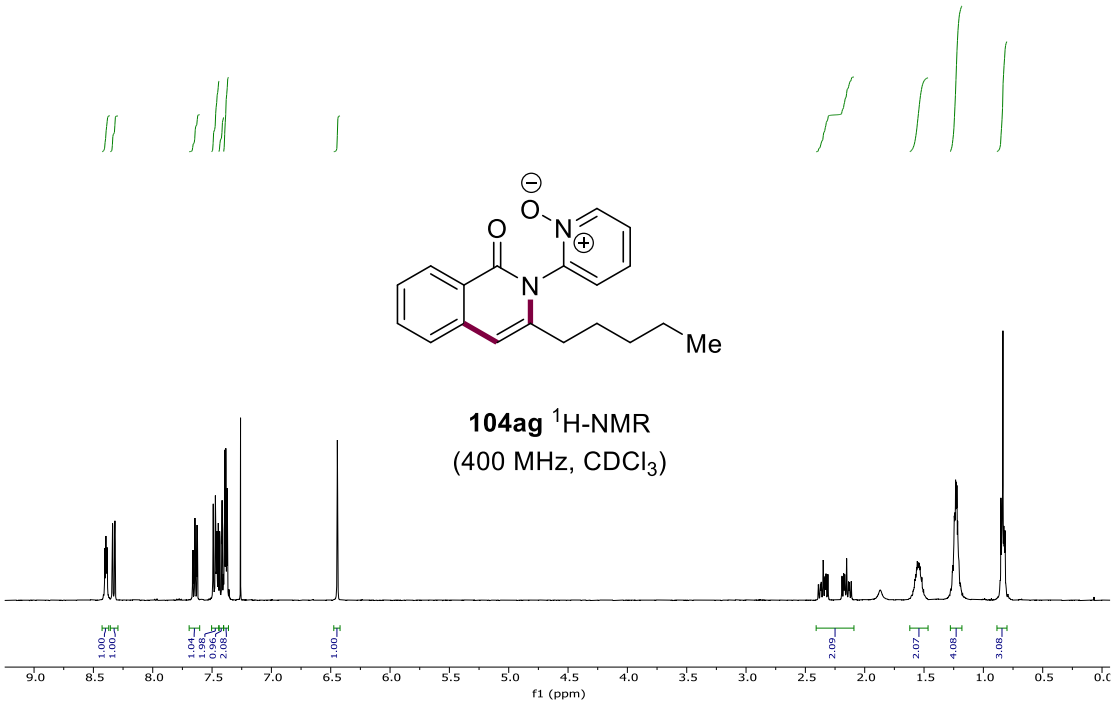

104ag ^{1}H-NMR
(400 MHz, $CDCl_3$)

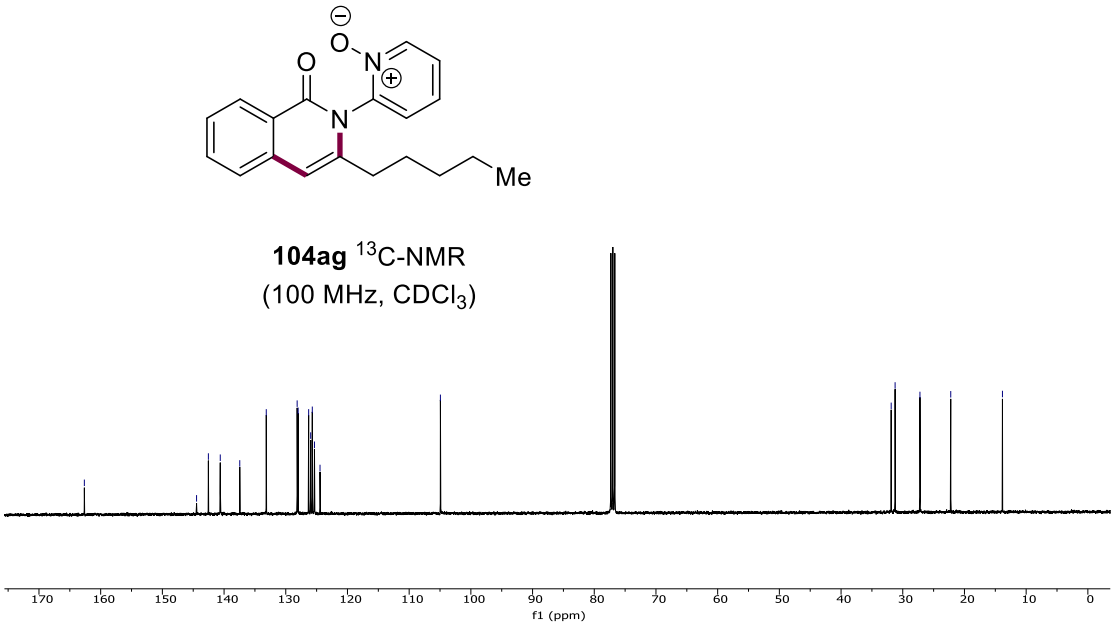

104ag ^{13}C-NMR
(100 MHz, $CDCl_3$)

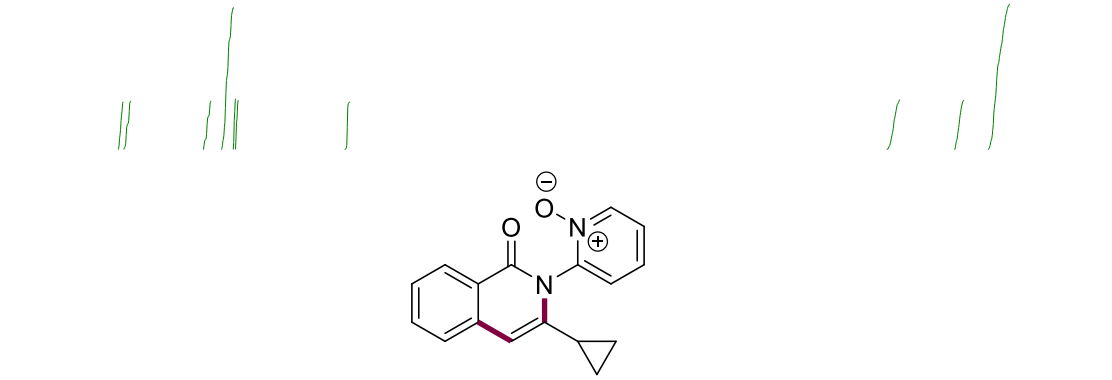

104ah ^{1}H-NMR
(300 MHz, $CDCl_3$)

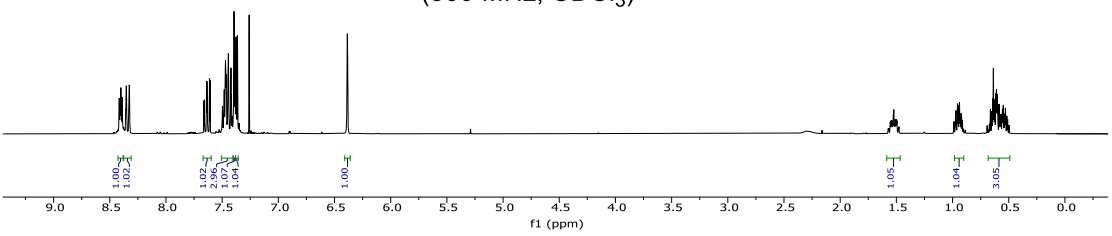

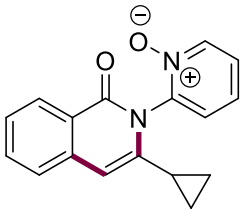

104ah ^{13}C-NMR
(125 MHz, $CDCl_3$)

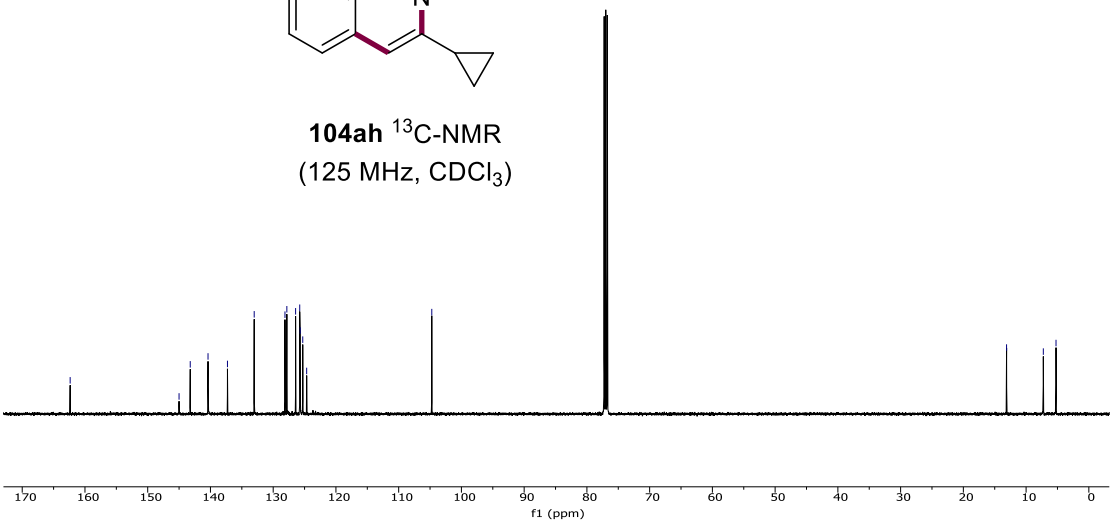

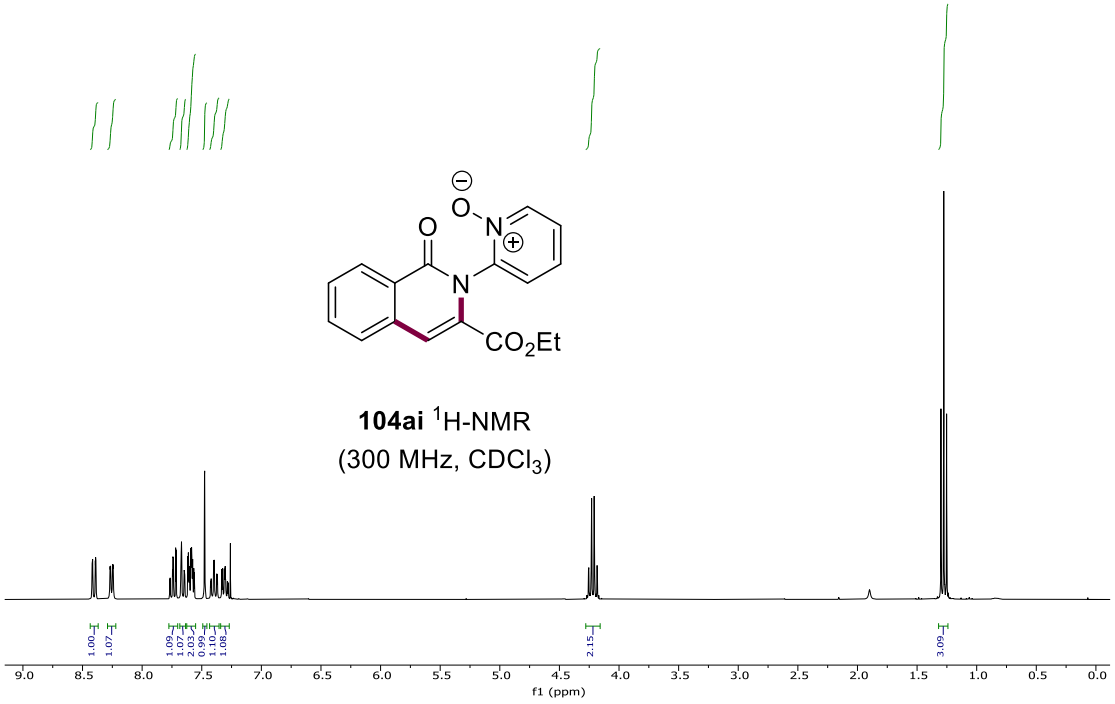
O
N
N
CO2Et
104ai 1H-NMR
(300 MHz, CDCl3)
f1 (ppm)

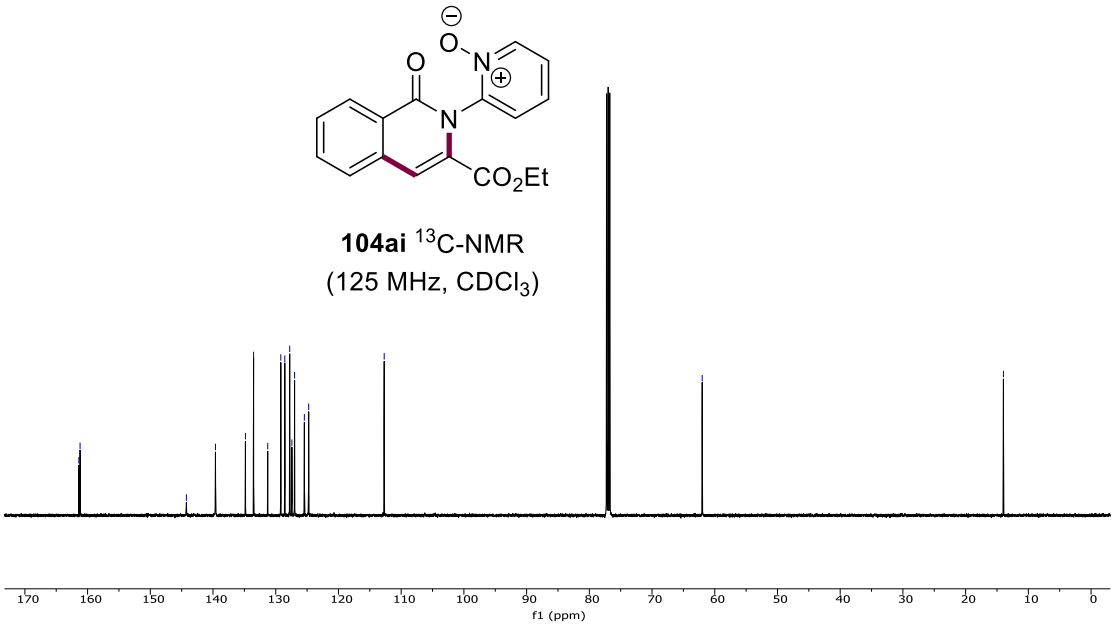
O
N
N
CO2Et
104ai 13C-NMR
(125 MHz, CDCl3)
f1 (ppm)

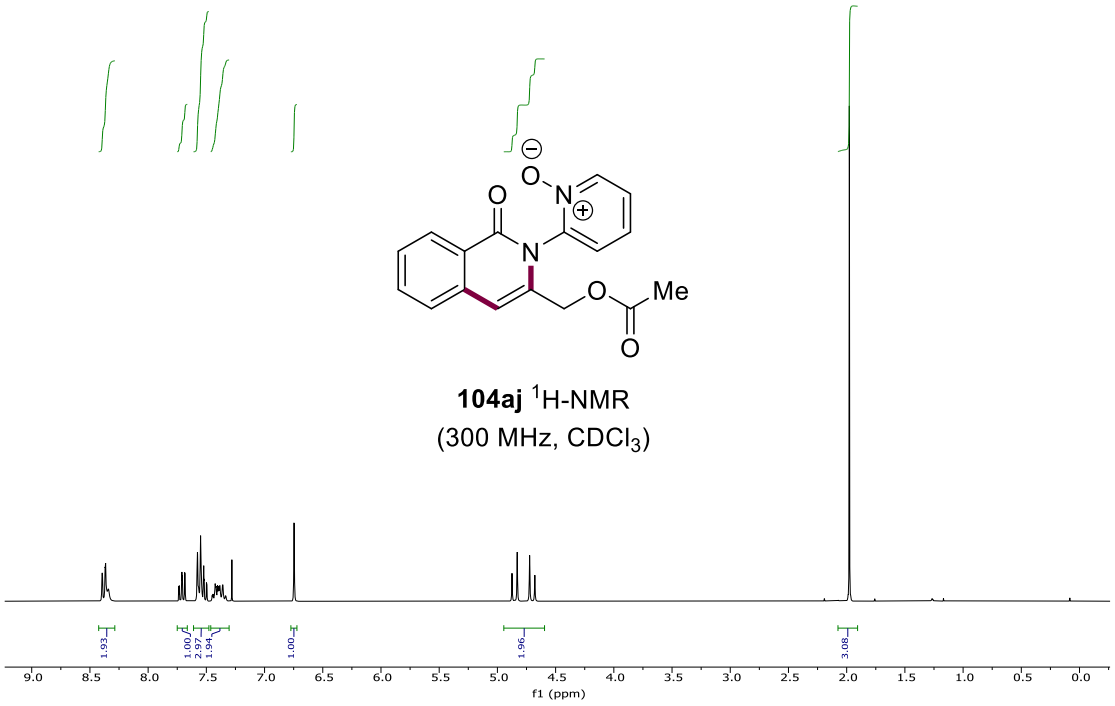

104aj ^{1}H-NMR
(300 MHz, $CDCl_3$)

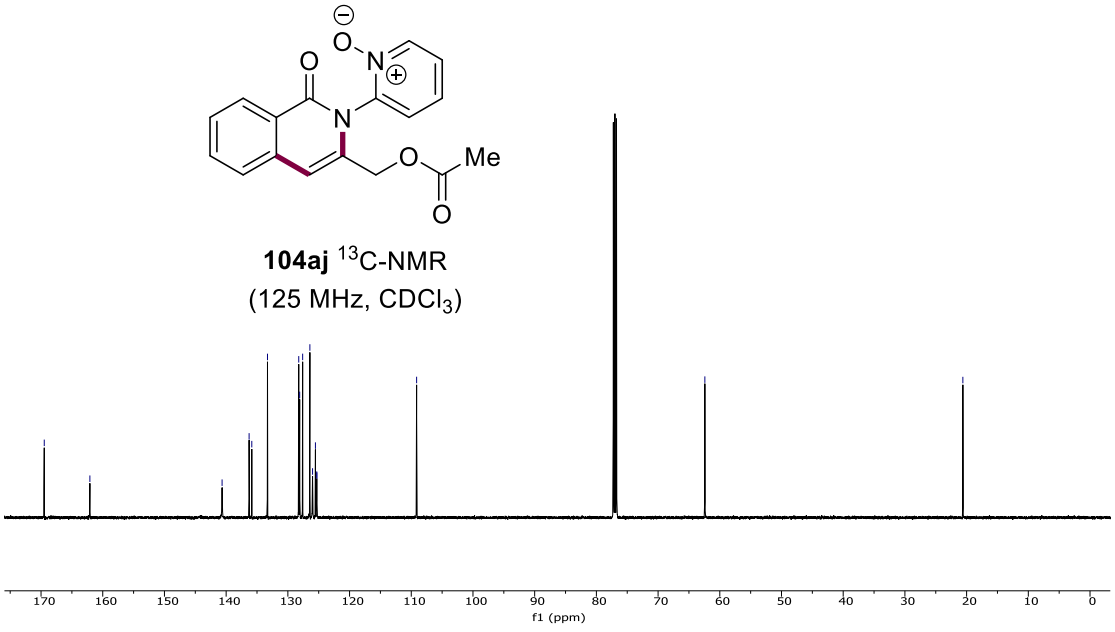

104aj ^{13}C-NMR
(125 MHz, $CDCl_3$)

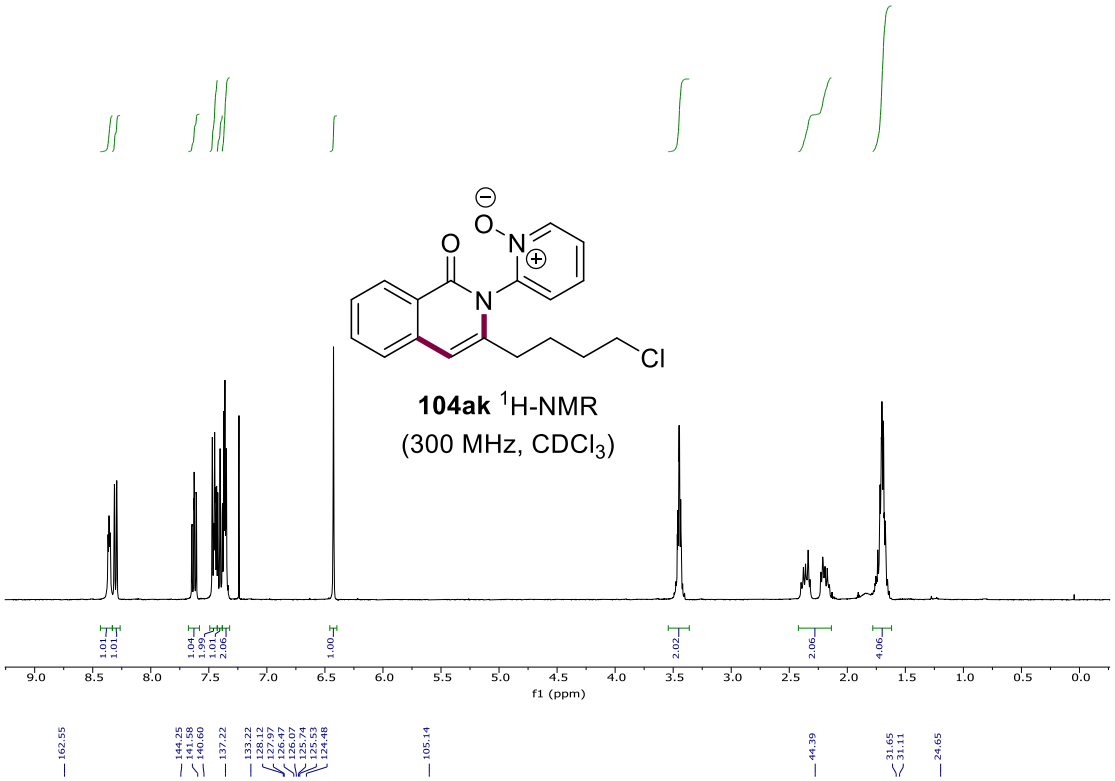
O
N
N
Cl
104ak 1H-NMR
(300 MHz, CDCl3)
f1 (ppm)

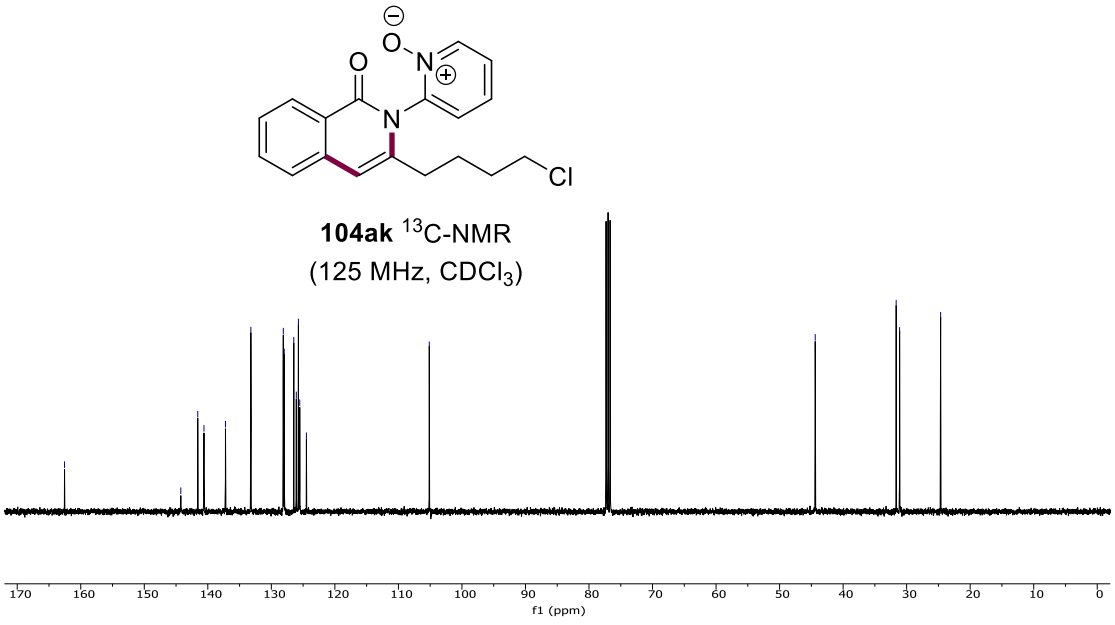
O
N
N
Cl
104ak 13C-NMR
(125 MHz, CDCl3)
f1 (ppm)

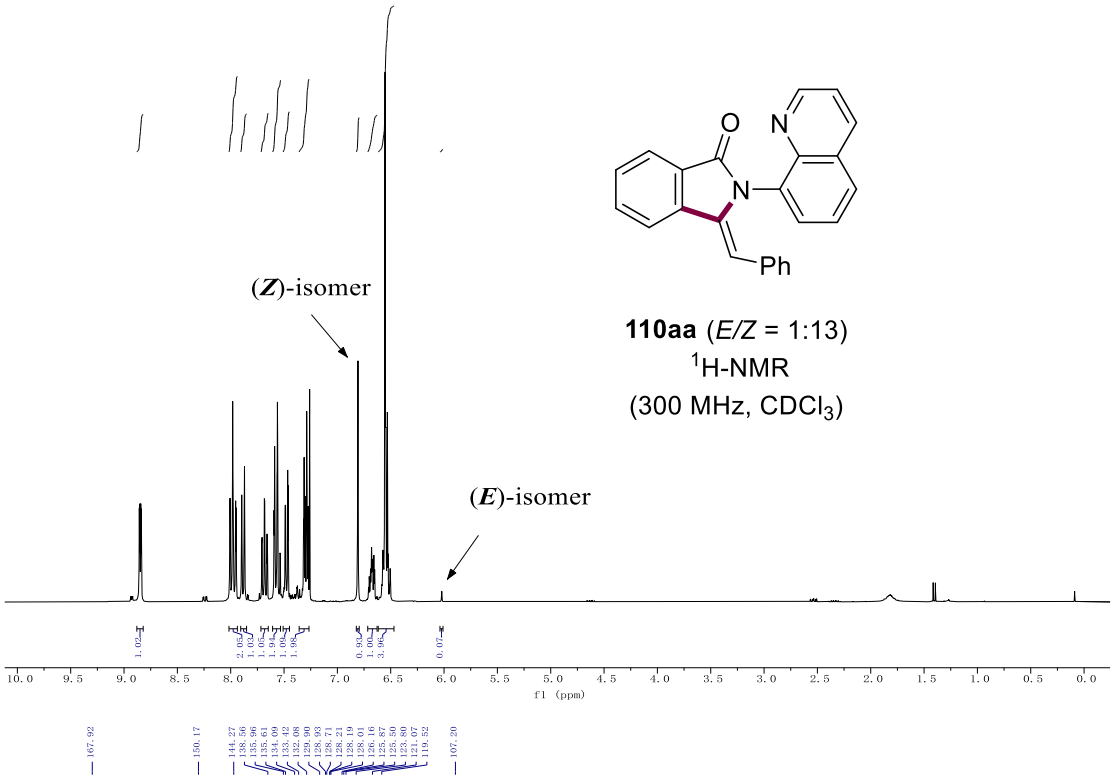
O
N
N
Ph
(Z)-isomer
(E)-isomer
110aa (E/Z = 1:13)
1H-NMR
(300 MHz, CDCl3)
f1 (ppm)

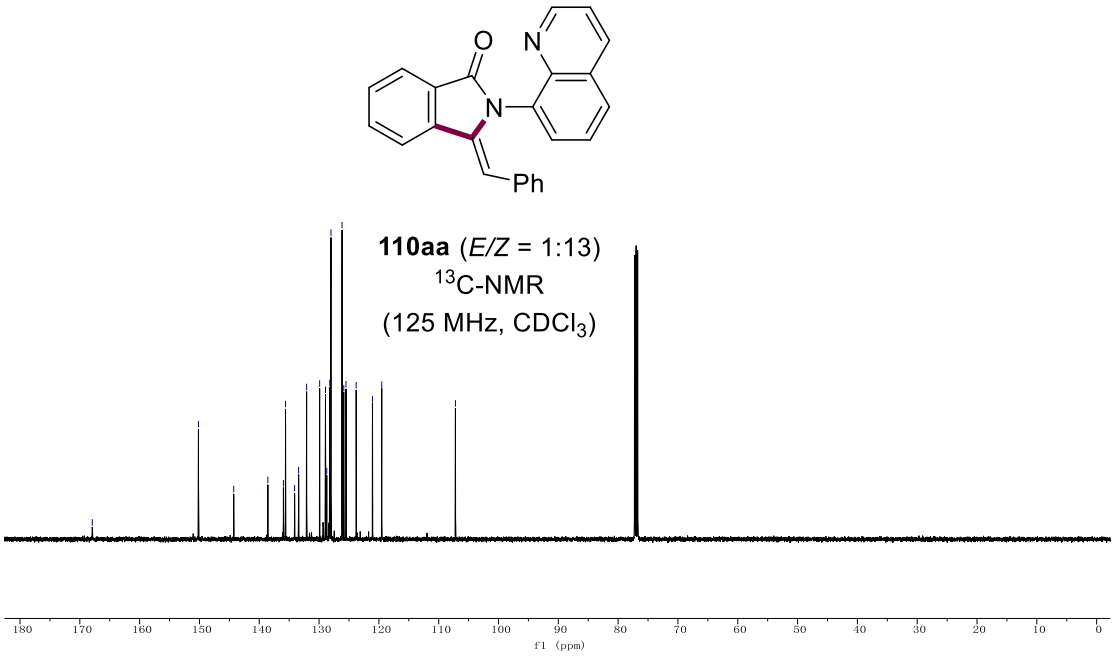
O
N
N
Ph
110aa (E/Z = 1:13)
13C-NMR
(125 MHz, CDCl3)
f1 (ppm)

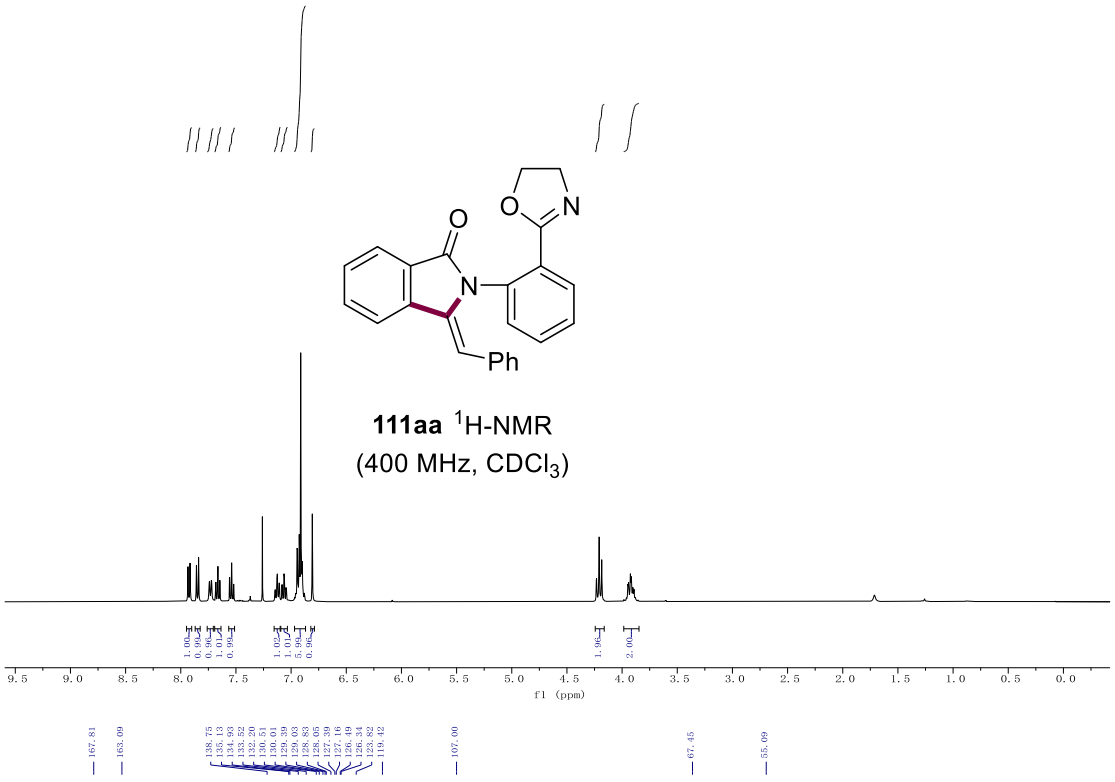

111aa ^{1}H-NMR
(400 MHz, $CDCl_3$)

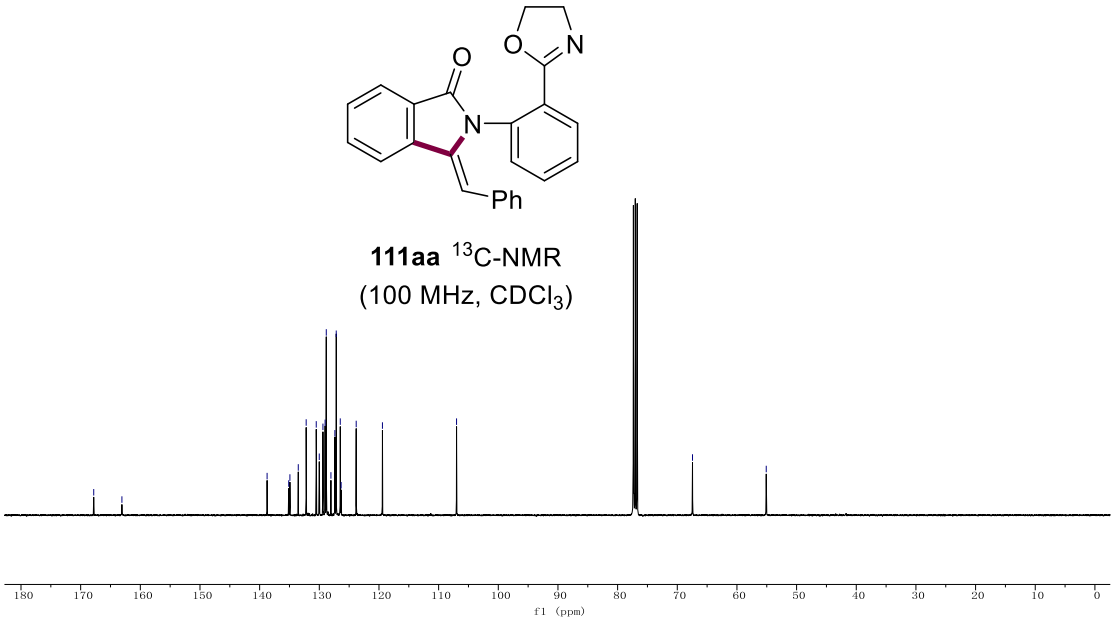

111aa ^{13}C-NMR
(100 MHz, $CDCl_3$)

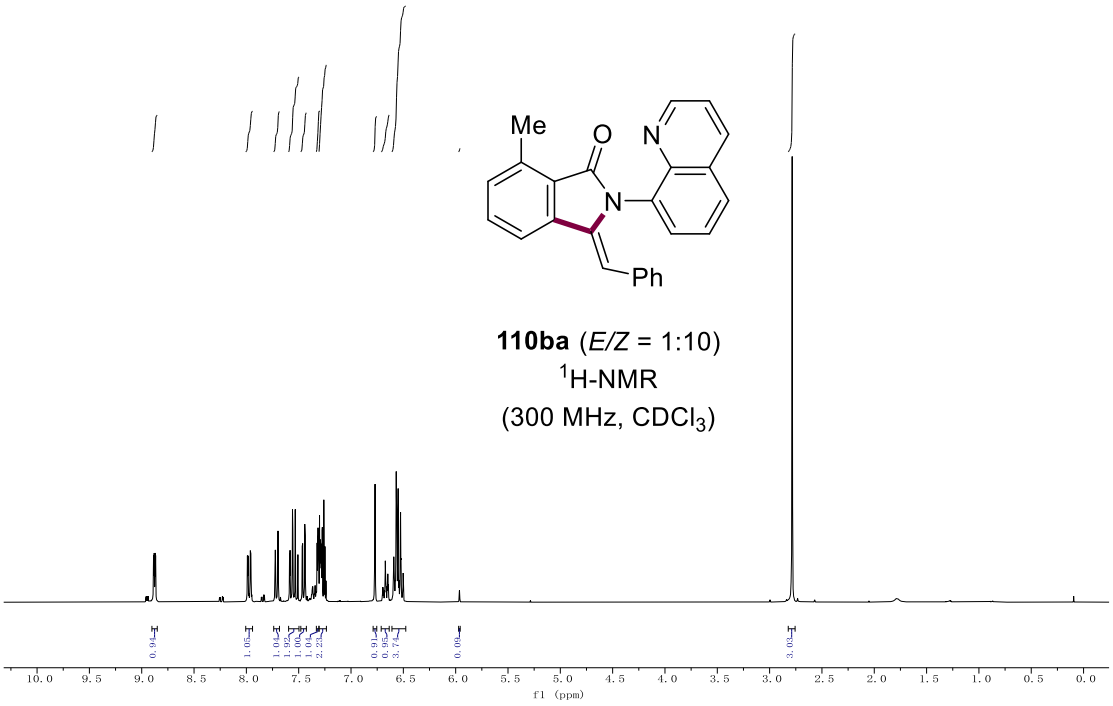

110ba (*E*/*Z* = 1:10)
^{1}H-NMR
(300 MHz, $CDCl_3$)

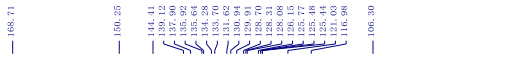

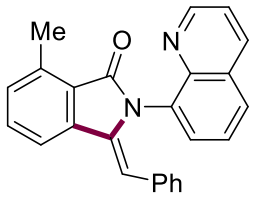

110ba (*E*/*Z* = 1:10)
^{13}C-NMR
(125 MHz, $CDCl_3$)

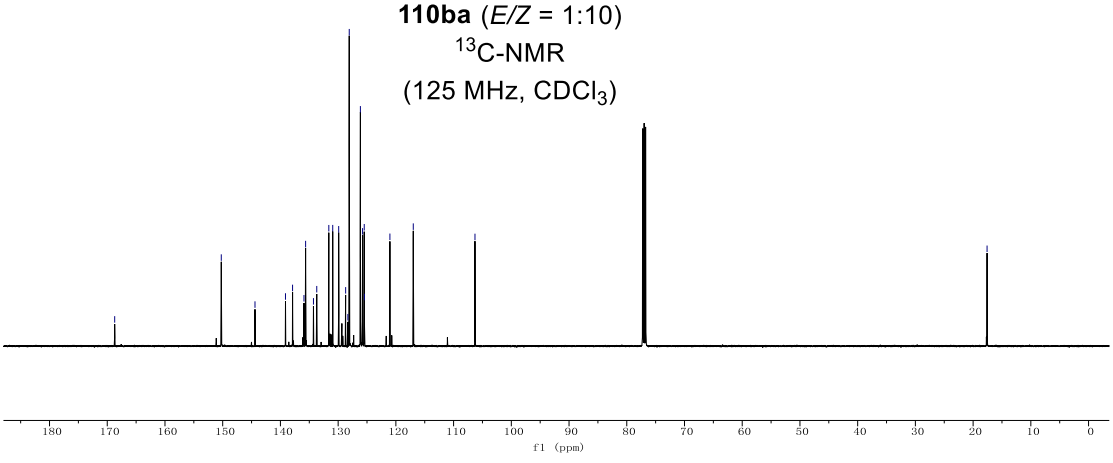

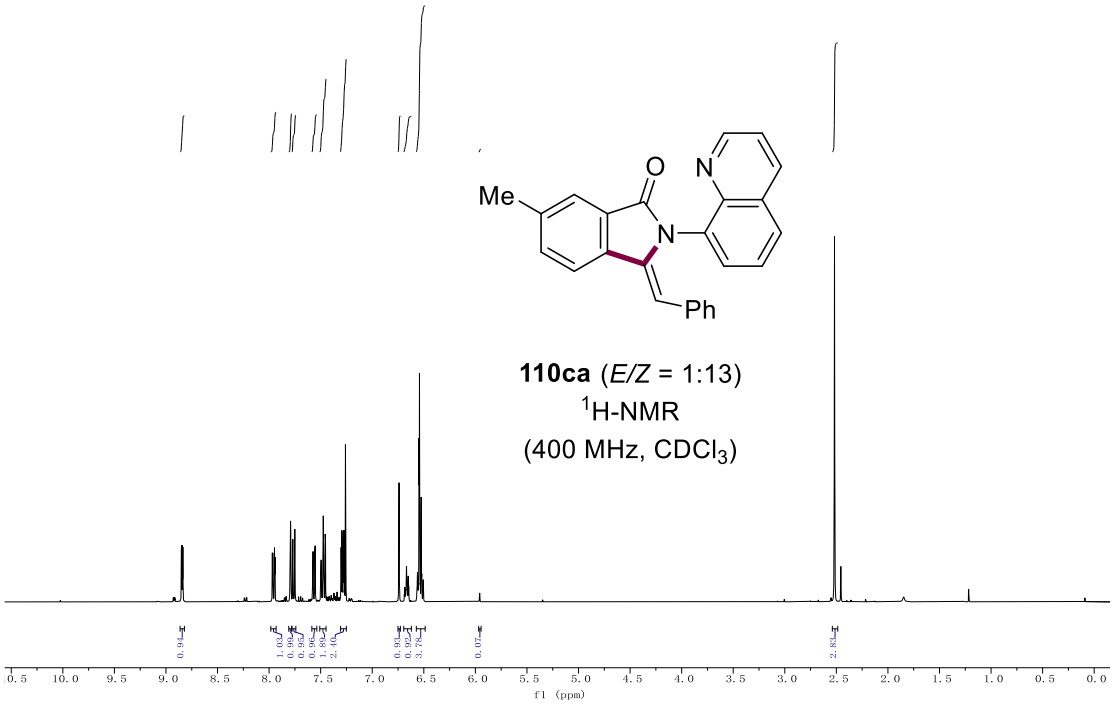

110ca (*E*/*Z* = 1:13)
^{1}H-NMR
(400 MHz, $CDCl_3$)

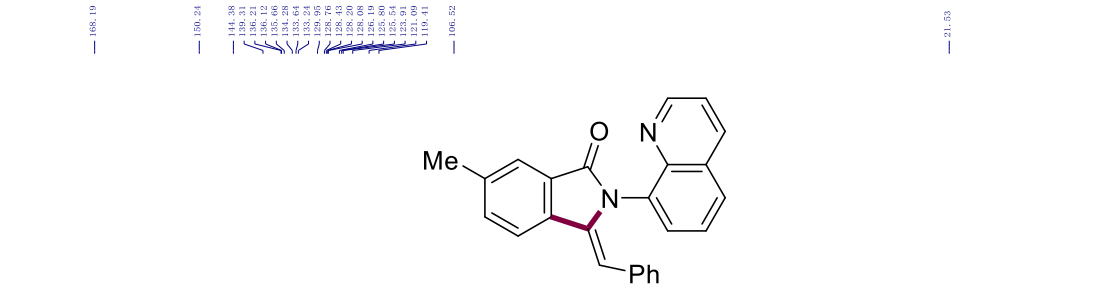

110ca (*E*/*Z* = 1:13)
^{13}C-NMR
(100 MHz, $CDCl_3$)

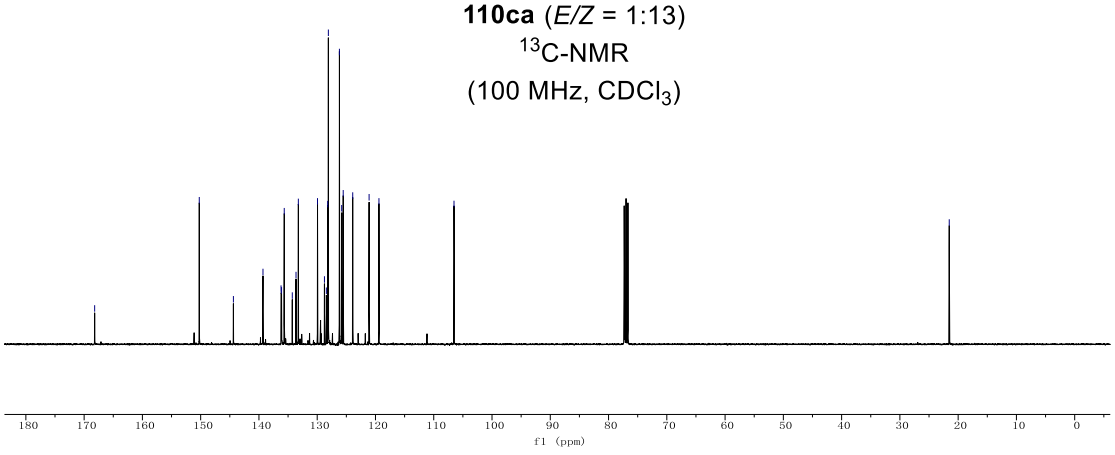

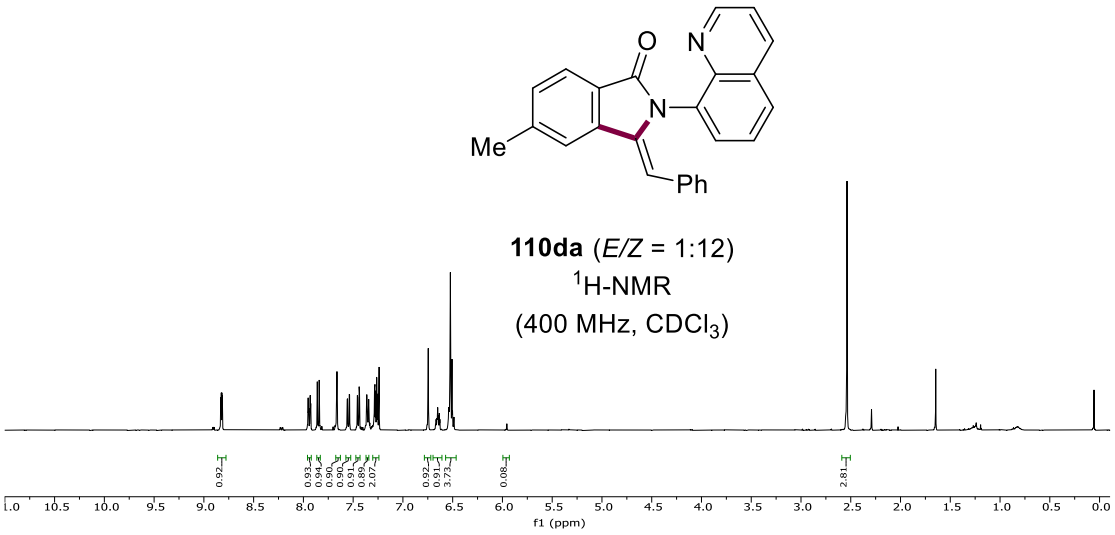

110da (*E/Z* = 1:12)
^{1}H-NMR
(400 MHz, $CDCl_3$)

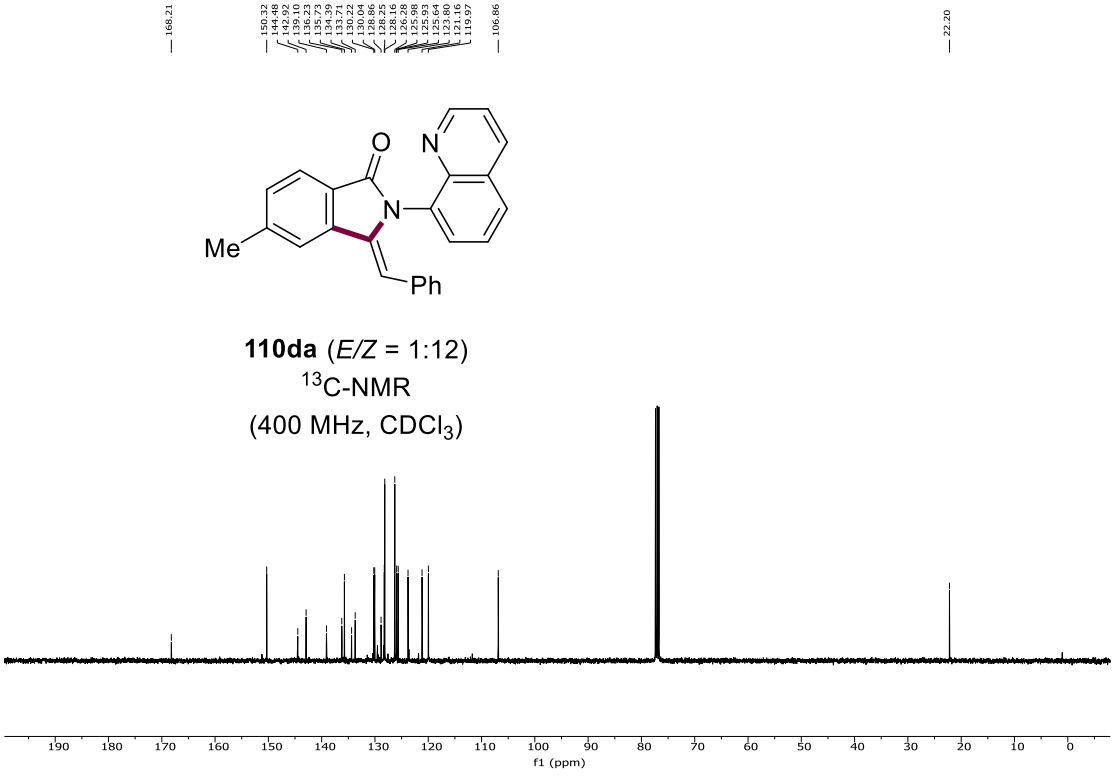

110da (*E/Z* = 1:12)
^{13}C-NMR
(400 MHz, $CDCl_3$)

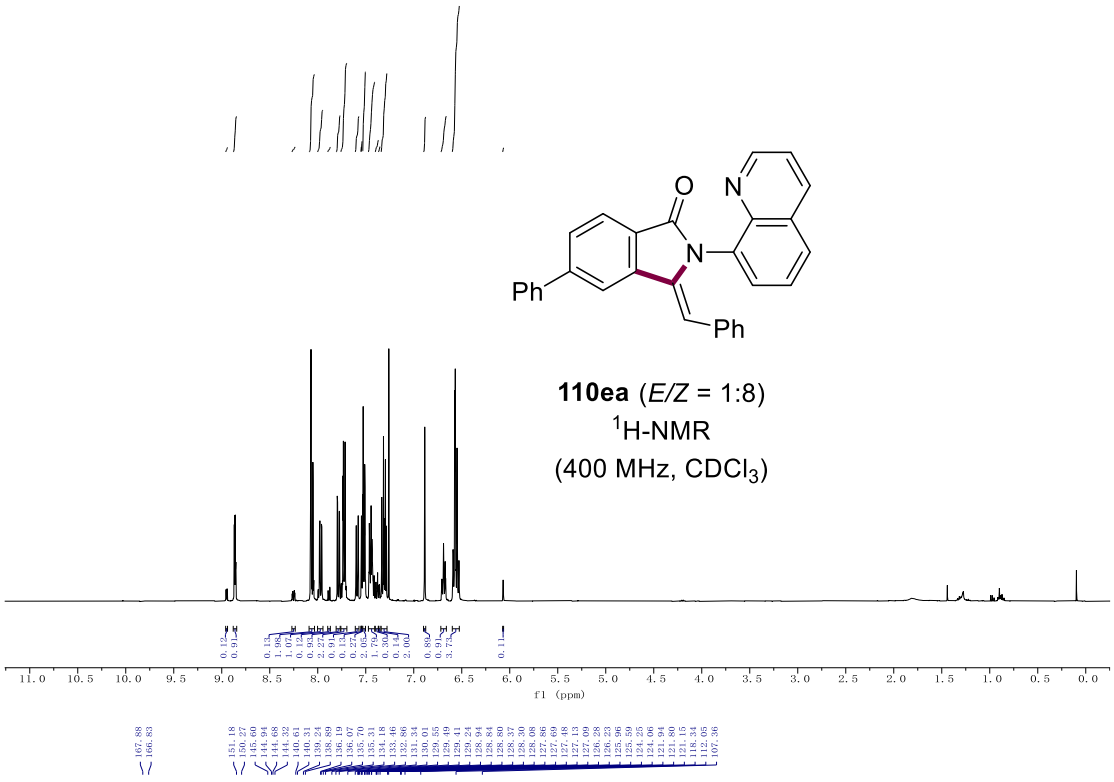
O
N
N
Ph
Ph
110ea (*E/Z* = 1:8)
^{1}H-NMR
(400 MHz, $CDCl_3$)
f1 (ppm)

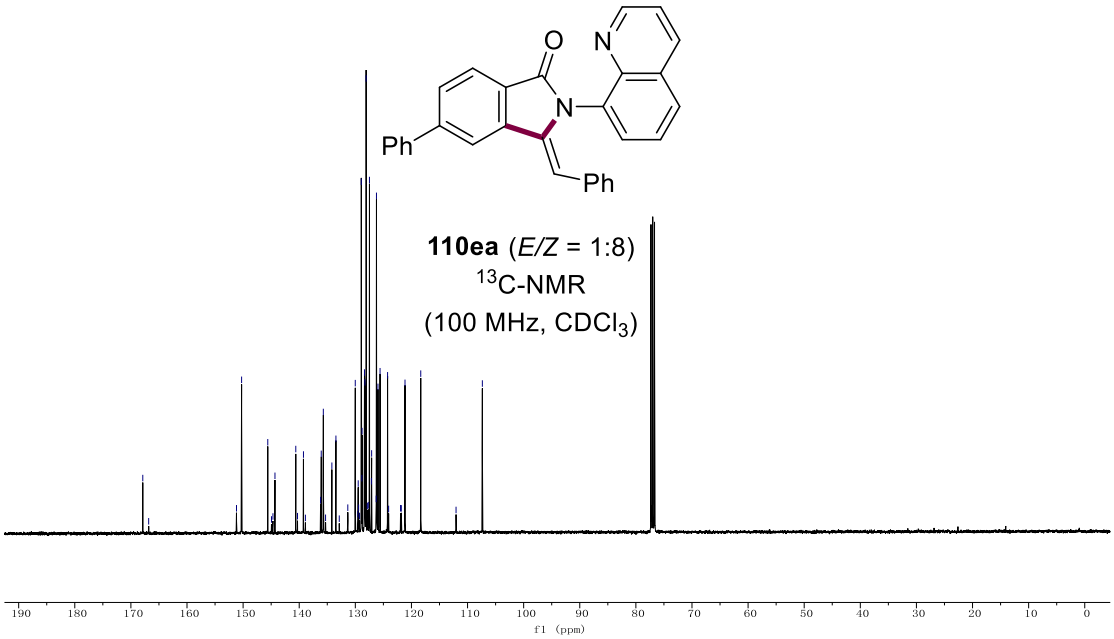
O
N
N
Ph
Ph
110ea (*E/Z* = 1:8)
^{13}C-NMR
(100 MHz, $CDCl_3$)
f1 (ppm)

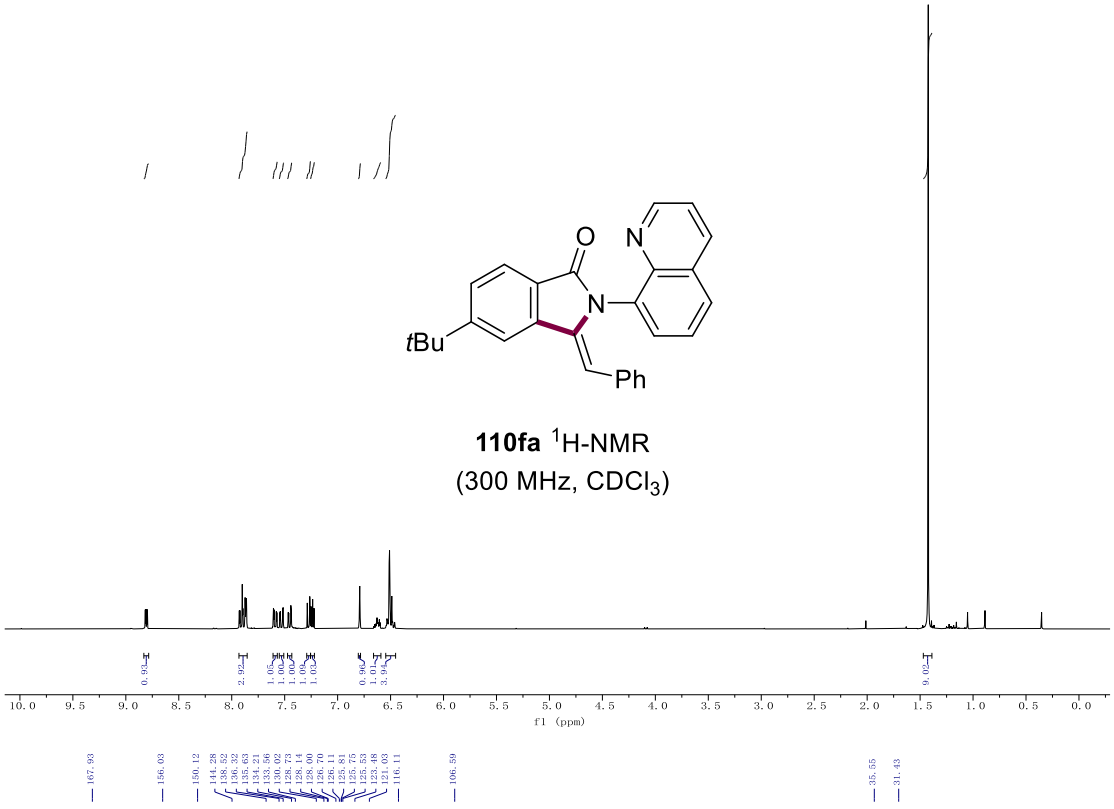

110fa ^{1}H-NMR
(300 MHz, $CDCl_3$)

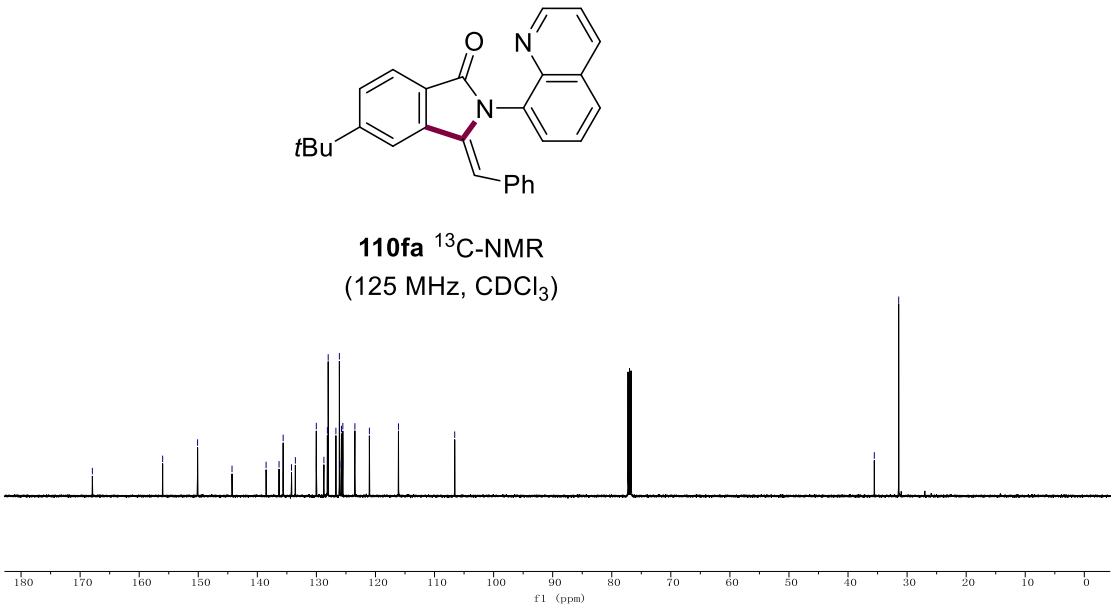

110fa ^{13}C-NMR
(125 MHz, $CDCl_3$)

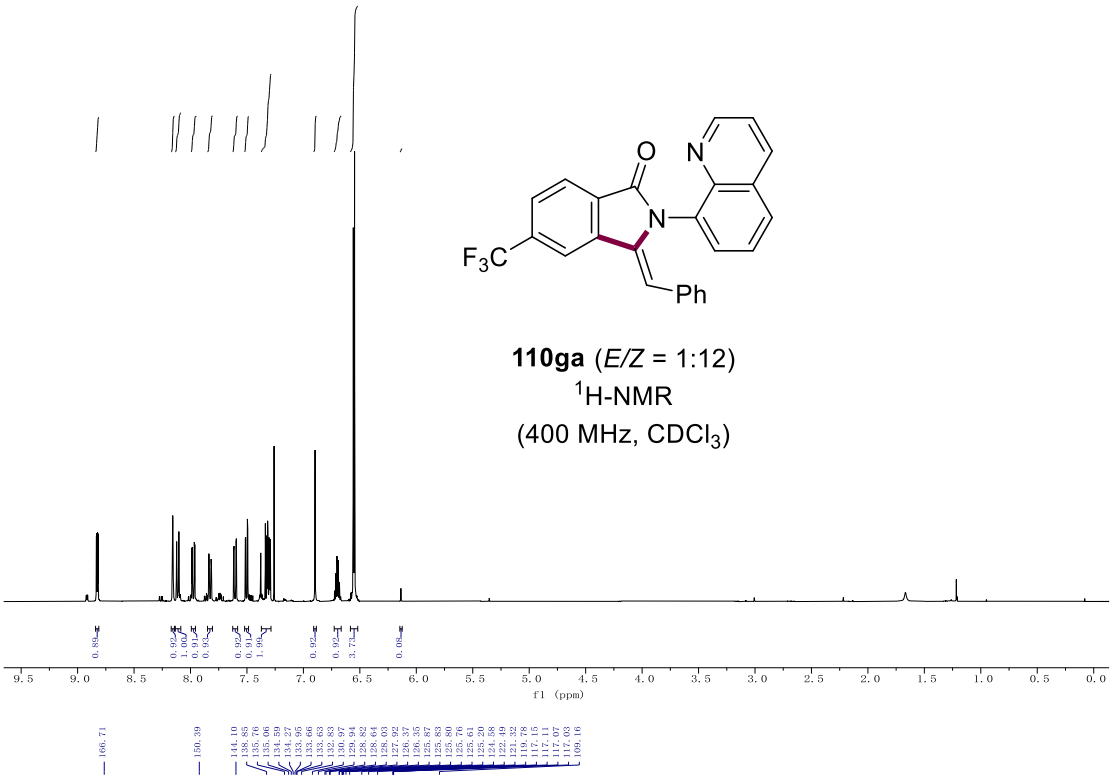

110ga (*E/Z* = 1:12)
^{1}H-NMR
(400 MHz, $CDCl_3$)

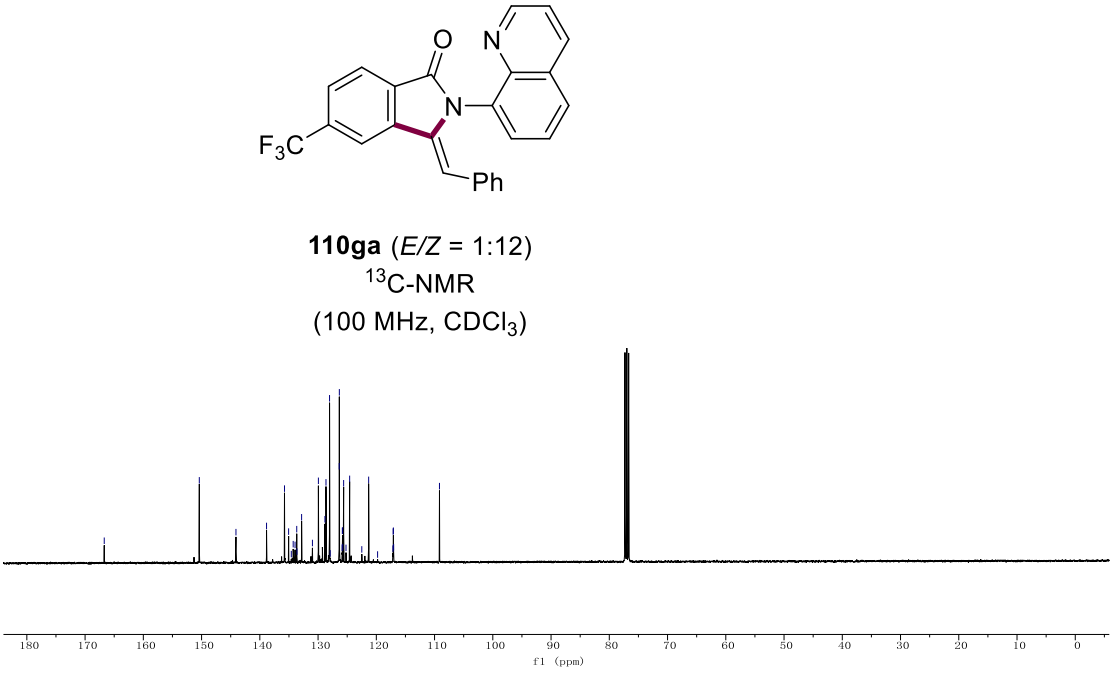

110ga (*E/Z* = 1:12)
^{13}C-NMR
(100 MHz, $CDCl_3$)

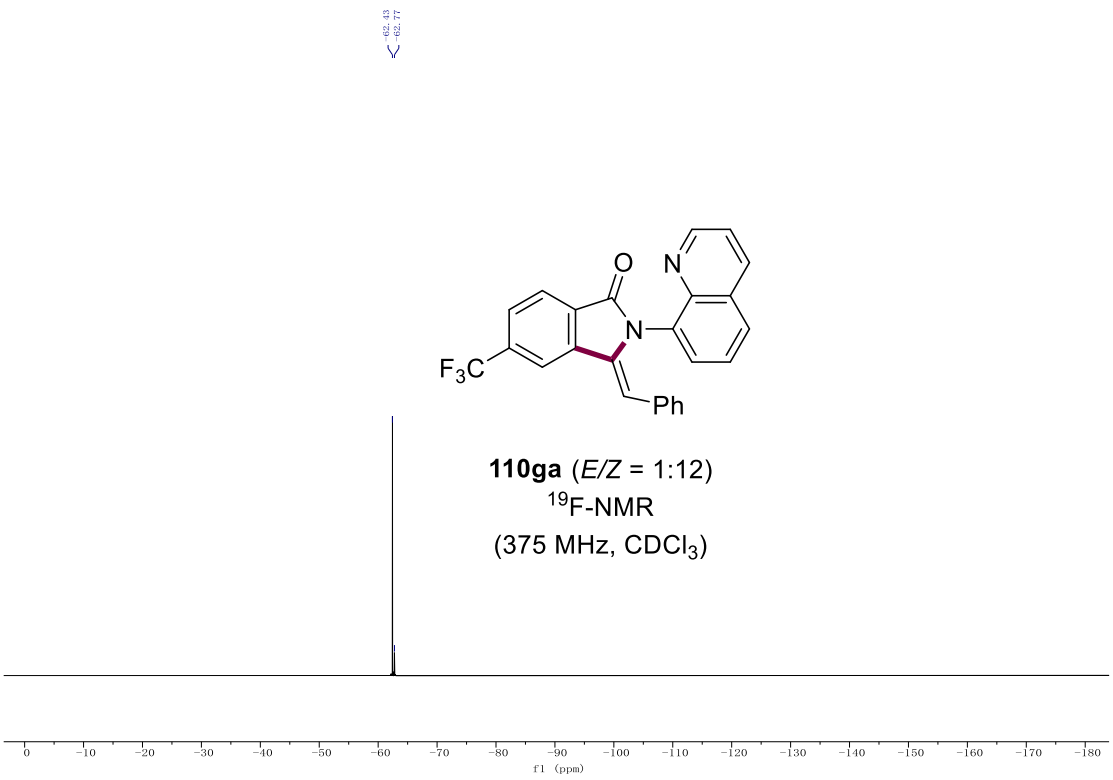
-62.43
-62.77
O
N
N
F3C
Ph
110ga (E/Z = 1:12)
19F-NMR
(375 MHz, CDCl3)
0
−10
−20
−30
−40
−50
−60
−70
−80
−90
−100
−110
−120
−130
−140
−150
−160
−170
−180
f1 (ppm)

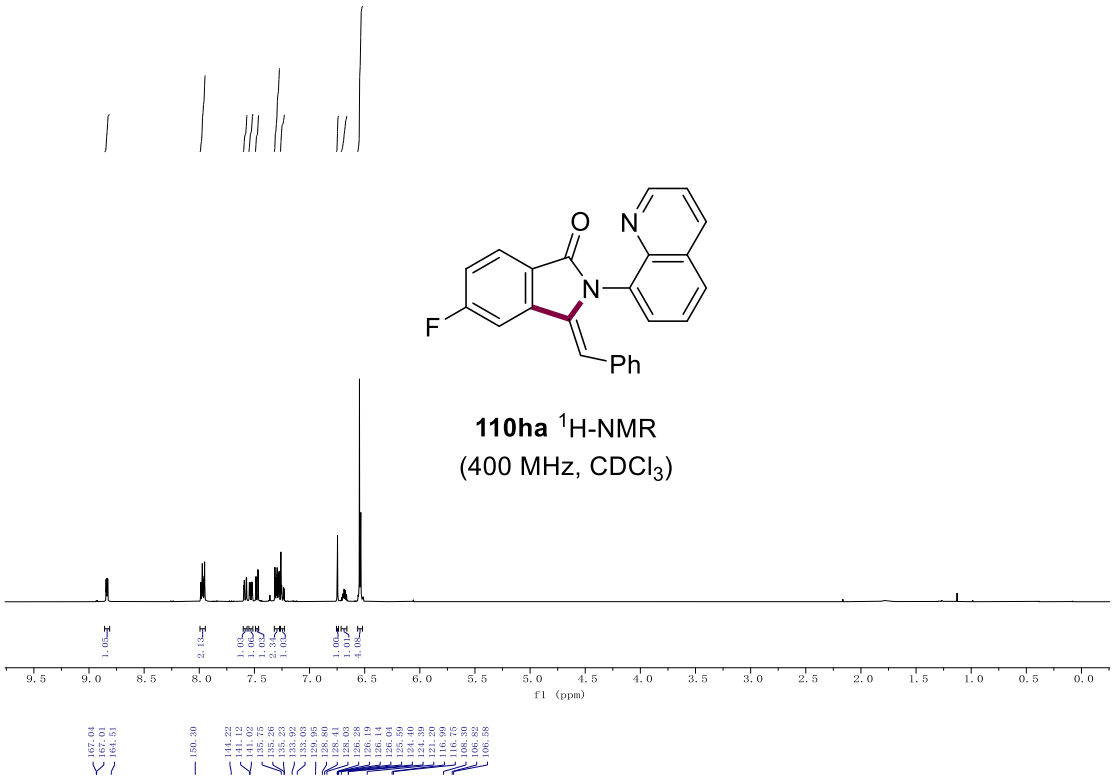

110ha ^{1}H-NMR
(400 MHz, $CDCl_3$)

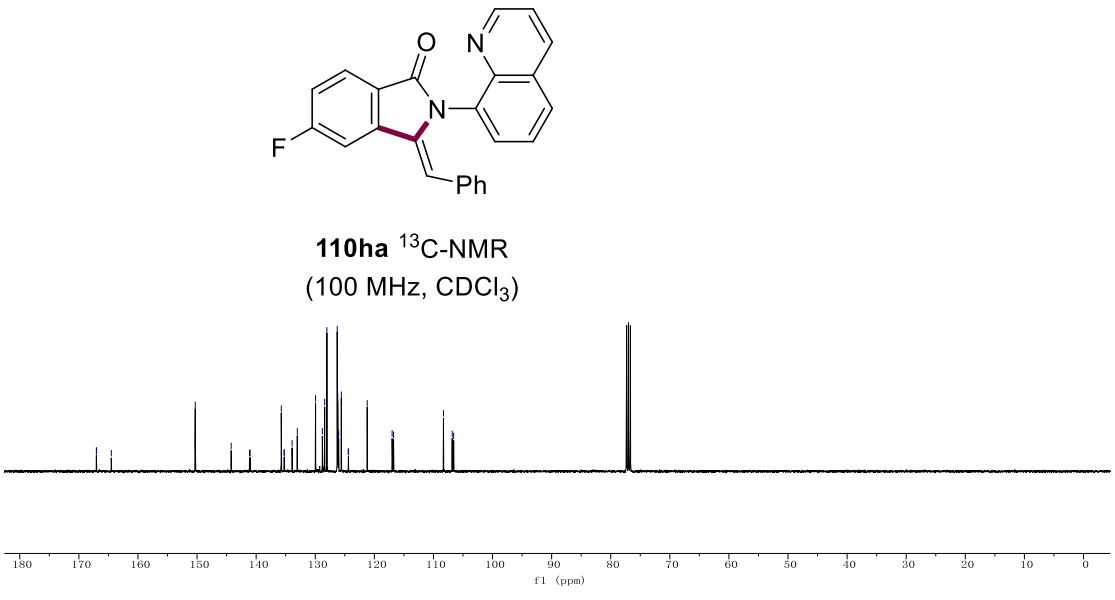

110ha ^{13}C-NMR
(100 MHz, $CDCl_3$)

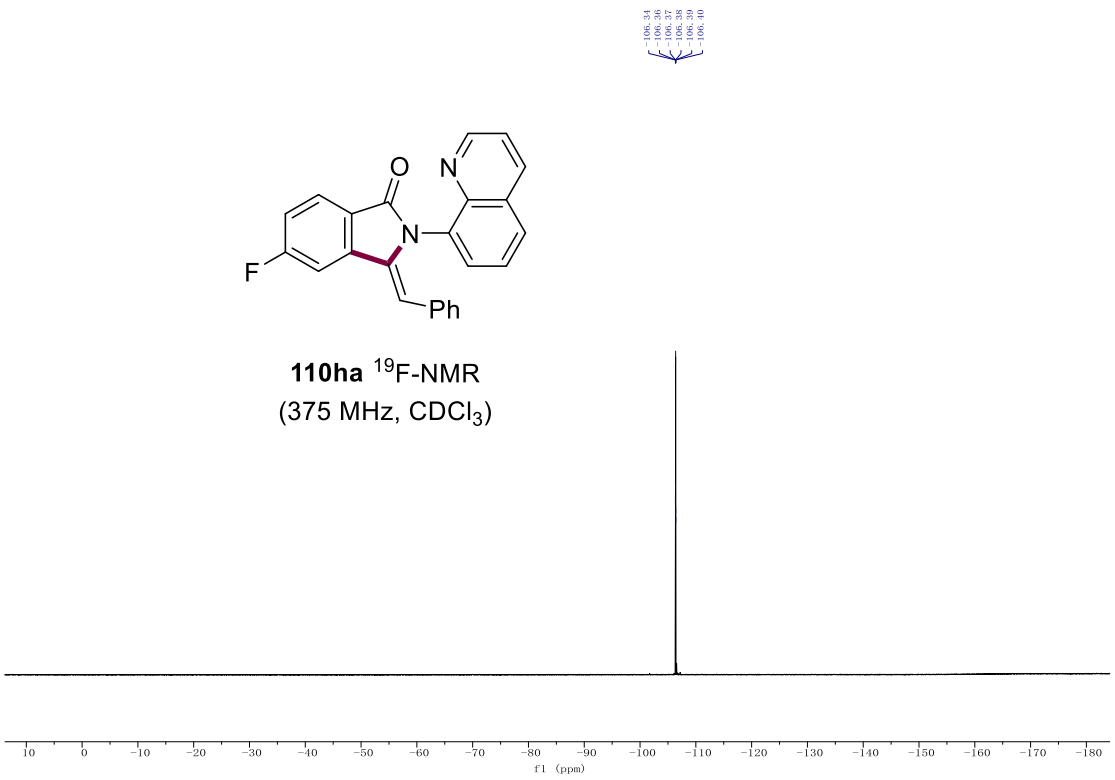

110ha ^{19}F-NMR
(375 MHz, $CDCl_3$)

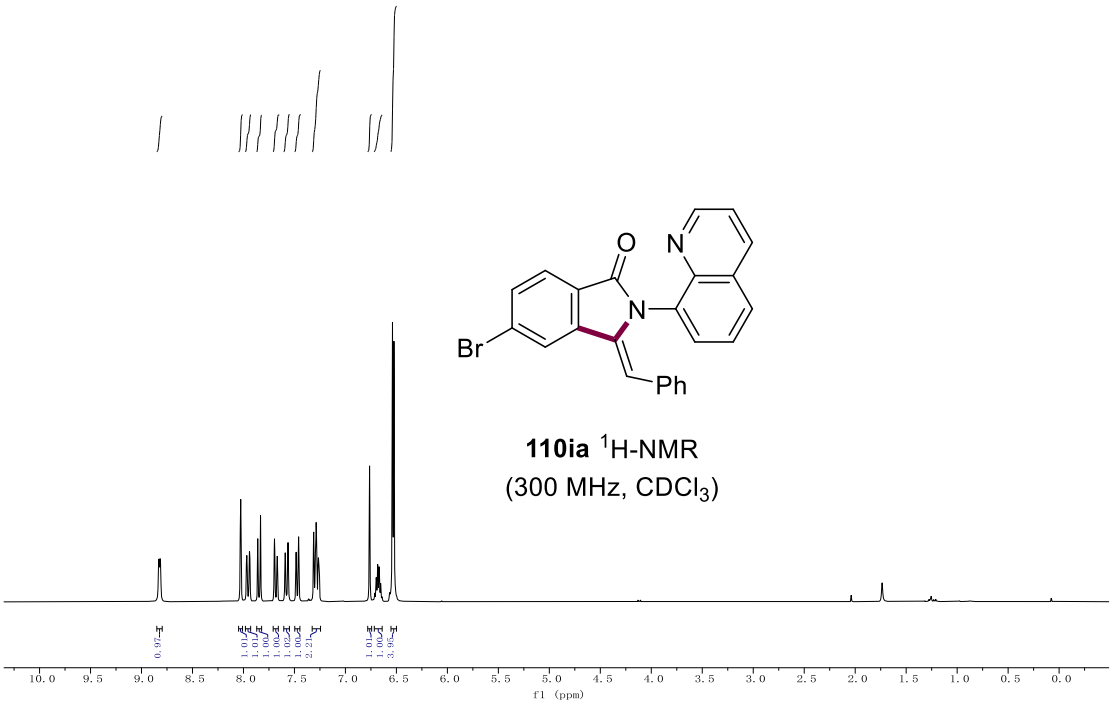

110ia ^{1}H-NMR
(300 MHz, $CDCl_3$)

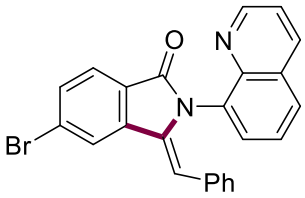

110ia ^{13}C-NMR
(125 MHz, $CDCl_3$)

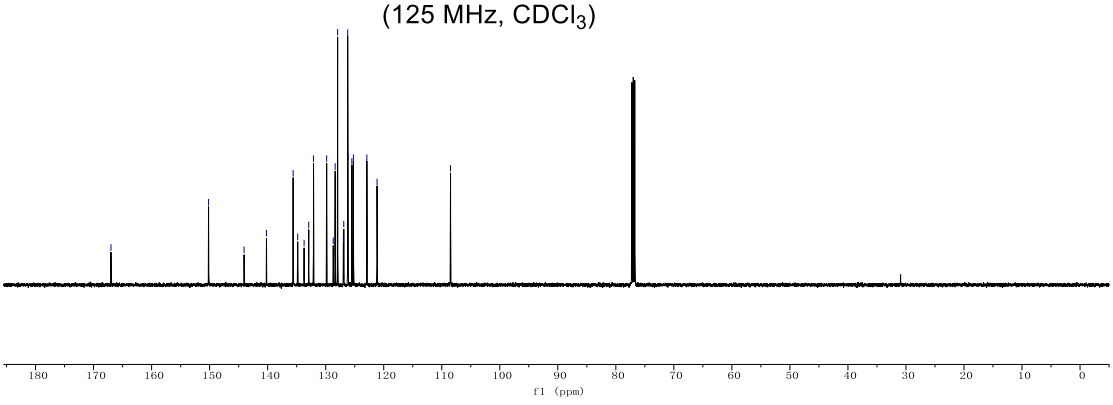

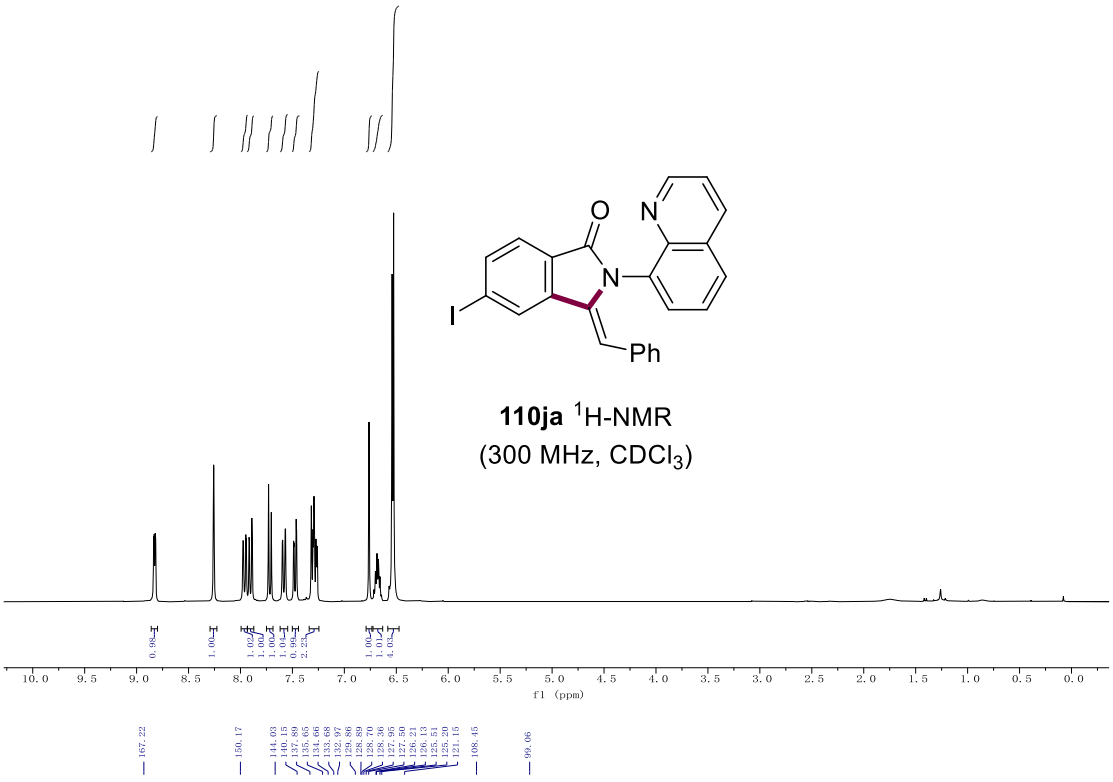

110ja ^{1}H-NMR
(300 MHz, $CDCl_3$)

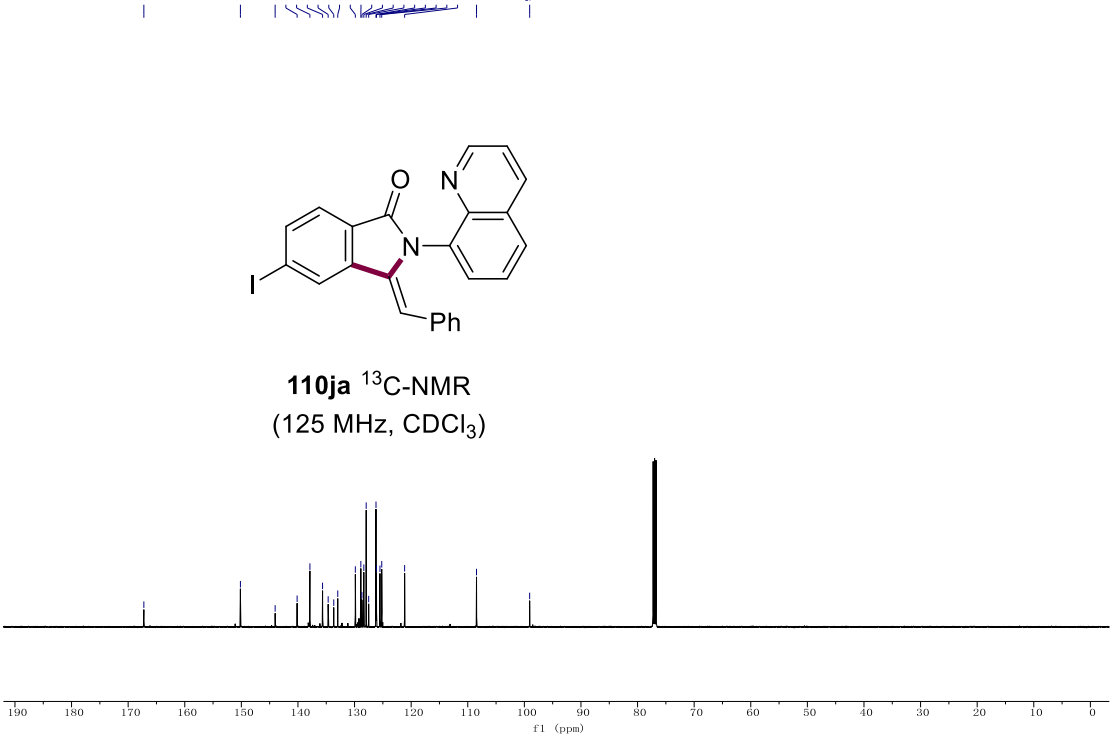

110ja ^{13}C-NMR
(125 MHz, $CDCl_3$)

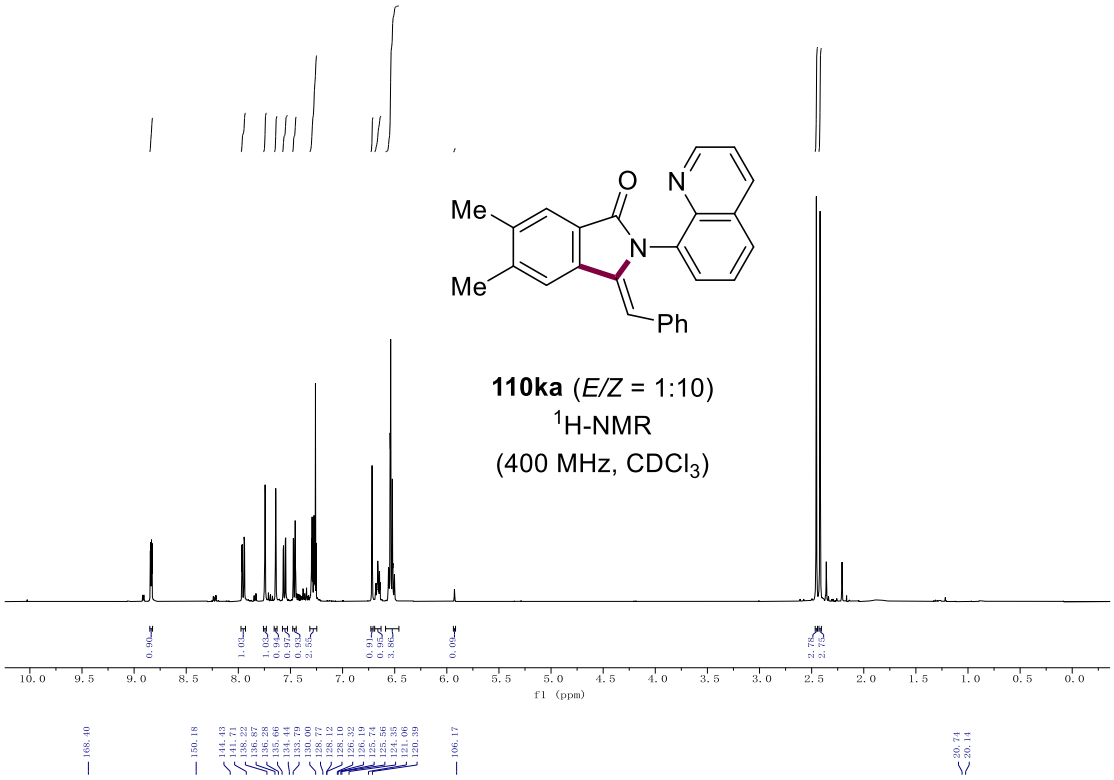
Me
Me
O
N
N
Ph
110ka (*E*/*Z* = 1:10)
^{1}H-NMR
(400 MHz, $CDCl_3$)
f1 (ppm)

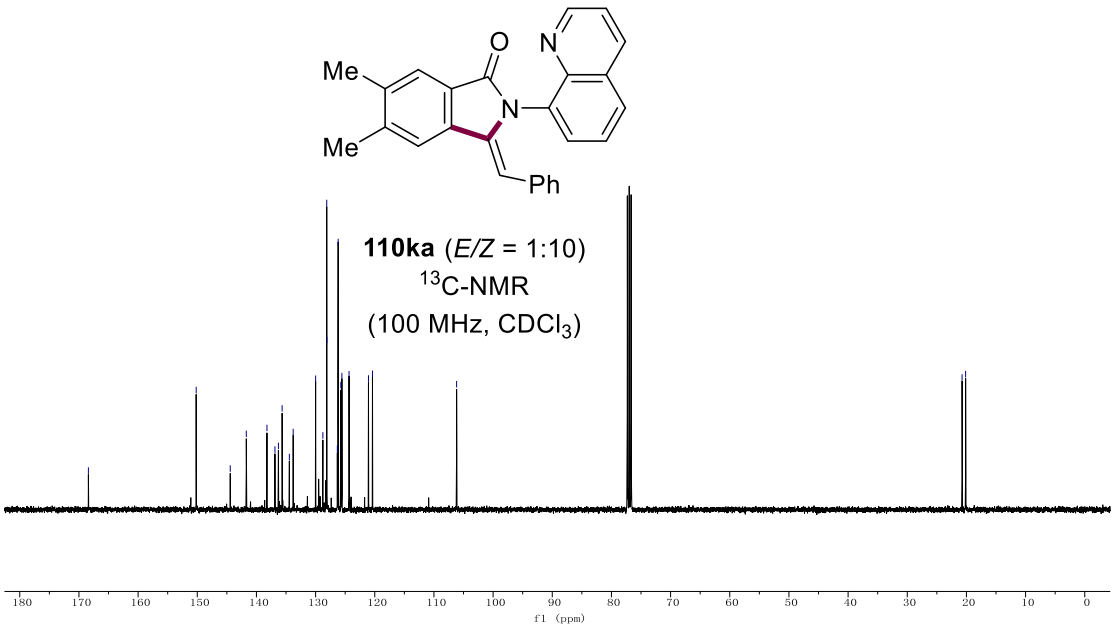
Me
Me
O
N
N
Ph
110ka (*E*/*Z* = 1:10)
^{13}C-NMR
(100 MHz, $CDCl_3$)
f1 (ppm)

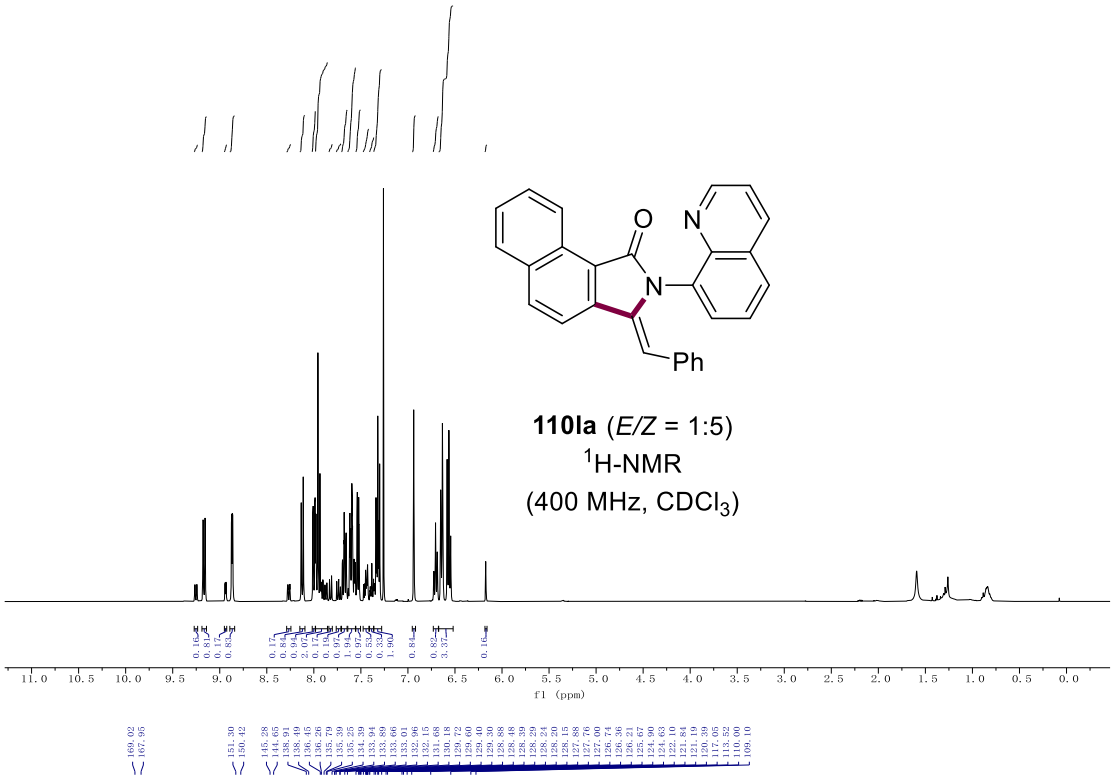

110la (*E*/*Z* = 1:5)
^{1}H-NMR
(400 MHz, $CDCl_3$)

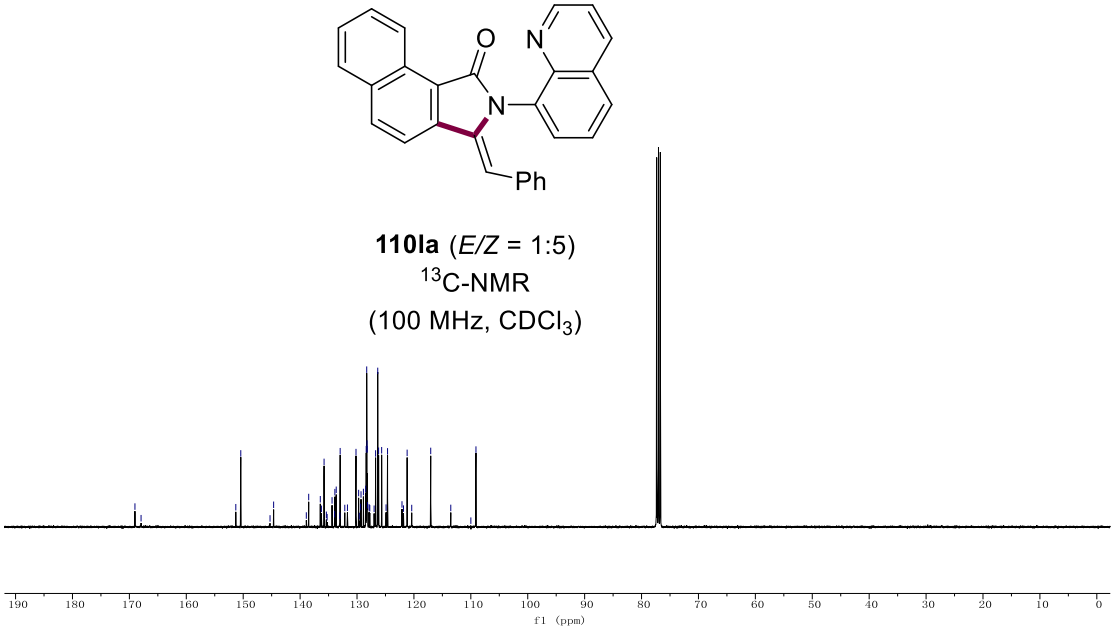

110la (*E*/*Z* = 1:5)
^{13}C-NMR
(100 MHz, $CDCl_3$)

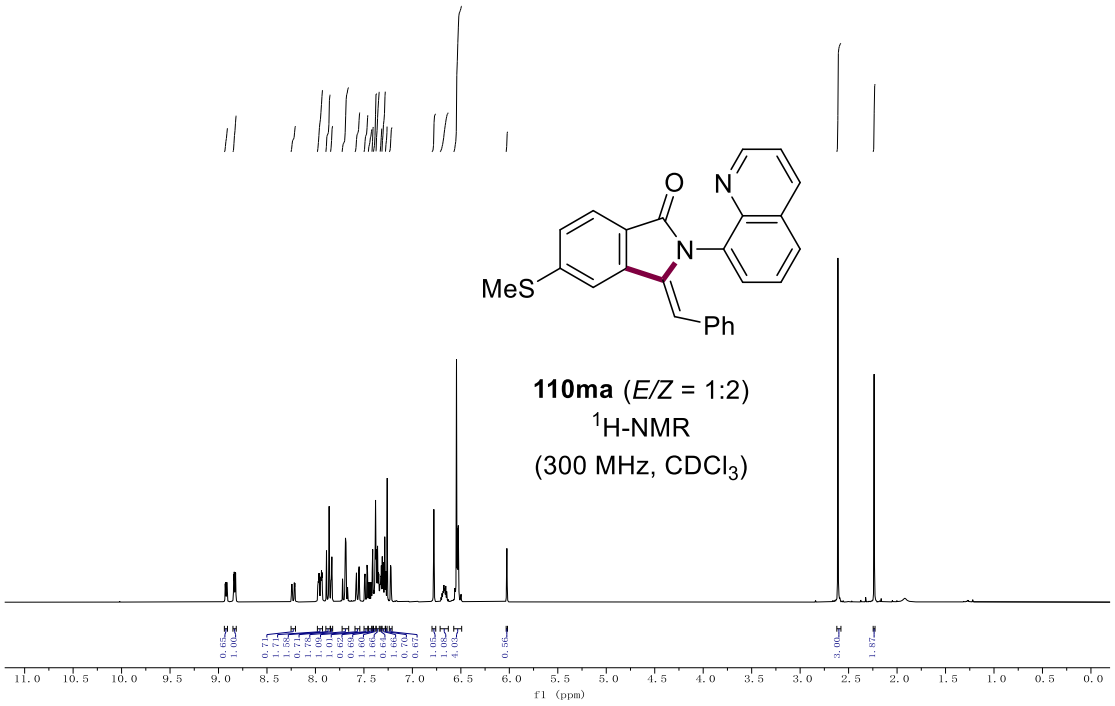
O
N
N
MeS
Ph
110ma (*E/Z* = 1:2)
^{1}H-NMR
(300 MHz, $CDCl_3$)
f1 (ppm)

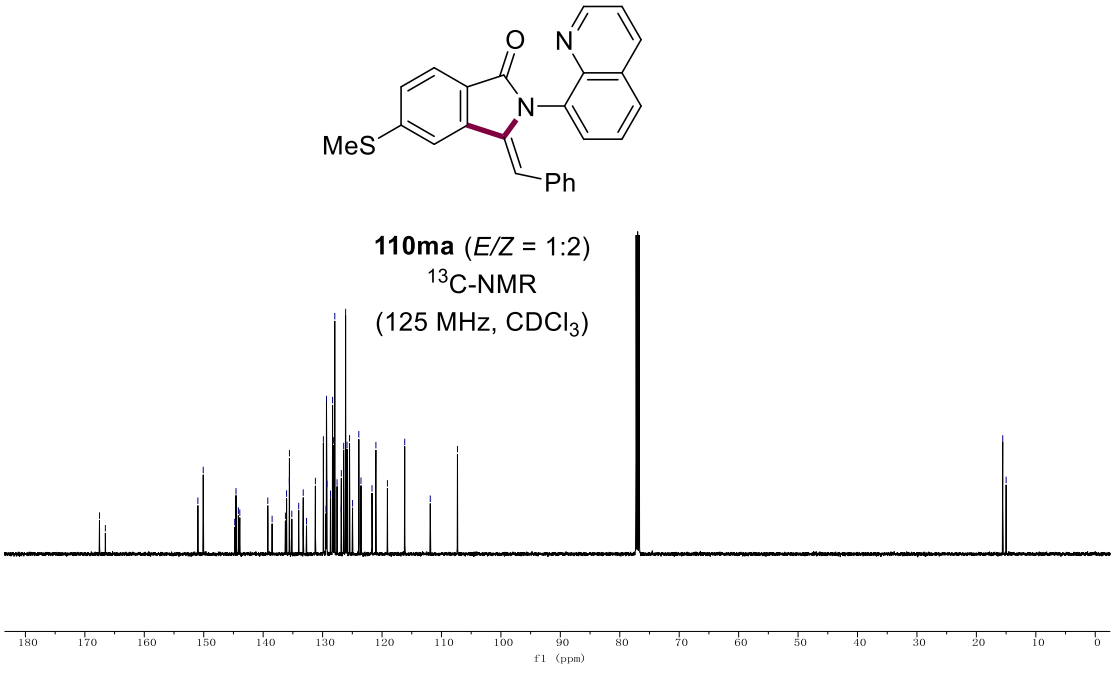
O
N
N
MeS
Ph
110ma (*E/Z* = 1:2)
^{13}C-NMR
(125 MHz, $CDCl_3$)
f1 (ppm)

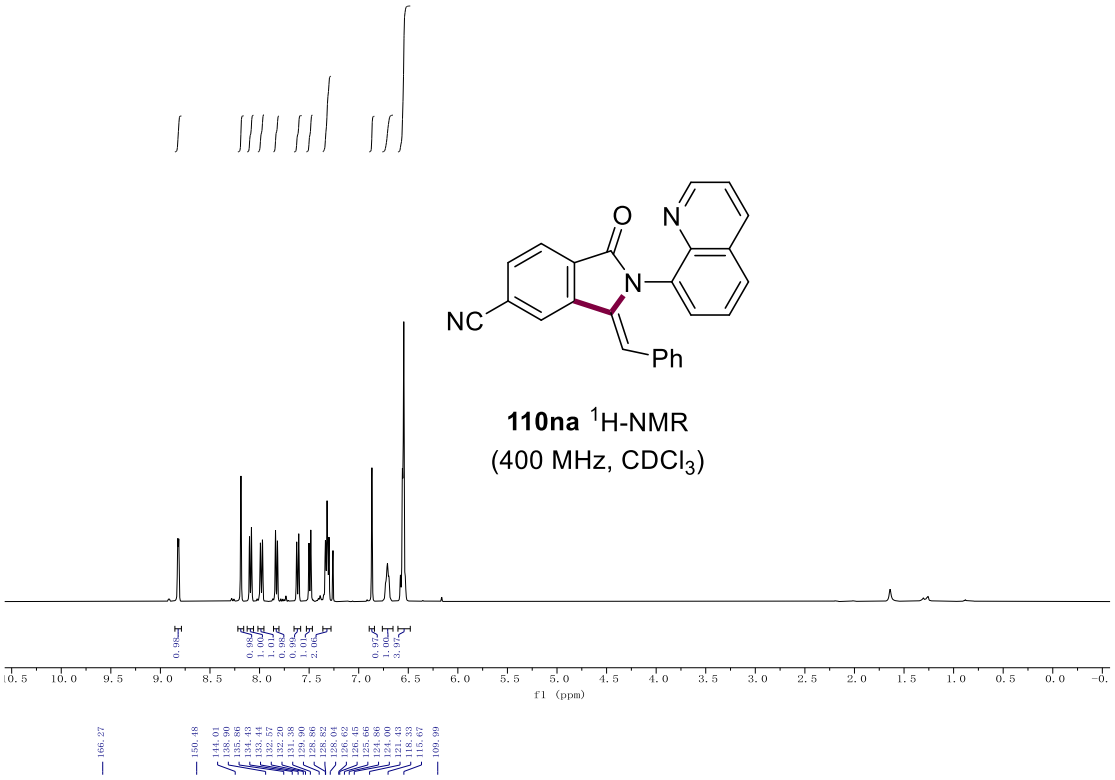
O
N
N
NC
Ph
110na 1H-NMR
(400 MHz, CDCl3)
f1 (ppm)

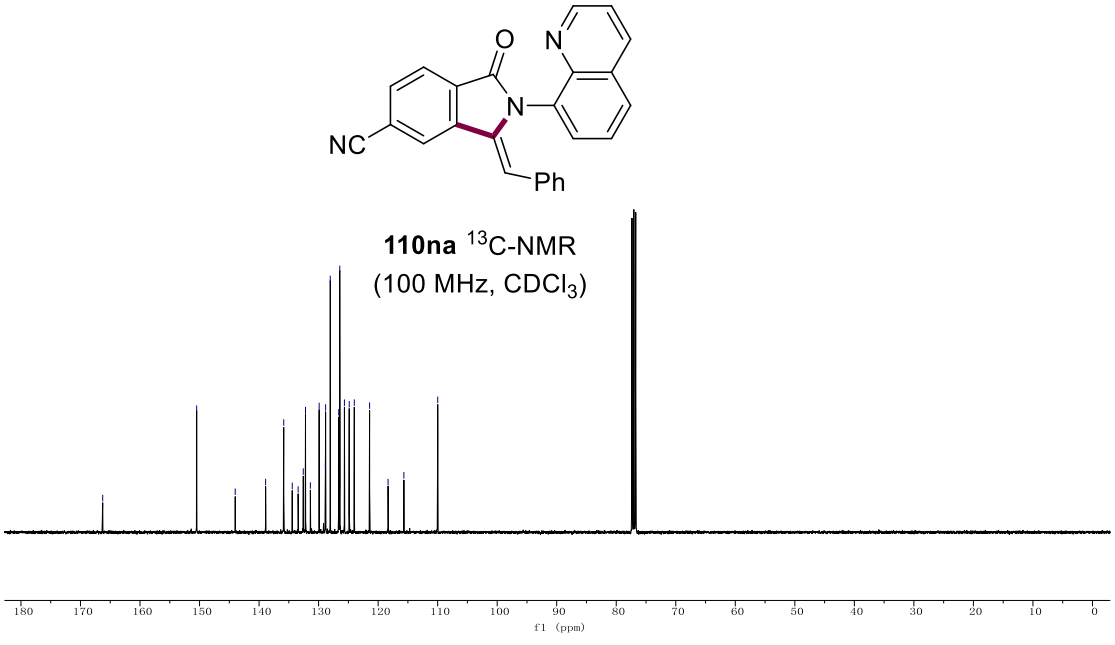
O
N
N
NC
Ph
110na 13C-NMR
(100 MHz, CDCl3)
f1 (ppm)

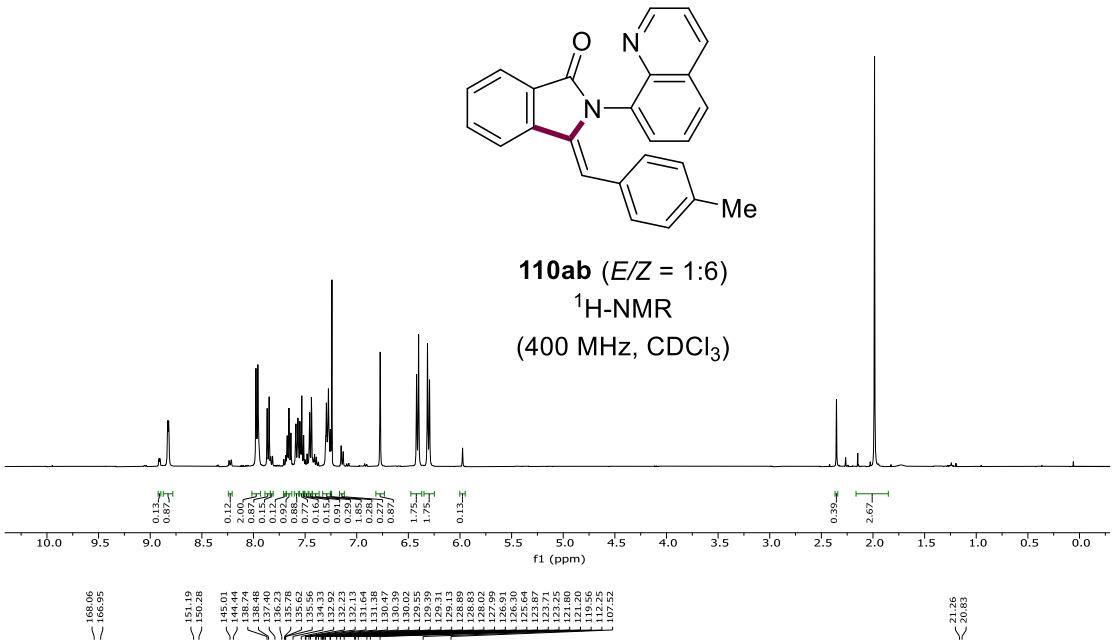

110ab (*E*/*Z* = 1:6)
^{1}H-NMR
(400 MHz, $CDCl_3$)

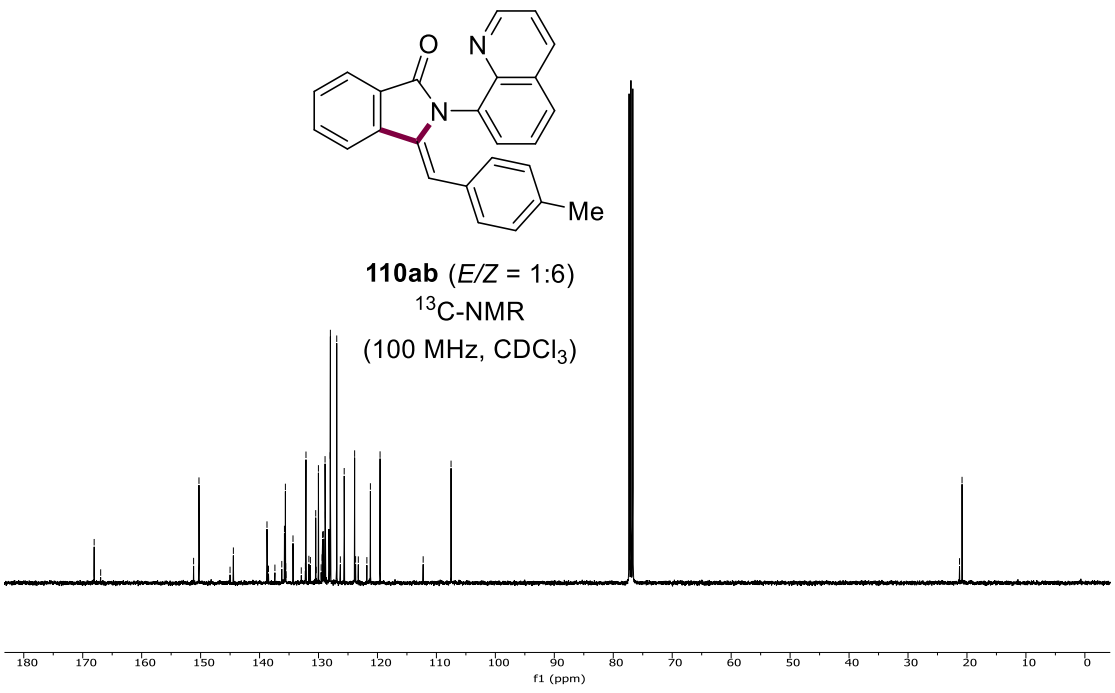

110ab (*E*/*Z* = 1:6)
^{13}C-NMR
(100 MHz, $CDCl_3$)

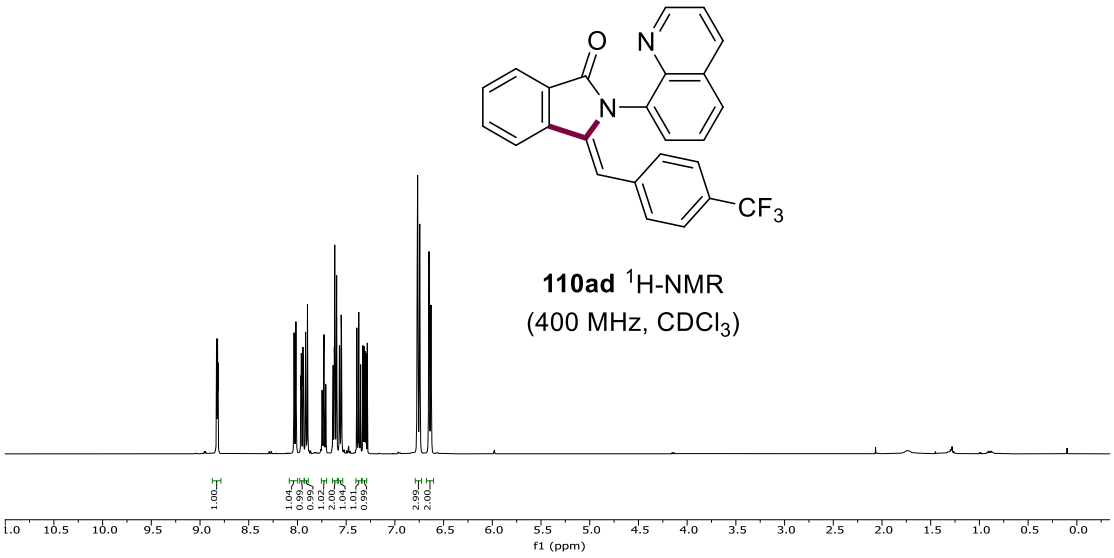
O
N
N
CF3
110ad 1H-NMR
(400 MHz, CDCl3)
f1 (ppm)

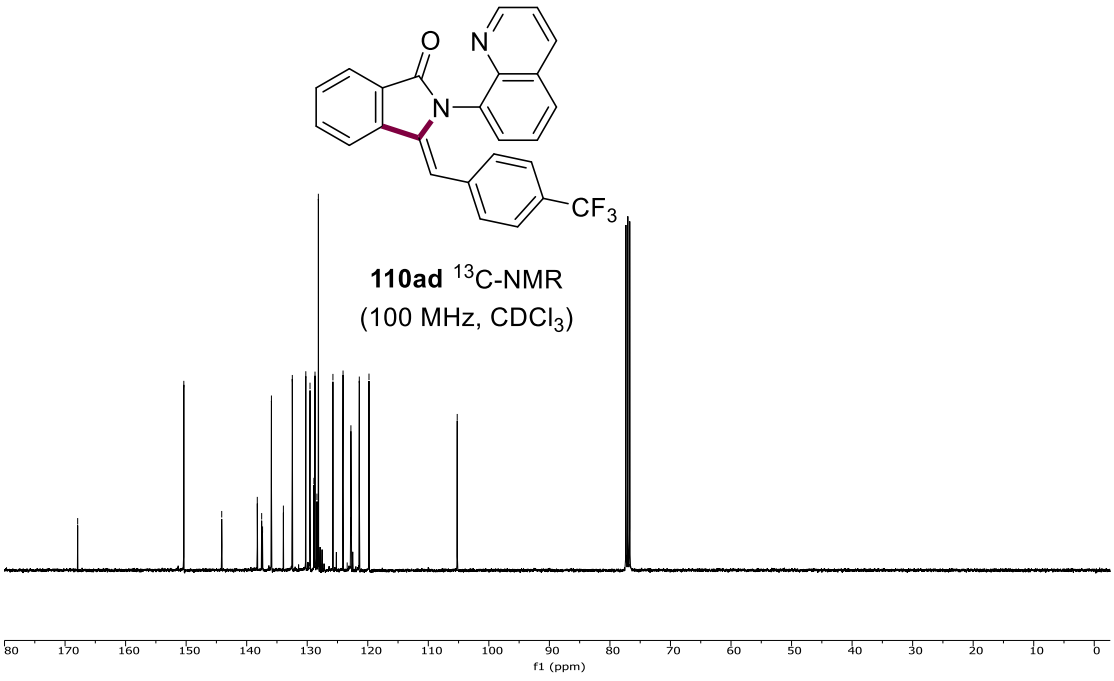
O
N
N
CF3
110ad 13C-NMR
(100 MHz, CDCl3)
f1 (ppm)

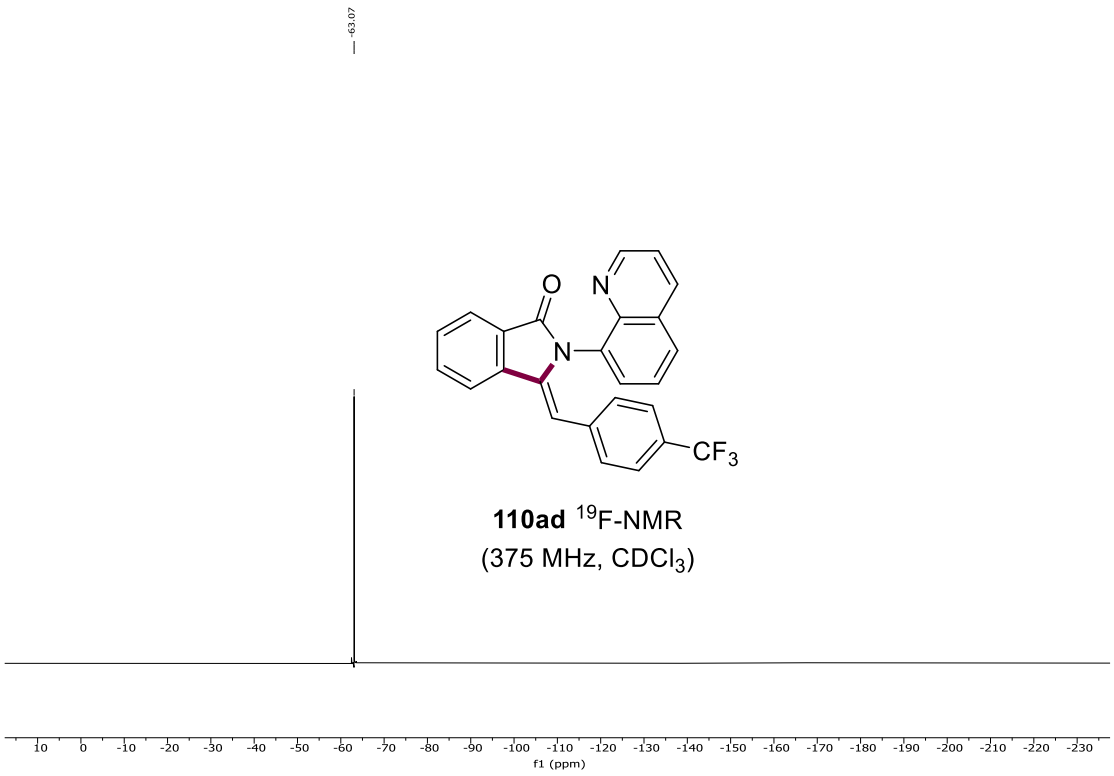

110ad ^{19}F-NMR
(375 MHz, $CDCl_3$)

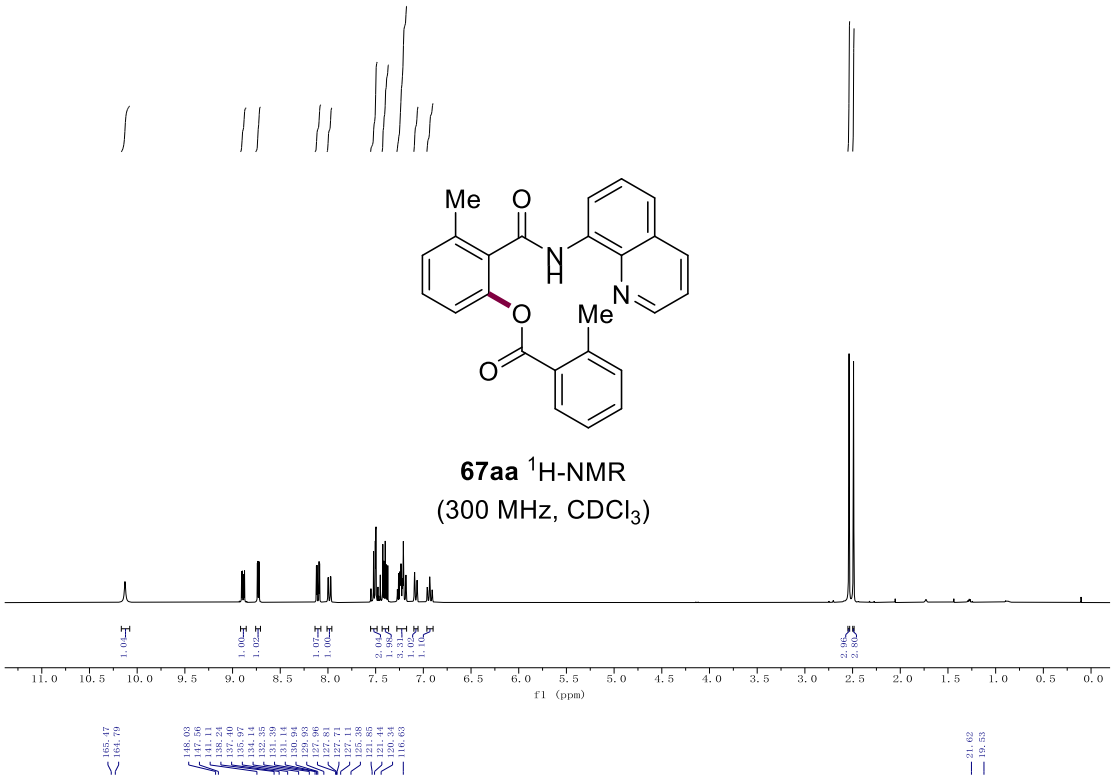

67aa ^{1}H-NMR
(300 MHz, $CDCl_3$)

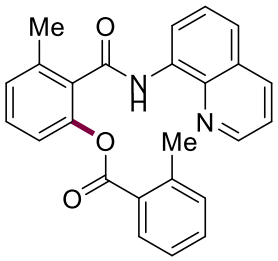

67aa ^{13}C-NMR
(125 MHz, $CDCl_3$)

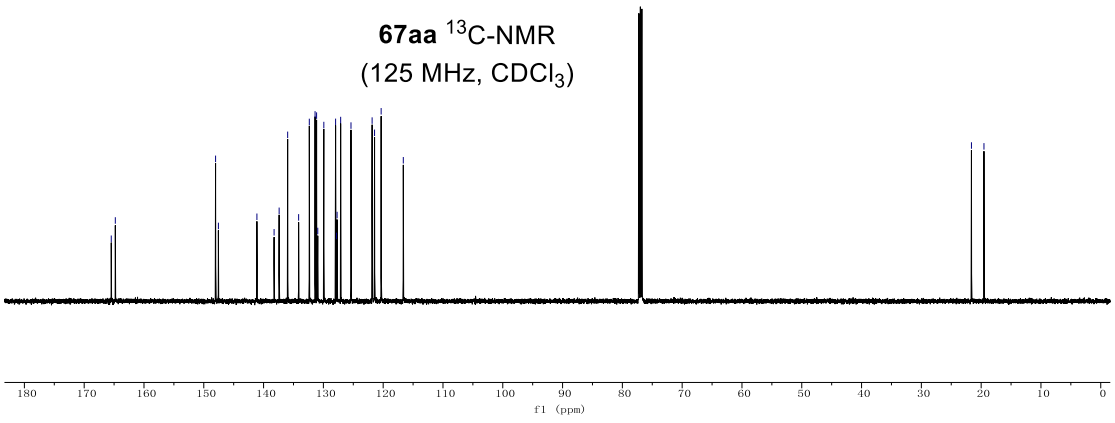

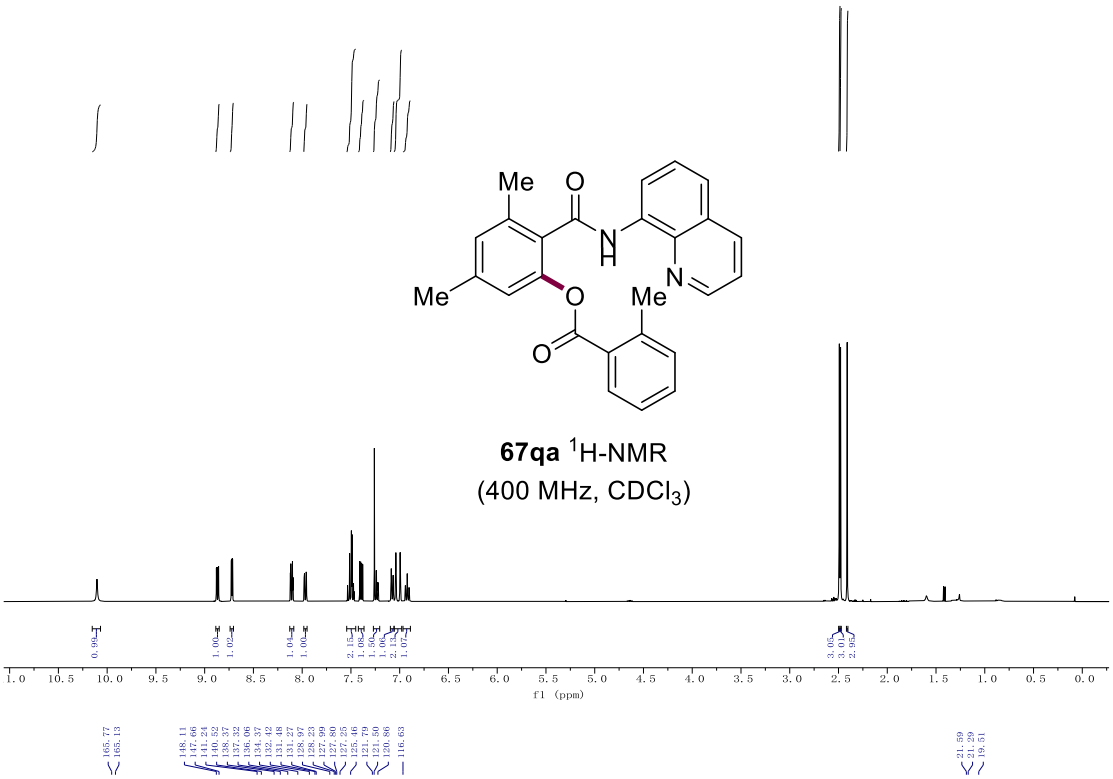

67qa ^{1}H-NMR
(400 MHz, $CDCl_3$)

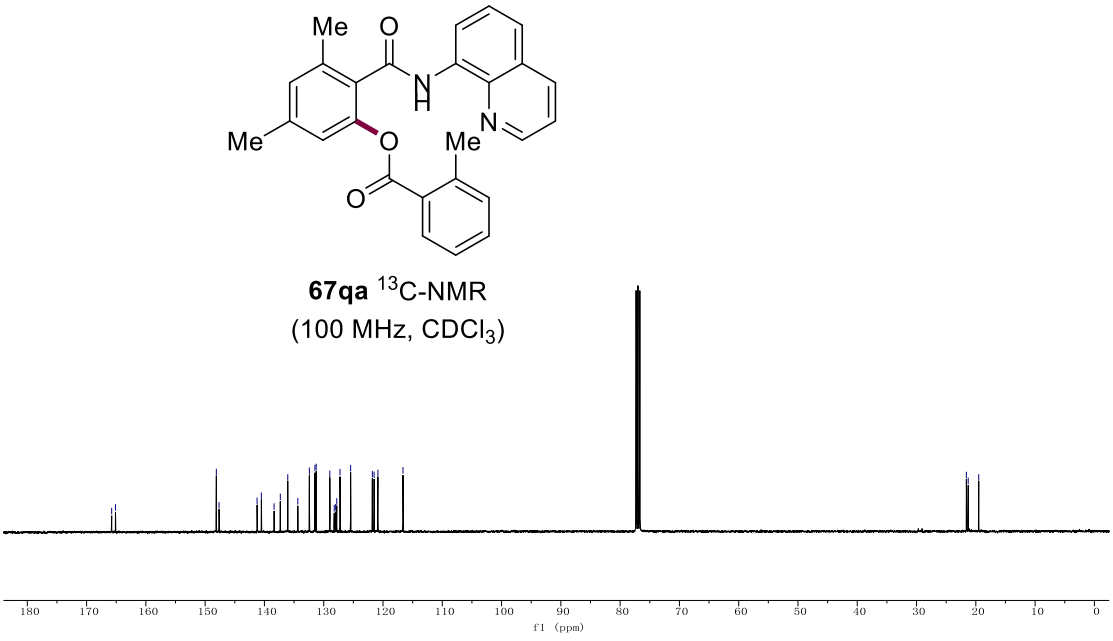

67qa ^{13}C-NMR
(100 MHz, $CDCl_3$)

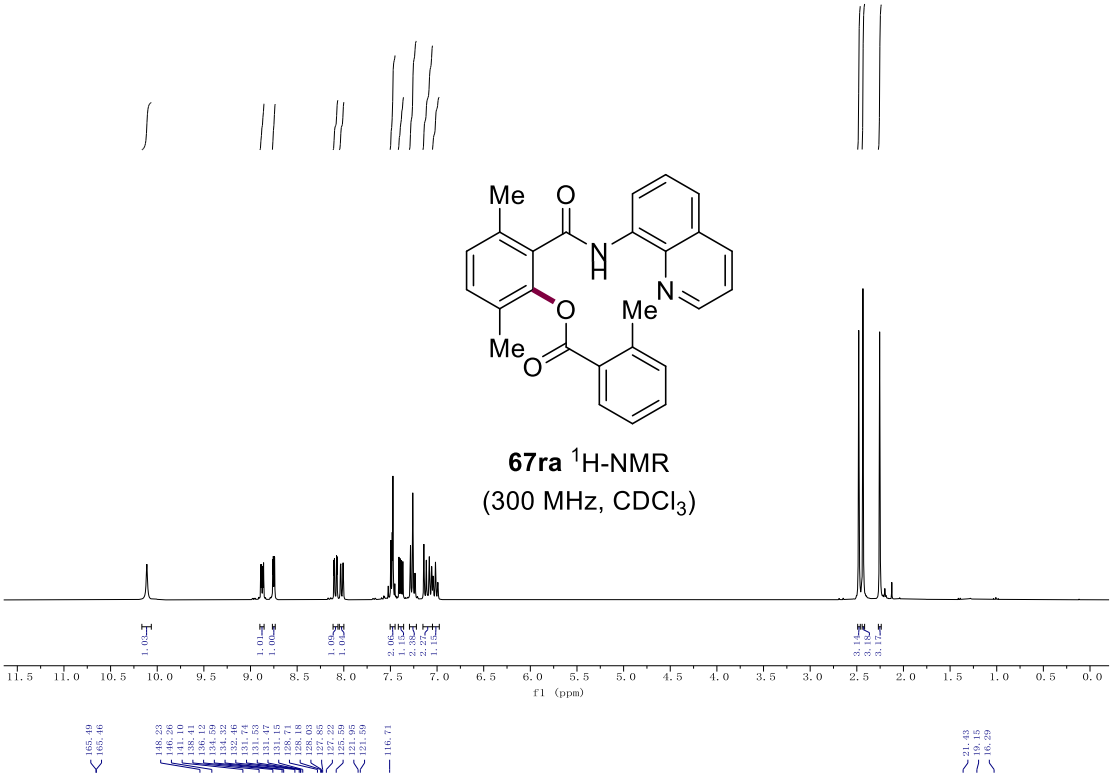

67ra ^{1}H-NMR
(300 MHz, $CDCl_3$)

67ra ^{13}C-NMR
(75 MHz, $CDCl_3$)

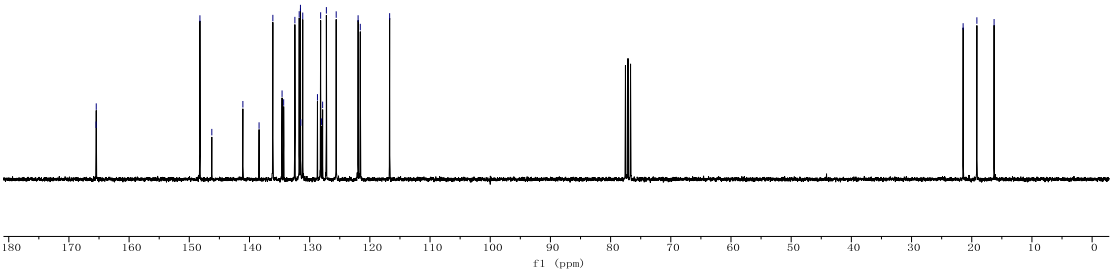

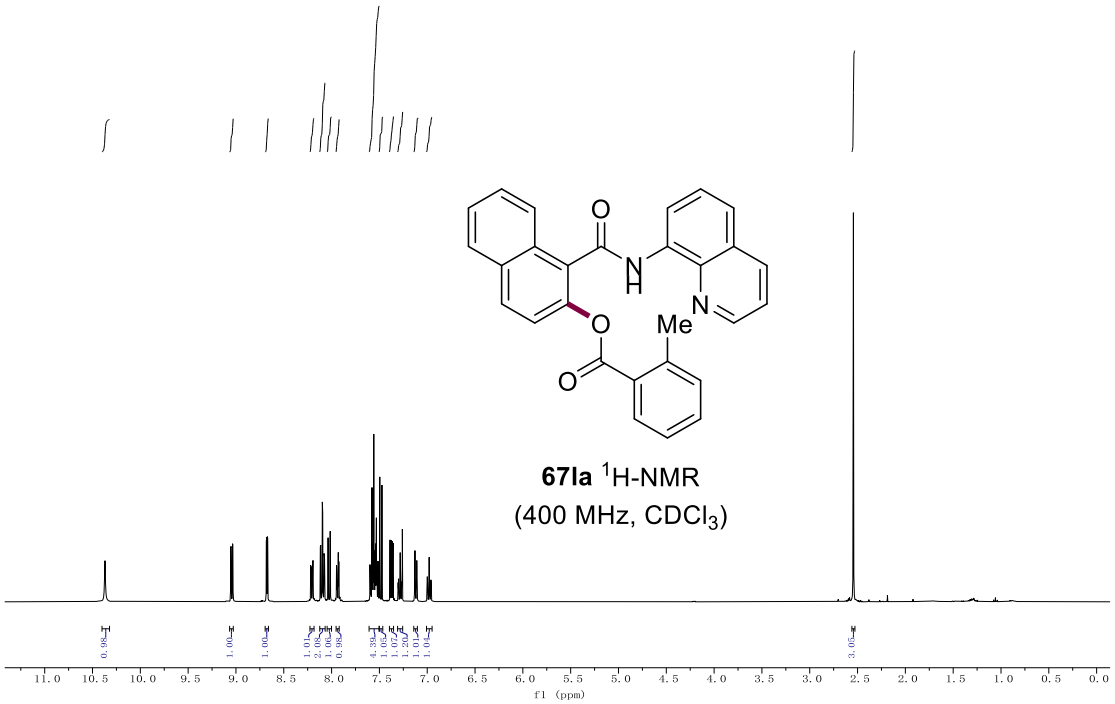

67la ^{1}H-NMR
(400 MHz, $CDCl_3$)

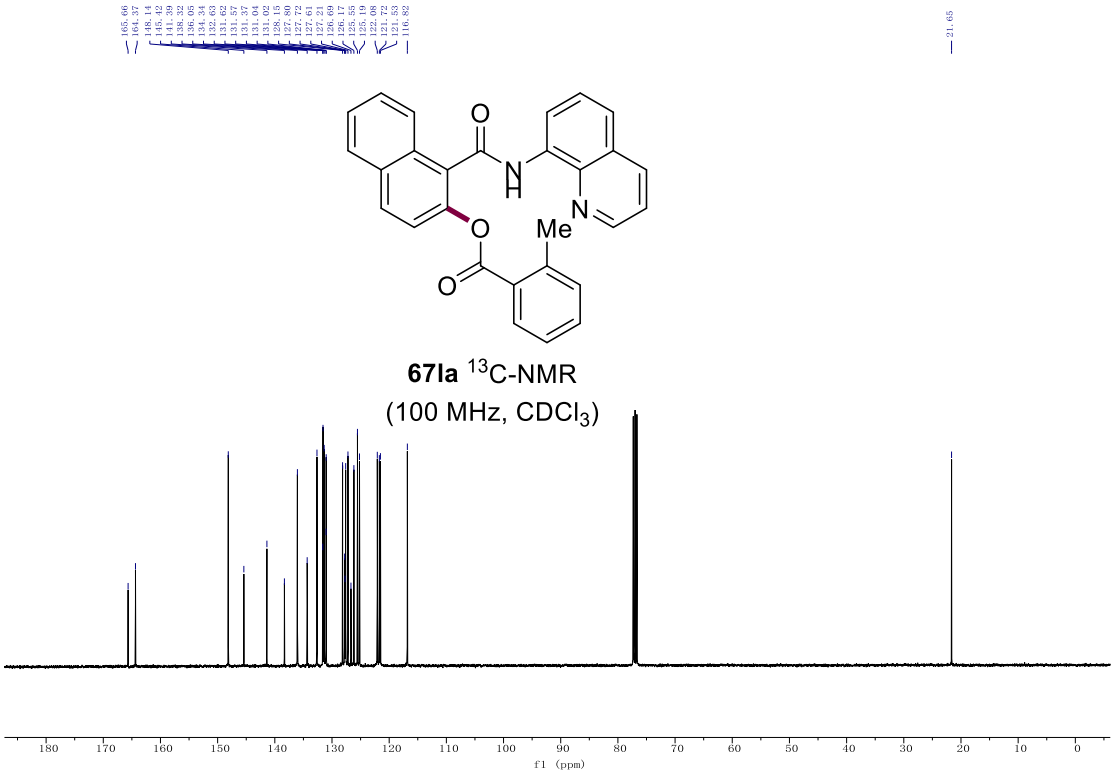

67la ^{13}C-NMR
(100 MHz, $CDCl_3$)

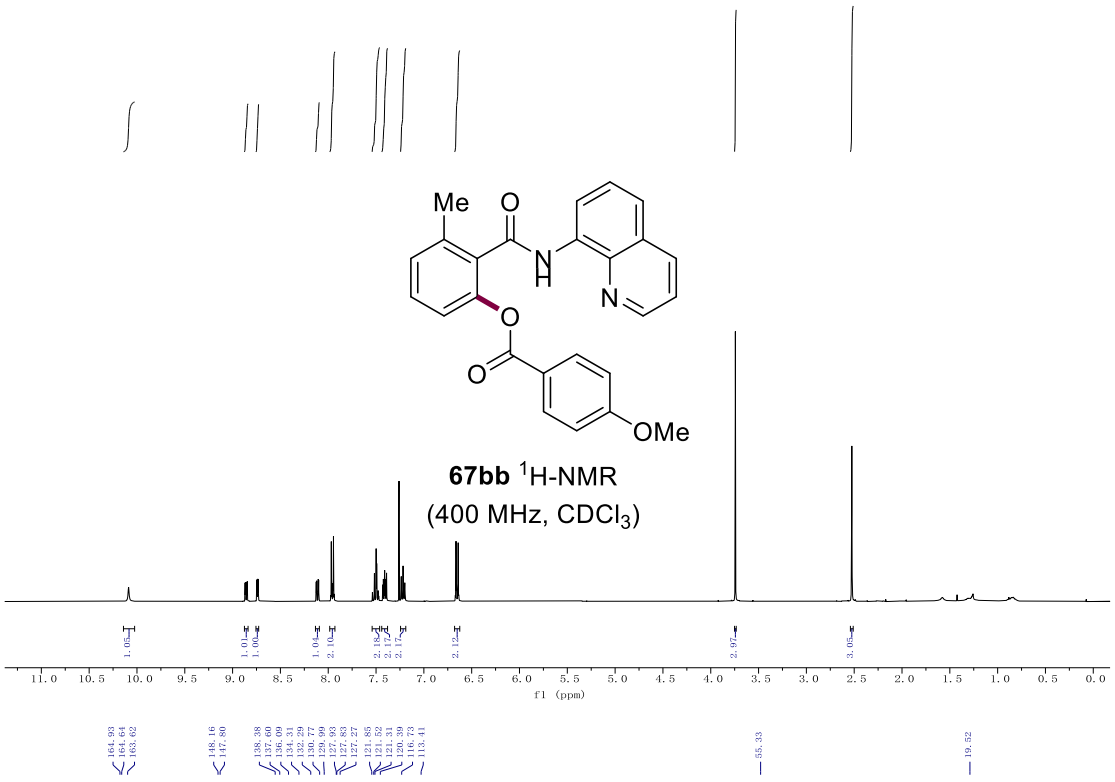
Me
O
N
H
N
O
O
OMe
67bb ^{1}H-NMR
(400 MHz, $CDCl_3$)
f1 (ppm)

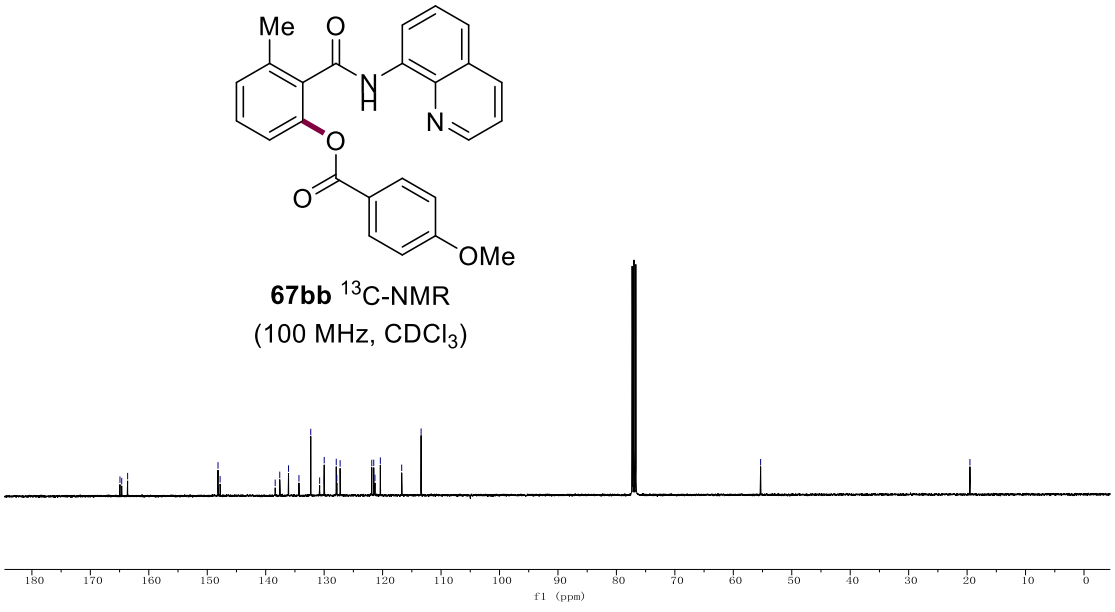
Me
O
N
H
N
O
O
OMe
67bb ^{13}C-NMR
(100 MHz, $CDCl_3$)
f1 (ppm)

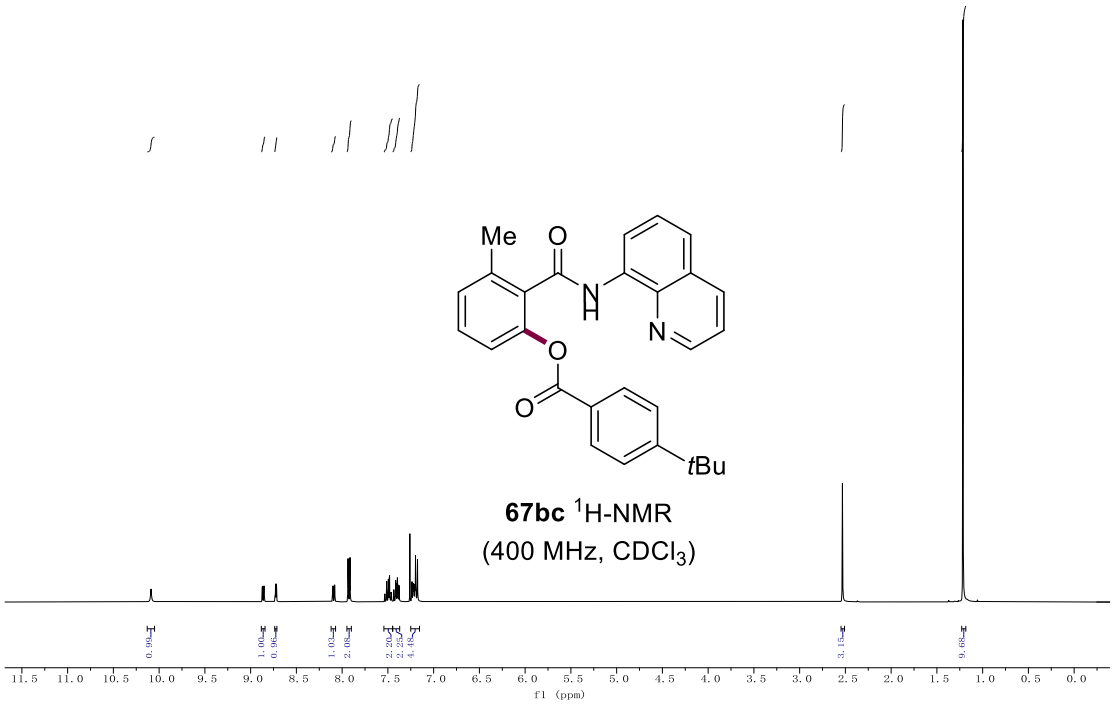

67bc ^{1}H-NMR
(400 MHz, $CDCl_3$)

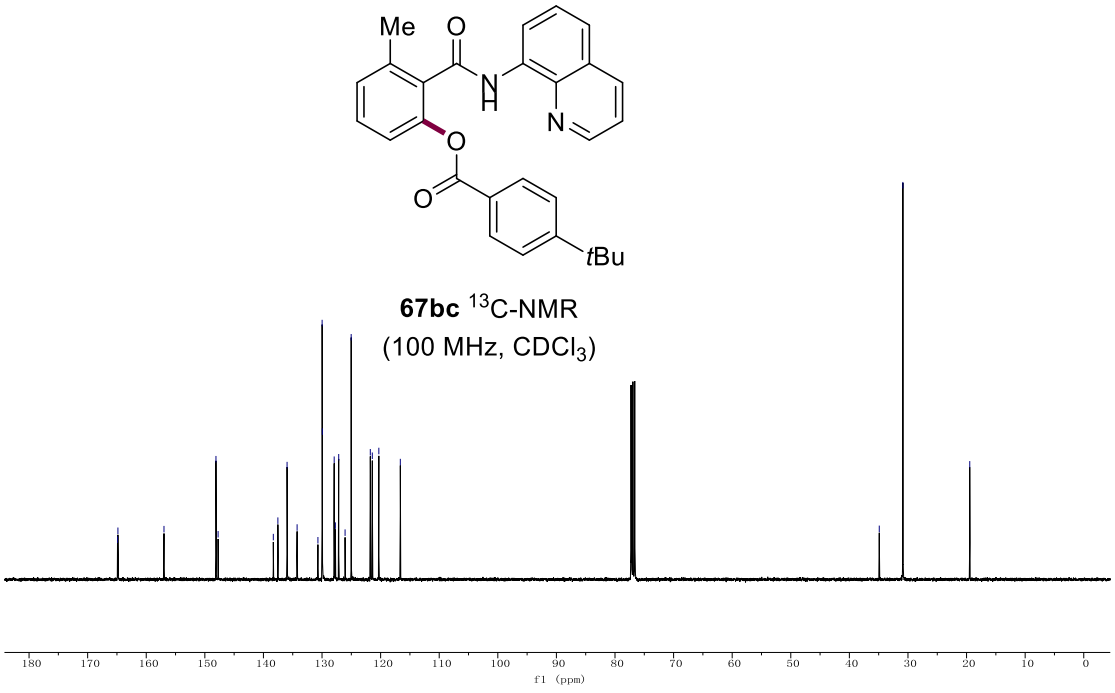

67bc ^{13}C-NMR
(100 MHz, $CDCl_3$)

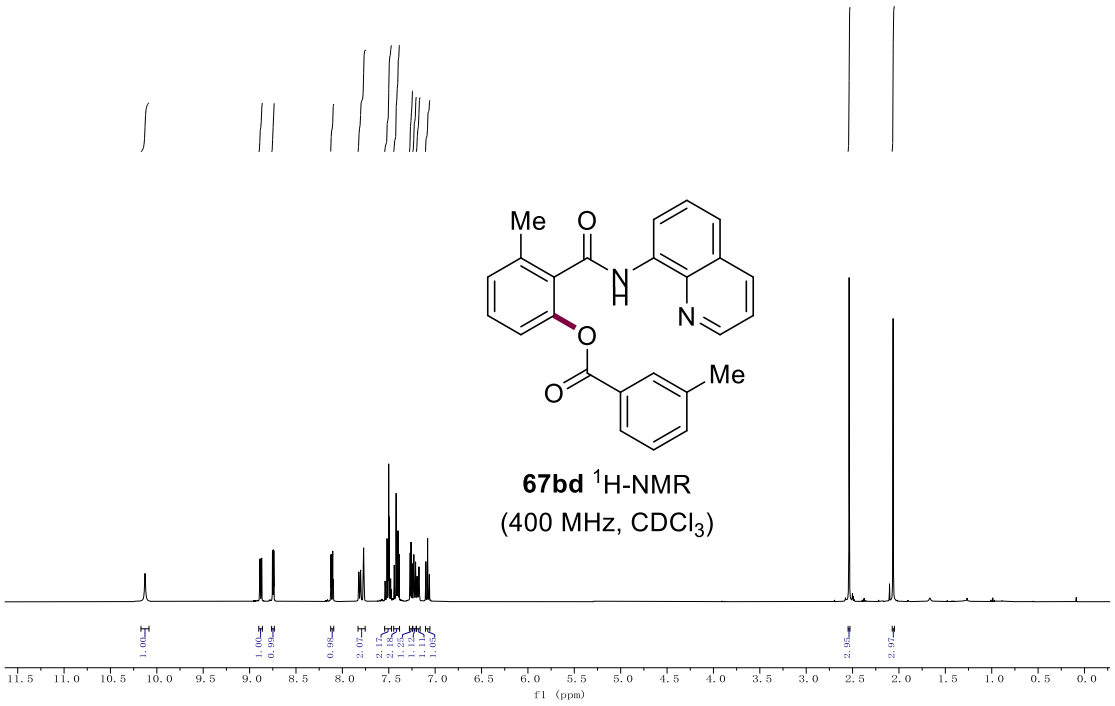

67bd ^{1}H-NMR
(400 MHz, $CDCl_3$)

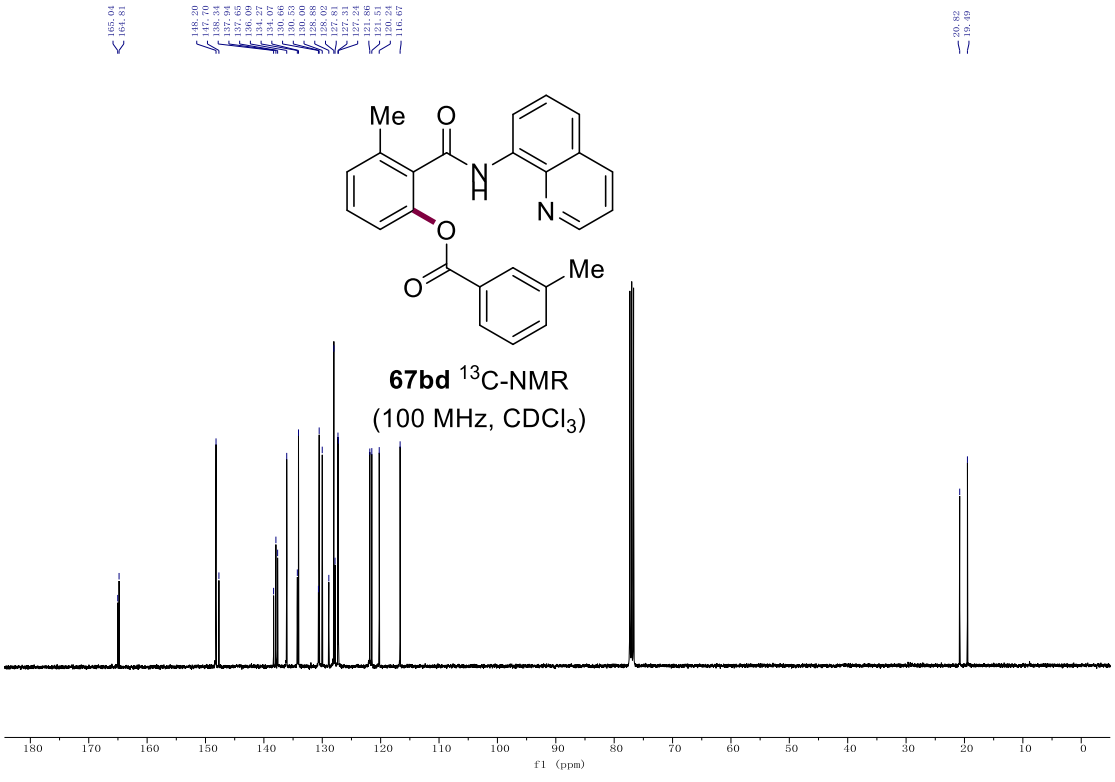

67bd ^{13}C-NMR
(100 MHz, $CDCl_3$)

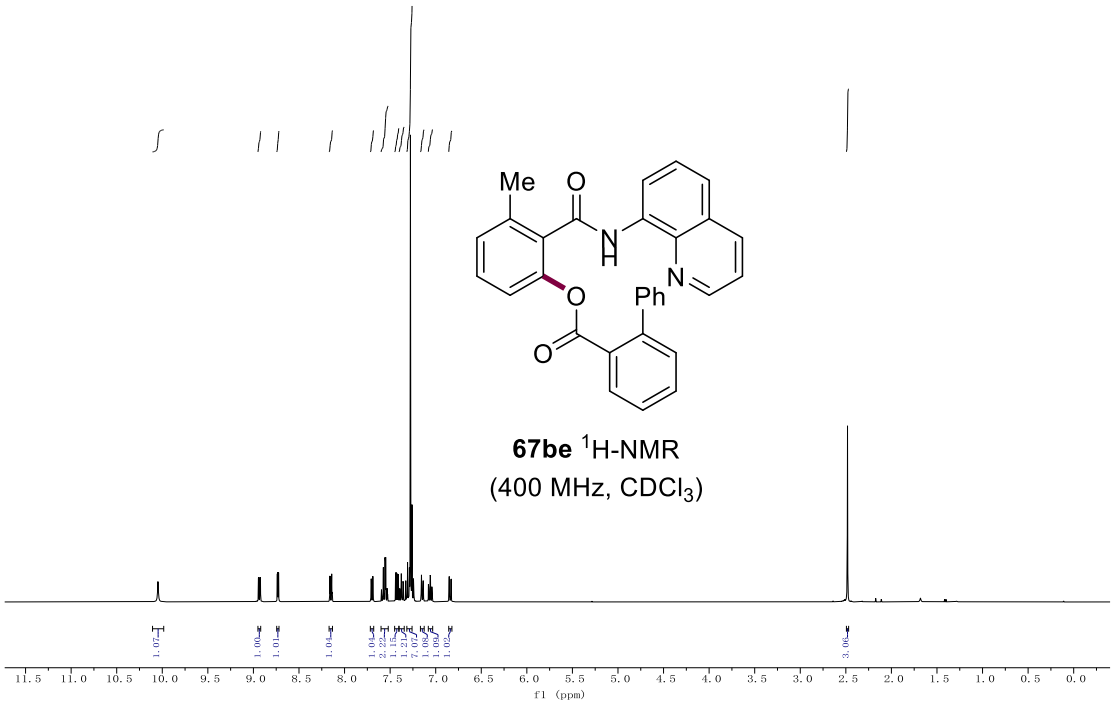

67be ^{1}H-NMR
(400 MHz, $CDCl_3$)

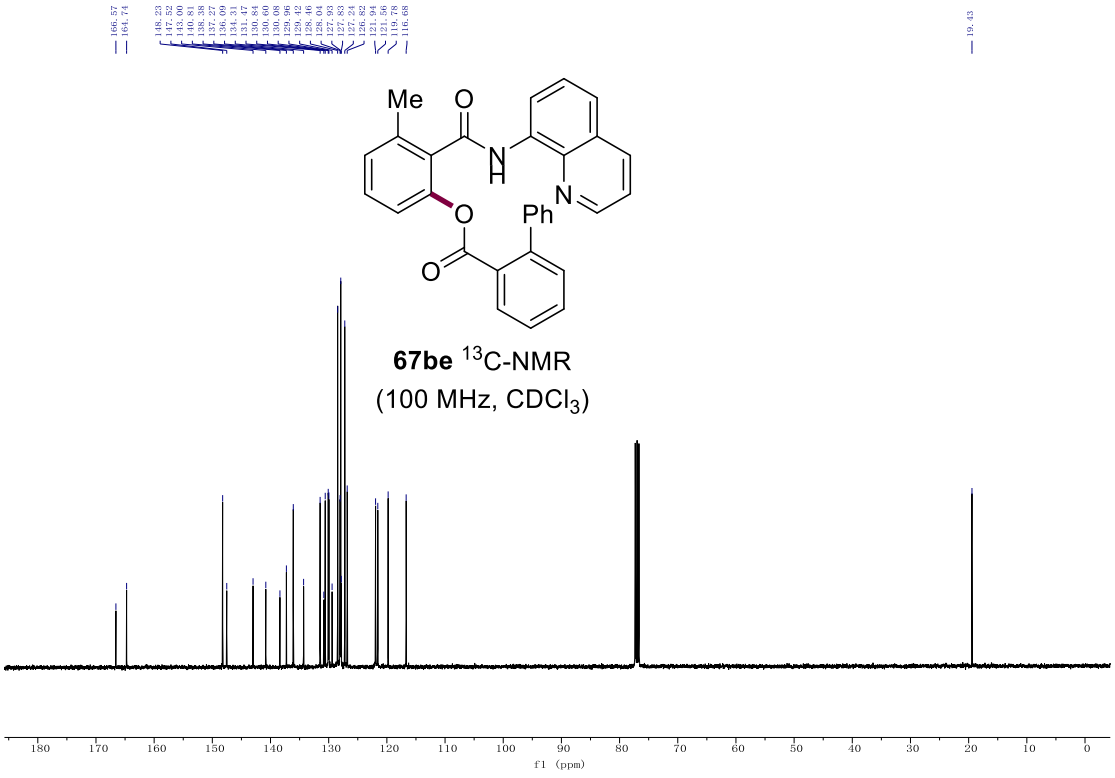

67be ^{13}C-NMR
(100 MHz, $CDCl_3$)

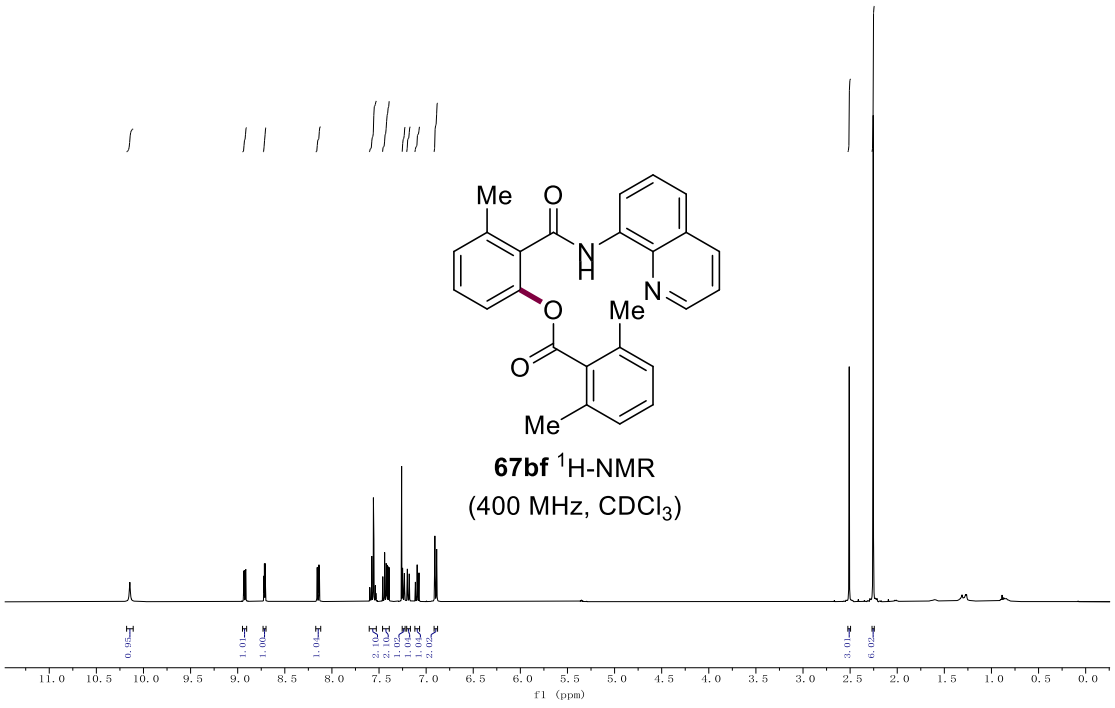

67bf ^{1}H-NMR
(400 MHz, $CDCl_3$)

67bf ^{13}C-NMR
(100 MHz, $CDCl_3$)

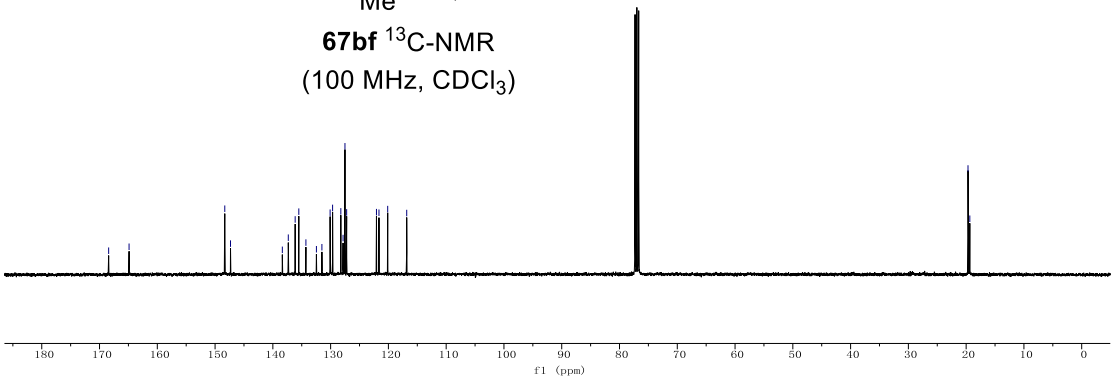

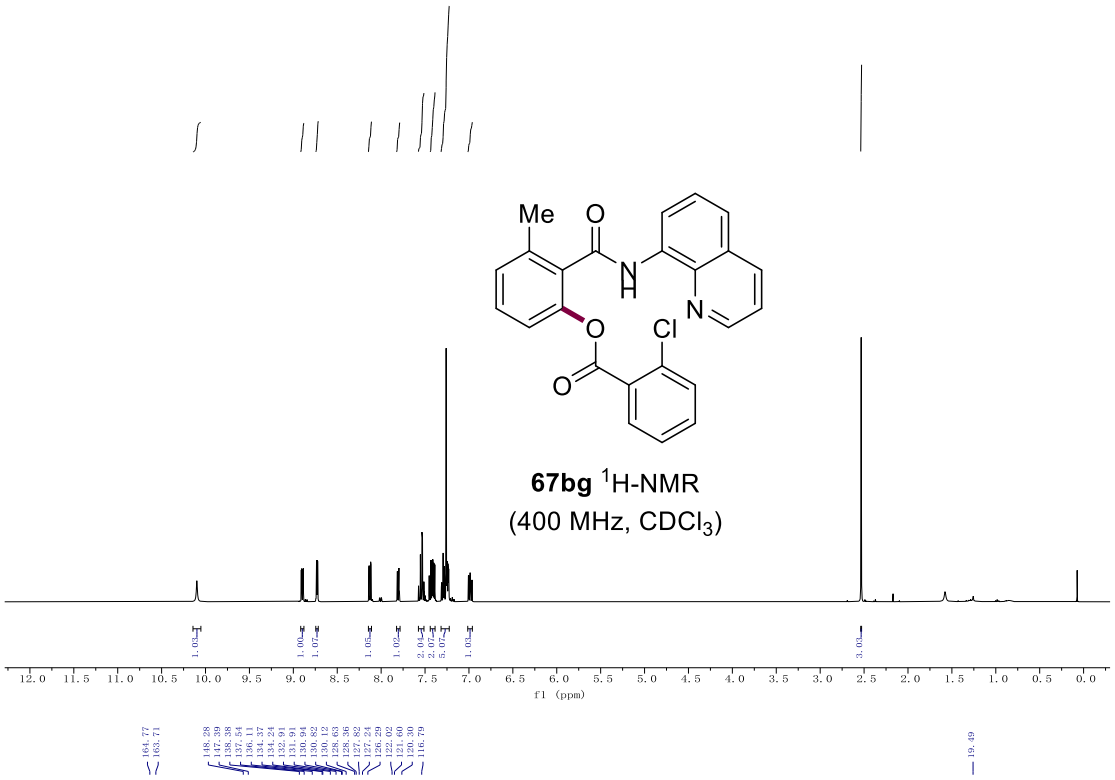

67bg ^{1}H-NMR
(400 MHz, $CDCl_3$)

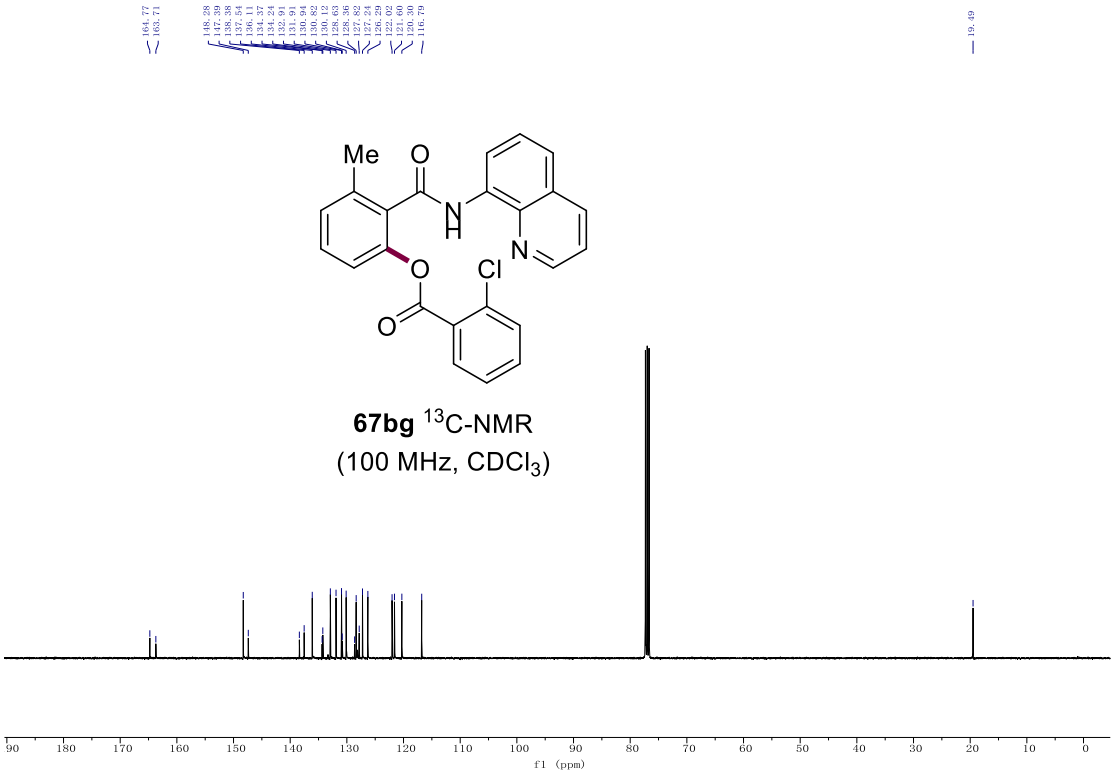

67bg ^{13}C-NMR
(100 MHz, $CDCl_3$)

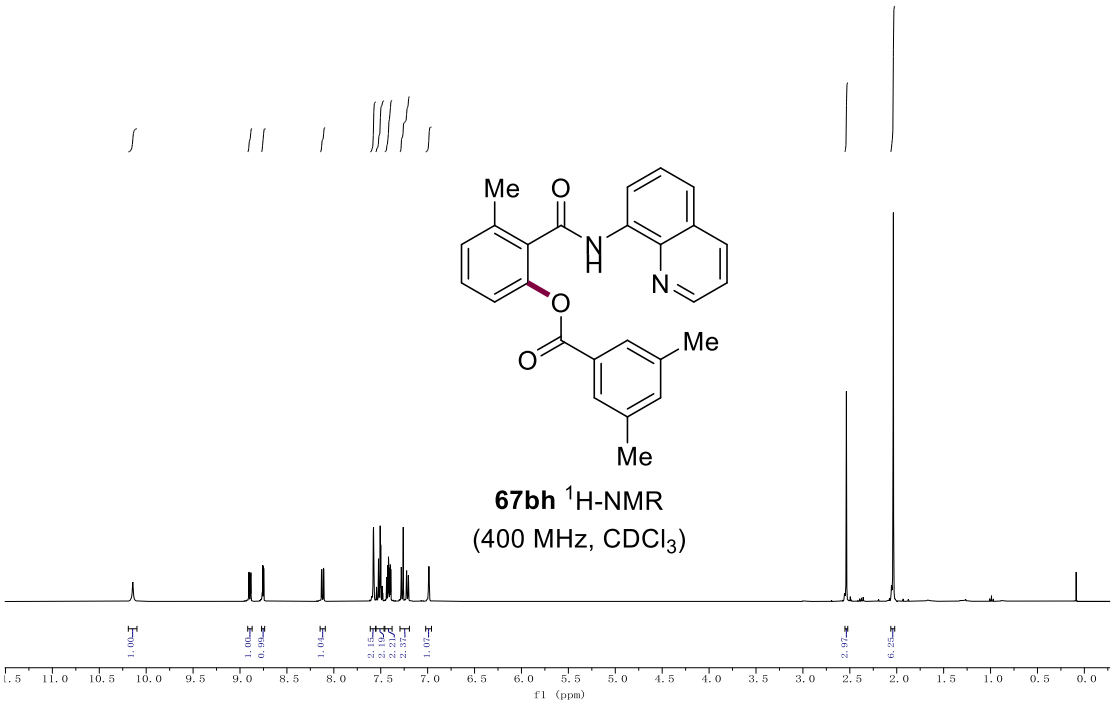

67bh ^{1}H-NMR
(400 MHz, $CDCl_3$)

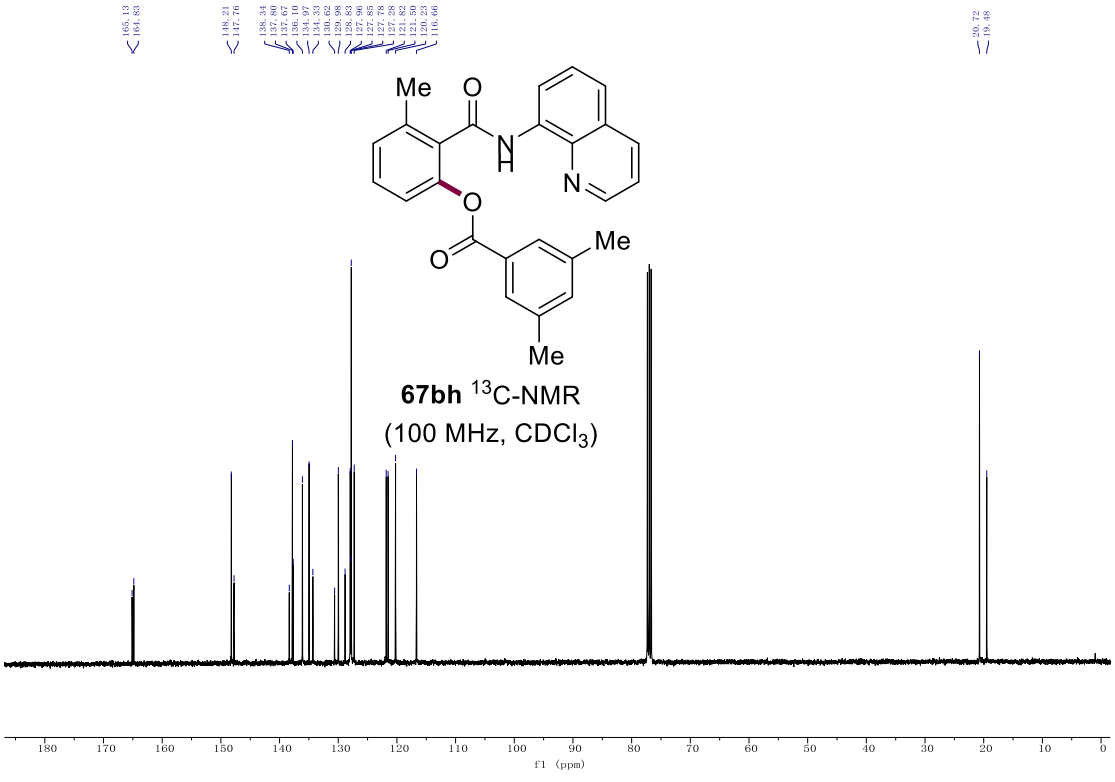

67bh ^{13}C-NMR
(100 MHz, $CDCl_3$)

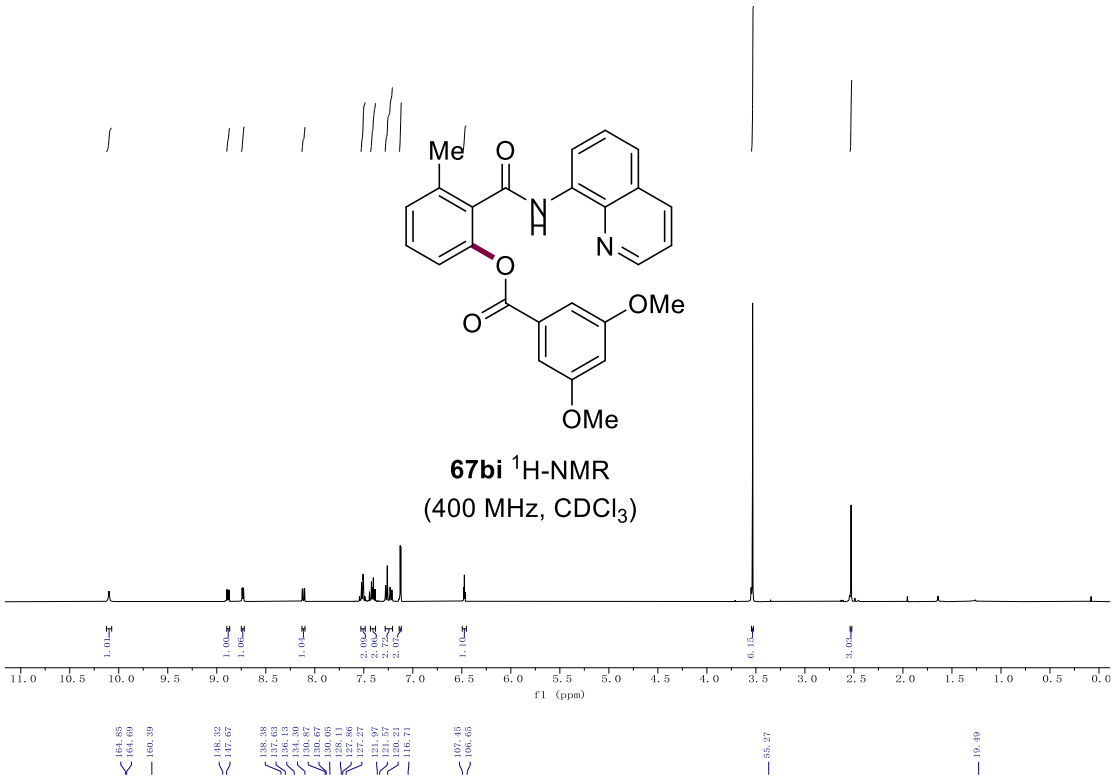

67bi ^{1}H-NMR
(400 MHz, $CDCl_3$)

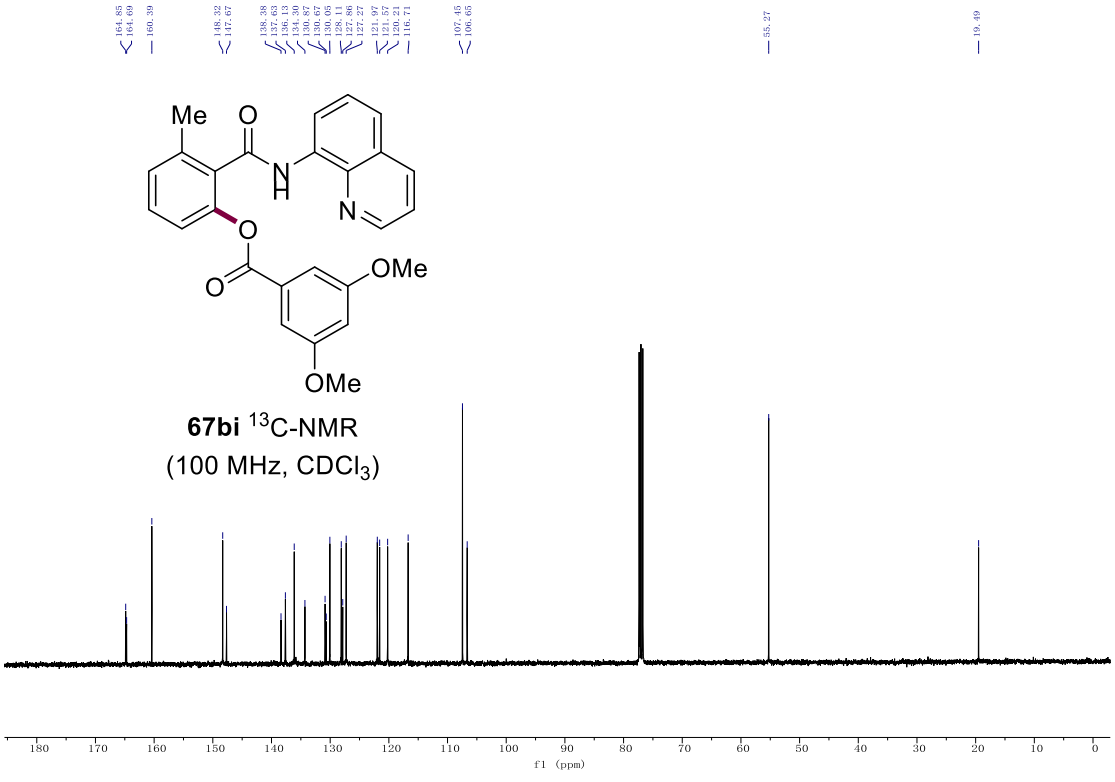

67bi ^{13}C-NMR
(100 MHz, $CDCl_3$)

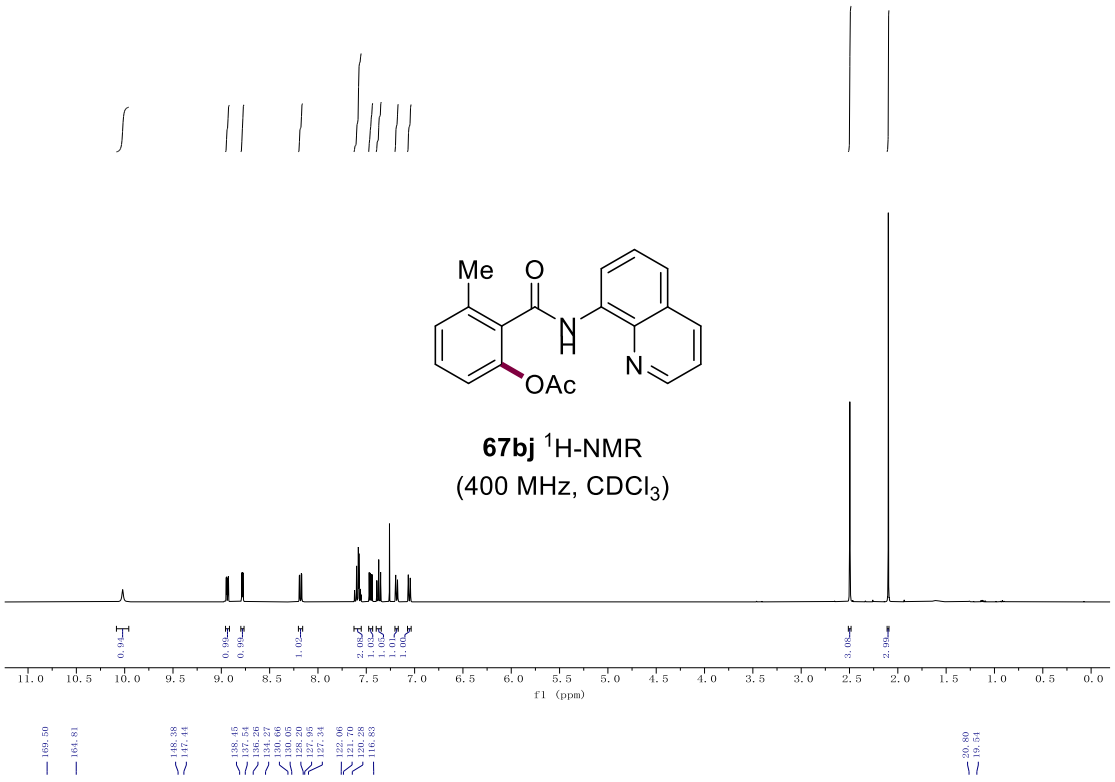

67bj ^{1}H-NMR
(400 MHz, $CDCl_3$)

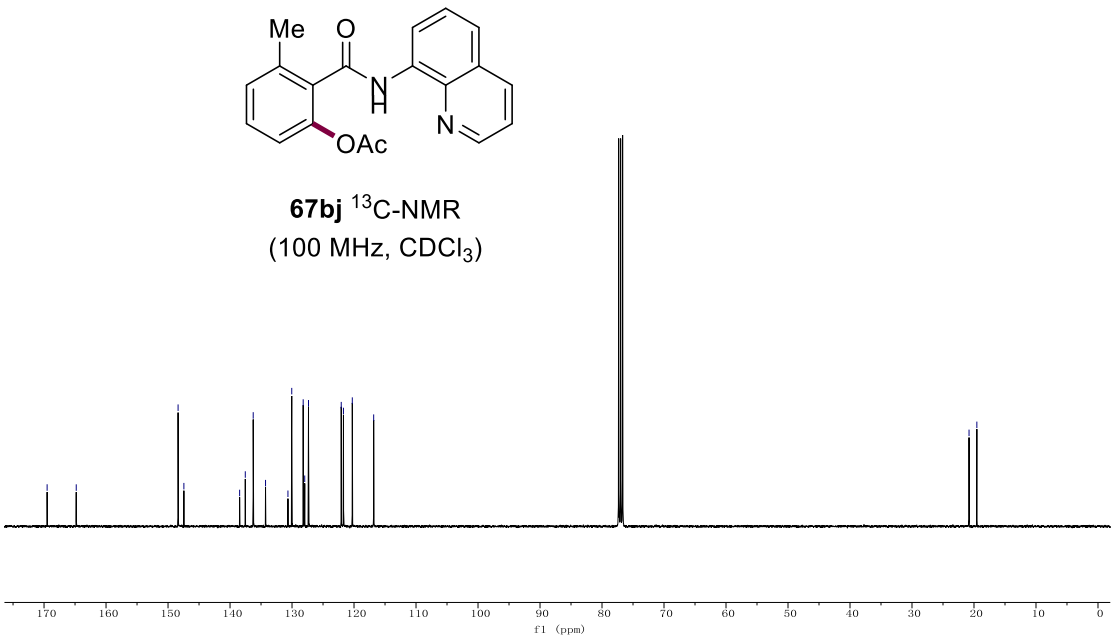

67bj ^{13}C-NMR
(100 MHz, $CDCl_3$)

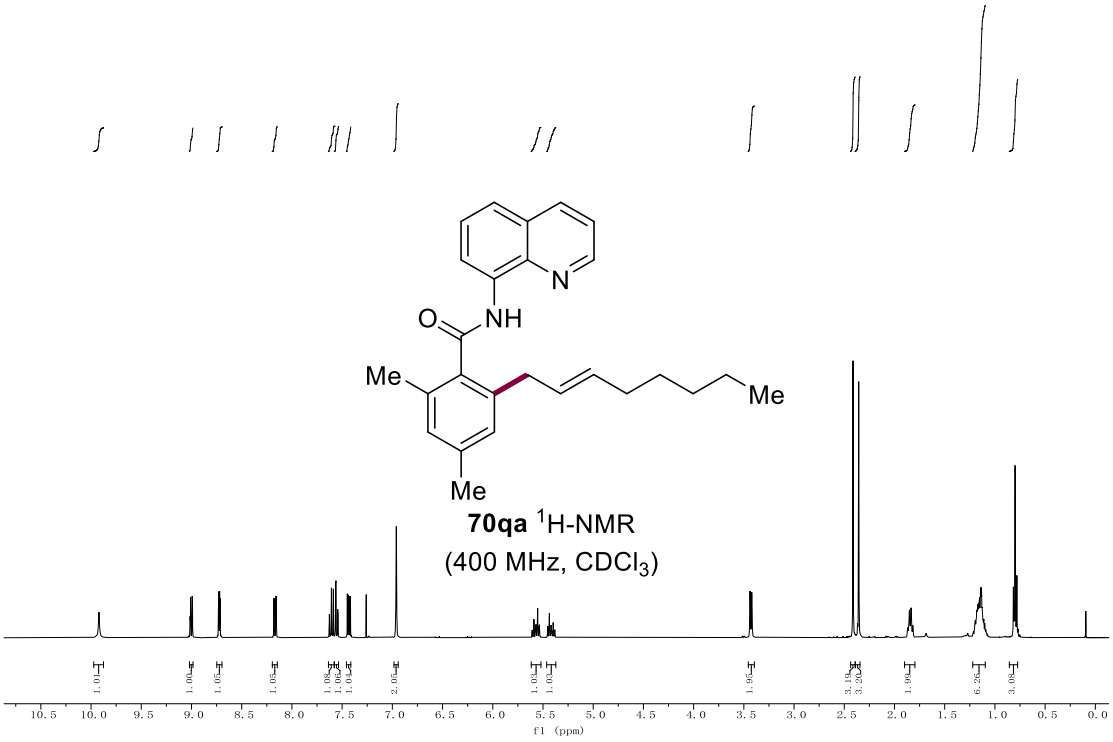

70qa ^{1}H-NMR
(400 MHz, $CDCl_3$)

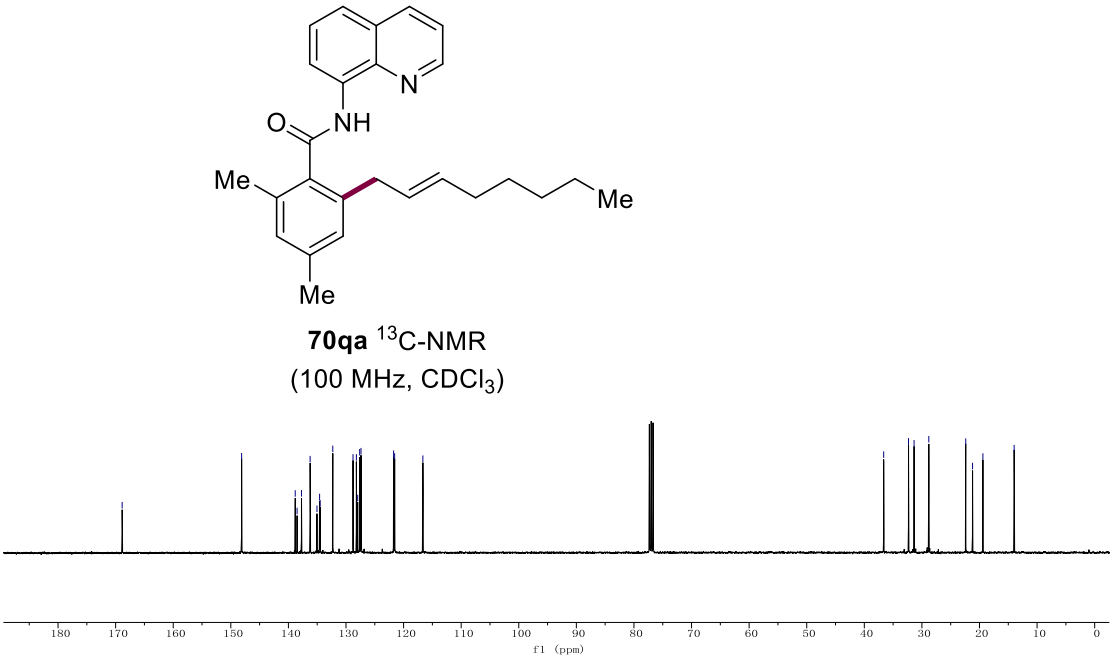

70qa ^{13}C-NMR
(100 MHz, $CDCl_3$)

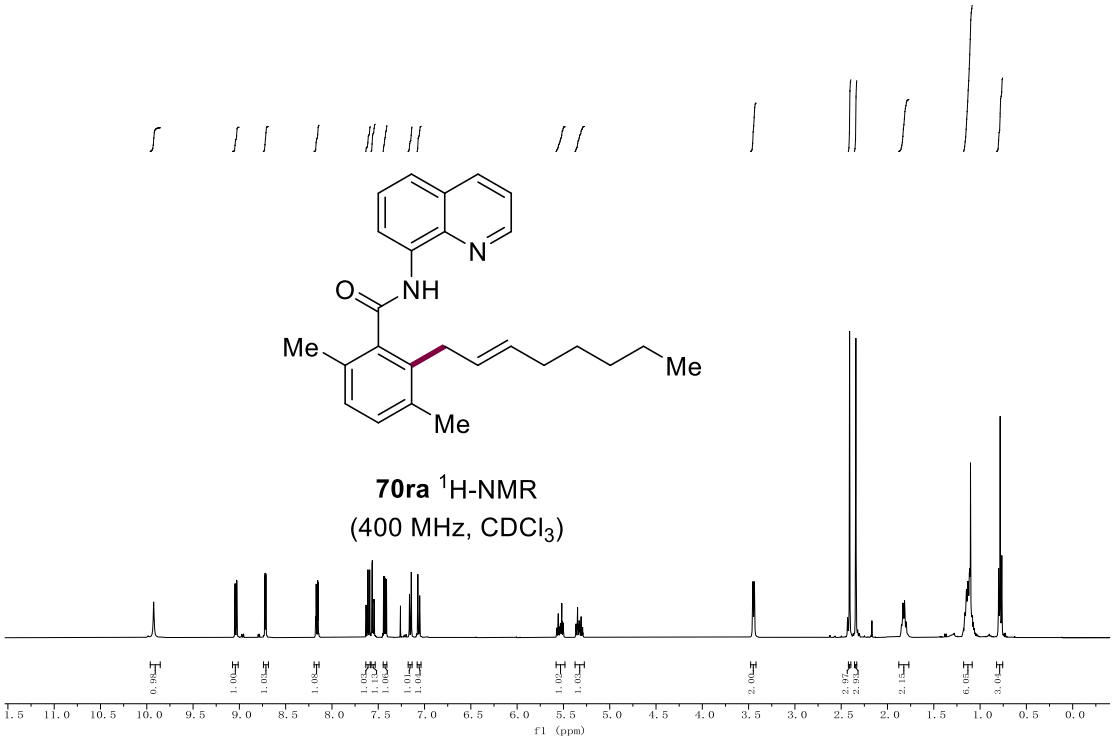

70ra ^{1}H-NMR
(400 MHz, $CDCl_3$)

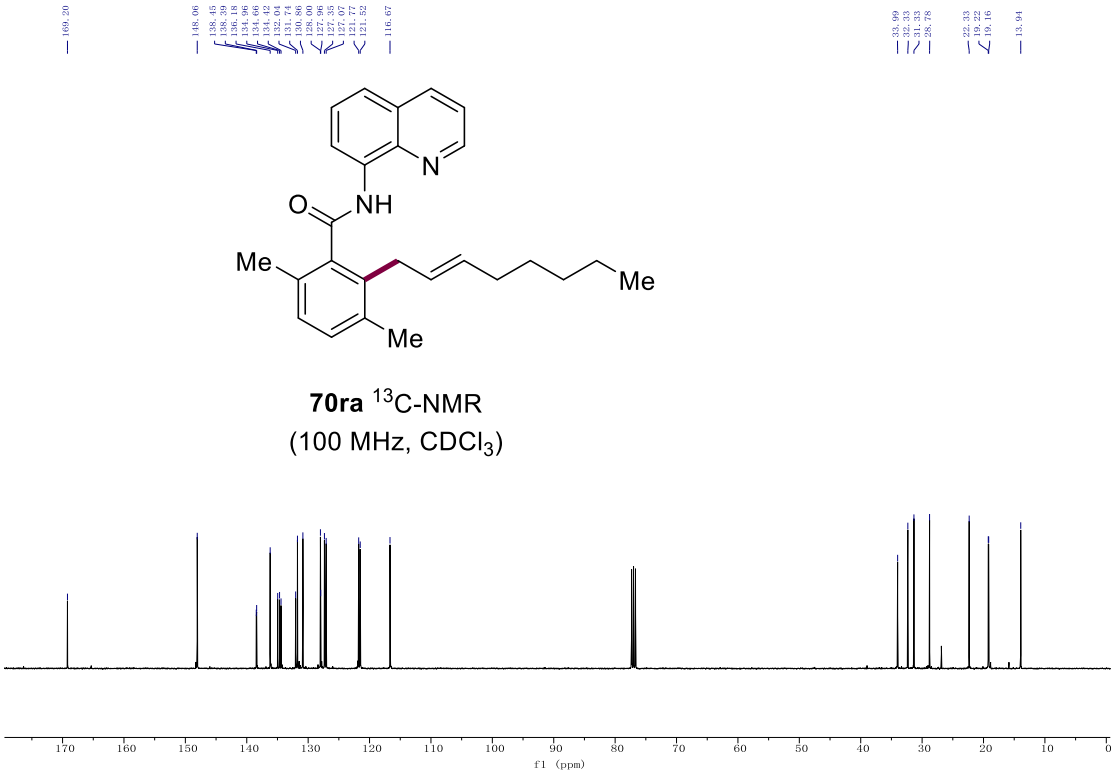

70ra ^{13}C-NMR
(100 MHz, $CDCl_3$)

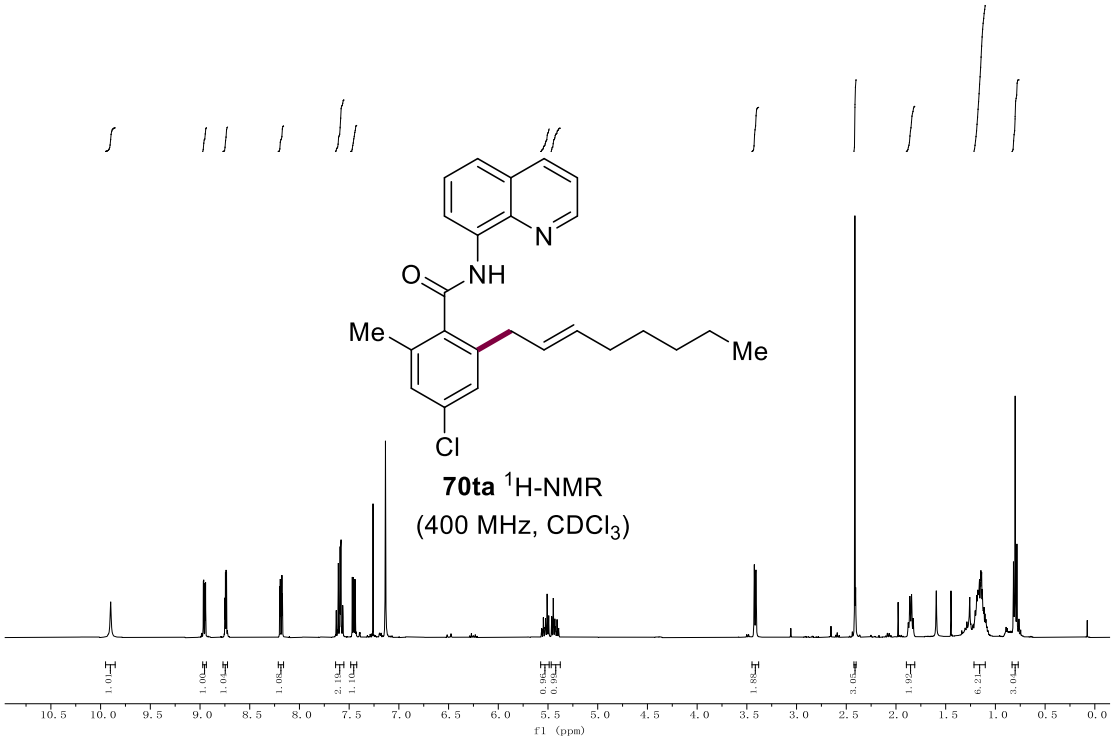
N
O
NH
Me
Me
Cl
70ta 1H-NMR
(400 MHz, CDCl3)
f1 (ppm)

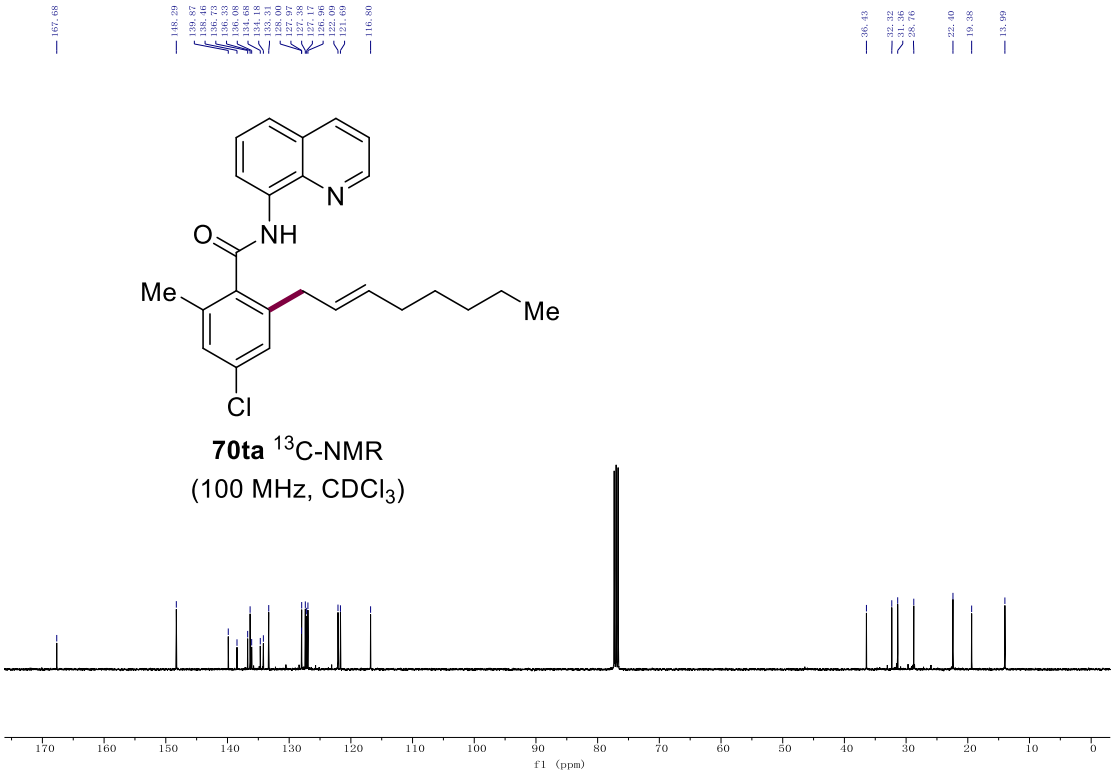
N
O
NH
Me
Me
Cl
70ta 13C-NMR
(100 MHz, CDCl3)
f1 (ppm)

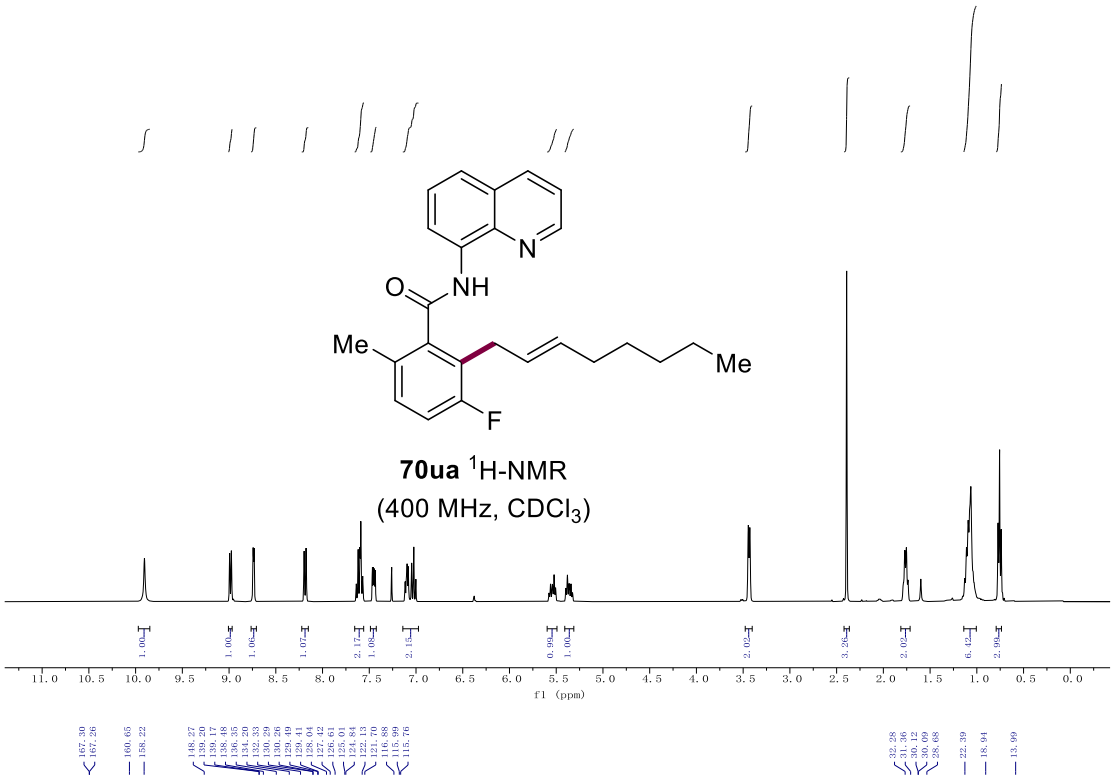
N
O
NH
Me
Me
F
70ua 1H-NMR
(400 MHz, CDCl3)
f1 (ppm)

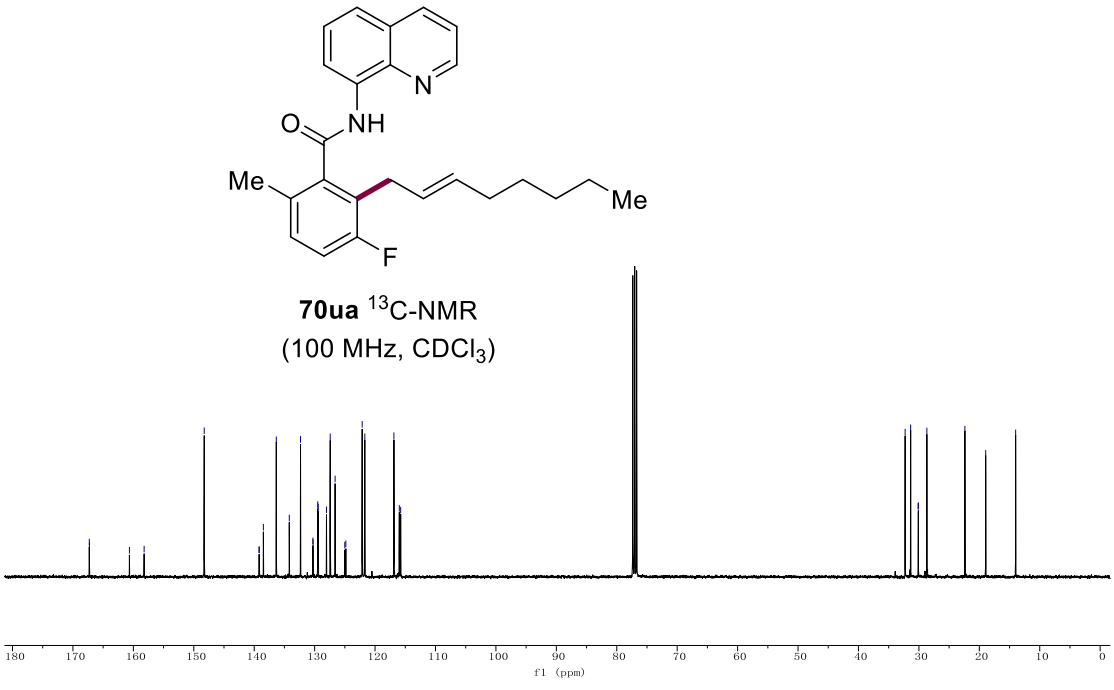
N
O
NH
Me
Me
F
70ua 13C-NMR
(100 MHz, CDCl3)
f1 (ppm)

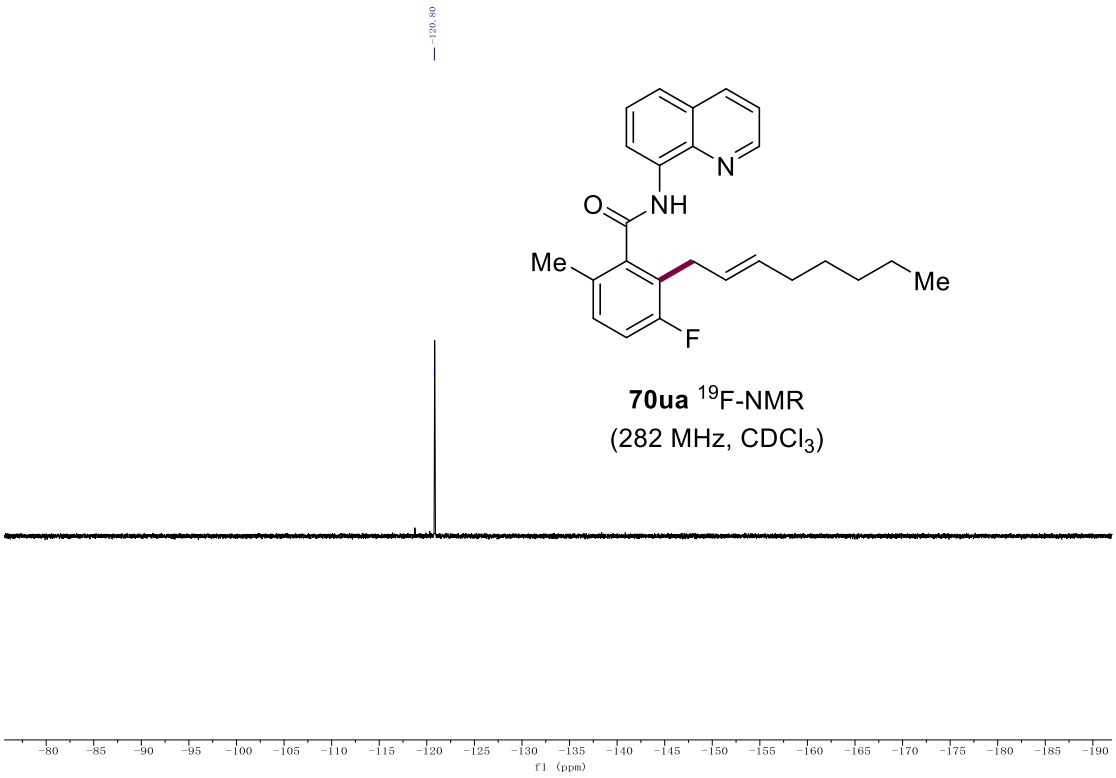

70ua ^{19}F-NMR
(282 MHz, $CDCl_3$)

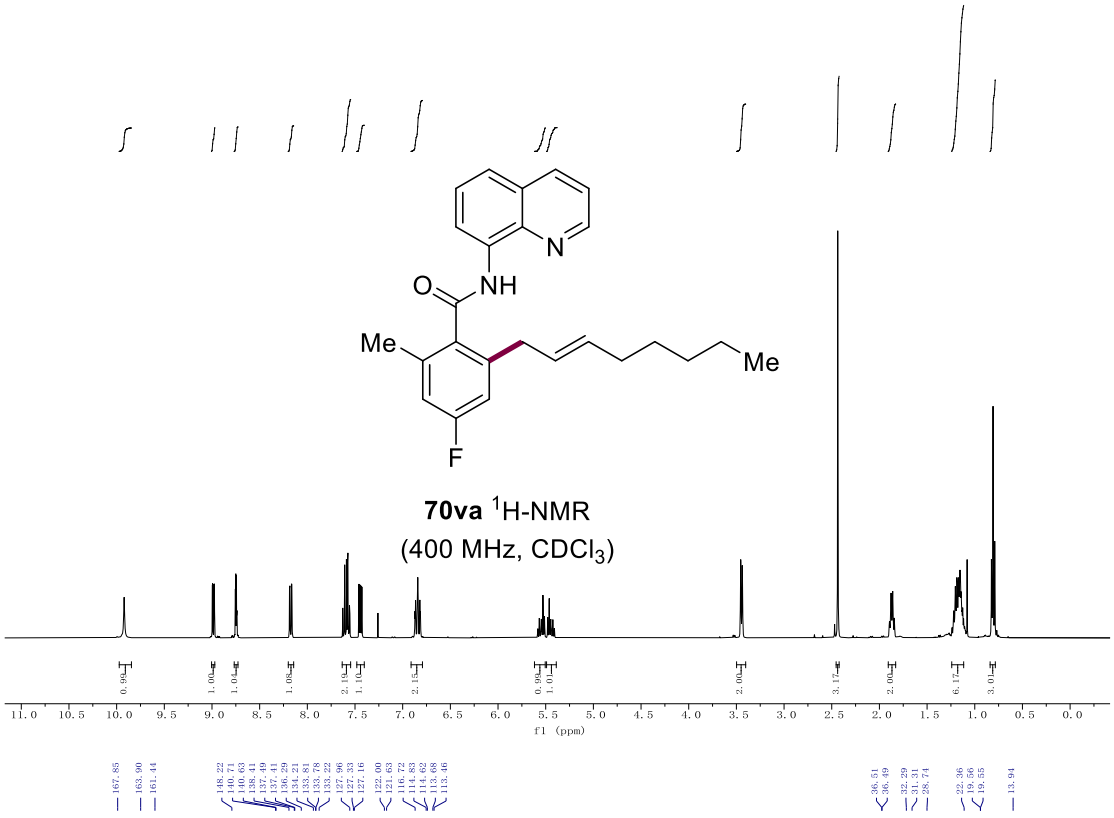

70va ^{1}H-NMR
(400 MHz, $CDCl_3$)

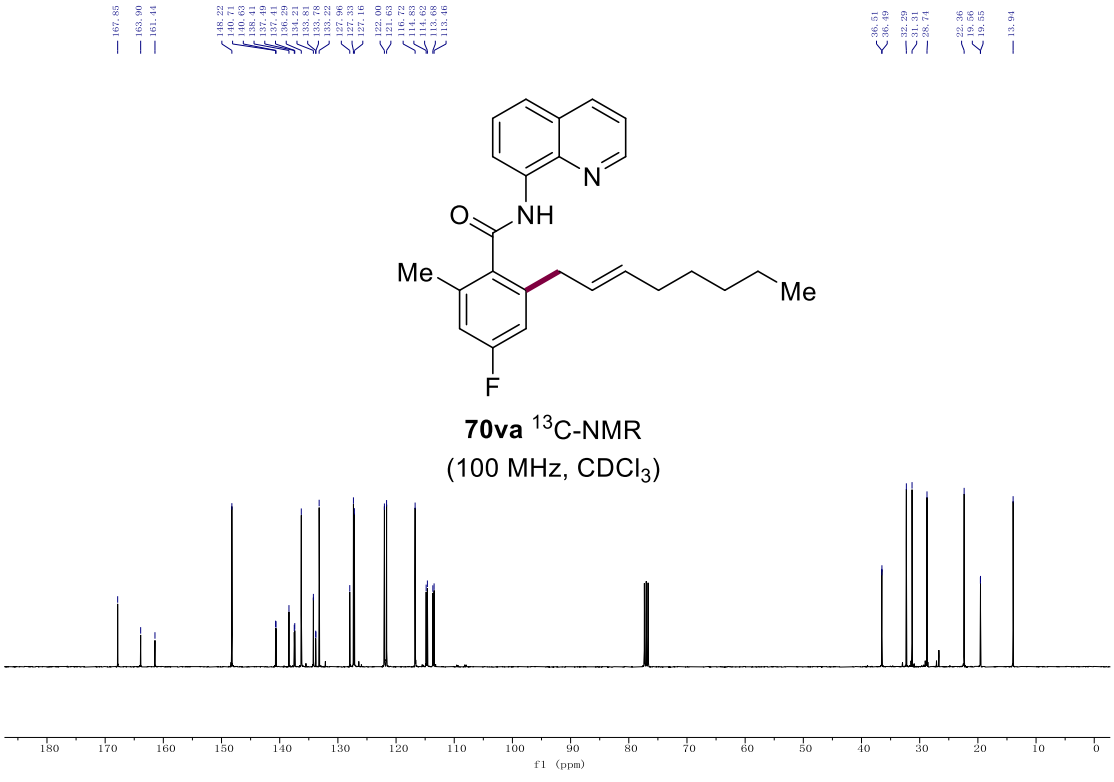

70va ^{13}C-NMR
(100 MHz, $CDCl_3$)

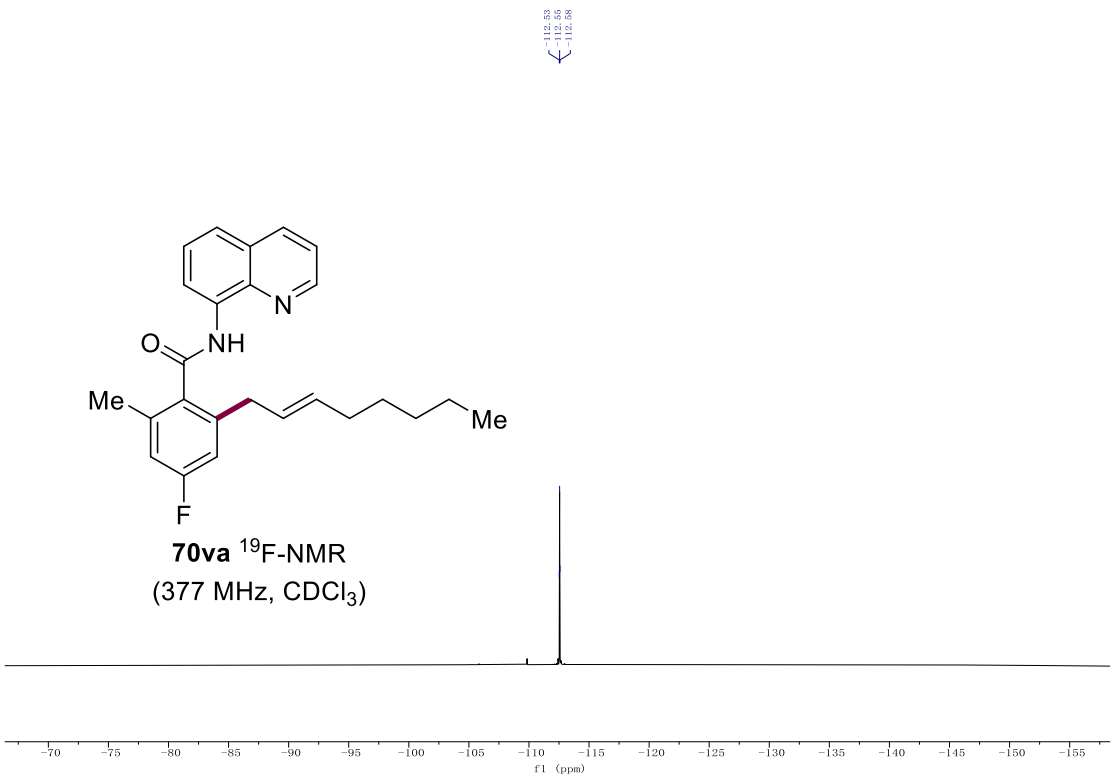
-112.53
-112.55
-112.58
N
O
NH
Me
Me
F
70va 19F-NMR
(377 MHz, CDCl3)
−70
−75
−80
−85
−90
−95
−100
−105
−110
−115
−120
−125
−130
−135
−140
−145
−150
−155
f1 (ppm)

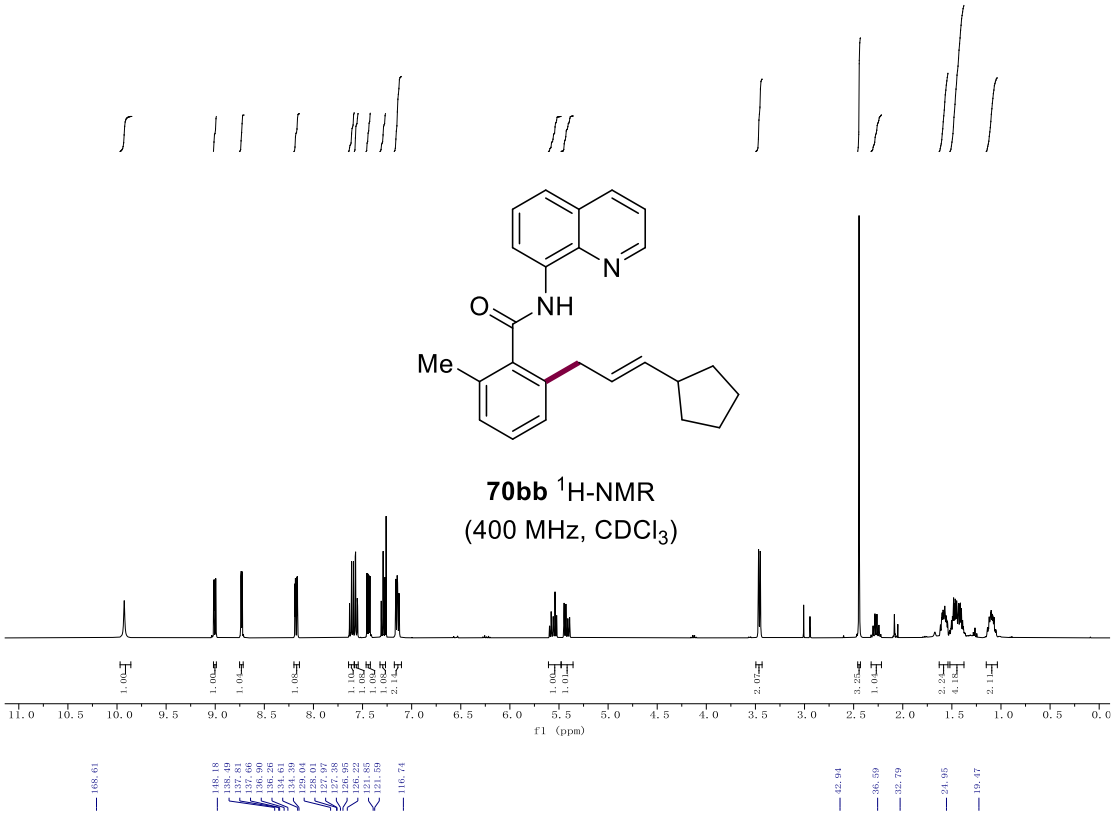

70bb ^{1}H-NMR
(400 MHz, $CDCl_3$)

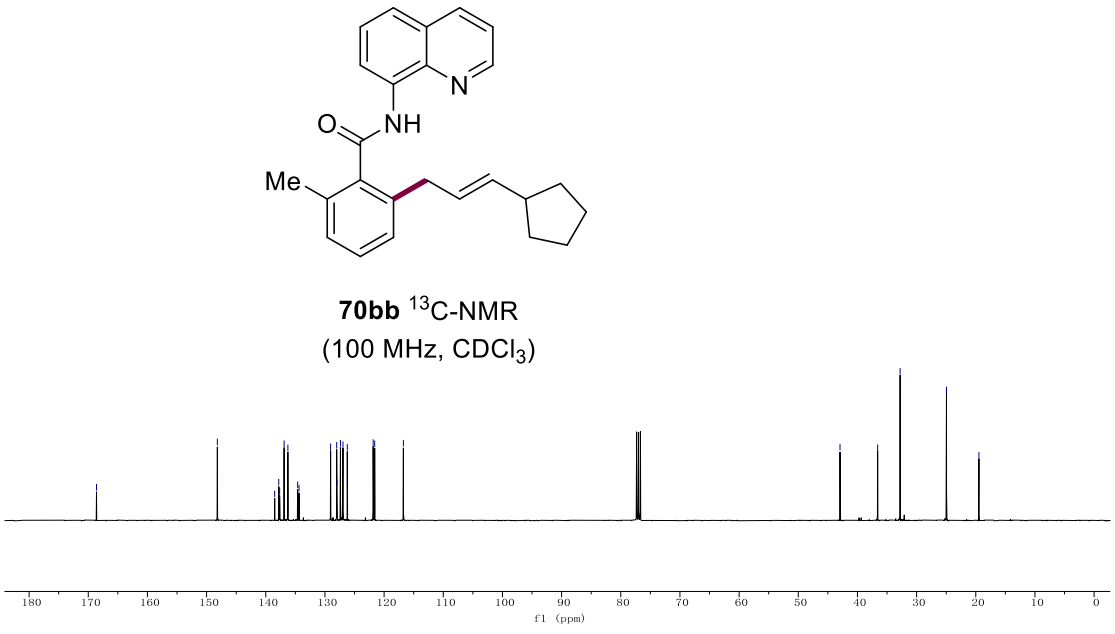

70bb ^{13}C-NMR
(100 MHz, $CDCl_3$)

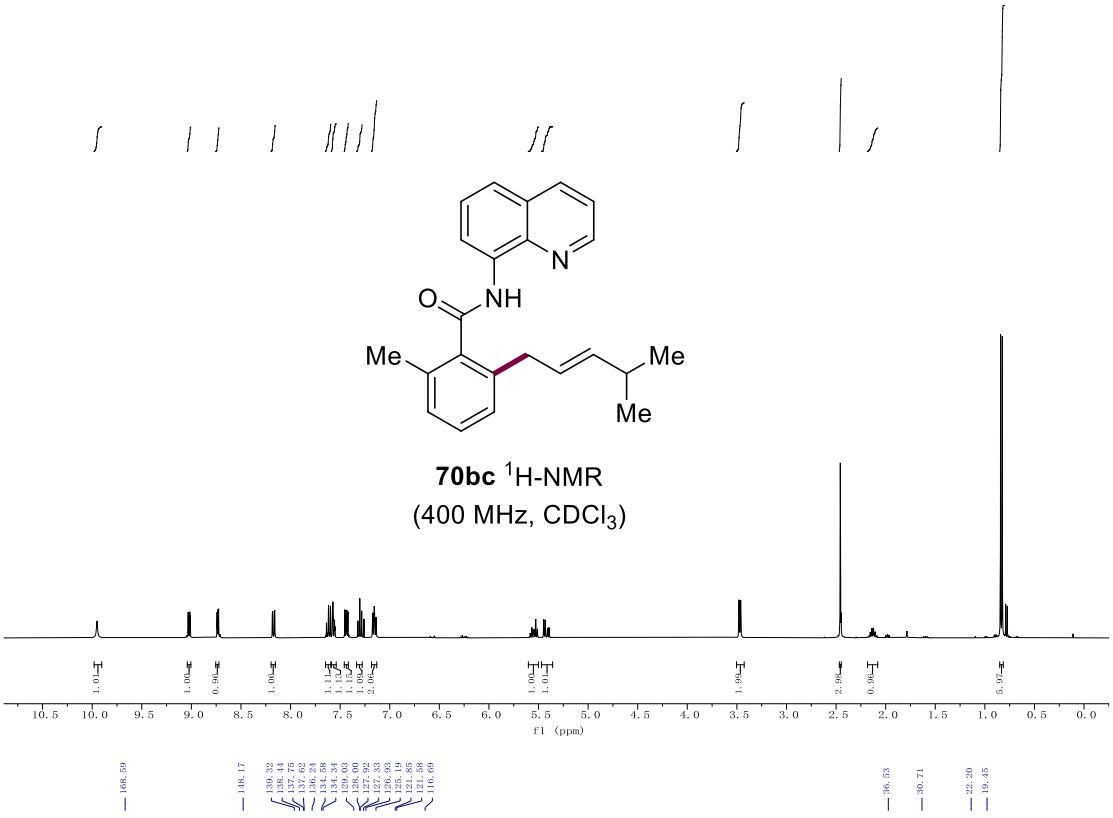

70bc ^{1}H-NMR
(400 MHz, $CDCl_3$)

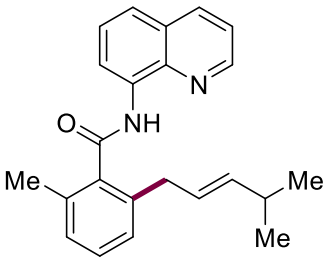

70bc ^{13}C-NMR
(100 MHz, $CDCl_3$)

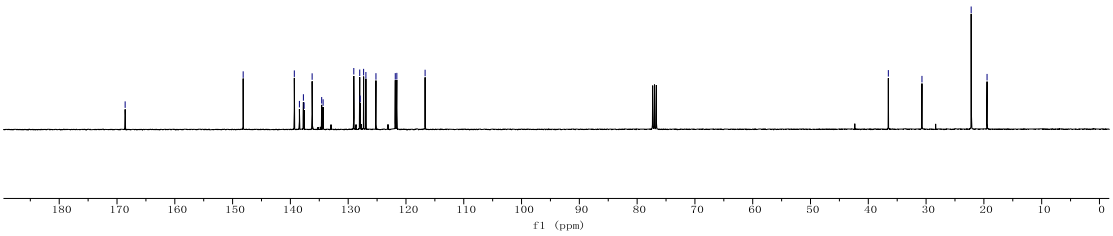

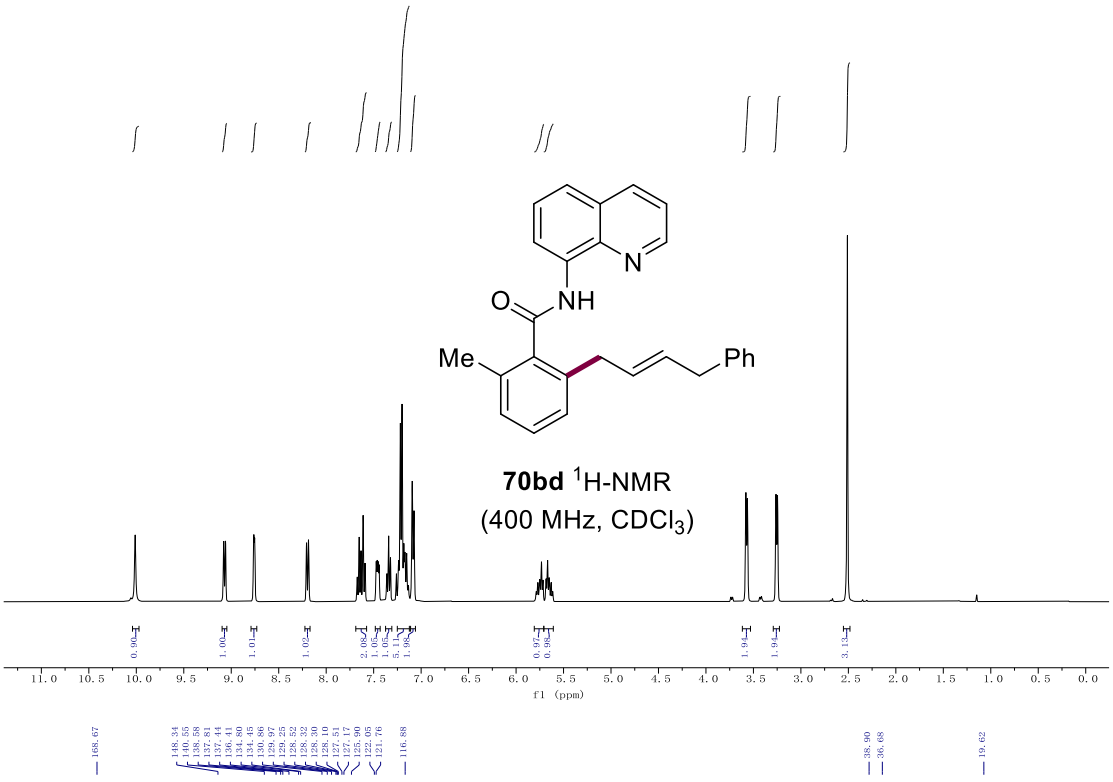

70bd ^{1}H-NMR
(400 MHz, $CDCl_3$)

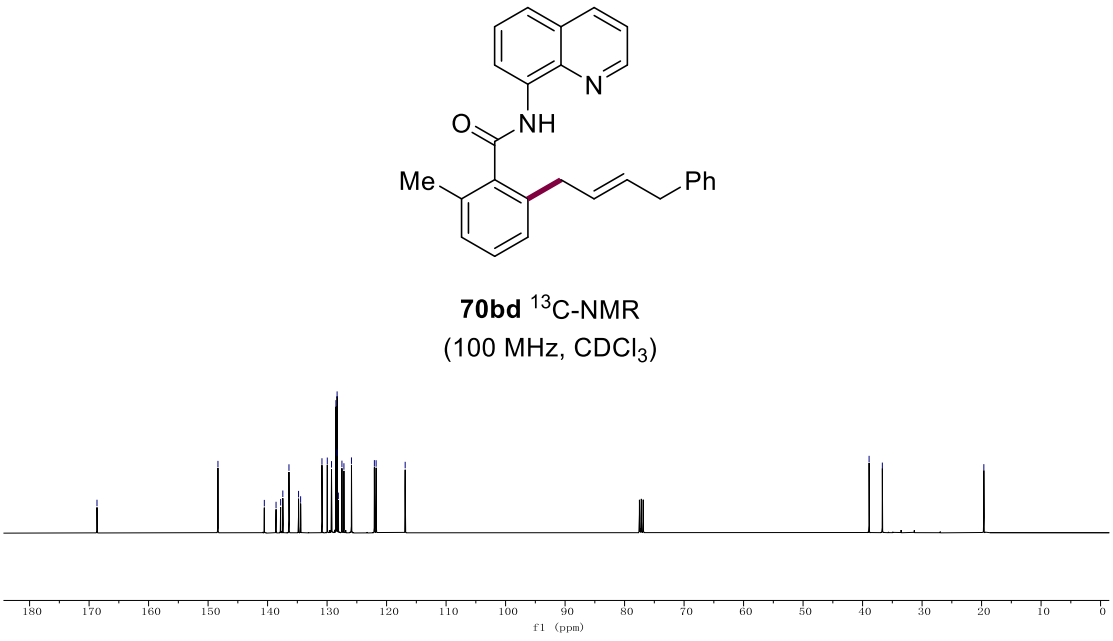

70bd ^{13}C-NMR
(100 MHz, $CDCl_3$)

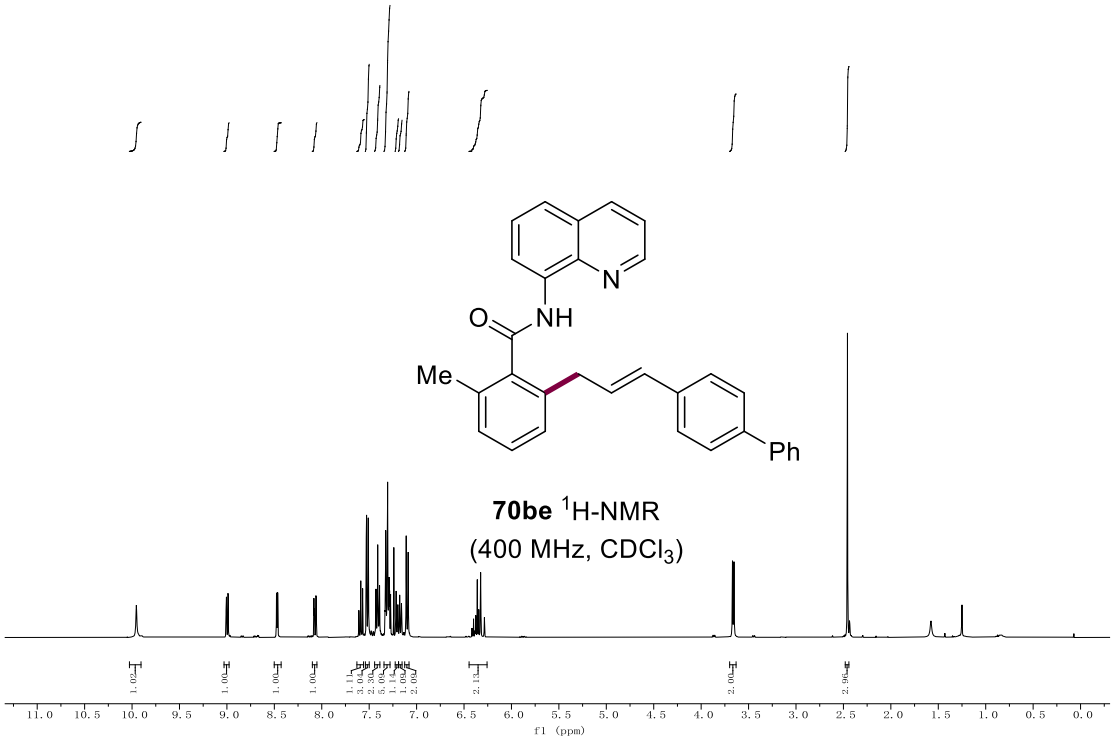
N
O
NH
Me
Ph
70be ^{1}H-NMR
(400 MHz, CDCl$_3$)
f1 (ppm)

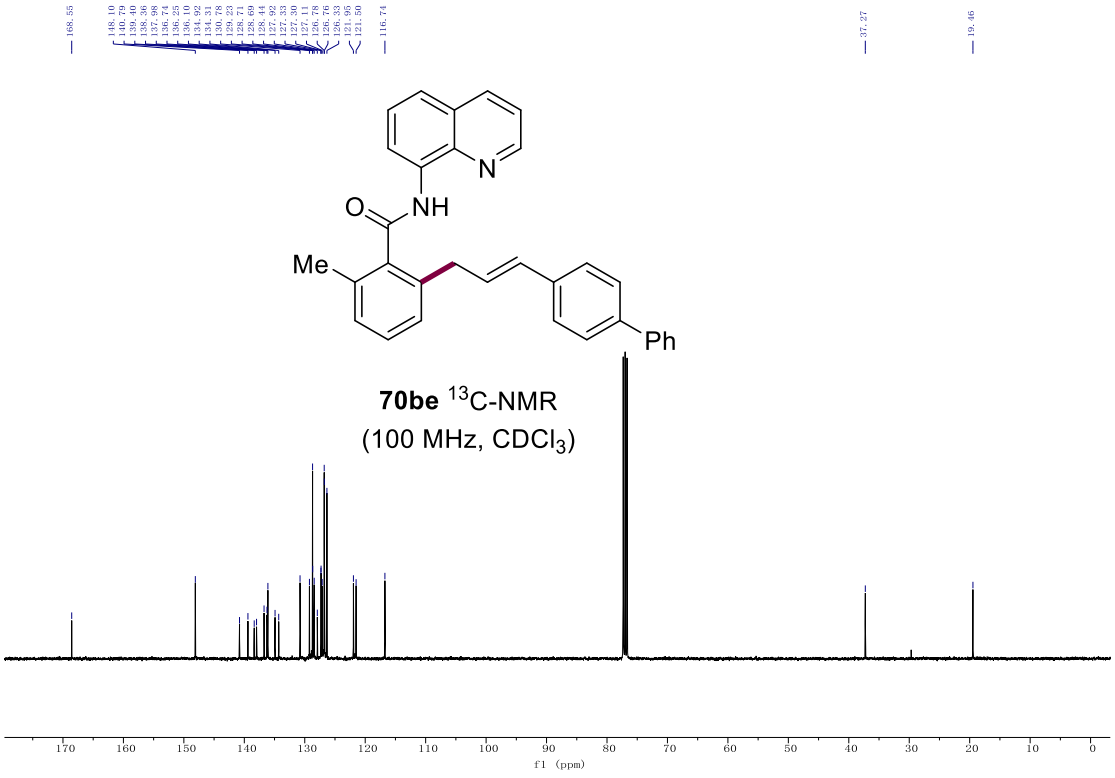
N
O
NH
Me
Ph
70be ^{13}C-NMR
(100 MHz, CDCl$_3$)
f1 (ppm)

Acknowledgement

I would like to take this chance to express my gratitude to all the people have supported me during last four years. First and foremost, I'd like to thank Prof. Dr. Lutz Ackermann for the opportunity to work in this excellent group. Your guidance in chemistry and mentorship of scientific research are essential for my doctoral research.

Secondly, I'd like to thank Prof. Shoubhik Das for being my second supervisor. I'm grateful for all the time you have taken for our meetings and kindly suggestions you provided for my chemistry and life as well.

I gratefully acknowledge China Scholarship Council (CSC) for the financial support during my research stay in Germany.

I would also like to extend my gratitude to all the group members I have the opportunity to collaborate: Dr. Youai Qiu, Uttam Dhawa, Tjark Meyer, Leonardo Massignan, Julia Struwe, Alexj Scheremetjew, Maximilian Stangier, Dr. Lar Finger, Dr. Nicolas Sauermann, Dr. Torben Rogge, Dr. João C. A. de Oliveira, Dr. Tomasz Wdowik, Jiping Hao and Weizhao Li.

I would like to thank all the people who have proofread and helped me correcting this thesis: Dr. Xuefeng Tan, Valentin Müller, Zhigao Shen, Shou-Kun Zhang, Jiayu Mo, Uttam Dhawa, Jun Wu and Wen Wei. I would like to thank all the people who previously helped me correcting manuscripts, supporting information, posters, abstracts and proposals for me: Shou-Kun Zhang, Uttam Dhawa, Zhigao Shen, Jiayu Mo, Wei Wang, Dr. Torben Rogge, Dr. Youai Qiu, Dr. Svenja Warratz, Dr. Ramesh Chandra Samanta, Tjark Meyer, Leonardo Massignan, Julia Struwe, Alexj Scheremetjew, Maximilian Stangier, Ralf Alexander Steinbock, Dr. Weijun Kong, Dr. Xuefeng Tan, Dr. Lar Finger and Dr. Cuiju Zhu.

Furthermore, I am grateful to Gabriele Keil-Knepel for all the kind and patient support regarding all the administrative tasks and other requirements necessary to my research and life in Germany. I particularly thank Stefan Beußhausen and Karsten Rauch for all their kindly support, which contributes to our excellent working conditions

in the lab. Additionally, I thank the analytical departments of IOBC for the swift and precise handling of countless of analytical samples and their kind support.

I'd like to take the chance to express my gratitude to my former supervisor Prof. Xiaonian Li and Prof. Chunshan Lu. The meetings with Prof. Xiaonian Li have always been the highlights of my master study.

Last but not least, I would like to thank my family for their understanding and constantly support in the last four years. Especially to my mother Jixiang Liu, my wife Mengdan Liu and my daughter Youran Tian, you are the delight of my life.